supplemento ai
rendiconti
del Circolo matematico di Palermo

VIIth International Conference in "Stochastic Geometry, Convex Bodies, Empirical Measures & Applications to Mechanics and Engineering Train-Transport"

Messina, April 22-24, 2009

Edited by:
GIUSEPPE CARISTI

serie II - numero 81 - anno 2009

sede della società: Palermo - Via Archirafi, 34

SUPPLEMENTO

AI

RENDICONTI DEL CIRCOLO MATEMATICO DI PALERMO

DIREZIONE E REDAZIONE
Via Archirafi, 34 - Tel. 0916040266 - 90123 Palermo (Italia)
E-mail: vetro@math.unipa.it

Tipografia «A.C.» s.n.c. - Via Filippo Marini, 15 - Tel. e Fax 091422758 - 90128 Palermo
e-mail: tipografiaac@tin.it

SUPPLEMENTO

AI

RENDICONTI DEL CIRCOLO MATEMATICO DI PALERMO

DIRETTORE: **P. VETRO**

VIIth INTERNATIONAL CONFERENCE IN "STOCHASTIC GEOMETRY, CONVEX BODIES, EMPIRICAL MEASURES & APPLICATIONS TO MECHANICS AND ENGINEERING TRAIN-TRANSPORT"

Messina, April 22-24, 2009

Edited by:
Giuseppe Caristi

SERIE II - NUMERO 81 - ANNO 2009



P A L E R M O
S E D E D E L L A S O C I E T À
VIA ARCHIRAFI, 34

CONFERENCE DATA

Messina, 22nd – 24th April, 2009

Scientific Committee

M.I. Stoka (Torino - Italia); D. Bosq (Paris - France); V. Capasso (Milano - Italia);
G. Caristi (Messina - Italia); R. Corradetti (Torino - Italia); P. Deheuvels (Paris - France);
A. Duma (Hagen - Germany); A. Florian (Salisburg - Austria);
P. Gruber (Wien - Austria); D. Lo Bosco (Reggio Calabria - Italia);
G. Restuccia (Messina - Italia)

Host Organizations

University of Messina - Faculty of Economics

Organizing Committee

G. Caristi; D. Barilla; V. Bonanzinga; G. Leonardi; A. Puglisi; S. Saccà.

Supported by

Sicily Region
Assembly Regional Sicilian
Province of Messina
Municipality of Messina
University of Reggio Calabria - Faculty of Engineering
Department DIMET of University of Reggio Calabria
Bonino Pulejo Foundation - Messina
Franca and Diego de Castro Foundation - Torino
N.G.I. Shipping Company
Carige Bank

Dedicated to Professor Marius Stoka
on occasion of his 75th birthday



Prof. Marius I. Stoka

UNION MATEMATICA ARGENTINA
CASILLA DE CORREO 3588
BUENOS AIRES
REPUBLICA ARGENTINA

BUENOS AIRES, November 12. 1978

Professor MARIUS STOKA
Department of Mathematics
Université des Sciences Sociales
Place Anatole France
31070 TOULOUSE CEDEX

Dear professor Stoka:

The last month of october I was absent of Buenos Aires, so that I find your letter of 21.9.78 just a few days ago, at my return to Buenos Aires. I beg pardon for the delay in answering it.

Unfortunately the two journals: "Revista de Matemática y Fisica Teórica de la Universidad de Tucumán" and "Mathematicae Notae" (from Rosario), have at present (two or three years ago) interrupted their publication (by lack of financial support). The editors communicate to me that they expect to follow with their publication, but there is not any certainty. The only remaining argentine mathematical journal is the "Revista de la Unión Matemática Argentina", but it appears only two times in the year and at present has so much material that the waiting time is the order of two years.

Given these circumstances, please let me know if you prefer that I send back to you the manuscript of Grimaldi and Tanasi, or if I may submit it to the Revista de la Unión.Mat. Arg. or to the other argentine Journals if in the meantime they reappear.

I have been very glad of having again news from you: in the last time I did not have your addresse.

With best regards

Yours sincerely

L.A.Santaló

L.A.Santaló
Cochabamba 780
1150 BUENOS AIRES, Argentina.-

Preface

The seventh International Conference on "Stochastic Geometry, Convex Bodies, Empirical Measure & Applications to Mechanics and Engineering Train-Transport" took place in Messina from April 22nd to April 24th .

This volume collect the Proceedings of the seventh Conference, organized by the Research Group on Integral Geometry, Geometrical Probabilities and Convex Bodies, together Faculty of Economics of Messina University and it is dedicated to Professor Marius Stoka on occasion of his 75th birthday.

The conference was sponsored by the following:

- Messina University - Faculty of Economics
- Sicily Region
- Province of Messina
- Municipality of Messina
- Reggio Calabria University - Faculty of Engineering
- Department DIMET of Reggio Calabria University
- Bonino Pulejo Foundation - Messina
- Franca e Diego De Castro Foundation - Torino
- N.G.I. Shipping Company
- Carige Bank

Our grateful acknowledgements.

We want to thank the *Scientific Committee of the Journal* "Rendiconti del Circolo Matematico di Palermo" for accepting to publish the Proceedings of the Conference in a supplement of the Journal.

Giuseppe Caristi

Contents

Preface pag. 11

Barilla D. - Leonardi G. - Puglisi A. – *Risk analysis of hazardous materials transportation by railway* » 15

Bäsel U. – *Geometric probabilities for a cluster of needles and a lattice of rectangles* » 29

Bonanzinga V. - Sorrenti L. – *Geometric probabilities of Buffon type in the euclidean plane* » 39

Bonanzinga V. - Sorrenti L. – *Geometric probabilities for cubic lattices with cubic obstacles* » 47

Bosq D. – *On estimation of the support in metric spaces* » 55

Böttcher R. – *Geometrical probabilities using the principle of inclusion-exclusion* » 59

Caristi G. – *Random lattice in the euclidean space* E_3 » 69

Čerin Z. - Gianella G. M. – *On* $D(-4)$ *and* $D(8)$ *triples from Pell and Pell-Lucas numbers* » 73

Chiricosta S. – *Dall'impresa agricola alla bioenergy farm: potenzialità e prospettive di sviluppo del biogas* » 85

Chiricosta S. - Saccà S. – *Valorizzazione e diffusione della filiera biogas in Europa ed in Italia* » 97

Cirà A. - Maggio G. - Carlucci F. – *Contingent valuation e stima della domanda di turismo naturalistico nelle aree protette* » 107

Corriere F. - Lo Bosco D. – *The design of waiting areas to optimize the storage capacity in the marine intermodal terminals* » 121

Czinkota I. - Kertész B. - Kovács A. - Hajdók I. – *Particle size distribution curve calculation using limited domains of settling functions* » 131

Duma A. - Rizzo S. – *Chord length distribution functions for an arbitrary triangle* » 141

Duma A. - Wecker M. – *The generalized Buffon-experiment with multiple intersections for the lattice of Buffon and a bunch as test body* » 159

Failla G. – *Quadratic Plücker relations for Hankel varieties* » 171

Grasso F. - Cucurullo L. – *Statistical tourism analysis and market strategies* 181

Heinrich L. – *Central limit theorems for motion-invariant Poisson hyperplanes in expanding convex bodies* » 187

Heinrich L. – *On lower bounds of second-order chord power integrals of convex discs* » 213

Imbesi M. – *Graphs arising from ideals of mixed products* » 223

La Barbiera M. – *Minimal vertex covers and matching problems on planar graphs* » 237

Lanfranchi M. - Giannetto C. - Puglisi A. – *Risk in agricultural firm: a mathematical approach* » 247

Marchisio M. - Perduca V. – *On some explicit semi-stable degenerations of toric varieties* » 261

Marino D. - Trapasso R. – *Assessing the quality of local development through an input-output model* » 273

Mucciardi M. – *A distance decay model for local spatial statistics* » 289

Praticò F. G. - Moro A. - Ammendola R. – *Rail track substructure resistance to Hazmat spillage: an experimental study* » 299

Praticò F. G. - Moro A. - Ammendola R.- Dattola V. – *Assessing rail track sub-ballast resistance through density testing: experiments* » 311

Praticò F. G. - Ammendola R.- Moro A. - Dattola V. – *Joint density and related performance in HMA subballast* » 323

Puglisi A. – *On Pareto minimum solutions* » 333

Restuccia G. – *On a simple class of staircase polytopes* » 337

Staglianò P. L. – *Computing the integral closure of powers of mixed products ideals* » 345

Streit S. – *Statistical tests for point processes obtained from martingale central limit theorems* » 353

Zhou J. - Zhou C. - Ma F. – *Isoperimetric deficit upper limit of a planar convex set* » 363

Zirilli A. - Alibrandi A. – *A permutation approach to evaluate hyperhomocysteinemia in epileptic patients* » 369

RENDICONTI DEL CIRCOLO MATEMATICO DI PALERMO
Serie II, Suppl. 81 (2009), pp. 15-27

Risk analysis of Hazardous Materials transportation by railway

D. Barilla[*]*, G. Leonardi*[**] *and A. Puglisi*[*]

[*]Departement SEA Faculty of Economiy – University of Messina
Email: dbarilla@unime.it, puglisia@unime.it

[**]Department DIMET Faculty of Engineering – University of Reggio Calabria
Email: giovanni.leonardi@unirc.it

ABSTRACT

In the present paper we propose a methodological approach for the characterization of railway routes, on which to base a decision support system (DSS) for identifying minimum risk routes.
Risk analysis assumes a fundamental importance in the transport of dangerous goods in order to identify possible alternative routes and choose among these the route of minimum risk.
It is necessary to appropriately integrate risk analysis with planning and transport management to prevent a potential danger being transformed into a real event.
The illustrated model aims to estimate the risk for hazardous material transportation by rail using a stochastic geometry approach.

Keywords: railway, hazmat, stochastic geometry, risk.

1. INTRODUCTION

One of the greatest risks connected with industrial development is that of the production, distribution and storage of materials which can cause damage to people and to the environment, in the event of accidental leakage.
The use of these types of materials certainly generates economic benefits; nevertheless the term “hazardous” is an indicative that negative and damaging consequences can result from an accident event, which takes place in activities where hazardous materials are present. If such an event occurs, the consequences can affect our society and environment.
Unfortunately, in most cases, attention is paid only to risks connected with production and, thus, to industrial plants, while the risk linked to the transportation of dangerous goods (HazMats) is often overlooked.
The transport of HazMat is an important, complex and socially and environmentally very sensitive problem; a problem involving in general a plethora of parameters: economic, social and environmental.
Generally HazMats have to be transported from a point of origin to one or more destination points. The origin points are fixed facilities where the HazMats are produced, stored, or distributed. The HazMats are then transported from a production facility to storage, distribution, or another facility where the HazMat is required.

Typically, the transporter will wish to use the lowest cost route. It is also required that the route(s) taken be chosen to minimise exposure to hazard in the event of an accident. In most cases, "*risk"* and safety interests conflict with economic interests, rendering the decision-making process a complex task.
The problem that arises when transporting HazMats is how to select a route where economic and risk issues are considered. On one hand the HazMat transport has to be economically feasible for the stakeholders directly involved in this activity. On the other hand, the HazMat transport must pursue safe transport by minimizing the risk throughout the whole transportation process.

2. Risk prevention in hazardous material transportation by rail

The new Eurostat Regulations on rail transportation (EC n.91/2003) has provided for the collection of information on hazardous material transportation since 2004, but only for larger rail companies. Before this date only partial data is available, referring to certain years.
The categories shown in table 1 are the ones defined in international regulations on hazardous material transportation by rail, usually known as RID.

Table 1 – Hazardous materials by category transported in 2005.

RID Classification	Tonnage		Tonnage-km	
	Absolute value	%	Absolute value	%
Explosives	2.603	0,1	887	0,1
Compressed, liquid or dissolved gases	1.393.745	30,6	712.272	43,5
Inflammable liquids	1.431.198	31,4	343.527	21,0
Inflammable solids	111.630	2,4	96.987	5,9
Spontaneously inflammable material	45.906	1,0	7.437	0,5
Material producing inflammable gases on contact with water	15.700	0,3	5.250	0,3
Comburent substances	40.014	0,9	13.603	0,8
Organic peroxides	4.280	0,1	594	0,0
Toxic substances	482.242	10,6	168.967	10,3
Infective substances	-	-	-	-
Radioactive material	221	0,0	37	0,0
Corrosive material	682.050	15,0	191.377	11,7
Other dangerous substances	351.229	7,7	96.450	5,9
Total	**4.560.818**	**100,0**	**1.637.388**	**100,0**

We can see that the main hazardous materials transported by rail are solid compressed, liquid or dissolved gases (making up 30,6% of tonnage and 43,5% of tonnage-kilometre) and inflammable liquids (accounting for 31,4% in terms of tonnage and 21,0% of tonnage-kilometre). In particular, in 2005 hazardous goods accounted for a fairly significant proportion of goods transported by rail, 6.6% of tonnage and 8.1% of tonnage-kilometre.

Table 2 – Hazardous materials transported and relative percentages in 2004-05.

Merci	2004		2005	
	Tonnellate	Migliaia di Tonnellate-Km	Tonnellate	Migliaia di Tonnellate-Km
Totale merci	75.479.200	21.047.129	68.675.526	20.129.995
Merci pericolose	5.803.471	1.722.024	4.560.818	1.637.388
Incidenza % merci pericolose sul totale	**7,7**	**8,2**	**6,6**	**8,1**

In view of a probable gradual increase in the quantity of hazardous goods transported by rail, it is necessary to identify an appropriate methodology for the evaluation of risk in order to optimize route selection. In this optimization process it is not sufficient to make a cost-benefit analysis without taking into account the impact that a potential accident could have on the biotic and abiotic components of the area in question.

These impacts are associated with the pollution effects on people and the environment, resulting from the continuous (non-instantaneous) emission of pollutants around a vehicle involved in an accident. This polluting activity is very complex and stochastic, governed to a large extent by the meteorological conditions (mainly winds) prevailing at the time and site of the accident. The affected area in this case is relatively very large. As a consequence, the quantification and evaluation of related costs is a difficult problem not yet satisfactorily resolved. It is possible to distinguish two types of effect from an accident involving vehicles transporting hazardous materials:

a) Injuries to people and physical damage as a result of the shock of an explosion associated with an accident. The severity of these effects is inversely proportional to the distance from the site of the explosion, and in general these effects are not influenced by the prevailing meteorological conditions. The resulting damage is confined to a circle centred at the site of the explosion and having a radius of a few hundred meters (in more serious incidents).
b) Contamination of humans and the environment resulting from the emission of airborne pollution that can be carried many kilometres by the wind. The resulting effects can be considerably widespread and depend both on the meteorological conditions at the time of the accident and the distribution of population around it.

It is obvious that the effects of an explosion, as opposed to low emission effects, are directly felt by people (society). As a consequence, the vicinity of a route along which hazardous materials are transported to an urban site creates serious social problems for the people living there, mainly associated with the anxiety caused by the expectancy of an accident [J. Karkazis , T.B. Boffey].

The importance of risk analysis, in terms of the probability of an unfavourable event occurring and the seriousness of its consequences, is thus of great importance in order to minimize damage (social and environmental costs) deriving from accidents involving this means of transport.

3. Risk Analysis

Risk can be defined as the expected consequences associated with a given activity. Considering an activity with only one event with potential consequences risk R the probability that this event will occur (accident) is thus P multiplied by the consequences given the event occurs C.

$$R = P \cdot C \tag{1}$$

For an activity with n events the risk is defined by:

$$R = \Sigma (P_i \cdot C_i)$$

where P_i and C_i are the probability and consequence of event i.

Or more general we have:

$$R = \Sigma (P_i \cdot C_i^{\alpha})$$

where α is a weight factor of consequences (depending on social perception of gravity of the consequences).

Equation (1) can also be written as:

$$R = P \cdot V \cdot N$$

where C is defined as: $C = V \cdot N$

- V is the *vulnerability*, defined as the resistance of people, infrastructures, buildings and goods when the emergency occurs.
- N is the *exposure*, that can be defined as the elements (people, goods and infrastructures) affected during and after the event.

Considering the equation (1) two types of measure for risk reduction may be defined:

1) *prevention*, which consists in reducing the level of P;
2) *protection*, which consists in reducing the level of M.

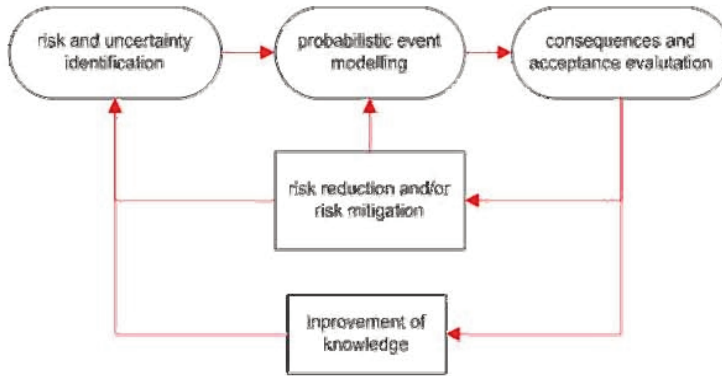


Figure 1 - Principal flow diagram of risk assessment.

The risk value R thus estimated can be considered in an absolute sense or as representing a term of comparison between various alternatives, both in order to evaluate whether the risk is more or less tolerable and in order to compare various solutions, hypothesising various routes between two fixed points in the rail network and evaluating the risk value of each one.

4. ROUTE OPTIMIZATION FOR HAZARDOUS MATERIAL TRANSPORT

4.1 - Network efficiency and overall reliability of the rail system.

There are other parameters which measure the reliability and efficiency of the system as a whole. These generally refer to the whole of the transport network analysed; considering full usability of the system in question and service flexibility as the objective, it is possible to resort to specific indicators which show the particular link between the transport network analysed and the correlated supply availability, if needed, of alternative routes.

Following this method, a particular index of network usability and service flexibility can be based on the number of arcs (or branches) of the graph in which the network can be schematized, thus leading in the definition of an appropriate connectivity index β, resulting from the relationship between the number of existing arcs and the maximum possible number in the network; the greater the number of existing arcs, the more interconnected are the nodes of the graph.

The greater the network connection, the easier it is for each carrier to change destination or route; this is of great importance for example when particular events limit the accessibility of certain arcs, because satisfactory interconnection of the network allows for the continuation of a journey following alternative arcs or nodes, even in the event of critical conditions in some elements (from a structural or functional point of view), thus guaranteeing the movement foreseen.

In general, both for passenger and freight transportation, the problem of network reliability and efficiency can be mathematically schematized by referring to two classes of characteristic variables: *movement demand* D and *supply resistance capacity* R. According to this methodological approach, the conditions of *system reliability* will be very if R > D and, thus, if the relationships M = R - D > 0 (*safety margin*) and $\Phi = R/D > 1$ (*safety factor*) are respected.

Knowing the *probability functions* of the aleatory variables R and D, the probability that the *extreme vulnerability limit* is reached is expressed by the integral sum of the probabilities that the safety factor Φ is contained in the interval [0,1];

$$P_r = \int_0^1 f_\Phi(\Phi) d\Phi$$

where f_Φ is the density function of the probability of variable Φ, while the corresponding reliability is measured by the expression:

$$P_a = 1 - P_r$$

On the basis of the above we can clearly see that the conditions of *network efficiency* and *overall quality* of service are, thus, structurally linked to the characteristics of *reliability* and *vulnerability of each individual route.*

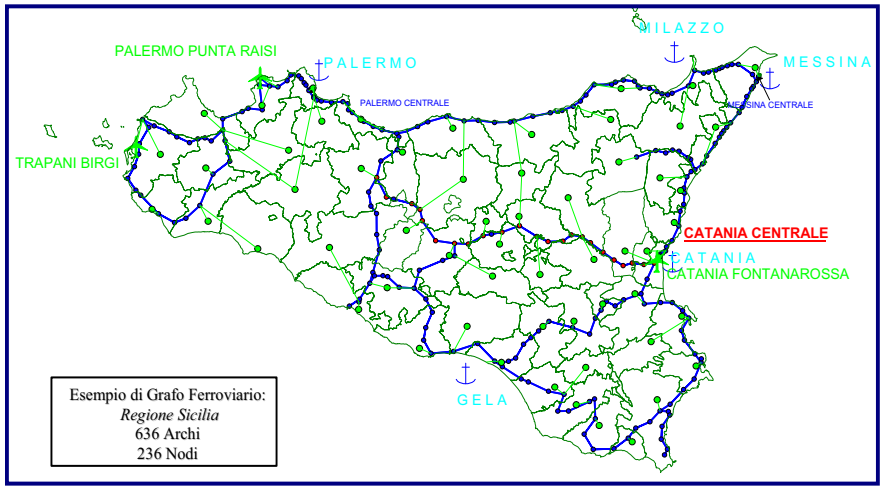


Figure 2 – Example of railway network.

The normal functioning conditions of the rail network can sometimes be disrupted by particular factors dependent on the complex *"environment-infrastructure-vehicle-man"* system, which does not allow free movement of trains because of obstacles along the line.
In these critical situations we need to identify appropriate alternative routes in order to ensure an efficient transportation service to the final destination for each of the origin-destination O-D connections affected by the event in question.
In order to identify the lowest risk route between O and D it is necessary to identify the "risk factors" (hazard, vulnerability and exposure) to be considered when planning routes.

4.2 - Risk estimation

From a methodological viewpoint, the problem of accident risk estimation can be adequately approached by using the theory of *geometric probabilities* to estimate the probability of an accident. Indeed, considering the graph showing the network as an union set of geometric shapes (squares, triangles equilaterals, etc.) forming appropriate *lattices* $\Re$, in the geometric space in question, it is possible to use particular *test-bodies* (segments of varying length *l*, rectangles with sides *a* and *b*, etc.), representing trains, in order to study the relative movement in $\Re$ and any interferences generated by obstacles (of established shape and dimensions) along the prefigured route O-D. In the railway field, these test-bodies, for the analyses we propose to carry out below, may be taken as segments of an appropriate length *l* (in order to schematize a train with a high number of carriages, as happens for example in the composition of a freight train).
Moreover, in order to simplify the calculations, $\Re$ will be presumed to be square, as will the obstacles (squares, having sides of dimension 2*a*) and, finally, a segment of constant length will be used as a corpo-test.

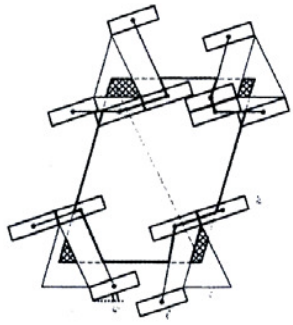


Figure 3 -

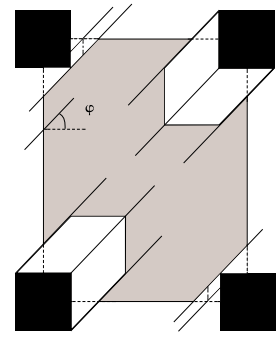


Figure 4 -

Calculation of the probability of interference of the test-body with the obstacles in the lattice

Given this, we thus consider in the Euclidian plane referring to a system of orthogonal axes, a lattice $\Re$ formed by regular polygons identical to one another, the centres of which are points distributed in a regular way. For example the lattice $\Re$(A, *a*) shown in Figure 5,

which is made up of the squares Q with sides $2a$ with centres at points $\mathrm{M_{h,k}} = (h\mathrm{A}, k\mathrm{A}), (h, k \in \sqcup)$ and sides parallel to the coordinated axes.

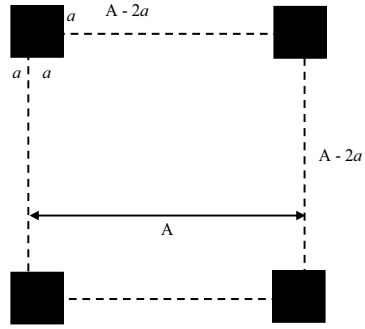


Figure 5 -

Let T be a geometric figure of well established shape and dimensions but of *aleatory position* (test-body).
We assume that T is a segment *s* of constant length *l*. In this case we choose *P* as midpoint of *s* and *d* the support line of *s*.
Below we will determine the probability p_t that the test-body considered, that is to say a segment *s* of length *l* forming the angle φ with axis Ox (Figure 4), does not intersect the squares *Q* of the lattice $\Re(\mathrm{A}, a)$, representing the obstacles along the route.
To this end we consider points $M_{0,0} = (0, 0)$; $M_{1,0} = (\mathrm{A}, 0)$; $M_{0,1} = (0, \mathrm{A})$; $M_{1,1} = (\mathrm{A}, \mathrm{A})$; and the square $\mathrm{C_0}$ with its vertexes at these points (Figure 5).
Indicating with *M* the set of segments *s* which has its midpoint in the square C_0 and with *N* the set of segments *s* wholly contained in C_0 but which do not intersect the four squares Q with their centres at points $M_{0,0}$, $M_{1,0}$, $M_{0,1}$, $M_{1,1}$, we have:

$$\mathrm{p_t} = \frac{\mu(N)}{\mu(M)}, \tag{2}$$

where μ is the *Lebesgue measure.*
The measurements $\mu(N)$ and $\mu(M)$ are calculated using *Poincaré's elementary kinematic measure* in the Euclidian plane

$$\mathrm{dk} = \mathrm{dx} \wedge \mathrm{dy} \wedge \mathrm{d}\varphi\,, \tag{3}$$

where *x* and *y* are the coordinates of the midpoint of segment *s* and φ the angle between the axis Ox and the support line *d* of segment *s*.

Theorem 1. If $l \le A - 2a$ with $A > 2\left(\sqrt{2}+1\right)a$, the probability p_t is:

$$p_t = 1 - \frac{4a^2}{A^2} - \frac{8al}{\pi A_2}. \tag{4}$$

Proof. Taking into account the symmetries, it is sufficient to consider the values of φ in the interval $[0, \pi/4]$. Then:

$$\mu(\mathrm{M}) = \int_0^{\frac{\pi}{4}} d\varphi \iint_{\{(x,y)\in C_0\}} dxdy = \int_0^{\frac{\pi}{4}} area\left(C_0\right) d\varphi = \frac{\pi}{4} A^2\,. \tag{5}$$

We prove the formula (3) considering the following limitations for l:

1) $l \le 2a$;

2) $2a \le l \le 2\sqrt{2}a$;

3) $3\sqrt{2}a \le l \le A - 2a$.

Denoting with $\hat{C}_0(\varphi)$ the figure (contained in C_0) defined by the following property: the point P is in $\hat{C}_0(\varphi)$ if and only if P is in C_0 as midpoint of a segment s that gives an angle φ with the axis Ox not intersecting the four squares Q of centres $M_{0,0}$, $M_{1,0}$, $M_{0,1}$, $M_{1,1}$.

In the first case we have (Figure 6):

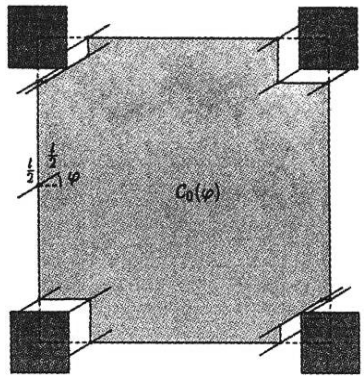


Figure 6 -

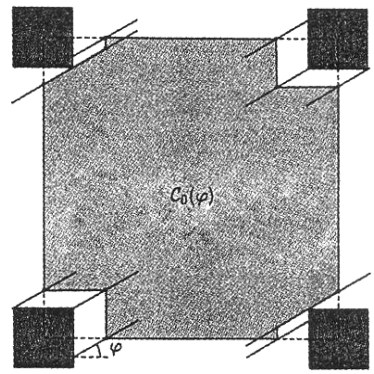


Figure 7 -

$$area\hat{C}_0(\varphi) = A^2 - 2\left(a + \frac{l}{2}\cos\varphi\right)\left(a + \frac{l}{2}\sin\varphi\right) -$$

$$+2 \cdot \frac{\left(2a - l/2\sin\varphi\right)\frac{l}{2}\cos\varphi}{2} - 2 \cdot \frac{\left(2a - l/2\cos\varphi\right)\frac{l}{2}\sin\varphi}{2} - 2a^2 = \qquad (6)$$

$$A^2 - 4a^2 - 2al\left(\sin\varphi + \cos\varphi\right),$$

hence:

$$\mu(\mathrm{N}) = \int_0^{\frac{\pi}{4}} d\varphi \iint_{\{(x,y)\in\hat{C}_0(\varphi)\}} dxdy = \int_0^{\frac{\pi}{4}} \left[area\hat{C}_0(\varphi)\right] d\varphi = \frac{\pi}{4}\left(A^2 - 4a^2\right) - 2al \, . \qquad (7)$$

By substituting (5) and (7) in formula (2) we get the probability (4).

In the 2°) case, putting $\varphi_0 = \arccos\frac{2a}{l}$ and taking into account the condition $2a \le l \le 2\sqrt{2}a$, hence $0 \le \varphi_0 \le \pi/4$.

Then we have to consider the following ranges of variation for the angle φ: $[0, \varphi_0], [\varphi_0, \pi/4]$.

If $\varphi \in [0, \varphi_0]$ we have (Figure 7):

$$area\hat{C}_0(\varphi) = A\cdot(A - l\cos\varphi - 2a) + 2\cdot\frac{\left(2A - 4a - \frac{l}{2}\sin\varphi - a\tan\varphi\right)\left(\frac{l}{2}\cos\varphi + a\right)}{2} +$$

$$+\left(\frac{l}{2}\cos\varphi - a\right)\cdot\left(\frac{l}{2}\sin\varphi - a\tan\varphi\right) = A^2 - 4a_2 - 2al(\sin\varphi + \cos\varphi).$$

If $\varphi \in [\varphi_0, \pi/4]$, we have (Figure 6):

$$area\hat{C}_0(\varphi) = A(A - 2a - l\sin\varphi) + l^2\sin\varphi\cos\varphi +$$

$$(2a + l\sin\varphi)(A - 2a - l\cos\varphi) = A^2 - 4a^2 - 2al(\sin\varphi + \cos\varphi),$$

That is the same expression of $area\hat{C}_0(\phi)$ when $\varphi \in [0, \varphi_0]$ and of $area\hat{C}_0[\varphi]$ in the first case. Then the measure μ = (N) is given by formula (7) and we have the probability (4).

In the 3°) case, let φ_1 in [0, π/4] with $\sin\varphi_1 = \frac{2a}{l}$.

Then we have to consider the following ranges of variation for the angle φ: [0, φ_1] and [φ_1, π/4].

If $\varphi \in [0, \varphi_1]$, we have (Figure 7):

$$area\hat{C}_0(\varphi) = A(A - l\cos\varphi - 2a) + 2a(2A - 4a - 2a\tan\varphi) +$$

$$+(l\cos\varphi - 2a)(A - 2a - 2a\tan\varphi) = A^2 - 4a^2 - 2al(\sin\varphi + \cos\varphi).$$

If $\varphi \in [\varphi_1, \pi/4]$, we have (Figure 8):

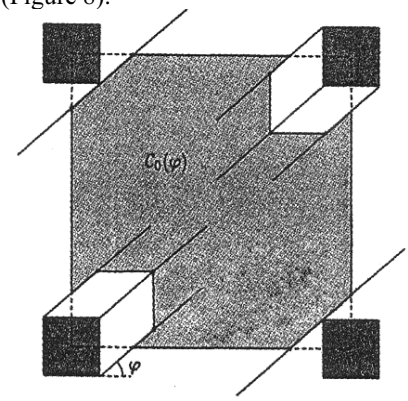


Figure 8

$$area\hat{C}_0(\varphi) = 2(A - 2a - 2a\cot g\varphi)\left(\frac{l}{2}\sin\chi\varphi - a\right) + \left(2A - 4a - 2\mathrm{cotg}\varphi - \frac{l}{2}\cos\varphi\right)\left(2a - \frac{l}{2}\sin\varphi\right) +$$

$$+a\tan\varphi(2A - 3a - l\cos\varphi) + \left(\frac{l}{2}\sin\varphi - a\tan\varphi\right)(2A - 2a - l\cos\varphi) +$$

$$+\left(\frac{l}{2} - \frac{a}{\cos\varphi}\right)^2\sin\varphi\cos\varphi + (A - 2a - l\sin\varphi)A = A^2 - 4a^2 - 2al(\sin\varphi + \cos\varphi),$$

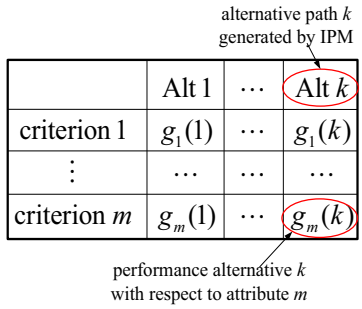
Hence the same expression of $area\hat{C}_0(\varphi)$ when $\varphi \in [0, \varphi_1]$ and of $area\hat{C}_0(\varphi)$ in the first case.
Then the measure $\mu = (N)$ is given by formula (7) and we have formula (4).

4.3 - Choice of the lowest risk route

Risk analysis of different alternatives to achieve the elimination of unacceptable alternatives and to find the route with minimal risk is achieved through Multi-Criteria Analysis (MCA).
All multi-criteria problems have some common characteristics, which can be listed in the following points:

- objectives/attributes are multiple, the decision-making has to define objectives and/or remarkable attributes to analyse the problem;
- conflicts among the criteria, the criteria are clash with one another;
- measurement units are incommensurable, every objective and/or attribute is measured using different units.[Leonardi]

The solutions to these problems may concern both the creation of the best alternative and the choice of the most satisfactory alternative within a default set of alternatives.
To focus the problem there are, therefore, two possible set of alternatives: one contains a finite number of alternatives, while the other contains an endless number of them. Then it is possible to divide the multi-criteria problems into two categories, on the basis of the number of alternatives. A finite number of alternatives concerns the multi-attribute problems, an endless number of alternatives concerns the multi-objective problems.
The multi-objective analysis can be associated with problems that have a set of alternatives that are not predetermined. Therefore, it has a solution of continuous type, where several objectives are pursued simulyaneously. The multi-attribute analysis is associated with problems that have a finite number of predetermined alternatives. Each alternative is associated with a level of satisfaction of the attributes (not necessarily quantifiable) on the basis of which the final decision is assumed. The problem concerns the selection of the alternative, not its creation.
Since, in this case, the choice is limited to a finite and discrete number of alternative routes previously identified, the model refers to the multi-attribute.
Once the choice set is defined, it is necessary to choose the assessment criteria depending on the objectives to be pursued and, consequently, the indicators for measuring the performance of different alternatives.
So the MADM (Multi Attribute Decision Making) problem can be represented by a valuation matrix:



The objectives that will be used as criteria in the route optimization model presented in this research study are: *minimization of travel time, minimization of travel distance, minimization of risk for the population and minimization of risk related to a natural hazard*. [Avendano]
The objectives are not fixed; they reflect the interests of the stakeholders involved in the decision-making process. However, in order to give an understandable explanation of the proposed method, each of these objectives will be described below:

a) *minimization of travel time and minimization of travel distance.*
In order to reduce costs, private or public companies responsible for HazMat transportation often use of the shortest routes available. The shortest route available can be identified as the route with the lowest travel distance and/or travel time (Zografos and Davis: 1989; Leonelli, Bonvicini *et al.*: 2000; Fabiano, Curro *et al.*: 2002). The travel distance is simply the length of each arc. The total travel distance is the sum of length values of every arc in the route.

$$d_{route} = \sum_{arc \in route} l_{arc}$$

where:

l_{arc} = length of each arc.

The travel time required for a given arc can be estimated by dividing the length of the arc by the arc speed. Impedance time values can be added to the estimated arc travel time value. The total travel time for a given arc will be the sum of the simple arc travel time and the impedance time attributed to its end node.

$$t_{route} = \sum_{arc \in route} \left[\left(l_{arc} \times \overline{v}_{arc} \right) + t_{arc} \right]$$

where: $\overline{v}$ = average speed for each arc;
t_{arc} = average waiting time at arc node.

b) minimization of risk for the population

The approach to risk calculation for the population in relation to a HazMat transport accident used in this document is based on the approach proposed by Zografos and Androutsopoulos (2004). The risk for the population is defined as the product of the probability of the HazMat transport accident and the population being exposed. The probability of the HazMat transport accident is proportional to the accident probability on each arc, estimated as previously illustrated (4), and the rate of vehicles transporting HazMat.

$$ap_{\text{arc}} = hp_{arc} \times hm$$

where: ap_{arc} = accident probability on each arc involving a HazMat transport;
hp_{arc} = accident probability for each arc in the transport network;
hm = rate of vehicles transporting HazMat.

The population exposed is the population situated within the impact area of the accident. The mathematical equation used for calculating the population exposed is as follows:

$$Rpop_{\text{route}} = \sum_{arc \in route} \left(hp_{arc} \times hm \times p\left(ex\right)_{arc} \right)$$

where: $p(ex)_{\text{arc}}$ = number of persons exposed to an accident event along one arc;

The risk over the whole route will be the summation of the risk values of every arc in the route. This risk measure will indicate the number of persons expected to be injured or killed in the event of a HazMat accident occurring. The evaluation of this objective should result in choosing the route with the lowest values of risk for the population.

c) minimization of risk related to a natural hazard

If the vulnerability of infrastructures (bridges, viaducts, etc.) to the natural hazard is known, the route selection for the transport of HazMat should also consider these risk factors (the hazard and vulnerability to the hazard). Consider the case of an earthquake; the amount of debris produced by the collapse of structures during the earthquake event increases the hazard of an accident occurring, and therefore the hazard of fire.

In the case where two routes are available for the transport of HazMat for example, one of the routes has a low accident rate but with high structure vulnerability to earthquakes; the second route, on the other hand, has a high accident rate, but low structure vulnerability to earthquakes. The question is now, which route should be used for the HazMat transport? The output required from such a model is the degree of infrastructure damage expected in the event of an earthquake, i.e. the specific risk for bridges in the event of an earthquake. The value assigned to each arc can be labelled as earthquake-structure risk score, making reference to the fact that the natural hazard considered is related to an earthquake and the vulnerability is based on buildings. The route optimization equation will then be:

$$Rb_{\text{route}} = \sum_{arc \in route} Rb_{arc}$$

where: Rb_{route} = qualitative risk measure of the amount of expected structure damage in the event of an earthquake along the route;
Rb_{arc} = earthquake-structure specific risk score assigned to each arc.

5. CONCLUSIONS

The methodology proposed in this paper wants to integrate stochastic geometric probability with risk analysis.
In dangerous material transportation the principal problem is to estimate the probability of accident. So we proposed to estimate the probability of accident in railway transport as the probability to find an obstacle along the path.
The obtained results can easily be applied to more complex cases, by studying various geometric figures in order to work on schemes similar to the reality of infrastructure to analyze.
Also, the model can be customized to other case studies (road transportation) and easily adapted to different infrastructural network.

References

[1] Castillo J. E. A., (2004). *Route Optimization for Hazardous Materials Transport*, Thesis submitted to the International Institute for Geo-information Science and Earth Observation", Master of Science in Urban Planning and Land Administration, The Netherlands.
[2] Duma A. and Stoka M. (Paris 2004), *Geometric probabilities for quadratic lattices with quadratic obstacles*, Annales de l'I.S.U.P., vol. XXXXVIII, Fas. 1-2, pp. 19-42.
[3] Duma A. and Stoka M. (Paris 2005), *Geometric probabilities for triangular lattices with triangular obstacles*, Annales de l'I.S.U.P., vol. XLIX, Fas. 2-3, pp. 57-72.
[4] Duma A. and Stoka M. (2008), *Probabilità Geometriche per reticoli esagonali con ostacoli esagonali*, Suppl. Rendiconti del Circolo Matematico di Palermo, serie II, n. 80, pp. 153-160.
[5] Fabiano B., F. Curro, E. Palazzi and R. Pastorino, (2002). *A framework for risk assessment and decision-making strategies in dangerous good transportation* Journal of Hazardous Materials 93(1): 1-15.
[6] Leonardi G., (2001). *Using the multi-dimensional fuzzy analysis for the project optimization of the infrastructural interventions on transport network.* Supplementi dei Rendiconti del Circolo Matematico di Palermo, vol. 70, pp. 95-108.
[7] Leonelli P., S. Bonvicini and G. Spadoni, (2000). *Hazardous materials transportation: a risk-analysis based routing methodology*, Journal of Hazardous Materials 71(1-3): 283-300.
[8] Ministero dei Trasporti, (2005). *Conto Nazionale Trasporti*.
[9] Zografos K. G. and C. F. Davis, (1989). *Multi-Objective Programming Approach For Routing Hazardous Materials*. Journal of Transportation engineering 115(6): 661-673.
[10] Zografos K. G. and K. N. Androutsopoulos, (2004). *A heuristic algorithm for solving hazardousmaterials distribution problems*. European Journal of Operational Research 152(2): 507-519.

RENDICONTI DEL CIRCOLO MATEMATICO DI PALERMO
Serie II, Suppl. 81 (2009), pp. 29-38

GEOMETRIC PROBABILITIES FOR A CLUSTER OF NEEDLES AND A LATTICE OF RECTANGLES

Uwe BÄSEL

Abstract

A cluster of n needles ($1 \leq n < \infty$) is dropped at random onto a plane lattice of rectangles. Each needle is fixed at one end in the cluster centre and can rotate independently about this centre.

The distribution of the relative number of needles intersecting the lattice is shown to converge uniformly to the limit distribution as $n \to \infty$.

AMS Classification: 60D05, 52A22, 78M05

AMS 2000 Subject Classification: Geometric probability, stochastic geometry, random sets and random convex sets, method of moments

1 Introduction

We consider a cluster $\mathcal{Z}_n$ of n needles thrown at random onto a plane lattice $\mathcal{R}_{a,\,b}$ of rectangles (see figure 1). The fundamental cell of $\mathcal{R}_{a,\,b}$ is a rectangle with side lengths a and b. All needles of $\mathcal{Z}_n$ are connected in the centre of $\mathcal{Z}_n$. Each needle has equal length 1.

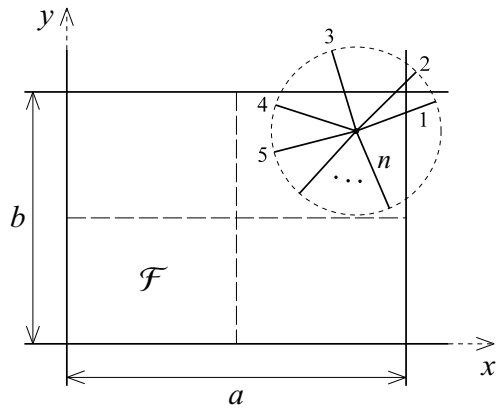


Figure 1: Lattice $\mathcal{R}_{a,\,b}$ and cluster $\mathcal{Z}_n$

We assume $\min(a,b) \geq 2$ so that the cluster $\mathcal{Z}_n$ can intersect at most one of the vertical lines of $\mathcal{R}_{a,b}$ and (at the same time) one of the horizontal lines of $\mathcal{R}_{a,b}$ (except sets with measure zero). A *random throw of* $\mathcal{Z}_n$ *onto* $\mathcal{R}_{a,b}$ is defined as follows: After throwing $\mathcal{Z}_n$ onto $\mathcal{R}_{a,b}$ the coordinates x and y of the center point are random variables uniformly distributed in $[0,a]$ and $[0,b]$ resp.; the angle ϕ_i between the x-axis and the needle i is for $i \in \{1,\ldots,n\}$ a random variable uniformly distributed in $[0,2\pi]$. All $n+2$ random variables are stochastically independent. In the following $\lambda := 1/a$ and $\mu := 1/b$ with $0 \leq \lambda, \mu \leq 1/2$ will be used.

2 Intersection probabilities

The intersection probabilities for this problem are derived in [2]. In this section the results are summarised, that are necessary for the following investigations.

$p_n(i)$, $i \in \{0,\ldots,2n\}$, denotes the probability of exactly i intersections between $\mathcal{Z}_n$ and $\mathcal{R}_{a,b}$. Due to existing symmetries it is sufficient to consider only the subset $\mathcal{F}$ of the fundamental cell (figure 1). For the calculations it is necessary to consider $\mathcal{F}$ as union of five subsets $\mathcal{F}_1,\ldots,\mathcal{F}_5$ (see figure 2):

$$\begin{aligned}
\mathcal{F}_1 &= \{(x,y) \in \mathbb{R}^2 \,|\, 1 \leq x \leq a/2,\, 1 \leq y \leq b/2\}\,,\\
\mathcal{F}_2 &= \{(x,y) \in \mathbb{R}^2 \,|\, 0 \leq x \leq 1,\, 1 \leq y \leq b/2\}\,,\\
\mathcal{F}_3 &= \{(x,y) \in \mathbb{R}^2 \,|\, 1 \leq x \leq a/2,\, 0 \leq y \leq 1\}\,,\\
\mathcal{F}_4 &= \{(x,y) \in \mathbb{R}^2 \,|\, 0 \leq x \leq 1,\, \sqrt{1-x^2} \leq y \leq 1\}\,,\\
\mathcal{F}_5 &= \{(x,y) \in \mathbb{R}^2 \,|\, 0 \leq x \leq 1,\, 0 \leq y \leq \sqrt{1-x^2}\,\}\,.
\end{aligned}$$

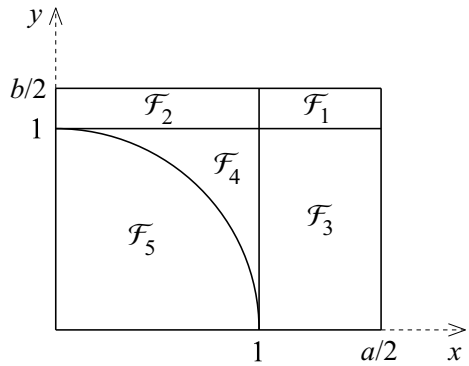


Figure 2: $\mathcal{F} = \mathcal{F}_1 \cup \ldots \cup \mathcal{F}_5$

With $p_n(i\,|\,(x,y))$ we denote the conditional probability, that $\mathcal{Z}_n$ with centre point $(x,y) \in \mathcal{F}$ has exactly i intersections with $\mathcal{R}_{a,\,b}$. Considering the case distinctions for the subsets $\mathcal{F}_m$ the probabilities are calculated with

$$\begin{aligned} p_n(i) &= \iint_{\mathcal{F}} p_n(i\,|\,(x,y)) f_1(x) f_2(y)\,\mathrm{d}x\,\mathrm{d}y \\ &= \sum_{m=1}^{5} \iint_{\mathcal{F}_m} p_n(i\,|\,(x,y)) f_1(x) f_2(y)\,\mathrm{d}x\,\mathrm{d}y\,, \end{aligned} \tag{1}$$

where

$$f_1(x) = \begin{cases} 2/a & \text{for } 0 \le x \le a/2\,, \\ 0 & \text{else}\,, \end{cases} \quad \text{and} \quad f_2(y) = \begin{cases} 2/b & \text{for } 0 \le y \le b/2\,, \\ 0 & \text{else} \end{cases}$$

are the density functions of x and y. We get

$$\begin{aligned} p_n(i) &= \frac{4}{ab} \sum_{m=1}^{5} \iint_{\mathcal{F}_m} p_n(i\,|\,(x,y))\,\mathrm{d}x\,\mathrm{d}y \\ &= 4\lambda\mu \sum_{m=1}^{5} \iint_{\mathcal{F}_m} p_n(i\,|\,(x,y))\,\mathrm{d}x\,\mathrm{d}y\,. \end{aligned} \tag{2}$$

The conditional intersection probabilities for centre point $(x,y) \in \mathcal{F}_1$ are given by

$$p_n(0\,|\,(x,y)) = 1\,, \quad p_n(1\,|\,(x,y)) = 0\,, \quad p_n(2\,|\,(x,y)) = 0\,.$$

For $(x,y) \in \mathcal{F}_m\,,\ m \in \{2,3,4\}$, we have

$$\begin{aligned} p_n(i\,|\,(x,y)) &= \binom{n}{i} q_1(x,y)^i\,(1 - q_1(x,y))^{n-i}\,, \quad i \in \{0,1,\ldots,n\}\,, \\ p_n(i\,|\,(x,y)) &= 0\,, \quad i \in \{n+1,\ldots,2n\}\,, \end{aligned}$$

with

$$q_1(x,y) = \begin{cases} \dfrac{1}{\pi} \arccos x\,, & \text{if } (x,y) \in \mathcal{F}_2\,, \\ \dfrac{1}{\pi} \arccos y\,, & \text{if } (x,y) \in \mathcal{F}_3\,, \\ \dfrac{1}{\pi}(\arccos x + \arccos y)\,, & \text{if } (x,y) \in \mathcal{F}_4\,. \end{cases}$$

For $(x,y) \in \mathcal{F}_5$, we have

$$p_n(i\,|\,(x,y)) \;=\; \sum_{j=0}^{[i/2]} \binom{n}{i-j} \binom{i-j}{j} q_2^j\, q_1^{i-2j}\, [1-q_1-q_2]^{n-i+j}\,, \qquad i \in \{0,1,\ldots,2n\}\,, \tag{3}$$

where $q_1 = q_1(x,y) = 1/2$, $q_2 = q_2(x,y) = \frac{1}{2\pi}(\arccos y - \arcsin x)$ and $[i/2]$ denotes the integer part of $i/2$.

3 Distribution functions

In the following let X_n denote the ratio

$$\frac{\text{number of intersections between } \mathcal{Z}_n \text{ and } \mathcal{R}_{a,\,b}}{n}\,.$$

We shall investigate the asymptotic behaviour of the distribution functions

$$F_n(x) \;=\; P(X_n \le x) \;=\; \begin{cases} 0 & \text{for} \quad -\infty < x < 0\,, \\ \displaystyle\sum_{i=0}^{[nx]} p_n(i) & \text{for} \quad 0 \le x < 2\,, \\ 1 & \text{for} \quad 2 \le x < \infty\,, \end{cases} \tag{4}$$

as $n \to \infty$, where $p_n(i)$ is defined by (2).

Theorem. *As $n \to \infty$, the random variables X_n converge weakly to the random variable X, whose distribution function is given by*

$$F(x) = \begin{cases} 0 \quad \textit{for} \quad -\infty < x < 0\,, \\ 1 - 2(\lambda+\mu)\cos\pi x + 2(2\cos\pi x - \pi x \sin\pi x)\lambda\mu \quad \textit{for} \quad 0 \le x < \frac{1}{2}\,, \\ 1 + 2\pi(x-1)\lambda\mu\sin\pi x \quad \textit{for} \quad \frac{1}{2} \le x < 1\,, \\ 1 \quad \textit{for} \quad 1 \le x < \infty\,. \end{cases}$$

Moreover, it holds the uniform convergence $\lim_{n\to\infty} \sup_{x\in\mathbb{R}} |F_n(x) - F(x)| = 0$.

Proof. The proof of the weak convergence is based on the method of moments. According to the Fréchet-Shohat theorem (see e.g. [4, pp. 81/82]) we have to show that for each $k \in \mathbb{N}$ the sequence of moments $\mathrm{E}(X_n^k) = \int_{-\infty}^{\infty} x^k \,\mathrm{d}F_n(x)$ converges to $\mathrm{E}(X^k) = \int_{-\infty}^{\infty} x^k \,\mathrm{d}F(x)$ as $n \to \infty$ and the

moments $\mathrm{E}(X^k)$, $k \in \mathbb{N}$, uniquely determine F.

Since F is a distribution function that is constant outside the interval $[0,1]$, it is uniquely determined by its moments. These moments are given by

$$\begin{aligned}\mathrm{E}(X^k) &= [2\pi(\lambda+\mu) - 6\pi\lambda\mu] \int_0^{1/2} x^k \sin \pi x \,\mathrm{d}x \\ &\quad - 2\pi^2\lambda\mu \int_0^{1/2} x^{k+1} \cos \pi x \,\mathrm{d}x \\ &\quad + 2\pi\lambda\mu \int_{1/2}^{1} x^k \left[\sin \pi x - \pi(1-x)\cos \pi x\right] \mathrm{d}x \,, \; k \in \mathbb{N} \,. \quad (5)\end{aligned}$$

For the moments $\mathrm{E}(X_n^k)$, $k \in \mathbb{N}$, we find

$$\begin{aligned}\mathrm{E}(X_n^k) &= \int_{-\infty}^{\infty} x^k \,\mathrm{d}F_n(x) \;=\; \sum_{i=0}^{2n} \left(\frac{i}{n}\right)^k p_n(i) \\ &= \sum_{i=0}^{2n} \left(\frac{i}{n}\right)^k 4\lambda\mu \sum_{m=1}^{5} \iint_{\mathcal{F}_m} p_n(i \,|\, (x,y)) \,\mathrm{d}x \,\mathrm{d}y \\ &= 4\lambda\mu \sum_{m=1}^{5} \iint_{\mathcal{F}_m} \sum_{i=0}^{2n} \left(\frac{i}{n}\right)^k p_n(i \,|\, (x,y)) \,\mathrm{d}x \,\mathrm{d}y \\ &= 4\lambda\mu \sum_{m=1}^{5} \iint_{\mathcal{F}_m} \mathrm{E}(X_n^k \,|\, (x,y)) \,\mathrm{d}x \,\mathrm{d}y \,,\end{aligned}$$

where $\mathrm{E}(X_n^k \,|\, (x,y))$ is the conditional k-th moment of X_n given the cluster centre in (x,y).

Now let us consider the subsets $\mathcal{F}_1, \ldots, \mathcal{F}_5$:

For centre point $(x,y) \in \mathcal{F}_1$ and any $k \in \mathbb{N}$ we have $\mathrm{E}(X^k \,|\, (x,y)) = 0$ and therefore

$$\lim_{n\to\infty} \iint_{\mathcal{F}_1} \mathrm{E}(X_n^k \,|\, (x,y)) \,\mathrm{d}x \,\mathrm{d}y = 0 \,.$$

For centre point $(x,y) \in \mathcal{F}_m$, $m \in \{2,3,4\}$, and $i \in \{n+1, \ldots, 2n\}$ all conditional probabilities $p_n(i \,|\, (x,y)) = 0$. Hence we have

$$\begin{aligned}\mathrm{E}(X_n^k \,|\, (x,y)) &= \sum_{i=0}^{n} \left(\frac{i}{n}\right)^k p_n(i \,|\, (x,y)) \\ &= \sum_{i=0}^{n} \left(\frac{i}{n}\right)^k \binom{n}{i} q_1(x,y)^i (1 - q_1(x,y))^{n-i} \,.\end{aligned}$$

$\mathrm{E}(X_n^k \,|\, (x,y))$ is the Bernstein polynomial of the function x^k. In the interval $0 \le q_1(x,y) \le 1$ it converges uniformly to $q_1(x,y)^k$ as $n \to \infty$ (see e.g. [3, p. 222]). It follows that $\mathrm{E}(X_n^k \,|\, (x,y))$ converges uniformly to $q_1(x,y)^k$ in $\mathcal{F}_m$, $m \in \{2,3,4\}$, that is

$$\lim_{n\to\infty} \sup_{(x,\,y)\,\in\,\mathcal{F}_m} |\mathrm{E}(X_n^k \,|\, (x,y)) - q_1(x,y)^k| = 0\,, \quad k \in \mathbb{N}\,.$$

Owing to the uniform convergence we can exchange limit and integral and get

$$\begin{aligned}\lim_{n\to\infty} \iint_{\mathcal{F}_m} \mathrm{E}(X_n^k \,|\, (x,y))\,\mathrm{d}x\,\mathrm{d}y &= \iint_{\mathcal{F}_m} \lim_{n\to\infty} \mathrm{E}(X_n^k \,|\, (x,y))\,\mathrm{d}x\,\mathrm{d}y \\ &= \iint_{\mathcal{F}_m} q_1(x,y)^k\,\mathrm{d}x\,\mathrm{d}y\,, \quad m \in \{2,3,4\}\,.\end{aligned}$$

For $(x,y) \in \mathcal{F}_2$ we have $q_1(x,y) = \frac{1}{\pi}\arccos x$, hence

$$\begin{aligned}\lim_{n\to\infty} \iint_{\mathcal{F}_2} \mathrm{E}(X_n^k \,|\, (x,y))\,\mathrm{d}x\,\mathrm{d}y &= \int_{y=1}^{b/2} \int_{x=0}^{1} \Big(\frac{\arccos x}{\pi}\Big)^k \,\mathrm{d}x\,\mathrm{d}y \\ = (b/2-1)\pi \int_0^{1/2} u^k \sin \pi u\,\mathrm{d}u &= \frac{1-2\mu}{2\mu}\,\pi \int_0^{1/2} u^k \sin \pi u\,\mathrm{d}u\,.\end{aligned}$$

For $(x,y) \in \mathcal{F}_3$ we have $q_1(x,y) = \frac{1}{\pi}\arccos y$, hence

$$\begin{aligned}\lim_{n\to\infty} \iint_{\mathcal{F}_3} \mathrm{E}(X_n^k \,|\, (x,y))\,\mathrm{d}x\,\mathrm{d}y &= \int_{x=1}^{a/2} \int_{y=0}^{1} \Big(\frac{\arccos y}{\pi}\Big)^k \,\mathrm{d}y\,\mathrm{d}x \\ = (a/2-1)\pi \int_0^{1/2} u^k \sin \pi u\,\mathrm{d}u &= \frac{1-2\lambda}{2\lambda}\,\pi \int_0^{1/2} u^k \sin \pi u\,\mathrm{d}u\,.\end{aligned}$$

For $(x,y) \in \mathcal{F}_4$ we have $q_1(x,y) = \frac{1}{\pi}(\arccos x + \arccos y)$ and therefore

$$\begin{aligned}&\lim_{n\to\infty} \iint_{\mathcal{F}_4} \mathrm{E}(X_n^k \,|\, (x,y))\,\mathrm{d}x\,\mathrm{d}y \\ &\qquad = \int_{y=0}^{1} \int_{x=\sqrt{1-y^2}}^{1} \left(\frac{\arccos x + \arccos y}{\pi}\right)^k \,\mathrm{d}x\,\mathrm{d}y\,.\end{aligned}$$

For centre point $(x,y) \in \mathcal{F}_5$ we have

$$\mathrm{E}(X_n^k \,|\, (x,y)) = \sum_{i=0}^{2n} \left(\frac{i}{n}\right)^k \, p_n(i \,|\, (x,y)) \tag{6}$$

with

$$p_n(i \,|\, (x,y)) = \sum_{j=0}^{[i/2]} \binom{n}{i-j} \binom{i-j}{j} q_2^j \, q_1^{i-2j} \, (1-q_1-q_2)^{n-i+j} \,,$$

where $q_1 = q_1(x,y) = 1/2$ and $q_2 = q_2(x,y) = \frac{1}{2\pi}(\arccos y - \arcsin x)$. Using the lemma in [3, p. 219] we show that $\mathrm{E}(X_n^k \,|\, (x,y)) \to (q_1(x,y)+2q_2(x,y))^k$ uniformly as $n \to \infty$. At first we may write the expectation (6) as

$$\mathrm{E}(X_n^k \,|\, (x,y)) = \int_{t=0}^{2} t^k \,\mathrm{d}F_n(t \,|\, (x,y)) \,, \tag{7}$$

where $F_n(t \,|\, (x,y))$ is the conditional distribution of the random variable X_n for fixed cluster centre (x,y).

By Z_i, $i \in \{1, \ldots, n\}$, we denote the random number of intersections between needle i and $\mathcal{R}_{a,b}$ given the cluster center in (x,y) and by M_n the arithmetic mean $(Z_1 + \ldots + Z_n)/n$. We have $\mathrm{E}(Z_i) = q_1 + 2q_2$, $\mathrm{E}(Z_i^2) = q_1 + 4q_2$ and therefore $\mathrm{Var}(Z_i) = \mathrm{E}(Z_i^2) - [\mathrm{E}(Z_i)]^2 = q_1 + 4q_2 - (q_1 + 2q_2)^2$. Furthermore we find

$$\mathrm{E}(M_n) = \mathrm{E}(Z_1/n) + \ldots + \mathrm{E}(Z_n/n) = \mathrm{E}(Z_1) = q_1 + 2q_2 \,.$$

Since the random variables $Z_1, \ldots, Z_n$ are independent and identically distributed we have

$$\begin{aligned} \mathrm{Var}(M_n) &= \mathrm{Var}(Z_1/n) + \ldots + \mathrm{Var}(Z_n/n) \\ &= \frac{1}{n}\,\mathrm{Var}(Z_1) \;=\; \frac{q_1 + 4q_2 - (q_1+2q_2)^2}{n} \,. \end{aligned}$$

We put $\mathcal{D} := \{(q_1, q_2) \in \mathbb{R} \,|\, 0 \le q_1 \le 1,\, 0 \le q_2 \le 1 - q_1\}$. The function $g : \mathcal{D} \to \mathbb{R}$, $g(q_1, q_2) := q_1 + 4q_2 - (q_1 + 2q_2)^2$ has its maximum in the point $(1/2,\, 0)$ with $g(1/2,\, 0) = 1$. Hence $\mathrm{Var}(M_n) \le 1/n$ and therefore $\mathrm{Var}(M_n) \to 0$ as $n \to \infty$. From [3, p. 219] it follows that (7) converges uniformly to $(q_1 + 2q_2)^k$ as $n \to \infty$.

Now we get

$$\begin{aligned} \lim_{n\to\infty} \iint_{\mathcal{F}_5} \mathrm{E}(X_n^k \,|\, (x,y))\,\mathrm{d}x\,\mathrm{d}y \;&=\; \iint_{\mathcal{F}_5} \lim_{n\to\infty} \mathrm{E}(X_n^k \,|\, (x,y))\,\mathrm{d}x\,\mathrm{d}y \\ &= \iint_{\mathcal{F}_5} [q_1(x,y) + 2\,q_2(x,y)]^k \,\mathrm{d}x\,\mathrm{d}y \\ &= \int_{y=0}^{1} \int_{x=0}^{\sqrt{1-y^2}} \left(\frac{\arccos x + \arccos y}{\pi}\right)^k \mathrm{d}x\,\mathrm{d}y \,. \end{aligned}$$

The sum of the integrals for $\mathcal{F}_4$ and $\mathcal{F}_5$ is given by

$$\lim_{n\to\infty} \iint_{\mathcal{F}_4 \cup \mathcal{F}_5} \mathrm{E}(X_n^k \mid (x,y))\,\mathrm{d}x\,\mathrm{d}y = \int_{y=0}^{1}\int_{x=0}^{1} \left(\frac{\arccos x + \arccos y}{\pi}\right)^k \mathrm{d}x\,\mathrm{d}y\,.$$

We simplify this integral, that we denote by I_{45}. With the substitutions $\arccos x = \pi u$ and $\arccos y = \pi v$ ($\mathrm{d}x = -\pi \sin \pi u\ \mathrm{d}u$ and $\mathrm{d}y = -\pi \sin \pi v\ \mathrm{d}v$) it follows, that

$$I_{45} = \int_0^{1/2}\int_0^{1/2} (u+v)^k \sin \pi u \sin \pi v\ \mathrm{d}u\,\mathrm{d}v\,.$$

With $z := u + v$ and considering v as a constant we get $\mathrm{d}z = \mathrm{d}u$ and

$$I_{45} = \int_{v=0}^{1/2}\int_{z=v}^{v+1/2} z^k\ \sin \pi(z-v)\ \sin \pi v\ \mathrm{d}z\,\mathrm{d}v\,.$$

Changing the order of integrations gives

$$\begin{aligned} I_{45} &= \int_{z=0}^{1/2} z^k \int_{v=0}^{z} \sin \pi(z-v)\ \sin \pi v\ \mathrm{d}z\,\mathrm{d}v \\ &\quad + \int_{z=1/2}^{1} z^k \int_{v=z-1/2}^{1/2} \sin \pi(z-v)\ \sin \pi v\ \mathrm{d}z\,\mathrm{d}v\,. \end{aligned}$$

The calculation of the inner integrals yields

$$\begin{aligned} I_{45} &= \frac{\pi}{2}\int_0^{1/2} z^k\,[\sin \pi z - \pi z \cos \pi z]\,\mathrm{d}z \\ &\quad + \frac{\pi}{2}\int_{1/2}^{1} z^k\,[\sin \pi z - \pi(1-z)\cos \pi z]\,\mathrm{d}z\,. \end{aligned}$$

As summary of the preceding results we get

$$\begin{aligned} \lim_{n\to\infty} \mathrm{E}(X_n^k) &= 4\lambda\mu \left(\frac{1-2\mu}{2\mu}\,\pi \int_0^{1/2} x^k \sin \pi x\ \mathrm{d}x \right. \\ &\quad + \frac{1-2\lambda}{2\lambda}\,\pi \int_0^{1/2} x^k \sin \pi x\ \mathrm{d}x \\ &\quad + \frac{\pi}{2}\int_0^{1/2} x^k\,[\sin \pi x - \pi x \cos \pi x]\,\mathrm{d}x \\ &\quad \left. + \frac{\pi}{2}\int_{1/2}^{1} x^k\,[\sin \pi x - \pi(1-x)\cos \pi x]\,\mathrm{d}x \right) \end{aligned}$$

$$
\begin{aligned}
= \quad & [2\pi(\lambda+\mu) - 6\pi\lambda\mu] \int_0^{1/2} x^k \sin \pi x \, \mathrm{d}x \\
& - 2\pi^2 \lambda\mu \int_0^{1/2} x^{k+1} \cos \pi x \, \mathrm{d}x \\
& + 2\pi\lambda\mu \int_{1/2}^{1} x^k \left[\sin \pi x - \pi(1-x)\cos \pi x\right] \mathrm{d}x \, . \qquad (8)
\end{aligned}
$$

The comparison of (8) with (5) shows, that $\lim_{n\to\infty} \mathrm{E}(X_n^k) = \mathrm{E}(X^k)$ for $k \in \mathbb{N}$. It follows that F_n converges weakly to F as $n \to \infty$.

From the weak convergence it follows that F_n converges uniformly to F in all points of continuity of F. F is a continuous function, if $\lambda = 1/2$ and $\mu = 1/2$. If $\lambda \neq 1/2$ or $\mu \neq 1/2$, F is continuous except in the point 0. For this case we consider the convergence of $F_n(0)$ as $n \to \infty$. The probability that $\mathcal{Z}_n$ does not intersect $\mathcal{R}_{a,\,b}$ is given by

$$
p_n(0) = 4\lambda\mu \iint_{\mathcal{F}} p_n(0 \,|\, (x,y)) \, \mathrm{d}x \, \mathrm{d}y = 4\lambda\mu \iint_{\mathcal{F}} q_0(x,y)^n \, \mathrm{d}x \, \mathrm{d}y \, ,
$$

where $q_0(x,y)$ denotes the probability that a single needle with one end point in the cluster centre (x,y) has no intersections with $\mathcal{R}_{a,\,b}$. For almost every $(x,y) \in \mathcal{F} \setminus \mathcal{F}_1$ we have $q_0(x,y) < 1$ and therefore $q_0(x,y)^n \to 0$ as $n \to \infty$. For every $(x,y) \in \mathcal{F}_1$ we have $q_0(x,y) = 1$. With Lebesgue's dominated convergence theorem we find

$$
\begin{aligned}
\lim_{n\to\infty} p_n(0) \quad &= \quad 4\lambda\mu \lim_{n\to\infty} \iint_{\mathcal{F}} q_0(x,y)^n \, \mathrm{d}x \, \mathrm{d}y \;=\; 4\lambda\mu \iint_{\mathcal{F}_1} \mathrm{d}x \, \mathrm{d}y \\
&= \quad (1-2\lambda)(1-2\mu) \, .
\end{aligned}
$$

It follows that $F_n(0) \to F(0)$ as $n \to \infty$. Hence the convergence $F_n \to F$ is completely uniform. So the proof is complete. □

Acknowledgment

The author is grateful to Lothar Heinrich (University of Augsburg) for the fruitful discussion. Especially the proposed use of the Fréchet-Shohat theorem led to a simplification of the proof.

References

[1] Stoka, M.: Probabilités géométriques de type 'Buffon' dans le plan euclidien. *Atti Accad. Sci. Torino* **110** (1975/76) 53-59.

[2] Bäsel, U.; Duma, A.: Buffon's Problem with a Cluster of Needles and a Lattice of Rectangles. *Fernuniversität Hagen: Seminarberichte aus der Fakultät für Mathematik und Informatik.* **81** (2008) 1-11. Accepted for publication in *General Mathematics, Sibiu.*

[3] Feller, W.: *An Introduction to Probability Theory and Its Applications,* Vol. II, 2nd edn. John Wiley & Sons, New York, 1971.

[4] Galambos, J.: *Advanced Probability Theory,* 2nd edn. Marcel Dekker, New York, Basel, Hong Kong, 1995.

Uwe BÄSEL

Leipzig University of Applied Sciences
Department of Mechanical
and Energy Engineering,
04251 Leipzig, Germany

baesel@me.htwk-leipzig.de

RENDICONTI DEL CIRCOLO MATEMATICO DI PALERMO
Serie II, Suppl. 81 (2009), pp. 39-46

GEOMETRIC PROBABILITIES OF BUFFON TYPE IN THE EUCLIDEAN PLANE

VITTORIA BONANZINGA AND LOREDANA SORRENTI

Abstract: We solve problems of Buffon type for two different lattices: a lattice $\mathfrak{R}_1 = \mathfrak{R}(A, B, a, b)$ of rectangles of sides A and B and with obstacles parallelograms of sides $2a$ and $2b$ and angle $\alpha \in]0; \frac{\pi}{2}]$ with the barycentre on the vertexes of a rectangular tile; a lattice $\mathfrak{R}_2$ with elementary tile a parallelogram $\mathcal{P}$ of sides a and b and angle $\alpha \in]0; \frac{\pi}{2}[$. We consider a line segment and a circle as test bodies .

AMS 2000 Subject Classifications: Geometric probability, stochastic geometry, random sets, random convex sets and integral geometry.
AMS Classification: 60D05, 52A22.

Introduction

Geometric probabilities of different test bodies and lattices are considered in many papers, for instance in [5], [8] and [10]. In some recent bibliography, lattices with obstacles ([2], [3], [4]) and problems of Buffon type with multiple intersections ([1],[6],[7]) are considered.
In the first section of the paper we consider a lattice $\mathfrak{R}_1 = \mathfrak{R}(A, B, a, b)$ of rectangles of sides A and B and with obstacles parallelograms of sides $2a$ and $2b$ and angle $\alpha \in]0; \frac{\pi}{2}]$ with the barycentre on the vertexes of a rectangular tile. We compute the probability of intersection of a line segment with the sides of $\mathfrak{R}_1$.
In the second section of the paper we study problems of Buffon type with multiple intersections for a lattice $\mathfrak{R}_2$ of parallelograms and a circle as test body.

1. Geometric probabilities of a line segment for a lattice with obstacles

In the Euclidean plane E_2, referred to a system of perpendicular axes Oxy, let $\mathfrak{R}_1 = \mathfrak{R}(A, B, a, b)$ be a lattice of rectangles of sides A and B and with obstacles parallelograms of sides $2a$ and $2b$ and angle $\alpha \in]0; \frac{\pi}{2}]$ with the barycentres in the points $M_{h,k} = (hA, kB), k \in \mathbb{Z}$, a side of the obstacle is parallel to the axis x, and the other side forms an angle α with

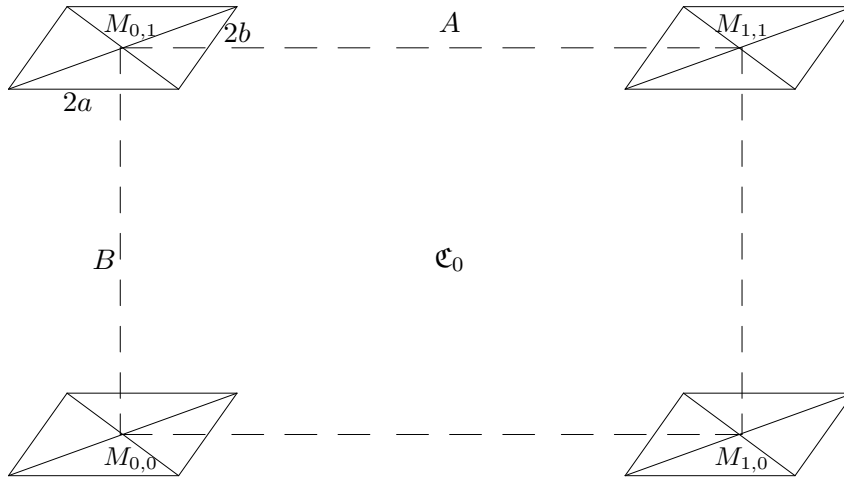


FIGURE 1

the axis x (see figure 1). Let T be a "test body", Q its barycentre and $\mathbf{d}$ a line through Q, intrinsically related to T. We determine the probability p_{T} that T does not intersect the lattice $\mathfrak{R}(A, B, a, b)$, when T is a line segment, with constant length l. In order to compute this probability we consider the points $M_{0,0} = (0, 0)$, $M_{1,0} = (A, 0)$, $M_{0,1} = (0, B)$, $M_{1,1} = (A, B)$ and the rectangle $\mathfrak{C}_0$ with vertexes these points. We denote by $\mathcal{M}$ the set of test bodies T having the barycentre inside the rectangle $\mathfrak{C}_0$ and $\mathcal{N}$ the set of test bodies T entirely contained in $\mathfrak{C}_0$, but not intersecting any parallelogram $\mathcal{P}$ with barycentre in $M_{0,0}$, $M_{1,0}$, $M_{0,1}$, $M_{1,1}$. We use a well-known Stoka's formula in order to compute the probability p_{T}, (see [10], [2]):

$$p_{\mathrm{T}} = \frac{\mu(\mathcal{N})}{\mu(\mathcal{M})}, \tag{1}$$

where μ is the Lebesgue measure. The measures $\mu(\mathcal{M})$ and $\mu(\mathcal{N})$ are computed using the elementary kinematic measure in the Euclidean plane E_2 ([9]):

$$dK = dx \wedge dy \wedge d\varphi, \tag{2}$$

where x and y are the coordinates of the point $R \in \mathrm{T}$, φ the angle between the Ox axis and the line $\mathbf{d}$.
In the following results we study the problem when T is a segment s and $\mathbf{d}$ the support line of s.

Theorem 1. *If $l \leq \min(2a, 2b\sin\alpha)$ the probability that a segment s, with constant length l, uniformly distributed in a bounded region of the Euclidean plane, does not intersect any parallelogram $\mathcal{P}$ of the lattice $\mathfrak{R}(A, B, a, b)$ is:*

$$p_s = 1 - \frac{4ab\sin\alpha}{AB} - \frac{4lb\sin\alpha}{AB\pi} - \frac{4al}{AB\pi} + \frac{4lb\cos\alpha}{AB\pi}. \tag{3}$$

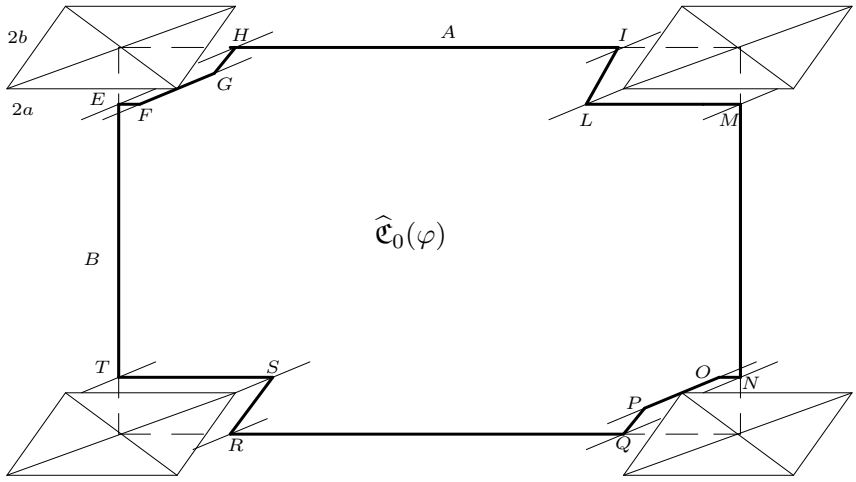
Proof. Taking into account the symmetries we may assume that $\varphi \in [0, \frac{\pi}{2}]$. Then:

$$\mu(\mathcal{M}) = \int_0^{\frac{\pi}{2}} d\varphi \int\int_{\{(x,y)\in\mathfrak{C}_0\}} dxdy = \int_0^{\frac{\pi}{2}} (\text{Area}\mathfrak{C}_0)d\varphi = \frac{AB\pi}{2}. \tag{4}$$

In order to compute $\mu(\mathcal{M})$ we denote by $\widehat{\mathfrak{C}}_0(\varphi)$ the figure, within $\mathfrak{C}_0$, with the following property: a point Q is inside $\widehat{\mathfrak{C}}_0(\varphi)$, if and only if, the line segment s with barycentre Q and forming an angle φ with the Ox axis is entirely contained within $\mathfrak{C}_0$, but does not intersect any parallelogram $\mathcal{P}$ with center $M_{0,0}$, $M_{1,0}$, $M_{0,1}$, $M_{1,1}$. Then we can compute the area $\widehat{\mathfrak{C}}_0(\varphi)$ represented in figure 2:

$$\text{Area } \widehat{\mathfrak{C}}_0(\varphi) = A \cdot B - 4ab\sin\alpha - 2al\sin\varphi - 2lb\sin(\alpha - \varphi). \tag{5}$$

Hence



$$\mathfrak{R}_1 = \mathfrak{R}(A, B, a, b)$$

FIGURE 2

$$(6)\quad \mu(\mathcal{N}) = \int_0^{\frac{\pi}{2}} d\varphi \int_{\{(x,y)\in\widehat{\mathfrak{C}}_0(\varphi)\}} dxdy = \int_0^{\frac{\pi}{2}} (\text{ Area } \widehat{\mathfrak{C}}_0(\varphi))d\varphi =$$
$$= \int_0^{\frac{\pi}{2}} (A\cdot B - 4ab\sin\alpha - 2al\sin\varphi - 2bl\sin\alpha\cos\varphi +$$
$$+2bl\cos\alpha\sin\varphi)d\varphi =$$
$$= (A\cdot B - 4ab\sin\alpha)\cdot\frac{\pi}{2} - 2bl\sin\alpha - 2al + 2bl\cos\alpha.$$

Then, by substituting (6) and (4) in (1) we obtain (3). □

Remark 2. If $A = B$, $a = b$ and $\alpha = \frac{\pi}{2}$ it follows from (3):

$$(7)\qquad p_s = 1 - \frac{4a^2}{A^2} - \frac{8al}{A^2\pi},$$

that is Duma and Stoka's result for quadratic lattices with quadratic obstacles [2].

In what follows we will denote by d_1 the smallest diagonal of the obstacle, that is:

$$(8)\qquad d_1 = \sqrt{4a^2 + 4b^2 - 4ab\cos\alpha}.$$

Theorem 3. *If* $\min(2a, 2b\sin\alpha) \le l \le d_1$ *the probability that a segment* s*, with constant width* l*, uniformly distributed in a bounded region of the plane, does not intersect any parallelogram* $\mathcal{P}$ *of the lattice* $\mathfrak{R}(A, B, a, b)$ *is:*

$$(9)\quad p_s = 1 - \frac{4bl\cos(\psi_0 - \alpha) - 4bl\cos\alpha\cos\psi_0 - 4bl\sin\alpha\sin\psi_0}{\pi\cdot A\cdot B} +$$
$$-\frac{4bl\cos\alpha + 4al + 4bl\sin\alpha}{\pi\cdot A\cdot B},$$

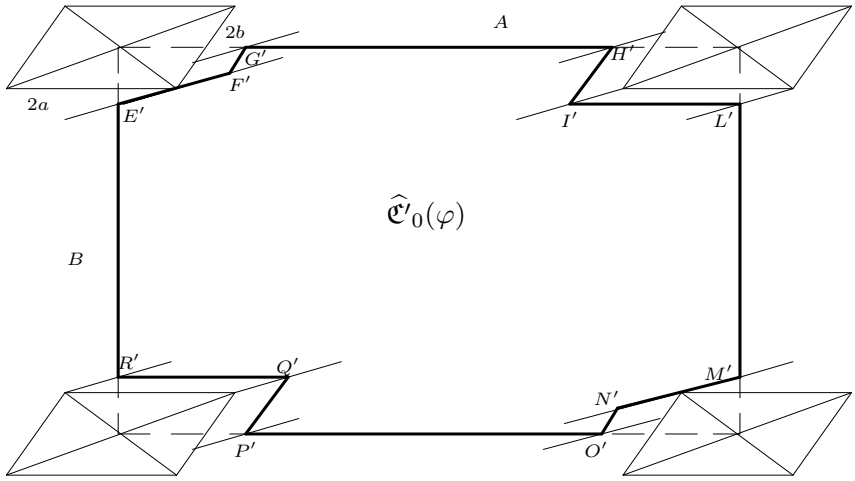
where $\psi_0 = \arccos\left(\frac{2\sqrt{a^2+b^2-ab\cos\alpha-b^2\sin^2\alpha}}{l}\right)$.

Proof. Taking into account the symmetries we may assume that $\varphi \in [0, \frac{\pi}{2}]$. Then:

$$(10)\ \mu(\mathcal{M}) = \int_0^{\frac{\pi}{2}} d\varphi \int\int_{\{(x,y)\in\mathfrak{C}_0\}} dxdy = \int_0^{\frac{\pi}{2}} \text{Area}\mathfrak{C}_0 d\varphi = \frac{AB\pi}{2}.$$

In order to compute $\mu(\mathcal{M})$ we denote by $\widehat{\mathfrak{C}'}_0(\varphi)$ the figure, within $\mathfrak{C}_0$ with the following property: a point Q is inside $\widehat{\mathfrak{C}'}_0(\varphi)$ if and only if the line segment s, with barycentre Q and forming an angle φ with the Ox axis, is entirely contained within $\mathfrak{C}_0$ but does not intersect any parallelogram $\mathcal{P}$ with center $M_{0,0}$, $M_{1,0}$, $M_{0,1}$, $M_{1,1}$. Then we have:

$$(11)\quad \mu(\mathcal{N}) = \int_0^{\frac{\pi}{2}} d\varphi \int_{\{(x,y)\in\widehat{\mathfrak{C}'}_0(\varphi)\}} dxdy = \int_0^{\frac{\pi}{2}} \text{ Area } \widehat{\mathfrak{C}'}_0(\varphi)d\varphi.$$



$$\mathfrak{R}_1 = \mathfrak{R}(A, B, a, b)$$

FIGURE 3

In order to compute $\mu(\mathcal{N})$ we distinguish two cases:
First Case. If $0 \leq \varphi \leq \psi_0$, then $\widehat{\mathfrak{C}'}_0(\varphi)$ is the plane surface represented in figure 3. Then:

$$\text{Area } \widehat{\mathfrak{C}'}_0(\varphi) = A \cdot B - 4ab\sin\alpha - 2bl\sin(\alpha - \varphi) - 2al\sin\varphi. \tag{12}$$

Second Case. If $\psi_0 \leq \varphi \leq \frac{\pi}{2}$, then $\widehat{\mathfrak{C}'}_0(\varphi)$ is the plane surface represented in figure 2, that is:

$$\widehat{\mathfrak{C}'}_0(\varphi) = \widehat{\mathfrak{C}}_0(\varphi). \tag{13}$$

Then

$$\begin{aligned} \text{Area } \widehat{\mathfrak{C}'}_0(\varphi) &= \text{Area } \widehat{\mathfrak{C}}_0(\varphi) = \\ &= A \cdot B - 4ab\sin\alpha - 2al\sin\varphi - 2bl\sin\alpha\cos\varphi + \\ &\quad +2bl\cos\alpha\sin\varphi. \end{aligned} \tag{14}$$

Then

$$
\begin{aligned}
(15)\,\mu(\mathcal{N}) &= \int_0^{\psi_0} (A\cdot B - 4ab\sin\alpha - 2bl\sin(\alpha-\varphi) - 2al\sin\varphi)d\varphi + \\
&\quad \int_{\psi_0}^{\frac{\pi}{2}} (A\cdot B - 4ab\sin\alpha - 2al\sin\varphi - 2bl\sin\alpha\cos\varphi + \\
&\quad +2bl\cos\alpha\sin\varphi)d\varphi = \\
&= 2bl\cos\alpha\cos\psi_0 + 2bl\sin\alpha\sin\psi_0 + 4ab\psi_0\sin\alpha + AB\psi_0 + \\
&\quad -2bl\sin\alpha - 2al\cos\psi_0 + \frac{AB(\pi-2\psi_0)}{2} - 2al + \\
&\quad +2bl\cos\alpha - 4ab\psi_0\cos\alpha + 2al\cos\psi_0 + \\
&\quad -2\pi ab\sin\alpha - 2bl\cos(\alpha-\psi_0).
\end{aligned}
$$

Then by substituting (15) and (10) in (1) we obtain (9).

Remark 4. If $A = B$, $a = b$ and $\alpha = \frac{\pi}{2}$ it follows from (9):

$$p_s = 1 - \frac{4a^2}{A^2} - \frac{8al}{A^2\pi}, \tag{16}$$

that is Duma and Stoka's result for quadratic lattices with quadratic obstacles [2].

2. A problem of Buffon type with multiple intersections for a lattice of parallelograms

Let be given in the Euclidean plane E_2 a lattice $\mathfrak{R}_2$, whose fundamental tile is a parallelogram $\mathcal{P}$ with sides a and b and angle $\alpha \in]0, \frac{\pi}{2}[$, as in figure 4. In [7] A. Duma and M. Stoka consider the lattice of figure 4 and they

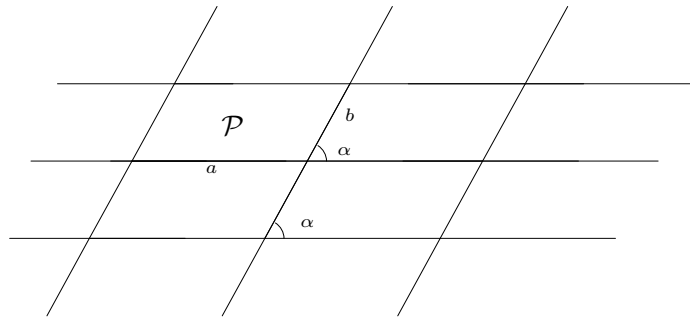


Figure 4

compute the probability of multiple intersections with a line segment as

test body.
We study the probability of multiple intersections of a circle $\mathcal{C}$ with the sides of $\mathfrak{R}_2$. We denote by p_i the probability that the circle $\mathcal{C}$ intersects i times the sides of the lattice.

Theorem 5. *If $2r < \min(a\sin\alpha, b\sin\alpha)$, the probabilities that a circle $\mathcal{C}$ of constant radius r, uniformly distributed in a bounded region of the plane intersects i times the sides of the lattice $\mathfrak{R}_2$ are*

$$p_i = 0 \text{ for } i \notin \{2,4\}; \tag{17}$$

$$p_2 = \frac{r}{abt_1t_2}\left(a+b-\frac{2r}{t_1t_2}-\frac{3r}{2t_1^2t_2}-\frac{r}{t_1}-\frac{r}{t_2}\right); \tag{18}$$

$$p_4 = \frac{r^2}{abt_1t_2}\left(\frac{1}{t_1t_2}-\frac{3}{2t_1^2t_2}+\frac{1}{t_1}+\frac{1}{t_2}\right); \tag{19}$$

where $t_1 = \sin\frac{\alpha}{2}$, $t_2 = \cos\frac{\alpha}{2}$.

Proof. We note the a circle $\mathcal{C}$ with constant radius r and such that $2r < \min(a\sin\alpha, b\sin\beta)$ never intersects i times the sides of $\mathfrak{R}_2$, when $i \notin \{2,4\}$, then (17) holds.
We denote by $\mathcal{M}$ the set of circles of constant radius r with center C belonging to $\mathcal{P}$. Then the circle intersects two times, respectively four times, the sides of the parallelogram $\mathcal{P}$ if and only if $C \in P_2$ or $C \in P_4$ (see figure 5). Hence, putting

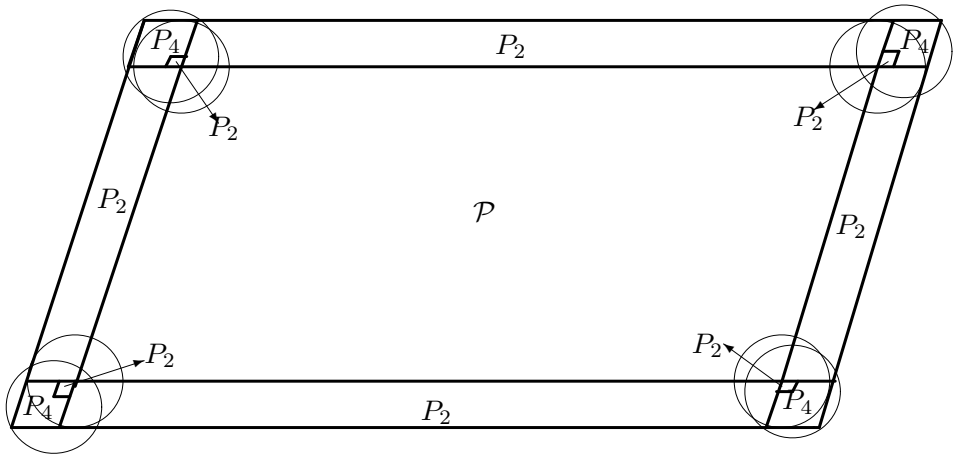


FIGURE 5

$$\mathcal{N}_i = \{(x,y) \in P_i\}, \text{ for } i \in \{2,4\} \tag{20}$$

we have

$$p_2 = \frac{\mu(\mathcal{N}_2)}{\mu(\mathcal{M})}, \tag{21}$$

$$p_4 = \frac{\mu(\mathcal{N}_4)}{\mu(\mathcal{M})}. \tag{22}$$

where μ is the Lebesgue measure in the Euclidean plane.

Remark 6. It follows from Theorem 5 that the total probability of intersection is

$$p_{tot} = p_2 + p_4 = \frac{2r(a+b)}{ab\sin\alpha} - \frac{4r^2}{ab\sin^2\alpha}, \tag{23}$$

which coincides with the formula obtained in [11] by Stoka.

References

[1] V. Bonanzinga and L. Sorrenti, *Buffon type problems with multiple intersections for rectangle in the Euclidean plane*, Pub. Inst. Stat. Univ. Paris. LII fasc. 3, pp. 61-69, 2008.

[2] A. Duma and M. Stoka, *Geometric Probabilities for quadratic obstacles*, Pub. Inst. Stat. Univ. Paris. XXXXVIII fasc.1-2, pp. 19-42, 2004.

[3] A. Duma and M. Stoka, *Geometric Probabilities for triangular lattices with quadratic obstacles*, Pub. Inst. Stat. Univ. Paris. XLIX, fasc.2-3, pp. 57-72, 2005.

[4] A. Duma and M. Stoka, *Probabilitá geometriche per reticoli esagonali con ostacoli esagonali*, Suppl. Rendiconti del Circolo Mat. di Palermo, VI International Conference of Stochastic Geometry, Convex Bodies, Empirical Measure & Applications to Mechanics and Engeneering of Train-Transport, serie II, 80, pp. 153-159, 2008.

[5] A. Duma and M. Stoka, *Problems of Buffon type for the Dirichlet-Voronoi lattice*, Pub. Inst. Stat. Univ. Paris, XXXXVII, fasc 1-2, pp. 91-108, 2003.

[6] A. Duma and M. Stoka, *Problems of Buffon type with multiple intersections for lattices of equilateral triangles*, Pub. Inst. Stat. Univ. Paris. LI fasc. 3, pp. 3-15, 2007.

[7] A. Duma and M. Stoka, *Problems of Buffon type with multiple intersections for lattices of parallelograms*, Rendinconti del Circolo Mat. di Palermo, Serie II, Tomo LV, pp. 241-248, 2006.

[8] A. Duma, *Problems of Buffon type for non-small Needles*, Suppl. Rendinconti del Circolo Mat. di Palermo, Serie II, Tomo XLVIII, pp. 23-40, 1999.

[9] H. Poincaré, *Calcul des probabilités*, Carré, Paris, 1912.

[10] M. I. Stoka, *Probabilitiés géométriques de type "Buffon" dans le plane euclidien*, Atti Acc. Sci. Torino, pp. 53-59, 1975-76.

[11] M. I. Stoka, *Sur quelques problems de probabilitiés géométriques pour des réseaux dans l'espace euclideien E_n*, Pub. Inst. Stat. Univ. Paris, XXXIV, 3, 31-50, 1989.

Vittoria BONANZINGA,
University of Reggio Calabria,
Faculty of Engineering-DIMET,
via Graziella (Feo di Vito),
vittoria.bonanzinga@unirc.it
vittoria.bonanzinga@tin.it

Loredana SORRENTI,
University of Reggio Calabria,
Faculty of Engineering-DIMET,
via Graziella (Feo di Vito),
sorrenti.loredana@tiscali.it
loredana.sorrenti@unirc.it

RENDICONTI DEL CIRCOLO MATEMATICO DI PALERMO
Serie II, Suppl. 81 (2009), pp. 47-53

GEOMETRIC PROBABILITIES FOR CUBIC LATTICES WITH CUBIC OBSTACLES

VITTORIA BONANZINGA AND LOREDANA SORRENTI

Abstract: In this paper we present solutions for problems of Buffon type for a cubic lattice $\mathfrak{R}(L,a)$ consisting of cubic obstacles with edges $2a$, having as symmetry center the points $M_{h,k,l} = (hL, kL, lL)$, $h,k,l \in \mathbb{Z}$ and the faces parallel to the coordinate planes and the lattice $\mathfrak{R}'(L,a)$ obtained by $\mathfrak{R}(L,a)$ adding the plane portions delimited by the following segments: $\{(x, kL, lL) : x \in [hL+a, (h+1)L-a]\}$, $\{(hL, y, lL) : y \in [hL+a, (h+1)L-a]\}$, $\{(hL, kL, z) : z \in [hL+a, (h+1)L-a]\}$, $h,k,l \in \mathbb{Z}$.

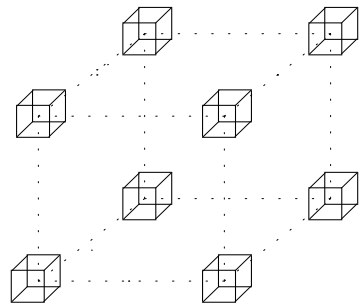
AMS 2000 Subject Classifications: Geometric probability, stochastic geometry, random sets, random convex sets and integral geometry.
AMS Classification: 60D05, 52A22.

1. Introduction

In a previous paper [3], A. Duma and M. Stoka compute the probability that a test body T does not intersect a lattice consisting by squares with quadratic obstacles, in the Euclidean plane E_2, in several cases, when T is a circle or a line segment. In this paper we consider the analogue problem in the Euclidean space E_3. Let be given, in the Euclidean space E_3, a system of perpendicular axes, a lattice $\mathfrak{R}(L,a)$ consisting by cubes C with edges $2a$ having as symmetry center the points $M_{h,k,l} = (hL, kL, lL)$, $h,k,l \in \mathbb{Z}$ and the edges parallel to the coordinate axes, as in figure 1. Let T be a test body with centroid P and oriented axis of rotation $\mathbf{d}$. Our main goal is to answer to the following:

Question 1. *If T is a test body placed with random position in the lattice, what is the probability p_T that T does not intersect the lattice $\mathfrak{R}(L,a)$?*

In order to compute the desired probability we consider the points $M_{0,0,0}$, $M_{L,0,0}$, $M_{0,L,0}$, $M_{L,L,0}$, $M_{0,0,L}$, $M_{L,0,L}$, $M_{0,L,L}$, $M_{L,L,L}$, and the cube $\mathfrak{C}_0$ with vertexes these points. We denote by $\mathcal{M}$ the set of the test bodies having the barycenter in the cube $\mathfrak{C}_0$ and by $\mathcal{N}$ the set of test bodies completely lying within $\mathfrak{C}_0$, but not intersecting the eight cubes C with



$\mathfrak{R}(L,a)$

FIGURE 1

symmetry center the points $M_{0,0,0}$, $M_{L,0,0}$, $M_{0,L,0}$, $M_{L,L,0}$, $M_{0,0,L}$, $M_{L,0,L}$, $M_{0,L,L}$, $M_{L,L,L}$. We have:

$$p_T = \frac{\mu(\mathcal{N})}{\mu(\mathcal{M})} \tag{1}$$

where μ is the Lebesgue measure (see [3]). The measures $\mu(\mathcal{M})$ and $\mu(\mathcal{N})$ are computed using the elementary Kinematic measure of the Euclidean space E_3 [4]:

$$dK = dx \wedge dy \wedge dz \wedge d\Omega \wedge d\varphi \tag{2}$$

where x, y, z are the coordinates of the midpoint of T, $d\Omega$ the element of the solid angle.

$$d\Omega = |\sin\theta| d\psi \wedge d\theta \tag{3}$$

and φ the angle of rotation, $0 \leq \varphi \leq 2\pi$, $0 \leq \psi \leq 2\pi$, $0 \leq \theta \leq \frac{\pi}{2}$. The oriented axis of rotation is the support line of T.

2. Geometric probability of intersection for spheres

In the following, we consider the probability p_T that a sphere T does not intersect the lattice $\mathfrak{R}(L,a)$, when T is a sphere with constant radius r placed with random position in the lattice.

Theorem 1. *If $L > 2a$, the probability p_S that a sphere S with random position and constant radius r, uniformly distributed in a limited region of*

the space E_3, does not intersect the lattice $\mathfrak{R}(L,a)$ is:

$$p_S = 1 - \tfrac{4\pi a r^2 + 20a^2 r + 16a^3}{L^3} - \tfrac{2\pi r^3}{3L^3} + \\ - \tfrac{4a}{L} + \tfrac{12a^2}{L^2}, \qquad \text{if } r \le \frac{L-2a}{2}; \tag{4}$$

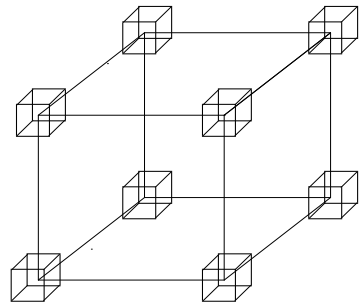
$$p_S = 1 - \tfrac{8a^2}{L^3} + \tfrac{12a^2}{L^2} - \tfrac{6a}{L} + \\ - \left(\tfrac{1}{L} + \tfrac{2a^2}{L^3} - \tfrac{4a}{L^2}\right)\sqrt{4r^2 - (L-2a)^2} + \\ -2\beta r\left(\tfrac{1}{L^2} - \tfrac{2a}{L^3}\right), \qquad \text{if } \frac{L-2a}{2} < r < \frac{L-2a}{\sqrt{2}}; \tag{5}$$

$$p_S = 0, \qquad \text{if } r \ge \frac{L-2a}{\sqrt{2}}, \tag{6}$$

where $\beta = \frac{\pi}{2} - 2\arccos\left(\frac{L-2a}{2r}\right)$.

Proof. See [1]. □

Now we consider the lattice $\mathfrak{R}'(L,a)$ obtained by $\mathcal{R}(L,a)$ adding the plane portions delimited by the following segments: $\{(x,kL,lL) : x \in [hL+a,(h+1)L-a]\}$, $\{(hL,y,lL) : y \in [hL+a,(h+1)L-a]\}$, $\{(hL,kL,z) : z \in [hL+a,(h+1)L-a]\}$, $h,k,l \in \mathbb{Z}$ (see figure 2).



$\mathfrak{R}'(L,a)$

FIGURE 2

Theorem 2. *If $L > 4a$, the probability p_S that a sphere S with radius r does not intersect one of the edges of $\mathfrak{R}'(L,a)$ is the following:*

$$p_S = 1 - \frac{16a^3-4a^2r+4ar^2(\pi-5)+4r^3(4-\pi)}{L^3} + \\ - \frac{2\pi r^3}{3L^3} - \frac{8ar-12a^2-8r^2}{L^2} - \frac{4a+2r}{L}, \qquad \text{if } r < a \tag{7}$$

$$p_S = 1 - \frac{2\pi a^2}{3L^3} - \frac{6r}{L} + \frac{12r^2}{L^2} - \frac{8r^3}{L^3}, \qquad \text{if } a \le r < \frac{L}{2} \tag{8}$$

$$p_S = 0, \qquad \text{if } r \ge \frac{L}{2}. \tag{9}$$

Proof. See [1]. □

Remark 3. If $a = 0$, then $\mathfrak{R}'(L,a)$ is a lattice whose fundamental tile is a cube with edge L. In this case, it follows from Theorem 2 that:

$$p_S = 1 - \frac{6r}{L} + \frac{12r^2}{L^2} - \frac{8r^3}{L^3}. \tag{10}$$

Then the probability of intersection for a sphere with diameter $2r < L$ is

$$p'_S = \frac{6r}{L} - \frac{12r^2}{L^2} + \frac{8r^3}{L^3}. \tag{11}$$

Remark 4. In [2] A. Duma and M. Stoka determined the following formula for computing the probability of intersection of an arbitrary convex test body K with constant width k, with a lattice of planes whose fundamental cell is a rectangular parallelepiped, with sides a, b, c:

$$p_K^{(3)} = \frac{k(ab+bc+ca)}{abc} - \frac{k^2(a+b+c)}{abc} + \frac{k^3}{abc}, \tag{12}$$

which coincides with the formula obtained by M. Stoka in [6] for a sphere with diameter k. If $k = 2r$ and $a = b = c = L$ formula (12) coincides with formula (11).

3. Geometric probability of intersection of a small line segment with $\mathfrak{R}'(L,a)$

In the following, the probability that a line segment s does not intersect one of the planes or of the obstacles of the cubic lattice $\mathfrak{R}'(L,a)$ with side L, with cubic obstacles with sides $2a$ (see figure 2), is computed.

Theorem 5. *If $l \le a$, the probability that a segment s of length l, uniformly distributed in a bounded region of the space, does not intersect the cubes C of the lattice $\mathfrak{R}'(L,a)$ is*

$$p_s = 1 - \frac{3l}{2L} + \frac{2l^2}{\pi L^2} - \frac{l^3}{4\pi L^3} - \frac{8a^3}{L^3} \tag{13}$$

Proof. We use the kinematic measure in E_3 given by (2), where x, y, z are the coordinates of the midpoint of s. The oriented axis of rotation is the line support of s. We denote by $\mathfrak{C}_1$ the solid with the following property: a point P in inside $\mathfrak{C}_1$, if and only if, the line segment with barycenter P belongs to $\mathfrak{C}_0$ and does not intersect any obstacle. We have:

$$\begin{aligned}(14)\quad \mu(\mathcal{M}) &= \int_0^{2\pi} d\varphi \int_0^{\pi} d\psi \int_0^{\frac{\pi}{2}} \sin\theta d\theta \int_{\{(x,y,z)\in\mathfrak{C}_0\}} dxdydz = \\ &= 2\pi^2 \cdot (\text{Volume of } \mathfrak{C}_0) = 2\pi^2 L^3,\end{aligned}$$

$$\begin{aligned}(15)\quad \mu(\mathcal{N}) &= \int_0^{2\pi} d\varphi \int_0^{\pi} d\psi \int_0^{\frac{\pi}{2}} \sin\theta d\theta \int_{\{(x,y,z)\in\mathfrak{C}_1\}} dxdydz = \\ &= \int_0^{2\pi} d\varphi \int_0^{\pi} d\psi \int_0^{\frac{\pi}{2}} V(\theta,\varphi)\sin\theta d\theta,\end{aligned}$$

where $V(\theta, \varphi)$ is the volume of the solid obtained considering the line segment s in all limit positions.
In order to compute $\mu(\mathcal{N})$ we note that:

$$(16)\qquad V(\theta,\varphi) = V_{\mathcal{C}} - \sum_{i=1}^{8} V_i,$$

where $V_{\mathcal{C}}$ is the volume of the solid $\mathcal{C}$ with vertexes the following points:

$$M_1\left(\frac{l}{2}\cos\varphi\sin\theta, \frac{l}{2}\sin\varphi\sin\theta, \frac{l}{2}\cos\theta\right),$$

$$N_1\left(L - \frac{l}{2}\cos\varphi\sin\theta, \frac{l}{2}\sin\varphi\sin\theta, \frac{l}{2}\cos\theta\right),$$

$$P_1\left(L - \frac{l}{2}\cos\varphi\sin\theta, L - \frac{l}{2}\sin\varphi\sin\theta, \frac{l}{2}\cos\theta\right),$$

$$Q_1\left(\frac{l}{2}\cos\varphi\sin\theta, L - \frac{l}{2}\sin\varphi\sin\theta, \frac{l}{2}\cos\theta\right),$$

$$M_2\left(\frac{l}{2}\cos\varphi\sin\theta, \frac{l}{2}\sin\varphi\sin\theta, L - \frac{l}{2}\cos\theta\right),$$

$$N_2\left(L - \frac{l}{2}\cos\varphi\sin\theta, \frac{l}{2}\sin\varphi\sin\theta, L - \frac{l}{2}\cos\theta\right),$$

$$P_2\left(L - \frac{l}{2}\cos\varphi\sin\theta, L - \frac{l}{2}\sin\varphi\sin\theta, L - \frac{l}{2}\cos\theta\right),$$

$$Q_2\left(\frac{l}{2}\cos\varphi\sin\theta, L - \frac{l}{2}\sin\varphi\sin\theta, L - \frac{l}{2}\cos\theta\right).$$

$$(17)\qquad V_C = \int_{\frac{l}{2}\cos\varphi\sin\theta}^{L-\frac{l}{2}\cos\varphi\sin\theta} dx \int_{\frac{l}{2}\sin\varphi\sin\theta}^{L-\frac{l}{2}\sin\varphi\sin\theta} dy \int_{\frac{l}{2}\cos\varphi}^{L-\frac{l}{2}\cos\varphi} dz =$$
$$= (L - l\cos\varphi\sin\theta)\,(L - l\sin\varphi\sin\theta)(L - l\cos\theta).$$

Denoting by x_P, y_P, z_P the coordinates of a point P, we have:

$$(18)\qquad V_1 = \int_{x_{N_1}-a}^{x_{N_1}} dx \int_{y_{N_1}}^{y_{N_1}+a} dy \int_{z_{N_1}}^{z_{N_1}+a} dz,$$

$$(19)\qquad V_2 = \int_{x_{P_1}-a}^{x_{P_1}} dx \int_{y_{P_1}-a}^{y_{P_1}} \int_{z_{P_1}}^{z_{P_1}+a} dz,$$

$$(20)\qquad V_3 = \int_{x_{Q_1}}^{x_{Q_1}+a} dx \int_{y_{Q_1}-a}^{y_{Q_1}} \int_{z_{Q_1}}^{z_{Q_1}+a} dz,$$

$$(21)\qquad V_4 = \int_{x_{M_1}}^{x_{M_1}+a} dx \int_{y_{M_1}}^{y_{M_1}+a} \int_{z_{M_1}}^{z_{M_1}+a} dz,$$

$$(22)\qquad V_5 = \int_{x_{P_2}-a}^{x_{P_2}} dx \int_{y_{P_2}-a}^{y_{P_2}} \int_{z_{P_2}}^{z_{P_2}+a} dz,$$

$$(23)\qquad V_6 = \int_{x_{N_2}-a}^{x_{N_2}} dx \int_{y_{N_2}}^{y_{N_2}+a} \int_{z_{N_2}-a}^{z_{N_2}} dz,$$

$$(24)\qquad V_7 = \int_{x_{Q_2}}^{x_{Q_2}+a} dx \int_{y_{Q_2}-a}^{y_{Q_2}} \int_{z_{Q_2}-a}^{z_{Q_2}} dz,$$

$$(25)\qquad V_8 = \int_{x_{M_2}}^{x_{M_2}+a} dx \int_{y_{M_2}}^{y_{M_2}+a} \int_{z_{M_2}-a}^{z_{M_2}} dz.$$

Then by substituting the formulas (18)-(25) in (16) we obtain:

$$(26)\quad V(\theta,\varphi) = L^3 - L^2 l\sin\varphi\sin\theta - lL^2\cos\varphi\sin\theta - lL^2\cos\theta + $$
$$+ l^2 L\sin^2\theta\sin\varphi\cos\varphi + Ll^2\sin\theta\cos\theta\sin\varphi +$$
$$+ l^2 L\cos\varphi\cos\theta\sin\theta - l^3\sin^2\theta\cos\theta\sin\varphi\cos\varphi - 8a^3.$$

It follows from (15) that:

$$(27)\qquad \mu(\mathcal{N}) = \pi^2 L^3 - \frac{3\pi^2 l L^2}{2} + 2\pi l^2 L - \frac{\pi l^3}{4} - 8\pi^2 a^3.$$

Then, by substituting (27) and (14) in (1) we obtain formula (13). □

Remark 6. In [5] M. Stoka computed the following formula for computing the probability that a line segment does not intersect the sides of a lattice of planes whose fundamental cell is a rectangular parallelepiped, with sides

a, b, c:

$$p = 1 - \frac{(ab + ac + bc)l}{2abc} + \frac{2(a + b + c)l^2}{3\pi abc} - \frac{l^3}{4\pi abc} \tag{28}$$

If $a = b = c = L$ formula (28) coincides with formula (13).

References

[1] V. Bonanzinga and L. Sorrenti, *Geometric probabilities for three-dimensional tessellations and raster classifications*, Applied and Industrial Mathematics in Italy III (AIMI III), selected contributions from the 9th Conference SIMAI (to appear).

[2] A. Duma and M. Stoka, *Geometric probabilities for convex bodies of revolution in the euclidean space E_3*, Rend. Circ. Mat. Palermo, serie II-Suppl. **65** (2000), pp.109-115.

[3] A. Duma and M. Stoka, *Geometric probabilities for quadratic lattices with quadratic obstacles*, Ann. I.S.U.P., **48**, 1-2 (2004), 19-42.

[4] L. A. Santaló, *Integral Geometry and Geometric Probability*, 1976, Addison Wesley, Mass.

[5] M. Stoka, Probabilitá e Geometria, Herbita (1982).

[6] M. Stoka, *Sur quelques problèmes de probabilités géométriques pour des réseaux dans l'espace euclidien E_n*, Pub. Inst. Stat. Univ. Paris, XXXIV, fasc. 3, (1989).

Vittoria BONANZINGA,
University of Reggio Calabria,
Faculty of Engineering-DIMET,
via Graziella (Feo di Vito),
vittoria.bonanzinga@unirc.it
vittoria.bonanzinga@tin.it

Loredana SORRENTI,
University of Reggio Calabria,
Faculty of Engineering-DIMET,
via Graziella (Feo di Vito),
sorrenti.loredana@tiscali.it
loredana.sorrenti@unirc.it

RENDICONTI DEL CIRCOLO MATEMATICO DI PALERMO
Serie II, Suppl. 81 (2009), pp. 55-58

ON ESTIMATION OF THE SUPPORT IN METRIC SPACES

Denis Bosq

Université Pierre et Marie Curie

Abstract

Let $Z = (X, Y)$ be a random vector with values in the cartesian product of separable metric spaces and such that $Y = \varphi(X)$.

Let P_Z be the distribution of Z. We construct a statistical estimator of the support of P_Z. For that purpose we use a statistic which vanishes outside the support.

The rate of convergence of the estimator is sharp.

AMS subject classification: 62G
Keywords : support, nonparametric estimation, metric space

1 Notation and assumptions

Let X and Y be random variables, defined on the probability space $(\Omega, \mathcal{A}, P)$ with values in the separable metric spaces E (with metric d) and F (with metric δ) respectively.

Suppose that there exists $\varphi : E \longmapsto F$ continuous and such that

$$Y = \varphi(X), \tag{1}$$

then, under regularity conditions, φ characterizes the support of (X, Y). A typical example is the case where E is a compact space, X has a strictly positive continuous density on E, with respect to some finite measure and φ is a homeomorphism. Then the support of (X, Y) is the graph of φ.

We want to estimate φ from independent copies (X_i, Y_i), $1 \leq i \leq n$ of (X, Y). To this aim, we consider a kernel $K : \mathbb{R}_+ \longmapsto \mathbb{R}_+$ and a sequence $(h_n) \to 0^+$, and we define the statistic

$$(2) \qquad g_n(x,y) = \frac{1}{n}\sum_{i=1}^{n} K\left(\frac{d(x,X_i)}{h_n}\right) K\left(\frac{\delta(y,Y_i)}{h_n}\right), \quad x \in E, y \in F.$$

In order to study g_n we make the following assumptions:

- K is a bounded measurable function such that $K(u) = 0$ if $u \geq a$ and $K(u) \geq \beta > 0$ if $u \leq \alpha < a$.
- φ satisfies the Lipschitz condition

$$\delta(\varphi(x'), \varphi(x)) \leq c'_{\varphi} d(x,x') \; ; \; x, x' \in E$$

and we set $c_\varphi = \max(1, c'_\varphi)$.

Finally we put

$$V(x,\varepsilon) = \{y \; : \; \delta(y, \varphi(x)) < \varepsilon \} \; ; \; \varepsilon > 0, \; x \in E$$

Then we have the following results:

Proposition 1

$$(3) \qquad y \notin V(x, 2ac_\varphi h_n) \Rightarrow g_n(x,y) = 0$$

and

$$(4) \qquad y \in V(x, \frac{\alpha h_n}{1+c_\varphi}) \Rightarrow g_n(x,y) \geq \frac{\beta^2}{n}\sum_{i=1}^{n} \mathbb{I}_{d(x,X_i) < \frac{\alpha h_n}{1+c\varphi}}.$$

2 Estimating φ

One defines an estimator of φ by

$$(5) \qquad g_n(x, \varphi_n(x)) = \max_{y \in F} g_n(x,y), \; x \in E.$$

We suppose that φ_n does exist and that it is possible to choose a measurable version of $\varphi_n(x)$ for all x. These facts can be directly verified for each (reasonable) choice of K.

Using Proposition 1, one obtains:

Proposition 2

$$P\left(\delta(\varphi_n(x), \varphi(x)) \geq 2ac_\varphi h_n\ \right) \leq (1-p_n)^n \tag{6}$$

where

$$p_n = P\left(d(x, X) < \frac{\alpha h_n}{1 + c_\varphi}\right). \tag{7}$$

Corollary 1

If $np_n \to \infty$

$$\limsup h_n^{-1}\delta(\varphi_n(x), \varphi(x)) < 2ac_\varphi \tag{8}$$

in probability.

If $\frac{np_n}{\log n} \to \infty$

$$\limsup h_n^{-1}\delta(\varphi_n(x), \varphi(x)) < 2ac_\varphi \tag{9}$$

almost completely.

We give some examples of application:

Examples

1. If E is an interval in $\mathbb{R}$ and X has a continuous density in a neighbourhood of x then $p_n \simeq h_n$ and the choice $h_n = \frac{\log n \cdot \log\log n}{n}$ gives

$$\limsup \frac{n}{\log n \cdot \log\log n}\delta\left(\varphi_n(x), \varphi(x)\ \right) < 2ac_\varphi \quad \text{a.c.}$$

2. In $\mathbb{R}^k$ $(k \geq 1)$, similar results hold, i.e. the rate is $n^{1/k}$ up to a logarithm.

3. In an infinite dimensional space, the situation is more intricate. In general the rate is logarithmic. For example, if E is a separable Hilbert space and X is a gaussian random variable satisfying the Grenander condition (cf [4] p. 375-382) the rate is $\mathcal{O}\left((\log n)^{-\gamma}\ \right)$ $(\gamma > 0)$.
In a general space a good rate can be obtained if a special "fractal condition" holds (cf [3] p. 121).

4. Now, suppose that $E = F = C([0,1])$ the Banach space of continuous functions on [0,1], equipped with the uniform norm. If $X =$

$(\max(0, W_t),\ 0 \leq t \leq 1)$ where (W_t) is a standard Wiener process and φ is a bounded linear operator on $C[0,1]$ then, since

$$P\left(\sup_{0\leq t\leq 1} |X_t| \leq \varepsilon\right) = \sqrt{\frac{2}{\pi}} \int_0^{\varepsilon} \exp(-\frac{u^2}{2})\, du \sim_{\varepsilon\to 0} \sqrt{\frac{2}{\pi}}\varepsilon,$$

(cf [2]), the rate is the same as in the real case.

3 Discussion and extensions

It is noteworthy that, since $Y_i = \varphi(X_i)$, φ is perfectly known at $X_1, \cdots, X_n$. Thus, at least in the real case, it is easy to construct an estimator by interpolation. However, such a method does not provide a better rate of convergence.

Now, a more suitable form of our model should be

$$Y_{in} = \varphi(X_{in}) + \varepsilon_{in}\ ;\ 1 \leq i \leq n,\ n \geq 1$$

where ε_{in} is a "small" noise.

Then, under mild regularity conditions, and if

$$\sum_{n\geq 1} nP\left(\delta(0, \varepsilon_{in}) > \frac{\alpha}{2} h_n\right) < \infty,$$

(8) and (9) hold with $4ac_\varphi$ instead of $2ac_\varphi$ and consequently, one may reach the same rate as in model (1).

Another extension consists in replacement of (1) by the implicit relation

$$\Psi(X, Y) = 0.$$

Finally, other modes of convergence (L^p, uniform) may be considered.
The proofs will appear elsewhere.

References

[1] D. Bosq. Estimating the support of a probability distribution. *Rend. Circ. Mat. Palermo 2*, Suppl. 80:17–29, 2008.

[2] D. Bosq and H.T. Nguyen. *A course in stochastic processes*, volume 34 of *Theory and Decision Library. Series B: Mathematical and Statistical Methods.* Kluwer Academic Publishers Group, Dordrecht, 1996. Stochastic models and statistical inference.

[3] F. Ferraty, V. Nuñez Anton, and P. Vieu. *Regression No Parametrica: Desde la Dimension Uno Hasta la Dimension Infinita.* Servicio Editorial de la Universidad del Pais Vasco, Bilbao, 2001.

[4] U. Grenander. *Abstract inference.* Wiley, New York, 1981.

RENDICONTI DEL CIRCOLO MATEMATICO DI PALERMO
Serie II, Suppl. 81 (2009), pp. 59-68

Geometrical Probabilities using the Principle of Inclusion-Exclusion

Roger Böttcher

Mathematics Subject Classification (2000). 60D05, 65C05, 68U20.

Abstract. In the outlook of [1] the question is arisen, whether it is possible or how to minimize the number of necessary integrals to calculate a proper amount of geometric probabilities?—Here we consider a particular type of lattice, where together with the Principle of Inclusion-Exclusion (PIE) only basic measures, i.e. only two separated elements of the lattice are involved at a time, are necessary to create general formulas for geometrical probabilities of arbitrary long segments, which are randomly intersecting this sort of lattice exactly k times.

Introduction

The geometrical probabilities treating in [1] are a special case of a wider class of lattices, which we will introduce and investigate here. Once more we ask for the probabilities of exactly k intersections between a randomly placed, arbitrary long straight segment on the convex hull on such a lattice with the lattice itself. It is very useful to create the required measures for this sets of events in a sense of an "assembly system"—this will reduce the number of integrals and focus more on the inner structure of the measures. Very often we like to gain the measure of a union of events and very often we have a sufficient knowledge of the intersections of sets of events. So this is a good place to bring the "sieve method" into play:

Principle of Inclusion-Exclusion (PIE). *If S_1, S_2, ..., S_n, $n \in \mathbb{N}$, are measureable sets, then we have*

$$\mu\Big(\bigcup_{i=1}^{n} S_i\Big) = \sum_{k=1}^{n}(-1)^{k-1} \sum_{I \in \binom{\{1,2,\dots,n\}}{k}} \mu\Big(\bigcap_{i \in I} S_i\Big) \tag{1}$$

$$= \sum_{\emptyset \neq I \subseteq \{1,2,\dots,n\}} (-1)^{|I|-1}\, \mu\Big(\bigcap_{i \in I} S_i\Big) \tag{2}$$

$$= \sum_{k=1}^{n} \sum_{1 \le i_1 < i_2 < \dots < i_k \le n} (-1)^{k-1}\, \mu(S_{i_1} \cap S_{i_2} \cap \dots \cap S_{i_k})\,, \tag{3}$$

where $|I|$ is the cardinality of the index set I, and $\mu : S \mapsto \mathbb{R}$ is a common measure. The expression $\binom{\{1,2,\dots,n\}}{k}$ in (1) denotes all subsets of $\mathbb{N}_n$ containing k elements.

These three equations, see for example [8] or [10], are expressing all the same: How to count or measure a union of sets only by the way looking for intersections of it. Now it is our task to provide this principle with a just geometrical as stochastic meaning as well, searching for geometrical measures and probabilities.

1 Sequential Lattices

Now we introduce sequential lattices which — in brief — have a geometrical structure like a ladder. So, two elements of this lattices can only be connected by a straight segment hitting all other elements lying "between" this two elements.

Definition 1.1 (Sequential Lattice)**.** *Assume there are $n+1$, $n \in \mathbb{N}_0$, non closed curves K_ν, $1 \le \nu \le n+1$, given in the plane. If there exist a set $I \subset \mathbb{N}$ of indices in such a way that*

$$K_i \cap \mathcal{N} \neq \emptyset \ \wedge \ K_j \cap \mathcal{N} \neq \emptyset \ \implies \ K_\nu \cap \mathcal{N} \neq \emptyset \ \text{ for all } \ i \le \nu \le j \,,\ i,\nu,j \in I \,,$$

holds for any line segment $\mathcal{N}$ in the plane, then $\mathcal{L} := \cup_{i\in I} K_i$ is called a ***sequential lattice****. We will denote by $\mathcal{C}(\mathcal{L})$ the convex hull of such a lattice. Thus $\mathcal{C}(\mathcal{L})$ can be structured by n cells $\mathcal{Z}_\nu := \mathcal{C}(K_\nu \cup K_{\nu+1})$ for $\nu = 1, ..., n$. The curves K_ν are called the elements of the lattice.*

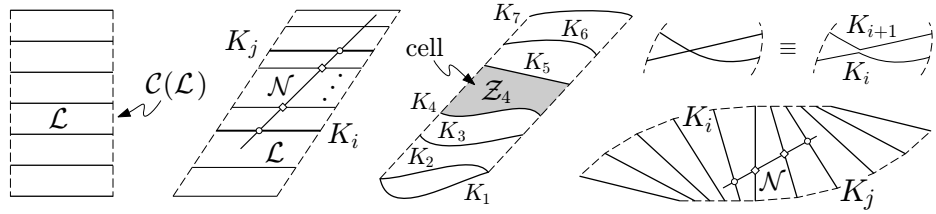


Fig. 1: Definition and Examples for Sequential Lattices

The pictures in figure 1 show the concept of sequential lattices and depict some examples of them. If an element of a sequential lattice intersect another element we will assume that there are two elements only touching each other, see on the right hand side of figure 1—so far possible, otherwise the property to be sequential vanishes. Together with the test element this defines a wide class of lattices.

1.1 Measures and Probabilities

Problem. (Line Segment on Sequential Lattice.) *We are searching for the geometrical probabilities p_k that a straight segment $\mathcal{N}$ of arbitrary length which is randomly placed on the convex hull $\mathcal{C}$ of a sequential lattice $\mathcal{L}$ intersect exactly k elements of it with $1 \le k \le n+1$.*

If the elements of the lattices $\mathcal{L}$ are itself straight segments we can equalize the integer k directly to the number of intersections between $\mathcal{N}$ and $\mathcal{L}$, having in mind that collinear segments $\mathcal{N}$ to any $\mathcal{K} \in \mathcal{L}$ are of zero measure. So we define:

$$p_k := p(\#(\mathcal{N} \cap \mathcal{L}) = k) \ \text{ with } \ \#(\mathcal{N} \cap \mathcal{L}) := \big|\, \{\, j \,|\, \mathcal{N} \cap K_j \neq \emptyset \,\} \,\big| \,, \qquad (4)$$

where $|\cdot|$ is the cardinality of the (here discrete) set of indices of elementes. Thus, $\#$ counts the number of elements of the lattice $\mathcal{L}$ which are hit by the segment $\mathcal{N}$.

To tackle these question we construct the following family of sets of segments $\mathcal{N}$:

- $D_i := \{\mathcal{N} \,|\, \mathcal{N} \cap K_i \neq \emptyset\}$, i.e. all segments $\mathcal{N}$ intersecting (at least) the i-th element of the lattice: $K_i \in \mathcal{L}$, $i = 1, ..., n+1$,
- $U_k^i := \{\mathcal{N} \,|\, \mathcal{N} \cap K_i \neq \emptyset \wedge \mathcal{N} \cap K_{i+k-1} \neq \emptyset\}$, $k = 1, ..., n+1$, $i = 1, ..., n-k+2$, i.e. all segments $\mathcal{N}$ which hit (at least) the k fixed elements K_i, K_{i+1}, ..., K_{i+k-1} of $\mathcal{L}$, so we have $U_k^i = D_i \cap D_{i+k-1}$,
- M_k, $k = 1, ..., n+1$, containing all segments $\mathcal{N}$ which intersect at least k elements of $\mathcal{L}$, so there is $M_k := \{\mathcal{N} \,|\, \#(\mathcal{N} \cap \mathcal{L}) \geq k\} = \bigcup_{i=1}^{n-k+2} U_k^i$,
- finally the set S_k, $k = 1, ..., n+1$, contains all segments $\mathcal{N}$ intersecting *exactly* k elements of $\mathcal{L}$: $S_k := \{\mathcal{N} \,|\, \#(\mathcal{N} \cap \mathcal{L}) = k\}$.

Obviously there is the following chain of subsets

$$M_{n+1} \subset M_n \subset ... \subset M_k \subset ... \subset M_1 \tag{5}$$

as well as the differences

$$S_k = M_k \backslash M_{k+1} \text{ of sets for } 1 \leq k \leq n, \text{ and } S_{n+1} = M_{n+1}. \tag{6}$$

To shorten notation we continue to write for

$$\mu(U_k^i) = \mu(D_i \cap D_{i+k-1}) =: u_{i,i+k-1} \tag{7}$$

and in particular

$$\mu(U_1^i) = \mu(D_i) =: u_i \tag{8}$$

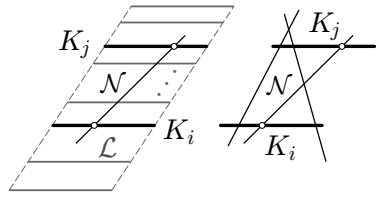


Fig. 2: $u_{i,i+k-1} = \mu(U_k^i)$

due to the fact that this measures have a just as clear as easy meaning: $u_{i,j}$ denotes exactly the measure of all segments $\mathcal{N}$ cutting the elements K_i and K_j of $\mathcal{L}$! And in general this geometrical configuration is as well seizable as calculable *separated* from the lattice—so this measures are worthy to get a special symbol and deserve our attention, see fig. 2. Since the lattice $\mathcal{L}$ is sequential, we have

$$U_k^i = D_i \cap D_{i+k-1} = D_i \cap D_{i+1} \cap ... \cap D_{i+k-2} \cap D_{i+k-1}\,, \tag{9}$$

and the measure of such a set can be treated by the following auxiliary theorem:

Lemma 1.2. *Given a family $\mathcal{A} = \{A_i\}_{i \in \mathbb{N}_m}$, $m \geq 1$, of measureable sets A_i with the property*

$$i < j \,:\, A_i \cap A_j = A_i \cap A_{i+1} \cap ... \cap A_{j-1} \cap A_j\,. \tag{10}$$

Then the measure for the union $\cup\mathcal{A} := \bigcup_{i=1}^m A_i$ is

$$\mu(\cup\mathcal{A}) = \sum_{i=1}^{m} \mu(A_i) - \sum_{i=1}^{m-1} \mu(A_i \cap A_{i+1})\,. \tag{11}$$

Note: In the equivalent expression

$$\mu(\cup\mathcal{A}) \;=\; \sum_{i=1}^{m-1} \;\mu(A_i) - \mu(A_i \cap A_{i+1}) \;\; + \mu(A_m) \;=\; \sum_{i=1}^{m-1} \;\mu(A_i \backslash A_{i+1}) \;\; + \mu(A_m)$$

of equation (11) it becomes clear that the part of the difference $A_i \backslash \cup_{k>i} A_k$ has to be added successively to receive the final measure. Figure 3 shows an example of such a family of sets in form of a Venn diagram.

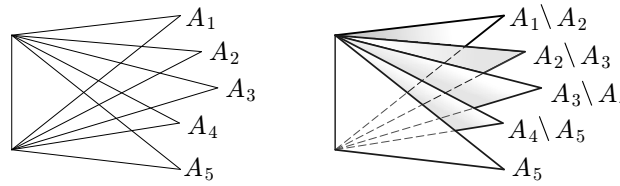


Fig. 3: Example of an actual family $\mathcal{A}$ with $m \;=\; 5$

Proof. Induction: The beginning for one set $m = 1$ is easy to see. Now the reason of induction comes from the **(PIE)**: i.e. due to (3) we have

$$\mu(\cup\mathcal{A} \cup A_{m+1}) \;=\; \mu(\cup\mathcal{A}) \;+\; \mu(A_{m+1}) \;-\; \mu(\cup\mathcal{A} \cap A_{m+1})\,. \qquad (*)$$

And within this formula there is

$$\cup\mathcal{A} \cap A_{m+1} \;=\; \bigcup_{i=1}^{m} (A_i \cap A_{m+1}) \;=\; A_m \cap A_{m+1}\,;$$

this is according to the following argumentation:

$$\begin{array}{ll} \text{let} & x \in A_i \cap A_{m+1} \;\text{ for } i \text{ with } \; 1 \le i \le m \\ \Rightarrow & x \in A_i \cap A_{i+1} \cap \ldots \cap A_m \cap A_{m+1} \;\; \text{(due to the property of } \mathcal{A}) \\ \Rightarrow & x \in A_m \cap A_{m+1}\,, \end{array}$$

so that $\cup\mathcal{A} \cap A_{m+1} \subset A_m \cap A_{m+1}$; the other direction of the relation of subsets is obvious, so the assertion $\cup\mathcal{A} \cap A_{m+1} = A_m \cap A_{m+1}$ holds. Now together with equation (*) we have the final conclusion

$$\begin{aligned} \mu(\cup\mathcal{A} \cup A_{m+1}) &= \mu(\cup\mathcal{A}) \;+\; \mu(A_{m+1}) \;-\; \mu(A_m \cap A_{m+1}) \\ &= \sum_{i=1}^{m} \mu(A_i) + \mu(A_{m+1}) \;-\; \sum_{i=1}^{m-1} \mu(A_i \cap A_{i+1}) - \mu(A_m \cap A_{m+1}) \\ &= \sum_{i=1}^{m+1} \mu(A_i) \;-\; \sum_{i=1}^{(m+1)-1} \;\mu(A_i \cap A_{i+1})\,. \end{aligned}$$

□

The mensionable fact of this lemma is, that the measure of the unification $\cup\mathcal{A} = \cup(A_i)_{i\in\mathbb{N}_m}$ can simply be seized by a sum of measures of the sets A_i itself and a sum of measures of set intersections $A_i \cap A_{i+1}$ of at most two neighbouring sets!

So due to the property (9) of the family $\{U_k^i\}_{i\in\mathbb{N}_{n+1}}$ and lemma 1.2 with $m = n+1$ for the unification $M_k = \cup_i U_k^i$ we have the measure

$$\begin{aligned}\mu(M_k) &= \sum_{i=1}^{n-k+2} \mu(U_k^i) - \sum_{i=1}^{n-k+1} \mu(U_k^i \cap U_k^{i+1}) \\ &= \sum_{i=1}^{n-k+2} \mu(D_i \cap D_{i+k-1}) - \sum_{i=1}^{n-k+1} \mu(D_i \cap D_{i+k}) \\ &= \sum_{i=1}^{n-k+2} u_{i,i+k-1} - \sum_{i=1}^{n-k+1} u_{i,i+k} = \Omega_{k-1} - \Omega_k \end{aligned} \tag{12}$$

with the meaningful abbreviation

$$\Omega_\nu := \sum_{i=1}^{n-\nu+1} u_{i,\,i+\nu}\,, \tag{13}$$

which is just the sum of all basic measures of test bodies intersecting the separated elements K_i and $K_{i+\nu}$ of the lattice! Hence we get easily the further measures

$$\mu(S_k) = \mu(M_k) - \mu(M_{k+1}) = \Omega_{k-1} - 2\,\Omega_k + \Omega_{k+1}\,,\ k = 1, ..., n, \tag{14}$$

$$\mu(S_{n+1}) = \mu(M_{n+1}) = u_{1,n+1} = \Omega_n\,. \tag{15}$$

Under the definition of $\Omega_\nu := 0$ for $\nu > n$ it is possible to write for all $1 \le k \le n+1$ this relations in the way $\mu(S_k) = \Omega_{k-1} - 2\,\Omega_k + \Omega_{k+1}$.

Corollary 1.3. *Consider a sequential lattice $\mathcal{L}$ with n cells and the convex hull $\mathcal{C}$. A randomly placed line segment $\mathcal{N}$ on the convex hull $\mathcal{C}$ intersects exactly k elements of the lattice $\mathcal{L}$ with the geometrical probability*

$$p_k = \frac{\Omega_{k+1} - 2\,\Omega_k + \Omega_{k-1}}{\mu(C)}\,, \tag{16}$$

where $\mu(C)$ is the measure of the set $C := \{\,\mathcal{N}\,|\,\mathcal{N}\cap\mathcal{C} \neq \emptyset\,\}$ of all segments in the plane which have at least one point in common with the convex hull $\mathcal{C}$, and Ω_k is the sum of "basic measures of distance k" according to expression (13).

Proof. The asserted geometrical probability is due to Stoka's formula the ratio $p_k = \frac{\mu(S_k)}{\mu(C)}$ of the measures of the set C of all considered events and the set S_k with the measure according to (14) and (15) respectively. □

Note: The function $p(k) = p_k$ can be considered as the density of the random variable

$$X\,:\,C \longrightarrow \mathbb{N}_{n+1}\,,\ \mathcal{N} \longmapsto \#\{\,\mathcal{N}\cap\mathcal{L}\,\}\,. \tag{17}$$

1.2 Mean Values

The question for the expected value of the random variable X in (17) answers the following theorem:

Theorem 1.4. *The mean number of intersections between a randomly placed segment $\mathcal{N}$ on the convex hull $\mathcal{C}$ of a sequential lattice $\mathcal{L}$ with n cells with the elements of this lattice itself is*

$$E(X) \;=\; \Omega_0/\mu(\mathcal{C}\cap\mathcal{N}\neq\emptyset)\,,$$

where Ω_0 denotes according to (13) and (8) the sum of the measures, which $\mathcal{N}$ is cutting the singular elements of $\mathcal{L}$.

Proof. The expected value is $E(X)=\sum_{k=1}^{n+1} k p_k$ with $p_k=\frac{\mu(S_k)}{\mu(C)}$ and the set C as introduced above, thus we have to show that $\sum_{k=1}^{n+1} k\mu(S_k)=\sum_{i=1}^{n+1} u_i=\Omega_0$ holds. A proof by induction is a cumbersome work, because arising the number of cells by one, all the measures of the previous lattice are changed. So due to the telescopic character of the sum over the products $k\cdot\mu(S_k)$ we look directly at the inner structure of the sum for $E(X)$. Here with (14) and (15) we have:

$$\begin{array}{rcl}
\sum_{k=1}^{n+1} k\cdot\mu(S_k) \;=\; & 1\cdot\Omega_0 & \overbrace{-\,1\cdot 2\,\Omega_1 \;+\; 1\cdot\Omega_2}^{=0} \\
+\; 2\cdot\Omega_1 & -\,2\cdot 2\,\Omega_2 \;+\; 2\cdot\Omega_3 & \\
+\; 3\cdot\Omega_2 & -\,3\cdot 2\,\Omega_3 \;+\; 3\cdot\Omega_4 & +\;\ldots \\
+\;\ldots & -\,\ldots \;+\; (k-1)\cdot\Omega_k & \\
+\;\ldots & -\,k\cdot 2\,\Omega_k \;+\;\ldots & \\
+\;(k+1)\cdot\Omega_k & -\,\ldots \;+\;\ldots & +\;\ldots \\
+\;\ldots & -\,\ldots \;+\; (n-1)\cdot\Omega_n & \\
+\;\ldots & -\,n\cdot 2\,\Omega_n \;+\;\ldots & \\
+\;(n+1)\cdot\Omega_n\,. &&
\end{array}$$

□

For lattices consisting of straight line segments as elements with the lengths L_i, $i=1,\ldots,n+1$, we can conclude this proposition:

Corollary 1.5. *If a line segment $\mathcal{N}$ of length l is randomly placed on the convex hull $\mathcal{C}$ of a sequential lattice $\mathcal{L}$ with n cells then the mean number of intersections between $\mathcal{N}$ and $\mathcal{L}$ will be*

$$E(X) \;=\; 2\,l\,L/\mu(\mathcal{C}\cap\mathcal{N}\neq\emptyset)\,,$$

where $L=\sum_{i=1}^{n+1} L_i$ is the total length of all elements of the lattice $\mathcal{L}$.

Note I: Especially this is a new and shorter proof of theorem 6.7.1, p. 167, in [1]; now without the necessity to take any case distinctions into account within the formula of the geometrical probabilities p_k!

Note II: As a summary, all this relations of mean values are reflections of the formula of Poincaré $\int_{\Gamma_0 \cap \mathcal{N}} k \, dN = 2\, l\, L$. Here $\Gamma_0 \subset \mathcal{C}$ is a curve lying inside a convex domain $\mathcal{C}$—this represents our lattice $\mathcal{L}$ of total length L. Now the integral over the number k of cuts and the kinematic density dN of non-oriented segments $\mathcal{N}$ of length l represents the numerator in our quotient of the mean value of cuts, see [9], chapter 7. Together with the basic result $\mu(\mathcal{C} \cap \mathcal{N} \neq \emptyset) = \pi F + l\, U$, see [9], chapter 6, section 4, where F denotes the area and U the perimeter of the convex set $\mathcal{C}$, we have simply $E(X) = \frac{2\, l L}{\pi F + l\, U}$ for the mean number of intersections.

2 Applications

The benefit of the theorem 1.3 depends mainly on the number of basic measures which are available. A "basic measures" means a formula for the $u_{i,i+\nu}$ in (7) expressing the measure of the set of all segments hitting both elements K_i and $K_{i+\nu}$ separated of the lattice in the plane at all. In the papers [2] and [3] there are applications for a crown and a bundle of half-lines according to fig. 4.

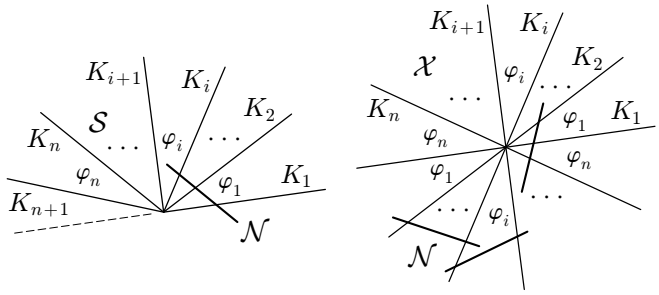


Fig. 4: crown $\mathcal{S}$ and bundle $\mathcal{X}$ of segments K_i with randomly placed needles $\mathcal{N}$

Here the "basic measure" gathers all segments $\mathcal{N}$ of length l hitting two half-lines K_i and K_j with $\varphi_{i,j} = \measuredangle(K_i, K_j)$ inside the lattice. And this is according to [9], chapter 6, section 4, expressable by the formula

$$\mu\big(\{\mathcal{N} \,|\, \mathcal{N} \cap K_i \neq \emptyset \,\wedge\, \mathcal{N} \cap K_j \neq \emptyset\}\big) \;=\; \tfrac{l^2}{4} \cdot \big[\, 1 \,+\, (\pi - \varphi_{i,j}) \,\cot \varphi_{i,j} \,\big] \,. \qquad \text{(S)}$$

So, guided by the lemma 1.2 and the result of (12) for the measure of M_k and S_k we get sums of (S) in form of

$$\mu(S_k) \;=\; \sum_{\nu=0}^{2} (-1)^\nu \binom{2}{\nu} \sum_{i=1}^{n-k+\nu} w_{\varphi_{i,k-\nu+i}} \,,\; k = 2, ..., n+1, \;\text{ and}$$

$$\mu(S_k^*) \;=\; 2 \sum_{\nu=0}^{2} (-1)^\nu \binom{2}{\nu} \sum_{i=1}^{n} w_{\varphi_{i,k-\nu+i}} \,,\; k = 2, ..., n,$$

for the measure of sets S_k and S_k^* of all line segments intersecting exactly k elements of the crown and bundle of half-lines respectively; for the complete examination see [2]. Even in the case that a lattice as a whole is not of sequential type it is

sometimes possible to separate the lattice into small sequential parts which works very well for sufficient small test elements. In [3] we study a *finite* triangular lattice and small, randomly placed needles on it, where the formulas for the geometrical probabilities p_k of exactly one, two, and three cuts between the lattice and the line segments are derived with the method of locally introduced sequential lattices.

3 Outlook

A closer look to the theorem 1.3 and its proof and to the above mentioned applications shows that there is nothing particular for the elements of a sequential lattices to be curved or for the test elements to be line segments respectively. So we can also consider convex sets for the elements of the lattices or the test bodies as well—even in this case the structure of the expression (16) for the p_k describing the geometrical probability that such a test body hits exactly k elements of the lattice still holds.

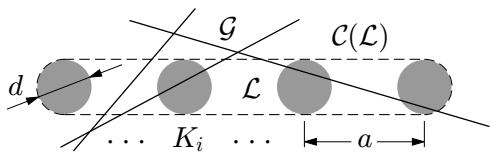


Fig. 5: Lattice $\mathcal{L}$ of circles with n cells and randomly placed lines $\mathcal{G}$ intersecting $\mathcal{C}(\mathcal{L})$

As an example we consider the lattice $\mathcal{L}$ of circles in fig. 5 and randomly drawn lines in the plane. Here the elements of the lattice are the convex sets K_i, $i = 1, ..., n+1$, of the circles. For such a geometrical configuration we will proof the following result:

Theorem 3.1. *Let $\mathcal{L}$ be the lattice of $n+1$ circles of diameter d and each a units apart. Then a randomly placed line $\mathcal{G}$ in the plane crossing the convex hull $\mathcal{C}(\mathcal{L})$ of the lattice will intersect exactly k circles with the geometrical probability*

$$p_k \;=\; \frac{\big(1-\frac{(k+1)-1}{n}\big)\,\psi_{k+1} - 2\cdot\big(1-\frac{(k)-1}{n}\big)\,\psi_k + \big(1-\frac{(k-1)-1}{n}\big)\,\psi_{k-1}}{\frac{1}{n}\cdot\frac{\pi}{2}+\alpha} \qquad (18)$$

for $1 \le k \le n+1$ with

$$\psi_k \;:=\; \begin{cases} \pi/2 & \text{for } k=0,\\ \operatorname{arccot}\sqrt{\alpha_k^2-1} + \sqrt{\alpha_k^2-1} - \alpha_k & \text{for } 1\le k\le n,\\ 0 & \text{for } k>n, \end{cases}$$

and the parameter and its multiple $\alpha := \frac{a}{d} > 1$ and $\alpha_k = k\cdot\alpha$ respectively.

Proof. As already mentioned above there is no special argument in the proof of equation (16) concerning curves that exclude convex sets for elements of the lattices as well. Thus according to corollar 1.3 we have

$$p_k \;=\; \big(\Omega_{k+1} - 2\,\Omega_k + \Omega_{k-1}\big)/\mu(C)\,, \qquad (*)$$

where $C = \{\mathcal{G} \mid \mathcal{C}(\mathcal{L}) \cap \mathcal{G} \neq \emptyset\}$ is the set of all lines in the plane intersecting the convex hull of the lattice $\mathcal{L}$ and due to equation (13) we have

$$\Omega_k \;=\; \sum_{i=1}^{n-k+1} u_{i,\,i+k} \;=\; (n-k+1)\cdot \Psi_k \tag{19}$$

for the sum of the basic measures Ψ_k. Now, here these basic measures $u_{i,\,i+k}$ capture all lines $\mathcal{G}$ which meets the circles K_i *and* K_{i+k}, separated of the lattice. Since this depends only on the distance $k\,a$ of the circles, the basic measures becomes independent of the place within the lattice and we have

$$\Psi_k := u_{i,\,i+k} = L_{\mathrm{i}} - L_{\mathrm{e}}\,,\; k \geq 1\,,$$

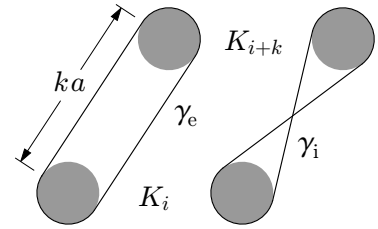


Fig. 6: external and internal cover

see fig. 6. According to [9], chapter 3, section 3, L_{i} and L_{e} denote the lengths of the internal and external cover γ_{i} and γ_{e} of the circles K_i and K_{i+k} respectively. An elementary calculation yields immediately the following difference of lengths

$$\begin{aligned}\Psi_k \;&=\; L_{\mathrm{i}} - L_{\mathrm{e}} \;=\; d\cdot\big(2\pi - 2\arccos\tfrac{d}{k\,a}\big) + 2\sqrt{(k\,a)^2 - d^2} - \big(2\,k\,a + \pi\,d\big)\\ &=\; 2\,d\cdot\big[\operatorname{arccot}\sqrt{(\tfrac{k\,a}{d})^2 - 1} \;+\; \sqrt{(\tfrac{k\,a}{d})^2 - 1} \;-\; \tfrac{k\,a}{d}\big]\,.\end{aligned} \tag{20}$$

For $k = 0$ we have simply to consider the case $\mathcal{G} \cap K_i \neq \emptyset$. Once more according to [9], chapter 3, section 2, the measure for lines that intersect a convex set is equal to the length of its boundary, so we get $\Psi_0 = \mu(\mathcal{G} \cap K_i \neq \emptyset) = 2d \cdot \frac{\pi}{2}$. In the same sense we gain due to the perimeter $\pi d + 2na$ of the convex hull $\mathcal{C}(\mathcal{L})$:

$$\mu(C) \;=\; L\big(\mathcal{C}(\mathcal{L})\big) \;=\; 2\,d\cdot\big[\,\tfrac{\pi}{2} + n\,\tfrac{a}{d}\big]\,. \tag{21}$$

All that remains is to put the terms (20) into (19) and furthermore the expressions (19) for the "distances" $k+1$, k, and $k-1$ as numerator and (21) as denominator, respectively, into the ratio for p_k in (*). □

Note I: To complete the geometrical probabilities in theorem 3.1 for no cuts at all between the randomly drawn line and the circles in the lattice we have

$$p_0 \;=\; \big(\tfrac{1}{n}\cdot\tfrac{\pi}{2} + \alpha\big)^{-1}\cdot\Big(\operatorname{arccot}\sqrt{\alpha^2 - 1} + \sqrt{\alpha^2 - 1} - \tfrac{\pi}{2}\Big)$$

as a consequence of $p_0 = 1 - \sum_{k=1}^{n+1} p_k$ or due to $\mu(S_0) = n\cdot(L_{\mathrm{i}} - 2\pi d)$ for the measure of all lines passing a cell of the lattice without hitting a circle. (Here L_{i} is the length of the internal cover for two circles, i.e. for the distance $k = 1$.)

Note II: The mean number of intersections between a randomly placed line $\mathcal{G}$ and the lattice of circles is according to theorem 1.4 the fraction $\Omega_0/\mu(\mathcal{C} \cap \mathcal{G} \neq \emptyset) = (n+1)\cdot\Psi_0/\mu(\mathcal{C} \cap \mathcal{G} \neq \emptyset) = (1 + \frac{1}{n})\cdot\frac{\pi}{2}/(\frac{1}{n}\cdot\frac{\pi}{2} + \alpha)$.

Conclusion: The short examinations of this paper shows how important the so called basic measures are in order to compute geometrical probabilities of multiple intersections within sequential lattices using the formula (16). Beside this, for non-small needles the combination of the sums Ω_ν with $\nu = k+1$, k, and $k-1$ makes it necessary to investigate case distinctions! In the large examination of non-small needles hitting rectangular lattices in [1], e.g., the basic measures concern line segments intersecting parallel segments in the plane—there the case distinctions originate from the combination of measures of sets of such segments "connecting" parallel elements of the lattice which are $(k+1)a$, ka, and $(k-1)a$ units apart!

Bibliography

[1] **Böttcher, R.**, Geometrische Wahrscheinlichkeiten vom Buffonschen Typ in begrenzten Gittern, FernUniversität in Hagen, 2005, German version in world wide web: http://deposit.fernuni-hagen.de/volltexte/2006/39/

[2] **Böttcher, R.**, Geometrische Wahrscheinlichkeiten nach dem Prinzip der Inklusion-Exklusion I, Seminarberichte Mathematik, FernUniversität in Hagen, S.101-126, Band 81, 2008

[3] **Böttcher, R.**, Geometrische Wahrscheinlichkeiten nach dem Prinzip der Inklusion-Exklusion II, Seminarberichte Mathematik, FernUniversität in Hagen, Band 82, 2009, to appear

[4] **Duma, A.**, **Stoka, M. I.**, Schnitte eines 'kleinen' gleichseitigen Dreiecks mit den Gittern von Buffon und Laplace, Seminarberichte Mathematik, FernUniversität in Hagen, S.13-22, Band 79, 2008

[5] **Duma, A.**, **Stoka, M. I.**, Problems of Buffon Type with multiple intersections for lattices of parallelograms, Rendiconti del Circolo Mat. di Palermo, Serie II, Tomo LV, pp. 241-248, 2006

[6] **Duma, A.**, Problems of Buffon type for 'non-small' Needles, Supp. Rendiconti del Circolo Mat. di Palermo, Serie II, Tomo XLVIII, pp. 23-40, 1999

[7] **Duma, A.**, Problems of Buffon type for 'non-small' Needles (II), Rev. Roumaine Math. Pures Appl., Tom XLIII, 1-2, pp. 121-135, 1998

[8] **Matoušek, J.**, **Nešetřil, J.**, Invitation to Discrete Mathematics, Oxford University Press, Oxford, 1998

[9] **Santaló, L. A.**, Integral Geometry and Geometric Probability, Addison-Wesley, London, 1976

[10] **Stanley, R. P.**, Enumerative Combinatorics, Cambridge University Press, Cambridge, 1997

[11] **Stoka, M. I.**, Problems of Buffon Type for Convex Test Bodies, Conf. Semin. Mat. Univ. Bari, No. 268, 1-17, 1998

Roger Böttcher
FB Mathematik u. Informatik der Fernuniversität in Hagen
D-58084 Hagen
Roger.Boettcher@FernUni-Hagen.de

RENDICONTI DEL CIRCOLO MATEMATICO DI PALERMO
Serie II, Suppl. 81 (2009), pp. 69-72

Random Lattice in the Euclidean Space E_3

Giuseppe Caristi
Departement SEA - University of Messina

Abstract

In this note we compute the probability $p_{S,R}$ that a random segment S whose length l is a bounded random variable Δ, and moments $E(\Delta)$, $E(\Delta^2)$, $E(\Delta^3)$, intersects a lattice R obtained by partitioning E_3 with a family of elementary tiles of a right prism, of height c, whose base is a right angled triangle of catheti a and $b = a\tan\alpha$ $(0 < \alpha < \pi/2)$.

AMS Classification: 60D05, 52A22.
Key words: Geometric Probability, Random Sets, Random Convex Sets and Integral Geometry.

1 Introduction

In 1733, at meeting of the Académie desc Sciencs de Paris, Buffon posed a problem that later on should become known as the famous "Buffon needle problem": in a room, the fbor of which is merely divided by parallel lines, at a distance a apart, a needle of lenght $l < a$ is allowed to fall at random: which is the probability that the needle intersects one of the lines?

The solution, determined by Buffon by means of empirical methods, was $p = 2l/\pi a$. The problem and its solution were published in 1777, in the "Comptes rendus del l'Académie des sciences de Paris".

In 1812, Laplace extended the problem by considering a room paved with equal tiles, shaped as rectangles of sides a and b, with $l < \min(a, b)$. The solution was $p = \frac{2l(a+b)-l^2}{\pi ab}$, and it is obvious that the probability of Buffon can be obtained from that of Laplace by letting $b \to +\infty$.

We restate now these problems in a slightly different from, which will be useful for several defferent extensions. In the classical problem of Buffon type, we have always referred to a test body T, uniformly distributed in the Euclidean space.

Obviously all the results are essentially tied to our particular definition of random positioning of a body in the space and to the choice of the elementary Kinematic measure wich provides invariance of probability statement under a special group of trasformations. Other definitions are possible and these lead to different results.

For Example we might need anisotropically distributed test bodies (see e.g. [1], [3]), or we can find invariance under rotation and traslation too demanding, and we can relax this condition (see [2]). In this order of idea in this note we compute the probability $p_{S,R}$ that a random segment S whose lenght l is a bounded random variable Δ, and known moment $E(\Delta)$, $E(\Delta^2)$, $E(\Delta^3)$, intersects a lattice R obtained by partitioning E_3 with a family of elementary tiles consists of a right prism, of height c, whose base is a right angled triangle of catheti a and $b = a\tan\alpha$ $(0 < \alpha < \pi/2)$.

2 The Lattice R

Let us denote by E_3 the Euclidean space. By a lattice R in E_3 we understand a sequence of closed and connected sets $\{C_n\}_{n\in N}$ such that

1. $\cup_{n\in N}\ C_n = E_3$,
2. $Int(C_i) \cap Int(C_j) = \emptyset,\ \ \forall i, j \in N$ and $i \neq j$,
3. $C_n = \gamma_n(C_0)$, $\forall n \notin N$, where γ_n are the elements of a discrete subgroup of the group of motions in E_3 that leaves in variant the lattice.

The domain C_0 is usually called the fundamental tile (or cell) of R. Let K be a convex body (which means here a compact convex set) which we shall call test body. A general problem of Buffon type can be stated as follows:

"Which is the probability $p_{K,R}$ that the random convex body K, or more precisely, the random congruent copy of K, meets some of the boundary points of at least one of the domains C_n?"

In the following part of the paper we shall deal with a lattice R obtaining E_3 where each elementary tile consists of a right prism, of height c, was base is a right angled triangle of catheti a and $b = a\tan\alpha$ $(0 < \alpha < \pi/2)$.

Let

$$C_0(R) := \{(x, y, z) \in E_3 : 0 \leq x \leq a, 0 \leq y \leq (a - x)\tan\alpha, 0 \leq z \leq c\},$$

then R is obteined as

$$R := R^1 \cup R^2 \cup R^3 \cup R^4,$$

where the elementary lattice R^i are defined as follows

$$R^1 := \{x = na, n \in Z\},$$

$$R^2 := \{y = nb, n \in Z\},$$

$$R^3 := \{x - z\cot\xi - na\sin\alpha = 0, n \in Z\},$$

$$R^4 := \{y = (a-x)n\tan\alpha, n \in Z\}.$$

3 Main Result

With notation of before we obtaion the following result

Theorem 1 *The probability $p_{S,R}$ that a random segment S whose lenght l is a bounded random variable Δ, with upper boundary $l < \min(b\cos\alpha, c)$, and known moments $E(\Delta)$, $E(\Delta^2)$, $E(\Delta^3)$, intersects the lattice R is the following:*

$$p_{S,R} = \frac{ab + (1+\cos\alpha)ac + (1+\sin\alpha)bc}{2abc}E(\Delta) - \frac{1}{3\pi abc}\Lambda_1 E(\Delta^2) + \Lambda_2 E(\Delta^3),$$

where we put

$$\Lambda_1 := 2(1+\cos\alpha)a + 2(1+\sin\alpha)b + \left[3 + (\pi-\alpha)\cot\alpha + \left(\frac{\pi}{2}+\alpha\right)\tan\alpha\right]c,$$

and,

$$\Lambda_2 := \frac{3 + (\pi-\alpha)\cot\alpha + (\pi/2+\alpha)}{8\pi abc}$$

Proof. The upper boundary of Δ assures that S is always small when compared to the elementary tile of R. Let $f(\delta)$ be the density of Δ and $p(R/\delta)$ the probability that S intersects a cell of R given the condition $\Delta = \delta$. Then the probability $p_{S,R}$ that S intersects at least one of the planes of the lattice can be computed as ■

$$p_{S,R} = \int_0^D p(R\,|\delta)\, f\,(\delta)\, d\delta.$$

Hence, a long computation ensures that

$$p_{S,R} = \frac{ab + (1+\cos\alpha)ac + (1+\sin\alpha)bc}{2abc}\int_0^D \delta f\,(\delta)\, d\delta - \frac{1}{3\pi abc}\Lambda_1\int_0^D \delta^2 f\,(\delta)\, d\delta + \Lambda_2\int_0^D \delta^3 f\,(\delta)\, d\delta.$$

which is the stated formula

References

[1] A. Duma, A. Rizzo: The Buffon needle problem in a magnetic field, suppl. Rend. Circ. Mat. Palermo, serie II, 35, 1994, pp. 127-142.

[2] H. Solomon: Geometric probability, soc. for Ind and Appl.Math, 1978.

[3] M. I. Stoka: Il problema dellàgo di Buffon nella teoria delle probabilità geometriche, Conf. Semin. Mat. Univ. Bari, 190, 1983.

RENDICONTI DEL CIRCOLO MATEMATICO DI PALERMO
Serie II, Suppl. 81 (2009), pp. 73-83

ON $D(-4)$ AND $D(8)$ TRIPLES FROM PELL AND PELL-LUCAS NUMBERS

ZVONKO ČERIN AND GIAN MARIO GIANELLA

Abstract. In this paper four examples of infinite double sequences of triples of natural numbers with the property that the product of any two of them increased by a fixed integer n is a square of a number are given. Two double sequences are built such that each of its triples starts with an odd indexed Pell number for $n = -4$ while the other two double sequences are built such that each of its triples starts with an odd indexed Pell-Lucas number for $n = 8$. We show many interesting properties of these double sequences and various methods how to get complete squares from them. Some geometric invariants for the associated tetrahedra are also computed. Many 3×3 matrices with rows from these double sequences of triples have nice determinants.

1. Introduction

For an integer $n \in \mathbb{Z}$ and a natural number $m \in \mathbb{N}$, we say that $a \in \mathbb{N}^m$ is a $D(n)$-m-tuple provided $a_i\, a_j + n$ is a square for each pair of different indices i and j.

The first $D(1)$-quadruple (1, 3, 8, 120) was discovered by Fermat. Later, Davenport and Baker [6] proved that it can not be extended to a $D(1)$-quintuple while Hoggatt and Bergum [7] noticed the existence of a whole sequence $(F_{2k},\, F_{2k+2},\, F_{2n+4},\, 4\, F_{2n+1}\, F_{2n+2}\, F_{2n+3})$ of $D(1)$-quadruples built from Fibonacci numbers with the Fermat quadruple as the initial term.

On the other hand, Brown [1] showed the nonexistence of the $D(n)$-quadruples when an integer n is of the form $4\,k + 2$. The folklore conjecture is that the same holds when $n \in \Gamma$, where Γ is the set

$$\{-4,\, -3,\, -1,\, 3,\, 5,\, 8,\, 12,\, 20\}.$$

The recent research in this part of number theory thus can go into the search of new examples of $D(n)$-m-tuples for various values of m and n or the proof of their nonexistence. Of course, the above exceptional values for the number n are very interesting in an attempt to settle the conjecture.

1991 *Mathematics Subject Classification.* Primary 11B37, 11B39, 11D09.

Key words and phrases. property $D(n)$, Pell numbers, Pell-Lucas numbers, square, determinant, tetrahedron, volume, vector cross-product.

Another task is to explore properties of special $D(n)$-m-tuples like the above Hoggatt-Bergum $D(1)$-quadruples from Fibonacci numbers.

In [2] the authors considered the numbers $n = -4$ and $n = 8$ from the set Γ and constructed two infinite sequences of $D(-4)$-triples and two infinite sequences of $D(8)$-triples from Pell and Pell-Lucas numbers and explored several of their properties.

In this paper we shall extend and improve these results by constructing pairs of double sequences $\alpha = \{\alpha(k, n)\}$ and $\beta = \{\beta(k, n)\}$ of $D(-4)$-triples and $\gamma = \{\gamma(k, n)\}$ and $\delta = \{\delta(k, n)\}$ of $D(8)$-triples, where $k \in \mathbb{N}^* = \{0\} \cup \mathbb{N}$ and $n \in \mathbb{Z}$. For $n = 0$, we get the above sequences in [2].

The double sequences α, β, γ and δ are built from the Pell and Pell-Lucas numbers such that the triples $\alpha(k, n)$ and $\beta(k, n)$ start with the odd indexed Pell number P_{2k+1} while the triples $\gamma(k, n)$ and $\delta(k, n)$ start with the odd indexed Pell-Lucas number Q_{2k+1}. The Pell and Pell-Lucas sequences of natural numbers P_n and Q_n are defined by the recurrence relations

$$P_0 = 0, \qquad P_1 = 2, \qquad P_n = 2\,P_{n-1} + P_{n-2} \ \text{ for } n \geqslant 2,$$

and

$$Q_0 = 2, \qquad Q_1 = 2, \qquad Q_n = 2\,Q_{n-1} + Q_{n-2} \ \text{ for } n \geqslant 2.$$

The numbers Q_k make the integer sequence $A002203$ from [8] while the numbers $\frac{1}{2}P_k$ make $A000129$. The authors studied some sums of these numbers in the recent articles [3], [4] and [5].

The aim of this article is to explore some properties of the double sequences α, β, γ and δ. Since the triples of natural numbers can be used as rows of 3×3 matrices or as coordinates of points in the 3-dimensional Euclidean space we examine what happens when these are from our double sequences. In some cases it is possible to compute closed forms of their determinants, volumes, vector cross-products and to find other interesting relationships.

2. The double sequences α and β

Let $\pi_u = P_{2k+u}$ and $\varrho_u = Q_{2k+u}$ for a (fixed) $k \in \mathbb{N}^*$ and a $u \in \mathbb{N}^*$. Let $\alpha, \beta : \mathbb{N}^* \times \mathbb{Z} \to \mathbb{N}^3$ be the functions defined by

$$A = \alpha(k, n) = (\pi_1,\ \pi_1\,n^2 + 2\,\varrho_1\,n + 2\,\pi_1,\ \pi_1\,n^2 + 2\,\pi_2\,n + \pi_3),$$
$$B = \beta(k, n) = (\pi_1,\ \pi_1\,n^2 + 2\,\pi_2\,n + \pi_3,\ \pi_1\,n^2 + 2\,\varrho_2\,n + 2\,\pi_3).$$

Theorem 1. *The triples A and B are the $D(-4)$-triples.*

Proof. Since $A_1 = B_1$, $A_3 = B_2$, this follows from $A_1\,A_2 - 4 = (\pi_1\,n + \varrho_1)^2$, $A_2\,A_3 - 4 = (\pi_1\,n^2 + (\varrho_2 + \pi_0)\,n + \varrho_2)^2$, $B_2\,B_3 - 4 = (\pi_1\,n^2 + \pi_3\,n + \varrho_3)^2$,

$$A_3\,A_1 - 4 = (\pi_1\,n + \pi_2)^2, \quad \text{and} \quad B_3\,B_1 - 4 = (\pi_1\,n + \varrho_2)^2.$$

□

Let $\widetilde{\alpha}, \widetilde{\beta} : \mathbb{N}^* \times \mathbb{Z} \to \mathbb{N}^3$ be the functions defined by

$$\widetilde{A} = \widetilde{\alpha}(k, n) = (\pi_1 n^2 + (\varrho_2 + \pi_0) n + \varrho_2, \pi_1 n + \pi_2, \pi_1 n + \varrho_1),$$

$$\widetilde{B} = \widetilde{\beta}(k, n) = (\pi_1 n^2 + \pi_3 n + \varrho_3, \pi_1 n + \varrho_2, \pi_1 n + \pi_2).$$

Hence, the coordinates of $\widetilde{X}$ for $X = A, B$ satisfy the following relations:

$$\widetilde{X}_1 = \sqrt{X_2 X_3 - 4}, \quad \widetilde{X}_2 = \sqrt{X_3 X_1 - 4}, \quad \widetilde{X}_3 = \sqrt{X_1 X_2 - 4}.$$

Let $\sigma_1, \sigma_2, \sigma_3 : \mathbb{N}^3 \to \mathbb{N}$ be the basic symmetric functions defined for $x = (a, b, c)$ by $\sigma_1(x) = a + b + c$, $\sigma_2(x) = b c + c a + a b$, $\sigma_3(x) = a b c$.

The linear expressions involving symmetric functions σ_1 and σ_2 of the triples A and B are the source of many complete squares as the following theorem shows.

Theorem 2. *For $k \in \mathbb{N}^*$ and $n, a, b \in \mathbb{Z}$, the following identities hold:*

$$a(b\,\sigma_1(A) + a) + b^2(\sigma_2(A) - 4) = (b\,[\widetilde{A}_1 + \pi_1] + a)^2,$$

$$a(b\,\sigma_1(B) + a) + b^2(\sigma_2(B) - 4) = (b\,[\widetilde{B}_1 + \pi_1] + a)^2.$$

Proof. Let $\varphi = 1 + \sqrt{2}$ and $\psi = 1 - \sqrt{2} = -\frac{1}{\varphi}$. Let $a_\pm = 3 \pm 2\sqrt{2}$, $b_\pm = 23 \pm 16\sqrt{2}$, $c_\pm = 57 \pm 40\sqrt{2}$, $u = K^4 + a_-$, $v = 7\,K^4 - 43 + 30\sqrt{2}$, $w = 51\,b\,K^8 + 2(14 - 9\sqrt{2})\,a\,K^6 - 2\,b_-\,b\,K^4 + 2(78 - 55\sqrt{2})\,a\,K^2 + 3(1041 - 736\sqrt{2})\,b$ and $s = 7\,b\,K^4 + (8 - 5\sqrt{2})\,a\,K^2 + c_-\,b$.

Since $P_j = \frac{\varphi^j - \psi^j}{\sqrt{2}}$ and $Q_j = \varphi^j + \psi^j$, after the substitutions $\psi = -\frac{1}{\varphi}$ and $K = \varphi^k$, the left hand side $a\,b\,\sigma_1(A) + b^2\,\sigma_2(A) - 4\,b^2 + a^2$ becomes

$$\tfrac{a_+\,b^2\,u^2\,n^4}{2\,K^4} + \tfrac{(11+8\sqrt{2})u\,v\,b^2\,n^3}{7\,K^4} + \tfrac{b_+\,w\,b\,n^2}{34\,K^4} + \tfrac{(7+5\sqrt{2})s\,b\,v\,n}{7\,K^4} + \tfrac{c_+\,s^2}{98\,K^4}.$$

However, this is precisely the right hand side $(b\,[\widetilde{A}_1 + \pi_1] + a)^2$. □

In particular, when $b = 1$ and $a = 0$ and $b = 1$ and $a = \pm 2$ we obtain the following statement.

Corollary 1. *For each $(k, n) \in \mathbb{N}^* \times \mathbb{Z}$, the triples A and B satisfy*

$$\sigma_2(A) - 4 = (\widetilde{A}_1 + \pi_1)^2, \qquad \sigma_2(B) - 4 = (\widetilde{B}_1 + \pi_1)^2,$$

$$\sigma_2(A) \pm 2\,\sigma_1(A) = (\widetilde{A}_1 + \pi_1 \pm 2)^2, \qquad \sigma_2(B) \pm 2\,\sigma_1(B) = (\widetilde{B}_1 + \pi_1 \pm 2)^2.$$

For triples a, b and c of numbers, let $[a, b, c]$ denote the 3×3 matrix whose rows are a, b and c. In the next result we determine the value of the determinants of the matrices whose rows are the members of the double sequences α and β and show their invariance with respect to the translation of the second variable.

Theorem 3. *For all a, b, $c \in \mathbb{N}^*$ and all u, v, w, x, $y \in \mathbb{Z}$ it holds:*

$$\begin{aligned}\det([\alpha(a,\, u+x),\, \alpha(b,\, v+x),\, \alpha(c,\, w+x)]) &= \\ \det([\beta(a,\, u+y),\, \beta(b,\, v+y),\, \beta(c,\, w+y)]) &= \\ 4[(P_{2a+1}\, u^2 + 2\, P_{2a+1}\, v\, w + 2\, Q_{2a+1}\, u)\, P_{2(b-c)} + & \\ (P_{2b+1}\, v^2 + 2\, P_{2b+1}\, w\, u + 2\, Q_{2b+1}\, v)\, P_{2(c-a)} & \\ + (P_{2c+1}\, w^2 + 2\, P_{2c+1}\, u\, v + 2\, Q_{2c+1}\, w)\, P_{2(a-b)}] & \\ - 2(v-w)(w-u)(u-v) P_{2a+1}\, P_{2b+1}\, P_{2c+1}. &\end{aligned}$$

Proof. For a $k \in \mathbb{N}^*$, let us write $a_k = P_{2\,a+k}$, $A_k = Q_{2\,a+k}$, etc. Then the first determinant is of the form $P\, x^2 + Q\, x + R$, where R is the cyclic sum

$$\begin{aligned}\sum [2\, u\, b_1\, c_1 (v^2 - w^2)(A_0 + 2\, a_0 - a_2) + u(b_3\, c_1 - b_1\, c_3) & \\ (u\, a_1 + 4\, a_0 + 2\, A_0) + 4\, a_1 (2\, b_0\, c_2 - b_2\, C_0 + B_0\, c_2 - 2\, b_2\, c_0)\, v\, w]. &\end{aligned}$$

Since $P = Q = 0$ and $A_0 + 2\, a_0 - a_2 = -a_1$, $4\, a_0 + 2\, A_0 = 2\, A_1$, $b_3\, c_1 - b_1\, c_3 = 4\, P_{2(b-c)}$ and $2\, b_0\, c_2 - b_2\, C_0 + B_0\, c_2 - 2\, b_2\, c_0 = 4\, P_{2(b-c)}$, we immediately get the above equality. The second determinant has the same value. □

Let us introduce three binary operations $\odot$, $\triangleright$ and $\triangleleft$ on the set $\mathbb{N}^3$ of triples of natural numbers by the rules

$$(a,\, b,\, c) \odot (u,\, v,\, w) = (a\, u,\, b\, v,\, c\, w),$$

$$(a,\, b,\, c) \triangleright (u,\, v,\, w) = (a\, v,\, b\, w,\, c\, u),$$

and

$$(a,\, b,\, c) \triangleleft (u,\, v,\, w) = (a\, w,\, b\, u,\, c\, v).$$

The next result shows that the double sequences α and β are miraculously connected with respect to the products $\odot$, $\triangleright$ and $\triangleleft$. In fact, the theorem holds also for the pairs $(\alpha,\, \alpha)$, $(\beta,\, \beta)$ and $(\beta,\, \alpha)$ with similar factors.

Theorem 4. *For all n, u, $v \in \mathbb{N}^*$, all a, $b \in \mathbb{Z}$ and each $\diamond \in \{\odot, \triangleright, \triangleleft\}$ the determinant of the matrix with the rows the triples $\alpha(n,\, a) \diamond \beta(n,\, b)$, $\alpha(n+u,\, a) \diamond \beta(n+u,\, b)$ and $\alpha(n+u\,v,\, a) \diamond \beta(n+u\,v,\, b)$ is independent of the value n. These determinants are equal to $64\, P_{2u}\, P_{2\,u\,v}\, P_{2\,u(v-1)}$ multiplied by*

$$-2\,[a(a+1)(b^2+3\,b+1) - (b+1)(b+2)],\ a(a-b)(b+2)(a\,b+a+b-1)$$

and $-(a+1)(b+1)(a-b-2)(a\,b+2\,a-2)$.

Proof. This could be proved by the same method that was used in the proof of Theorem 2. □

3. The double sequences γ and δ

The functions γ, $\delta : \mathbb{N}^* \times \mathbb{Z} \to \mathbb{N}^3$ are defined by the rule

$$C = \gamma(k,\, n) = (\varrho_1,\ \varrho_1\, n^2 + 2\,\pi_1\, n + 2\,\varrho_1, \varrho_1\, n^2 + 2\,\varrho_2\, n + \varrho_3),$$

$$D = \delta(k,\, n) = (\varrho_1,\ \varrho_1\, n^2 + 2\,\varrho_2\, n + \varrho_3, \varrho_1\, n^2 + 2\,\pi_2\, n + 2\,\varrho_3).$$

Theorem 5. *The triples C and D are the $D(8)$-triples.*

Proof. Since $C_1 = D_1$, $C_3 = D_2$, this follows from $C_1\, C_2 + 8 = (\varrho_1\, n + \varrho_0)^2$,

$$C_2\, C_3 + 8 = (\varrho_1\, n^2 + (\pi_3 - \pi_0)\, n + 2\,\pi_2)^2,\ C_3\, C_1 + 8 = (\varrho_1\, n + \varrho_2)^2,$$

$$D_2\, D_3 + 8 = (\varrho_1\, n^2 + \varrho_3\, n + 2\,\pi_3)^2, \quad \text{and} \quad D_3\, D_1 + 8 = (\varrho_1\, n + 2\,\pi_2)^2.$$

□

Let $\widetilde{\gamma}$, $\widetilde{\delta} : \mathbb{N}^* \times \mathbb{Z} \to \mathbb{N}^3$ be the functions defined by

$$\widetilde{C} = \widetilde{\gamma}(k,\, n) = (\varrho_1\, n^2 + (\pi_3 - \pi_0)\, n + 2\,\pi_2,\ \varrho_1\, n + \varrho_2,\ \varrho_1\, n + \varrho_0),$$

$$\widetilde{D} = \widetilde{\delta}(k,\, n) = (\varrho_1\, n^2 + \varrho_3\, n + 2\,\pi_3,\ \varrho_1\, n + 2\,\pi_2,\ \varrho_1\, n + \varrho_2).$$

Hence, the coordinates of $\widetilde{Y}$ for $Y = C$, D satisfy the following relations:

$$\widetilde{Y}_1 = \sqrt{Y_2\, Y_3 + 8}, \quad \widetilde{Y}_2 = \sqrt{Y_3\, Y_1 + 8}, \quad \widetilde{Y}_3 = \sqrt{Y_1\, Y_2 + 8}.$$

The linear expressions involving symmetric functions σ_1 and σ_2 of the triples C and D are also the source of many complete squares as the following theorem shows. Its proof is analogous to the proof of Theorem 2.

Theorem 6. *For $k \in \mathbb{N}^*$ and n, a, $b \in \mathbb{Z}$, the following identities hold:*

$$a(b\,\sigma_1(C) + a) + b^2(\sigma_2(C) + 8) = (b\,[\widetilde{C}_1 + \varrho_1] + a)^2,$$

$$a(b\,\sigma_1(D) + a) + b^2(\sigma_2(D) + 8) = (b\,[\widetilde{D}_1 + \varrho_1] + a)^2.$$

In particular, when $b = 1$ and $a = 0$ and $b = 1$ and $a = \pm 1$ we obtain the following statement.

Corollary 2. *For each $(k,\, n) \in \mathbb{N}^* \times \mathbb{Z}$, the triples C and D satisfy*

$$\sigma_2(C) + 8 = (\widetilde{C}_1 + \pi_1)^2, \qquad \sigma_2(C) \pm \sigma_1(C) + 9 = (\widetilde{C}_1 + \pi_1 \pm 1)^2,$$

$$\sigma_2(D) + 8 = (\widetilde{D}_1 + \pi_1)^2, \qquad \sigma_2(D) \pm \sigma_1(D) + 9 = (\widetilde{D}_1 + \pi_1 \pm 1)^2.$$

In the following result we compute the value of the determinants of the matrices whose rows are members of the double sequences γ and δ and show their invariance with respect to the translation of the second variable.

Theorem 7. *For all a, b, $c \in \mathbb{N}^*$ and all u, v, w, x, $y \in \mathbb{Z}$ it holds:*

$$\begin{aligned}\det([\gamma(a,\, u+x),\, \gamma(b,\, v+x),\, \gamma(c,\, w+x)]) = \\ \det([\delta(a,\, u+y),\, \delta(b,\, v+y),\, \delta(c,\, w+y)]) = \\ -8[(Q_{2a+1}\,u^2 + 2\,Q_{2a+1}\,v\,w + 4\,P_{2a+1}\,u)\,P_{2(b-c)} + \\ (Q_{2b+1}\,v^2 + 2\,Q_{2b+1}\,w\,u + 4\,P_{2b+1}\,v)\,P_{2(c-a)} \\ + (Q_{2c+1}\,w^2 + 2\,Q_{2c+1}\,u\,v + 4\,P_{2c+1}\,w)\,P_{2(a-b)}] \\ - 2(v-w)(w-u)(u-v)Q_{2a+1}\,Q_{2b+1}\,Q_{2c+1}.\end{aligned}$$

The following theorem shows that the double sequences C and D are also connected with respect to the products $\odot$, $\triangleright$ and $\triangleleft$.

Theorem 8. *For all n, u, $v \in \mathbb{N}^*$, all a, $b \in \mathbb{Z}$ and each $\diamond \in \{\odot, \triangleright, \triangleleft\}$ the determinant of the matrix with the rows the triples $\gamma(n,\, a) \diamond \delta(n,\, b)$, $\gamma(n+u,\, a) \diamond \delta(n+u,\, b)$ and $\gamma(n+u\,v,\, a) \diamond \delta(n+u\,v,\, b)$ is independent of the value n. These determinants are equal to -8 times the corresponding value for the double sequences α and β (see Theorem 4).*

We can also consider analogues of Theorems 4 and 8 for the pairs $(\alpha,\, \gamma)$, $(\alpha,\, \delta)$, $(\beta,\, \gamma)$ and $(\beta,\, \delta)$ and the products $\odot$, $\triangleright$ and $\triangleleft$ but with somewhat more complicated expressions.

4. Determinants

Here we attempt to find some simple cases of the determinants from the members of the three among the double sequences α, β, γ and δ. For a $u \in \mathbb{N}^*$, let $A_{\underline{u}} = \alpha(k,\, n+u)$. The symbols $B_{\underline{u}}$, $C_{\underline{u}}$ and $D_{\underline{u}}$ have similar meaning. For a, b, $c \in \mathbb{N}^3$, let $|a,\, b,\, c|$ be the determinant $\det([a,\, b,\, c])$.

Theorem 9. *For all $k \in \mathbb{N}^*$ and all $n \in \mathbb{Z}$, the following identities hold:*

$$|A,\, B,\, C| = 8(\varrho_2 + \pi_0), \quad |A_{\underline{2}},\, B_{\underline{1}},\, C| = 0, \quad |A,\, B_{\underline{1}},\, C_{\underline{2}}| = 32\,\pi_0,$$

$$|A,\, B,\, D| = 8(\pi_2 - \varrho_0), \quad |A_{\underline{2}},\, B_{\underline{1}},\, D| = 0, \quad |A_{\underline{2}},\, B,\, D_{\underline{1}}| = 8(\varrho_0 - \pi_2),$$

$$|C,\, D,\, A| = -8(2\,\pi_2 + \varrho_0), \quad |C_{\underline{2}},\, D_{\underline{1}},\, A| = 0, \quad |C,\, D_{\underline{1}},\, A_{\underline{2}}| = -32\,\varrho_0,$$

$$|C,\, D,\, B| = -8(2\,\pi_1 + \varrho_0),\ |C_{\underline{2}},\, D_{\underline{1}},\, B| = 0,\ |C_{\underline{2}},\, D,\, B_{\underline{1}}| = 8(2\,\pi_1 + \varrho_0).$$

Proof. Let us use the notation $\pi_m = P_{2\,k+m}$ and $\varrho_m = Q_{2\,k+m}$ for every $m \in \mathbb{N}^*$. The determinant $|A,\, B,\, C|$ has the form $P\,n^2 + Q\,n + R$, where P, Q and R are $-4\varrho_1\,\pi_2^2 + (6\varrho_2 + 2\varrho_0)\,\pi_2\,\pi_1 - 2\,\varrho_2\,(\varrho_2 + \varrho_0 + 2\,\varrho_1)\,\pi_1 + 4\varrho_2\,\varrho_1^2$, $(4\varrho_1 + 2\varrho_3)\,\pi_2\,\pi_1 - 4\varrho_2\,\pi_1^2 - 4\,\varrho_1\,\pi_3\,\pi_2 - (2\varrho_3\,\varrho_1 + \pi_3\,\varrho_0 - \pi_3\,\varrho_2)\,\pi_1 + 4\varrho_1^2\,\pi_3$, and $(\pi_3 - 2\,\pi_1)(\pi_1\,\varrho_3 - \pi_3\,\varrho_1)$. Now it is easy to check that $P = Q = 0$ and $R = 8(\varrho_2 + \pi_0)$. □

5. Squares from double sequences $\widetilde{\alpha}$, $\widetilde{\beta}$, $\widetilde{\gamma}$ and $\widetilde{\delta}$

There are many expressions built from double sequences $\widetilde{\alpha}$, $\widetilde{\beta}$, $\widetilde{\gamma}$ and $\widetilde{\delta}$ that are complete squares. Here we give only few simple examples.

$$\sigma_1(\widetilde{A}\odot\widetilde{A})+8=\tfrac{1}{2}\,\sigma_1(A\odot A)+4=\tfrac{1}{2}(\sigma_1(\widetilde{A}\odot\widetilde{A})+\sigma_2(A))+2=(\widetilde{A}_1+\pi_1)^2,$$

$$\sigma_1(\widetilde{B}\odot\widetilde{B})+8=\tfrac{1}{2}\,\sigma_1(B\odot B)+4=\tfrac{1}{2}(\sigma_1(\widetilde{B}\odot\widetilde{B})+\sigma_2(B))+2=(\widetilde{B}_1+\pi_1)^2,$$

$$\sigma_1(\widetilde{C}\odot\widetilde{C})-16=\tfrac{1}{2}\,\sigma_1(C\odot C)-8=\tfrac{1}{2}(\sigma_1(\widetilde{C}\odot\widetilde{C})+\sigma_2(C))-4=(\widetilde{C}_1+\varrho_1)^2,$$

$$\sigma_1(\widetilde{D}\odot\widetilde{D})-16=\tfrac{1}{2}\,\sigma_1(D\odot D)-8=\tfrac{1}{2}(\sigma_1(\widetilde{D}\odot\widetilde{D})+\sigma_2(D))-4=(\widetilde{D}_1+\varrho_1)^2.$$

Of course, we can use also the other two products $\triangleright$ and $\triangleleft$ and also the double sequences α, β, γ and δ. Hence, from all these double sequences and the three products using linear expressions of the kind exemplified above we can get many squares. This seems quite natural if we remember that the members of these double sequences have the properties $D(-4)$ and $D(8)$.

We can compute the determinants of the matrices with rows from the members of the double sequences $\widetilde{\alpha}$, $\widetilde{\beta}$, $\widetilde{\gamma}$ and $\widetilde{\delta}$ using the following relations. For a, b, $c\in\mathbb{N}^*$ and u, v, $w\in\mathbb{Z}$, let $\mathfrak{a}_1=\alpha(a,\,u)$, $\mathfrak{a}_2=\alpha(b,\,v)$ and $\mathfrak{a}_3=\alpha(c,\,w)$. The symbols $\mathfrak{b}_i$, $\mathfrak{c}_i$, $\mathfrak{d}_i$, $\widetilde{\mathfrak{a}}_i$, $\widetilde{\mathfrak{b}}_i$, $\widetilde{\mathfrak{c}}_i$ and $\widetilde{\mathfrak{d}}_i$ for $i=1,\,2,\,3$ are defined similarly.

Theorem 10. *For all a, b, $c\in\mathbb{N}^*$ and all u, v, $w\in\mathbb{Z}$, it holds:*

$$\frac{|\widetilde{\mathfrak{a}}_1,\,\widetilde{\mathfrak{a}}_2,\,\widetilde{\mathfrak{a}}_3|}{|\mathfrak{a}_1,\,\mathfrak{a}_2,\,\mathfrak{a}_3|}=\frac{|\widetilde{\mathfrak{b}}_1,\,\widetilde{\mathfrak{b}}_2,\,\widetilde{\mathfrak{b}}_3|}{|\mathfrak{b}_1,\,\mathfrak{b}_2,\,\mathfrak{b}_3|}=\frac{|\widetilde{\mathfrak{c}}_1,\,\widetilde{\mathfrak{c}}_2,\,\widetilde{\mathfrak{c}}_3|}{|\mathfrak{c}_1,\,\mathfrak{c}_2,\,\mathfrak{c}_3|}=\frac{|\widetilde{\mathfrak{d}}_1,\,\widetilde{\mathfrak{d}}_2,\,\widetilde{\mathfrak{d}}_3|}{|\mathfrak{d}_1,\,\mathfrak{d}_2,\,\mathfrak{d}_3|}=-\frac{1}{2}.$$

Next we shall consider some simple cases of the determinants from the members of the three among the double sequences $\widetilde{\alpha}$, $\widetilde{\beta}$, $\widetilde{\gamma}$ and $\widetilde{\delta}$. Note that these are all opposite of half the values given in Theorem 9.

Theorem 11. *For all $k\in\mathbb{N}^*$ and all $n\in\mathbb{Z}$, the following identities hold:*

$$|\widetilde{A},\,\widetilde{B},\,\widetilde{C}|=-4(\varrho_2+\pi_0),\quad |\widetilde{A}_{\underline{2}},\,\widetilde{B}_{\underline{1}},\,\widetilde{C}|=0,\quad |\widetilde{A},\,\widetilde{B}_{\underline{1}},\,\widetilde{C}_{\underline{2}}|=-16\,\pi_0,$$

$$|\widetilde{A},\,\widetilde{B},\,\widetilde{D}|=4(\varrho_0-\pi_2),\quad |\widetilde{A}_{\underline{2}},\,\widetilde{B}_{\underline{1}},\,\widetilde{D}|=0,\quad |\widetilde{A}_{\underline{2}},\,\widetilde{B},\,\widetilde{D}_{\underline{1}}|=4(\pi_2-\varrho_0),$$

$$|\widetilde{C},\,\widetilde{D},\,\widetilde{A}|=4(2\,\pi_2+\varrho_0),\quad |\widetilde{C}_{\underline{2}},\,\widetilde{D}_{\underline{1}},\,\widetilde{A}|=0,\quad |\widetilde{C},\,\widetilde{D}_{\underline{1}},\,\widetilde{A}_{\underline{2}}|=16\,\varrho_0,$$

$$|\widetilde{C},\,\widetilde{D},\,\widetilde{B}|=4(2\,\pi_1+\varrho_0),\ |\widetilde{C}_{\underline{2}},\,\widetilde{D}_{\underline{1}},\,\widetilde{B}|=0,\ |\widetilde{C}_{\underline{2}},\,\widetilde{D},\,\widetilde{B}_{\underline{1}}|=-4(2\,\pi_1+\varrho_0).$$

Here we present the analogues of the Theorems 4 and 8 for the double sequences $\widetilde{\alpha}$, $\widetilde{\beta}$, $\widetilde{\gamma}$ and $\widetilde{\delta}$. Since the factors are rather complicated we give explicit values only in two cases.

Theorem 12. *For all n, u, $v \in \mathbb{N}^*$, all a, $b \in \mathbb{Z}$ and each $\diamond \in \{\odot, \triangleright, \triangleleft\}$ the determinant of the matrix with the rows either the triples $\widetilde{\alpha}(n, a) \diamond \widetilde{\beta}(n, b)$, $\widetilde{\alpha}(n+u, a) \diamond \widetilde{\beta}(n+u, b)$ and $\widetilde{\alpha}(n+u\,v, a) \diamond \widetilde{\beta}(n+u\,v, b)$ or the triples $\widetilde{\gamma}(n, a) \diamond \widetilde{\delta}(n, b)$, $\widetilde{\gamma}(n+u, a) \diamond \widetilde{\delta}(n+u, b)$ and $\widetilde{\gamma}(n+u\,v, a) \diamond \widetilde{\delta}(n+u\,v, b)$ does not dependent of the value n. For $\diamond = \odot$, the determinants are equal to $8\,P_{2u}\,P_{2\,u\,v}\,P_{2\,u(v-1)}$ multiplied by M and $-8\,M$, where M is*

$$a(3+2\,b)(a^2 - a\,b + b^2 + 2\,b - 3) + b^3 + 4\,b^2 + b + 2.$$

6. The geometry of the eight double sequences

In this section the members of our eight double sequences being triples of (real) numbers are considered as points in the 3-dimensional Euclidean space.

For a $k \in \mathbb{N}^*$ and a, b, c, $d \in \mathbb{Z}$, let T_α, T_β, T_γ and T_δ be the tetrahedra

$$\alpha(k, a)\alpha(k, b)\alpha(k, c)\alpha(k+1, d), \quad \beta(k, a)\beta(k, b)\beta(k, c)\beta(k+1, d),$$

$$\gamma(k, a)\gamma(k, b)\gamma(k, c)\gamma(k+1, d), \quad \delta(k, a)\delta(k, b)\delta(k, c)\delta(k+1, d).$$

The tetrahedra $T_{\widetilde{\alpha}}$, $T_{\widetilde{\beta}}$, $T_{\widetilde{\gamma}}$ and $T_{\widetilde{\delta}}$ are defined similarly.

Theorem 13. *For all $k \in \mathbb{N}^*$ and all a, b, c, $d \in \mathbb{Z}$, the tetrahedra T_α and T_β have the oriented volume $\frac{2\,\pi_1^2\,\pi_2(b-c)(c-a)(a-b)}{3}$ while $\frac{2\,\varrho_1^2\,\varrho_2(b-c)(c-a)(a-b)}{3}$ is the oriented volume of the tetrahedra T_γ and T_δ.*

Proof. Recall that the four points $T_i(x_i, y_i, z_i)$ $(i = 1, 2, 3, 4)$ determine a tetrahedron with the oriented volume

$$\frac{1}{6}\begin{vmatrix} x_1 & y_1 & z_1 & 1 \\ x_2 & y_2 & z_2 & 1 \\ x_3 & y_3 & z_3 & 1 \\ x_4 & y_4 & z_4 & 1 \end{vmatrix}.$$

When we substitute the above quadruples of points into this determinant after some tedious work we get the above values. □

The following result shows that the tetrahedra T_α, T_β, T_γ and T_δ have twice larger volumes and opposite orientation from the tetrahedra $T_{\widetilde{\alpha}}$, $T_{\widetilde{\beta}}$, $T_{\widetilde{\gamma}}$ and $T_{\widetilde{\delta}}$.

Theorem 14. *For all $k \in \mathbb{N}^*$ and all a, b, c, $d \in \mathbb{Z}$, the following holds: $|T_{\widetilde{\alpha}}| = |T_{\widetilde{\beta}}| = -\frac{|T_\alpha|}{2}$ and $|T_{\widetilde{\gamma}}| = |T_{\widetilde{\delta}}| = -\frac{|T_\gamma|}{2}$.*

We examine the volume of the tetrahedra from the the centroids of our eight tetrahedra.

Theorem 15. *For all $k \in \mathbb{N}^*$ and all a, b, c, $d \in \mathbb{Z}$, the tetrahedron whose vertices are the centroids of the tetrahedra T_α, T_β, T_γ and T_δ has the oriented volume $\frac{(\pi_2-\varrho_0)(a+b+c-3\,d-14)}{6}$. If instead we use the centroids of the tetrahedra $T_{\widetilde{\alpha}}$, $T_{\widetilde{\beta}}$, $T_{\widetilde{\gamma}}$ and $T_{\widetilde{\delta}}$, then the oriented volume is $\frac{(\pi_2-\varrho_0)(14+3\,d-a-b-c)}{12}$.*

For points E, F, G and H in the 3-dimensional Euclidean space E^3, let $|EFGH|$ denote the oriented volume of the tetrahedron $EFGH$. For a $k \in \mathbb{N}^*$ and a, $b \in \mathbb{Z}$, let $T_{\alpha\beta}$ denote the tetrahedron

$$\alpha(k,\,a)\alpha(k+1,\,a)\beta(k,\,b)\beta(k+1,\,b).$$

We similarly define tetrahedra $T_{\alpha\gamma}$, $T_{\alpha\delta}$, $T_{\beta\gamma}$, $T_{\beta\delta}$ and $T_{\gamma\delta}$ and $T_{\widetilde{\alpha}\widetilde{\beta}}$, $T_{\widetilde{\alpha}\widetilde{\gamma}}$, $T_{\widetilde{\alpha}\widetilde{\delta}}$, $T_{\widetilde{\beta}\widetilde{\gamma}}$, $T_{\widetilde{\beta}\widetilde{\delta}}$, and $T_{\widetilde{\gamma}\widetilde{\delta}}$. Notice that $|T_{\alpha\beta}| = -2\,|T_{\widetilde{\alpha}\widetilde{\beta}}|$ and that the analogous relation holds for the remaining five pairs of tetrahedra.

Theorem 16. *For each $k \in \mathbb{N}^*$ and all a, $b \in \mathbb{Z}$, the oriented volumes of the tetrahedra are the following:*

$$|T_{\alpha\beta}| = \frac{32\,\pi_2(b-a+1)^2}{3},\ |T_{\alpha\gamma}| = \frac{16(b-a)(\varrho_1(a-b)+4\,\pi_3)}{3},$$

$$|T_{\alpha\delta}| = \frac{16(b-a+1)(\varrho_1(a-b)+13\,\varrho_1+6\,\varrho_0)}{3},$$

$$|T_{\beta\gamma}| = \frac{16(b-a-1)(\varrho_1(a-b)+3\,\varrho_3)}{3},$$

$$|T_{\beta\delta}| = \frac{16(b-a)(\varrho_1\,(a-b)-4\,\pi_3)}{3},\quad |T_{\gamma\delta}| = -\frac{64\,\varrho_2(b-a+1)^2}{3}.$$

Theorem 17. *The oriented volume of the tetrahedron from the centroids of the tetrahedra $T_{\alpha\beta}$, $T_{\beta\gamma}$, $T_{\gamma\delta}$ and $T_{\delta\alpha}$ is equal to $\frac{(b-a)(b-a-1)\varrho_1^2\,\varrho_3}{12}$. The oriented volume of the tetrahedron from the centroids of the tetrahedra $T_{\widetilde{\alpha}\widetilde{\beta}}$, $T_{\widetilde{\beta}\widetilde{\gamma}}$, $T_{\widetilde{\gamma}\widetilde{\delta}}$ and $T_{\widetilde{\delta}\widetilde{\alpha}}$ is equal to $\frac{(a-b)(b-a-1)\varrho_1^2\,\varrho_3}{24}$.*

The tetrahedra $\Omega(k,\,a,\,b,\,c,\,d)$ and $\widetilde{\Omega}(k,\,a,\,b,\,c,\,d)$ whose vertices are the triples $\alpha(k,\,a)$, $\beta(k,\,b)$, $\gamma(k,\,c)$ and $\delta(k,\,d)$ and $\widetilde{\alpha}(k,\,a)$, $\widetilde{\beta}(k,\,b)$, $\widetilde{\gamma}(k,\,c)$ and $\widetilde{\delta}(k,\,d)$ have nice oriented volumes.

Theorem 18. *For $k \in \mathbb{N}^*$ and a, b, c, $d \in \mathbb{Z}$, the tetrahedron $\Omega(k,\,a,\,b,\,c,\,d)$ has the oriented volume $V = \frac{\pi_0(b-a+1)(c-d-1)(\pi_1\,\varrho_1(c+d-a-b)+8)}{3}$ while the tetrahedron $\widetilde{\Omega}(k,\,a,\,b,\,c,\,d)$ has the oriented volume $-\frac{V}{2}$.*

7. Vector cross-products

We close with three theorems about the vector cross-products of two vectors that are members of our eight double sequences.

For an integer a, let $\mathfrak{a}$ and $\mathfrak{b}$ denote vectors $-4((a+2)(a-1),\, a+1,\, -a)$ and $-4(a(a+3),\, a+2,\, -a-1)$.

Theorem 19. *For all $n,\, k \in \mathbb{N}^*$ and all $a \in \mathbb{Z}$, the vector cross-products are as follows:* $\alpha(n,\, a) \times \alpha(n+k,\, a) = \pi_0\, \mathfrak{a}$, $\quad \beta(n,\, a) \times \beta(n+k,\, a) = \pi_0\, \mathfrak{b}$,

$$\gamma(n,\, a) \times \gamma(n+k,\, a) = -2\,\pi_0\, \mathfrak{a}, \quad \delta(n,\, a) \times \delta(n+k,\, a) = -2\,\pi_0\, \mathfrak{b},$$

$$\alpha(n,\, a) \times \gamma(n+k,\, a) = \varrho_0\, \mathfrak{a}, \quad \beta(n,\, a) \times \delta(n+k,\, a) = \varrho_0\, \mathfrak{b}.$$

Proof. Let $\varphi^n = H$, $\psi^n = K$, $\varphi^k = M$, $\psi^k = N$. The vector cross-product $\alpha(n,\, a) \times \alpha(n+k,\, a)$ simplifies to

$$2\sqrt{2}\left(N^2 - M^2\right)\, H^2\, K^2\left((a+2)\,(a-1)\,,\, a+1,\, -a\right),$$

that we recognize as $-4\,\pi_0((a+2)(a-1),\, a+1,\, -a)$. □

For an integer a, let $\mathfrak{c}$ and $\mathfrak{d}$ denote vectors $2(1,\, a^2-2,\, 1-2\,a-a^2)$ and $-2(-1,\, 1-2\,a-a^2,\, 2+4\,a+a^2)$.

Theorem 20. *For all $n,\, k \in \mathbb{N}^*$ and all $a \in \mathbb{Z}$, the vector cross-products are as follows:* $\widetilde{\alpha}(n,\, a) \times \widetilde{\alpha}(n+k,\, a) = \pi_0\, \mathfrak{c}$, $\quad \widetilde{\beta}(n,\, a) \times \widetilde{\beta}(n+k,\, a) = \pi_0\, \mathfrak{d}$,

$$\widetilde{\gamma}(n,\, a) \times \widetilde{\gamma}(n+k,\, a) = -2\,\pi_0\, \mathfrak{c}, \quad \widetilde{\delta}(n,\, a) \times \widetilde{\delta}(n+k,\, a) = -2\,\pi_0\, \mathfrak{d},$$

$$\widetilde{\alpha}(n,\, a) \times \widetilde{\gamma}(n+k,\, a) = \varrho_0\, \mathfrak{c}, \quad \widetilde{\beta}(n,\, a) \times \widetilde{\delta}(n+k,\, a) = \varrho_0\, \mathfrak{d}.$$

Theorem 21. *For all $k \in \mathbb{N}^*$ and $n \in \mathbb{Z}$, we have*

$$(A \times C) \times (B \times D) = -64\,(1,\, n^2+n+2,\, n^2+3\,n+4),$$

$$(\widetilde{A} \times \widetilde{C}) \times (\widetilde{B} \times \widetilde{D}) = 16\,(2\,n^2+4\,n+5,\, 2\,n+3,\, 2\,n+1).$$

Some results in this paper are stated without proof because of the space limitation.

References

[1] E. Brown, *Sets in which $x\,y+k$ is always a square*, Mathematics of Computation, **45** (1985), 613-620.

[2] Z. Čerin and G. M. Gianella, *On Diophantine triples from Pell and Pell-Lucas numbers*, Acc. Sc. Torino - Atti Sci. Fis. 143 (2009), (to appear).

[3] Z. Čerin and G. M. Gianella, *On sums of squares of Pell-Lucas numbers*, INTEGERS: Electronic Journal of Combinatorial Number Theory, **6** (2006), A15.

[4] Z. Čerin and G. M. Gianella, *Formulas for sums of squares and products of Pell numbers*, Acc. Sc. Torino - Atti Sci. Fis. 140 (2006), 113-122.

[5] Z. Čerin and G. M. Gianella, *On sums of Pell numbers*, Acc. Sc. Torino - Atti Sci. Fis. 141 (2007), 23-31.

[6] H. Davenport and A. Baker, *The equations* $3x^2 - 2 = y^2$ *and* $8x^2 - 7 = z^2$, Quart. J. Math. Oxford Ser. (2) **20** (1969), 129-137.
[7] V. E. Hoggatt and G. E. Bergum, *A problem of Fermat and the Fibonacci sequence*, Fibonacci Quart. **15** (1977), 323-330.
[8] N. Sloane, *On-Line Encyclopedia of Integer Sequences*, `http://www.research. att.com/~njas/sequences/`.

Kopernikova 7, 10010 Zagreb, CROATIA
E-mail address: `cerin@math.hr`

Dipartimento di Matematica, Università di Torino, via C. Alberto 10, 10123 Torino, ITALIA
E-mail address: `gianella@dm.unito.it`

RENDICONTI DEL CIRCOLO MATEMATICO DI PALERMO
Serie II, Suppl. 81 (2009), pp. 85-95

DALL'IMPRESA AGRICOLA ALLA BIOENERGY FARM: *potenzialità e prospettive di sviluppo del biogas*

S. Chiricosta
- Dipartimento S.E.A.- Università degli studi di Messina

INTRODUZIONE

Lo sviluppo della società umana, un tempo imperniato su un'economia basata fondamentalmente su risorse agricole, molto delocalizzate ma in linea di principio inesauribili, si è avviato, in maniera graduale ed inarrestabile, verso un'economia basata su risorse minerarie, molto localizzate, apparentemente più vantaggiose, ma esauribili. (1).

Questa tendenza sta causando danni irreparabili al pianeta ed all'Umanità intera, quali:

- ***il progressivo esaurimento delle riserve fossili, principalmente, di quelle petrolifere;***
- ***un riscaldamento globale sempre più difficile da controllare;***
- ***una crescente incapacità dell'ambiente di assorbire i rifiuti generati dalla attività industriale, ingannata dal miraggio di uno sviluppo "illimitato"***.

Anche la stessa agricoltura, diventata sempre più di tipo intensivo, ha generato, come qualsiasi altra attività produttiva umana, impatti sull'ambiente la cui effettiva incidenza è difficilmente quantificabile con precisione.

Si pone, pertanto, in modo sempre più pressante, anche per il Mondo Agricolo, la questione della **"sostenibilità ambientale".**

Oltre a ciò, i recenti aumenti dei prezzi dei prodotti petroliferi e l'insicurezza crescente, riguardo alla loro disponibilità a lungo termine, stanno creando ulteriori problemi, specialmente, per le imprese agricole, già oltremodo provate da una remunerativitá complessiva del settore sempre più bassa che, come conseguenza, ha determinato:

- ***una progressiva contrazione delle superfici agrarie e del numero di aziende;***
- ***una continua riduzione degli addetti, considerati soggetti deboli delle filiere agroalimentari;***
- ***un graduale abbandono dei giovani dalle campagne, seguita da una persistente carenza di manodopera, sempre più rimpiazzata con manovalanza extracomunitaria.***

Il problema principale dell'agricoltura, oggi, è determinato dalla costante flessione dei ricavi, considerato che, d'altra parte, i costi si fanno sempre maggiori, e ciò determina una progressiva perdita di **"redditività"** dell'impresa agricola(2). Ed, infatti, i prezzi delle derrate alimentari crescono ogni giorno di più; di conseguenza, i consumi si riducono e le tanto decantate produzioni biologiche non rappresentano effettivamente quella soluzione globale, tanto agognata dagli imprenditori agricoli, in quanto destinate, sempre per questioni economiche, solamente ad un mercato di nicchia.

Davanti a questo insieme di difficoltà si impone come non più procrastinabile la necessità di una revisione critica dei concetti che hanno, sin qui, guidato lo sviluppo agricolo della società umana.

TRASFORMAZIONE DELLE FILIERE AGRICOLE IN BIOENERGY FARM.

In particolare, per il settore agricolo, appare essenziale l'apertura verso una fase nuova, rispetto al passato, che riqualifichi gli imprenditori agricoli mediante una rivalutazione della peculiarità ed esclusività della loro "terra" intesa non soltanto come elemento di produzione di alimenti, ma anche di una vasta gamma di materie prime per l'industria e l'energia, provenienti dalle biomasse che essi stessi coltivano. Il comparto agricolo-forestale può svolgere un ruolo determinante nella produzione di biocombustibili in sostituzione dei tradizionali combustibili fossili. Attraverso processi chimici già sperimentati si possono produrre combustibili e materiali organici (polimeri, materiali plastici, lubrificanti, ecc.) in grado di sostituire prodotti simili derivati dal petrolio.

In questo senso, il terreno agricolo può essere considerato anche come ***"giacimento di energia"*** e gli agricoltori diventano, essi stessi, produttori di energia da biomasse, ossia di una risorsa territoriale a spiccata valenza locale, col duplice vantaggio di produrre un reddito addizionale per la propria azienda agricola e di tutelare l'ambiente grazie all'utilizzo di fonti rinnovabili..

Questa nuova forma di agricoltura detta **"agro-energia"** si propone, prepotentemente, come l'unico mezzo, valido e realmente alternativo, per coniugare **"sostenibilità e redditività",** mediante la chiusura di un ciclo geobiochimico che vede l'affermazione dell'impresa agricola nel nuovo ed imprescindibile ruolo di "anello di congiunzione" tra le attività produttive, il complesso dei consumi ed il sistema "ambiente".

Tali prospettive stanno facendo emergere una nuova tipologia di impresa agricola, la ***"bioenergy-farm"*** dedicata alla produzione di colture cerealicole, oleaginose, crucifere, biomasse e materiali legnosi (comprendenti anche prodotti residuali e colture specializzate) e reflui di allevamenti zootecnici convertiti in prodotti energetici.

Gli interessi economici che ruotano attorno a questo nuovo ***"paradigma agro-energetico"*** sono enormi tanto che esso si è affermato, in breve tempo, sulla scena mondiale, presentando innumerevoli vantaggi immediati e tutti egualmente importanti: *crea posti di lavoro; rivitalizza l'economia; combatte l'erosione del territorio; riduce la dipendenza dai combustibili importati; non genera gas serra e, quindi, lavora a favore del trattato di Kyoto* (3).

Le opportunità offerte dalle filiere agro energetiche, in materia di bioenergie, sono state evidenziate in diversi documenti, sia comunitari che nazionali; dei quali i principali sono elencati in Tabella I.

Ma un forte impulso alle filiere bioenergetiche è arrivato con la riforma della PAC, attuata nel 2003 (4), che concede il sostegno al reddito svincolato dalla produzione agricola.

Tabella I° - Le principali norme emanate dall'U.E. e dall'Italia

Unione Europea

-Libro Verde dell'U.E. che riporta il Piano d'azione per la biomassa;
-Dir. 2001/77/CE per la promozione dell'energia elettrica da fonti di energia rinnovabile, recepita in Italia con dlgs 29/12/2003 n°387;
- Decisione del Consiglio del 25/03/2002 sulla deroga per l'esenzione da accise per il biodiesel in Italia;
- Decisione del Consiglio del 25/04/2002 per la ratifica del Protocollo di Kyoto da parte dell'U.E.;
- Dir.25/03/2002 sulla promozione dell'uso dei biocarburanti;
-Dir. 2003/30/CE per la promozione dell'uso dei biocarburanti da trazione;
-Dir. 2003/96/CE riguardante la tassazione dei prodotti energetici e dell'elettricità recepite in Italia (legge 06/81);
-Dir. 2004/8/CE sulla promozione della cogenerazione basata su una domanda di calore utile nel mercato interno dell'energia;
-Reg.(CE) 1973/2004 del 29/10/2004 che stabilisce le modalità di applicazione per gli aiuti accoppiati e per il regime delle produzioni a scopo non alimentare effettuate su superfici ritirate dalla produzione e l'uso di superfici ritirate dalla produzione allo scopo di ottenere materie prime;
-Reg.(CE) 1782/2003 del 29/09/2003 che prevede il regime di aiuto per le colture energetiche;
-Comunicazione CE 2005 n°268 detta"Biomass Action Plan" che fissa le misure per promuovere ed incrementare l'uso delle biomasse nei settori del riscaldamento, dell'elettricità e dei trasporti.(L'obiettivo è di raddoppiare l'attuale contributo delle biomasse, pari al 4% dell'energia primaria dell'Ue25- passando dai 69 Mtep del 2003 a 186-189 Mtep nel 2010 e a 215-239 Mtep nel 2020);
-Comunicazione CE 2006 "Strategia della UE per i biocarburanti".

Italia

1997- Programma Nazionale per le Energie Rinnovabili da Biomasse (PNERB);
1998-Programma Nazionale per la Valorizzazione delle Biomasse Agricole e Forestali (PNVBAF);
2000-Programma Nazionale Biocombustibili (PROBIO);
-Legge 01/06/2002 n°120 di ratifica del Protocollo di Kyoto del Dicembre 1997;
-Dlgs n°128 del 30/05/2005 recante "Attuazione 2003/30/CE relativa alla promozione dell'uso dei biocarburanti o di altri carburanti rinnovabili nei trasporti";
- Legge n°266/05 (Finanziaria del 2006);
-Dpcm del 23/02/2006 che istituisce un tavolo di filiera per le bioenergie;
- Legge n°81 dell'11/03/2006;

Infatti, i produttori agricoli possono adeguare le loro produzioni alle esigenze del mercato energetico. Ed essendo, tali produzioni, equiparate alle attività connesse, possono beneficiare dello speciale regime di ***"aiuto alle colture energetiche"*** con un incentivo pari a 45€/ettaro (3). Gli orientamenti comunitari più recenti su queste tematiche sono emersi nel vertice di Bruxelles del Marzo 2007. In quella occasione gli Stati Membri dell'U.E. hanno sottoscritto un accordo vincolante con il quale si impegnavano, entro il 2020, a produrre il 20% dell' energia consumata nell'U.E.-27 mediante fonti energetiche rinnovabili. E' un obiettivo ambizioso che trova l'Italia impreparata ad affrontare i cambiamenti strutturali ed organizzativi richiesti e, tuttora, alle prese con forti ritardi su parametri fissati nelle precedenti direttive.
Infatti, la produzione di energia da fonti rinnovabili, in Italia, ha rappresentato, nel 2006, appena il 7,10% (13,95 MTep) della domanda lorda totale di energia pari a 195,6 MTep. ed, in particolare, nell'ambito delle rinnovabili, le biomasse hanno rappresentato una quantità di poco più del 2,1%(4,05 MTep), davvero esigua ma dalle potenzialità enormi(5).
Com'è noto, la biomassa, intesa come ***"sostanza organica, in forma non fossile, derivante direttamente o indirettamente dalla fotosintesi clorofilliana",*** rappresenta una forma naturale di accumulo di energia solare

che consente alle piante di assorbire, anidride carbonica dall'aria, acqua e le sostanze nutrienti presenti nei terreni, per trasformarle in materiale organico utile alla crescita della pianta (carboidrati, lignina, proteine, lipidi) oltre ad un numero praticamente illimitato di prodotti secondari di ogni tipo[1].
Pertanto, la biomassa, se usata, in maniera ciclica, per scopi energetici, rappresenta una importante risorsa locale, rinnovabile e rispettosa dell'ambiente, costituita da una grande quantità di materiali, di natura estremamente eterogenea, come:

- ***Le colture arbore*** *(es.:pioppo, salice, eucalipto)****, arbustive*** *(es.:la ginestra)****, erbacee*** *(es.: il sorgo zuccherino)****;***
- ***I sottoprodotti derivanti dalle diverse fasi produttive e distributive del "sistema foresta-legno"*** *(frascami, ramaglie, trucioli, segatura, ecc.)****;***
- ***I residui e gli scarti delle lavorazioni agro-industriali*** *(vinacce, sanse, panelli oleosi, borlande,ecc.)****;***
- ***I reflui degli allevamenti zootecnici;***
- ***Residui di aziende agroalimentari;***
- ***Scarti mercatali;***
- ***La frazione organica, esclusa la plastica, dei rifiuti solidi civili ed industriali.***

Le biomasse si possono considerare risorse primarie inesauribili nel tempo purché vengano impiegate ad un ritmo complessivamente non superiore alle capacità di rinnovamento biologico; in realtà esse non sono infinite quantitativamente, ma per ogni specie vegetale utilizzata la disponibilità trova un limite nella superficie ad essa destinata, nonché in vincoli climatici ed ambientali che tendono a limitare, in ogni regione, le specie che vi possono crescere con convenienza ed economia. Per tale motivo occorre definire delle priorità, operare delle scelte, per orientare le agrienergie verso quelle forme che riescano a realizzare il miglior valore aggiunto per le imprese agricole nel rispetto della sostenibilità ambientale e sociale (7).La produzione di biomasse rappresenta sicuramente un'opportunità per il settore agricolo**,** infatti esse hanno caratteristiche interessanti in quanto:
- trovano diversi impieghi e danno luogo a diversi prodotti energetici (bioetanolo, biodiesel, biogas, compost, ecc.);
-possono avere diffusione ubiquitaria sul territorio perché le specie impiegate sono numerose;
- le ricadute ambientali della loro coltivazione e del loro utilizzo sono positive per via della neutralità, ai fini del bilancio della CO_2, e delle ridotte emissioni;

[1] L'energia in essa contenuta è, quindi, energia solare ***"fissata"*** dai vegetali per mezzo della fotosintesi clorofilliana. E' stato calcolato che, in questo modo, vengono immobilizzate, complessivamente, circa 200 miliardi di tonnellate di carbonio all'anno, con un contenuto energetico equivalente a 70 miliardi di tonnellate di petrolio: ossia l'equivalente di circa 7 volte l'attuale fabbisogno energetico mondiale (6)

- sono costituite da materia organica contraddistinta da elevata biodegradabilità e, pertanto, non si pone il rischio di poter inquinare o contaminare l'ambiente;
- rappresentano un'alternativa per diversificare la propria azienda agricola;
- implicano un forte impegno degli operatori, a qualsiasi livello, per la loro diffusione sul territorio;
- offrono la possibilità di integrazione fra diverse attività per il perseguimento di obiettivi comuni e di interesse per la collettività, con buone ricadute economiche;
- costituiscono uno stimolo per l'economia rurale su base locale, contribuendo al loro sviluppo e creando notevoli benefici occupazionali;
- contribuiscono a ridurre la dipendenza dalle importazioni di combustibili fossili, a diversificare le fonti di approvvigionamento energetico ed a stabilizzare le emissioni in atmosfera di gas serra.

ASPETTI TECNOLOGICI DELLE BIOMASSE

Ad ogni tipologia di biomassa, a seconda del contenuto di umidità e del suo rapporto Carbonio/Azoto, corrisponde una tecnologia di conversione più adatta che dà luogo a specifici prodotti utilizzabili in particolari settori di utenza.
I processi di conversione delle biomasse, allo stato attuale più utilizzate, sono:

- ***combustione diretta;***
- ***carbonizzazione;***
- ***gassificazione;***
- ***pirolisi;***
- ***fermentazione alcoolica;***
- ***digestione aerobica;***
- ***digestione anaerobica;***
- ***estrazione di oli con produzione di biodiesel;***
- ***steam explosion;***
- ***bioconversione diretta mediante microorganismi fotosintetici.***

Non tutte le suddette tecnologie hanno raggiunto lo stesso grado di maturità o possono essere impiegate senza problemi. Alcune possono considerarsi giunte ad un livello di sviluppo tale da consentirne l'utilizzazione su scala industriale, altre, invece, necessitano di ulteriore sperimentazione al fine di aumentarne i rendimenti e di diminuirne i costi. Gli imprenditori agricoli sono pronti a dare il loro contributo scegliendo, fra le varie opportunità possibili, quelle che meglio rispondono alle esigenze di ciascuna realtà produttiva(8).
E' certo, però, che fra tutti i processi possibili, quello riguardante la digestione anaerobica, sotto il profilo strategico è l'investimento che appare più interessante per le imprese zootecniche perché non richiede, necessariamente, la coltivazione di una biomassa *"ad hoc"* che potrebbe, in ogni caso, entrare in competizione con le produzioni alimentari *("cibo o combustibile")* ma si propone, viceversa, come un mezzo, quanto mai utile, per lo smaltimento di una materia prima senza costo, il refluo, che, comunque, va eliminato e che,

certamente, costituisce un oneroso fardello per l'azienda che lo produce in quanto obbligata a dotarsi di un impianto di depurazione per dismetterlo; funzione che, nel caso specifico, verrebbe svolta dal digestore dell'impianto di digestione anaerobica con la produzione di un utile combustibile gassoso.
In Italia la maggiore spinta verso la digestione anaerobica sembra provenire dalla cosiddetta ***"Direttiva Nitrati"***. Questa, nell'ottica di proteggere le acque dall'inquinamento di nitrati da fonte agricola, tra le altre disposizioni, regolamenta, in maniera piuttosto restrittiva, la possibilità di spandere i reflui zootecnici su terreni agricoli, imponendo la necessità di un trattamento preliminare(9).

LA DIGESTIONE ANAEROBICA
È un processo di conversione di tipo biochimico che consiste nella demolizione, ad opera di microrganismi anaerobici, di sostanze organiche complesse (lipidi, protidi, glucidi) contenute nei vegetali e nei sottoprodotti di origine animale, con conseguente produzione di un "biogas", combustibile ad alto rendimento energetico avente un potere calorifico di circa 5500 Kcal/ Nm^3 (23000Kj/Nm^3) la cui costituzione è sotto indicata:

Tabella II- Composizione tipica del biogas

Componenti	***% volumetrica su s.s.***
Metano	**45-55**
Anidride Carbonica	**45-55**
Azoto	**1-12**
Ossigeno	**0-3**
Idrogeno solforato	**0,01-0,05**
Composti in tracce (*Idrocarburi paraffinici, aromatici, anidride solforosa).*	**0,1-0,5**

Le tecniche di digestione anaerobica possono suddividersi in due gruppi:
-***Digestione ad umido (wet)***, quando il substrato in digestione ha un contenuto di solidi solubili (SS) ≤10%;
-***Digestione a secco (dry)***, quando il substrato in digestione ha un contenuto di solidi solubili (SS) ≥ 20%.
Processi con valori di secco intermedi vengono definiti "processi a semisecco".
Importante parametro di funzionamento dell'intero processo digestivo è **la temperatura** che condiziona la velocità di sviluppo dei batteri e, di conseguenza, la velocità stessa di digestione del refluo, ossia il ***tempo di ritenzione,*** espresso in giorni, della permanenza delle deiezioni nel digestore.La digestione anaerobica può essere sostenuta da diversi tipi di batteri. I "criofili" che lavorano a bassa temperatura (8-12°C), i "mesofili" (34-40°C), i "termofili"(55°C) ed i "termofili spinti" (70°C). I migliori, perché più resistenti sono i batteri mesofili, cui bisogna assicurare condizioni ambientali stabili, rimescolando di continuo il liquame, a temperatura costante, mantenendo l'ambiente riscaldato con l'uso di parte dell'energia termica

prodotta dall'impianto stesso(10). Corrispondentemente la digestione anaerobica può essere condotta:
- *in condizioni psicrofile (circa 10-25°C);*
- *in condizioni mesofile (circa 35-37°C);*
- *in condizioni termofile (circa 55°C)..*

L'impiego iniziale della digestione anaerobica a temperatura ambiente, ossia in condizioni psicrofile, soluzione semplice ma molto lenta è stata ormai abbandonata considerato che conduce, in circa 40-60 giorni, ad un minor rendimento nella produzione di biogas, a causa della parziale perdita, con le sostanze volatili, di materia organica in parte degradata.
Lo sviluppo tecnologico odierno si caratterizza per una pronunciata accelerazione della velocità di produzione del biogas e, pertanto, ci si avvia sempre più verso tipologie di digestioni anaerobiche mesofile o termofile.
La scelta della condizione di fermentazione mesofila, è dettata, principalmente dalla mancanza di una fonte di calore supplementare a basso prezzo tale da consentire al fermentatore di raggiungere i 55°C della digestione termofila e da una semplicità di gestione dell'impianto, specialmente se esso viene affidato direttamente all'allevatore.
La digestione termofila si fa preferire in quanto, alla temperatura di 55°C, il liquame subisce una completa sterilizzazione degli agenti patogeni, un'abbattimento fino al 97% degli odori, la riduzione della volatilità degli odori rispetto al liquame fresco e l'aumento del potere fertilizzante (*organicazione dell'azoto*)(11).
Purtuttavia, i processi in condizioni mesofile, a causa della loro ricordata semplicità di gestione, sono stati ulteriormente migliorati allo scopo di ridurre il tempo di formazione del biogas a non più di 20-30 giorni, pervenendo, oggi, fondamentalmente a due tipi di digestione mesofila accelerata:
- ***Digestione per frazione solida flottata e sedimentata e fanghi di supero***: in cui il liquame, senza miscelazione, viene digerito con un tempo di ritenzione massimo di 15-20 giorni;
- ***Digestione in impianti ad alto carico di tipo CSTR (Completely Stirred Tank Reactor)***: in cui, in reattori,sia a semplice che a doppio stadio, dotati di sistemi di miscelazione oltre che di riscaldamento, la digestione del liquame viene portata a compimento in poco più di due settimane (11).

E' chiaro, inoltre, che, al di là del sistema di digestione anaerobica adottato, il rendimento di produzione del biogas risulta sempre condizionato da fattori sostanzialmente biochimici quali: *il rapporto C/N, il pH del substrato, il contenuto in acqua, il tipo di batteri presenti nei liquami* (12,13).
La digestione anaerobica si può suddividere in quattro fasi:

1- ***Idrolisi,*** mediante la quale le molecole organiche, per azione di *batteri idrolitici*, subiscono scissione in composti più semplici quali monosaccaridi, amminoacidi ed acidi grassi;
2- ***Acidogenesi,*** nel corso della quale, avviene l'ulteriore scissione, per

mezzo di *batteri acidogeni*, in molecole ancora più semplici, come acidi grassi volatili (ad es.: ac. acetico, propionico, butirrico, ecc.), con produzione di NH_3, CO_2 e H_2S, quali sottoprodotti;

3- ***Acetogenesi,*** dove le molecole semplici prodotte nel precedente stadio sono ulteriormente digerite, mediante l'azione di *batteri acetogeni*, con produzione di CO_2, H_2 e, principalmente, acido acetico;
4- ***Metanogenesi***, nel corso della quale, per mezzo di *batteri metanigeni*, sia *di tipo acetoclastico,*(agenti sull'acido acetico) che *di tipo idrogenotrofo*, (agenti su CO_2 e H_2) conducono alla produzione finale di una miscela di metano, anidride carbonica ed acqua.

La prima fase è, ancora, "aerobica", grazie all'ossigeno inizialmente disciolto nella biomassa, e, perciò, il principale gas che si produce è CO_2 .La seconda fase è caratterizzata da una forte diminuzione dell' O_2 disponibile che porta l'ambiente in condizioni anaerobiche. Si ha ancora grande produzione di CO_2 ed, in misura minore, di H_2. Nella terza fase, anaerobica, inizia la formazione di CH_4 che, considerata la sua scarsa solubilità in acqua, si libera completamente, allo stato gassoso, mentre contemporaneamente si ha una decisa riduzione della CO_2 prodotta, che, col procedere della digestione, partecipa, dissolvendosi nell'ambiente acquoso del substrato, all'equilibrio dei carbonati presenti nella biomassa in reazione. Anche il contenuto di azoto, inizialmente elevato nella prima fase aerobica del processo, decresce molto velocemente durante il passaggio alla seconda e, soprattutto, alla terza fase anaerobica. La produzione di biogas non avviene in modo costante, durante il processo di digestione anaerobica; il livello massimo viene raggiunto durante la fase centrale del processo. Nelle fasi iniziali e finali del processo, infatti, la produzione di biogas è minore perché, all'inizio, i batteri non si sono ancora riprodotti abbastanza e, alla fine, resta solamente il materiale più difficilmente digeribile.Nella quarta fase, la produzione di biogas raggiunge condizioni di quasi stazionarietà e la composizione del biogas non varia più. Le interazioni tra le diverse specie batteriche sono molteplici ed i prodotti del metabolismo di alcune specie possono essere utilizzati da altre specie come substrato o come fattori di crescita(14).

La composizione chimica del biogas varia molto a seconda delle condizioni di processo, delle sostanze che vengono immesse nel fermentatore, della temperatura di funzionamento, della *'salute'* dei ceppi batteriologici, del pH del substrato, ecc.. Tutti questi fattori devono essere perfettamente coordinati ed armonizzati tra loro per una produzione soddisfacente di biogas che risulti, alla fine, costituito principalmente da metano ed anidride carbonica.

Il processo di digestione può essere suddiviso in ***processo monostadio*** quando la fase di idrolisi, fermentazione acida e metanigena avvengono contemporaneamente in un unico reattore; e ***processo bistadio*** quando si ha un primo stadio durante il quale il substrato viene idrolizzato e

contemporaneamente avviene la fase acida, mentre la fase metanigena avviene in un secondo momento.
Un' ulteriore suddivisione dei processi di digestione anaerobica può essere fatta in base al tipo di alimentazione del reattore, che può essere continua o in cumuli ***(batch)*** ed in base al fatto che il substrato all'interno del reattore, venga miscelato o scorra sequenzialmente attraversando fasi via via diverse ***(pug flow)***(15). Per la captazione del biogas possono essere usati sia sistemi ***"attivi"*** che ***"passivi"***.Con i primi si fornisce artificialmente un gradiente di pressione mediante soffianti o compressori. Nei sistemi passivi, invece, si sfrutta il gradiente di pressione che si instaura naturalmente all'interno della biomassa, a seguito dei processi di generazione di biogas.I sistemi di captazione attiva sono, generalmente, più efficienti di quelli passivi. I condotti di estrazione del biogas sono, normalmente distribuiti su tutta la superficie dell'impianto, in modo da evitare zone di ristagno del gas. La loro spaziatura reciproca e la loro profondità dipendono dalle condizioni operative e dalle caratteristiche dell'impianto stesso (16).
Gli impianti di produzione di biogas di uso e applicazione più frequente, sono assimilabili a tre distinte tipologie, aventi ciascuna peculiarità particolari e per questo adatte ciascuna a specifiche e differenti realtà aziendali.
Nel caso di utilizzo di liquami zootecnici, costituiti dalla sola frazione liquida delle deiezioni, preventivamente separata da solidi grossolani, non tecnicamente biodegradabili in tempi tecnici ragionevoli, si utilizza un tipo di digestore assolutamente privo di organi di miscelazione interni e si deve prediligere un tipo di impianto avente la conformazione a canale del tipo ***"plug-flow"*** ossia con un *flusso a pistone.*
Quando la digestione anaerobica viene condotta con le deiezioni tal quali (frazione liquida + frazione solida), è necessario utilizzare un digestore cilindrico, dotato di impianto di miscelazione ad elica, di pompa di ricircolo esterna temporizzata e di un sistema di bocchette di fondo per ottenere la movimentazione del liquame e l'effetto up-flow e rompicrosta. Il digestore viene alimentato giornalmente con liquame fresco, mentre quello digerito uscirà dopo un tempo medio di permanenza in vasca di circa 20/25 giorni. Questa conformazioneè detta di tipo ***"up-flow miscelato".***
Infine, quando si fa avvenire la digestione anaerobica di liquami zootecnici tal quali mescolati ad opportuna biomassa anche in grandi quantità (codigestione), e spesso oltre il limite di pompabilità, bisogna utilizzare un impianto del tipo ***"super-flow"***, adatto proprio per biomasse super dense.
Il rendimento in biogas, e di conseguenza, quello energetico del processo, è molto variabile e dipende dalla biodegradabilità del substrato trattato, come indicato nella tabella III.
In genere, durante la digestione anaerobica, si ottiene una riduzione di almeno il 50% dei solidi volatili (SV) alimentati.. Naturalmente non tutto il biogas ottenuto può essere utilizzato. Circa il 30%, infatti, deve essere bruciato per

assicurare il mantenimento della temperatura del digestore, mentre il resto del biogas, raccolto, essiccato, compresso ed immagazzinato, costituisce la ***"produzione netta"*** che può essere valorizzata per l'utilizzazione(17).

TabellaIII -Biomasse e scarti organici avviabili a digestione anaerobica e loro resa in biogas (m^3 di sostanze volatili per tonnellata di materiale s.s.)

Materiali	***m^3 biogas per tonnellata***
Deiezioni animali (bovini, suini, avicunicoli)	200-500
Residui colturali (paglia, colletti barbabietole, ecc.)	350 – 400
Scarti organici agroindustriali (siero, scarti vegetali, lieviti, fanghi e reflui di distillerie, birrerie, cantine, ecc.)	400-800
Scarti organici di macellazione (grassi, sangue, contenuto stomacale e viscerale, fanghi di flottazione, ecc.)	550-1000
Fanghi di depurazione	250-350
Frazione organica dei rifiuti solidi urbani	400-600
Colture energetiche (mais, sorgo zuccherino, ecc.)	550-750

Si è potuto stabilire sperimentalmente che, in condizioni ottimali, possono essere prodotti dalla stabulazione di un bovino, in media, 1-2 m^3 di biogas/giorno e che per ottenere 1 m^3 di gas, a partire da suini o da avicoli, sono necessarie le stabulazioni rispettivamente di 4-10 capi e 50-100 capi.
Nella stima del potenziale reale vanno considerate, per ogni comparto, solo quelle aziende con un numero di capi allevati pari o superiori al "numero minimo" individuato come accettabile nel rispetto dei criteri di economicità di ogni investimento. Nello specifico, ipotizzando una vita utile del digestore di 10 anni, è stato stimato che, per l'implementazione di sistemi di recupero energetico fattibili, sul piano tecnico-economico, siano necessarie aziende con 350 capi per bovini, 1000 capi per suini e 25000 capi per avicoli (18).

CONCLUSIONI

Da quanto detto si evince che si può contrastare efficacemente la perdita di redditività dell'impresa agricola mediante un'opportuna trasformazione di filiera che tenga conto delle enormi potenzialità bioenergetiche fin qui trascurate.
Dal quadro panoramico tracciato sulle possibilità offerte dalle biomasse si deduce che la digestione anaerobica con produzione di biogas presenta molteplici vantaggi:

- ***Rappresenta una valida alternativa ad altri trattamenti energivori*** costituendo, di fatto, una doppia economia (energia non consumata ed energia prodotta);

- ***Permette di disinquinare la parte organica dei reflui***, dal momento che tutte le sostanze fermentescibili sono trasformate in biogas che può sostituirsi ai combustibili fossili classici (olio, carbone, gas naturale);
- ***Stabilizza l'effluente digerito***, eliminando, al termine del processo di fermentazione, germi patogeni e cattivi odori e lasciando integri i principali elementi nutritivi (azoto, fosforo e potassio) già presenti nella materia prima. L'effluente diventa, pertanto, un ottimo fertilizzante, ricco d'azoto in forma direttamente assimilabile dalle piante,già pronto per la fase di concimazione dei terreni agricoli;
- ***Restituisce un residuo che può essere impiegato come integratore alimentare per alimenti zootecnici e per la piscicoltura***;
- ***Elimina il rischio di una degradazione anaerobica non controllata*** che genererebbe emissioni di grosse quantità di metano, gas ad effetto climalterante circa 20 volte superiore a quello della CO_2;
- ***Offre la possibilità di accedere ai contributi*** che incentivano gli operatori ad investire in questo nuovo settore.

BIBLIOGRAFIA

1)Bardi U., *Agrienergia. Un nuovo paradigma per le energie rinnovabili*, Conferenza Renewables 2004, Evora, Portogallo.
2) www.agrienergia.it
3)Rosa F.- Sinergie e multifunzionalità delle produzioni agro-energetiche- Agriregionieuropa Anno3, Numero 9- Giugno 2007.
4) Reg. Com. 1782/2003
5) Giuca S: - Le biomasse nella politica energetica comunitaria e nazionale.-Giornata di studio su "Cambiamenti climatici e bioenergie in agricoltura"-Pescara 10/07/2007.
6) www.itabia.it "Conoscere le biomasse".
7) Berton M. Le imprese agrienergetiche come modelli organizzativi delle filiere bioenergetiche in Convegno su "L'autonomia energetica dei territori rurali ed i finanziamenti del programma Energia Intelligente Europa- Torreano di Martignacco (UD) 12/06/2007.
8)Astuto P. Bilancio energetico ed efficienza ambientale- Giugliano 2/10/2006.
9) Direttiva 91/676/CE recepita in Italia con Dlgs 152 del 11/05/1999.
10)Piccinini S.-Le tecnologie di produzione del biogas- CRPA-Reggio E. 30/05/2007
11) Movendi srl-Plus Energy- Recupero di un impianto a biogas- Nogara 5 Novembre 2005.
12) Collivignarelli C., Sorlini S., Mari M:- Recupero di biogas in impianti di digestione anaerobica di reflui suinicoli-RS Rifiuti solidi, vol.XV, n°5, Sett.-Ott. 2001, p.35
13)Paoli L.-Energie rinnovabili: Impieghi su piccola scala. Il Rostro Ed.,2001,p.62.
14) Navarotto P.- Energie rinnovabili in agricoltura:il biogas-IREF Milano 23/01/2007.
15) Piccinini S:- Biogas: Produzione e prospettive in Italia- Convegno Nazionale sulla bioenergia- Roma, 12 Maggio 2004
16)RotaG.-Impianti recupero di biogas-http://www.rotaguido.it/prodotti/recupero-biogas.html
17)Fabbri C., Piccinini S.- Gestione dei reflui zootecnici, digestione anaerobica e recupero del biogas- UNACOMA- Bologna, 27 Aprile 2006.
18) Piccioni E. Biomasse da energia- Filiera biogas- Grosseto 14-15/06/2006

RENDICONTI DEL CIRCOLO MATEMATICO DI PALERMO
Serie II, Suppl. 81 (2009), pp. 97-106

VALORIZZAZIONE E DIFFUSIONE DELLA FILIERA BIOGAS IN EUROPA ED IN ITALIA

S. Chiricosta, S. Saccà
Università degli Studi di Messina
Dipartimento di Studi e Ricerche Economico-aziendali ed Ambientali
Email: salvatore.chiricosta@unime.it, ssacca@unime.it

1. INTRODUZIONE

È, oramai, ampiamente assodato come le biomasse possano rappresentare una grande opportunità per il comparto agricolo-forestale soprattutto perché una loro appropriata utilizzazione potrebbe permettere la realizzazione di un valore aggiunto per le imprese del settore pur nel rispetto della sostenibilità ambientale e sociale.
Dall'esame di insieme delle varie tecnologie disponibili (Fig.1) è stato evidenziato come la produzione di biogas, rispetto ad altri possibili processi di conversione, produca tutta una serie di vantaggi non solo di natura economica ma anche di tipo energetico, ambientale ed agricolo.
Le materie prime utilizzabili per alimentare una filiera di biogas possono essere sia reflui di aziende zootecniche che residui industriali o municipali a base organica che vengono sottoposte a digestione anaerobica. Ciò per mezzo della possibilità tecnica della co-digestione che permette la realizzazione di un sistema di recupero integrato sia di biomasse agro-zootecniche che di reflui civili e grazie, anche, ai significativi incentivi assegnati alle energie rinnovabili.
Da questo punto di vista gli scenari che possono essere attuati sono molteplici ed ognuno di essi può portare a risultati economici ed a conseguenze, sull'assetto organizzativo delle aziende, differenti, considerato che il biogas prodotto può avere molteplici utilizzazioni, come:
-***combustione diretta in caldaia,*** con produzione di sola energia termica;
-***combustione in motori azionanti gruppi elettrogeni*** per la produzione di sola energia elettrica;
-***combustione in cogeneratori*** per la produzione combinata di energia elettrica e di energia termica;
-***uso per autotrazione come metano al 95-97%***;
- ***immissione,*** dopo opportuna purificazione, ***nella rete di distribuzione del gas naturale*** (1).

2. DIFFUSIONE DEGLI IMPIANTI DI BIOGAS IN EUROPA

A tal proposito bisogna sottolineare come l'U.E. abbia avviato un aggressivo programma di sviluppo per cercare di incentivare la diffusione di colture energetiche e l'utilizzo di residui agro-industriali e zootecnici e di biomasse acquatiche, con l'obiettivo di raddoppiare o triplicare, in pochi anni , il contributo di questa fonte energetica.

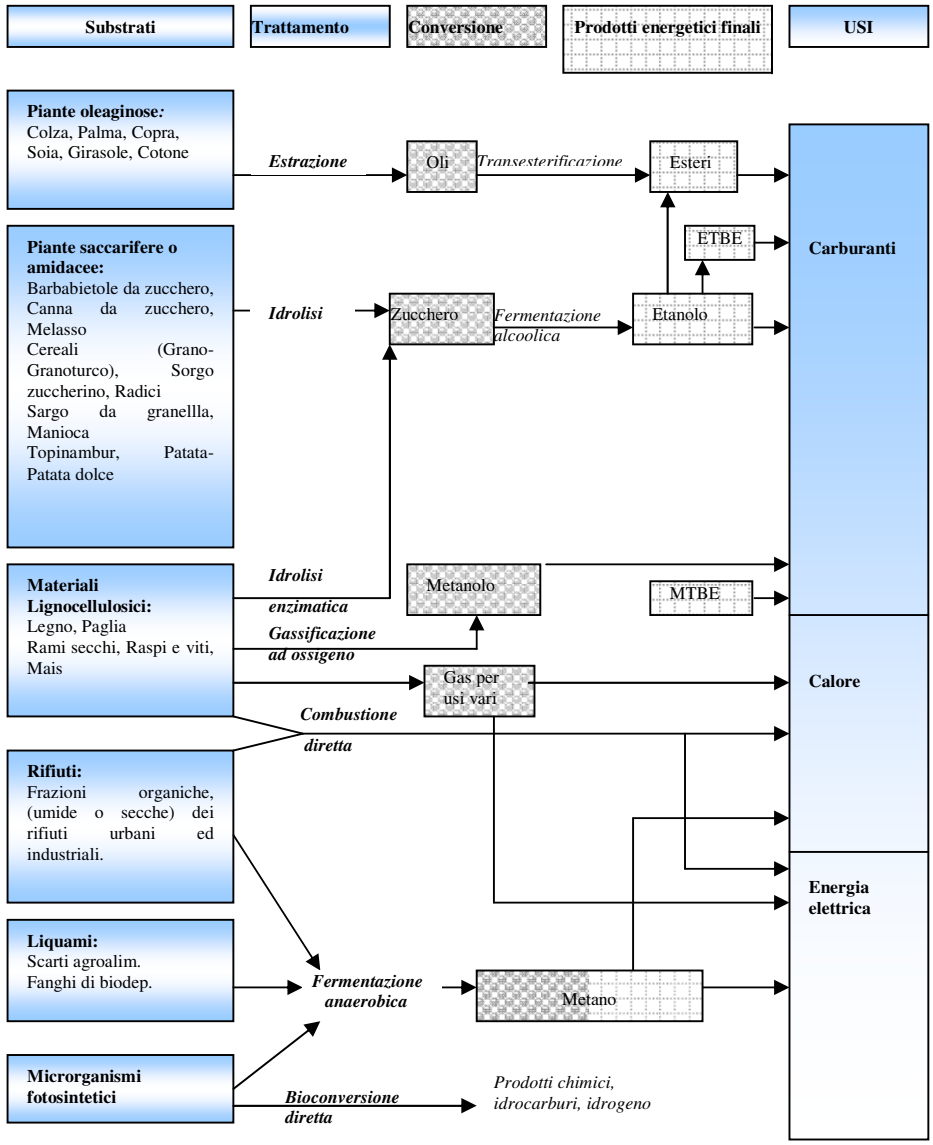


Fig.1- Schema dei principali processi di conversione di biomasse in prodotti energetici e loro usi finali.

In Europa, i primi ad accorgersi di questa realtà sono stati i tedeschi che vantano, in materia, oramai un'esperienza quasi trentennale (2).

La diffusione della digestione anaerobica è incominciata nel settore della stabilizzazione dei fanghi di depurazione urbani ed attualmente si stimano circa 6600 digestori operativi. In particolare:

- circa 1600 digestori operativi nella stabilizzazione dei fanghi di depurazione;

- oltre 400 impianti di biogas per il trattamento delle acque reflue industriali ad alto carico organico;
- circa 450 impianti operativi nel recupero di biogas dalle discariche per rifiuti solidi urbani;
- quasi 4000 impianti operanti su liquami zootecnici in particolare in Germania (oltre 3700), Austria, Italia, Danimarca, Svizzera e Svezia;
- circa 130 impianti trattano frazione urbana di rifiuti urbani e/o residui organici industriali.

Nella tabella seguente è riportata la produzione di biogas, a livello dell'Europa-27, suddivisa per nazione ed espressa in MTep.

Tab.I°- *Produzione di biogas (espressa in MTep) nelle nazioni dell'U.E.-27, variazione percentuale nel biennio 2004/2005 e ripartizione dell'energia prodotta tra calore (MTep) ed elettricità (Gwh).*

Paese	***2004***	***2005***	***Var% 2004/2005***	***Prod. Calore (Mtep) 2005***	***Prod. Elettrica (Gwh) 2005***
Gran Bretagna	1491,70	1782,60	16,32%	0,066	4783
Germania	1294,70	1594,40	18,80%	0,084	5564
Italia	335,50	376,50	10,89%	0,037	1313
Spagna	295,10	316,90	6,88%	0,014	879
Francia	207,00	209,00	0,96%	0,055	460
Olanda	126,20	126,20	0,00%	0,023	261
Svezia	105,10	105,10	0,00%	0,031	32
Altri	422,00	448,00	5,80%	0,114	1184
TOTALE	**4277,30**	**4958,70**		**0,424**	**14476**

Fonte:*Biogas Barometer, 2006*

La produzione di biogas, nel 2005, è stata complessivamente di quasi 5 milioni di TEP, di cui :

- 3,17 MTep, pari al 64%, ha avuto origine dal trattamento di discariche di rsu.;
- 0,93 MTep, corrispondenti al 18,8% , provenienti da fanghi di depurazione industriali e civili;
- 0,85% MTep, equivalenti al 17,2% da altre fonti, ivi compresi i liquami zootecnici ed altri impianti agricoli dedicati (3).

In termini di produzione primaria, la Gran Bretagna e la Germania hanno fatto registrare un forte incremento tanto che la loro produzione di biogas è raddoppiata nel corso degli ultimi quattro anni ed adesso occupano i primi due posti, seguiti, a grande distanza, da Italia e Spagna, e questi, a loro volta, da Francia, Paesi Bassi, Svezia, Austria, Belgio, Danimarca, Lussemburgo (Tabella I°).

Circa gli usi finali, solo il 9% del biogas prodotto è stato utilizzato per la produzione di calore, mentre, la maggior parte, è stato utilizzato per produrre energia elettrica che, nel 2005, è ammontata a 14,5 miliardi di kWh.

Sulla base dell'attuale trend, che ipotizza maggiori sforzi anche da parte delle altre Nazioni, potenzialmente forti produttori come Italia, Spagna e Francia, si stima che

la produzione al 2010 sfiorerà i 9,0 MTep senza, peraltro, raggiungere i 15 MTep tanto auspicati (4).
La graduatoria riflette la situazione degli interventi governativi che sono stati più disponibili proprio in Germania e Gran Bretagna.
Infatti il governo tedesco ha fissato un prezzo per l'energia elettrica da biogas di 0,215 €/KWh ed eroga, in genere, anche una sovvenzione che parte da un minimo del 25% del costo dell'investimento. E, difatti, in questo Paese si sta verificando un notevole incremento di impianti. I dati, che nel 2005 dichiaravano circa 2700 impianti esistenti, con una potenza elettrica installata di oltre 665 MW, a distanza di soli due anni, nel 2007, evidenziano già 3711 digestori anaerobici agricoli di media e piccola dimensione che operano nella produzione di elettricità in unità di cogenerazione, con una potenza elettrica complessiva di 1270 MW (5).
In Gran Bretagna la produzione di energia elettrica da biogas ha beneficiato particolarmente del sistema nazionale dei certificati verdi a partire dal 2002. Il recupero di biogas dalle discariche per rifiuti rappresenta in questa Nazione la fonte più importante di energia alternativa da biomasse.
In Lussemburgo viene erogata una sovvenzione pari al 60% del costo dell'investimento ed è possibile ricavare fino ad un massimo di 0,10€/KWh per l'energia venduta.
In Olanda l'energia immessa in rete ha un valore pari a 0,08 €/KWh, ma la nuova normativa, che dovrebbe entrare in vigore a breve, prevede incentivi dello stesso tipo di quelli erogati in Germania.
Ancora più contenuto l'incentivo stanziato in Belgio pari a 0,07 €/KWh, ma a questo deve aggiungersi un "bonus" pari a 0,05 €/KWh termico ceduto per sistemi di teleriscaldamento, per cui si raggiunge un ricavo massimo totale sull'energia venduta pari a 0,12 €/KWh. Bisogna osservare, però, che non viene erogata alcuna sovvenzione per la costruzione degli impianti di digestione anaerobica.
In Francia, infine, l'energia immessa in rete è retribuita con soli 0,05 €/KWh e ciò spiega lo scarso interesse che questo tipo di incentivi ha suscitato nel comparto agricolo (6).

3. DIFFUSIONE DEGLI IMPIANTI DI BIOGAS IN ITALIA

In Italia, le prime applicazioni relative ad impianti di produzione di biogas da fermentazione anaerobica di materiali organici di origine agricola, avvenute alla metà degli anni '70, erano finalizzate, prevalentemente, a risolvere i problemi relativi agli allevamenti intensivi dei suini. Tali esperienze, supportate da sperimentazioni e ricerche, non hanno dato risultati significativi , al punto che, anche per fattori esterni, quali ad esempio la non cedibilità a terzi dell'energia prodotta, i pochi impianti costruiti avevano perso gradualmente interesse fino ad essere abbandonati (7).
Recentemente una scelta politica, molto chiara e netta, a favore delle agro-energie, ha riportato in auge la valorizzazione delle biomasse a fini energetici agevolata, a livello nazionale, dall' emissione di strumenti incentivanti quali:

-***Finanziamenti a bando*** per lo sviluppo e la valorizzazione a fini energetici di biomasse[1].
-***Accesso prioritario al sistema di distribuzione dell'energia elettrica*** concesso all'elettricità fornita da impianti che utilizzano biomasse solide e biogas che hanno ottenuto dal Gestore dei Servizi Elettrici (GSE) la ***"qualifica"*** di *Impianti Alimentati da Fonti Rinnovabili* (IAFR)[2]*;*
-***Utilizzo di Certificati Verdi*** che attestano l'avvenuta produzione di una certa quantità di elettricità da impianti IAFR*;*
I Certificati Verdi (CV), secondo quanto disposto dall'art.5, comma 1 del DM 11/11/99, sono veri e propri titoli, di valore pari o multiplo di 100 MWh, attestanti la produzione di energia elettrica da IAFR, negoziabili sul mercato elettrico ed emessi e controllati dal GSE. Essi possono essere emessi:
- ***a consuntivo***: Il produttore/importatore chiede al GRTN il rilascio dei CV in base alla sua produzione dell'anno precedente;
- ***a preventivo***: Il produttore/importatore chiede al GRTN il rilascio dei CV in base alla produzione attesa per quello stesso anno o per quello successivo, salvo verifica "a posteriori" sulla effettiva produzione dell'impianto dell'anno precedente.
Gli operatori possono adempiere all'obbligo di immissione nel sistema elettrico di energia rinnovabile, imposto dal Decreto Bersani, con le seguenti modalità:
- producendo direttamente energia rinnovabile;
- acquistando un numero corrispondente di CV dal GRTN;
- acquistando un numero corrispondente di CV da altri produttori mediante contratti bilaterali o contrattazioni sul mercato elettrico.
Di conseguenza i CV possono essere scambiati:

---

[1] A questo proposito, infatti, bisogna ricordare che, la Direttiva 96/92/CE, recante le norme comuni per il mercato dell'energia elettrica, recepita in Italia dal Dlgs 16/03/1999 n°79, noto come "Decreto Bersani", ha posto particolare attenzione all'integrazione tra obiettivi economici ed ambientali, allo sviluppo delle FER ed ai vincoli di emissione dei gas serra imposti dal Protocollo di Kyoto.Per incentivare la produzione di e.e. da fonti rinnovabili il Decreto Bersani aveva inizialmente previsto per gli operatori l'obbligo di immettere nel sistema elettrico nazionale, nell'anno successivo, una percentuale di energia rinnovabile pari al 2% dell'energia eccedente i 100 GWh prodotti o importati nell'anno di riferimento. Il Decreto del Ministero dell'Industria, del Commercio e dell'Artigianato (MICA) dell'11/11/1999 ha dato attuazione all'art. 11 del Decreto Bersani introducendo proprio i Certificati Verdi in sostituzione del vecchio e superato criterio di incentivazione tariffaria noto come Cip 6/92.

[2] La procedura per ottenere il rilascio dei Certificati Verdi consiste nel:
-richiedere al GSE il riconoscimento IAFR;
- avuto il riconoscimento, si può richiedere al GSE l'emissione dei Certificati Verdi per l'anno in corso;
- per gli anni successivi all'entrata in produzione dell'impianto, deve essere presentata la dichiarazione fatta dall'Ufficio Tecnico Imposta di Fabbricazione (UTIF) che dimostrerà la produzione effettiva.
Inizialmente il diritto a ricevere i CV valeva per gli 8 anni successivi al periodo di avviamento e collaudo degli impianti.

- su un apposito mercato dal Gestore del Mercato Elettrico tra i soggetti obbligati a consegnarli al GRTN ed i soggetti titolati a riceverli dal GRTN in quanto produttori di elettricità da fonti energetiche rinnovabili (FER);
- mediante contratti bilaterali tra soggetti detentori di CV ed i soggetti all'obbligo.

Successivamente il Dlgs 387 del 29/12/2003, in attuazione della Direttiva 2001/77/CE, ha reso operativa in Italia la suddetta direttiva ed, in particolare, per l'incentivazione della produzione da FER col sistema dei CV, ha previsto:

- a decorrere dal 2004 e fino al 2006, l'incremento annuale pari a 0,35%, rispetto alla base del 2%, fissata dal Dlgs 16/3/1999 n°79, della quota minima di elettricità prodotta da impianti alimentati da FER che, nell'anno successivo, deve essere immessa nel sistema elettrico (art.4);
- l'inclusione dei rifiuti tra le fonti energetiche ammesse a beneficiare del regime riservato alle FER (art.17);
- la razionalizzazione e semplificazione delle procedure autorizzative per la costruzione degli impianti alimentari dalle FER (art.12);
- l'introduzione delle centrali ibride, che producono e.e. utilizzando sia fonti non rinnovabili che rinnovabili, ivi inclusi gli impianti di co-combustione;
- la modifica del valore minimo dei CV da 100MWh a 50 MWh.

Nel mercato dei CV, la domanda è costituita dall'obbligo per produttori ed importatori di immettere annualmente una quota di energia prodotta da FER che, nel biennio 2002-2003 è stata pari al 2% di quanto prodotto e/o importato da fonti convenzionali nell'anno precedente; successivamente, nel triennio 2004-2006, è stata incrementata dello 0,35% per anno e per i successivi trienni 2007-2009 e 2010-2012 l'incremento sarà uguale o superiore.

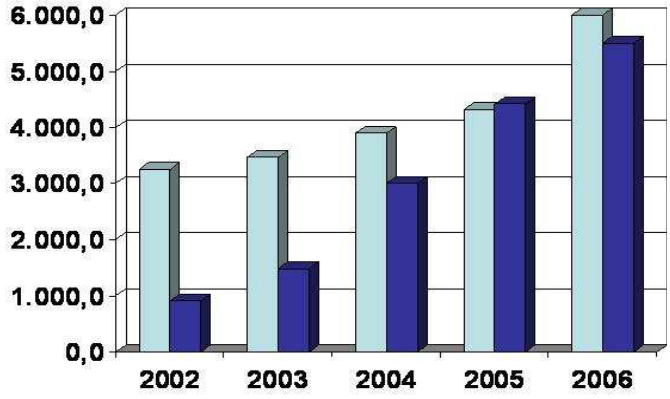


Fig.2 – Andamento della domanda ( ) e dell'offerta (, espressa in Gwh, di Certificati Verdi nel quinquennio 2002-2006.

Il prezzo dei CV è variabile ed è fissato di anno in anno sulla base degli incentivi concessi. Dall'andamento, riportato in figura 2, si evince che domanda e offerta

tendono ad equipararsi nel tempo e ciò sta comportando, di conseguenza, una riduzione del prezzo dei CV sul mercato (Fig. 3).

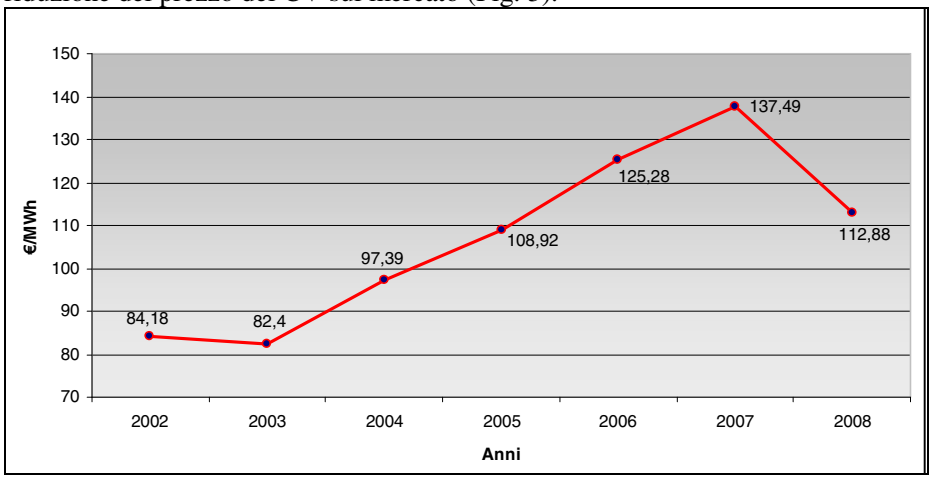


Fig.3 – Variazione del prezzo dei Certificati Verdi nel periodo 2002-2008.

La legge prevede due categorie distinte di incentivo a secondo che la potenza elettrica degli impianti sia superiore o inferiore a 1MW.
Nel primo caso *(>1MW)* la forma del beneficio economico viene calcolata per ciascun impianto attraverso il riconoscimento di Certificati Verdi (1 per ogni MW) in numero pari all'energia elettrica prodotta nell'anno precedente, moltiplicata per il coefficiente 1,8.
Nel secondo caso *(<1MW)* il produttore ha diritto, in alternativa, ai certificati verdi e, su specifica richiesta, a una tariffa fissa omnicomprensiva pari a 0,30€/KWh. In pratica si tratta di un meccanismo simile al *"conto energia"* applicato attualmente all'energia elettrica prodotta da pannelli fotovoltaici.
Questa forma di sostegno può essere riconosciuta a precise condizioni:
- che le biomasse ed il biogas derivino da prodotti agricoli, da allevamento e forestali, inclusi i sottoprodotti;
- che questi prodotti siano ottenuti nell'ambito di intese di filiera o contratti quadro così come disciplinati dagli art. 9 e 10 del dlgs 102/2005;
- che questi prodotti siano ottenuti da filiere corte, cioè quelle in cui i prodotti sono ricavati entro un raggio di 70 Km dall'impianto che li utilizza per generare elettricità.

Dopo un tribolato iter parlamentare, il 28 Novembre 2007 sono stati approvati i nuovi ***"Certificati Verdi"*** di tipo agricolo, previsti nella conversione in legge con modificazioni del dlgs 159/2007, meglio conosciuto come *"collegato alla finanziaria"*.
E' previsto dall'art.30-bis della finanziaria 2008, al comma 7, che, a partire dallo stesso anno e fino al raggiungimento dell'obiettivo minimo della copertura del 25% del consumo interno di energia elettrica da fonti energetiche rinnovabili, il GSE, su richiesta del produttore, ritiri i Certificati Verdi in scadenza nell'anno, oltre a quelli necessari ad assolvere all'obbligo della quota minima, ad un prezzo medio pari a

quello riconosciuto nell'anno precedente dal GSE. Ciò significa che non si correrà alcun rischio di mancato collocamento dei certificati, considerato, in pratica, l'obbligo del ritiro da parte del GSE.
In entrambi i casi la legge prevede una durata dei Certificati Verdi per un periodo di 15 anni (Dlgs 152/2006) dalla data di esercizio commerciale dell'impianto (Qualifica IAFR presso GRTN). Ogni 3 anni con decreto dei Ministri competenti potrà essere aggiornato sia il coefficiente di moltiplicazione, relativamente agli impianti sopra al MW, sia la tariffa omnicomprensiva.
Per i medesimi impianti, qualunque sia la potenza elettrica, è previsto che l'accesso agli incentivi, limitato solo alle aziende che garantiranno la tracciabilità e la rintracciabilità di filiera, sia cumulabile con altri incentivi pubblici di natura nazionale, regionale, locale o comunitaria in conto capitale o conto interessi con capitalizzazione anticipata, non eccedenti il 40% del costo dell'investimento(8).
In Italia si contano circa 1350 impianti industriali che mediante l'utilizzazione di biomasse contribuiscono già alla produzione di energia elettrica (103 MW) e di energia termica (1240 MW). All'ENEL, a seguito dei provvedimenti legislativi per la promozione degli investimenti e l'incentivazione all'autoproduzione di elettricità (CIP 6/92), sono state inoltrate proposte di convenzione per la produzione di energia elettrica dalle biomasse per circa 700 MW (60 MW biogas; 306,2 MW residui agricoli; 196 MW rifiuti solidi urbani; 129,3 MW altri rifiuti).
Tenuto conto delle possibilità ulteriori offerte da coltivazioni dedicate, anche in terreni marginali, che, in Italia, hanno un'estensione complessiva stimata pari a 3 milioni di ettari, in grado di offrire una produzione annua di biomassa secca di 10 t/ettaro (con potere calorifico inferiore di 4000 Kcal/Kg), si ritiene tecnicamente fattibile l'attivazione, per il 2010, di impianti per complessivi circa 2500 MW.
Si ha diritto a tale incentivazione per un periodo di 15 anni (Dlgs. 152/2006) dalla data di esercizio commerciale dell'impianto (Qualifica IAFR presso GRTN)
Il biogas adesso è una realtà che lentamente si sta diffondendo anche in Italia. Gli impianti di digestione anaerobica sono ormai tecnologicamente collaudati. Da un punto di vista economico sono investimenti che rientrano in tempi contenuti anche se non adeguatamente supportati. Un caso italiano tra i più noti è l'azienda Mengoli di Bologna che ha saputo sfruttare i vantaggi connessi con la presenza nelle vicinanze di agroindustrie che producono scarti fermentescibili in ambiente anaerobico. Anche se non totalmente gratuiti, questo insieme di materie prime consentono di alimentare un codigestore da 350 KWe di potenza installata.(9).
Secondo un censimento del GSE al 30/06/ 2008 erano operanti in Italia 362 impianti di digestione anaerobica per la produzione di biogas : 202 alimentati con effluenti zootecnici (di cui 88 impianti semplificati che utilizzano solo liquame suino e bovino), 121 con fanghi di depurazione civile, 10 con la frazione organica dei r.s.u., 22 alimentati con reflui agro-industriali ed, infine, 7 con altre tipologie di substrato (10). L'area con maggior numero di impianti è la Lombardia (72), seguita dal Trentino-Alto Adige (34) e dall'Emilia-Romagna (28), il Veneto(23) ed il Piemonte (16).
La Confagricoltura, nell'ultima edizione di "Vegetalia" svoltasi a Cremona, ha presentato il progetto ***"Dalla Terra alla Luce"***, nel quale si prevede un

investimento di 180 milioni di euro per la realizzazione di altri 30 nuovi impianti in otto regioni italiane (Lombardia, Piemonte, Emilia-Romagna,Veneto, Toscana, Umbria, Puglia e Calabria) alimentati con fonti rinnovabili di origine agricola con una produzione complessiva di 53 MW elettrici e 20 MW termici, secondo il seguente prospetto:

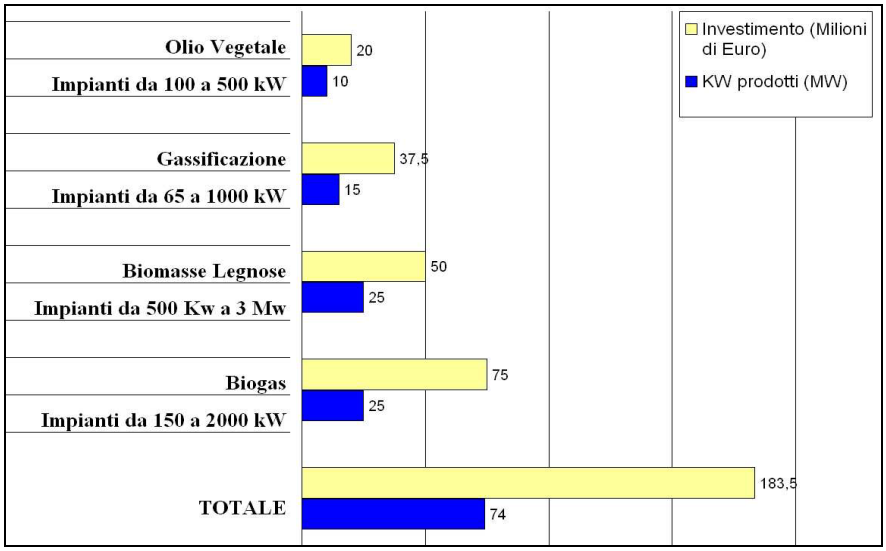


Fig.4- Prospetto riassuntivo del progetto "Dalla Terra alla Luce".

La forma di finanziamento ipotizzata prevede l'impiego di 80 milioni di euro in 15 anni, con un costo medio annuo di 5,5 milioni di euro e con un frazionamento dell'importo totale decrescente negli anni a seconda del piano di ammortamento. Per la cessione dell'energia prodotta sono già stati presi contatti fra Confagricoltura ed apposite società di Trading (Edison, Iride) che consentiranno di commercializzare l'energia prodotta (11).

Come si può osservare da questo progetto, è proprio il settore del biogas che beneficerà dell'investimento più cospicuo per la produzione complessiva di 25 MW mediante impianti da 150 e fino a 2000 kW.

Negli ultimi anni sta crescendo l'utilizzo della digestione anaerobica nel trattamento della frazione organica raccolta in modo differenziato oppure separata da appositi impianti di preselezione della frazione organica dei r.s.u. (FORSU) in miscela con altri scarti organici industriali o con liquami zootecnici (co-digestione).

Relativamente all'uso del biogas la cogenerazione, ossia la produzione contemporanea di calore ed elettricità, è attualmente l'impiego prevalente.

CONCLUSIONI

Negli ultimi dieci anni nei vari Paesi Europei sono state messe a punto tecnologie più efficienti e con rese migliori in biogas rispetto al passato e si sono via via

sviluppate politiche di sostegno finalizzate ad incrementare la produzione energetica da fonti alternative.
Anche nel nostro Paese sono state intraprese iniziative di incentivazione per cercare di dare un impulso consistente alla produzione di energia da fonti rinnovabili.
Lo sfruttamento a fini energetici delle biomasse, con la tecnologia della digestione anaerobica, può assumere un ruolo strategico, contribuendo ad uno sviluppo sostenibile ed equilibrato del nostro pianeta. In particolare, il settore zootecnico può rappresentare un punto di forza per la produzione, su larga scala, di biogas in Italia. I vantaggi sono, infatti, molteplici:

- miglioramento della "sostenibilità ambientale" degli allevamenti;
- riduzione dei problemi ambientali legati alla emissione in atmosfera di metano, ammoniaca, composti organici volatili (COV) non metanici, del livello di odore;
- integrazione al reddito "dall'energia verde";
-possibilità di produrre biogas esclusivamente per autoconsumo creando, in tal modo, un sistema produttivo "integrato" perfettamente ecosostenibile.

BIBLIOGRAFIA

[1] - Piccinini S.-Le tecnologie di produzione del biogas-CRPA-Reggio E. 30/05/2007;
[2] - Terrosi M.P. Il gas dell'alleanza tra rifiuti e batteri- Energy- Enel S.p.A.-2009;
[3] - Sala C.– Produzione di Biogas in Europa- Master bioenergia Weblog23/05/2008;
[4] - Libro Bianco per la valorizzazione energetica delle fonti rinnovabili Roma- Aprile 1999;
[5] - Soldano M.- Biogas: Situazione e prospettive- Ravenna 03/12/2008;
[6] - Olivier Bertrand- Energia: La Francia ha scoperto il biogas agricolo-Agricoltura Nuova 29/04/2004 p.17;
[7] - Mengoli M. – Biogas da reflui zootecnici e da materiali vegetali di origine agricola- Palazzo Trinci- Foligno 25/10/2007;
[8] - Berton M.-L'Informatore agrario n°45-30 Nov.-6Dic.2007;
[9] - Patacca S., Frascarelli A.- Biogas: Esempio di applicazione aziendale. Perugia 21/02/2007 p.114-122;
[10] - Dati GSE al 30/06/2008;
[11] - Bernardelli M.- Agroenergie, decollano i microimpianti. Terra e Vita 17/02/2007 pag.14.

RENDICONTI DEL CIRCOLO MATEMATICO DI PALERMO
Serie II, Suppl. 81 (2009), pp. 107-119

CONTINGENT VALUATION E STIMA DELLA DOMANDA DI TURISMO NATURALISTICO NELLE AREE PROTETTE

Andrea Cirà, Gaetano Maggio, Fabio Carlucci

ABSTRACT

Il dibattito sulla valorizzazione e lo sfruttamento delle risorse turistiche si inquadra, in generale, in un'ottica di accresciuta sensibilità alle problematiche ambientali che ha coinvolto l'attenzione di politici, operatori economici e popolazione residente. In particolare la gestione di aree protette risponde, anche, alla necessità di proporre e coordinare modelli di sviluppo sostenibile che coniughino la tutela ambientale con lo sviluppo sociale ed economico, fornendo alle comunità locali fonti di reddito alternative.

Focalizzeremo la nostra attenzione sul territorio del Parco delle Madonie e il lavoro rientra nell'ambito di una ricerca più ampia, il cui obiettivo principale consiste nel definire se esistono le condizioni per la creazione di un sistema turistico integrato che coinvolga quella parte del comprensorio più marginale dal punto di vista economico, che coincide con il territorio dei comuni posti ad altitudini maggiori. Infatti, essendo ormai fallito il tentativo – più volte annunciato da politici ed esponenti delle pubbliche amministrazioni locali – di produrre sviluppo locale mediante la ricerca di forme di integrazione con il sistema turistico balneare ormai consolidatosi lungo la fascia costiera del parco, i comuni montani si trovano nella difficile situazione di doversi inventare processi di specializzazione turistica basati sulla fruizione delle risorse naturali e tendenti, dal punto di vista economico, a massimizzare la spesa dei turisti non residenti.

Le azioni di policy individuate avranno un impatto sull'economia locale che sarà misurato, in sede di previsione, utilizzando tecniche di tipo ACB. Per poter produrre questo esercizio valutativo sarà necessario poter disporre non solo delle statistiche riguardanti i flussi turistici attuali, ma anche di una possibile previsione sulle potenzialità della domanda in relazione ai servizi turistici esistenti o da creare in futuro.

Lo scopo ovviamente è quello di produrre una prima stima della spesa turistica (attuale e potenziale) legata alla capacità attrattiva dell'area naturale mediante la predisposizione delle seguenti fasi dell'indagine: a) individuazione delle caratteristiche

socio economiche e delle preferenze individuali dell'attuale domanda turistica nei comuni del parco; b) ricostruzione della curva di domanda sia per il turismo escursionistico che per il turismo stanziale e stima della spesa attuale; c) previsione del possibile incremento di domanda e di spesa turistica che può verificarsi in seguito a possibili ipotesi di riorganizzazione delle attività ricettive e dei servizi connessi.

Il presente lavoro, quindi, riporta i risultati di una recente indagine sulla domanda turistica effettuata sul territorio del parco ed è da considerare come una fase di pre-testing. I risultati ottenuti sono molto incoraggianti in termini di possibilità di creare percorsi di crescita basati sulla attenta fruizione delle risorse naturalistiche e danno precise indicazioni sulle modalità di intervento da proporre per il potenziamento/riadeguamento dell'offerta locale e sugli elementi di stimolo della domanda di turismo naturalistico (*ecotourism*). L'utilizzo della *Contigent Valuation*, inoltre, si è rivelata un potente strumento di indagine in quanto ha permesso di mostrare l'esistenza di una buona disponibilità a pagare per la fruizione del servizio turistico in area parco, che caratterizza una domanda turistica potenziale tuttora in massima parte inespressa che andrebbe intercettata mediante intelligenti interventi di marketing turistico territoriale.

1. Le politiche di sviluppo nelle aree naturali tra opportunità e vincoli economici

Le politiche ambientali si trovano ancora oggi ad affrontare, in alcuni parchi naturali, il problema di una difficile coesistenza con le esigenze di sviluppo socio economico delle comunità locali. E' sentita, infatti, l'esigenza di porre maggiore attenzione sia all'approfondimento dell'analisi sulle dinamiche territoriali che hanno generato profondi cambiamenti nella struttura organizzativa, sociale e produttiva di questi territori, sia alla definizione di strategie di sviluppo sostenibili, che concentrandosi sulla ricostruzione delle identità locali, possano consentire la valorizzazione delle risorse naturali, culturali ed umane in modo da potere individuare traiettorie economicamente produttive e durevoli nel tempo.

Posto in questi termini il problema va affrontato in un'ottica di sviluppo locale, nella quale il ruolo centrale è giocato dal territorio in quanto fattore in grado di incidere sulle dinamiche evolutive dei processi economici e sociali già in atto.

Negli ultimi anni si è assistito, in generale, a politiche tendenti a favorire un aumento degli investimenti pubblici e privati per lo sviluppo del settore turistico, perché ritenuto capace di esprimere un'azione trainante sull'economia locale, agendo

positivamente anche in termini di riduzione dei livelli di disoccupazione. Questa scelta precisa dell'operatore pubblico tendente a costituire, in alcuni casi, una sorta di specializzazione turistica del territorio, ha reso evidente la necessità di approfondire meglio la relazione tra turismo e crescita e tra turismo e sviluppo locale, indagando quali implicazioni economiche e quali prospettive di crescita di lungo periodo possono effettivamente essere generati. I risultati derivanti da un recente filone di studi sviluppatosi in Italia e all'estero (cfr. fra gli altri Lanza, 1995; Lanza, Temple e Urga, 2002; Pigliaru, 1997) sono confortanti, nel senso che il settore turistico può in alcuni casi assicurare tassi di crescita uguali se non superiori a quelli che caratterizzano il settore industriale. La spiegazione di questo fenomeno è riconducibile principalmente a due aspetti legati alla possibile alternativa specializzazione di un territorio o di una economia nel settore industriale o nel settore turistico: l'innovazione tecnologica (che notoriamente caratterizza il primo come settore leader) e l'andamento nel tempo dei prezzi relativi ai beni prodotti dai due settori. In particolare, partendo un semplice modello di crescita endogeno, alcuni autori (Pigliaru et al., 2007) giungono alla conclusione che nonostante il settore industriale sia più favorito grazie ad un tasso tecnologico più elevato, questa situazione potrebbe venire ribaltata nel momento in cui si considera il rapporto di scambio tra il prezzo del bene turistico e il prezzo del bene industriale. In particolare quando la variazione dei prezzi relativi (cioè il rapporto tra prezzi turistici e prezzi industriali) risulti più favorevole al prodotto turistico e riesce a compensare il gap tecnologico esistente tra i due settori. Ulteriori approfondimenti dell'analisi hanno considerato la possibilità di trasferimenti di tecnologia tra settori, dal settore leader a quello turistico, in particolare evidenziando la possibilità di ulteriori vantaggi in termini di crescita per quest'ultimo.

Il legame con le possibilità di sviluppo locale risulterebbero più stretti quando si approfondisce la relazione tra turismo e risorse naturali. Infatti, le forme di turismo che si basano sullo sfruttamento di risorse naturali esauribili e non riproducibili di qualità elevata rispondono a regole di mercato specifiche, caratterizzandosi come *snob goods* a causa della rarità di offerta e della bassa elasticità di sostituzione rispetto al turismo che si basa invece su risorse sfruttate intensamente e con caratteristiche qualitative inferiori (ad esempio il prodotto balneare). Di conseguenza il prezzo della prima tipologia di servizi turistici dovrebbe registrare dinamiche più favorevoli rispetto alle altre. Esistono, quindi, anche ragioni economiche che rendono conveniente adottare un'ottica conservativa o comunque una gestione "cauta" del bene naturale al di là delle finalità di politica protezionistica proprie dell'ente gestore del parco naturale.

In estrema sintesi l'aumento dello sfruttamento della risorsa naturale, ambientale o paesaggistica a fini turistici, comporta un peggioramento della qualità della risorsa stessa. In presenza di una domanda con preferenze caratterizzate da avversione all'affollamento (Butler, 1991), diviene fondamentale riuscire a determinare qual è il grado di sfruttamento ottimale, cioè quel livello di fruizione turistica che concilia redditività commerciale e mantenimento dell'integrità qualitativa delle risorse naturali disponibili. Come si sa, il meccanismo di mercato non conduce spontaneamente a scelte sostenibili nel tempo (Candela, 1996), ecco perché è necessario l'intervento pubblico, che dovrebbe svolgersi in un'ottica di mobilitazione degli attori locali e di concertazione delle strategie da perseguire. dei gruppi di interesse e in definitiva il successo in termini di realizzabilità delle azioni di policies prescelte.

Il lavoro è così strutturato: il prossimo paragrafo riporta una breve descrizione del modello utilizzato per l'analisi della domanda turistica attuale e potenziale, il paragrafo 3 espone i tratti salienti della costruzione del questionario somministrato e le modalità seguite per l'individuazione del campione indagato, nel paragrafo 4 vengono illustrati i risultati delle stime, infine nel paragrafo 5 seguono alcuni iniziali suggerimenti di policy per l'operatore pubblico che verranno approfonditi in un successivo lavoro attualmente in corso di redazione[1].

2. Obiettivo dell'analisi e descrizione del modello utilizzato

Obiettivo della nostra ricerca empirica è stabilire se i visitatori del parco sono disposti a pagare per mantenere e migliorare le condizioni di fruizione turistica dell'area. Inoltre è di particolare interesse stabilire se l'offerta di una gamma più ampia e qualitativamente diversa di servizi turistici può contribuire ad aumentare il numero e la durata delle visite nel parco. A tal fine è stata condotta un'indagine campionaria volta ad analizzare l'esistenza ed il livello della disponibilità a pagare degli attuali utenti, nonché il tipo di servizi utilizzati.

Al fine di determinare se esiste un reale interesse, da parte degli attuali fruitori, alla prosecuzione dell'attività di "conservazione e di tutela" delle risorse ambientali e paesaggistiche svolta dall'Ente parco, si è pensato di adottare la metodologia della *contingent valuation* (CV). Infatti, la presenza contemporanea di valori d'uso e di non uso e la difficoltà di applicare tecniche di stima indirette, vista la mancanza di beni che

[1] Sebbene il lavoro sia frutto di una ricerca comune dei tre autori, i paragrafi 1,3,e 5 sono redatti G. Maggio, il paragrafo 4 da A. Cirà ed il paragrafo 2 da F. Carlucci.

presentano caratteristiche simili a quello oggetto di analisi, riducono fortemente la classe degli strumenti che possono essere utilizzati per stimare il valore economico del paesaggio agrario[2].

Un quesito rilevante che si pone quando si parla di politiche di conservazione del paesaggio riguarda, in particolare, l'individuazione degli strumenti e dei metodi da utilizzare per finanziare l'attività stessa degli enti di gestione dei parchi naturali. Gli studi quantitativi finalizzati a rilevare questo particolare aspetto, proposti in letteratura, sono ancora pochi, così come viene anche messo in evidenza nel lavoro di Cicia e Scarpa (1993) nel quale viene effettuata una ottima rassegna della letteratura in merito alla disponibilità a pagare per il paesaggio rurale. Una conclusione comune a quasi tutti gli studi è la convenienza alla protezione del patrimonio naturalistico. Infatti, moltiplicando la stima della disponibilità a pagare per il numero di individui della popolazione campionata e dividendo tale risultato per la superficie coltivata, si ottengono valori superiori al reddito che si ritrae dal solo sfruttamento del suolo per usi commerciali. Ciò vuol dire che, il valore sociale di questo bene non di mercato è di entità elevata, quindi le politiche di finanziamento agli agricoltori, per le pratiche che permettono di conservare certe forme di paesaggio, sono giustificabili, non solo da un punto di vista sociale, ma anche con riferimento alla efficiente allocazione delle risorse finanziarie.

Sotto l'aspetto puramente economico il problema può essere inquadrato in una prospettiva di più ampio spettro che riguarda la massimizzazione dell'utilità del consumatore.

---

[2] Per valore d'uso s'intende l'utilità attribuita da ciascun utente alla fruizione della risorsa naturale. L'esistenza di una risorsa naturale comporta la possibilità di godere sia di benefici diretti, nel nostro caso specifico derivanti dalle possibilità di crescita dei flussi turistici, dalla possibilità di specializzazione in attività produttive di tipo biologico ecc., sia di benefici indiretti, quali ad esempio maggiore salubrità dell'ambiente. Un altro aspetto del valore d'uso dell'ambiente è quello della possibilità di poter utilizzare in qualunque momento la risorsa ambientale. Questa particolare forma del valore d'uso viene chiamata anche valore d'opzione. Il valore di non uso viene visto sotto una duplice forma, la prima costituita da valore che può essere attribuito al bene quale patrimonio da trasmettere alle generazioni future, la seconda quale valore da attribuire all'esistenza di un bene unico ed irriproducibile nel caso in cui venga definitivamente perso, in altri termini si attribuisce un valore ad un bene indipendentemente dall'uso che se ne fa poiché esso produce un benessere in un soggetto soltanto per il fatto di esistere. Nessuno dei due valori si concretizza in un prezzo di mercato poiché, essendo l'ambiente un bene pubblico, non può essere scambiato in maniera efficiente sul mercato per i motivi sopra detti. La letteratura offre spunti diversi per la valutazione dei beni pubblici utilizzando tecniche di stima indirette e tecniche dirette. Le prime si basano sul concetto delle "preferenze rivelate", si cerca cioè di inferire il valore di una particolare caratteristica di un bene pubblico esaminando la domanda di un altro bene scambiato sul mercato che presenta la stessa caratteristica, rientrano in questo filone il metodo dei prezzi edonici (Gilley and Pace 1995) e quello dei costi di viaggio (Font 2000). I metodi di stima diretti, basati sulle "preferenze dichiarate", vengono usati quando si tratta di stimare la disponibilità a pagare per un bene pubblico che ha un insieme di caratteristiche che rendono il bene oggetto di analisi unico e che quindi non possono essere considerate separatamente. Fra le tecniche di stima indiretta la più utilizzata è proprio il metodo di valutazione contingente.

Assumiamo che la funzione di utilità indiretta di un singolo consumatore dipenda dal suo reddito *y*, dalle caratteristiche del bene extra mercato da valutare *a* (nel nostro caso il parco) e da altre variabili inclusi i prezzi di mercato e gli attributi dell'individuo che modificano le sue preferenze. In questi casi, la letteratura sulla *Contingent Valuation* ha suggerito differenti metodi per la stima della disponibilità a pagare (DAP). In questo lavoro, utilizzeremo il metodo RUM (*Random Utility Maximization*) basato sull'utilità stocastica. Tale approccio differisce dalle analisi classiche delle funzioni di utilità del consumatore poiché non vengono stimate funzioni secondarie come la funzione di domanda o di spesa. Tale metodo permette quindi di creare un collegamento diretto fra il modello di tipo statistico per l'analisi dei dati osservati ed il corrispondente modello di preferenze microeconomiche della popolazione osservata.

In un'ottica microeconomica il problema della massimizzazione dell'utilità si presenta nella seguente maniera. Ad un individuo viene proposto di pagare un prezzo *P* come contributo per il mantenimento del parco e il miglioramento dei servizi in esso disponibili, spiegando in che modo è possibile coglierne l'utilità.

Formalmente, possiamo rappresentare il problema nella seguente maniera, il soggetto intervistato confronta due alternative. La prima corrisponde alla scelta di contribuire per avere un parco curato, l'utilità di tale scelta viene identificata dalla seguente funzione: $u(y-P,a^1,s)$, dove P è il prezzo proposto agli individui per sostenere l'intervento, a^1 è il vettore delle caratteristiche che presenterebbe il bene ambientale manutenzionato ed s è un vettore di variabili socio economiche relative all'individuo intervistato.

La seconda alternativa individua la scelta di non contribuire al mantenimento del parco e quindi avere la seguente funzione di utilità: $u(y,a^0,s)$ dove a^0 è un vettore di fattori caratterizzanti un paesaggio non curato.

Sotto l'aspetto statistico possiamo riformulare il problema scomponendo le suddette funzioni di utilità in due parti, la prima rappresenta la componente deterministica che può essere scritta come $v(y,a,s)$, la seconda, che rappresenta la parte non osservabile della funzione di utilità, segue un comportamento stocastico ed è indicata con il simbolo ε. In altre parole, il modello RUM assume che mentre l'individuo conosce le proprie preferenze, il ricercatore non le conosce o non può rilevarle e quindi vengono trattate come casuali. Queste componenti non osservabili potrebbero essere caratteristiche

dell'individuo e/o attributi del bene e rappresentare quindi sia le diverse preferenze degli individui sia l'errore di misurazione ε.

È proprio quest'ultima, di cruciale importanza, che rappresenta l'idea di massimizzazione dell'utilità casuale (RUM). La nozione di RUM costituisce quindi il collegamento fra il modello economico di massimizzazione dell'utilità ed il modello statistico dei dati osservati.

Per i due scenari avremo rispettivamente che:

$$u(y-P,a^1,s)=v(y-P,a^1,s)+\varepsilon^1 \qquad [1]$$

per il p rimo caso, mentre nel secondo avremo:

$$u(y-P,a^0,s)=v(y-P,a^0,s)+\varepsilon^0$$

I soggetti intervistati, che assumiamo siano individui razionali, avranno un interesse a contribuire al mantenimento del parco se il miglioramento delle caratteristiche del parco ($a^1>a^0$) determinerà un accrescimento dell'utilità dell'individuo. Riprendendo il concetto Hicksiano di surplus equivalente H, possiamo formulare la seguente equazione: $u(y-H,a^1,s)=u(y,a^0,s)$. Essa mette in evidenza che affinchè un soggetto sia disposto a pagare una somma di denaro *H* per il mantenimento del parco è necessario che l'utilità che ritrae dal parco curato sia eguale all'utilità del soggetto in assenza di intervento.

In definitiva possiamo dire che un soggetto intervistato sarà disposto a pagare se viene verificata la seguente sequenza di condizioni:

$$u(y-P,a^0,s)\geq u(m,a^1,s)\rightarrow v(y-P,a^0,s)+\varepsilon^0\geq v(m,a^1,s)+\varepsilon^1\rightarrow$$

$$\rightarrow v(y-P,a^0,s)-v(m,a^1,s)\geq+\varepsilon^1-\varepsilon^0\rightarrow\Delta v\geq\Delta\varepsilon$$

Ciò vuol dire che affinché un soggetto dia un responso positivo alla disponibilità a pagare occorre che la variazione della componente deterministica sia maggiore uguale alla variazione della componente probabilistica. Traducendo questa affermazione in termini di probabilità di verificare una risposta positiva, se si propone ad un intervistato il pagamento di un prezzo *P* come contributo alla cura del parco, possiamo scrivere che:

$$\Pr(Si\mid P,a,s;\theta)=\Pr(\Delta v\geq\Delta\varepsilon;\theta)\equiv F_{\Delta\varepsilon}(\Delta v;\theta)$$

Dove θ indica un vettore di parametri che specificano la probabilità di responso positivo e $F_{\Delta\varepsilon}(\Delta v;\theta)$ rappresenta la funzione parametrica di distribuzione cumulata data dalla differenza delle due componenti deterministiche dell'utilità Δv.

Il problema che si pone è quello di stimare il vettore di parametri θ, a tal fine, nell'applicazione che verrà riportata nel paragrafo 5, utilizzeremo uno stimatore di massima verosimiglianza.

3. Costruzione del campione e predisposizione dei questionari

In questo lavoro si utilizzerà un modello di *Stated Preferences* per valutare la disponibilità a pagare dei visitatori del parco e il possibile ritorno economico che si potrebbe avere nel caso in cui l'Ente parco introducesse possibili forme di contribuzione per la fruizione delle zone attrezzate.

A tal fine sono stati distribuiti alcuni questionari ai visitatori ed ai residenti nei comuni dell'area del Parco[3] per comprendere se e quanto si è disposti a contribuire per il miglioramento del territorio protetto.

Il questionario somministrato agli intervistati è suddiviso in tre parti, nella prima sono state rilevate le variabili che possono darci indicazioni in merito alle preferenze dei visitatori. La seconda sezione mira a rilevare le caratteristiche socio economiche dei visitatori. Nella terza sezione sono stati inseriti quesiti utili a stabilire quali politiche di sviluppo turistico del territorio si presentano più adatte ad attrarre un maggior numero di visitatori e quali sono gli interventi economici che maggiormente rispondono alle preferenze di questi ultimi. Per ovvi motivi di sintesi in questo lavoro non saranno inserite analisi sull'intero set di domande effettuate e faremo solo alcune brevi considerazioni sugli interventi di policy che, comunque, saranno sviluppati in un prossimo lavoro.

4. Descrizioni dei risultati della stima del modello

Al fine di stimare la disponibilità a pagare dei visitatori si è costruita una funzione di utilità le cui variabili esplicative sono volte a rilevare se la scelta di fruire del parco

[3] La letteratura empirica suggerisce che il campione di soggetti selezionati deve essere costruito in maniera del tutto casuale, anche se rientrante fra coloro che saranno successivamente interessati dalle politiche oggetto di analisi. Abbiamo preferito, invece, somministrare i questionari a persone che potessero esprimere un giudizio di stima con sufficiente cognizione di causa derivante da una situazione di residenza e/o da precedenti occasioni di fruizione del territorio del parco delle Madonie e/o di altri parchi regionali. Si ritiene, infatti, che soltanto questa tipologia di individui può rispondere in maniera più oggettiva sulla validità e sulla convenienza degli interventi che possono essere prospettati in quanto ha già sedimentato la conoscenza sulle potenzialità offerte dall'area del parco quale luogo di fruizione naturalistica, di svago e di riposo e di conseguenza ha maturato adeguata riflessione sulla attribuzione di un valore monetario.

mediante il pagamento di una forma qualsiasi di contribuzione è condizionata oltre che dalla tariffa prevista anche da altri fattori soggettivi ed oggettivi del visitatore. Quindi, nella nostra funzione di utilità oltre alla variabile prezzo del pedaggio (*TICKET*) sono state inserite le variabili che di seguito vengono descritte.

Le variabili di scelta del parco determinate dai gusti e dalle abitudini del visitatore sono le seguenti.

I motivi della visita (*MOVI*), essa ci dice se il visitatore si reca nel parco per motivi di svago o di lavoro. Sotto l'aspetto teorico non è possibile fare alcuna assunzione sul segno che assumerà tale variabile, il suo utilizzo è volto semplicemente ad indagare se esiste una correlazione fra il motivo della visita e l'utilità che l'utente riceve quando soggiorna nel territorio del parco.

Le modalità di fruizione delle strutture ricettive (*UTSTRIC*), fornisce indicazioni sulle preferenze dei consumatori e quindi ci si attende che il loro utilizzo fornisca un'utilità aggiuntiva ai visitatori.

Fra le variabili di tipo socio-economico, a nostro avviso di rilievo per la definizione della funzione di utilità, abbiamo inserito le classi di reddito (REDDITO) dei visitatori, la composizione del nucleo familiare (NUCFAM), il titolo di studio (TITSTUD) che unitamente al variabile iscrizione ad associazioni ambientalistiche (ISCASAMB) ci fornisce una *proxy* della cultura del visitatore o del capofamiglia. A queste variabili, in linea teorica, ci si aspetta che sia collegata un'utilità positiva al crescere del rispettivo livello.

Nome Variabile	**Range**	**Segno atteso**
TICKET	1-4	-
MOVI	0-1	Nd
UTSTRIC	0-1	+
REDDITO	0- 30.000	+
NUCFAM	1-5	+
TITSTUD	1-3	+
ISCASAMB	0-1	+

A questo punto è possibile definire la funzione di utilità della fruizione del parco nella seguente maniera: *U=f(TICKET, MOVI, UTSTRIC, REDDITO, NUCFAM, TITSTUD, ISCASAMB)*, e partendo da essa è possibile definire la disponibilità a pagare (WTP) dei visitatori come descritto nel paragrafo 3.

La forma funzionale che utilizzeremo in questo lavoro per stimare gli effetti delle variabili personali e di policy sul livello e sulla cause di variazione della disponibilità a

pagare delle differenti categorie di soggetti intervistati è quella logit multinomiale. Questa forma funzionale presenta il vantaggio di avere un numero elevato di informazioni sia sulla disponibilità a pagare di ciascuna classe di soggetti intervistati, sia sugli effetti che una policy avrebbe sul livello di successo dell'intervento.

Inoltre è possibile segmentare la domanda per fasce tariffarie cosa difficile per altre forme funzionali di determinazione dei livelli di disponibilità a pagare utilizzate da altri autori, che utilizzano modelli come i normali logit o probit.

La funzione che si otterrà utilizzando un modello logit multinomiale sarà del tipo:

$$\log(P_i / P_{i \neq j}) = \alpha_i + \beta(X_i) \qquad \text{con } i=1,\ldots,j,\ldots,n$$

dove il primo membro indica il logaritmo della probabilità che il campione intervistato scelga di pagare un prezzo fra gli *n* disponibili, mentre il secondo membro indica il vettore di variabili *X* soggettive e di policy, collegati alla scelta *i*, che influiscono sulle scelte, e quindi, sulla funzione di utilità dell'individuo intervistato.

Nel nostro studio abbiamo indicato i=4, dato che quattro sono i livelli di tariffa sottoposti alla scelta dell'utente del parco (€ 1, 2, 2,5, 3). I risultati ottenuti dalla stima sono quelli riportati di seguito, da essi si vede che le variabili ritenute significative per la scelta degli utenti sono: *UTSTRIC, REDDITO, NUCFAM*, mentre le altre variabili sono statisticamente irrilevanti per la determinazione della disponibilità a pagare da parte dei visitatori del parco.

	1		2		3		4	
ristik	Coef.	P>|z|	Coef.	P>|z|	Coef.	P>|z|	Coef.	P>|z|
utstric	-1.708231	0.003	1.959993	0.018	1.809026	0.001	12.38848	0.003
reddito	.0009177	0.004	.0069087	0.000	.0038855	0.000	.0091752	0.003
nucfam	1.203455	0.002	7.209822	0.000	4.969266	0.000	5.478065	0.000
_cons	-8.341883	0.009	-78.86324	0.000	-47.97882	0.000	-113.342	0.002

I risultati della tabella sopra riportata mostrano come varia la disponibilità a pagare per ognuno dei differenti livelli di prezzo ogni qualvolta si modifica una delle variabili stimate come significative per la determinazione della DAP dei visitatori. In pratica è possibile seguire un simile ragionamento: supponiamo che vi sia un membro della famiglia in più, la probabilità che i visitatori scelgano di pagare il prezzo 1 anziché 0, aumenta di 1,203. Osservando tutti i livelli tariffari possiamo inoltre dire che, in genere, i visitatori con un maggior numero di familiari sono maggiormente disposti a pagare un prezzo più alto per sostenere il parco.

5. Considerazioni conclusive e suggerimenti di policy

La ricerca ha messo in evidenza alcuni aspetti specifici che caratterizzano quella componente della domanda turistica sensibile agli aspetti ambientali e paesistici delle località turistiche.

Gli elementi della domanda che la nostra analisi ha permesso di isolare sono correlati da un lato alle caratteristiche socio economiche dei visitatori e dall'altro ad elementi di offerta. In particolare il reddito procapite, la composizione del nucleo familiare e la tipologia e qualità delle strutture ricettive hanno mostrato un elevato grado di significatività statistica.

Quanto alla prima variabile è nota la correlazione esistente tra l'incremento della disponibilità di spesa e l'utilità legata alla fruizione delle risorse turistiche locali. Per livelli più elevati di reddito disponibile la curva di domanda si sposta verso l'esterno e individua nuove situazioni di equilibrio microeconomico caratterizzate dalla probabile disponibilità ad acquistare i medesimi livelli di servizi ad un prezzo superiore.

La rilevante significatività della variabile "composizione del nucleo familiare" và interpretata in relazione alle caratteristiche sociali del target che si indirizza verso le aree protette, dato che le "famiglie con bambini" costituiscono una marcata componente dell'attuale flusso di visitatori.

Sia con riferimento alla prima che alla seconda delle variabili citate, i risultati predetti dal modello appaiono coerenti con l'evidenza empirica che rileva l'esistenza di una componente specifica della domanda (i nuclei familiari) nella quale emergono più che in altri segmenti della stessa domanda quelle componenti sociali e psicologiche che producono una crescente sensibilità alle problematiche ambientali e di conservazione delle risorse paesistiche e naturali non riproducibili.

Una riflessione più approfondita merita il ruolo assunto dalla variabile collegata all'utilizzo delle strutture ricettive. Questa, elemento basilare del sistema di offerta di una località turistica, viene considerata nel modello come fattore che permette di segmentare la domanda turistica naturalistica inizialmente considerata omogenea. Il nostro ragionamento deriva dalla constatazione che il segno del coefficiente della variabile *UTSTRIC* del modello stimato è diverso dal segno atteso in corrispondenza del solo livello più basso della tariffa proposta, mostrando invece assoluta coerenza in relazione agli altri tre livelli di tariffa. La nostra spiegazione è legata alla considerazione che l'utilità che complessivamente può essere tratta da una vacanza in un'area protetta non dipende solo dalla disponibilità e dal livello di integrità delle risorse, ma anche da altre dimensioni legate

alla fruizione dell'offerta, fra cui la qualità della ricettività e dei servizi complementari di cui il visitatore può disporre, elementi sui quali è necessario svolgere un supplemento di indagine. Anche se intuitivamente questa considerazione sembra ovvia, i risultati del modello ci dicono che le caratteristiche legate all'utilizzo delle strutture ricettive possono costituire uno stimolo in termini di richiamo di domanda turistica solo da un certo livello qualitativo in su. E' ragionevole, infatti, pensare che esiste un segmento medio-alto di visitatori la cui disponibilità di spesa maggiore e/o la cui struttura delle preferenza più sensibile ai servizi collegati all'offerta ricettiva mostra una tendenziale disponibilità a pagare crescente. Questa viene rilevata, nel modello, usando le fasce più alte di disponibilità a pagare (DAP). In maniera speculare esiste una parte della domanda poco sensibile alla fruizione dei servizi collegati alle strutture ricettive, generalmente caratterizzata da disponibilità di spesa inferiore che utilizza meno la stessa offerta ricettiva e che si rivela sensibile alla fruizione delle sole risorse naturalistiche presenti.

In sede di indicazioni di policy, non si può non rimarcare la necessità di stimolare un maggiore collegamento tra gli interventi finanziari per l'adeguamento del sistema di offerta locale e di marketing del territorio con gli elementi che caratterizzano le specificità del target turistico di riferimento alcune delle quali rilevate dalla presente analisi.

Il mantenimento di elevati livelli qualitativi del patrimonio naturale non rinnovabile è l'aspetto che più di altri emerge dall'analisi e, anche soltanto da un punto di vista strettamente economico, le risorse pubbliche spese a tal fine risultano giustificate dall'esistenza di elevati livelli di disponibilità a pagare da parte degli individui. Peraltro, la sensibilità ambientale nei paesi sviluppati è tendenzialmente crescente di conseguenza è da attendersi anche un aumento del volume del flusso di visitatori che si dirigono verso le aree protette.

A questa condizione basilare va aggiunta l'esigenza di stimolare una maggiore diversificazione dell'attività ricettiva vera e propria verso quelle categorie di servizi specificamente individuati dalle analisi sulla domanda di turismo naturalistico. Ospitalità diffusa, contesti abitativi comodi ma abilmente connotanti le caratteristiche rurali dei luoghi. A questi va aggiunta la creazione e diffusione di itinerari culturali ed enogastronomici, l'individuazione di percorsi sportivi e aree attrezzate per i più piccoli e tutto ciò che può essere collegato alle particolari specificità di ogni territorio.

Riferimenti bibliografici principali:

Calia, P. e E. Strazzera (2000), "Bias and Efficiency of Single vs. Double Bound Models for Contingent Valuation Studies: a Monte Carlo Analysis", *Applied Economics*, 32, 1329-1336, Routledge.

Strazzera, E., M. Genius, R. Scarpa e G. Hutchinson (2001): "The Effect of Protest Votes on the Estimates of Willingness to Pay for Use Values of Recreational Sites", Note di Lavoro FEEM, 95.0, and II world congress of Environmental and Resource Economics, Monterey, USA, June 2002.

Strazzera, E., S. Balia e R. Brau (2002): "Modelling Participation and Valuation Choices in the Market of Cultural Goods", Università di Cagliari.

Brandon, K.E. e M. Wells, (1992) "Planning for people and parks: design dilemmas", World Development, vol.20, n.4

The British Council-Ass. Italia-Inghilterra (a cura di) (1996) "National Parks: a Viability or Liability?", Atti dell'incontro di studio su salvaguardia e valorizzazione ambientale, Cagliari

Gilley O. W., Pace R. K. (1995), "Improving hedonic estimation with an inequality restricted estimator" Review of Economics and Statistics Volume: 77, Issue: 4, November, pp. 609-621

Font A. R. (2000), "Mass Tourism and the Demand for Protected Natural Areas: A Travel Cost Approach", Journal of Environmental Economics and Management Volume: 39, Issue: 1, January, pp. 97-116

Hanemann M. and Kanninen B. (1999), "The statistical analysis of discrete response CV data", in Bateman I. J. and Willis K. G., Valuing environmental preferences, Oxford University Press.

Scheyvens, R. (1999). "Ecotourism and the empowerment of local communities", Tourism Management.

Mackoy, R., & Osland, G. (2004), "Lodge selection and satisfaction: Attributes valued by ecotourists", Journal of Tourism Studies.

Lawton, L. (2001), "Ecotourism in public protected areas", in D. Weaver (Ed.), Encyclopedia of ecotourism. Wallingford, UK, CAB International.

Goodwin, H. (2002), "Local community involvement in tourism around National Parks: Opportunities and constraints", Current Issues in Tourism, 5.

Fennell, D. (1999). "Ecotourism: An introduction". London, Routledge.

Navrud, S., & Vondolia, G. (2005),"Using contingent valuation to price ecotourism sites in developing countries", Tourism, 53.

Pigliaru F., Brau R., Lanza A. (2007), "How Fast are Small Tourism Countries Growing? The 1980-2003 Evidence" in Feem WP n.1.

RENDICONTI DEL CIRCOLO MATEMATICO DI PALERMO
Serie II, Suppl. 81 (2009), pp. 121-130

THE DESIGN OF WAITING AREAS TO OPTIMIZE THE STORAGE CAPACITY IN THE MARINE INTERMODAL TERMINALS

Ferdinando Corriere (*)
Dario Lo Bosco (**)

ABSTRACT

The appropriate sizing of storage areas to optimize the management of intermodal transport, the adoption of environment protection systems and the appropriate flow's regulations inside manoeuvre's zones can solve many problems encountered today in a intermodal marine terminal.

For these reasons the "integrated design" of storage areas for vehicles and containers is considered essential to ensure efficiency and functionality for all harbour-system.

So is here proposed a simulative model as a tool for a more correct design of waiting areas by considering the real stochastic conditions of the process of the arrivals.

For the sizing of areas for containers in the harbours, it is necessary to report the storage capacity in terms of TEU that can be stored (and handled) in the unit of time, e.g. in one year, with the extension of sites for storage of boxes and furniture with the other specific operating parameters.

The sizing of storage areas of the goods date constitutes a delicate problem the frequent shortage of the areas available. The ability to warehouse of the terminal is essentially determined from the interrelation between fixed and static parameters in the short period which the extension of the storage area, the height of the overlapping batteries of container (defined also like number of "shooting"), the means of movements and, at last, a series of parameters that can vary the efficiency's degree according to of the operatives of the terminal.

The optimal level of use is caught up when it is employed approximately the 60-65% of the maximum storage capacity; account is kept, therefore, of a sure tolerance necessary in order to make forehead to eventual peaks of traffic in the periods in which the volume of container in the terminal or advanced to that mean. By use of the Sartor expression (1997), it is possible to find out the capacity of traffic C of a terminal for container in a period of reference (generally one year) and this can be useful in order to define the requirements of areas to assign to the storage.

(*) Associate Professor at University of Palermo.
(**) Full Professor at University of Reggio Calabria.

1 The size of storage areas for vehicles waiting.

The correct sizing of storage areas (parking spaces near the landing-stage), the adoption of passive protection systems (sonic barriers, green works, etc.) and the adjustment (also by the realization of appropriate infrastructure) of the flows entering and out coming from the terminal, it can help to solve many problems in the intermodal infrastructures.

In other words the "integrated design" of transport infrastructure and the proper size of each element is considered essential to ensure the functionality of the system as a whole.

The evaluation of the operational capacity that must be allocated for parking areas in order to achieve an appropriate supply for the demand of service, it should be done primarily by evaluating the number of elements waiting for service (length of the queue). Such variable, obviously, depends by the characteristics of the service (frequency and ability of the ships) and by the medium rate and distribution of the arrivals, the typologies of the vehicles etc..

By the knowledge of the parking ability (the maximum number of vehicles that can at the same time engage the area of accumulate in normal conditions of exercise), the dimensioning of the infrastructure could be carried out making use of the relation.

$$A = (a\ N_s)/\ u \qquad (1)$$

where:

- A = Surface of plan in m^2 of storage area.
- a = Area of medium occupation of vehicle in m^2 (equal to the weighted average of the areas employed by vehicles at the same time present in the area).
- N_s = the maximum number of vehicles that can stop at the same time in the area.
- u = Coefficient of use in the area.

The average area of occupation can be estimated as the sum of two terms that are the average area of employ and the average area of franc between the vehicles.

The dimensioning of storage area is carried out imposing the condition of equilibrium between the number of at the same time present vehicles in queue N_q in the area in the more unfavorable conditions [(1)] and the N_s number that characterizes the storage capacity to avoid queues and congestion on the

[(1)] Really, it can be imposed that the number of queuing vehicles N_q don't exceed (with a given probability's degree) the number of average places N_s the factor "a" assumes the significance of service-level index for the projecting area.

arteries of connection with the city or background ways. The problem becomes, then, to calculate, in a methodologically corrected way, the N_q number of vehicles in waiting, that is, the total length of the queue L_q.

In the extension of this note it will be exposed a criterion for the appraisal of the length of the queue of the vehicles in waiting according to the medium rate the arrivals of the vehicles Γ and the medium rate service μ; in particular the so-called method of the "bulk service" will be exposed that permits to estimate the length of the queue, for sizing the accumulate area.

It is emphasized, however, that the formulation of the problem here considered refers to normal conditions of exercise of the system; in absence, that is, of interruptions due to atmospheric causes or trade-union agitations, even if it can be take account of these circumstances indirectly making reference to values opportunely reduced of the medium rate service μ, for the determination of the L_q value that could be taken place in such circumstances.

Generally, for the aims of sizing, is appropriate to refer to conditions of normal exercise of the system, otherwise remarkable over sizing of infrastructures could be obtained.

2. Determination of the length of the queue by the method of Markov chains in the case of a system of service groups (bulk service)

The evaluation of the length of the queue can be made by reference to a system of service groups (bulk service). Consider the system with a Poisson distribution of the arrivals, a distribution of negative exponential of time service, a standby system with a single channel server providing the service to groups of users of size r (or less than r).

The time of service for the user group in question is identified by a distribution function of exponential negative; users arrive with a simple the Poisson rate r, one at a time[(2)].

The system of service groups (bulk service) is represented by a process of arrivals of Erlang type and in fact, when the server is available (ship at the dock), accept a group of r customers from the queue and provide the service in collective form, the length of service for this group is described by an

[(2)] Generally the block system are classified on the basis of the distribution's type of the time of arrivals and of the service time. It is used the Kendall codex that assumes the structure AIB/m; where A and B point at the distributions of t_a and t_s (for the positions A and B, codex M seems a negative exponential distribution, E an Erlang distribution with parameter r, D a uniform variable, and, finally G a common variable). The position m seems the number of channels in service (in the study case 1 channel serves r users at a time).

exponential distribution of parameter μ (the rate the service).

If, once available, serving finds less than r customers in queue, then it will wait for until will accumulate a total of r customers and it will accept then them in group and so on.

Therefore a service system type M/M/1 conditioned supplying the service to groups of r customers, is equivalent to a system E/M/1 where the distribution of the arrivals is described from a function of Erlang of parameter r and therefore the functions of density of the interval of the arrivals t and the time of service x is respective:

$$a(t) = \frac{r\Gamma\left(r\Gamma t\right)^{r-1} e^{-r\Gamma t}}{\left(r-1\right)!} \qquad t\geq O \qquad (2)$$

$$b(x) = \mu e^{-\mu x} \qquad x\geq;O \qquad (3)$$

where Γ is the average rate of arrivals of vehicles in the accumulation and μ is the average rate of service (rate of departure of the ships).

Shown so the system of service and operating with the method of the states of equilibrium due to Markov, to assess the probability P_n of finding n users in the system, we consider the following equations of equilibrium:

$$\left(\Gamma+\mu\right)\cdot p_n = \mu\cdot p_{n+r} + \Gamma\cdot p_{n-1} \qquad n\geq 1 \qquad (4)$$

$$\Gamma\cdot p_0 = \mu\left(p_1 + ...p_n\right) \qquad (5)$$

The above balance equations allow me, through the application of the method of functional transformation z (z-transformation), to achieve the equation of state which expresses the probability of having n users in the system.

$$p_n = \left(1-1/z_0\right)\cdot\left(1/z_0\right)^n \qquad n\geq 1 \qquad (6)$$

The z_o variable that appears in the expression above is solution of:

$$r\cdot\Phi\cdot z^{r+1} - \left(1+r\cdot\Phi\right)\cdot z^r + 1 = 0 \qquad (7)$$

where we defined $\Phi = \Gamma/\mu r$ because this system can be served simultaneously up to r users in a time period of duration $1/\mu$ [sec.].

The (7) is a polynomial of degree r +1, therefore it admits r +1 solutions, one of these will be at the point z = 1, r-1 are such that $|z|<1$ and only one, called z_o, that will be $|z_o| > 1$ and this is the only one that interests us.

Identified the P_n distribution, the number of elements N_q (vehicles) waiting the service is assessed by the expression:

$$N_q = \sum_n n\cdot p_{n+1} \qquad (8)$$

that, therefore, provides the stationary queue length in the non-saturation

conditions; otherwise when the demand exceeds the supply, it is necessary to calculate the length of the queue in the non-stationary conditions, this can be effected by multiplying the excess of vehicles for the ending time sovrasaturazione. The total length of the queue will be, in this case, the sum of the queue of stationary and non stationary. The waiting time in queue is then evaluated based on the known expression:

$$W_q = N_q / \Gamma \cdot m \tag{9}$$

being m the number of channels of access (with m = 1 if the system has only one channel that serves up to r users at a time). The Fig 1 shows a family of curves N_q (r) obtained by means of (8) according to the hourly rate of service and allocated size of the group that is served (average capacity of vessels in service in terms of cars transportable).

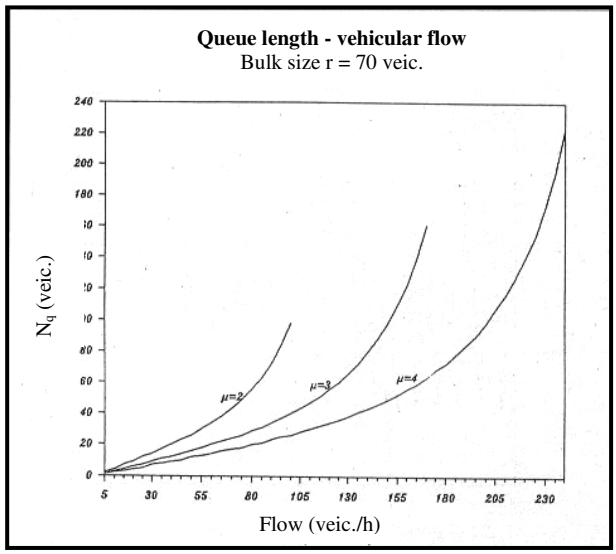


Fig 1 - Relationship between number of vehicles in queue and vehicular flow for different service rates μ [ship/h], with size of the group served equal to 70 veic, according to the theory of Markov.

The length in meters of the queue L_q (Γ) in expectation of service is obtained by multiplying the variable N_q for the average length of employment of the vehicles in the system or, as in the case considered here, the weighted average of the lengths of the vehicles that make up the flow (Fig. 2).

The weighted average of the lengths taken to be equal to 6,65 m, having split the flow into three vehicle classes and having taken on the basis of investigations conducted for a case studied.

- 60% passenger cars (average length 4 m.)
- 25% trucks and commercial vehicles (average length 8 m)
- 15% T.I.R. (average length 15 m).

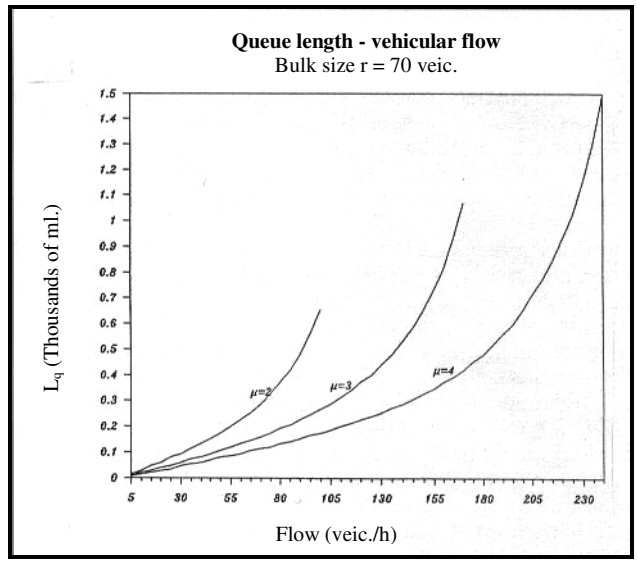


Fig. 2 - Relationship between the length of the queue in thousands of metres and vehicular flow for different service rates μ [ship / h], with size of the group served equal to 70 veic ,according to the Markov's theory.

The families of curves, shown in Figg. 1 and 2, respectively represent the number of vehicles in queue and the length of the same queue for different values of the average hourly rate of service μ, given the size of the group being served (average capacity of ships in terms of transport vehicles for each trip), also the same curves arrivals rate and ability offered from the equal system to 0,75 are limited to a advanced end of the relationship between medium.

Then by the position N_S = Nq it is possible the optimal size of the waiting area.

3 The storage capacity of areas for containers

For the sizing of storage areas for containers in the port areas, it is necessary to report the storage capacity in terms of TEU that can be stored (and handled) in the unit of time, eg. in one year, with the extension of sites for

storage of boxes and furniture with the other operating parameters specific to the site.

The UTI (Intermodal Transport Unit) is a conventional size that the homogenised different types of unit load. On the basis of statistical averages is approximately valid, the following equivalence in volume terms: 1 UTI = 2,6 TEU. So a swap bodies of class A (UTI), with dimensions 13,6-2,55-2,67 m, has an external volume of 93 m^3, while a TEU (twenty equivalent unit) is a unit equivalent to 20 feet (about 6 meters in length) and has a volume of about 36 m^3. The sizing of storage areas of the goods date constitutes a delicate problem the frequent shortage of the areas available. The ability to warehouse of the terminal is essentially determined from the interrelation between fixed and static parameters in the short period which the extension of the storage area, the height of the overlapping batteries of container (defined also like number of "shooting"), the means of movements and, at last, a series of parameters that can vary the efficiency degree according to of the operatives of the terminal.

The ability expresses, therefore, the measure of the volume of cases you furnish (UTI or TEU) that day, month or year) inside of the destined harbour area can be storage in a prefixed interval of time (accumulate to it of the container.

The optimal level of use is caught up when it is employed approximately the 60-65% of the maximum storage capacity; account is kept, therefore, of a sure tolerance necessary in order to make forehead to eventual peaks of traffic in the periods in which the volume of container in the terminal or advanced to that mean.

The following expression (Sartor 1997) expresses the ability to traffic C of the one terminal for container in a period of reference (generally year) and can be useful in order to define the requirements of areas to assign to the storage:

$$\mathbf{C = (a \bullet h \bullet s \bullet d)/(g \bullet p)} \tag{10}$$

in which:
- **a** is the area expressed in m^2 or in equivalent TEU destined to the storage;
- **h** is the theoretical degree of overlap of the containers;
- **s** is the coefficient of under use of the storage-area (normally inferior of one);
- **d** is the number of days in considered period (i.e. 365 if the period is a year);
- **g** is the medium time of parking of the container in the terminal (in days);
- **p** is the peak-factor of the containers flows in the terminal (higher then one).

The storage area (**a**) depends directly from the used equipments: (portal crane or frontal crane).

The medium height (**h**) is the medium number of overlaps previewed for the containers. In the case of UTI for the arranged transport it would be

predispose specific areas for semi-owing and movable cases, not being previewed the overlap.

The coefficient of under-use (**s**) indicates a programmed margin of empty space in order to avoid a decrease of operating efficiency: Practically a rate of under use is defined, as an example of 30% that it implies 70% as space available for the warehouse, such percentage is exactly the coefficient of under use **s**.

The medium time of pauses (**g**) remarkably influences the ability to a terminal, in fact every slot available comes used n times the year and therefore the rate I re-use depends from the times of pauses of every container.

The ability of a terminal is inversely proportional to the medium stop's time; when the times of pause are very short, their variations make change much capacity, while in the case of time the sensitivity of capacity to their change is less.

Where the stop's time are very variable, and this occurs under conditions of high utilization of the terminal, the operators have difficulties in operation daily.

The peak factor (**p**) represents the extent of the excess volume of container, defined as the ratio between the peak value and the average flow in a given period.

Almost all variables in (10) may be considered of deterministic type, except for the average time to render **g** and the factor of peak **p**, which must consider variables of stochastic type and dependent by the rate of arrivals Γ and of service μ.

4 Example of calculation

Some surveys provide valuable information for sizing the storage of a container terminal. In the example in the table below indicates the areas of space for medium-sized containers of 20 '(TEU) and the corresponding number according to the handling equipment used in relation to an area of 18,000 m^2.

	Average footprint area of container [m^2]	
Means of handling	20' (TEU)	n. TEU
Gantry cranes	16,7	1080
Crane front	18	1000

Table 1 Average space for containers and No of TEU (for each level) for the storage yard with area of 18,000 m^2.

The following table show the annual storage capacity offered by a container terminal in relation to the means of handling employees.

Terminals equipped with gantry cranes are obviously a storage capacity higher than those using crane front.

			Terminal equipped whit	
			Frontal cranes	Gantry cranes
Average degree of container's overlap	h_0 h_p	empty 38% full 62%	5 3	5 3
Theoretical degree of overlap	h		3,76	3,76
Theoretical storage capacity (TEU)	C_t		3760	4060
Coefficient of under use	s		0,7	0,95
Effective storage capacity	$C_t \bullet s$		2632	3872
Medium time of container's parking	g_v g_p	empty full	9,91 3,91	9,91 3,91
	g	Weight average	6,19	6,19
Peak factor	p		1,179	1,179
$L_0 = s/p$			0,594	0,806
Terminal traffic capacity -TEU/year	**C**		**131.636**	**192.903**

Table 2 Calculating example of the storage capacity for containers 20' (storage area equal to 18,000 m^2, d = 365 days)

In conclusion, if you have an estimate of traffic in terms of TEU equivalent handled (TEU / year), it calculates the percentage of actual deposit of the full and empty obtain the storage capacity necessary for the terminal. Depending on the storage capacity (which also depends on the type of crane to be used) one can determine the area required as indicated.

By the impossibility to assess really the influence of all factors, the result, of course, can be considered reliable only if the assumptions made on the various coefficients are proving unfounded.

5 Conclusions

In this paper is shown a method to size the areas of accumulation of rubberised vehicles based on the determination of the number of queuing vehicles N_q simultaneously present in the most adverse conditions and the number N_s which characterizes the area parking capacity to avoid queuing on connecting roads whit urban areas. The method described allows to determine the number N_q of vehicles waiting or the total length of L_q queue, by imposing an equilibrium state in the system between the average rate of arrivals and service with a certain degree of probability α that represents the level of service.

The design of storage areas of the containers is, otherwise, to relate the storage capacity of the area with the capacity of traffic (or annual handling) by some variables that reflect the real operating conditions of the marine terminal.

6 Bibliography

[1] E. KOENIGSBERG "Cyclic queues", Operations Research Quarterly, 1958.
[2] P. J BURKE "The output of a queuing system", *Operations Research, 1966*
[3] K. M CHANDY "The analysis and solutions for general queuing networks", *Proc. Sixth annual Princeton Conference on Information Sciences and Systems, Princeton University, press Itd, 1972*
[4] W J. GORDON, G F NEWELL "Closed queuing systems with Exponential servers", *Operations Research, 1967.*
[5] "Introduzione alla simulazione discreta", *Boringheri editore, 1978.*
[6] J R G IAEZZOLLA JACKSON "Jobshop like queuing systems", *Management Science, 1963.*
[7] JUNUICHI IMAKITA "A techno-economic analyse; Southport transport system", *Gower, 1978*
[8] J F KINGMAN "Markov population processes", *Journal of Applied Probability, 1969*
[9] L KLEINROCK "Queuing Systems Volume l: Theory", A Willey-lnterscience Publication John Willey & Sons, New York, 1975
[10] A. NUZZOLO " La capacità di sosta nei terminal per container", *Trasporti Industriali, n. 241, 1979.*
[11] P RIVETT "Model Building for decision analysis", *John Willey & Sons. 1980.*
[12] R. W VICKERMAN "Spatial economic behaviour", *The Mac Millan press Itd, 1980.*
[13] STRETTO DI MESSINA s.p.a. "Legge n. 1158 del 17/12/1971 per un collegamento viario e ferroviario fra la Sicilia e il continente - Rapporto di fattibilità – Vol. 8", *1986.*
[14] F. CORRIERE "Il dimensionamento delle aree di sosta per il traghettamento dei mezzi gommati attraverso lo stretto di Messina", *Le Strade n° 1282, Febbraio 1992.*
[15] P. SARTOR "La capacità delle aree di sosta nei terminal container", *Trasporti europei , n°7, 58-62 Dic. 1997.*

RENDICONTI DEL CIRCOLO MATEMATICO DI PALERMO
Serie II, Suppl. 81 (2009), pp. 131-140

Particle Size Distribution curve calculation using limited domains of settling functions.

Czinkota I, Kertész B, Kovács A, Hajdók I

Szent István University, Dept. of Soil Science and Agricultural Chemistry, Páter Károly u. 1., H-2103 Gödöllő, Hungary;

Abstract

The determination of particle size distribution (PSD) is one of the most important fundamental physical property of soils, which determines the physical, chemical, mechanical, geotechnical, moreover the environmental behavior. Although the measurement of PSD using different techniques is commonly performed in soil labs there are two important problems not solved: automation and continuous PSD curve generation.

. In this paper we introduce a new evaluation method, for the big number of measured density data points named Method of FInite Tangents or shortly: the "FIT method". Because the whole system can be managed as the aggregation of many mono-disperse systems, it is possible to divide the measured density-time function into grain-size fractions with tangent lines drawn to finite but optional points. For calculating the settling speed of given fraction, these tangent lines are very good tools, because the changing speed of density is equal to the multiplication of settling speed and mass of given fraction. The settling speed of all fractions is calculable using the Stokes law, so thus the mass of all floating fraction is calculable. Because the soil-suspension is a poly-disperse system, the measured density decreasing can be considered as an integration of finite mono-disperse system, which means that it can be interpreted as the sum of linear density vs. time functions. If the mass of all grain-size fractions are known, the particle size distributions are calculable easily.
This mathematical method is relatively easy to program, and the intervals of grain-size fractions are freely adjustable, so using this program, almost all particle size distribution systems are calculable, not only the uniform distribution. Using an appropriate controller and calculating program, the particle size distribution can be calculated immediately after downloading the measured data, or using the stored database and particle size distribution can be calculable. Using this technique does not require more sample preparation than past methods. The automated reading requires less manpower to perform the measurement - which also reduces human error sources - but provides very detailed PSD data that has advantages like revealing multi-modality in the particle-size distribution – among others.

Keywords: soil texture, particle-size distribution, automated, aerometry,

INRTODUCTION

Soil moisture and contaminant transport, erosion etc. models are widely used all over the world to solve wide range of problems on the fields of geology, soil sciences, environmental geotechnics, contaminant hydrogeology. The mentioned models require a big amount of input data. The measurements to obtain soil hydraulic, transport and other data are not only time-consuming but costly, as well, that is why for many applications, the prediction of these properties by pedotransfer functions (PTFs) can be a competitive alternative. In many cases the need of input parameters lead to the application of soil property databases (such as Envirobrowser of GEOREF, Inc.) which is a wrong alternative, since it is neither based on the behavior of the actual soil (medium) nor on the characteristics of the permeant liquid (water, dilutant, contaminants, etc.).

Particle-size distribution (PSD) is a fundamental physical property of soils, correlated to many other soil properties. As there is continuous interest in predicting more complex soil physical and chemical properties from easily measured soil characteristics it also became a key input parameter to the PTFs.

PSD is not only a key parameter of PTFs but it is the basis of petrologic classification of loose sediments (silts, sands, gravels, etc.). Despite a number of recognized international standards, soil texture data are rarely compatible across national frontiers, which make them difficult to use.

Traditionally used measurement methods in particle size analysis

There are several principles widely used for particle size analysis in different fields of life. The methods can be classified into two groups: methods based on the settling of particles and all the other methods.

Different methods exist and are applied to determine soil PSD. Gee and Bauder (1986) describe the principles of the most basic and widely used methods. Alternative methods have been developed and proposed by e.g. Stuyt (1992); Oliveira et al. (1997) and Starr et al. (2000). Despite a number of recognized international standards, soil texture data are rarely compatible across national frontiers, which makes it difficult to use such data. Most existing PTFs adhere to the FAO/USDA system. FAO (1990) and USDA (1951) define clay as the particle-size fraction <2 µm, silt as the fraction between 2 and 50 µm and sand as the fraction between 50 and 2000 µm. Nemes et al. (1999), however, gave examples for countries where soils are classified in a different manner. In most of those cases, the silt/sand boundary is defined differently – at 20 µm – as adopted by the International Society of Soil Science (ISSS, 1929). Nemes et al. (2002) introduced a quasi-continuous measurement method, but the data management was not correctly solved. Kovács et al. (2004) published a nimproved version of this measurement technique. In this paper we showed an possible solution how to generate PSD curves using continuous measured data, based on physical equations and using limited domain of settling function.

METHODS BASED ON SETTLING OF PARTICLES

The methods based on settling particles from soil suspension use the Stokes-law to determine the position of particles of different size in the suspension. The Stokes law describes the settling velocity of the particles in a fluid from which the vertical settling path of the particles can be calculated during a time interval:

$$v = \frac{2g \cdot (\rho_p - \rho_w) \cdot r^2}{9\eta},$$

where v is the settling velocity, $\rho_{p\ and}$ ρ_w are the particle- and fluidum densities, r is the radius of the particle and η of the dynamic viscosity.
The settling path can be achieved considering constant settling velocities from:

$$h = \frac{۲g \cdot (\rho_p - \rho_w) \cdot r^۲}{۹\eta} \cdot t$$

where h is the settling path and t is the time interval of settling.

THE ASTA APPROACH – THE DIGITAL AREOMETER

In the previous stage of technical realizations the developers worked out a good, stabile and linear signal generator for water level measurement and were able to minimize the size electronic parts of the device with low energy consumption. This made the building of electronics into the body of the areometer a more competitive alternative as the traditional hydrostatic ASTA measuring principle. A solution for parallel measurements (using USB interface) was also developed, which made possible to develop the ASTA digital areometer with returning to the old, standard hydrometer measurement principle, but with introduction of the continuous measurement ability and achieving much higher accuracy then before.

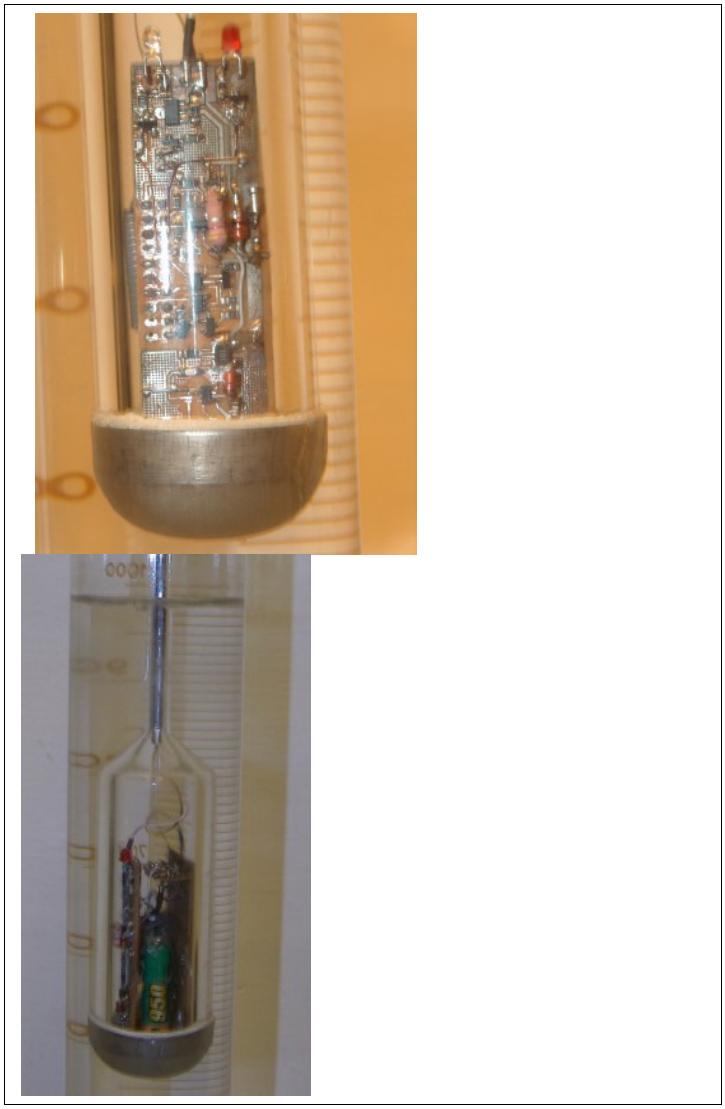


Fig 1. The picture of the equipment.

The instrument head detects the decreasing of liquid level difference, which represents the decreasing density of the suspension.

PHISICAL METHOD

This method is based on the realization, that changing of the average density of a suspension can be measured during the deposition of particles, where the density of particles is larger than the density of the liquid; and that deposition speed is dependent on the particle-size. The density of a suspension can be described with the measurement of the change of force derived from change of the hydrostatic pressure that acts on a cylinder that sinks into the suspension.
Density of the suspension can be turned directly into digital signals with the use of an electric device that measures force, which practically can be an analytical scale. These signals are transmitted through a communication line into a computer. The computer can accept signals from multiple measurement cells in parallel. Data are evaluated quasi-continuously during the measurement as well as after the end of a measurement. Change of density as a function of time can be followed on screen from the beginning of the measurement, as well as the particle-size distribution calculated by a evaluation software. A theoretical outline of the equipment can be seen in Figure 1.
By calculating the speed of deposition of different particle-sizes, relation between time and density of the suspension containing different particle-sizes can be calculated. The evaluating program needs to calculate this in a reverse direction. In the following the deduction of this relation will be briefly shown.
Reduction of lifting power that acts on the floating cylinder as a result of deposing particles needs to be taken into consideration during the calculations. Figure 2 shows the outline of the measurement cell. According to the law of Stokes, deposition speed of particles can be unambiguously calculated from particle size and other constants of the system. Therefore it is satisfactory to calculate only the speed-concentration function of the system. This requires the following steps of calculation.
In a homogenous, monodispersed suspension, *G* lifting power acts on a measurement cylinder with a given volume, as:

$$G = A \cdot l \cdot g$$

where:
A = cross-section of floating cylinder, m^2
l = height of floating cylinder, m
g = gravity acceleration, 9.81 $m.s^{-2}$
ρ = density of suspension, kg ▪ m^{-3}.
Density of the suspension is determined by the density of the liquid, the density of suspended particles and the concentration of the suspended particles:

$$\rho = \rho_w + c \cdot \left(\rho_p - \rho_w \right)$$

where:
ρ_w = density of liquid, kg ▪ m^{-3}
ρ_p = density of suspended particles, kg ▪ m^{-3}
c = concentration of suspended particles, kg particles/kg suspension.

When the particles in the suspension are settling with speed v, they move $v \cdot \Delta t$ distance downward during t time. Concentration of the suspended particles changes Δc around the measurement cylinder during this time:

$$\Delta c = c \cdot \frac{l - v \cdot \Delta t}{l}$$

This relationship can be interpreted only while the value of $v \cdot \Delta t$ does not exceed the height of the floating cylinder. Particles that arrive lower than the bottom of the floating cylinder, no longer influence the lifting power that acts on the floating cylinder. The above function would give zero instead of negative values, therefore the following correction is needed:

$$\Delta c = c \cdot \frac{\left[abs\left(l - v \cdot \Delta t\right) + \left(l - v \cdot \Delta t\right)\right]}{۲ \cdot l}$$

Lifting power changes during t time which is related to the density change ($\Delta\rho$) of the suspension in the following way:

$$\Delta G = A \cdot l \cdot g . \Delta\rho$$

where:

$$\Delta\rho = \left(\rho_p - \rho_w\right) \cdot c \cdot \frac{\left[abs\left(l - v \cdot \Delta t\right) + \left(l - v \cdot \Delta t\right)\right]}{۲ \cdot l}$$

In a heterodispersed suspension the i_{th} fraction from n particle fractions of different size (sinking with different speed) causes ΔG_i change in lifting power during t time.

$$\Delta G_i = \frac{۱}{۲} \cdot A \cdot g \cdot \left(\rho_p - \rho_w\right) \cdot c_i \cdot \frac{\left[abs\left(l - v_i \cdot \Delta t\right) + \left(l - v_i \cdot \Delta t\right)\right]}{۲ \cdot l}$$

The total change of lifting power in a heterogeneous suspension is the sum of changes for all fractions.

$$\Delta G = \frac{1}{2} \cdot A \cdot g \cdot \left(\rho_p - \rho_w\right) \cdot \sum_{i=1}^{n} \left\{ c_i \cdot \frac{\left[abs\left(l - v_i \cdot \Delta t\right) + \left(l - v_i \cdot \Delta t\right)\right]}{2 \cdot l} \right\}$$

During a measurement, G is measured as a function of deposition time. Due to the large number of measurement points – provided by the possibility of using of very small time steps - it is possible to determine the concentration of each fraction separately, described with v_i deposition speed, using regression calculations. It is possible to define the proportion of more than hundred fractions of a sample which provides a quasi-continuous curve of particle-size distribution.

EVALUATION OF DENSITY CHANGES IN TIME USING THE "FIT" METHOD. THE PSD DETERMINATION USING FINITE TANGENTS

The hydrostatic approach and therefore the ASTA device generates the soil suspension density vs. time curve. The big number of measured data points led to the introduction of a new evaluation method, the Method of FInite Tangents or shortly: the "FIT method".

To better understand the basic idea of the FIT method let us investigate the density changes in a mono- and a bi-disperse system. In a monodisperse system all the particles have the same density and size, meanwhile the bi-disperse system consists of a larger and a smaller grain agglomeration.

When the speed of deposition is continuous (derived form Stokes-law), then in case of a mono-disperse system the changing of density is linear, until the last particle – which was found in the highest position at the beginning of the measurement – merged under the reference-point. After that the density is constant, and equal with the density of the pure liquid. (Fig. 3., Curve 1.).

When the mono-disperse system is made from smaller particles, then the density-time function is similar, but the settlement of the liquid and the reaching of constant density needs longer/more time (Fig. 3., Curve 2.). In the case of bi-disperse system, both processes happens together, which results an integrated curve of the two density-time functions (Fig. 3., Curve 3.) (Czinkota et. al, 2002).

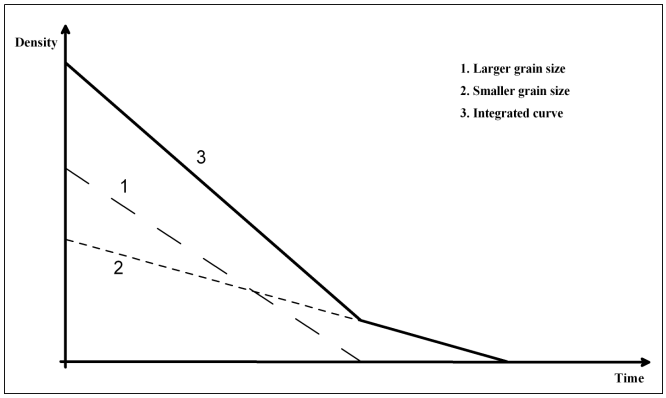


Fig. 3. Density-time characteristics of mono- and bi-disperse systems

This hypothesis is only true, while the particles do not disturb each other's movement, namely the suspension is weak enough.

Because the whole system can be managed as the aggregation of many mono-disperse systems, it is possible to divide the measured density-time function into grain-size fractions with tangent lines drawn to finite but optional points

The intersection point of the tangent line and the ordinate is proportional with the quantity of particles in the suspension, and the distance between the breakpoints of the tangent lines along the abscissa gives the maximum time which is needed by the particle of given size to merge under the reference point.

Knowing the density and the viscosity of the liquid the average particle size can be calculated using the Stokes-law:

$$r[\mu m] = 10^6 \cdot \sqrt{\frac{9 \cdot \eta[Pa.s] \cdot h[m]}{2 \cdot g\left[\frac{m}{s^2}\right] \cdot (\rho - \rho_w)\left[\frac{kg}{m^3}\right] \cdot t[s]}}$$

The traditional PSD curve is obtained after norming the amount of substance defined by the ordinate intersections of particle-size fractions.

Algorithm and programming:

The measured data: measurement time t (t_1, t_2, …t_i, …t_n) and the connecting density values ρ (ρ_1, ρ_2, … ρ_i, … ρ_n).A fragmented line must be fitted on these data pairs. The component line features the sum of all settling fractions in the given time. The t_0 the time is when the last particle of given fraction leaves the bottom of the areometer. In Fig3. it is t_a (the crossing of a line and t-axis) in case of a fraction, and t_b in case of b fraction. All component lines have a known point. This is $\rho=0$, $t=t_a$ point, in case of the smallest fraction. While next fraction, it is the sum of last two fraction, in the Fig3. (ρ_b, t_b) *point.* ρ_b is calculable by substitute t_b in the function of a line. For calculating the parameters of best fitting fragmented line, a regression formula must be derived, what describe a line, crossing a given point.

The equation of line*:* $\rho = a.t + b$ *(5)*

Substituate the (ρ_0, t_0) into the equation and express b: $b = \rho_0 - a.t_0$ (6)

Substituate (6) equation into (5): $\rho = a.t - a.t_0 + \rho_0$ rearranged : $\rho - \rho_0 = a.(t - t_0)$ (7)

Transforming the variable: $y = \rho - \rho_0$ and $x = t - t_0$ (8)

In further derivation the y means the transformed measured data and y_c the transformed calculated data. Using transformed variables (8) the equation of line is the following: $y_c = a.x$ (9)

The regression means, the a parameter must be determine if sum of squere the difference of measured and calculated y values (SQ) are minimum.

$$SQ = \sum_{i=1}^{n} \left(y_i - y_{ci} \right)^2 \quad (10)$$

Transforming (10) equation: $$SQ = \sum_{i=1}^{n} \left(y_i^2 - 2 \cdot y_i \cdot y_{ci} + y_{ci}^2 \right) \quad (11)$$

Substitute (9) into (11): $$SQ = \sum_{i=1}^{n} \left(y_i^2 - 2 \cdot y_i \cdot a \cdot x_i + a^2 \cdot x_i^2 \right) \quad (12)$$

The order of sum is changeable: $$SQ = \sum_{i=1}^{n} y_i^2 - 2 \cdot a \cdot \sum_{i=1}^{n} \left(y_i \cdot x_i \right) + a^2 \cdot \sum_{i=1}^{n} x_i^2 \quad (13)$$

The derivative is taken with respect to a have to be 0 if the original function is in minimum: $$\frac{dSQ}{da} = -2 \cdot \sum_{i=1}^{n} \left(y_i \cdot x_i \right) + 2 \cdot a \cdot \sum_{i=1}^{n} x_i^2 = 0 \quad (14)$$

Expressing a from (14) a value can be calculated : $$a = \frac{\sum_{i=1}^{n} \left(y_i \cdot x_i \right)}{\sum_{i=1}^{n} x_i^2} \quad (15)$$

Substituting back the original values using (8) a and using (6) b parameters can be determined:

$$a = \frac{\sum_{i=1}^{n}\left((\rho_i - \rho_0)\cdot(t_i - t_0)\right)}{\sum_{i=1}^{n}(t_i - t_0)^2} \qquad b = \rho_0 - a \cdot t_0 \tag{16}$$

The derived functions can be used to calculate the mass of predetermined particle size fraction.

The steps of calculation:

1. Calculation of t_0 values of the predetermined fraction based on Stokes law.
2. Determination of parameters of rectangle component lines using (16) equations.
3. Repeat 2. step on each in increasing order of predetermined particle size fraction
4. The cumulated particle size distribution values are the b values of every component lines.

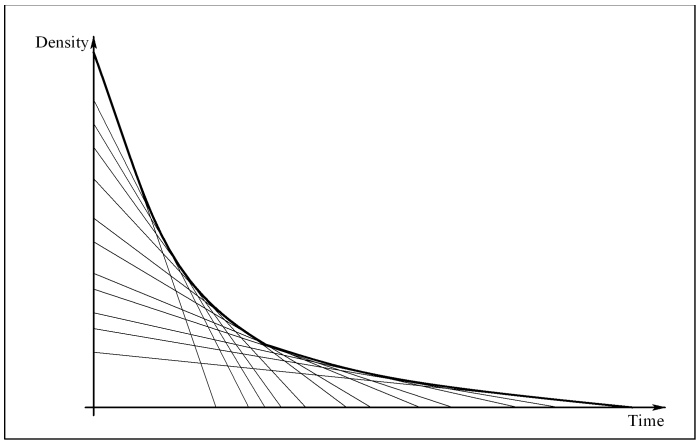


Fig 5. The calculation of tangent lines.

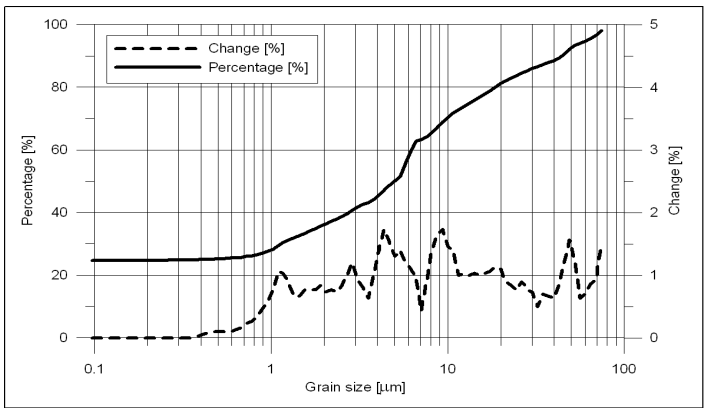


Fig. 6. Evaluation of density vs. time curve using the FIT-method

CONCLUSIONS

Considering the demand on automation of particle size distribution determination the introduction of new testing equipment was decided. After an overview and evaluation of the standardized methods a new principle was chosen to work on. The hydrostatic principle was found adequate to make automated measurements and to create high-resolution PSD curves. To control the theory pilot-test were done in one cylinder and multi-cylinder scales using the Automated Soil Texture Analyzer (ASTA). The high-resolution measurement results gave the opportunity to develop a new evaluation method: the method of finite tangents (FIT-method). The mentioned device and method lead to finer measurements of particle size distribution and hopefully will give the opportunity of better understanding the environmental, geotechnical, etc. behavior of loose sediments.

ACKNOWLEDGEMENTS

This work has been supported by the Hungarian Scientific Research Foundation OTKA under grant No. T 32506 and T037667

REFERENCES

Gee, G.W. and J.W. Bauder. 1986. Particle-size analysis. p. 383-411. In A. Klute (ed.) Methods of soil analysis. Part 1. 2nd ed. Agron Monogr. 9. ASA and SSSA, Madison, Wisconsin.

Stuyt, L.C.P.M. 1992. The water acceptance of wrapped subsurface drains. Ph.D. Thesis, Agricultural University of Wageningen, The Netherlands. (LU-1468) 305p.

Oliveira, J.C.M., C.M.P. Vaz, K. Reichardt and D. Swartzendruber. 1997. Improved soil particle-size analysis by gamma ray attenuation. Soil Sci. Soc. Am. J. 61: 23-26.

Starr, G.C., P. Barak, B. Lowery and M. Avila-Segura. 2000. Soil particle concentrations and size analysis using a dielectric method. Soil Sci. Soc. Am. J. 64: 858-866.

FAO (Food and Agriculture Organisation). 1990. Guidelines for soil descriptions. (3rd ed.). FAO/ISRIC, Rome.

USDA (United States Department of Agriculture). 1951. Soil Survey Manual. U.S. Dept. Agriculture Handbook No. 18. Washington, DC.

Nemes, A., J.H.M. Wösten, A. Lilly and J.H. Oude Voshaar. 1999. Evaluation of different procedures to interpolate particle-size distributions to achieve compatibility within soil databases. Geoderma 90: 187-202.

Nemes A. - Czinkota I. - Czinkota Gy. - Tolner L. - Kovács B. (2002): Outline of an automated system for quasy-continous measurement of particle size distribution. Agrokémia és Talajtan, 51. 37-46.

Kovács B. - Czinkota I. - Tolner L. - Czinkota Gy. (2004): The determination of particle size distribution (PSD) of clayey and silty formations using the hydrostatic method. Acta mineralogica-petrographica 45. 29-34.

RENDICONTI DEL CIRCOLO MATEMATICO DI PALERMO
Serie II, Suppl. 81 (2009), pp. 141-157

Chord length distribution functions for an arbitrary triangle

Andrei Duma – Sebastiano Rizzo

Dedicated to Professor M. Stoka on occasion of his 75th birthday

Abstract

We consider an arbitrary triangle $\mathbf{D}$ with the side lengths a, b, c, the angles A, B, C and the heights h_a, h_b, h_c. Let $\mathcal{R}_d$ be the lattice of Buffon type consisting of parallel straight lines. For the real number s, which is less or equal to the diameter $\max(a, b, c)$ of D, p_s determines the probability, that the arbitrarily thrown triangle intersects a segment of length greater or equal to s out of any straight line of $\mathcal{R}_d$. We calculate p_s for the case, that $\max(a, b, c)$ is less than the distance between any two adjoining straight lines of $\mathcal{R}_d$. (In this case $\mathbf{D}$ is said (cf. [1]) to be small respective $\mathcal{R}_d$). As a result we get the distribution of secants in the triangle $\mathbf{D}$, i.e. we determine the function F, which assigns to every s the probability, that any secant in $\mathbf{D}$ has a length of less or equal to s. Particularly in the case of an equilateral triangle $\mathbf{D}$ we get the results of [2] .

AMS 2000 Subject Classification : Geometric probability, stochastic geometry, random sets, random convex sets and integral geometry.
AMS Classification : 60D05, 52A22.

§ 0. Introduzione

Consideriamo un triangolo qualsiasi $\mathbf{D}$ con i lati di lunghezza a, b, c, gli angoli di ampiezza A, B, C e siano h_a, h_b, h_c le lunghezze delle altezze corrispondenti. Sia $\mathcal{R}_d$ il reticolo di Buffon formato da rette parallele aventi distanza costante d l'una dall'altra.
Se s è un numero reale non negativo minore o uguale del $\max\{a, b, c\}$, troveremo la probabilità p_s che il triangolo aleatorio $\mathbf{D}$ distribuito uniformemente nel piano intersechi su una retta di $\mathcal{R}_d$ un segmento di lunghezza maggiore o uguale ad s.

§ 1. I casi possibili

Senza ledere la generalità possiamo supporre $a \leq b \leq c$ e quindi $c \leq d$. Ne segue $h_a \geq h_b \geq h_c$, $A \leq B \leq C$, $h_b \leq a$ e $h_a \leq b$.
Nel seguito, per affrontare i calcoli, occorre distinguere i casi $C \leq \frac{\pi}{2}$ e $C \geq \frac{\pi}{2}$. Confrontando s con le lunghezze a, b, c, h_a, h_b, h_c e anche tenendo conto della relazione tra a e h_a, dobbiamo considerare diversi casi che scaturiscono dalla combinazione di ciascuna delle due ipotesi $I : C \leq \frac{\pi}{2}$ e $II : C \geq \frac{\pi}{2}$ con i seguenti casi: $1 : s \leq h_c$, $2 : h_c \leq s \leq h_b$, $3 : h_b \leq s \leq \min(a, h_a)$, $4 : a \leq s \leq h_a$, $5 : h_a \leq s \leq a$, $6 : \max(a, h_a) \leq s \leq b$, $7 : b \leq s \leq c$.
Si ottengono cosi 14 casi che indichiamo con I.1, I.2 ,. . ., I.7, II.1, II.2, . . ., II.7 ; alcuni di essi si possono studiare insieme.
Nel seguito si rinuncerà ad alcuni semplici calcoli, preferendo dare ampio spazio alle idee geometriche che saranno illustrate con le opportune figure.

Come cellula fondamentale $\mathcal{F}$ consideriamo una striscia illimitata di larghezza d avente come asse di simmetria una retta $\mathfrak{g}$ del reticolo. La frontiera di $\mathbf{D}$ e la retta $\mathfrak{g}$ hanno l'orientazione indicata nella figura 1. Con abuso di notazione indichiamo con A, B e C anche i vertici del triangolo $\mathbf{D}$. Sia φ l'angolo tra $\mathfrak{g}$ e il lato AB.

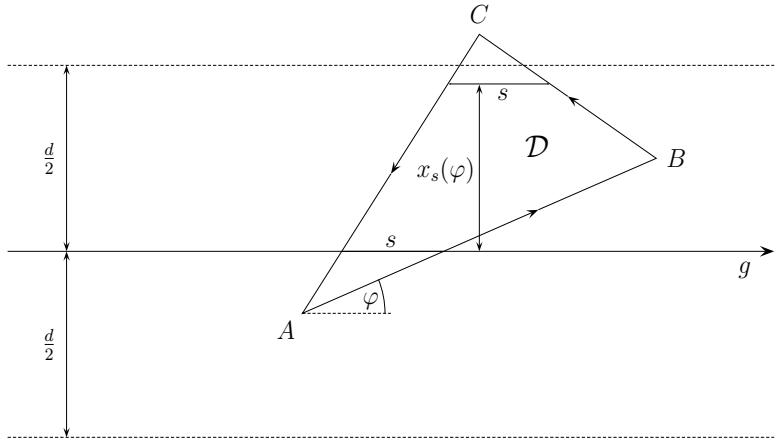


Figura 1: $C \le \frac{\pi}{2}$ e $0 \le \varphi \le B$

Poichè vogliamo considerare ogni posizione possibile di $\mathbf{D}$ una volta e solo una volta, occorre considerare $\varphi \in [0, \pi]$. Fissando un valore di φ, sia $x_s(\varphi)$ la distanza tra due corde parallele di $\mathbf{D}$ entrambe di lunghezza s, delle quali una giace su $\mathfrak{g}$. (Ovviamente solo corde comprese tra queste due hanno lunghezza maggiore o uguale ad s.)
Per calcolare la probabilità p_s utilizzeremo la nota formula di Stoka, che in questo caso è il rapporto tra la misura delle rette parallele a $\mathfrak{g}$ comprese tra le due corde considerate e la misura delle rette parallele a $\mathfrak{g}$ e situate nella cellula fondamentale $\mathcal{F}$.

$$p_s = \int_0^\pi x_s(\varphi)d\varphi \Big/ \int_0^\pi d\, d\varphi = \frac{1}{\pi d}\int_0^\pi x_s(\varphi)d\varphi \ . \tag{1}$$

Nei paragrafi successivi troveremo in tutti i casi l'espressione della funzione x_s e quindi della probabilità richiesta.

§ 2. Casi I.1 e II.1: $s \le h_c$ con C arbitrario

L'espressione di $x_s(\varphi)$ cambia a seconda che φ appartenga a $[0, B]$ oppure a $[B, \pi - A]$ oppure a $[\pi - A, \pi]$.
Se $\varphi \in [0, B]$, utilizzando la figura 1, otteniamo

$$\begin{aligned} x_s(\varphi) &= \sin(A+\varphi)\Big[b - s\Big(\frac{\sin\varphi}{\sin A} + \frac{\sin(B-\varphi)}{\sin C}\Big)\Big] \\ &= b\sin(A+\varphi) - \frac{s}{2}\Big[\cot A + \cot C - \frac{\cos(A+2\varphi)}{\sin A} + \frac{\cos(A-B+2\varphi)}{\sin C}\Big] \ . \end{aligned}$$

Se $\varphi \in [B, \pi - A]$, con l'aiuto della figura 2, risulta

$$x_s(\varphi) = \sin\varphi\Big[c - s\Big(\frac{\sin(A+\varphi)}{\sin A} + \frac{\sin(\varphi - B)}{\sin B}\Big)\Big]$$
$$= c\sin\varphi - \frac{s}{2}\Big[\cot A + \cot B - \frac{\cos(A+2\varphi)}{\sin A} - \frac{\cos(2\varphi - B)}{\sin B}\Big] .$$

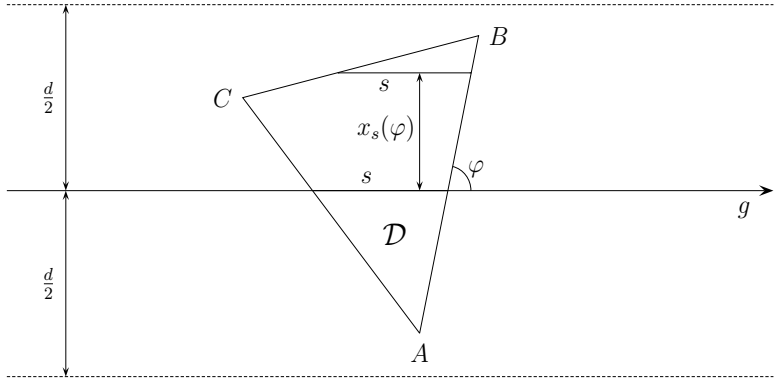


Figura 2: $C \le \frac{\pi}{2}$ e $B \le \varphi \le \pi - A$

Infine se $\varphi \in [\pi - A, \pi]$, utilizzando la figura 3

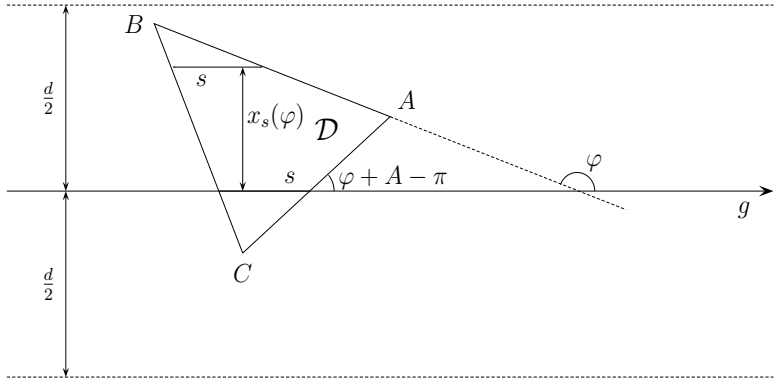


Figura 3: $C \le \frac{\pi}{2}$ e $\pi - A \le \varphi \le \pi$

si ha:

$$x_s(\varphi) = \sin(\varphi - B)\Big[a - s\Big(\frac{\sin\varphi}{\sin B} - \frac{\sin(A+\varphi)}{\sin C}\Big)\Big]$$
$$= a\sin(\varphi - B) - \frac{s}{2}\Big[\cot B + \cot C - \frac{\cos(2\varphi - B)}{\sin B} + \frac{\cos(A - B + 2\varphi)}{\sin C}\Big] .$$

Osserviamo che l'ampiezza di C non gioca alcun ruolo nel calcolo di x_s, cioè esso rimane invariato anche se $C \geq \frac{\pi}{2}$. Risulta

$$\int_0^{\pi} x_s(\varphi)d\varphi = \left(\int_0^{B} + \int_B^{\pi-A} + \int_{\pi-A}^{\pi}\right) x_s(\varphi)d\varphi = \ldots = a(\cos B + \cos C) + b(\cos C + \cos A) +$$
$$c(\cos A + \cos B) - \frac{s}{2}\left[3 + A(\cot B + \cot C) + B(\cot C + \cot A) + C(\cot A + \cot B)\right] =$$
$$a + b + c - \frac{s}{2}\left[3 + \frac{A\sin^2 A + B\sin^2 B + C\sin^2 C}{\sin A \sin B \sin C}\right],$$

e così, dalla formula (1), si ottiene

$$p_s = \frac{1}{\pi d}\left[a + b + c - \frac{s}{2}\Big(3 + \frac{A\sin^2 A + B\sin^2 B + C\sin^2 C}{\sin A \sin B \sin C}\Big)\right]. \tag{2}$$

Nel caso particolare $a = b = c = l$ e $s \leq \frac{l\sqrt{3}}{2} = h_a$ si ottiene il risultato della proposizione 1 del lavoro [2]. Aggiungendo l'ipotesi $s = 0$ si ottiene il classico risultato di Stoka (v. [4]).

§ 3. **Casi** I.2 e II.2 : $h_c \leq s \leq h_b$ e C **arbitrario**

Sul lato AB di **D** consideriamo i punti C_1 e C_2 tali che i segmenti CC_1 e CC_2 hanno entrambi lunghezza s. Indichiamo con φ_1 l'angolo tra $\mathfrak{g}$ e AB per cui il segmento CC_2

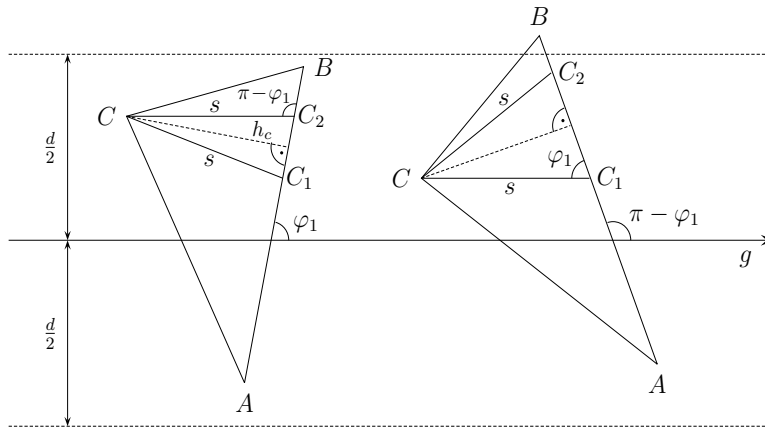


Figura 4: $C \leq \frac{\pi}{2}$ e definizione di φ_1

è parallelo a $\mathfrak{g}$.

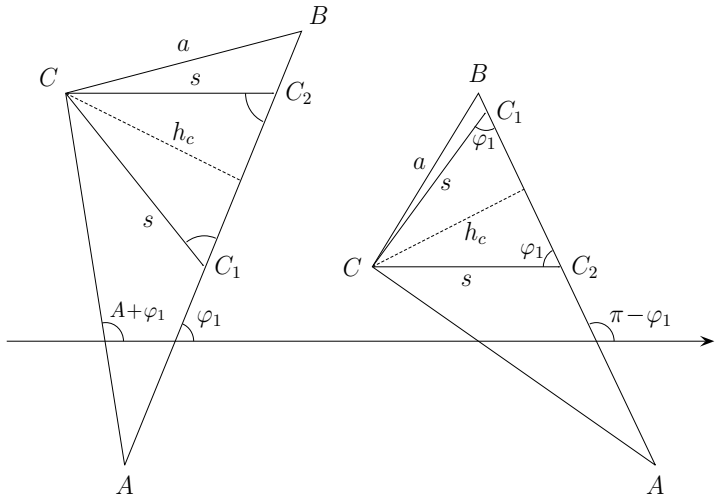


Figura 5: $C \geq \frac{\pi}{2}$ e definizione di φ_1

Dalle figure 4 e 5 si vede che $s \sin\varphi_1 = h_c = b \sin A = a \sin B$, e quindi $\varphi_1 \geq B \geq A$ nonché $\pi - \varphi_1 \leq \pi - A$.

Se φ è tale che la retta parallela a $\mathfrak{g}$ condotta da C intersechi AB tra C_1 e C_2, allora essa interseca in $\mathbf{D}$ una corda di lunghezza minore di s e dunque $x_s(\varphi) = 0$. Quindi la funzione x_s è nulla nel sottointervallo $[\varphi_1, \pi - \varphi_1]$ di $[B, \pi - A]$. Su $[0, \varphi_1] \cup [\pi - \varphi_1, \pi]$ le espressioni di x_s sono identiche a quelle dei casi I.1 e II.1. Ne segue

$$\int_0^\pi x_s(\varphi)d\varphi = \left(\int_0^B + \int_B^{\varphi_1} + \int_{\pi-\varphi_1}^{\pi-A} + \int_{\pi-A}^{\pi} \right) x_s(\varphi)d\varphi = \ldots = a + b + c$$

$$-2c\cos\varphi_1 - \frac{s}{2}\left[3 + \frac{A\sin^2 A + B\sin^2 B + C\sin^2 C}{\sin A \sin B \sin C} + (2\varphi_1 - \pi - \sin 2\varphi_1)\frac{\sin C}{\sin A \sin B}\right],$$

e perciò

(3)
$$p_s = \frac{1}{\pi d}\left\{a+b+c-2c\cos\varphi_1 - \frac{s}{2}\left[3 + \frac{A\sin^2 A + B\sin^2 B + C\sin^2 C}{\sin A \sin B \sin C} + (2\varphi_1 - \pi - \sin 2\varphi_1)\frac{\sin C}{\sin A \sin B}\right]\right\}.$$

Osseriamo che nel caso limite $s = h_c$ le formule (2) e (3) forniscono lo stesso risultato poichè $\varphi_1 = \frac{\pi}{2}$.

§ 4. Caso I.3 : $h_b \le s \le \min(a, h_a)$ **e** $C \le \frac{\pi}{2}$

Denotiamo con $\varphi_0 \in [0, B]$ l'angolo tra $\mathfrak{g}$ e AB, tale che la parallela a $\mathfrak{g}$ condotta da B forma una corda di **D** di lunghezza s che si trova tra AB e h_B (v. fig. 6).

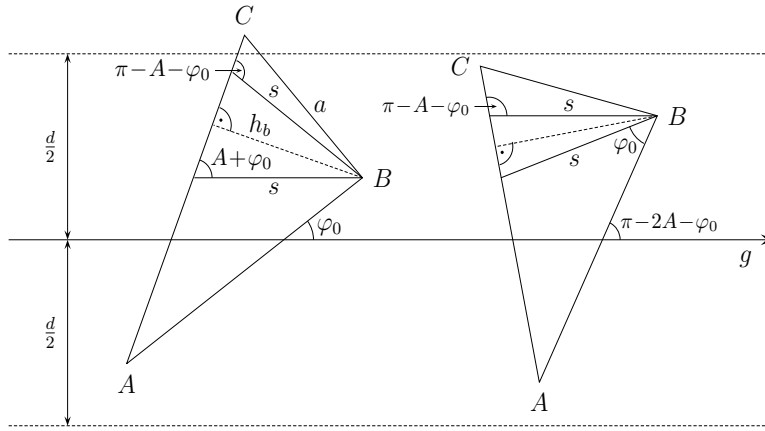


Figura 6: $h_b \le s \le h_a$ e definizione di φ_0

Si ha $\varphi_0 \le \pi - 2A - \varphi_0 \le B$, $\varphi_0 = \arcsin\left(\frac{a \sin C}{s}\right) - A = \arcsin\left(\frac{c \sin A}{s}\right) - A$ e $x_s(\varphi) = 0$ se $\varphi \in [\varphi_0, \pi - 2A - \varphi_0]$. L'angolo φ_1 definito come nel caso precedente, gioca il medesimo ruolo. Risulta

$$\int_0^{\pi} x_s(\varphi)d\varphi = \left(\int_0^{\varphi_0} + \int_{\pi-2A-\varphi_0}^{B}\right) x_s(\varphi)d\varphi + \left(\int_0^{\varphi_1} + \int_{\pi-\varphi_1}^{\pi-A}\right) x_s(\varphi)d\varphi + \int_{\pi-A}^{\pi} x_s(\varphi)d\varphi =$$

$$a + b + c - 2(b\cos(A+\varphi_0) + c\cos\varphi_1) - \frac{s}{2}\left[3 + \frac{A\sin^2 A + B\sin^2 B + C\sin^2 C}{\sin A \sin B \sin C}\right.$$

$$\left. + (2(A+\varphi_0) - \pi)\frac{\sin B}{\sin A \sin C} + (2\varphi_1 - \pi - \sin 2\varphi_1)\frac{\sin C}{\sin A \sin B}\right]$$

e allora

$$p_s = \frac{1}{\pi d}\left\{a + b + c - 2[b\cos(A+\varphi_0) + c\cos\varphi_1] - \frac{s}{2}\left[3 + \frac{A\sin^2 A + B\sin^2 B + C\sin^2 C}{\sin A \sin B \sin C}\right.\right.$$

(4)

$$\left.\left. + (2(A+\varphi_0) - \pi)\frac{\sin B}{\sin A \sin C} + (2\varphi_1 - \pi - \sin 2\varphi_1)\frac{\sin C}{\sin A \sin B}\right]\right\}.$$

Nel caso limite $s = h_b$ si ha $A + \varphi_0 = \frac{\pi}{2}$, e (4) si riduce a (3).

§ 5. **Caso** II.3 : $h_b \le s \le \min(a, h_a)$ **e** $C \ge \frac{\pi}{2}$

Ora l'angolo φ_0 definito come nel caso precedente, non gioca alcun ruolo, poichè si ha $B \le \varphi_1 \le \varphi_0 < 2\pi - A - \varphi_0 \le \pi - \varphi_1$ (e $x_s(\varphi)$ è nulla se $\varphi \in [\varphi_1,\, \pi - \varphi_1]$), poichè si ha $\sin\varphi_0 = \frac{(b+CC^*)\sin A}{s} \ge \frac{b\sin A}{s} = \sin\varphi_1$ (v. fig. 7).

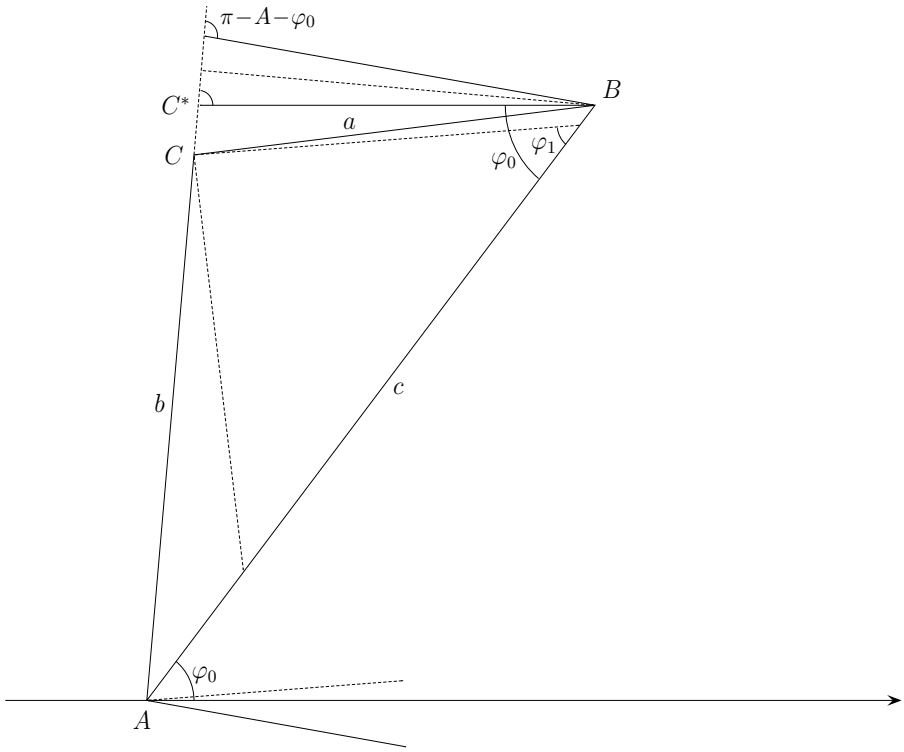


Figura 7: $h_b \le s \le \min(a, h_a)$ r $C \ge \frac{\pi}{2}$

Dal punto di visto geometrico ciò significa che le rette passanti per B segano **D** in corde di lunghezza maggiore di a e quindi di s. Per tale motivo p_s si calcola in questo caso con la formula (3).

§ 6. Casi I.4 **e** II.4 : $a \le s \le h_a$ (C arbitrario)

Con gli angoli φ_0 e φ_1 introdotti precedemente si ha $A \le \varphi_1 \le B$ e $\varphi_0 + A \le C$ e quindi $\pi - 2A - \varphi_0 \ge \pi - 2A - C + A = \pi - A - C = B$, poichè $a \le s$. Tali disuguaglianze così come la disuguaglianza $\varphi_0 \le \varphi_1$ sono evidenti dalle figure 8 e 9:

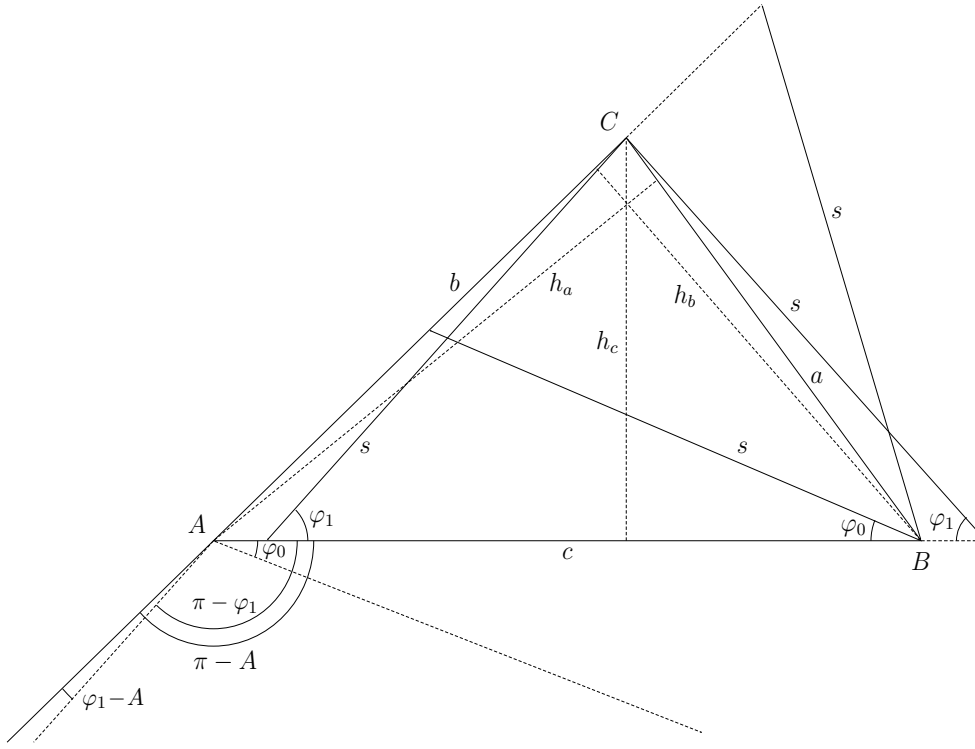


Figura 8: $a \le s \le h_a$ e $C \le \frac{\pi}{2}$

Poichè $x_s(\varphi) = 0$ se $\varphi \in [\varphi_0\,, \pi - \varphi_1]$, si ha

$$\int_0^{\pi} x_s(\varphi)d\varphi = \left(\int_0^{\varphi_0} + \int_{\pi-\varphi_1}^{\pi-A} + \int_{\pi-A}^{\pi} \right) x_s(\varphi)d\varphi = a(\cos B + \cos C) + b(\cos A - \cos(A + \varphi_0))$$

$$+c(\cos A - \cos\varphi_1) - \frac{s}{2}\Big[\varphi_0(\cot C + \cot A) + (\varphi_1 - A)(\cot A + \cot B) + A(\cot B + \cot C)\Big]$$

$$-\frac{s}{4}\left[4 + \frac{\sin(A - B + 2\varphi_0)}{\sin C} - \frac{\sin(A + 2\varphi_0)}{\sin A} + \frac{\sin(A - 2\varphi_1)}{\sin A} - \frac{\sin(B + 2\varphi_1)}{\sin B}\right],$$

e quindi

$$(5)\qquad p_s = \frac{1}{\pi d}\left\{ a(\cos B + \cos C) + b(\cos A - \cos(A+\varphi_0)) + c(\cos A - \cos\varphi_1) \right.$$
$$-\frac{s}{2}\left[\varphi_0(\cot C + \cot A) + (\varphi_1 - A)(\cot A + \cot B) + A(\cot B + \cot C)\right]$$
$$\left. -\frac{s}{4}\left[4 + \frac{\sin(A-B+2\varphi_0)}{\sin C} - \frac{\sin(A+2\varphi_0)}{\sin A} + \frac{\sin(A-2\varphi_1)}{\sin A} - \frac{\sin(B+2\varphi_1)}{\sin B}\right]\right\}.$$

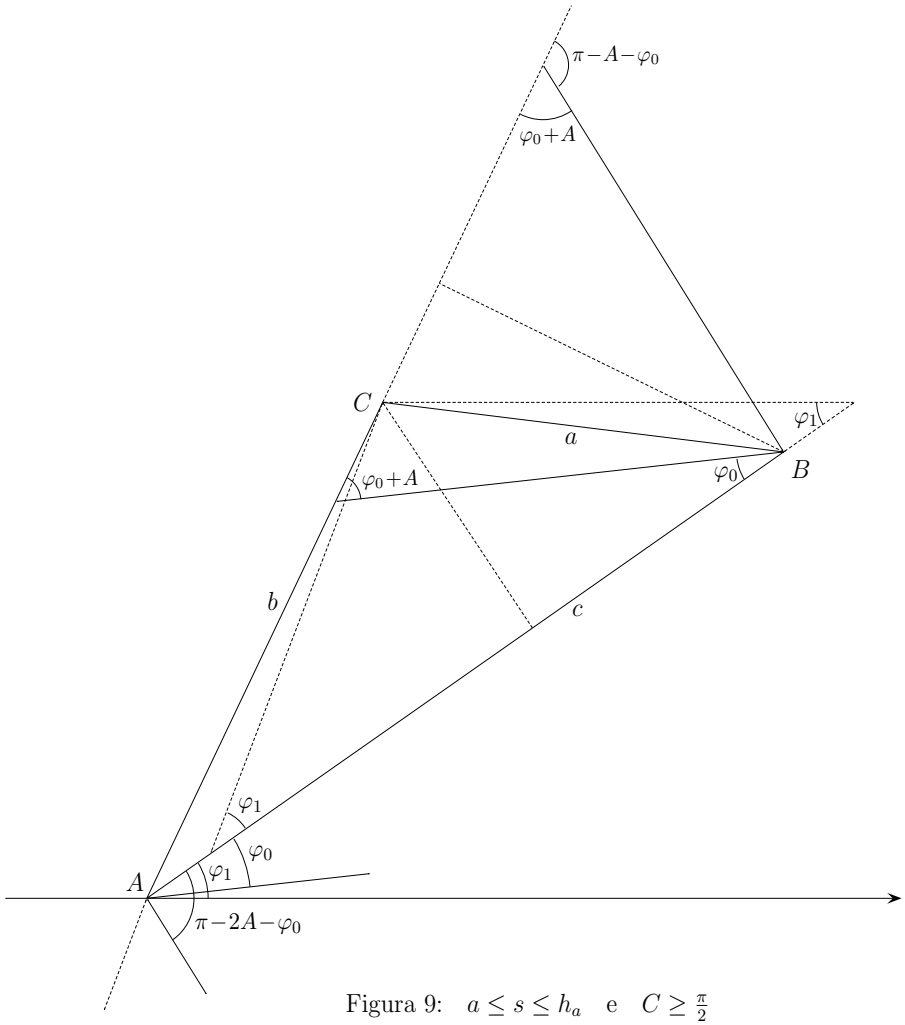


Figura 9: $a \le s \le h_a$ e $C \ge \frac{\pi}{2}$

Se $s = a$ si ha $\varphi_1 = B$, $\varphi_0 = C - A$ e $\pi - 2A - \varphi_0 = B$, e il valore p_a si può calcolare sia con la formula (5) che con la formula (3).

§ 7. Caso I.5 : $h_a \le s \le a$ **e** $C \le \frac{\pi}{2}$

Questo caso differisce dal caso I.3 solo per il comportamento della funzione x_s nell'intervallo $[\pi - A, \pi]$. Poichè $h_a \le s \le a$ esistono due angoli φ_2 e $\pi + 2B - \varphi_2$ con $\varphi_2 \le \pi + 2B - \varphi_2$ per i quali le parallele a $\mathfrak{g}$ condotte da A determinano in $\mathbf{D}$ corde di lunghezza s (v. fig. 10).

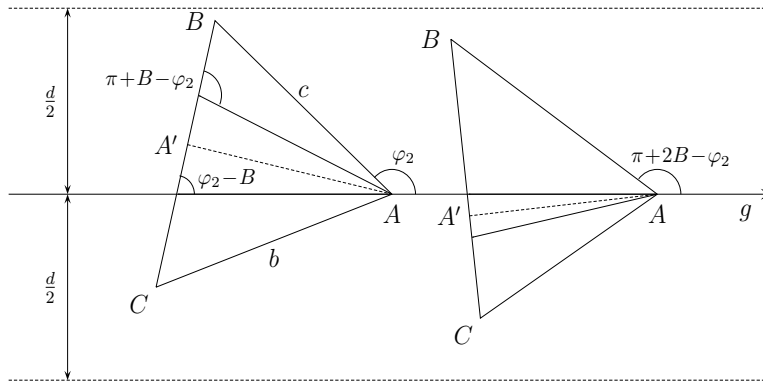


Figura 10: $h_a \le s \le a$ e la definizione di φ_2

Dalla stessa figura si vede che $s\sin(\varphi_2 - B) = c\sin B = b\sin C$ e $\varphi_2 + A \ge \pi \Rightarrow \varphi_2 \ge \pi - A = B + C \ge 2B \Rightarrow \pi + 2B - \varphi_2 \le \pi$. Come conseguenza $x_s(\varphi) = 0$ se $\varphi \in [\varphi_0, \pi - 2A - \varphi_0] \cup [\varphi_1, \pi - \varphi_1] \cup [\varphi_2, \pi + 2B - \varphi_2]$. Risulta

$$\int_0^{\pi} x_s(\varphi)d\varphi = \left(\int_0^{\varphi_0} + \int_{\pi-2A-\varphi_0}^{B} + \int_B^{\varphi_1} + \int_{\pi-\varphi_1}^{\pi-A} + \int_{\pi-A}^{\varphi_2} + \int_{\pi+2B-\varphi_2}^{\pi} \right) x_s(\varphi)d\varphi =$$

$$\ldots = a(\cos B + \cos C - 2\cos(\varphi_2 - B)) + b(\cos C + \cos A - 2\cos(A + \varphi_0))$$

$$+c(\cos A + \cos B - 2\cos\varphi_1) - \frac{s}{2}\Big[3 + (\cot A + \cot B)(2\varphi_1 - A - B - \sin 2\varphi_1)$$

$$+(\cot B + \cot C)(2\varphi_2 + A - 2B - \pi - \sin(2\varphi_2 - 2B))$$

$$+(\cot C + \cot A)(2\varphi_0 + 2A + B - \pi - \sin(2A + 2\varphi_0))\Big] = \ldots \ ,$$

e cosi

$$(6) \qquad p_s = \frac{1}{\pi d}\left\{ a + b + c - 2\Big[b\cos(A + \varphi_0) + c\cos\varphi_1 + a\cos(\varphi_2 - B)\Big] \right.$$

$$-\frac{s}{2}\left[3 + \frac{A\sin^2 A + B\sin^2 B + C\sin^2 C}{\sin A\sin B\sin C} + (2(A + \varphi_0) - \pi)\frac{\sin B}{\sin A\sin C}\right.$$

$$\left.\left. +(2\varphi_1 - \pi - 2\sin\varphi_1)\frac{\sin C}{\sin A\sin B} + (2(\varphi_2 - B) - \pi - \sin(2\varphi_2 - 2B))\frac{\sin A}{\sin B\sin C}\right]\right\}.$$

Osserviamo che se **D** è un triangolo equilatero di lato l e $s \in \left[\frac{l\sqrt{3}}{2}, l\right]$ la (6) diventa la formula (2) del lavoro [2]. Osserviamo inoltre che se $h_a = s = a$ e quindi $\varphi_2 = \frac{\pi}{2} + B$, la formula (6) coincide con la (4).

§ 8. Caso II.5 : $h_a \le s \le a$ **e** $C \ge \frac{\pi}{2}$

Come nel caso II.4 si ha $B \le \varphi_1 \le \varphi_0 \le \pi - 2A - \varphi_0 \le \pi - \varphi_1 < \pi - A$. $\varphi_2 - B < \frac{\pi}{2}$, $\varphi_1 < \frac{\pi}{2}$ e $\sin(\varphi_2 - B) = \frac{c \sin B}{s} = \frac{b \sin C}{s} \ge \frac{b \sin A}{s} = \sin \varphi_1$ si ha $\varphi_1 \le \varphi_2 - B < \varphi_2$. Utilizzando la seguente figura e le relative notazioni

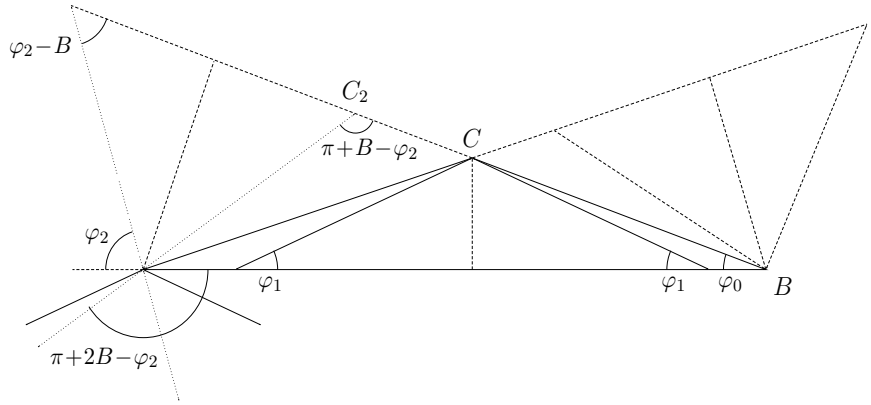


Figura 11: $h_a \le s \le a$ e $C \ge \frac{\pi}{2}$

otteniamo la relazione

$$\frac{a}{\sin \varphi_1} \ge \frac{a}{\sin(\varphi_2 - B)} = \frac{C_2 B}{\sin(\varphi_2 - 2B)} = \frac{C_2 C + a}{\sin(\varphi_2 - 2B)} = \frac{s}{\sin B} \ge \frac{a}{\sin(\varphi_2 - 2B)} .$$

Da cui segue $\sin(\pi - \varphi_1) = \sin \varphi_1 \le \sin(\varphi_2 - 2B) = \sin(\pi + 2B - \varphi_2)$ e poichè gli angoli $\pi - \varphi_1$ e $\pi + 2B - \varphi_2$ sono ottusi, si ha $\pi + 2B - \varphi_2 \le \pi - \varphi_1$. La funzione x_s è nulla nel sottointervallo $[\varphi_1, \pi - \varphi_1]$ di $[B, \pi - A]$; dunque il calcolo della probabilità p_s in questo caso coincide con quello visto nel § 3 e quindi il risultato è fornito dalla formula (3).

§ 9. Caso I.6 : $\max(a, h_a) \le s \le b$ **e** $C \le \frac{\pi}{2}$

Definendo gli angoli φ_0, φ_1 e φ_2 come nei casi precedenti e osservando la figura 12 si ha $\varphi_0 \le \varphi_1 \le B \le \pi - 2A - \varphi_0 \le \pi - \varphi_1 \le \pi - A \le \varphi_2 \le \pi + 2B - \varphi_2 \le \pi$.

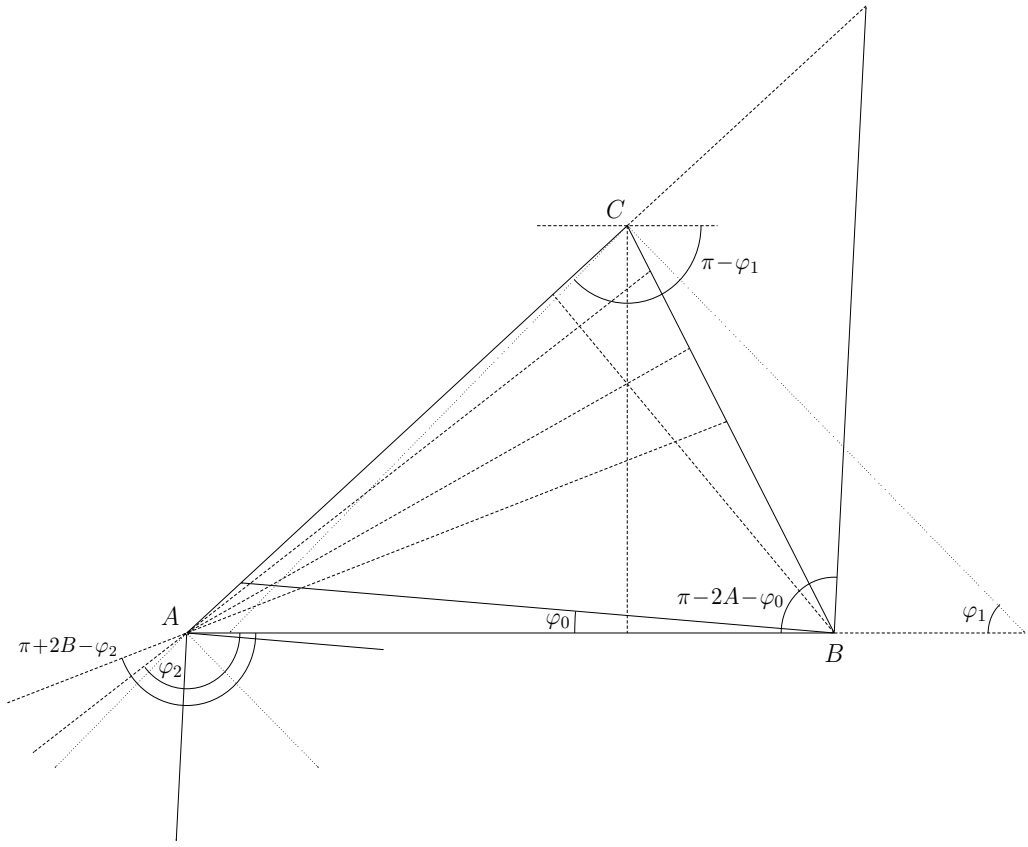


Figura 12: $\max(a, h_a) \le s \le b$ e $C \le \frac{\pi}{2}$

Essendo la funzione x_s nulla in $[\varphi_0\,, \pi - \varphi_1] \cup [\varphi_2\,, \pi + 2B - \varphi_2]$, si ha

$$\int_0^{\pi} x_s(\varphi)d\varphi = a + b + c - (b\cos(A+\varphi_0) + c\cos\varphi_1 + 2a\cos(\varphi_2 - B))$$

$$-\frac{s}{2}\left[2 + \frac{A\sin^2 A + B\sin^2 B + C\sin^2 C}{\sin A\sin B\sin C} - (B-\varphi_0)\frac{\sin B}{\sin A\sin C}\right.$$

$$-(\pi - B - \varphi_1)\frac{\sin C}{\sin A\sin B} - (\pi + 2B - 2\varphi_2 + \sin(2\varphi_2 - 2B))\frac{\sin A}{\sin B\sin C}$$

$$\left.+\frac{\sin(A - B + 2\varphi_0)}{2\sin C} - \frac{\sin(A+2\varphi_0)}{2\sin A} + \frac{\sin(A-2\varphi_1)}{2\sin A} - \frac{\sin(B+2\varphi_1)}{2\sin B}\right]$$

e quindi la probabilità cercata è

$$
\begin{aligned}
(7)\qquad p_s = \frac{1}{\pi d}\Bigg\{ & a+b+c-(b\cos(A+\varphi_0)+c\cos\varphi_1+2a\cos(\varphi_2-B)) \\
& -\frac{s}{2}\Bigg[2+\frac{A\sin^2 A+B\sin^2 B+C\sin^2 C}{\sin A\sin B\sin C}-(B-\varphi_0)\frac{\sin B}{\sin A\sin C}-(\pi-B-\varphi_1)\frac{\sin C}{\sin A\sin B} \\
& -(\pi+2B-2\varphi_2+\sin(2\varphi_2-2B))\frac{\sin A}{\sin B\sin C}+\frac{\sin(A-B+2\varphi_0)}{2\sin C}-\frac{\sin(A+2\varphi_0)}{2\sin A} \\
& +\frac{\sin(A-2\varphi_1)}{2\sin A}-\frac{\sin(B+2\varphi_1)}{2\sin B}\Bigg]\Bigg\}.
\end{aligned}
$$

Osserviamo che le formule(5) e (7), rispettivamente (6) e (7), forniscono lo stesso risultato se $a \le h_a = s$, rispettivamente $h_a \le a = s$.

§ 10. Caso II.6 : $\max(a, h_a) \le s \le b$ **e** $C \ge \frac{\pi}{2}$

Come si vede anche dalla figura 13 in questo caso valgano le seguenti disuguaglianze

$$0 < \varphi_0 \le \varphi_1 \le B \le \varphi_2 \le \pi - 2A - \varphi_0 \le \pi + 2B - \varphi_2 \le \pi - \varphi_1 \le \pi - A \le \pi\ .$$

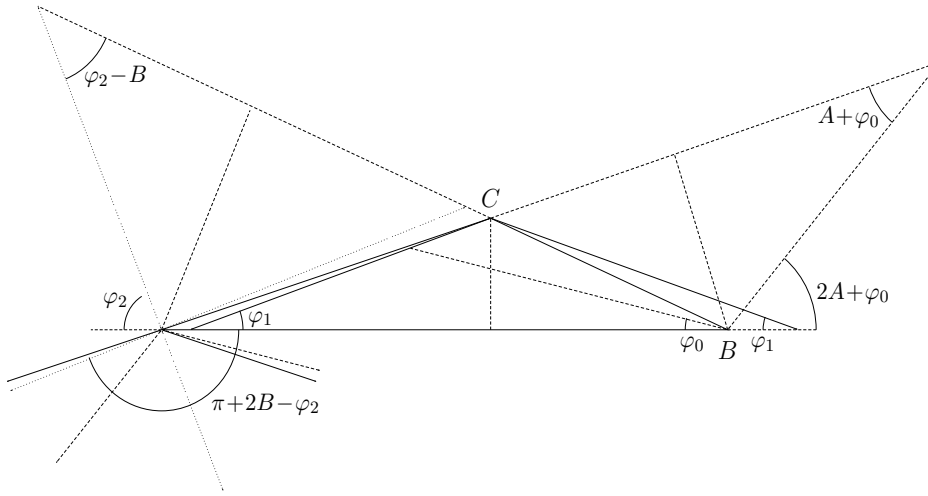


Figura 13: $\max(ah_a) \le s \le b$ e $C \ge \frac{\pi}{2}$

Poichè in questo caso x_s non è nulla solo negli intervalli $[0, \varphi_0]$ (sottointervallo di $[0, B]$), $[\pi - \varphi_1\,, \pi - A]$ (sottointervallo di $[B,\, \pi - A]$) e $[\pi - A,\, \pi]$, il calcolo di $\int_0^{\pi} x_s(\varphi)d\varphi$ è identico a quello del §6. Ne segue che l'espressione della probabilità p_s è fornita dalla formula (5).

§ 11. Casi I.7 **e** II.7 : $b \leq s \leq c$ (C arbitrario)
Nel caso $C \leq \frac{\pi}{2}$ possiamo utilizzare la figura 14 per ottenere le seguenti disuguaglianze:

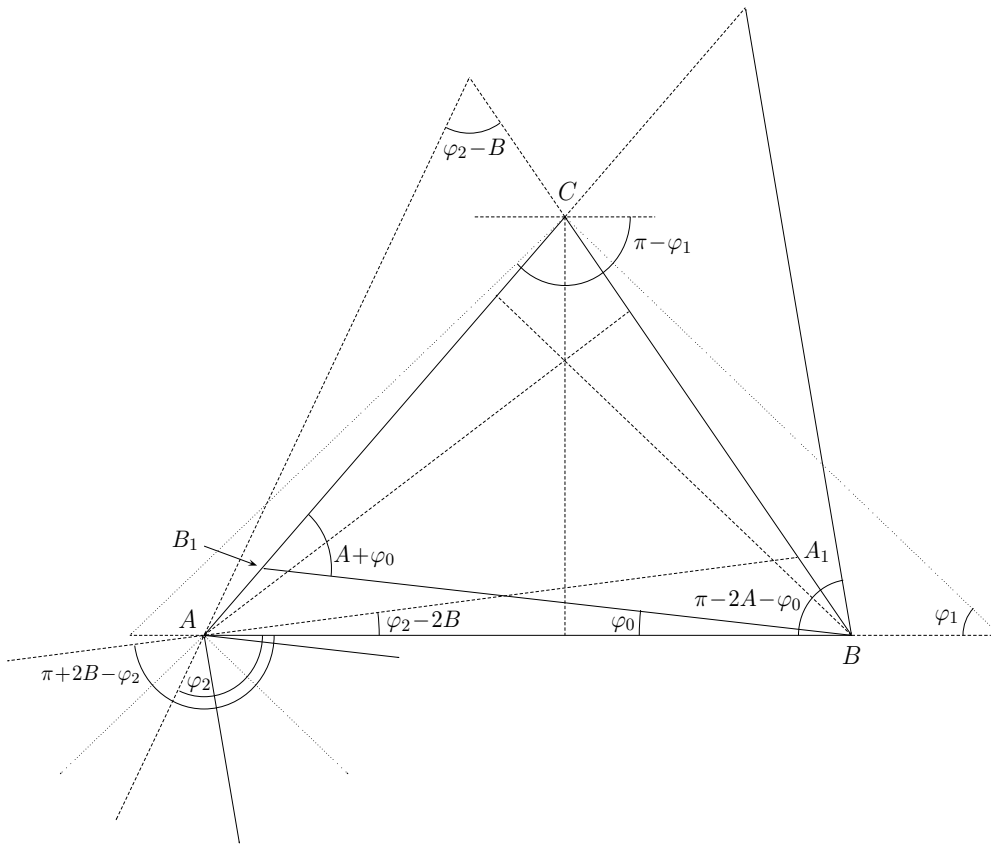


Figura 14: $b \leq s \leq c$ e $C \leq \frac{\pi}{2}$

$$(*) \qquad \varphi_0 \leq \varphi_1 \leq A \leq B \leq \varphi_2 \leq \pi - A \leq \pi - \varphi_1 \leq \pi + 2B - \varphi_2 \leq \pi \ .$$

È bene notare che le disuguaglianze $(*)$ (cosi come tutte quelle considerate nei paragrafi precedenti) si possono stabilire direttamente anche utilizzando le note proprietà delle funzioni trigonometriche:

- $\sin\varphi_0 = \dfrac{\overline{AB_1}\sin A}{s} \le \dfrac{b\sin A}{s} = \sin\varphi_1 \Rightarrow \varphi_0 \le \varphi_1$,
- $\sin\varphi_1 = \dfrac{b\sin A}{s} \le \sin A \Rightarrow \varphi_1 \le A$ e cosi $\pi - A \le \pi - \varphi_1$,
- $\sin(\varphi_2 - B) = \dfrac{c\sin B}{s} \ge \sin B \Rightarrow \varphi_2 - B \ge B \Rightarrow \varphi_2 \ge 2B$, poiche $\varphi_2 - B \le \dfrac{\pi}{2}$,
- $\dfrac{\sin(\varphi_2 - 2B)}{s} \le \dfrac{\sin(\varphi_2 - 2B)}{|\overline{A_1B}|} = \dfrac{\sin B}{s} \le \dfrac{\sin\varphi_1}{s} \Rightarrow \varphi_2 - 2B \le \varphi_1 \iff$
  $\pi - \varphi_1 \le \pi + 2B - \varphi_2$.

Da $(*)$ segue che $x_s(\varphi)$ è nulla su $[0,\pi] \setminus ([0,\varphi_0] \cup [\pi + 2B - \varphi_2\,, \pi]$. Si ha

$$\int_0^{\pi} x_s(\varphi)d\varphi = \int_0^{\varphi_0} x_s(\varphi)d\varphi + \int_{\pi+2B-\varphi_2}^{\pi} x_s(\varphi)d\varphi = b(\cos A - \cos(A+\varphi_0))$$

$$+a(\cos B - \cos(\varphi_2 - B)) - \frac{s}{2}\Bigg[(\cot A + \cot C)\varphi_0 + (\cot B + \cot C)(\varphi_2 - 2B) + 1$$

$$+\frac{\sin(A - B + 2\varphi_0)}{2\sin C} - \frac{\sin(A+2\varphi_0)}{2\sin A} + \frac{\sin(3B - 2\varphi_2)}{2\sin B} - \frac{\sin(A + 3B - 2\varphi_2)}{2\sin C}\Bigg] ,$$

e quindi

$$(8) \qquad p_s = \frac{1}{\pi d}\Bigg\{b(\cos A - \cos(A+\varphi_0)) + a(\cos B - \cos(\varphi_2 - B))$$

$$-\frac{s}{2}\Bigg[(\cot A + \cot C)\varphi_0 + (\cot B + \cot C)(\varphi_2 - 2B) + 1 + \frac{\sin(A - B + 2\varphi_0)}{2\sin C}$$

$$-\frac{\sin(A+2\varphi_0)}{2\sin A} + \frac{\sin(3B - 2\varphi_2)}{2\sin B} - \frac{\sin(A + 3B - 2\varphi_2)}{2\sin C}\Bigg]\Bigg\}.$$

Se $s = b$ si ha $\varphi_1 = A$ e $\varphi_2 - B = C$, quindi $\varphi_2 = \pi - A$; ne segue che per tali valori le formule (7) e (8) coincidono.

Sia ora $C \ge \frac{\pi}{2}$. Utilizzando le stesse argomentazioni e anche la Figura 15 si ottiene la stessa catena di disugualianze $(*)$. La formula (8) è valida anche in questo caso.

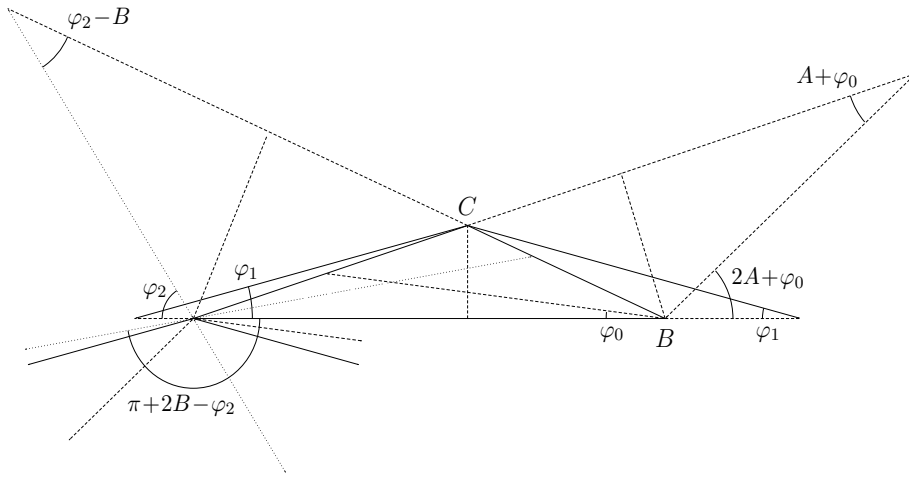


Figura 15: $b \le s \le c$ e $C \ge \frac{\pi}{2}$

§ 12. Risultato principale

Abbiamo dimostrato il seguente

Theorema: La probabilità p_s, che un triangolo **D** di lati a, b, c, angoli $A \le B \le C$ e altezze $h_a \ge h_b \ge h_c$ uniformemente distribuito in una regione limitata del piano euclideo intersechi su una retta del reticolo di Buffon $\mathcal{R}_d$ un segmento di lunghezza maggiore o uguale ad s, con $0 \le s \le c \le d$, si calcola, tenendo conto di tutti i casi possibili, con le formula (2), (3), ..., (8). Gli angoli φ_0, φ_1, φ_2 che intervengono in tali formule sono univocamente determinati nell'intervallo $\left[0, \frac{\pi}{2}\right]$ dalle formule

$$\sin(\varphi_0 + A) = \frac{a \sin C}{s} \ . \quad \sin\varphi_1 = \frac{b \sin A}{s} \quad \text{e} \quad \sin(\varphi_2 - B) = \frac{b \sin C}{s} \ .$$

§ 13. Distribuzione della corda nel triangolo

La funzione F di distribuzione della corda nel triangolo **D** associa ad ogni $s \in [0, c]$ la probabilità che una corda arbitraria in **D** abbia una lunghezza minore o uguale di s. Cioè

$$F(s) = 1 - p_s/p_0 \ . \tag{9}$$

Si osservi esplicitamente che la funzione **F** non dipende dalla distanza d tra le rette del reticolo.

La densita $f = F'$ della distribuzione della corda è costante solo nei casi I.1 e II.1, poichè nei casi rimanenti φ_0, φ_1 e φ_2 sono funzioni non lineari di s.

Bibliografia

[1] **Duma, A.:** Problems of Buffon type for "non small" needles, *Rend. Circ. Mat. Palermo, Serie II, Tomo XLVIII, pp. 23-40, 1999.*

[2] **Duma, A. - Stoka M.I.:** Schnitte eines "kleinen" gleichseitigen Dreiecks mit den Gittern von Buffon und Laplace, *Seminarberichte der Fernuniversität, pp. 13-22, 2008.*

[3] **Pettineo, M.:** Geometric probability problems for lattices of Buffon and Laplace, *VI International Conference "Stochastic geometry, convex bodies, empirical measure and applications to mechanics and engineering of train-transport", Milazzo, 2007.*

[4] **Stoka, M.I.:** Probabilités géométriques de type "Buffon" dans le plan euclidien, *Atti Acc. Sci. Torino, 110, pp. 53-59, 1975-76.*

Andrei Duma
Fakultät für
Mathematik und Informatik
FernUniversität in Hagen
58084 Hagen
Germany

Sebastiano Rizzo
Dipartimento di Matematica
Università del Salento
Via per Arnesano
73100 Lecce
Italy

RENDICONTI DEL CIRCOLO MATEMATICO DI PALERMO
Serie II, Suppl. 81 (2009), pp. 159-169

The generalized Buffon-experiment with multiple intersections for the lattice of Buffon and a bunch as test body

Andrei DUMA - Martin WECKER

Dedicated to Professor M. Stoka on occasion of his 75th birthday

1 Introduction

Let $\mathcal{R}_d$ be Buffon's lattice of equidistant parallel lines in the plane, where d denotes the distance between two adjacent lines of $\mathcal{R}_d$. A Bunch $\mathcal{B}$ is a plane figure consisting of n segments $s_1, ..., s_n$ of length $d_1 = d_{01}, ..., d_n = d_{0n}$, which have the same initial starting point Q_0 and the end points $Q_1, ..., Q_n$.

Let d_{ik} be the length of the segment $\overline{Q_iQ_k}$. If $d > \max_{0\leq i,k\leq n} d_{ik}$ let $P(q)$ ($q \in \{0, 1, ..., n\}$) be the probability that any straight line of $\mathcal{R}_d$ intersects q segments of the testbody $\mathcal{B}$ with random position and uniformly distributed in a bounded region of the plane.

For $n = 4$ we compute the probabilities $P(1), P(2), P(3)$ and $P(4)$ as functions of d_{ik} ($0 \leq i, k \leq 4$, $i \neq k$) and the range L of the convex closure of the set $\{Q_0, Q_1, ..., Q_4\}$. For this we have to consider seven cases as we will see later, but first we start with a few basic theorems which are well known from many books about integral geometry. All proofs of the following theorems can be found in [1] or [2].

1.1 The measure of lines in the plane

A straight line g in the plane is determined by an angle $\varphi \in [0, 2\pi)$ and $p \geq 0$ according to figure 1. Let $G := \{(p, \varphi) \,|\, p \in \mathbb{R}_+, \varphi \in [0, 2\pi)\} \subset \mathbb{R}^2$ be a set of lines, then the measure $m(G)$ of the set G is given by

$$m(G) := \int_G dpd\varphi. \tag{1}$$

In [1] it is shown that the measure m is the unique invariant measure under euclidean motions of G. If we have a set $K \subset \mathbb{R}^2$ we denote the set of all lines which intersect K as $G_K := \{g = (p, \varphi) \,|\, g \cap K \neq \emptyset\}$.

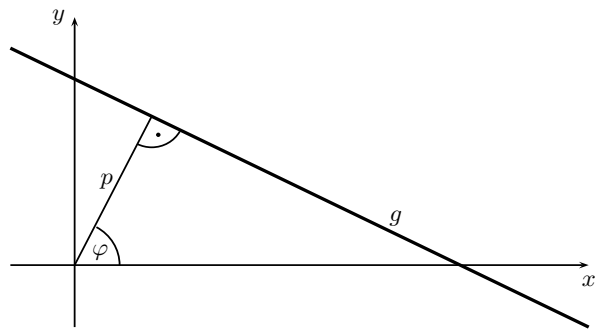


Figure 1: A line in the plane

1.2 Convex Sets

THEOREM 1.1. Let $K \subset \mathbb{R}^2$ be a bounded and convex set and let $L_{\partial K}$ be the length of the boundary ∂K, then we have

$$m(G_K) = L_{\partial K}.$$

Convex sets are very important for our purposes because if we have a bounded set $K \subset \mathbb{R}^2$ and the convex closure $H(K)$ of K then we have $m(G_K) = m(G_{H(K)})$. For our further investigations we have to apply theorem 1.1 to line segments and convex polygons.

1.3 Pairs of convex sets

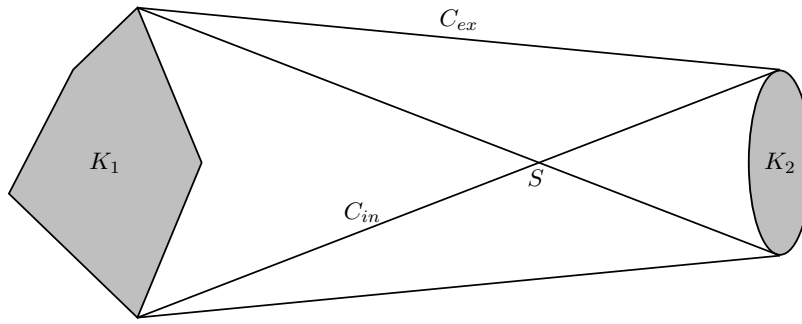


Figure 2: Two bounded convex sets

If we have two bounded convex sets K_1 and K_2, we are especially interested in the measure of all lines g which intersects K_1 and K_2. Before we can cite another important theorem from [1] we have to define some notations.

We define C_{ex} as the boundary of the convex closure $H(K_1 \cup K_2)$ of K_1 and K_2:

$$C_{ex} := \partial H(K_1 \cup K_2).$$

If we have $K_1 \cap K_2 = \emptyset$ we also need the so called inner curve C_{in}. The definition of C_{in} has to be done carefully, therefore we begin for all points $R \in H_0 := H(K_1 \cup K_2)$ with the closed curves

$$C_1(R) := \partial H(K_1 \cup \{R\}) \quad \text{and} \quad C_2(R) := \partial H(K_2 \cup \{R\})$$

and the set

$$U := \{R \in H_0 \,|\, (H(K_1 \cup \{R\}) \cap K_2) \subseteq \{R\} \text{ and } (H(K_2 \cup \{R\}) \cap K_1) \subseteq \{R\}\}.$$

Generally U contains points on the boundary of ∂K_1 or ∂K_2, but no points in $K_1 \setminus \partial K_1$ or $K_2 \setminus \partial K_2$. If we connect $C_1(R)$ and $C_2(R)$, we get a closed curve around K_1 and K_2, which intersects itself in R. Now we define C_{in} as the shortest of all these curves:

$$C_{in} := C_1(S) \cup C_2(S)$$

with $S \in U$ und $L_{C_1(S)} + L_{C_2(S)} = \min_{R \in U} (L_{C_1(R)} + L_{C_2(R)})$.

THEOREM 1.2. Let $K_1, K_2 \subset \mathbb{R}^2$ be two bounded and convex sets with $K_1 \cap K_2 = \emptyset$ and let L_{in} be the length of C_{in} and L_{ex} the length of C_{ex}, then we have:

(a) $m(G_{K_1} \cap G_{K_2}) = L_{in} - L_{ex}$

(b) $m(G_{K_1} \setminus G_{K_2}) = L_{\partial K_1} - (L_{in} - L_{ex})$ und $m(G_{K_2} \setminus G_{K_1}) = L_{\partial K_2} - (L_{in} - L_{ex})$

(c) $m(G_{H(K_1 \cup K_2)} \setminus (G_{K_1} \cup G_{K_2})) = L_{in} - (L_{\partial K_1} + L_{\partial K_2})$

We obeserve that in the case $K_1 \cap K_2 \neq \emptyset$ (a)-(c) stay valid if we set $L_{in} := L_{\partial K_1} + L_{\partial K_2}$. Now we apply this theorem to seven examples Ex1 - Ex7. In the first three examples K_1 and K_2 are two line segments and in the other examples K_1 is a line segment and K_2 is a convex polygon with four corners. For all examples we only compute the measure $m(G_{K_1} \cap G_{K_2}) = L_{in} - L_{ex}$ which we need later. We denote the euclidean distance between two points $A, B \in \mathbb{R}^2$ as $d(A, B)$.

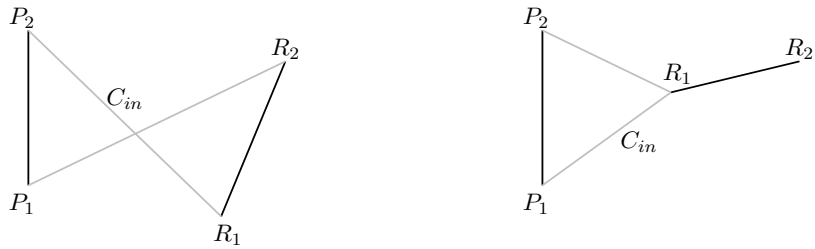


Figure 3: Examples Ex1 (left) and Ex2 (right)

(Ex1) The line segments $\overline{P_1R_2}$ and $\overline{P_2R_1}$ intersect each other. We have

$$L_{in} = d(P_1, P_2) + d(P_1, R_2) + d(P_2, R_1) + d(R_1, R_2)$$
$$L_{ex} = d(P_1, P_2) + d(P_1, R_1) + d(P_2, R_2) + d(R_1, R_2)$$

and with theorem 1.2 we get

$$m(G_{K_1} \cap G_{K_2}) = d(P_1, R_2) + d(P_2, R_1) - d(P_1, R_1) - d(P_2, R_2).$$

If the line segments $\overline{P_1R_1}$ and $\overline{P_2R_2}$ intersect each other, then we can change R_1 and R_2 and again we have the situation of Ex1.

(Ex2) The line segments $\overline{P_1R_2}$, $\overline{P_2R_1}$ and also $\overline{P_1R_1}$, $\overline{P_2R_2}$ do not intersect each other and we have $K_1 \cap K_2 = \emptyset$. We get

$$\begin{aligned} L_{in} &= d(P_1,P_2) + d(P_1,R_1) + d(P_2,R_1) + 2d(R_1,R_2) \\ L_{ex} &= d(P_1,P_2) + d(P_1,R_2) + d(P_2,R_2) \\ m(G_{K_1} \cap G_{K_2}) &= d(P_1,R_1) + d(P_2,R_1) + 2d(R_1,R_2) - d(P_1,R_2) - d(P_2,R_2). \end{aligned}$$

(Ex3) In this example we have $P_1 = R_1$. Since $K_1 \cap K_2 \neq \emptyset$ in this case, we have

$$\begin{aligned} L_{in} &= 2d(P_1,P_2) + 2d(P_1,R_2) \\ L_{ex} &= d(P_1,P_2) + d(R_1,R_2) + d(P_2,R_2) \\ m(G_{K_1} \cap G_{K_2}) &= d(P_1,P_2) + d(R_1,R_2) - d(P_2,R_2). \end{aligned}$$

In this example the line segments $\overline{P_1P_2}$ und $\overline{P_1R_2}$ are two sites of a triangle with corners P_1, P_2, R_2, it means for a triangle with sites $a = \overline{P_1P_2}, b = \overline{P_1R_2}$ and $c = \overline{P_2R_2}$ we have

$$m(G_a \cap G_b) = L_a + L_b - L_c.$$

In the following four examples Ex4 - Ex7 we have a line segment $K_1 = \overline{P_1P_2}$ and a convex polygon K_3 with corners $R_1, ..., R_4$. There may be more combinations of a line segment and a polygon than these four examples, but we only need Ex4 - Ex7 for our further computations.

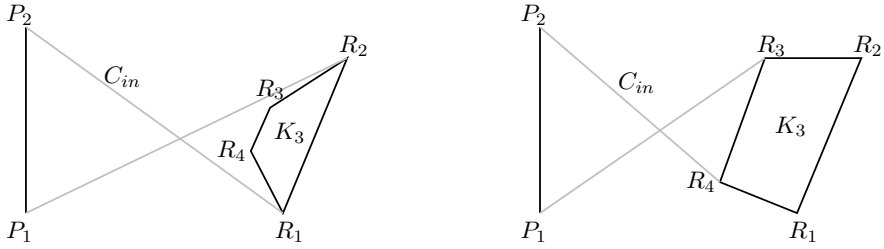


Figure 4: Examples Ex4 (left) and Ex5 (right)

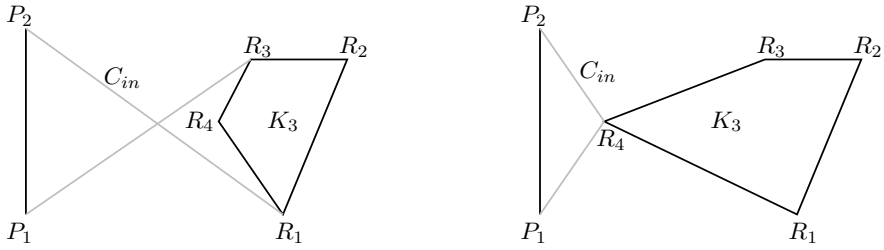


Figure 5: Examples Ex6 (left) and Ex7 (right)

(Ex4) In this example we have with the notation of figure 4

$$\begin{aligned} L_{in} &= d(P_1,P_2)+d(P_1,R_2)+d(P_2,R_1)+d(R_1,R_2)\\ L_{ex} &= d(P_1,P_2)+d(P_1,R_1)+d(R_1,R_2)+d(P_2,R_2)\\ m(G_{K_1}\cap G_{K_3}) &= d(P_1,R_2)+d(P_2,R_1)-d(P_1,R_1)-d(P_2,R_2). \end{aligned}$$

(Ex5) We have

$$\begin{aligned} L_{in} &= d(P_1,P_2)+d(P_1,R_3)+d(R_2,R_3)+d(P_2,R_4)+d(R_1,R_4)+d(R_1,R_2)\\ L_{ex} &= d(P_1,P_2)+d(P_1,R_1)+d(R_1,R_2)+d(P_2,R_2)\\ m(G_{K_1}\cap G_{K_3}) &= d(P_1,R_3)+d(R_2,R_3)+d(P_2,R_4)+d(R_1,R_4)\\ &\quad -d(P_1,R_1)-d(P_2,R_2). \end{aligned}$$

(Ex6) Here we have

$$\begin{aligned} L_{in} &= d(P_1,P_2)+d(P_1,R_3)+d(P_2,R_1)+d(R_1,R_2)+d(R_2,R_3)\\ L_{ex} &= d(P_1,P_2)+d(P_1,R_1)+d(R_1,R_2)+d(P_2,R_2)\\ m(G_{K_1}\cap G_{K_3}) &= d(P_1,R_3)+d(P_2,R_1)+d(R_2,R_3)-d(P_1,R_1)-d(P_2,R_2). \end{aligned}$$

(Ex7) In this case we have

$$\begin{aligned} L_{in} &= d(P_1,P_2)+d(P_1,R_4)+d(P_2,R_4)+L_{\partial K_3}\\ L_{ex} &= d(P_1,P_2)+d(P_1,R_1)+d(P_2,R_2)+d(R_1,R_2)\\ m(G_{K_1}\cap G_{K_3}) &= d(P_1,R_4)+d(P_2,R_4)+d(R_1,R_4)+d(R_3,R_4)+d(R_2,R_3)\\ &\quad -d(P_1,R_1)-d(P_2,R_2). \end{aligned}$$

1.4 Convex polygons in the lattice of Buffon

THEOREM 1.3. Let $\mathcal{R}_d$ be Buffon's lattice and let $K\subset\mathbb{R}^2$ be a convex polygon with corners $P_1,...,P_k$ and $d(P_i,P_j)\le d$ $(i,j\in\{1,...,k\})$. Since $d(P_i,P_j)\le d$ the polygon K intersects not more than one line of $\mathcal{R}_d$. The probability p that K intersects a line of $\mathcal{R}_d$ is given by

$$p=\frac{1}{\pi d}m(G_K)=\frac{1}{\pi d}L_{\partial K}.$$

Now we know all basics about the measure m which we need to calculate the probabilities $P(k)$ $(1\le k\le 4)$ for a bunch $\mathcal{B}$. But before we start, we outline some central ideas of our solution in the next section.

2 Methodology and central ideas

We want to show, how we can apply theorems 1.1 to 1.3 to calculate $P(k)$ $(1\le k\le 4)$ for a bunch $\mathcal{B}$ with $n=4$. First of all the boundary $\partial H(\mathcal{B})$ is a convex polygon, where $H(\mathcal{B})$ is the convex closure of $\mathcal{B}$. For any line g we have

$$g\cap\mathcal{B}\neq\emptyset\Leftrightarrow g\cap H(\mathcal{B})\neq\emptyset.$$

Any line g has exactly two intersection points with $\partial H(\mathcal{B})$. Let s_{ij} and s_{kl} be two line segments of ∂H, where $H := H(\mathcal{B})$. We define $G(q) := \{g \,|\, g \cap \mathcal{B} \text{ consists of } q \text{ points}\}$, $M(q) := m(G(q))$ and $M(q|s_{ij}s_{kl}) := m(G(q) \cap G_{s_{ij}} \cap G_{s_{kl}})$ for any $q \in \{1, ..., 4\}$.

It seems to be complicated to calculate the measure $M(q)$, but we can divide $M(q)$ into many measures which we will calculate later:

$$M(q) = \sum_{s_{ij}, s_{kl} \subset \partial H} M(q|s_{ij}s_{kl}) \quad (q = 1, ..., 4). \tag{2}$$

Once we have calculated $M(q)$ we get $P(q) = \frac{1}{\pi d} M(q)$ from theorem 1.3.

From now on our aim is to calculate the measure $M(q|s_{ij}s_{kl})$ for any $q \in \{1, ..., 4\}$ and any $s_{ij}, s_{kl} \subset \partial H$. We will develope a methodology only based on theorem 1.1 and 1.2. It is important to understand the core idea of our method, therefore we begin with the situation in figure 6. There we have a convex quadrangle K_0 with the corners R_1, R_2, R_3, R_4 and two points $S_1, S_2 \in K_0 \setminus \partial K_0$.

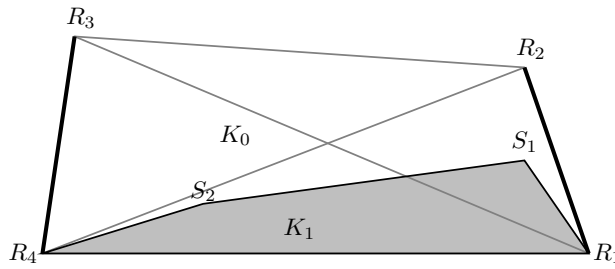


Figure 6: Illustration of the central idea

Now we want to calculate the measure of all lines which intersect $\overline{R_1R_2}$, $\overline{R_3R_4}$ and K_1, it means $m(G_{\overline{R_1R_2}} \cap G_{\overline{R_3R_4}} \cap G_{K_1})$. Since we have $K_1 \subset K_0$ any line $g \in G_{K_1}$ intersects two of the four sides of K_0. We see that $g \in G_{K_1}$ fulfill exactly one of the following four cases:

(i) g intersects intersects $\overline{R_2R_3}$ and K_1,
(ii) g intersects $\overline{R_1R_2}$ and $\overline{R_1R_4}$ and therefore also K_1,
(iii) g intersects $\overline{R_3R_4}$ and $\overline{R_1R_4}$ and therefore also K_1,
(iv) g intersects $\overline{R_1R_2}$, $\overline{R_3R_4}$ and K_1.

It is important to notice that generally $G_{K_1} \cap G_{\overline{R_2R_3}} \neq G_{\overline{R_1R_4}} \cap G_{\overline{R_2R_3}}$ because under some circumstances a line $g \in G_{K_1} \cap G_{\overline{R_2R_3}}$ can also intersect $\overline{R_1R_2}$ or $\overline{R_3R_4}$ instead of $\overline{R_1R_4}$. Now the idea is to divide G_{K_1} into four disjunct subsets and to calculate the measure of three subsets separately and to get the measure of (iv) as a difference of these measures and $m(G_{K_1})$.

It is obvious that a line $g \in G_{K_1}$ can only fulfill one of the four cases (i)-(iv) and the other way around any line $g \in G_{K_1}$ fulfill at least one of the cases (i)-(iv), so we have

$$\begin{aligned} m(G_{K_1}) = {} & m(G_{\overline{R_2R_3}} \cap G_{K_1}) + m(G_{\overline{R_1R_2}} \cap G_{\overline{R_1R_4}}) \\ & + m(G_{\overline{R_3R_4}} + G_{\overline{R_1R_4}}) + m(G_{\overline{R_1R_2}} \cap G_{\overline{R_3R_4}} \cap G_{K_1}) \end{aligned} \tag{3}$$

The measure on the left side of (3) and the first three measures on the right side can be computed with theorem 1.1 or 1.2 because we only have a convex set or pairs of convex sets. So we get $m(G_{\overline{R_1R_2}} \cap G_{\overline{R_3R_4}} \cap G_{K_1})$ as a difference of four known measures. Formula (3) is very important for our further investigations and we will need this formula in many variations. We can also apply (3) in the cases $R_1 = R_4$ or $R_2 = R_3$ because then we have $d(R_1, R_4) = 0$ (it means $m(G_{\overline{R_1R_2}} \cap G_{\overline{R_1R_4}}) = m(G_{\overline{R_3R_4}} + G_{\overline{R_1R_4}}) = 0$) or $d(R_2, R_3) = 0$ (it means $m(G_{\overline{R_2R_3}} \cap G_{K_1}) = 0$).

Now we compute the measure $M(q|s_{ij}s_{kl})$ for two examples to show how (3) will help us to calculate the probabilities $P(q)$ $(1 \leq q \leq n)$.

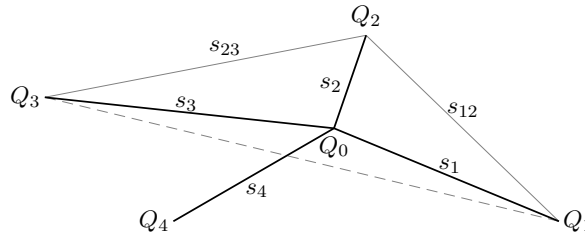


Figure 7: Application of formula (3), example 1

For the example in figure 7 we now calculate $M(q|s_{12}s_{23})$ $(1 \leq q \leq 4)$. Any line $g \in G_{s_{12}} \cap G_{s_{23}}$ has either one or three intersection points with $\mathcal{B}$. If $g \in G_{s_{12}} \cap G_{s_{23}} \cap G_{s_2}$ the line g has exactly one intersection point with $\mathcal{B}$ We apply theorem 1.2 to this set with $Q_2 = R_1 = R_4, Q_3 = R_2, Q_1 = R_3$ and $Q_0 = S_1 = S_2$ and we get

$$\begin{aligned} m(G_{s_{12}} \cap G_{s_{23}} \cap G_{s_2}) &= m(G_{s_2}) - m(G_{s_2} \cap G_{s_{13}}) \\ &= 2d_2 - (d_4 + d_3 + 2d_2 - d_{23} - d_{24}) \\ &= d_{23} + d_{24} - d_3 - d_4 \end{aligned}$$

where we apply theorem 1.2 (Ex2) to $m(G_{s_2} \cap G_{s_{13}})$. Then with $m(G_{s_{12}} \cap G_{s_{23}}) = d_{12} + d_{23} - d_{13}$ we have

$$\begin{aligned} &M(1|s_{12}s_{23}) = m(G_{s_{12}} \cap G_{s_{23}} \cap G_{s_2}) = d_{23} + d_{24} - d_3 - d_4, \\ &M(3|s_{12}s_{23}) = m(G_{s_{12}} \cap G_{s_{23}}) - m(G_{s_{12}} \cap G_{s_{23}} \cap G_{s_2}) = d_3 + d_4 + d_{12} - d_{13} - d_{24}, \\ &M(q|s_{12}s_{23}) = 0 \quad (q = 2, 4). \end{aligned}$$

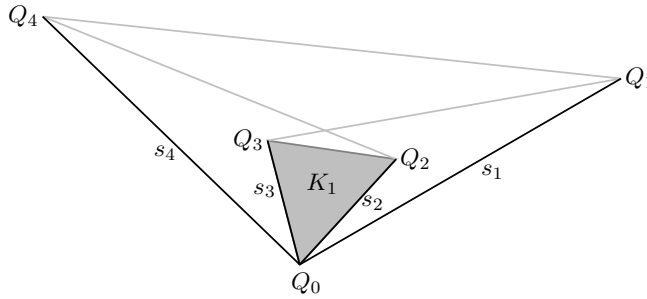


Figure 8: Application of formula (3), example 2

For the example in figure 8 we compute $M(q|s_1s_4)$ $(1 \leq q \leq 4)$. Any line $g \in G_{s_1} \cap G_{s_4}$ intersects at least s_1 and s_4 but it can also intersects s_2 and/or s_3.

We apply (3) with $Q_0 = R_1 = R_4, Q_1 = R_2, Q_4 = R_3, Q_2 = S_1$ and $Q_3 = S_2$ and we set $K_1 := H(Q_0, Q_2, Q_3)$. So we have $m(G_{s_1} \cap G_{s_4} \cap G_{K_1}) = m(G_{K_1}) - m(G_{s_{14}} \cap G_{K_1}) = d_1 + d_4 + d_{23} - d_{13} - d_{24}$ where we apply theorem 1.2 (Ex5) to $m(G_{s_{14}} \cap G_{K_1})$.

Since any line $g \in G_{s_1} \cap G_{s_4} \cap G_{K_1}$ has at least three common points with $\mathcal{B}$ we get

$$\begin{aligned} M(2|s_1s_4) &= m(G_{s_1} \cap G_{s_4}) - m(G_{s_1} \cap G_{s_4} \cap G_{K_1}) \\ &= (d_1 + d_4 - d_{14}) - (d_1 + d_4 + d_{23} - d_{13} - d_{24}) \\ &= d_{13} + d_{24} - d_{14} - d_{23}. \end{aligned}$$

For the calculation of $M(3|s_1s_4)$ we apply (3) with $K_2 := H(Q_0, Q_2) = s_2$ and $K_3 := H(Q_0, Q_3) = s_3$ instead of K_1. Then we get

$$\begin{aligned} m(G_{s_1} \cap G_{s_4} \cap G_{K_2}) &= m(G_{K_2}) - m(G_{s_{14}} \cap G_{K_2}) \\ &= 2d_2 - (2d_2 + d_{12} + d_{24} - d_1 - d_4) \\ &= d_1 + d_4 - d_{12} - d_{24}, \\ m(G_{s_1} \cap G_{s_4} \cap G_{K_3}) &= m(G_{K_3}) - m(G_{s_{14}} \cap G_{K_3}) \\ &= d_1 + d_4 - d_{13} - d_{34}. \end{aligned}$$

If we consider that $g \in (G_{s_1} \cap G_{s_4} \cap G_{K_1}) \setminus (G_{s_1} \cap G_{s_4} \cap G_{K_2})$ intersects s_1, s_3 and s_4 and $g \in (G_{s_1} \cap G_{s_4} \cap G_{K_1}) \setminus (G_{s_1} \cap G_{s_4} \cap G_{K_3})$ intersects s_1, s_2 and s_4 we get

$$\begin{aligned} M(3|s_1s_4) &= [m(G_{s_1} \cap G_{s_4} \cap G_{K_1}) - m(G_{s_1} \cap G_{s_4} \cap G_{K_2})] \\ &\quad + [m(G_{s_1} \cap G_{s_4} \cap G_{K_1}) - m(G_{s_1} \cap G_{s_4} \cap G_{K_3})] \\ &= (d_{12} + d_{23} - d_{13}) + (d_{23} + d_{34} - d_{24}) \\ &= 2d_{23} + d_{12} + d_{34} - d_{13} - d_{24}, \\ M(4|s_1s_4) &= m(G_{s_1} \cap G_{s_4}) - M(3|s_1s_4) - M(2|s_1s_4) \\ &= (d_1 + d_4 - d_{14}) - (2d_{23} + d_{12} + d_{34} - d_{13} - d_{24}) - (d_{13} + d_{24} - d_{14} - d_{23}) \\ &= d_1 + d_4 - d_{12} - d_{23} - d_{34}. \end{aligned}$$

3 Results

For a bunch $\mathcal{B}$ with $n = 4$ we have to consider seven different cases. All these cases can be computed with the same methods we have applied to the previous two examples and with (2). This sections contains the results of our calculations.

3.1 Case 1

In this case Q_1, Q_2, Q_3 and Q_4 are corners of $H(\mathcal{B})$ and it is shown in figure 7. We have the following results

$$P(1) = \frac{1}{\pi d}(2L - d_{13} - d_{24} - \sum_{k=1}^{4} d_k), \quad P(2) = \frac{1}{\pi d}(2(d_{13} + d_{24}) - L),$$

$$P(3) = \frac{1}{\pi d}(\sum_{k=1}^{4} d_k - d_{13} - d_{24}), \quad P(4) = 0.$$

3.2 Case 2

Here are Q_1, Q_2 and Q_3 corners of $H(\mathcal{B})$ and we have

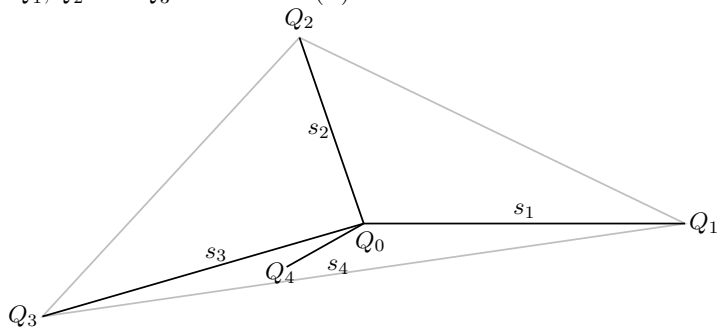


Figure 9: Case 2

$$P(1) = \frac{1}{\pi d}(2L - (d_{14} + d_{24} + d_{34}) - \sum_{k=1}^{4} d_k), \quad P(2) = \frac{1}{\pi d}(\,2(d_{14} + d_{24} + d_{34}) - L),$$

$$P(3) = \frac{1}{\pi d}(\sum_{k=1}^{4} d_k - (d_{14} + d_{24} + d_{34})), \quad P(4) = 0$$

3.3 Case 3

Q_0, Q_1, Q_2, Q_3 and Q_4 are corners of $H(\mathcal{B})$ in this case.

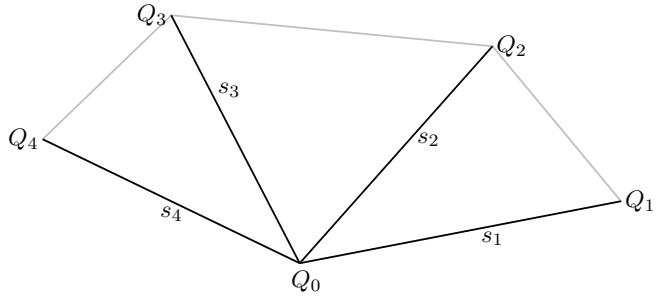


Figure 10: Case 3

$$P(1) = \frac{1}{\pi d}(L + d_{12} + d_{23} + d_{34} - d_{13} - d_{24} - d_2 - d_3),$$
$$P(2) = \frac{1}{\pi d}(2d_{13} + 2d_{24} - d_{12} - d_{23} - d_{34} - d_{14}),$$
$$P(3) = \frac{1}{\pi d}(2d_{14} + d_2 + d_3 - d_{13} - d_{24} - d_4 - d_1),$$
$$P(4) = \frac{1}{\pi d}(d_1 + d_4 - d_{14}).$$

3.4 Case 4

In this case we have Q_0, Q_1, Q_3, Q_4 as corners of $H(\mathcal{B})$ and the triangle $Q_1Q_3Q_4$ contains Q_2.

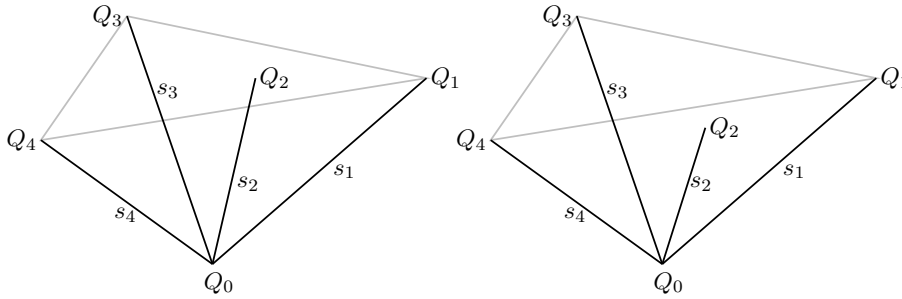


Figure 11: Case 4 (left) and case 5 (right)

$$
\begin{aligned}
P(1) &= \frac{1}{\pi d}(L + d_{13} + d_{34} - d_{12} - d_{23} - d_{24} - d_2 - d_3),\\
P(2) &= \frac{1}{\pi d}(2d_{12} + 2d_{23} + 2d_{24} - d_{13} - d_{14} - d_{34}),\\
P(3) &= \frac{1}{\pi d}(2d_{14} + d_2 + d_3 - d_{12} - d_{23} - d_{24} - d_1 - d_4),\\
P(4) &= \frac{1}{\pi d}(d_1 + d_4 - d_{14}).
\end{aligned}
$$

3.5 Case 5

Like in case 4 we have the corners Q_0, Q_1, Q_3 and Q_4 of $H(\mathcal{B})$ but as shown in figure 11 the triangle $Q_1Q_3Q_4$ does not contain Q_2. We get

$$
\begin{aligned}
P(1) &= \frac{1}{\pi d}(L + d_{13} + d_{34} - d_{14} - d_{23} - d_2 - d_3),\\
P(2) &= \frac{1}{\pi d}(2d_{14} + 2d_{23} - d_{12} - d_{13} - d_{24} - d_{34}),\\
P(3) &= \frac{1}{\pi d}(2d_{12} + 2d_{24} + d_2 + d_3 - d_{14} - d_{23} - d_1 - d_4),\\
P(4) &= \frac{1}{\pi d}(d_1 + d_4 - d_{12} - d_{24}).
\end{aligned}
$$

3.6 Case 6

In this case $H(\mathcal{B})$ has only three corners Q_0, Q_1 and Q_4 and the triangle $Q_1Q_3Q_4$ contains Q_2, so we calculate

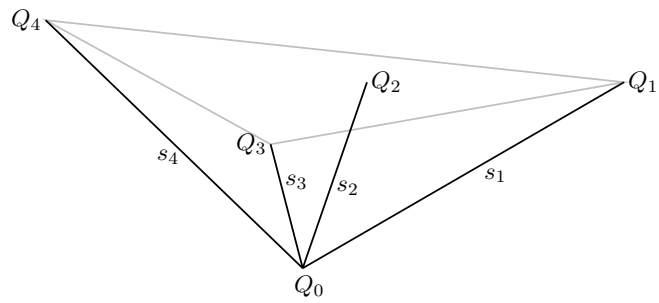


Figure 12: Case 6

$$P(1) = \frac{1}{\pi d}(L + d_{14} - d_{12} - d_{23} - d_{24} - d_2 - d_3),$$
$$P(2) = \frac{1}{\pi d}(2d_{12} + 2d_{23} + 2d_{24} - d_{13} - d_{14} - d_{34}),$$
$$P(3) = \frac{1}{\pi d}(2d_{13} + 2d_{34} + d_2 + d_3 - d_{12} - d_{23} - d_{24} - d_1 - d_4),$$
$$P(4) = \frac{1}{\pi d}(d_1 + d_4 - d_{13} - d_{34}).$$

3.7 Case 7

In this case Q_0, Q_1 and Q_4 are corners of $H(\mathcal{B})$ and s_{13} intersects s_{24}. It is shown in figure 8 and we get

$$P(1) = \frac{1}{\pi d}(L + d_{14} - d_{13} - d_{24} - d_2 - d_3),$$
$$P(2) = \frac{1}{\pi d}(2d_{13} + 2d_{24} - d_{12} - d_{14} - d_{23} - d_{34}),$$
$$P(3) = \frac{1}{\pi d}(2d_{12} + 2d_{23} + 2d_{34} + d_2 + d_3 - d_{13} - d_{24} - d_1 - d_4),$$
$$P(4) = \frac{1}{\pi d}(d_1 + d_4 - d_{12} - d_{23} - d_{34}).$$

References

[1] Santaló, Luis A.: 'Integral geometry and geometric probability', Cambridge University Press 2004, Second Edition

[2] Stoka, Marius: 'Probabilità e Geometria', Herbita editrice, Palermo 1982

Addresses

Andrei Duma
University of Hagen
Department of Mathematics
58084 Hagen, Germany
mathe.duma@fernuni-hagen.de

Martin Wecker
University of Hagen
Department of Mathematics
58084 Hagen, Germany
martinwecker@arcor.de

RENDICONTI DEL CIRCOLO MATEMATICO DI PALERMO
Serie II, Suppl. 81 (2009), pp. 171-180

QUADRATIC PLÜCKER RELATIONS FOR HANKEL VARIETIES

GIOIA FAILLA

Abstract. We explore combinatorial aspects of Plücker coordinates and the algebraic relations they satisfy, concerning Gröbner bases, subalgebras bases and connected semigroup rings. We give an application to the Hankel subvariety $H(1,n)$ of the grassmannian $\mathbb{G}(1,n)$, consisting of all Hankel lines of the projective space $\mathbb{P}^n$.

Introduction

Let R be any subalgebra of a polynomial ring with a finite Sagbi basis S. In this case, we say that S defines a flat degeneration from R to its initial algebra $\text{in}_\prec(R)$. The initial algebra $\text{in}_\prec(R)$ is generated by monomials, hence it corresponds to a toric variety. Geometrically, a finite Sagbi basis provides a flat family connecting the given variety $\text{Spec}(R)$ to the affine toric variety $\text{Spec}(\text{in}_\prec(R))$. It is known that there exists a deformation for the Grassmannian $\mathbb{G}(r,n)$ into a toric variety ([5], Chap.II). But, it is interesting to describe this degeneration explicitly for the presentation ideals of both algebras.

In this paper, following the point of view of [5], Chap.II, we apply combinatorial techniques to $H(1,n)$, the Hankel variety of Hankel lines of $\mathbb{P}^n$, subvariety of $\mathbb{G}(1,n)$, introduced in [4]. Since any Hankel line of $\mathbb{P}^n$ can be represented by a $2\times(n+1)$ Hankel matrix, results on subalgebras of maximal minors find here application.

More precisely, in Section n.1 we recall definitions and results on term orders represented by weight vectors and we give some descriptions of the degeneration of $\mathbb{G}(1,n)$ in terms of weight vectors.

In Section n.2 we consider the Hankel lines variety. We determine a Hankel weight matrix $2\times(n+1)$ starting from a weight vector which selects the main diagonal term of $2\times 2-$minors of a Hankel matrix and from the configuration $\mathcal{A}$ associated to the initial algebra $\text{in}_\prec(R)$, R being the subalgebra of the polynomial ring generated by the minors of an Hankel matrix. Since the generators of the presentations ideals of R and $\text{in}_\prec(R)$ can be written explicitly ([1],Section n.3 and Corollary 3.4), we describe the flat degeneration at the level of the presentation ideals, by using the Hankel weight vector obtained.

1. Plücker Relations

Let k be any field and $k[x_1, \ldots, x_n]$ be the polynomial ring in n variables. We recall some definitions and results about the representation of term orders by weight vectors.

Let $\omega = (\omega_1, \ldots, \omega_n) \in \mathbb{R}^n$ be a vector, $\mathbb{R}$ the real number field.

Definition 1.1. *Let $f \in k[\underline{x}] = k[x_1, \ldots, x_n]$ be a polynomial, $f = \sum c_i \underline{x}^{a_i}$, $a_i \in \mathbb{N}^n, a_i = (a_{i1}, \ldots, a_{in})$. We define the initial form $in_w(f)$ of f with respect to ω to be the sum of all terms $c_i \underline{x}^{a_i}$ of f such that the inner product $\omega \cdot a_i$ is maximal.*

Remark 1.2. *Let $e_1, \ldots, e_n$ be the canonical vectors of $\mathbb{R}^n$. Then $\omega \cdot e_i$ is the weight of the variable x_i.*

Definition 1.3. *For any ideal $I \subset k[\underline{x}]$, we define the initial ideal to be the ideal generated by all initial forms of I:*

$$in_\omega(I) = (in_\omega(f), f \in I)$$

Let $\omega \geq 0$ be, that is ω non negative, $(\omega_i \geq 0, \forall i)$, and let $\prec$ be an arbitrary term order on the monomials of $k[\underline{x}]$.

Definition 1.4. *We define a new term order $\prec_\omega$ as follows:*

$$\text{for } \alpha, \beta \in \mathbb{N}^n, \alpha \prec_\omega \beta \Leftrightarrow \omega \cdot \alpha < \omega \cdot \beta \text{ or } \omega \cdot \alpha = \omega \cdot \beta \text{ and } \alpha \prec \beta$$

Proposition 1.5. *Let G be a Gröbner bases (G.B.) of the ideal $I \subset k[\underline{x}$ with respect to $\prec_\omega$. Then $\{in_\omega(g), g \in G\}$ is a G.B. for $in_\omega(I)$ with respect to $\prec$ and $in_\prec(in_\omega(g), g \in G) = in_{\prec_\omega}(g \in G)$*

Proof. It follows by Proposition 1.5 and Corollary 1.9 of [5]. □

Now let $\mathcal{A} = \{\underline{a}_1, \underline{a}_2, \ldots, \underline{a}_n\} \subset N^d$ be a configuration of n points and let $\omega \in \mathbb{R}^d$ any weight vector that represents a term order in $k[\underline{t}] = k[t_1, \ldots, t_d]$.

Definition 1.6. *We call the vector $\omega' = \mathcal{A}^T\omega \in \mathbb{R}^n$ the weight vector induced by ω and by the matrix $\mathcal{A}$, where $\mathcal{A}$ is the $d \times n$ matrix that represents the set $\mathcal{A} \subset \mathbb{N}^n$ $\mathcal{A} = \begin{pmatrix} a_{11} & \ldots & a_{n1} \\ a_{12} & \ldots & a_{n2} \\ \vdots & \vdots & \vdots \\ a_{1d} & \ldots & a_{nd} \end{pmatrix}$, $\mathcal{A}^T$ is the transposed matrix $\mathcal{A}$ and*

$$\omega' = \mathcal{A}^T\omega = (a_{11}\omega_1 + \ldots + a_{1d}\omega_d, \ldots, a_{n1}\omega_1 + \ldots + a_{nd}\omega_d) \in \mathbb{R}^n$$

where $\omega = (\omega_1, \ldots \omega_d)$.

Now, let $\mathcal{F} = \{f_1, f_2, \ldots, f_n\}$ be a set of polynomials in $k[\underline{t}]$, let $R = k[\mathcal{F}]$ be the subalgebra they generated and fix a term order $\prec$ on $k[\underline{t}]$. Suppose $in_{\prec}(f_i) = \underline{t}^{a_i}$ and let $\mathcal{A} = \{\underline{a}_1, \underline{a}_2, \ldots, \underline{a}_n\} \subset N^d$. Consider the $k-$algebra epimorphism

$$h : k[\underline{x}] \to R$$
$$x_i \to f_i$$

where $k[\underline{x}] = k[x_1, \ldots, x_n]$ and denote $I = \mathrm{Ker}(h)$. Moreover consider the $k-$algebra epimorphism

$$h' : k[\underline{x}] \to in_{\prec}(R)$$
$$x_i \to in_{\prec}(f_i) = \underline{t}^{\underline{a}_i}$$

and denote by $I_{\mathcal{A}} = \mathrm{Ker}(h')$, the toric ideal of $in_{\prec}(R)$. Let ω be a weight vector that represents the term order $\prec$ on $k[\underline{t}]$.

Theorem 1.7. *The set $\mathcal{F} \subset k[\underline{t}]$ is a canonical basis of $R = k[\mathcal{F}]$ if and only if*

$$in_{\omega'}(I) = I_{\mathcal{A}}$$

where $\omega' = \mathcal{A}^T\omega$.

Proof. See [5], Theorem 11.4. □

Theorem 1.8. *Suppose $\mathcal{F}$ is a canonical basis for R. Then every reduced G.B. G of $I_{\mathcal{A}}$ lifts to a reduced G.B. G' of I, i.e., the elements of G are the initial forms (with respect to the weight vector $\mathcal{A}^T\omega$) of the elements of G'.*

Proof. [5], Corollary 11.6(1). □

Consider a $r \times s$ matrix (t_{ij}) of variables $r \leq s$. Let R be the subalgebra of $k[t_{11}, t_{12}, \ldots t_{rs}]$ generated by the $r \times r$ minors of the matrix (t_{ij}).
Its projective spectrum $\mathrm{Proj}(R)$ is the Grassmannian variety $G(r-1, s-1)$ of $r-$dimensional linear subspaces in the $s-$dimensional vector space k^s, k algebraic closed, presented in its usual Plücker embedding.

Definition 1.9. *Given a $r \times s$ matrix of variables* $A = \begin{pmatrix} t_{11} & \ldots & t_{1s} \\ t_{21} & \ldots & t_{2s} \\ \vdots & \vdots & \vdots \\ t_{r1} & \ldots & t_{rs} \end{pmatrix}$,
a weight vector w for A is a vector $w \in N^{r \times s}$, viewed as a $r \times s$ matrix

$$\omega = \begin{pmatrix} \omega_{11} & \ldots & \omega_{1s} \\ \omega_{21} & \ldots & \omega_{2s} \\ \vdots & \vdots & \vdots \\ \omega_{r1} & \ldots & \omega_{rs} \end{pmatrix}$$

and such that the weight of the entry (i, j) of A is ω_{ij}.

Remark 1.10. *The vector* $\alpha_{ij} = (0, 0, \ldots, 1, 0, \ldots, 0) \in N^{r\times s}$ *is the exponent vector of the* (i, j) *entry in the matrix* A. *Then* $w \cdot \alpha_{ij} = \omega_{ij}$

Example 1.11.

$$(1)\ \omega = (\omega_{ij}), \omega_{ij} = j^i \in \mathbb{N}$$

$$(2)\ \omega = (\omega_{ij}), \omega_{ij} = i + j^2 \in \mathbb{N}$$

are weight matrix vectors.

Now, let us assume $r = 2$ and $s = n$ and we consider the generic $2 \times n$ matrix $\begin{pmatrix} t_{11} & \ldots & t_{1n} \\ t_{21} & \ldots & t_{2n} \end{pmatrix}$

Proposition 1.12. *The weight matrix* (1) *of Example 1.11 represents the term order on* $k[t_{11}, \ldots, t_{1n}, t_{21}, \ldots, t_{2n}]$ *which selects the main diagonal term to be the initial term for each* 2×2 *minor of the matrix* $A = (t_{ij})$

Proof. Let $M_{i_1,i_2}, 1 \leq i_1 < i_2 \leq n$ be the 2×2 minor with column indices i_1, i_2, $i_1 < i_2$, that is $t_{1i_1}t_{2i_2} - t_{1i_2}t_{2i_1}$. If we apply the weight vector $\omega_{ij} = j^i$, we obtain

$$(\omega_{ij}) \cdot (\alpha_{1i_1} + \alpha_{2i_2}) = i_1 + i_2^2$$

$$(\omega_{ij}) \cdot (\alpha_{1i_2} + \alpha_{2i_1}) = i_2 + i_1^2$$

with $i_1 + i_2^2 > i_2 + i_1^2$. It follows $in_\omega(M_{i_1,i_2}) = t_{1i_1}t_{2i_2}$. □

We associate a new variable $[i_1, i_2]$ to be the 2×2 minor M_{i_1,i_2} with column indices $i_1 < i_2$ and consider the polynomial ring $k[[i_1, i_2], i_1 < i_2, 1 \leq i_1 < i_2 \leq n]$ generated by these $\binom{n}{2}$ brackets.

Let $I_{2,n}$ be the ideal of $k[[i_1, i_2], 1 \leq i_1 < i_2 \leq n]$ generated by the algebraic relations among the 2×2 minors. Note that $I_{2,n}$ is the kernel of the map:

$$k[[i_1, i_2], 1 \leq i_1 < i_2 \leq n] \to k[M_{i_1,i_2}, 1 \leq i_1 < i_2 \leq n]$$

$$[i_1, i_2] \to M_{i_1,i_2} = t_{1i_1}t_{2i_2} - t_{1i_2}t_{2i_1}.$$

The ideal $I_{2,n}$ is called the Grassmann-Plücker ideal.

The toric ideal $I_{\mathcal{A}_{2,n}}$ is the kernel of the map

$$k[[i_1, i_2], 1 \leq i_1 < i_2 \leq n] \to k[t_{11}t_{22}, t_{11}t_{23}, \ldots, t_{1(n-1)}t_{2n}] \subset k[t_{11}, t_{12}, \ldots, t_{2n}]$$

$$[i_1, i_2] \to t_{1i_1}t_{2i_2}.$$

The following theorem is a well known result, proved by many authors is different ways.

Theorem 1.13. *The set of* 2×2 *minors of a* $2 \times n$ *matrix of variables is a canonical basis (Sagbi basis) for the subalgebra* $R = k[t_{11}t_{22}, t_{11}t_{23}, \ldots, t_{1(n-1)}t_{2n}] \subset k[t_{11}, t_{12}, \ldots, t_{2n}]$ *they generate, with respect to any diagonal term order on* $k[t_{11}, t_{12} \ldots, t_{2n}]$.

Proof. See [5], Theorem 11.8. □

Then we can apply Theorem1.8, in order to connect the Gröbner bases of $I_{\mathcal{A}_{2,n}}$ and of $I_{2,n}$. First we have to calculate the weight vector ω'.
Let e_{ij} be the canonical vector in $\mathbb{N}^{2\times n}$ corresponding to the variable t_{ij}. The vectors configuration associated with the diagonal initial monomials $t_{1i_1}t_{2i_2}$ equals

$$\mathcal{A}_{2,n} = \{e_{1i_1} + e_{2i_2} : 1 \leq i_1 < i_2 \leq n\} \subset \mathbb{N}^{2\times n}.$$

We consider $\mathcal{A}_{2,n}$ as a $2n \times \binom{n}{2}$ matrix with rows:

$$e_{11} + e_{22} = (1, 0, \ldots, 0; 0, 1, 0, 0, \ldots, 0)$$
$$e_{11} + e_{23} = (1, 0, \ldots, 0; 0, 0, 1, 0, \ldots, 0)$$
$$\vdots$$
$$e_{1,n-1} + e_{2n} = (0, 0, \ldots, 0, 1; 0, 0, \ldots, 0, 1).$$

The transposed matrix $\mathcal{A}^T$ is a $\binom{n}{2} \times 2n$ matrix. A weight vector $\underline{\omega}$ is a $2 \times n$ matrix, viewed as a vector

$$(w_{11}, w_{12}, \ldots, w_{1n}; w_{21}, w_{22}, \ldots, w_{2n}).$$

Then $\omega' = \mathcal{A}_{2n}^T\omega = (\omega_{1i_1} + \omega_{2i_2}, 1 \leq i_1 < i_2 \leq n)^T$ is a $\binom{n}{2} \times 1$ matrix, i.e. a column vector:

$$\begin{pmatrix} 1 & 1 & \ldots & 0 \\ 0 & 0 & \ldots & 0 \\ \vdots & \vdots & \vdots & \vdots \\ 0 & 0 & \ldots & 0 \\ 0 & 0 & \ldots & 1 \\ 0 & 0 & \ldots & 0 \\ 1 & 0 & \ldots & 0 \\ 0 & 1 & \ldots & 0 \\ \vdots & \vdots & \vdots & \vdots \\ 0 & 0 & \ldots & 0 \\ 0 & 1 & \ldots & 1 \end{pmatrix}^T \begin{pmatrix} \omega_{11} \\ \omega_{12} \\ \vdots \\ \omega_{1n} \\ \omega_{21} \\ \omega_{22} \\ \vdots \\ \omega_{2n} \end{pmatrix} = \begin{pmatrix} \omega_{11} + \omega_{22} \\ \omega_{11} + \omega_{23} \\ \vdots \\ \omega_{1n-1} + \omega_{2n} \end{pmatrix} = \omega'$$

and $\omega'_{ij} = \omega_{1i} + \omega_{2j}$.

The mean of the theorem we want to prove is the deduction of informations on the toric ideal of the deformation $\text{in}_{\prec}R$, starting from the

Grassmann-Plücker ideal, well known in the literature (with its generators).

Theorem 1.14. *Let* $\begin{pmatrix} t_{11} & \dots & t_{1n} \\ t_{21} & \dots & t_{2n} \end{pmatrix}$ *be a generic matrix of variables. Let* $R = k[M_{1,2}, M_{1,3}, \dots, M_{n-1,n}]$ *be the subalgebra of* $k[t_{11}, \dots, t_{2n}]$ *generated by the minors and* $in_{\prec}(R) = k[t_{11}t_{22}, \dots, t_{1,n-1}t_{2n}]$ *the subalgebra of* $k[t_{11}, t_{12}, \dots, t_{2n}]$ *generated by the main diagonal terms of the minors. Then* $I_{\mathcal{A}_{2,n}}$ *is generated by a Gröbner basis of quadrics.*

Proof. The ideal $I_{2,n}$ is generated by the Plücker relations that are a Gröbner basis of $I_{2,n}$ with respect the term order $\prec$ on $k[[1,2], \dots, [n-1,n]]$ (see [5]). If we choose as weight vector $\omega_{ij} = j^i$, $\omega' = \omega_{1i} + \omega_{2j} = i + j^2$ that represents $\prec$. Then $\text{in}_{\prec}(I_{2,n}) = (\text{in}_{\prec}(g), g \in G)$ and $\text{in}_{\omega'}(I_{2,n}) = (\text{in}_{\omega'}(g), g \in G)$. Since $I_{2,n}$ is generated by a Gröbner basis of quadrics, $\text{in}_{\omega'}(I_{2,n})$ is generated in degree two. The assertion follows by Proposition 1.5, since $\text{in}_{\omega'}(I_{2,n}) = I_{\mathcal{A}_{2,n}}$. □

2. Hankel relations

Consider a generic $2 \times n$ Hankel matrix $H = \begin{pmatrix} t_{11} & t_{12} & \dots & t_{1n} \\ t_{12} & t_{13} & \dots & t_{1(n+1)} \end{pmatrix}$

Proposition 2.1. *The weight matrix* $\omega_{ij} = i + j^2$ *represents a term order on* $k[t_{11}, \dots, t_{1n}, t_{1(n+1)}]$ *which selects the main diagonal term to be the initial term for each* 2×2 *minor of the Hankel matrix* H.

Proof. Let $[i_1, i_2], 1 \le i_1 < i_2 \le n$ be the 2×2 minor with columns i_1, i_2, $(i_1 < i_2)$, that is $t_{1i_1}t_{1(i_2+1)} - t_{1(i_1+1)}t_{1i_2}$. If we apply the weight vector $\omega_{ij} = i + j^2$ we obtain

$$(\omega_{ij})(\alpha_{1i_1} + \alpha_{1(i_2+1)}) = i_1^2 + i_2^2 + 2i_2 + 3$$

$$(\omega_{ij})(\alpha_{1(i_1+1)} + \alpha_{1i_2}) = i_1^2 + i_2^2 + 2i_1 + 3.$$

Since $i_1 < i_2$, then

$$t_{1i_1}t_{1(i_2+1)} >_{\omega} t_{1(i_1+1)}t_{1i_2}.$$

□

As in Section n.1, we associate a new variable $[i_1, i_2]$ to the 2×2 minor with columns i_1, i_2, $i_1 < i_2$, in the Hankel matrix and consider the polynomial ring $k[[i_1, i_2], 1 \le i_1 < i_2 \le n]$ generated by these $\binom{n}{2}$ brackets.

Let $I^H_{2,n}$ be the ideal of $k[[i_1, i_2], 1 \le i_1 < i_2 \le n]$ generated by the algebraic relations among the 2×2 minors. We call the ideal $I^H_{2,n}$ the

Hankel-Grassmann-Plücker ideal. The toric ideal $I_{\mathcal{H}_{2,n}}$ is the kernel of the map

$$k[[i_1, i_2], 1 \leq i_1 < i_2 \leq n] \to k[t_{11}t_{13}, t_{11}t_{14}, \ldots, t_{1,n-1}t_{1(n+1)}]$$

$$[i_1, i_2] \to t_{1i_1}t_{1(i_2+1)}.$$

Then we have:

Theorem 2.2. *The set of 2×2 minors of an Hankel $2 \times n$ matrix of variables is a canonical basis (Sagbi basis) for the subalgebra they generate, with respect to any diagonal term order on $k[t_{11}, t_{12}, \ldots, t_{1(n)}, t_{1(n+1)}]$.*

Proof. See [1]. □

Theorem 2.3. *The ideal $I^H_{2,n}$ has a Gröbner basis of quadrics given by the following set of polynomials of $k[[1,2], \ldots, [n-1,n]]$ with respect to any diagonal term order and the lex order on the variables, $[1,2] \prec [1,3] \prec \ldots \prec [n-1,n]$:*

(a) $[i,j][h,k] - [i,k][h,j] + [i,h][k,j] \quad 1 \leq i < h < k < j \leq n$

(b) $[i,j][h,k] - [i,h-1][j+1,k] - [i,j+1][h,k-1] - [i+1,j][h-1,k] + [i+1,j+1][h-1,k-1] + [i,h][j+1,k-1] + [i+1,h-1][j,k] - [i+1,h][j,k-1]$

$1 \leq i < j < h < k \leq n,\ h - j > 1.$

Proof. See [1], Corollary 2.4. □

Theorem 2.4. *The toric ideal $I_{H_{2,n}}$ is generated by a Gröbner basis of quadrics given by the following set of binomials of $k[[12], \ldots, [n-1,n]]$:*

(c) $[i,j][h,k] - [i,k][h,j] \quad 1 \leq i < h < k < j \leq n$

(d) $[i,j][h,k] - [i,h-1][j+1,k] \quad 1 \leq i < j < h < k \leq n,\ h - j > 1.$

Proof. See [1], Section n.3. □

Then we can apply Theorem1.8, in order to connect the Gröbner bases of $I_{\mathcal{H}_{2,n}}$ and of $H_{2,n}$.
Let e_{ij} be the canonical vector of $\mathbb{N}^{n+1}$ corresponding to the variable t_{ij}. The vector configuration associated with the diagonal initial monomials $t_{1i_1}t_{1(i_2+1)}$ equals

$$\mathcal{H}_{2,n} = \{e_{1i_1} + e_{1(i_2+1)} : 1 \leq i_1 < i_2 \leq n\} \subset \mathbb{N}^{n+1}.$$

Theorem 2.5. *Let $\omega = (w_{ij})$ be a Hankel weight matrix. Then $\omega'_{i_1,i_2} = i_1 + i_2^2 + 2i_2 + 3$.*

Proof. We consider $\mathcal{H}_{2,n}$ as a $(n+1) \times \binom{n}{2}$ matrix:

$$\mathcal{H}_{2,n} = \begin{pmatrix} 1 & 1 & \dots & 1 & 0 & 0 & \dots & 0 & \dots & 0 \\ 0 & 0 & \dots & 0 & 1 & 1 & \dots & 1 & \dots & 0 \\ 1 & 0 & \dots & 0 & 0 & 0 & \dots & 0 & \dots & 0 \\ 0 & 1 & \dots & 0 & 1 & 0 & \dots & 0 & \dots & 0 \\ \vdots & \vdots & \dots & \vdots & 0 & 1 & \dots & \vdots & \dots & \vdots \\ \vdots & \vdots & \dots & \vdots & \vdots & 0 & \dots & \vdots & \dots & 0 \\ \vdots & \vdots & \dots & \vdots & \vdots & 0 & \dots & \vdots & \dots & 1 \\ \vdots & \vdots & \dots & 0 & \vdots & 0 & \dots & 0 & \dots & 0 \\ 0 & 0 & \dots & 1 & 0 & 0 & \dots & 1 & \dots & 1 \end{pmatrix}$$

and the transposed matrix $\mathcal{H}_{2,n}^T$. A Hankel weight vector ω is a $2 \times n$ matrix, that we can consider as a vector

$$\omega = (\omega_{11}, \omega_{12}, \dots, \omega_{1n}, \omega_{1(n+1)}) \in \mathbb{N}^{n+1} \text{ or a } 1 \times (n+1) \text{ matrix .}$$

Then $\omega' = \mathcal{H}_{2,n}^T \omega = (\omega_{1i_1} + \omega_{1i_2+1}, 1 \le i_1 < i_2 \le n)^T$ is the $\binom{n}{2} \times 1$ matrix:

$$\mathcal{H}_{2,n}^T \underline{\omega} = \begin{pmatrix} 1 & 0 & 1 & 0 & \dots & \dots & \dots & \dots & \dots & 0 \\ 1 & 0 & 0 & 1 & \dots & \dots & \dots & \dots & \dots & 0 \\ \vdots & \vdots & \vdots & \vdots & \vdots & \vdots & \vdots & \vdots & \vdots & \vdots \\ 1 & 0 & 0 & \dots & \dots & \dots & \dots & \dots & 0 & 1 \\ 0 & 1 & 0 & 1 & 0 & 0 & 0 & 0 & 0 & 0 \\ 0 & 1 & 0 & 0 & 1 & 0 & 0 & 0 & 0 & 0 \\ \vdots & \vdots & \vdots & \vdots & \vdots & \vdots & \vdots & \vdots & \vdots & \vdots \\ 0 & 1 & 0 & \dots & \dots & \dots & \dots & \dots & 0 & 1 \\ \vdots & \vdots & \vdots & \vdots & \vdots & \vdots & \vdots & \vdots & \vdots & \vdots \\ 0 & 0 & 0 & \dots & 0 & \dots & 0 & 1 & 0 & 1 \end{pmatrix} \begin{pmatrix} \omega_{11} \\ \omega_{12} \\ \vdots \\ \omega_{1(n+1)} \end{pmatrix} =$$

$$= \begin{pmatrix} \omega_{11} + \omega_{13} \\ \omega_{11} + \omega_{14} \\ \vdots \\ \omega_{1(n-1)} + \omega_{1(n+1)} \end{pmatrix} = \begin{pmatrix} \omega'_{11} \\ \omega'_{12} \\ \vdots \\ \omega'_{\binom{n}{2}} \end{pmatrix}.$$

Now we have achieved our goal taking in account that ω' is a weight vector on $k[[1,2], \dots, [n-1,n]]$, hence $\omega'_{i_1 i_2} = \omega_{1i_1} + \omega_{1(i_2+1)} = i_1 + i_2 + 2i_2 + 3$. □

Corollary 2.6. *Let ω be the Hankel weight vector $\omega_{ij} = i + j^2$. Then $\omega'_{ij} = \omega_{1i} + \omega_{1j} = i^2 + j^2 + 2j + 3$.*

Theorem 2.7. *Let* $H = \begin{pmatrix} t_{11} & \dots & t_{1n} \\ t_{12} & \dots & t_{1(n+1)} \end{pmatrix}$ *be a generic Hankel matrix of variables. Let* $k[M_{12}, M_{13}, \dots, M_{n-1,n}]$ *be the subalgebra of* $k[t_{11}, \dots, t_{1(n+1)}]$ *generated by the* 2×2 *minors of* H *and* $R = k[t_{11}t_{13}, \dots, t_{1(n-1)}t_{1(n+1)}]$ *the subalgebra of* $k[t_{11}, \dots, t_{1(n+1)}]$ *generated by the main diagonal terms of the minors. Then* $in_{\omega'}(I^H_{2,n}) = I_{\mathcal{H}_{2,n}}$.

Proof. We have to prove that the term order $\prec_{\omega'}$ coincides with the term order $\prec$ employed in theorems 2.3 and 2.4, then we apply Proposition 1.6. Let G be Gröbner basis of $I^H_{2,n}$. Then $\mathrm{in}_\prec I^H_{2,n} = (\mathrm{in}_\prec(g), g \in G) = (\mathrm{in}_{\prec_\omega}(g), g \in G)$. By Proposition 1.5, $\mathrm{in}_{\omega'}(I^H_{2,n}) = (\mathrm{in}_{\omega'}(g), g \in G)$. The ideal $I^H_{2,n}$ is generated by the Hankel-Plücker relations (a) and (b) of theorem 2.3. Now, we apply the weight vector $\omega' = (\omega'_{ij})$ with $\omega'_{ij} = i^2 + j^2 + 2j + 3$ (Corollary 2.6)to the set of polynomials (a). We have:

$$\omega' \cdot (\alpha_{ij} + \alpha_{hk}) = \omega' \cdot (\alpha_{i,h-1} + \alpha_{j+1,k}) = i^2 + j^2 + h^2 + k^2 + 2j + 2k + 6.$$

$$\omega' \cdot (\alpha_{i,j+1} + \alpha_{h,k-1}) = i^2 + j^2 + h^2 + k^2 + 2j + 2k + 6 + 2 + 2j - 2k.$$

Then

$$\omega' \cdot (\alpha_{ij} + \alpha_{hk}) > \omega' \cdot (\alpha_{i,j+1}\alpha_{h,k-1}), \text{ since } 2 + 2j - 2k < 0 \text{ for } k > j + 1 \ (1).$$

Moreover

$$\omega' \cdot (\alpha_{i+1,j} + \alpha_{h-1,k}) = i^2 + j^2 + h^2 + k^2 + 2j + 2k + 6 + 2 + 2i - 2h.$$

Then

$$\omega' \cdot (\alpha_{ij} + \alpha_{hk}) > \omega' \cdot (\alpha_{i+1,j} + \alpha_{h-1,k}), \text{ since } 2 + 2i - 2h < 0 \text{ for } h > j + 1 > i + 1 \ (2)$$

We conclude $\mathrm{in}'_\omega([i,j][h,k] - [i,k][h,j] + [i,h][k,j]) = [i,j][h,k] - [i,k][h,j]$. Now we apply ω' to the set (b).

$$\omega' \cdot (\alpha_{i+1,j+1} + \alpha_{h-1,k-1}) = i^2 + j^2 + h^2 + k^2 + 2j + 2k + 6 + 4 + 2i + 2j - 2h - 2k.$$

Then

$$\omega' \cdot (\alpha_{ij} + \alpha_{hk}) > \omega' \cdot (\alpha_{i+1,j+1} + \alpha_{h-1,k-1}), \text{ since } 4 + 2i + 2j - 2h - 2k < 0 \text{ for } (1) \text{ an}$$

Consider

$$\omega' \cdot (\alpha_{i,h} + \alpha_{j+1,k-1}) = i^2 + j^2 + h^2 + k^2 + 2j + 2k + 6 + 2h - 2k.$$

Then

$$\omega' \cdot (\alpha_{ij} + \alpha_{hk}) > \omega' \cdot (\alpha_{i,h} + \alpha_{j+1,k-1}), \text{ since } 2h - 2k < 0 \text{ for } k > h.$$

$$\omega' \cdot (\alpha_{i+1,h-1} + \alpha_{j,k}) = i^2 + j^2 + h^2 + k^2 + 2k + 6 + 2i.$$

We obtain

$$\omega' \cdot (\alpha_{ij} + \alpha_{hk}) > \omega' \cdot (\alpha_{i+1,h-1} + \alpha_{j,k}), \text{ since } 2j > 2i \text{ for } j > i.$$

Finally

$$\omega' \cdot (\alpha_{i+1,h} + \alpha_{j,k-1}) = i^2 + j^2 + h^2 + k^2 + 2k + 6 + 2i + 2h - 2k.$$

Then we obtain:

$\omega' \cdot (\alpha_{ij} + \alpha_{hk}) > \omega' \cdot (\alpha_{i+1,h} + \alpha_{j,k-1})$, since $2j > 2i + 2h - 2k$ for $k + j > h + i$.

We found that
$\text{in}'_\omega([i,j][h,k] - [i,h-1][j+1,k] - [i,j+1][h,k-1] - [i+1,j][h-1,k] + [i+1,j+1][h-1,k-1] + [i,h][j+1,k-1] + [i+1,h-1][j,k] - [i+1,h][j,k-1]) = (d)$
and the assertion of the theorem is achieved. □

References

[1] A. Conca, J. Herzog, G. Valla, *Sagbi bases with applications to blow-up algebras*, J.reine angew. Math.**474**(1996), 113 − 138.

[2] G. Failla, *Varietà di Hankel, sottovarietà di* $\mathbb{G}(r,m)$, Tesi di Dottorato di Ricerca in Matematica, Messina, 2008.

[3] G. Failla, S. Giuffrida , *On the Hankel lines variety* $H(1,n)$ *of* $\mathbb{G}(1,n)$, A.D.J.M, vol. 8, Number 2; p. 71-79, 2009.

[4] S. Giuffrida, R. Maggioni, *Hankel Planes*, J. of Pure and Appl. Algebra 209(2007), 119 − 138.

[5] B.Sturmfels,Groebner bases and Convex polytopes,Univ.Lect.Series,Vol.8, Amer.Math.Soc., 1995

Dipartimento di Matematica, Università di Messina, Contrada Papardo, salita Sperone, 31, 98166 Messina, Italy

E-mail address: gfailla@dipmat.unime.it

RENDICONTI DEL CIRCOLO MATEMATICO DI PALERMO
Serie II, Suppl. 81 (2009), pp. 181-186

Statistical tourism analysis and market strategies

Filippo Grasso* – Luigi Cucurullo**

*Department of "Scienze Economiche, finanziarie, sociali, ambientali, statistiche e del territorio" - University of Messina.
** PhD "controllo statistico di qualità" – University of Messina.

Abstract:

This work presents a statistical analysis of the tourist activities raised in Messinese territory and it thinks over the heated debate between the economy scholars and the dealers. In this work rises the need for a systematic connection between the economic system and the social-cultural transformations, as well as the need for defining a complex and in-depth picture of the tourist performance by the most effective and modern methodological instruments for the development of the territorial planning suitable strategies.

1. Analysis of the context and planning

A careful and timely strategic planning of the tourist flows is one of the most important bases for the definition of public and private sector politics.
To know the tourist statistics, as exact and quickly as possible, allows to consider scientifically the economic weight of the sector, and consequently to steer in real terms the incentive actions n favour of the public and private operators.
The Messinese territory is that which for its historical and morphological characteristics represents exhaustively the economic analysis of Sicilian tourism. As a consequence of this, this great property, not being distributed evenly all over the territory, forms tourist backgrounds different and separate from each other, that are projected on the market drawing the demand by the different sectors (rural, mountain, bathing and cultural tourism).
Without this important consideration, the analysis of the provincial statistics (positive statistics in comparison with those of the other Districts) could lead us into wrong conclusions and to believe that the whole regional territory is a breeding ground for tourist production. Really, what rises from the province of Messina, (one of the most desired provinces of the Sicilian tourism), is the presence of many magnets that scattered along the wide territory produce a considerable flow of tourists.
Among the proposed outcomes, it isn't considered the rest of the territory where the tourism isn't practised.
Two mountain ranges (Peloritani and Nebrodi) cross the territory, two different seas (Ionian and Tyrrhenian sea) are lapping on its coasts and it is bounded by the Etna Valley on the south-east.
All this added to the difficulty to establish links between the two sides contributed and keep on contributing to the formation and the sedimentation of the tourist systems independent from each other.

The tourist districts (PIT, Intermunicipal Associations, sheltered Areas, etc..), are so identified: Ionic Coast (I.C.); Peloritana Tyrrhenian Coast (T.C.1); Nebroidea Tyrrhenian Coast (T.C.2); Nebrodi Park (N.P); Aeolian Islands (A.I.); the City of Messina (ME), they allow to offer an economic schedule referred to the development of the main economic activity in the Messinese province, in fact, it is the tourist sector that drives the other connected sectors as the farming, the handicraft, the fishing and the transport.

The means to verify the characteristics, the peculiarities, variations, trends, interrelations and the directions of the complex realities in the tourist strategies are located not only in the analysis methodological choices but also in the possibility to dispose of a sufficient and reliable statistical documentation whose analysis has to take into consideration the design of connection instruments between the accommodation facilities and the terminals of territorial statistical survey (regional tourist services); the computerization of the regional statistical data processing.

The method of market strategy is referable to the planning method that includes three different but connected phases: the movement of the government where the targets' choices are made, the movement of the pure planning made to achieve the aims and, finally, the movement of information that permit the information gathering, its organization and elaboration to make the choices possible to be taken.

After all the pure elaboration of information will increase the rationality of the strategic decisions in the ambit of distribution and employment of the resources to which the sector's operators have to work.

2. Analysis of the statistical results

With its 1.011.415 arrivals registered in 2007 the Province of Messina confirms its position at the ranking top of the most longed Sicilian provinces for the holidaymakers and it reaches an increase of 44.001 units (+4,6 %) in comparison with those reached in 2005.

But the positive trend doesn't treat the six districts all equally, they develop differently. It is the case of the T.C.1 and ME districts that, as regards the arrivals, suffer a decline respectively of 3.650 units (-4,6%) and 6.841 units (-6,85%). On the contrary, the remaining districts register positive performances.

That which takes the lead is the I.C. district that boasts two of the biggest regional tourist magnets, Taormina and Naxos Gardens; the rise in the arrivals is equal to 28.398 units, followed by the T.C.2 district (+15.736), E.I. (+9.094) and N.P. (1.174).

As regards the per cent variations part of the Tyrrhenian zone registers the greatest increases. Here, in fact, three of the four districts have been able to apply operative development politics. The N.P., during the last years, directed its attention to the development of a mountain and rural tourism, by territory redevelopment, identification and promotion and today it starts to reap the rewards registering a rise in the arrivals of 9,67%. On the contrary, the T.C.2 district besides to increase its accommodation offer (in particular by the opening of several b&b) it has improved the maritime communications with the Aeolian Islands (by the rise in the "minicruises") and it has an increase in the arrivals of +13,44%. Finally, in the A.I district (+9,93% of the arrivals) with the expansion of its main seaports (Stromboli, Lipari, Vulcan and Salina) it has succeeded in rising the incoming proceeding from the centre and the north of Italy.

In comparison with the provincial average data the Ionic coast registers a +4,36% of arrivals and it shows that the strong increase of the tourist flows, that could be realized by the carrying out of the common politics from the two main tourist centres, Taormina and

Naxos Gardens (as the Sicilian tourism report of the Tourist OB hopes in 2006-2007) hasn't been still realized. (see tab.1)

Tab.n.1 Arrivals at the Province of Messina

Districts	**Arrivals**
Messina	6.841
Tyrrhenian Coast 1	3.650
Tyrrhenian Coast 2	15.736
Ionic Coast	28.398
Aeolian Islands	9.094
Nebrodi Park	1.174
Total	**64.893**

The positive trends as regards the arrivals, where the most of the districts show data above provincial average, aren't reaffirmed by the relative data to the tourist presences. With reference to this, in fact, the situation swung thanks to the two districts of ME and A.I. that surpassed the reference data.

Drawing generalizations from the results of the analysis, ME comes second with 51.336 presences and it is followed by A.I (18.427) and T.C. (5.119), while N.P. (-1.226) and T.C.1 (6.671) register a decrease in presences. (see tab.2).

Tab.n.2 Presences in the Province of Messina

Districts	**Presences**
Messina	51.336
Tyrrhenian coast 1	6.671
Tyrrhenian coast 2	5.199
Ionic Coast	82.400
Aeolian Islands	18.427
Nebrodi Park	1.226
Total	**165.259**

We can suppose that in districts as N.P. the attention has been directed to a greater visibility and to an increase in the "sightseeing" at the same district, but actually the instruments that encourage the tourists to stay in the territory aren't still mature (recreational, entertainment structures, performances planned during the year, etc..).

The territorial picture is very contradictory because of the Ionic side with the presence of the two most important tourist magnets, Taormina and Naxos Gardens that even if they are neighbouring districts don't succeed in carrying out of common politics for the relaunching and strengthening of their image to face the international tourist context.

The two country towns keep on developing differently without taking into consideration that the territorial planning and promotion should be unified in the interest of both of them.

In this context, the District of the Alcantara Valley, that has also become a Natural Park, deserves a particular attention thanks to its natural tourist attractions, as the Gorges and the presence of Etna. For its characteristics it should be treated as an unique case, in fact today, it has been positively considered for the establishment of the Alcantara Fluvial Park from the region.

As regards the Aeolian Islands, a recent French survey on the Mediterranean minor islands, justifies only the interventions directed towards the recovery of the current building property and of its consequent use for accommodation aims as the only one way for the enduring and balanced development of the Minor Islands.

The analysis of Italian presences in the districts shows a negative picture, as only the ME and A.I districts register some positive indexes with +17,10% (+45.187 units) and +4,40% (+12.137 units) and it's possible to suppose that the Aeolian data are undervalued because of above-mentioned problems of the hidden share. Other districts, excluding the T.C.2 district where there is some stability, register negative trends and in the I.C. district we've noticed a marked drop in Italian attendance equal to 69.886 (see.tab.3).

Tab.n.3 Compared data between the arrivals and the departures of Italian tourists in the provincial districts.

Districts	Arrivals	Departures
Messina	7.673	45.187
Tyrrhenian coast 1	1.987	1.897
Tyrrhenian coast 2	13.365	14.378
Ionic Coast	6.648	69.886
Aeolian Islands	6.773	12.137
Nebrodi Park	1.325	234
Total	**37.771**	**143.719**

Another aspect that has to be considered is the increase of the rural tourism. The agritouristic activity is a well-established reality, both for the accommodation activity and for the refreshment, and it has a fundamental role for the development of those inland areas characterized by the presence of several small centres rich of ancient traditions where today it's possible to find the ancient jobs and those typical products that distinguish a territory. From the data analysis emerges that 87 firms practise activities and in the course of some years will be added to them other 96 firms, owing authorization for the practice of the agritouristic activity and carrying out the works for the buildings readaptation. (see.tab.4 and 5).

Tab.n.4
Province of Messina
Firms owing the authorization for the practice of the agritouristic activity

	Firms n.	Bed n	Agri-campsite n,	Refreshment seat n.
Peloritan area	30	386	52	754
Nebrodi Area	51	748	26	1199
Aeolian Islands	6	56	0	74
Total	**87**	**1190**	**79**	**2027**

Tab.n.5
Province of Messina
Firms owing the sole permit for the practice of the agritouristic activity

	Firms n.	Bed n	Agri-campsite n,	Refreshment seat n.
Peloritan area	38	555	19	1033
Nebrodi Area	54	725	45	1241
Aeolian Islands	4	68	0	68
Total	**96**	**1348**	**64**	**2342**

In the end, this present work besides to have shown an analysis of the tourist sector in the Province of Messina highlights how this sector is the first cause for the territorial economic development. In fact, the solidity of the one-man businesses (81,1%) superior to national average solidity (66,6%) presents a relevant complex number of tourist facilities equal to 746 units, in all 40.934 beds that place the province of Messina to the top of Sicilian region wide.

Bibliography:

[1] - Assessorato al Turismo, Regione Siciliana – Il Turismo in Sicilia I flussi nazionali ed internazionali, 2005-2006. (Osservatorio Turistico della Regione Siciliana). Palermo 2007;

[2] - Bassi F.: Analisi di Mercato. Strumenti statistici per le decisioni di marketing, Ed. Carocci, 2008.

[3] - Dipartimento Turismo, Regione Siciliana – Dati statistici sui movimenti turistici, 2000-2008;

[4] - Parroco A. M .-Vaccina F. (a cura di), Isole Eolie, quanto turismo? Analisi

dei mercati turistici e sub – regionali. In: Studi statistici per il turismo vol. 3/200, Ed. Cleup, Padova.

[5] - Porretto A. – Nasca F.: La programmazione strategica del turismo, Ed. Pungitopo, 2009 – Palermo;

[6] - Lanfranchi M.: Agroalimentare e turismo: fattori aggreganti dell'identità rurale. Ed. Edas, Messina, 2008

[7] - Martini U – Ejarquev J.: Le nuove strategie di destination marketing. Come rafforzare la competitività delle regioni turistiche italiane. Ed. F.Angeli, 2008;

[8] - Micozzi G.: Marketing della cultura e del territorio. Ed. F.Angeli, 2006;

RENDICONTI DEL CIRCOLO MATEMATICO DI PALERMO
Serie II, Suppl. 81 (2009), pp. 187-212

Central Limit Theorems for Motion-Invariant Poisson Hyperplanes in Expanding Convex Bodies

LOTHAR HEINRICH

Dedicated to Professor Dr. Marius Stoka on the occasion of his 75th birthday

Abstract

It has been recently proved in Heinrich et al. [9] that the total number $\Psi_0(B^d_\varrho)$ of intersection points generated by a stationary process of d-dimensional Poisson hyperplanes in a ball B^d_ϱ with radius ϱ is asymptotically normally distributed for large ϱ. In the present paper we generalize this and other results by replacing B^d_ϱ by an expanding sampling window ϱK, where K is some fixed convex body with inner points. If the Poisson hyperplane process is additionally isotropic, the asymptotic variance of the scaled number $\Psi_0(\varrho K)/\varrho^{d-1/2}$ of intersection points in ϱK can be expressed in terms of a non-additive, motion-invariant ovoid functional of K, which is calculated explicitly for the unit ball B^d_1, ellipses and rectangles. Moreover, the method of $U-$statistics applied to the Poisson distributed number of hyperplanes hitting ϱK allows to derive multivariate central limit theorems for the vector of numbers of intersection $k-$flats $(k = 0, 1, \ldots, d-1)$ hitting ϱK as well as for the vector of their total $k-$volumes $(k = 0, 1, \ldots, d-1)$ within ϱK.

Keywords : Poisson hyperplanes, $k-$flat intersection process, hyperplane tessellation, intrinsic volumes, Crofton's formula, $U-$statistics, non-additive ovoid functionals

MCS 2000 : 60D05, 60F05, 52A40, 53C65

1 Preliminaries and notation

In the last fifteen years central limit theorems (briefly CLTs) for geometric functionals and measures associated with random tessellations of the d-dimensional Euclidean space $\mathbb{R}^d$ have been studied in various papers, see

e.g. [5], [17], [18], [1], [8], [9], [10], [19]. The investigation of Gaussian limits for empirical characteristics such as the total length of cell boundaries or the number of vertices of the cells contained in expanding regions is of great relevance for the statistical analysis of random tessellations (construction of confidence intervals for mean-value estimators or asymptotic goodness-of-fit tests). Voronoi-tessellations as well as random line or plane tessellations are bench mark models to describe real-world cell structures which arise in diverse disciplines, for example in material sciences, see [15] or [16], and in the modelling of telecommunication networks, see [8], [9]. For a lot of further applications of random tessellations and for the mathematical background from stochastic geometry and the theory of point processes we refer the reader to the monographs [16], [26], [12], [14], [23], and [4].

A CLT for the total number of vertices of convex polytopes induced by a stationary Poisson-Voronoi tessellation (briefly PVT) in cubes $[-n,n]^d$ has been first proved in [5], see also [7] for calculating exact asymptotic variances of these numbers in the case of $d=2$ and $d=3$.

An analogous result for motion-invariant Poisson line tessellations in growing circular regions in $\mathbb{R}^2$ was obtained by K. Paroux in [17] by employing the classical 'method of moments'. In Heinrich et al. [9] Paroux's CLT has been extended to stationary (not necessarily isotropic) Poisson hyperplane tessellations (briefly PHTs) in expanding spherical regions in $\mathbb{R}^d$ by applying Hoeffding's decomposition for U–statistics with Poisson distributed unboundedly growing samples sizes.

It should be noted that the probabilistic properties of PVTs and PHTs are quite different. So stationary PVTs are absolutely regular (or β-mixing) with exponentially decaying mixing coefficient being responsible for Gaussian approximations of mean-value estimates, see [5], [10]. On the other hand, stationary PHTs have 'long–range dependences' which entail slowly decaying correlations between distant parts of PHTs. This is seen, for example, from the explicitly known 'pair correlation function' of the point process of vertices in motion-invariant PHTs, see e.g. [7]. For the same reason the variance of the total k-volume of k-facets ($0 \le k \le d-1$) of a stationary PHTs contained in some large (convex) region of $\mathbb{R}^d$ grows significantly faster than its d-volume and depends additionally on its shape. The strong mixing properties of stationary Voronoi tessellations ensure that the corresponding variances increase proportional to the d-volume of the sampling region as it is known from many other classes of random set models, see e.g. [6].

In Section 2 we recall some notions from integral and stochastic geometry

needed in the sequel and introduce stationary (isotropic) Poisson hyperplane processes (briefly PHPs) in $\mathbb{R}^d$ without using the general theory of stationary hyperplane processes. In Section 3 we consider motion-invariant PHPs in an expanding convex region ϱK, where K is a convex body containing the origin as inner point. We formulate and prove a CLT for the joint distribution of the number of intersection points and the number of intersection k-flats ($k = 0, 1, \dots, d-1$) hitting ϱK as $\varrho \to \infty$. Section 4 is focused on proving Gaussian limits for the k-dimensional Lebesgue measure of the union of intersection k-flats (generated by intersection of $d-k$ hyperplanes) in ϱK for $k = 0, 1, \dots, d-1$. Note that for studying these random total k-volumes the convexity of K can be weakened. It is also noteworthy that in case of motion-invariant PHPs the rank of the corresponding asymptotic covariance matrix equals 1 in any dimension $d \geq 2$. Moreover, we show in Section 5 that the covariance matrix of the Gaussian limit in Section 3 has full rank for any $d \geq 2$. However, the entries of this covariance matrix strongly depend on the shape of K. In particular the asymptotic variance of each component is up to some constant a non-additive, motion-invariant ovoid functional which seems to be of interest in its own right. In Section 6 we give some estimates of these functionals and derive explicit formulas in case of balls ($d \geq 2$) and for ellipses and rectangles ($d = 2$).

At the end of this section we introduce some basic notation used repeatedly in this paper. Throughout, let $\mathfrak{B}^d$ be the $\sigma-$algebra of Borel sets in $\mathbb{R}^d$ and let $[\Omega, \mathfrak{A}, \mathsf{P}]$ be a common probability space on which all random objects are defined in this paper. The symbols E, Var and Cov are used for expectation, variance and covariance w.r.t. the probability measure P. Further, let $\langle x, y\rangle = \sum_{k=1}^d x_k y_k$ denote the scalar product of the coordinate vectors $x = (x_1, \dots, x_d)^\top$ and $y = (y_1, \dots, y_d)^\top$ in $\mathbb{R}^d$. By means of the Euclidean norm $\|\cdot\| = \sqrt{\langle \cdot, \cdot \rangle}$ we may define the closed ball $B_r^d = \{x \in \mathbb{R}^d : \|x\| \leq r\}$ with radius $r \geq 0$ centered at the origin and the unit sphere $\mathbf{S}^{d-1} = \{x \in \mathbb{R}^d : \|x\| = 1\}$ in $\mathbb{R}^d$, respectively. Furthermore, let $\mathbf{S}_+^{d-1} = \{(x_1, \dots, x_d)^\top \in \mathbf{S}^{d-1} : x_d \geq 0\}$ be the upper unit hemisphere and let $\nu_k(\cdot)$ denote the Lebesgue measure in $\mathbb{R}^k$ for $k = 0, 1, \dots, d$. This measure will also be used instead of the k-dimensional Hausdorff measure in $\mathbb{R}^d$ for $k = 0, 1, \dots, d-1$. As usual, $\nu_0(\cdot)$ coincides with the counting measure, i.e., $\nu_0(B) = \#B$. The d-volume of the unit ball is abbreviated by $\kappa_d = \nu_d(B_1^d)$ with

$$\kappa_{2k} = \frac{\pi^k}{k!} \quad \text{and} \quad \kappa_{2k+1} = \frac{2^{2k+1}\, k!\, \pi^k}{(2k+1)!} \quad \text{for} \quad k = 0, 1, \dots \ .$$

2 Stationary Poisson hyperplane processes in $\mathbb{R}^d$ and their k-flat intersection processes

An unoriented hyperplane in $\mathbb{R}^d$ can be represented in the parametrized form

$$H(p,v) = \{\, x \in \mathbb{R}^d : \langle x, v\rangle = p \,\}$$

with *orientation vector* $v \in \mathbf{S}_+^{d-1}$ (the normal unit vector of $H(p,v)$) and $p \in \mathbb{R}^1$ gives the signed perpendicular distance from the origin.

Definition A stationary *Poisson hyperplane process* $\Phi_{\lambda,\Theta}^{(d)}$ in $\mathbb{R}^d$ is defined to be a countable family $\{H(P_i,V_i) : i \geq 1\}$ of random $(d-1)-$dimensional affine linear subspaces of $\mathbb{R}^d$ (hyperplanes), where $\Psi = \{[P_i,V_i] : i \geq 1\}$ is a stationary independently marked Poisson point process on the real line $\mathbb{R}^1$ with intensity $0 < \lambda < \infty$ and mark distribution $\Theta(\cdot)$ (called *orientation distribution* of the PHP) given on the measurable mark space $[\mathbf{S}_+^{d-1}, \mathfrak{B}^d \cap \mathbf{S}_+^{d-1}]$.

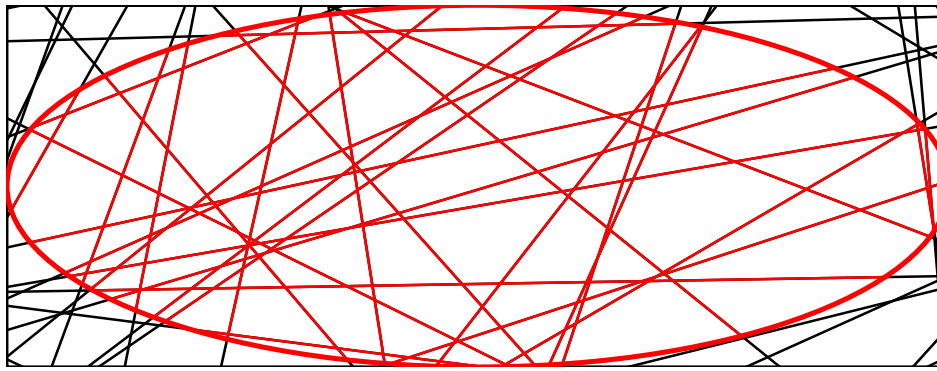


Figure 1: Motion-invariant Poisson line process in a rectangular and elliptic window

Note that non-stationary PHPs can be defined in the same way by letting Ψ an independently marked Poisson process with an intensity measure $\Lambda(\cdot)$ on $[\mathbb{R}^1, \mathfrak{B}^1]$ being not shift-invariant, see e.g. [24]. A stationary PHP $\Phi_{\lambda,\Theta}^{(d)}$ (or its orientation distribution $\Theta(\cdot)$) is called *non-degenerate*

if $\Theta(H(0,v)\cap \mathbf{S}_+^{d-1}) < 1$ for all $v \in \mathbf{S}_+^{d-1}$. This assumption on $\Theta(\cdot)$ ensures that the stationary k-flat intersection process

$$\Phi_{\lambda,\Theta}^{(d,k)} = \{H(P_{i_1}, V_{i_1}) \cap \cdots \cap H(P_{i_{d-k}}, V_{i_{d-k}}) \,:\, 1 \le i_1 < \cdots < i_{d-k}\}$$

has positive mean k-volume in the unit cube $[0,1]^d$ for each $k = 0, \ldots, d-1$, and the stationary PHT induced by $\Phi_{\lambda,\Theta}^{(d)}$ consists of bounded cells; see Chapter 10 in [23]. In this reference the reader can find a rigorous introduction into the general theory of stationary $k-$flat processes in $\mathbb{R}^d$ which are described there as point processes on the space $A(d,k)$ of all $k-$dimensional affine subspaces in $\mathbb{R}^d$, $0 \le k \le d-1$. A $(d-1)-$flat process is usually called hyperplane process. Sometimes the orientation distribution of a PHP is introduced as an even probability measure $\Theta^*(\cdot)$ on the entire sphere $\mathbf{S}^{d-1}$ which is then connected with $\Theta(\cdot)$ by $\Theta^*(B) = \frac{1}{2}\Big(\Theta(B\cap \mathbf{S}_+^{d-1}) + \Theta(-B\cap \mathbf{S}_+^{d-1})\Big)$ for any Borel set $B \subseteq \mathbf{S}^{d-1}$). The symmetry condition $\Theta^*(B) = \Theta^*(-B)$ expresses the identification of hyperplanes with antipodal orientation vectors. A stationary PHP $\Phi_{\lambda,\Theta}^{(d)}$ is said to be *isotropic* (or *motion-invariant*) if $\Theta(\cdot)$ is the uniform distribution $U(\cdot) = 2\,\nu_{d-1}(\cdot)/d\,\kappa_d$ on $\mathbf{S}_+^{d-1}$, i.e. $\Theta^*(\cdot)$ is the uniform distribution on $\mathbf{S}^{d-1}$. It turns out that the union sets

$$\Xi_{\lambda,\Theta}^{(d,k)} = \bigcup_{1\le i_1<\cdots<i_{d-k}} \bigcap_{j=1}^{d-k} H(P_{i_j}, V_{i_j}) \quad \text{for} \quad k = 0,1,\ldots,d-1$$

are stationary resp. motion-invariant random closed sets in $\mathbb{R}^d$, see [12], iff the PHP $\Phi_{\lambda,\Theta}^{(d)}$ does so in the above-defined sense. The intensity λ of $\Phi_{\lambda,\Theta}^{(d)}$ can be expressed by

$$\lambda = \frac{1}{2\,r}\,\mathsf{E}\#\{i \ge 1 : H(P_i,V_i)\cap B_r^d \ne \emptyset\} = \frac{1}{\nu_d(B)}\,\mathsf{E}\nu_{d-1}(\Xi_{\lambda,\Theta}^{(d,d-1)}\cap B)$$

for any $r > 0$ and any bounded $B \in \mathfrak{B}^d$.

Now we are in a position to introduce two functionals $\Psi_k^{(d)}(\cdot)$ and $\zeta_k^{(d)}(\cdot)$ on the family of sets $K_\varrho := \varrho\,K$, $\varrho \ge 1$, where K is convex and compact such that $B_\varepsilon^d \subseteq K$ for some $\varepsilon > 0$. For $k = 0,1,\ldots,d-1$ define

$$\Psi_k^{(d)}(K_\varrho) = \frac{1}{(d-k)\,!}\,{\sum_{i_1,\ldots,i_{d-k}\ge 1}}^{*}\,\chi\Big(\bigcap_{j=1}^{d-k} H(P_{i_j},V_{i_j})\cap K_\varrho\Big) \tag{2.1}$$

and

$$\zeta_k^{(d)}(K_\varrho) = \frac{1}{(d-k)\,!}\,{\sum_{i_1,\ldots,i_{d-k}\ge 1}}^{*}\,\nu_k\Big(\bigcap_{j=1}^{d-k} H(P_{i_j},V_{i_j})\cap K_\varrho\Big) \tag{2.2}$$

where $\chi(C) = 1$ for $C \neq \emptyset$ and $\chi(\emptyset) = 0$ and the asterisk in $\sum^*$ indicates that the sum runs over pairwise distinct indices $i_1, \ldots, i_{d-k} \geq 1$. Obviously, $\Psi_k^{(d)}(K_\varrho)$ counts the number of $k-$flats of $\Phi_{\lambda,\Theta}^{(d)}$ hitting K_ϱ, whereas $\zeta_k^{(d)}(K_\varrho)$ measures their the total $k-$volume in K_ϱ.

To determine expectations, variances and last but not least the asymptotic behaviour (as $\varrho \to \infty$) of (2.1) and (2.2) we consider the stationary independently marked Poisson process Ψ on $\mathbb{R}^1$ as a non-stationary Poisson process on the product space $\mathbb{R}^1 \times \mathbb{S}_+^{d-1}$. An equivalent formulation of the Poisson property of this point process enables us to argue as follows: Given the Poisson distributed number

$$N(K_\varrho) = \#\{i \geq 1 : H(P_i, V_i) \cap K_\varrho \neq \emptyset\} = \sum_{i \geq 1} \chi(H(P_i, V_i) \cap K_\varrho)$$

of hyperplanes hitting K_ϱ, say $N(K_\varrho) = n$, the random vectors $X_i^{(\varrho)} = (P_i, V_i)$, $i = 1, \ldots, n$, are (conditionally) independent of $N(K_\varrho)$ and independent identically distributed (briefly IID) with common distribution $Q_\Theta^{(\varrho)}(\cdot)$ which is defined, for $B \in \mathfrak{B}^1$ and $S \in \mathfrak{B}^d \cap \mathbb{S}_+^{d-1}$, by

$$Q_\Theta^{(\varrho)}(B \times S) = \frac{1}{b_\Theta(K)} \int_B \int_S \chi(H(\varrho^{-1}p, v) \cap K)\, \Theta(\mathrm{d}v)\, \mathrm{d}p\,,$$

where

$$b_\Theta(K) = \int_{\mathbb{R}^1} \int_{\mathbb{S}_+^{d-1}} \chi(H(p, v) \cap K)\, \Theta(\mathrm{d}v)\, \mathrm{d}p\,. \tag{2.3}$$

For brevity put $X_i = X_i^{(1)}$ for $i = 1, 2, \ldots$ and let X_0 denote the generic random vector with distribution $Q_\Theta^{(1)}(\cdot)$. Therefore we may write

$$\Psi_k^{(d)}(K_\varrho) \stackrel{\mathrm{d}}{=} \sum_{1 \leq i_1 < \cdots < i_{d-k} \leq N(K_\varrho)} \chi(\bigcap_{j=1}^{d-k} H(X_{i_j}^{(\varrho)}) \cap K_\varrho) \tag{2.4}$$

$$\zeta_k^{(d)}(K_\varrho) \stackrel{\mathrm{d}}{=} \sum_{1 \leq i_1 < \cdots < i_{d-k} \leq N(K_\varrho)} \nu_k(\bigcap_{j=1}^{d-k} H(X_{i_j}^{(\varrho)}) \cap K_\varrho)\,. \tag{2.5}$$

Here the symbol $\stackrel{\mathrm{d}}{=}$ indicates distributional equality. The expected number $\mathsf{E}N(K_\varrho)$ of hyperplanes hitting K can be calculated by means of Campbell's theorem, see e.g. [4] and leads to the following simple formula:

$$\mathsf{E}N(K_\varrho) = \mathsf{E}\sum_{i\geq 1}\chi(H(P_i,V_i)\cap K_\varrho) = \lambda\,\varrho\,b_\Theta(K)\;.$$

The integral $b_\Theta(K)$ defined in (2.3) can be rewritten as

$$b_\Theta(K) = \int_{\mathbb{S}^{d-1}_+}\big(\,h_K(v)+h_K(-v)\,\big)\,\Theta(\mathrm{d}v)\;,$$

where $h_K(v) = \max_{x\in K}\langle v,x\rangle$ denotes the *support function* of the convex body K. The last relation becomes clear since $h_K(v)$ equals just the distance of the support hyperplane with exterior normal unit vector u from the origin. The value of $b_\Theta(K)$ can be interpreted as 'direction-weighted breadth' of the convex body K w.r.t. the distribution $\Theta(\cdot)$.

If the PHP $\Phi^{(d)}_{\lambda,\Theta}$ is motion-invariant, i.e. $\Theta(\cdot)=U(\cdot)$, then $b_U(K)$ coincides with the *mean breadth* $b(K)$ of K which is a well-known from integral geometry, see [25], [20] and [23].

In what follows we put special emphasis on motion-invariant PHPs $\Phi^{(d)}_{\lambda,U}$. In this case the calculation of (conditional) expectations will be done by iterated application of *Crofton's formula* which can be written as follows:

$$\int_{\mathbb{S}^{d-1}_+}\int_{\mathbf{R}^1} V_k^{(d)}(H(p,v)\cap K)\,\mathrm{d}p\,U(\mathrm{d}v) = \frac{\kappa_{d-1}}{d\,\kappa_d}\,\frac{(k+1)\,\kappa_{k+1}}{\kappa_k}\,V_{k+1}^{(d)}(K) \quad (2.6)$$

for $k=0,1,\ldots,d-1$, where $V_k^{(d)}(K)$ is called the $k-$th *intrinsic volume* of the convex body $K\subset\mathbb{R}^d$, see Chapter 14 in [23]. These additive, motion-invariant and increasing ovoid functionals can be defined by the well-known *Steiner formula*

$$\nu_d(K+B_r^d) = \sum_{k=0}^{d} r^{d-k}\,\kappa_{d-k}\,V_k^{(d)}(K) \quad \text{for} \quad r\geq 0\;.$$

The intrinsic volumes of K are connected with *Minkowski's quermassintegrals* $W_k^{(d)}(K)$ by $\binom{d}{k}W_k^{(d)}(K) = \kappa_k\,V_{d-k}^{(d)}(K)$ for $k=0,1,\ldots,d-1$. We list some special cases:

$$V_0^{(d)}(K)=\chi(K)\;,\; V_1^{(d)}(K)=\frac{d\,\kappa_d}{2\,\kappa_{d-1}}\,b(K)\;,\; V_{d-1}^{(d)}(K)=\frac{1}{2}\,\nu_{d-1}(\partial K)\;,$$

$V_d^{(d)}(K) = \nu_d(K)$ and $V_k^{(d)}(K) = \nu_k(K)$ if $V_{k+1}^{(d)}(K) = 0$ for some $k \le d-1$.

Next, we calculate the mean values of (2.1) and (2.2). For doing this we use the distributional identities (2.4) and (2.5) and the well-known fact that the $(d-k)-$th factorial moment of the Poisson distributed number $N(K_\varrho)$ equals $(\mathsf{E}N(K_\varrho))^{d-k} = (\lambda\,\varrho\,b_\Theta(K))^{d-k}$ so that, for a stationary PHP,

$$\begin{aligned}\mathsf{E}\Psi_k^{(d)}(K_\varrho) &= \mathsf{E}\binom{N(K_\varrho)}{d-k}\,\mathsf{E}\chi(\bigcap_{i=1}^{d-k} H(X_i^{(\varrho)}) \cap K_\varrho) \\ &= (\lambda\,\varrho)^{d-k}\,\mu_\Theta^{(k,d)}(K)\,, \end{aligned} \tag{2.7}$$

where $\mu_\Theta^{(k,d)}(K)$ is defined by

$$(d-k)!\,\mu_\Theta^{(k,d)}(K) = (b_\Theta(K))^{d-k}\,\mathsf{P}(\bigcap_{i=1}^{d-k} H(X_i) \cap K \neq \emptyset)$$

$$= \int\limits_{\mathbb{S}_+^{d-1}} \int\limits_{\mathbf{R}^1} \cdots \int\limits_{\mathbb{S}_+^{d-1}} \int\limits_{\mathbf{R}^1} \chi(\bigcap_{i=1}^{d-k} H(p_i, v_i) \cap K)\,\mathrm{d}p_1\,\Theta(\mathrm{d}v_1) \cdots \mathrm{d}p_{d-k}\,\Theta(\mathrm{d}v_{d-k})\,.$$

If $\Theta(\cdot) = U(\cdot)$ we may apply Crofton's formula (2.6) $d-k$ times leading to

$$\begin{aligned}\mu_U^{(k,d)}(K) &= \prod_{j=0}^{d-k-1} \Big(\frac{\kappa_{d-1}}{d\,\kappa_d}\frac{(j+1)\,\kappa_{j+1}}{\kappa_j}\Big)\,\frac{V_{d-k}^{(d)}(K)}{(d-k)!} \\ &= \Big(\frac{\kappa_{d-1}}{d\,\kappa_d}\Big)^{d-k}\,\kappa_{d-k}\,V_{d-k}^{(d)}(K)\,. \end{aligned} \tag{2.8}$$

In the same way we find that

$$\begin{aligned}\mathsf{E}\zeta_k^{(d)}(K_\varrho) &= \frac{(\lambda\,\varrho\,b_\Theta(K))^{d-k}}{(d-k)!}\,\varrho^k\,\mathsf{E}\nu_k(\bigcap_{i=1}^{d-k} H(X_i) \cap K) \\ &= \lambda^{d-k}\,\lambda_\Theta^{(k,d)}\,\varrho^d\,\nu_d(K)\,, \end{aligned} \tag{2.9}$$

where $\lambda_\Theta^{(k,d)} =$

$$\int\limits_{\mathbb{S}_+^{d-1}} \int\limits_{\mathbf{R}^1} \cdots \int\limits_{\mathbb{S}_+^{d-1}} \int\limits_{\mathbf{R}^1} \nu_k(\bigcap_{i=1}^{d-k} H(p_i, v_i) \cap B_0)\,\mathrm{d}p_1\,\Theta(\mathrm{d}v_1) \cdots \mathrm{d}p_{d-k}\,\Theta(\mathrm{d}v_{d-k})\,.$$

Here, B_0 can be any bounded Borel set satisfying $\nu_d(B_0) = 1$. Again by multiple application of (2.6) it follows that

$$\lambda_U^{(k,d)} = \binom{d}{k} \frac{\kappa_d}{\kappa_k} \left(\frac{\kappa_{d-1}}{d\,\kappa_d} \right)^{d-k} . \tag{2.10}$$

Note that the relation (2.9) remains valid for any bounded $K \in \mathfrak{B}^d$ so that $\mathsf{E}\zeta_k^{(d)}(B_0) = \lambda^{d-k}\,\lambda_\Theta^{(k,d)}$ can be regarded as intensity of the random measure $\zeta_k^{(d)}(\cdot)$ as well as of the $k-$flat intersection process $\Psi_{\lambda,\Theta}^{(k,d)}$. Furthermore, one can rewrite $\lambda_\Theta^{(k,d)}$ as follows:

$$\begin{aligned} \lambda_\Theta^{(k,d)} &= \frac{1}{(d-k)!} \int\limits_{\mathbb{S}_+^{d-1}} \cdots \int\limits_{\mathbb{S}_+^{d-1}} \nabla_{d-k}(v_1, \ldots, v_{d-k})\, \Theta(\mathrm{d}v_1) \cdots \Theta(\mathrm{d}v_{d-k}) \\ &= V_{d-k}^{(d)}(Z_\Theta) \end{aligned}$$

for $k = 0, 1, \ldots, d-1$, where $\nabla_{d-k}(v_1, \ldots, v_{d-k})$ denotes the $(d-k)$-dimensional volume of the parallelotope spanned by $v_1, \ldots, v_{d-k} \in \mathbf{S}_+^{d-1}$ and Z_Θ is a centrally symmetric convex body uniquely determined by the orientation distribution $\Theta(\cdot)$ - called *associated zonoid* or *Steiner compact* in [12], see [23] for details.

At the end of this section we recall some basic facts on U-statistics. Let $Y_1, Y_2, \ldots$ be a sequence of IID random elements in some measurable space $[E, \mathfrak{E}]$ and, for fixed $m \geq 2$, let $f : E^m \to \mathbb{R}^1$ be a $\mathfrak{E}^m$-measurable symmetric function such that $\mathsf{E}|f(Y_1, \ldots, Y_m)| < \infty$. A U-statistic $U_n^{(m)}(f)$ of order $m \geq 1$ with *kernel function* f is defined by

$$U_n^{(m)}(f) = \sum_{1 \leq i_1 < \cdots < i_m \leq n} f(Y_{i_1}, \ldots, Y_{i_m}) \quad \text{for} \quad n \geq m\,.$$

The representations (2.4) and (2.5) reveal that $\Psi_k^{(d)}(K_\varrho)$ as well as $\zeta_k^{(d)}(K_\varrho)$ can treated as random U-statistics of order $d-k$ with Poisson distributed sample size $N(K_\varrho)$. In contrast to the standard case the kernel function $\chi(\bigcap_{i=1}^{d-k} H(y_i) \cap K_\varrho)$ resp. $\nu_k(\bigcap_{i=1}^{d-k} H(y_i) \cap K_\varrho)$ and the common distribution $Q_\Theta^{(\varrho)}(\cdot)$ of the Y_i's depend on the (mean) sample size.

The proofs of the CLTs we are going to present in Section 3 and Section 4 rely on Hoeffding's decomposition of U–statistics which allows to approximate $U_n^{(m)}(f)$ by a simple sum of independent random variables :

$$U_n^{(m)}(f) - \binom{n}{m}\mu = \binom{n-1}{m-1}\sum_{i=1}^{n}(\,g(Y_i)-\mu\,) + \binom{n}{m}R_n^{(m)}(f)\,, \quad (2.11)$$

where $\mu = \mathsf{E}f(Y_1,Y_2,\ldots,Y_m)$ and $g(y) = \mathsf{E}f_m(y,Y_2,\ldots,Y_m)$ is the conditional expectation of $f(Y_1,Y_2,\ldots,Y_m)$ given $Y_1 = y \in E$. The remainder term $R_n^{(m)}(f)$ contains sums of martingale difference sequences arising in Hoeffding's decomposition which in turn allows to prove the crucial estimate given in

Lemma 2.1 *Provided that* $\mathsf{E}f^2(Y_1,\ldots,Y_m) < \infty$ *we have*

$$\mathsf{E}\big(R_n^{(m)}(f)\big)^2 \le \frac{c_m}{n^2}\,\mathsf{E}\,f^2(Y_1,\ldots,Y_m) \quad \textit{for any} \quad n \ge m$$

and some positive constant c_m *only depending on the order* m.

This result is the main step in the proof of Hoeffding's CLT for U–statistics, see e.g. [3] or [9] for a sketch. In [3] the reader can find a lot of further details on U-statistics including weaker versions of Lemma 2.1.

3 CLTs for the number of intersection k-flats hitting ϱK

In this section we study the joint asymptotic behaviour (as $\varrho \to \infty$) of the centered and scaled random variables

$$\overline{\Psi}_{k,\varrho}^{(d)}(K) = \varrho^{-(d-k-1/2)}\left(\,\Psi_k^{(d)}(K_\varrho) - (\,\lambda\,\varrho\,)^{d-k}\,\mu_\Theta^{(k,d)}(K)\,\right) \quad (3.1)$$

for $k = 0,1,\ldots,d-1$ in case of a stationary PHP $\Psi_{\lambda,\Theta}^{(d)}$ with $\mu_\Theta^{(k,d)}(K)$ defined in (2.7). More precisely, we shall prove a multivariate CLT for the random vector $(\overline{\Psi}_{k,\varrho}^{(d)}(K))_{k=0}^{d-1}$ and determine the covariance matrix of the

Gaussian limiting vector in the particular case $\Theta(\cdot) = U(\cdot)$. To use results from the theory of U-statistics we introduce the conditional expectation

$$g_{\chi,\Theta}^{(k,d)}((p,v),K) = \mathsf{E}\chi(\bigcap_{i=1}^{d-k-1} H(X_i) \cap H(p,v) \cap K)$$

for $(p,v) \in \mathbb{R}^1 \times \mathbf{S}_+^{d-1}$. In analogy to (2.8) we apply Crofton's formula (2.6) $d-k-1$ times (with K replaced by $H(p,v) \cap K$) to derive a more explicit formula of the conditional expectation $g_{\chi,U}^{(k,d)}((p,v),K)$, namely

$$g_{\chi,U}^{(k,d)}((p,v),K) = a_k^{(d)} \, \frac{(d-k-1)!}{(b(K))^{d-k-1}} \, V_{d-k-1}^{(d)}(H(p,v) \cap K) \tag{3.2}$$

with

$$a_k^{(d)} = \Big(\frac{\kappa_{d-1}}{d\,\kappa_d}\Big)^{d-k-1} \kappa_{d-k-1} \quad \text{for} \quad k = 0,1,\ldots,d-1\,.$$

In the first step we calculate the asymptotic covariances

$$\sigma_{kl}^{(d)}(\Theta,K) = \lim_{\varrho\to\infty} \mathsf{Cov}(\,\overline{\Psi}_{k,\varrho}^{(d)}(K), \overline{\Psi}_{l,\varrho}^{(d)}(K)\,)\,.$$

For brevity, put $\sigma_{kl}^{(d)}(K) = \sigma_{kl}^{(d)}(U,K)$ for $k,l = 0,1,\ldots,d-1$.

Lemma 3.1 *Let $\Psi_{\lambda,\Theta}^{(d)}$ be a stationary PHP with non-degenerate orientation distribution $\Theta(\cdot)$. Then,*

$$\sigma_{kl}^{(d)}(\Theta,K) = \frac{(\,\lambda\, b_\Theta(K)\,)^{2d-k-l-1}}{(d-k-1)!\,(d-l-1)!}\, \mathsf{E} g_{\chi,\Theta}^{(k,d)}(X_0,K)\, g_{\chi,\Theta}^{(l,d)}(X_0,K) \tag{3.3}$$

and $\sigma_{kl}^{(d)}(\Theta,K) > 0$ for $k,l = 0,1,\ldots,d-1$.
In the particular case of a motion-invariant PHP $\Psi_{\lambda,U}^{(d)}$, we have

$$\begin{aligned} \sigma_{kl}^{(d)}(K) \;&=\; \lambda^{2d-k-l-1}\, a_k^{(d)}\, a_l^{(d)} \\ &\times \int\limits_{\mathbb{S}_+^{d-1}} \int\limits_{\mathbf{R}^1} V_{d-k-1}^{(d)}(H(p,v)\cap K)\, V_{d-l-1}^{(d)}(H(p,v)\cap K)\,\mathrm{d}p\, U(\mathrm{d}v)\,. \end{aligned} \tag{3.4}$$

Proof By symmetry of the kernel function $\chi(H(y_1) \cap \cdots \cap H(y_m) \cap K_\varrho)$ for $m = d-k$ and $m = d-l$ we may write

$$(d-k)!\,(d-l)!\;\mathsf{E}(\Psi_k^{(d)}(K_\varrho)\Psi_l^{(d)}(K_\varrho))$$

$$= \mathsf{E}\Big(\sum_{\substack{1\le i_p\le N(K_\varrho)\\ p=1,\dots,d-k}}^{*} \chi(\bigcap_{p=1}^{d-k} H(X_{i_p}^{(\varrho)}) \cap K_\varrho)\Big)\Big(\sum_{\substack{1\le j_q\le N(K_\varrho)\\ q=1,\dots,d-l}}^{*} \chi(\bigcap_{q=1}^{d-l} H(X_{j_q}^{(\varrho)}) \cap K_\varrho)\Big)$$

Some basic combinatorial relations combined with the independence assumptions made in (2.4) yield that, for $0 \le k \le l \le d-1$,

$$\mathsf{E}\big(\,\Psi_k^{(d)}(K_\varrho)\,\Psi_l^{(d)}(K_\varrho)\,\big) = \sum_{j=0}^{d-l} \frac{j!}{(d-k)!\,(d-l)!}\binom{d-k}{j}\binom{d-l}{j}$$

$$\times\quad \mathsf{E}\Big(\sum_{\substack{1\le i_r\le N(K_\varrho)\\ r=1,\dots,2d-k-l-j}}^{*} \chi(\bigcap_{p=1}^{d-k} H(X_{i_p}^{(\varrho)}) \cap K_\varrho)\,\chi(\bigcap_{q=d-k-j+1}^{2d-k-l-j} H(X_{i_q}^{(\varrho)}) \cap K_\varrho)\Big)$$

$$= \sum_{j=0}^{d-l} \frac{j!\,(2d-k-l-j)!}{(d-k)!\,(d-l)!}\binom{d-k}{j}\binom{d-l}{j}\mathsf{E}\binom{N(K_\varrho)}{2d-k-l-j}$$

$$\times\quad \mathsf{E}\Big(\,\chi(\bigcap_{p=1}^{d-k} H(X_p^{(\varrho)}) \cap K_\varrho)\,\chi(\bigcap_{q=d-k-j+1}^{2d-k-l-j} H(X_q^{(\varrho)}) \cap K_\varrho)\,\Big)$$

$$= \mathsf{E}\Psi_k^{(d)}(K_\varrho)\,\mathsf{E}\Psi_l^{(d)}(K_\varrho) + \sum_{j=1}^{d-l} \frac{\big(\,\lambda\, b_\Theta(K)\,\varrho\,\big)^{2d-k-l-j}}{j!\,(d-k-j)!\,(d-l-j)!}$$

$$\times\quad \mathsf{E}\Big(\,\chi(\bigcap_{p=1}^{d-k} H(X_p) \cap K)\,\chi(\bigcap_{q=d-k-j+1}^{2d-k-l-j} H(X_q) \cap K)\,\Big)\ .$$

Here, we have used that the summand for $j=0$ equals $\mathsf{E}\Psi_k^{(d)}(K_\varrho)\mathsf{E}\Psi_l^{(d)}(K_\varrho)$. Therefore, the covariance $\mathsf{Cov}(\Psi_k^{(d)}(K_\varrho), \Psi_l^{(d)}(K_\varrho))$ can be written as non-negative polynomial of degree $2d-k-l-1$ in $\varrho \ge 0$. Hence, in view of

(3.1), dividing this polynomial by $\varrho^{2d-k-l-1}$ yields $\mathsf{Cov}(\overline{\Psi}_{k,\varrho}^{(d)}(K), \overline{\Psi}_{l,\varrho}^{(d)}(K))$ which together with

$$\mathsf{E}\big(\chi(\bigcap_{p=1}^{d-k} H(X_p)\cap K_\varrho)\,\chi(\bigcap_{q=d-k}^{2d-k-l-1} H(X_q)\cap K)\big) = \mathsf{E}g_{\chi,\Theta}^{(k,d)}(X_0,K)\,g_{\chi,\Theta}^{(l,d)}(X_0,K)$$

implies the limiting relation (3.3).

Since $\chi(\bigcap_{q=d-k}^{2d-k-l-1} H(X_q)\cap K) \geq \chi(\bigcap_{q=d-k}^{2d-2k-1} H(X_q)\cap K)$ for $k \leq l$, we get

$$\mathsf{E}g_{\chi,\Theta}^{(k,d)}(X_0,K)\,g_{\chi,\Theta}^{(l,d)}(X_0,K) \geq \mathsf{E}(g_{\chi,\Theta}^{(k,d)}(X_0,K))^2 \geq (\mathsf{E}g_{\chi,\Theta}^{(k,d)}(X_0,K))^2$$

and the non-degeneracy of $\Theta(\cdot)$ entails that $\mathsf{E}\Psi_k^{(d)}(K) > 0$ for any convex body K with inner points, see Chapt. 14.2 in [23], so that, by (2.7), $\mathsf{E}(g_{\chi,\Theta}^{(k,d)}(X_0,K))^2 > 0$ for $k = 0,1,\ldots,d-1$.

Finally, relation (3.4) follows by combining (3.2) and (3.3), where the distribution of X_0 is $Q_U^{(1)}(\cdot)$ as defined in Sect. 2. Thus, Lemma 3.1 is proved. □

We now establish the announced multivariate CLT for the random counting variables (2.1). For this we consider the d-dimensional vector of centered and individually scaled counting variables (3.1). By $\mathcal{N}_d\big(o,\Sigma\big)$ we denote a d-dimensional Gaussian vector with mean vector $o = (0,\ldots,0)^\top$ and covariance matrix Σ and $\xrightarrow{\mathrm{d}}$ means convergence in distribution.

Theorem 3.1 *Let $\Psi_{\lambda,\Theta}^{(d)}$ be a stationary PHP with non-degenerate $\Theta(\cdot)$. Then,*

$$\big(\overline{\Psi}_{k,\varrho}^{(d)}(K)\big)_{k=0}^{d-1} \xrightarrow[\varrho\to\infty]{\mathrm{d}} \mathcal{N}_d\big(o,\Sigma_d(\Theta,K)\big)\,, \tag{3.5}$$

where the entries of the covariance matrix $\Sigma_d(\Theta,K) = \big(\sigma_{kl}^{(d)}(\Theta,K)\big)_{k,l=0}^{d-1}$ are given by the limits (3.3). If $\Theta(\cdot)$ is the uniform distribution on $\mathbf{S}_+^{d-1}$, then

$$\big(\overline{\Psi}_{k,\varrho}^{(d)}(K)\big)_{k=0}^{d-1} \xrightarrow[\varrho\to\infty]{\mathrm{d}} \mathcal{N}_d\big(o,\Sigma_d(K)\big)\,, \tag{3.6}$$

where $\mu_\Theta^{(k,d)}(K) = \mu_U^{(k,d)}(K)$ is as in (2.8) and $\Sigma_d(K) = \big(\sigma_{kl}^{(d)}(K)\big)_{k,l=0}^{d-1}$ is defined by (3.4).

Proof For notational ease put $N_\varrho = N(K_\varrho)$, $n_\varrho = \mathsf{E}N(K_\varrho) = \lambda\, b_\Theta(K)\, \varrho$ and $\mu_{d-k}(f) = \mathsf{E}f(X_1, \ldots, X_{d-k})$. We first apply the Hoeffding decomposition (2.11) to the counting variables (2.1): For $k = 0, 1, \ldots, d-1$,

$$\Psi_k^{(d)}(K_\varrho) - \mathsf{E}\Psi_k^{(d)}(K_\varrho) \stackrel{\mathrm{d}}{=} \left(\binom{N_\varrho}{d-k} - \frac{n_\varrho^{d-k}}{(d-k)!} \right) \mu_{d-k}(f)$$

$$+ \quad \binom{N_\varrho - 1}{d-k-1} \sum_{i=1}^{N_\varrho} \Big(g_{\chi,\Theta}^{(k,d)}(X_i, K) - \mu_{d-k}(f) \Big) + \binom{N_\varrho}{d-k} R_{N_\varrho}^{(d-k)}(f)\,,$$

where $f(X_1, \ldots, X_{d-k}) = \chi(H(X_1) \cap \cdots \cap H(X_{d-k}) \cap K)$ and the $X_1, X_2, \ldots$ are IID random vectors in $\mathbb{R}^1 \times \mathbf{S}_+^{d-1}$ with common distribution $Q_\Theta^{(1)}(\cdot)$.

Dividing both sides of the previous equality by $\varrho^{d-k-1/2}$ and some simple rearrangements on the left-hand side provide

$$\begin{aligned}
\overline{\Psi}_{k,\varrho}^{(d)}(K) \quad &\stackrel{\mathrm{d}}{=} \quad \frac{1}{\varrho^{d-k-1}} \binom{N_\varrho - 1}{d-k-1} \frac{1}{\sqrt{\varrho}} \Big(\sum_{i=1}^{N_\varrho} g_{\chi,\Theta}^{(k,d)}(X_i, K) - n_\varrho\, \mu_{d-k}(f) \Big) \\
&+ \quad \frac{\mu_{d-k}(f)}{\varrho^{d-k-1/2}} \left(\binom{N_\varrho}{d-k} - (N_\varrho - n_\varrho) \binom{N_\varrho - 1}{d-k-1} - \frac{n_\varrho^{d-k}}{(d-k)!} \right) \\
&+ \quad \frac{1}{\varrho^{d-k-1/2}} \binom{N_\varrho}{d-k} R_{N_\varrho}^{(d-k)}(f)\,.
\end{aligned}$$

Since N_ϱ is conditionally independent of $X_1, X_2, \ldots$, we find by Lemma 2.1 that

$$\mathsf{E}\Big(\big(R_{N_\varrho}^{(d-k)}(f) \big)^2 \mid N_\varrho = n \Big) \le \frac{c_{d-k}}{n^2}\, \mathsf{E}f^2(X_1, \ldots, X_{d-k}) \quad \text{for} \quad n \ge d-k\,.$$

Hence, we may proceed with

$$\begin{aligned}
\mathsf{E}\left(\binom{N_\varrho}{d-k} R_{N_\varrho}^{(d-k)}(f) \right)^2 \quad &= \quad \sum_{n \ge d-k} \binom{n}{d-k}^2 \mathsf{E}\Big(\big(R_{N_\varrho}^{(d-k)}(f) \big)^2 \mid N_\varrho = n \Big) \\
&\qquad \times \mathsf{P}(N_\varrho = n) \\
&\le \quad \frac{c_{d-k}\, \mathsf{E}f^2(X_1, \ldots, X_{d-k})}{(d-k)^2}\, \mathsf{E}\binom{N_\varrho - 1}{d-k-1}^2 .
\end{aligned}$$

Since $\mathsf{E}\big((N_\varrho-1)(N_\varrho-2)\cdots(N_\varrho-d+k+1)\big)^2$ is a polynomial of degree $2d-2k-2$ in n_ϱ, it follows that

$$\frac{1}{\varrho^{2d-2k-1}}\,\mathsf{E}\binom{N_\varrho-1}{d-k-1}^2 \underset{\varrho\to\infty}{\longrightarrow} 0\,.$$

Thus,

$$\frac{1}{\varrho^{d-k-1/2}}\binom{N_\varrho}{d-k}R_{N_\varrho}^{(d-k)}(f) \underset{\varrho\to\infty}{\overset{\mathsf{P}}{\longrightarrow}} 0\,, \tag{3.7}$$

where $\overset{\mathsf{P}}{\longrightarrow}$ denotes convergence in probability P. The validity of the limit

$$\frac{1}{\varrho^{d-k-1/2}}\left(\binom{N_\varrho}{d-k}-(N_\varrho-n_\varrho)\binom{N_\varrho-1}{d-k-1}-\frac{n_\varrho^{d-k}}{(d-k)!}\right) \underset{\varrho\to\infty}{\overset{\mathsf{P}}{\longrightarrow}} 0 \tag{3.8}$$

can be verified by repeating word by word the arguments used in Sect. 3 of [9] to treat the special case $K=B_1^d$. With

$$G_{k,\varrho}^{(d)}(K)=\varrho^{-1/2}\Big(\sum_{i=1}^{N_\varrho}g_{\chi,\Theta}^{(k,d)}(X_i,K)-n_\varrho\,\mu_{d-k}(f)\Big)\quad\text{for}\quad k=0,1,\dots,d-1$$

and by using that N_ϱ is Poisson distributed with mean $\lambda\,\varrho\,b_\Theta(K)$ and independent of $X_1,X_2,\dots$, it is easily checked that

$$\mathsf{E}G_{k,\varrho}^{(d)}(K)\,G_{l,\varrho}^{(d)}(K)=\lambda\,b_\Theta(K)\,\mathsf{E}g_{\chi,\Theta}^{(k,d)}(X_0,K)\,g_{\chi,\Theta}^{(l,d)}(X_0,K) \tag{3.9}$$

for $0\le k\le l\le d-1$ as well as $N_\varrho/\varrho \underset{\varrho\to\infty}{\overset{\mathsf{P}}{\longrightarrow}} \lambda\,b_\Theta(K)$, which in turn implies the limit

$$\frac{1}{\varrho^{d-k-1}}\binom{N_\varrho-1}{d-k-1} \underset{\varrho\to\infty}{\overset{\mathsf{P}}{\longrightarrow}} \frac{(\lambda\,b_\Theta(K))^{d-k-1}}{(d-k-1)!}\,.$$

Combining (3.7), (3.8), (3.9) for $k=l$, and the latter relation, we obtain with the above-introduced notation

$$\overline{\Psi}_{k,\varrho}^{(d)}(K)\overset{\mathrm{d}}{=}\frac{(\lambda\,b_\Theta(K))^{d-k-1}}{(d-k-1)!}\,G_{k,\varrho}^{(d)}(K)+Z_{k,\varrho}^{(d)}(K)\,,$$

where $Z_{k,\varrho}^{(d)}(K)$ disappears asymptotically as $\varrho \to \infty$, i.e. $Z_{k,\varrho}^{(d)}(K) \xrightarrow[\varrho\to\infty]{\mathsf{P}} 0$.

Recall that due to well-known Cramér-Wold device, see [2], the multivariate CLT (3.5) is equivalent to the univariate CLT

$$\sum_{k=0}^{d-1} t_k \overline{\Psi}_{k,\varrho}^{(d)}(K) \xrightarrow[\varrho\to\infty]{\mathrm{d}} \mathcal{N}\big(0, t^\top \Sigma_d(\Theta, K)\, t\big) \tag{3.10}$$

for all $t = (t_0, \ldots, t_{d-1})^\top \in \mathbb{R}^d \setminus \{o\}$. Slutsky's theorem, see also [2], tells us that on the left-hand side of (3.10) the random variables $\overline{\Psi}_{k,\varrho}^{(d)}(K)$ can be replaced by the scaled random sums $(\lambda\, b_\Theta(K))^{d-k-1}\, G_\varrho^{(k,d)}(K)/(d-k-1)!$ for $k = 0, 1, \ldots, d-1$ without changing the limit in distribution. In other words, we have to prove

$$H_\varrho^{(d)} = \varrho^{-1/2} \Big(\sum_{i=1}^{N_\varrho} h(X_i) - n_\varrho\, \mathsf{E}h(X_0) \Big) \xrightarrow[\varrho\to\infty]{\mathrm{d}} \mathcal{N}\big(0, t^\top \Sigma(\Theta, K)\, t\big) \tag{3.11}$$

for all $t = (t_0, \ldots, t_{d-1})^\top \in \mathbb{R}^d \setminus \{o\}$, where

$$h(X_i) = \sum_{k=0}^{d-1} t_k\, \frac{(\lambda\, b_\Theta(K))^{d-k-1}}{(d-k-1)!}\, g_{\chi,\Theta}^{(k,d)}(X_i, K) \quad \text{for} \quad i = 1, 2, \ldots .$$

This means that the proof of (3.5) can be put down to a CLT for sums of a Poisson distributed number of IID random variables. There are several results in the literature addressing this problem in great generality. However, we can do this in a simple way without referring to other results. Note that after a short calculation, using among others that $\mathsf{E}N_\varrho(N_\varrho - 1) = n_\varrho^2$, we arrive at

$$\mathsf{E}(H_\varrho^{(d)})^2 = \lambda\, b_\Theta(K)\, \mathsf{E}h^2(X_0) = \sum_{k=0}^{d-1} \sum_{l=0}^{d-1} t_k\, t_l\, \sigma_{kl}^{(d)} = t^\top \Sigma(\Theta, K)\, t$$

in accordance with the expressions of the asymptotic covariances in (3.3).

The characteristic function of $H_\varrho^{(d)}$ is easily obtained by using the independence assumptions and generating function $\mathsf{E}z^{N_\varrho} = \exp\{n_\varrho(z-1)\}$ for any complex z, so that

$$\mathsf{E}\exp\Big\{\mathrm{i}s\,H_\varrho^{(d)}\Big\} = \exp\left\{n_\varrho\left(\mathsf{E}\exp\Big\{\frac{\mathrm{i}s}{\sqrt{\varrho}}h(X_0)\Big\} - 1 - \frac{\mathrm{i}s}{\sqrt{\varrho}}\mathsf{E}h(X_0)\right)\right\}$$

whence, by applying the well-known inequality $\left| e^{\mathrm{i}x} - 1 - \mathrm{i}x - \frac{(\mathrm{i}x)^2}{2} \right| \le \frac{|x|^3}{6}$ for $x \in \mathbb{R}^1$, it follows that, for all $s \in \mathbb{R}^1$,

$$\mathsf{E}\exp\Big\{\mathrm{i}s\,H_\varrho^{(d)}\Big\} \underset{\varrho\to\infty}{\longrightarrow} \exp\Big\{-\frac{s^2}{2}\,\lambda\, b_\Theta(K)\,\mathsf{E}h^2(X_0)\Big\} = \exp\Big\{-\frac{s^2}{2}\,t^\top\Sigma(\Theta,K)\,t\Big\}\,,$$

which is equivalent to (3.11). Hence, the first assertion of Theorem 3.1 is proved. The second assertion is an immediate consequence of the first one and (3.4) which completes the proof of Theorem 3.1. □

4 CLTs for the total k-volume of intersection k-flats in ϱK

In continuation of the previous section we now consider the joint asymptotic behaviour (as $\varrho \to \infty$) of the centered and scaled random variables

$$\overline{\zeta}_{k,\varrho}^{(d)}(K) = \varrho^{-(d-1/2)}\left(\zeta_k^{(d)}(K_\varrho) - \lambda^{d-k}\,\lambda_\Theta^{(k,d)}\,\varrho^d\,\nu_d(K)\right) \tag{4.1}$$

for $k = 0, 1, \ldots, d-1$ for a stationary PHP $\Psi_{\lambda,\Theta}^{(d)}$, where $\lambda_\Theta^{(k,d)}$ defined by (2.9) resp. by (2.10) if the PHP is additionally isotropic. In order to argue along the line of the preceding section we need the conditional expectation

$$g_{\nu,\Theta}^{(k,d)}((p,v),K) = \mathsf{E}\nu_k(\overset{d-k-1}{\underset{i=1}{\cap}} H(X_i)\cap H(p,v)\cap K)$$

for $(p,v) \in \mathbb{R}^1 \times \mathbf{S}_+^{d-1}$. In order to evaluate $g_{\nu,U}^{(k,d)}((p,v),K)$ we apply Crofton's formula (2.6) - in analogy to (3.2) - $d-k-1$ times (with $H(p,v)\cap K$ instead of K) leading to

$$g_{\nu,U}^{(k,d)}((p,v),K) = \Big(\frac{\kappa_{d-1}}{d\,\kappa_d}\Big)^{d-k}\,\frac{d!\,\kappa_d}{k!\,\kappa_k}\,\frac{V_{d-1}^{(d)}(H(p,v)\cap K)}{(b(K))^{d-k-1}} \tag{4.2}$$

for $k = 0, 1, \ldots, d-1$. As in the foregoing section we first calculate the asymptotic covariances

$$\tau_{kl}^{(d)}(\Theta, K) = \lim_{\varrho \to \infty} \mathsf{Cov}(\overline{\zeta}_{k,\varrho}^{(d)}(K), \overline{\zeta}_{l,\varrho}^{(d)}(K)) .$$

For brevity, put $\tau_{kl}^{(d)}(K) = \tau_{kl}^{(d)}(U, K)$ for $k, l = 0, 1, \ldots, d-1$.

Lemma 4.1 *Let $\Psi_{\lambda,\Theta}^{(d)}$ be a stationary PHP with non-degenerate $\Theta(\cdot)$. Then,*

$$\tau_{kl}^{(d)}(\Theta, K) = \frac{\big(\lambda\, b_\Theta(K)\big)^{2d-k-l-1}}{(d-k-1)!\,(d-l-1)!}\, \mathsf{E} g_{\nu,\Theta}^{(k,d)}(X_0, K)\, g_{\nu,\Theta}^{(l,d)}(X_0, K) \qquad (4.3)$$

for $k, l = 0, 1, \ldots, d-1$.
In case of a motion-invariant PHP $\Psi_{\lambda,U}^{(d)}$, we get with $\lambda_U^{(k,d)}$ from (2.10) that

$$\begin{aligned} \tau_{kl}^{(d)}(K) &= \lambda^{2d-k-l-1}\, \lambda_U^{(k,d)}\, \lambda_U^{(l,d)}\, (d-k)\,(d-l) \\ &\quad \times \int\limits_{\mathbb{S}_+^{d-1}} \int\limits_{\mathbf{R}^1} \big(V_{d-1}^{(d)}(H(p,v) \cap K)\big)^2 \, \mathrm{d}p\, U(\mathrm{d}v) . \end{aligned} \qquad (4.4)$$

Proof The proof of Lemma 4.1 resembles that of Lemma 3.1 almost verbatim. We have to replace the kernel function $\chi(H(X_1^{(\varrho)}) \cap \cdots \cap H(X_1^{(\varrho)}) \cap K_\varrho)$ by $\nu_k(H(X_1^{(\varrho)}) \cap \cdots \cap H(X_1^{(\varrho)}) \cap K_\varrho)$ and then to take into account the different scaling

$$\begin{aligned} &\mathsf{E}\nu_k\big(\bigcap_{p=1}^{d-k} H(X_{i_p}^{(\varrho)}) \cap K_\varrho\big)\, \nu_l\big(\bigcap_{q=d-k-j+1}^{2d-k-l-j} H(X_{i_q}^{(\varrho)}) \cap K_\varrho\big)\Big) \\ = \;& \varrho^{k+l}\, \mathsf{E}\Big(\nu_k\big(\bigcap_{p=1}^{d-k} H(X_p) \cap K\big)\, \nu_l\big(\bigcap_{q=d-k-j+1}^{2d-k-l-j} H(X_q) \cap K\big)\Big) . \end{aligned}$$

Therefore, the covariance $\mathsf{Cov}\big(\zeta_k^{(d)}(K_\varrho)\, \zeta_l^{(d)}(K_\varrho)\big)$ represents a polynomial of degree $2d-1$ in ϱ, so that after dividing by ϱ^{2d-1} we get the limit (4.3) whence, by (4.2), it follows (4.4) completing the proof of Lemma 4.1. □

Theorem 4.1 *Let $\Psi^{(d)}_{\lambda,\Theta}$ be a stationary PHP with non-degenerate $\Theta(\cdot)$. Then,*

$$\big(\overline{\zeta}^{(d)}_{k,\varrho}(K)\big)_{k=0}^{d-1} \xrightarrow[\varrho\to\infty]{\mathrm{d}} \mathcal{N}_d\big(o, T_d(\Theta,K)\big)\,, \tag{4.5}$$

where the entries of the covariance matrix $T_d(\Theta,K) = \big(\tau^{(d)}_{kl}(\Theta,K)\big)_{k,l=0}^{d-1}$ are given by the limits (4.3). *If $\Theta(\cdot)$ is the uniform distribution on $\mathbf{S}^{d-1}_+$, then*

$$\big(\overline{\zeta}^{(d)}_{k,\varrho}(K)\big)_{k=0}^{d-1} \xrightarrow[\varrho\to\infty]{\mathrm{d}} \mathcal{N}_d\big(o, T_d(K)\big)\,, \tag{4.6}$$

where $\lambda^{(k,d)}_{\Theta} = \lambda^{(k,d)}_{U}$ is taken from (2.10) *and $T_d(K) = \big(\tau^{(d)}_{kl}(K)\big)_{k,l=0}^{d-1}$ is determined by* (4.4).

Employing Lemma 4.1, the proof of the CLT (4.5) (and likewise of (4.6)) coincides step by step - up to evident changes - with the proof of the first assertion of Theorem 3.1. For this reason the details of the proof of Theorem 4.1 are left to the reader. Instead we make some remarks on a more explicit representation of the conditional expectation $g^{(k,d)}_{\nu,\Theta}((p,v),K)$ the derivation of which can be found in [11].

Remark Let $\Psi^{(d)}_{\lambda,\Theta}$ be a stationary, non-degenerate PHP in $\mathbb{R}^d$. Then

$$g^{(k,d)}_{\nu,\Theta}((p,v),K) = \frac{(d-k-1)!}{(\,b_\Theta(K)\,)^{d-k-1}}\, V^{(d-1)}_{d-k-1}(Z^v_\Theta)\, V^{(d)}_{d-1}(H(p,v)\cap K)$$

for $k = 0,1,\dots,d-1$ and all $(p,v)\in\mathbb{R}^1\times\mathbf{S}^{d-1}_+$ such that $H(p,v)\cap K\neq\emptyset$, where Z^v_Θ denotes the image of the associated zonoid Z_Θ under orthogonal projection onto $H(0,v)$. With the notation introduced in at the end of Section 2, the intrinsic volume $V^{(d-1)}_{d-k-1}(Z^v_\Theta)$ is seen to be equal to

$$\frac{1}{(d-k-1)!}\int\limits_{\mathbb{S}^{d-1}_+}\cdots\int\limits_{\mathbb{S}^{d-1}_+}\nabla_{d-k}(v_1,\dots,v_{d-k-1},v)\,\Theta(\mathrm{d}v_1)\cdots\Theta(\mathrm{d}v_{d-k-1})\,.$$

Consequently, the covariance $\tau^{(d)}_{kl}(\Theta,K)$ in (4.3) admits the representation

$$\lambda^{2d-k-l-1}\int\limits_{\mathbb{S}^{d-1}_+}\int\limits_{\mathbb{R}^1}\big(V^{(d)}_{d-1}(H(p,v)\cap K)\big)^2\,\mathrm{d}p\,V^{(d-1)}_{d-k-1}(Z^v_\Theta)\,V^{(d-1)}_{d-l-1}(Z^v_\Theta)\,\Theta(\mathrm{d}v)$$

for $k,l = 0,1,\ldots,d-1$. In view of $V_{d-1}^{(d)}(H(p,v)\cap K) = \nu_{d-1}(H(p,v)\cap K)$, this formula as well as the CLT (4.5) hold for any bounded $K \in \mathfrak{B}^d$ satisfying $\nu_d(K) > 0$.

5 Some properties of the matrices $\Sigma_d(K)$ and $T_d(K)$

In this section we study the algebraic properties of the covariance matrices $\Sigma_d(K)$ and $T_d(K)$ defined in Theorem 3.1 and 4.1, respectively. Whereas the linear hull spanned by the columns of $T_d(K)$ is a one-dimensional subspace in $\mathbb{R}^d$ for any $d \geq 2$, the rank of $\Sigma_d(K)$ equals d, i.e. $\det(\Sigma_d(K)) > 0$.

Theorem 5.1 *Let $\Psi_{\lambda,U}^{(d)}$ be a motion-invariant PHP in $\mathbb{R}^d$ with intensity $\lambda > 0$, and let K be a convex body in $\mathbb{R}^d$ containing B_ε^d for some $\varepsilon > 0$. Then,*

(i) *the rank of $T_d(K)$ equals 1 for any $d \geq 2$ and, for $0 \leq k < l \leq d-1$,*

$$\frac{\overline{\zeta}_{l,\varrho}^{(d)}(K)}{\sqrt{\tau_{ll}^{(d)}(K)}} - \frac{\overline{\zeta}_{k,\varrho}^{(d)}(K)}{\sqrt{\tau_{kk}^{(d)}(K)}} \xrightarrow[\varrho\to\infty]{\mathsf{P}} 0\,, \tag{5.1}$$

(ii) *and $\Sigma_d(K)$ has full rank d, i.e. the inverse $(\,\Sigma_d(K)\,)^{-1}$ exists.*

Proof Clearly, (4.6) implies that $\tau_{kl}^{(d)}(K) = \sqrt{\tau_{kk}^{(d)}(K)\,\tau_{ll}^{(d)}(K)}$ for $0 \leq k,l \leq d-1$. This means that each column of the matrix $T_d(K)$ is a multiple of the column vector $\big(\sqrt{\tau_{kk}^{(d)}(K)}\big)_{k=0}^{d-1}$ proving (i). The relation (5.1) even holds in the quadratic mean since the shape of the limiting covariances (4.6) implies that

$$\mathsf{E}\Big(\sqrt{\tau_{kk}^{(d)}(K)}\,\overline{\zeta}_{l,\varrho}^{(d)}(K) - \sqrt{\tau_{ll}^{(d)}(K)}\,\overline{\zeta}_{k,\varrho}^{(d)}(K)\Big)^2 \underset{\varrho\to\infty}{\longrightarrow} 0\,.$$

Going back to the very definition of positive definiteness und making use of (3.4), our assertion (ii) means that

$$\sum_{k,l=0}^{d-1} t_k\,t_l\,\sigma_{kl}^{(d)}(K) \;=\; \mathsf{E}\Big(\sum_{k=0}^{d-1} s_k\,V_{d-k-1}^{(d)}(H(X_0)\cap K)\Big)^2 > 0 \tag{5.2}$$

for any $(t_0, t_1, \dots, t_{d-1}) \in \mathbb{R}^d \setminus \{o\}$ with $s_k = \lambda^{d-k-1} \sqrt{\lambda\, b(K)}\, a_k^{(d)}\, t_k$ for $k = 0, 1, \dots, d-1$. Equivalently, the (non-negative) double sum in the foregoing line attains zero iff $t_0 = \cdots = t_{d-1} = 0$. Assuming that the right-hand side of (5.2) disappears, i.e.,

$$\sum_{k=0}^{d-1} s_k\, V_{d-k-1}^{(d)}(H(p,v) \cap K) \;=\; 0 \tag{5.3}$$

for $(\nu_1 \times U)$-almost every $(p, v) \in \mathbb{R}^1 \times \mathbf{S}_+^{d-1}$ satisfying $H(p,v) \cap K \neq \emptyset$, we will prove that $s_0 = \cdots = s_{d-1} = 0$.

Let $e \in \partial K$ be an *extreme point* of K. Applying the characterization of extreme points given in [22], Lemma 1.4.6, we find, for any $\delta > 0$, a closed halfspace $H_{q,u}^+ = \{\, H(p,u) : p \geq q \,\}$ with $q = q(e,\delta) \in \mathbb{R}^1$ and $u = u(e,\delta) \in \mathrm{S}_+^{d-1}$ depending on (e,δ), such that

$$d(e,\delta) := \inf\{\|e-x\| : x \in H(q,u)\} > 0 \quad \text{and} \quad K \cap H_{q,u}^+ \subset B_\delta^d(e) := B_\delta^d + e\,.$$

Since $B_\varepsilon^d \subseteq K$, that part of the convex hull of $\{e\}$ and B_ε^d contained in the halfspace $H_{q,u}^+$ also belongs to $B_\delta^d(e)$. Therefore, by evident continuity arguments (shifting $H(q,u)$ closer to e and moving q slightly) we find an open interval $(\eta_1, \eta_2) \subset [q, q + d(e,\delta)]$ and a sufficiently small η-neighbourhood $W_\eta(q) := B_\eta^d(u) \cap \mathbf{S}_+^{d-1}$ of $u \in \mathbf{S}_+^{d-1}$ such that $V_{d-1}^{(d)}(H(p,v) \cap K) > 0$ and $V_1^{(d)}(H(p,v) \cap K) \leq V_1^{(d)}(B_\delta^d) = \delta\, d\kappa_d/\kappa_{d-1}$ for all $(p,v) \in (\eta_1, \eta_2) \times W_\eta(q)$. Note that the latter set has positive $(\nu_1 \times U)$-measure and $\delta > 0$ can be chosen arbitrarily small. Now we use a well-known known consequence of the Alexandrov-Fenchel inequality, see [22], Chapt. 6.4, which can be rewritten in terms of the intrinsic volumes $V_k^{(d)}(\cdot)$ as follows:

$$V_k^{(d)}(\cdot) \leq \left(V_j^{(d)}(\cdot)\right)^{k/j} \binom{d}{k} \frac{\kappa_d}{\kappa_{d-k}} \left(\binom{d}{j} \frac{\kappa_d}{\kappa_{d-j}}\right)^{-k/j} \tag{5.4}$$

for $0 \leq j \leq k \leq d-1$.

We first show that $s_{d-1} = 0$ in (5.3). Together with $V_0^{(d)}(H(p,v) \cap K) = 1$ it follows from (5.3) that

$$|s_{d-1}| \;\leq\; \sum_{k=1}^{d-1} |s_{d-k-1}|\; V_k^{(d)}(H(p,v) \cap K)\,. \tag{5.5}$$

Inequality (5.4) for $j = 1$ applied to $H(p,v) \cap K$ for $(p,v) \in (\eta_1, \eta_2) \times W_\eta(q)$ yields

$$V_k^{(d)}(H(p,v) \cap K) \leq \frac{\delta^k \, \kappa_d}{\kappa_{d-k}} \binom{d}{k} \quad \text{for} \quad 1 \leq k \leq d-1 \,. \tag{5.6}$$

Inserting these estimates on the right-hand side of (5.5) and letting $\delta \downarrow 0$ reveal that only $s_{d-1} = 0$ is possible. In the next step, we assume that $s_{d-1} = \cdots = s_{d-j} = 0$ for some $j \in \{1, \ldots, d-2\}$ so that then (5.3) implies

$$|s_{d-j-1}| \leq \sum_{k=j+1}^{d-1} |s_{d-k-1}| \, \frac{V_k^{(d)}(H(p,v) \cap K)}{V_j^{(d)}(H(p,v) \cap K)} \,. \tag{5.7}$$

Combining (5.4) with (5.5) (the latter for $k = j$) leads to the estimate

$$\frac{V_k^{(d)}(H(p,v) \cap K)}{V_j^{(d)}(H(p,v) \cap K)} \leq \delta^{k-j} \, \frac{j! \, (d-j)! \, \kappa_{d-j}}{k! \, (d-k)! \, \kappa_{d-k}} \quad \text{for} \quad (p,v) \in (\eta_1, \eta_2) \times W_\eta(q) \,,$$

which together with (5.7) enables us to conclude that $s_{d-j-1} = 0$. This proves (ii) and completes the proof of Theorem 5.1. □

6 Special cases and some inequalities

In this final section we derive some estimates and discuss extremal properties of the ovoid functionals

$$J_k^{(d)}(K) = \int\limits_{\mathrm{S}_+^{d-1}} \int\limits_{\mathbf{R}^1} \left(V_k^{(d)}(H(p,v) \cap K)\right)^2 \mathrm{d}p \, U(\mathrm{d}v) \quad , \quad k = 0, 1, \ldots, d-1 \,,$$

which are motion-invariant,non-decreasing and continuous, but not additive on the family of convex bodies in $\mathbb{R}^d$. A variant of the Blaschke–Petkantschin formula, see Theorem 8.6.4 in [23], allows to express $J_{d-1}^{(d)}(K)$ as dth–order *chord–power integral* of K. More precisely, it holds

$$J_{d-1}^{(d)}(K) = \frac{\kappa_{d-1}}{d} \int\limits_{A(d,1)} \left(V_1^{(d)}(K \cap g)\right)^d \mu_1^{(d)}(\mathrm{d}g) = \frac{(d-1) \, \kappa_{d-1}}{d \, \kappa_d} \int\limits_K \int\limits_K \frac{\mathrm{d}x \, \mathrm{d}y}{\|x-y\|} \,,$$

where $\mu_1^{(d)}(\cdot)$ denotes the (normalized) Haar measure w.r.t. rigid motions on the space $A(d,1)$ of all affine one-dimensional linear subspaces of $\mathbb{R}^d$. The second equality sign is seen from Theorem 7.2.7 in [23].

Next we provide closed expressions of $J_k^{(d)}(K)$ for balls B_r^d in any dimension $d \geq 2$, ellipses $E_{a,b} = \{(x_1,x_2) \in \mathbb{R}^2 : x_1^2/a^2 + x_2^2/b^2 \leq 1\}$ with numerical excentricity $\varepsilon = \sqrt{1-b^2/a^2} \in [0,1)$ (i.e. $a \geq b$) and planar rectangles $R_{a,b} = [-a,a] \times [-b,b]$.

Lemma 6.1 *For $k = 0,1,\ldots,d-1$,*

$$J_k^{(d)}(B_r^d) \;=\; \Big(\frac{(d-1)!\,\kappa_{d-1}}{(d-k-1)!\,\kappa_{d-k-1}}\Big)^2 \frac{(2\,r)^{2k+1}}{(2k+1)!}\,. \tag{6.1}$$

$$J_1^{(2)}(E_{a,b}) \;=\; \frac{32\,a\,b^2}{3\,\pi} \int_0^{\pi/2} \frac{\mathrm{d}\varphi}{\sqrt{1-\varepsilon^2\,\sin^2\varphi}}\,, \tag{6.2}$$

where the integral on the right-hand side is just the 'complete elliptic integral of first kind in Legendre form' $\mathrm{F}\big(\frac{\pi}{2},\varepsilon\big)$. Furthermore,

$$J_1^{(2)}(R_{a,b}) \;=\; \frac{16}{3\,\pi}\,\Big(\,I(a,b) + I(b,a)\,\Big)\;, \tag{6.3}$$

where

$$I(a,b) \;=\; 3\,a\,b^2\,\log\Big(\,\frac{\sqrt{a^2+b^2}+a}{b}\,\Big) - b^2\,\big(\,\sqrt{a^2+b^2}-b\,\big)\,.$$

The formulae (6.1) were derived in [9]. To calculate the functionals $J_1^{(2)}(E_{a,b})$ and $J_1^{(2)}(R_{a,b})$ (which are needed in cases as illustrated in Figure 1) one has to determine the lengths of all chords through $E_{a,b}$ and $R_{a,b}$, respectively. We omit these straightforward, but lengthy computations of integrals leading to (6.2) resp. (6.3). Interested readers can find the details in *http://www.math.uni-augsburg.de/stochastik/heinrich/papers/ cltmotinvphp.pdf*

In the particular case $a = b$ relation (6.2) coincides with (6.1) for $d = 2, k = 1, r = a$ and (6.3) results in

$$J_1^{(2)}(R_{a,a}) = \frac{32\,a^3}{3\,\pi}\,\Big(\,3\log(1+\sqrt{2}) + 1 - \sqrt{2}\,\Big) \approx 7.5712\,a^3\,.$$

Chord-power integrals and chord-length distributions play an important role in integral geometry, see [25], [20] and [23] and references therein. Using the Theorems 8.6.5 and 8.6.6 (due to E. B. Pfiefer) in [23] we deduce from the above representaion of $J_{d-1}^{(d)}(K)$ as dth–order chord–power integral the inequality

$$J_{d-1}^{(d)}(K) \le \frac{\big((d-1)!\,\kappa_{d-1}\big)^2}{(2d-1)!}\,\Big(\frac{2^d\,\nu_d(K)}{\kappa_d}\Big)^{(2d-1)/d} \tag{6.4}$$

for any convex body K in $\mathbb{R}^d$, where equality holds iff $K = B_r^d$, see [21] for related inequalities. Having in mind the variances (3.4) and (4.4) for $k = l = 1, d = 2$, it is intuitively clear that, for fixed area $\nu_2(K)$, the functional $J_1^{(2)}(K)$ may take arbitrarily small values when K becomes a long and thin strip. For example, fixing the area $A = \pi\,a\,b$ of the family of ellipses $E_{a,b}$ and setting $b = A/\pi\,a$, we get

$$J_1^{(2)}(E_{a,b}) = \frac{32\,A^2}{3\,\pi^3\,a}\,\mathrm{F}\Big(\frac{\pi}{2}, \sqrt{1 - A^2/\pi^2\,a^4}\Big) \underset{a\to\infty}{\longrightarrow} 0\,.$$

This means that long and thin planar convex discs K diminish the variance of $\overline{\Psi}_{0,\varrho}^{(d)}(K)$. Likewise, for fixed $\nu_d(K)$, the functional $J_{d-1}^{(d)}(K)$ can be minimized to zero in each dimension $d \ge 2$. In contrast to this, the functional $J_1^{(3)}(K)$ is bounded from below by $\pi\,\nu_3(K)$. This is rapidly seen by applying the isoperimetric inequality $\big(V_1^{(2)}(H(p,v)\cap K)\big)^2 \ge \pi\,V_2^{(2)}(H(p,v)\cap K)$, see [22], p. 323, for all planar convex bodies $H(p,v)\cap K$. Together with Crofton's formula (2.6) for $d = 3, k = 2$ we obtain

$$J_1^{(3)}(K) \ge \pi \int\limits_{\mathbb{S}_+^{d-1}} \int\limits_{\mathbf{R}^1} V_2^{(3)}(H(p,v)\cap K)\,\mathrm{d}p\,U(\mathrm{d}v) = \pi\,\nu_3(K)\,,$$

where the equality holds iff $K = B_r^3$.

To the best of the author's knowledge, sharp upper bounds of $J_k^{(d)}(K)$ $(2 \le k \le d-2,\, d \ge 4)$ in terms of intrinsic volumes of K seem to be unknown so far.

Acknowledgement

I wish to thank Dr. Ute Hahn (at present University of Aarhus) for simulating the Poisson line process in Figure 1.

References

[1] Baryshnikov, Yu. and Yukich, J. E. (2005). Gaussian limits for random measures in geometric probability. *Ann. Appl. Prob.* **15**, 213–253.

[2] Karr, A. F. (1993). *Probability.* Springer, New York.

[3] Koroljuk, V. S. and Borovskich, Yu. V. (1994). *Theory of U-Statistics.* Kluwer Academic Publishers, Dordrecht.

[4] Daley, D. J. and Vere-Jones, D. (1988). *An Introduction to the Theory of Point Processes.* Springer, New York.

[5] Heinrich, L. (1994). Normal approximation for some mean–value estimates of absolutely regular tessellations. *Math. Meth. Statist.* **3**, 1–24.

[6] Heinrich, L. and Molchanov, I. S. (1999). CLT for a class of random measures associated with germ–grain models. *Adv. Appl. Prob.* **31**, 283–314.

[7] Heinrich, L. and Muche, L. (2008). Second–order properties of the point process of nodes in a stationary Voronoi tessellation. *Math. Nachr.* **281**, 350–375.

[8] Heinrich, L., Schmidt, H. and Schmidt, V. (2005). Limit theorems for stationary tessellations with random inner cell stuctures. *Adv. Appl. Prob. (SGSA)* **37**, 25–47.

[9] Heinrich, L., Schmidt, H. and Schmidt, V. (2006). CLTs for Poisson hyperplane tessellations. *Ann. Appl. Prob.* **16**, 919–950.

[10] Heinrich, L., Schmidt, H. and Schmidt, V. (2007). Limit theorems for functionals on the facets of stationary random tessellations. *Bernoulli* **13**, 868–891.

[11] Heinrich, L. and Schertz, S. (2009). On asymptotic normality and asymptotic covariance matrices of stationary Poisson hyperplane processes. Report Inst. of Mathematics, Univ. Augsburg (in preparation)

[12] Matheron, G. (1975). *Random Sets and Integral Geometry.* J. Wiley & Sons, New York.

[13] Møller, J. (1989). Random tessellations in $\mathbb{R}^d$. *Adv. Appl. Prob.* **21**, 37–73.

[14] Møller, J. (1994). *Lectures on Random Voronoi Tessellations.* Lecture Notes in Statistics **87**, Springer, New York.

[15] Ohser, J. and Mücklich, F. (2000). *Statistical analysis of microstructures in material science.* J.Wiley & Sons, Chichester.

[16] Okabe, A., Boots, B., Sugihara, K. and Chiu, S. N. (2000). *Spatial Tessellations.* 2nd ed., J.Wiley & Sons, Chichester.

[17] Paroux, K. (1998). Quelques théorèmes centraux limites pour les processus poissoniens de droites dans le plan. *Adv. Appl. Prob.* **30**, 640–656.

[18] Penrose, M. D. and Yukich, J. E. (2001). CLTs for some graphs in computational geometry. *Ann. Appl. Prob.* **11**, 1005–1041.

[19] Penrose, M. D. (2007). Gaussian limits for random geometric measures. *Elect. J. Prob.* **12**, 989–1035.

[20] Santaló, L. A. (1976). *Integral Geometry and Geometric Probability.* Addison-Wesley, Reading (Mass.).

[21] Schneider, R. (1985). Inequalities for random flats meeting a convex body. *J. Appl. Prob.* **22**, 710–716.

[22] Schneider, R. (1993). *Convex Bodies: The Brunn-Minkowski Theory.* Cambridge University Press, Cambridge.

[23] Schneider, R. and Weil, W. (2008). *Stochastic and Integral Geometry.* Springer, Berlin.

[24] Schneider, R. (2003). Nonstationary Poisson hyperplanes and their induced tessellations. *Adv. Appl. Prob. (SGSA)* **35**, 139–158.

[25] Stoka, M. (1968). *Géométrie Intégrale.* Gauthier-Villars, Paris.

[26] Stoyan, D., Kendall, W. S. and Mecke, J. (1995). *Stochastic Geometry and its Applications.* 2nd ed., J. Wiley & Sons, Chichester.

Institute of Mathematics
University of Augsburg
D-86135 Augsburg, Germany
heinrich@math.uni-augsburg.de

RENDICONTI DEL CIRCOLO MATEMATICO DI PALERMO
Serie II, Suppl. 81 (2009), pp. 213-222

On Lower Bounds of Second-Order Chord Power Integrals of Convex Discs

LOTHAR HEINRICH

Abstract

For planar convex bodies K with positive area $A(K)$, boundary length $L(\partial K)$ and second-order chord power integral $I_2(K)$, we study the ratio $L(\partial K)\, I_2(K)/A^2(K)$ and give reasons supporting the conjecture that its uniform lower bound is $32/3$ attained exactly for circles. In particular, using the Ambartzumian-Pleijel representation of $I_2(K)$ we derive formulas for $I_2(K)$ in case of general triangles, rectangles, and regular N-gons. In these cases and for ellipses we can prove this inequality. A related conjecture is formulated for the class of convex N-gons which exhibits a strengthening of the isoperimetric inequality as well as of Carleman's inequality for convex N-gons. An extension to higher dimensions is discussed at the end of the paper.

Keywords : Poisson line process, isoperimetric inequality, Carleman's inequality, chord length distribution, regular N-gons, ellipses

MSC 2000: Primary 52A40 60G05 Secondary 52A07 52A22

1 Introduction - Posing the Problem

We consider a motion-invariant Poisson line tessellation $T_\lambda = \bigcup_{i\in\mathbb{Z}^1} g(P_i, \Phi_i)$ with line density λ in an increasing planar region ϱK with $1 \le \varrho \uparrow \infty$, where K is some fixed convex disc containing $\mathbf{o}$ as inner point. Here, $g(p,\varphi)$ denotes an unoriented straight line in a Cartesian x_1x_2-coordinate system with normal unit vector $(\cos\varphi, \sin\varphi)$ directed in the upper half-plane and signed perpendicular distance $p \in \mathbb{R}^1$ from the origin $\mathbf{o}$, formally written

$$g(p,\varphi) = \{\, (x_1,x_2) \in \mathbb{R}^2 : x_1\cos\varphi + x_2 \sin\varphi = p \,\} \quad , \quad \varphi \in [0,\pi) \quad , \quad p \in \mathbb{R}^1 \, .$$

T_λ is driven by an independently marked stationary Poisson process $\Pi_\lambda = \{[P_i, \Phi_i] : i \in \mathbb{Z}^1\}$ on the real line $\mathbb{R}^1$ with intensity λ and typical mark Φ_0 uniformly distributed on $[0,\pi)$, see Chapt. 3 in [5] for details.

Put

$$X_\varrho = \sqrt{\varrho}\,\Big(\,\frac{\Psi_L(\varrho\,K)}{L(\partial(\varrho\,K))} - \frac{\lambda}{\pi}\,\Big) \;\text{ and }\; Y_\varrho = \sqrt{\varrho}\,\Big(\,\frac{\Psi_V(\varrho\,K)}{A(\varrho\,K)} - \frac{\lambda^2}{\pi}\,\Big)\,,$$

where $\Psi_L(\varrho\,K)$ resp. $\Psi_V(\varrho\,K)$ denotes the total number of lines of T_λ hitting $\varrho\,K$ resp. the total number of line crossings generated by T_λ in $\varrho\,K$. In [3] we have proved the following bivariate central limit theorem :

$$\begin{pmatrix} X_\varrho \\ Y_\varrho \end{pmatrix} \underset{\varrho\to\infty}{\Longrightarrow} \mathcal{N}\left(\begin{pmatrix} 0 \\ 0 \end{pmatrix}, \begin{pmatrix} \frac{\lambda}{\pi\,L(\partial K)} & \frac{2\,\lambda^2}{\pi\,L(\partial K)} \\ \frac{2\,\lambda^2}{\pi\,L(\partial K)} & \frac{4\,\lambda^3}{\pi^3}\,\frac{I_2(K)}{A^2(K)} \end{pmatrix}\right) \tag{1}$$

with a strictly positive-definite covariance matrix in the Gaussian limit (1) implying that

$$\frac{I_2(K)}{A^2(K)} > \frac{\pi^2}{L(\partial K)} \approx \frac{9.8696}{L(\partial K)}\,. \tag{2}$$

Here, for $n = 0, 1, 2, \ldots,$

$$I_n(K) = \int_0^\pi \int_{\mathbb{R}^1} L^n(K \cap g(p,\varphi))\,\mathrm{d}p\,\mathrm{d}\varphi$$

denotes the nth-order *chord power integral* (briefly: CPI) of K.

From integral geometry it well-known, see [4] or [5], that $I_0(K) = L(\partial K)\,,$

$$I_1(K) = \pi\,A(K) \;\;,\;\; I_2(K) = \int_K \int_K \frac{\mathrm{d}x\,\mathrm{d}y}{\|y-x\|} \;\;,\;\; I_3(K) = 3\,A^2(K)\,.$$

Note that the CPIs $I_n(K)\,,\ n \geq 0\,,$ are connected with some unique *chord length distribution function* $C_K(x)\,,\ x \geq 0\,,$ such that the nth moment of C_K equals the ratio $I_n(K)/I_0(K)\,.$ However, C_K does not always determine completely the shape of the convex disc $K\,,$ as shown first by C.L. Mallows and J.M.C. Clark in 1970, see [4]. Nevertheless, in image analysis and other fields of application C_K and even only the first four CPIs $I_0(K), ..., I_4(K)$ are used to 'characterize' the shape of convex particles.

Further, we mention that the ratio $I_2(K)/A^2(K)$ can be interpreted as mean reciprocal Euclidean distance $\mathsf{E}\|P_K - Q_K\|^{-1}$ of two independent and

uniformly distributed points P_K and Q_K in K. This could be useful for computer-based simulations of the second-order CPI $I_2(K)$.

From the view point of *optimal experimental design* it is the aim to minimize the limiting variance of Y_ϱ in (1) given e.g. the perimeter $L(\partial K)$ or other side condition on K. In other words, we have to find the smallest possible ratio $I_2(K)/A^2(K)$ and the minimizing K, when $L(\partial K)$ is fixed.

In the rest of this paper we discuss several special cases which motivate in particular the lower estimate in

Conjecture I For any convex discs K with inner point the inclusion

$$\frac{10.6667}{L(\partial K)} \approx \frac{32}{3\,L(\partial K)} \le \frac{I_2(K)}{A^2(K)} \le \frac{16}{3\,\sqrt{\pi\,A(K)}} \tag{3}$$

holds which establishes a slight strengthening of the well-known isoperimetric inequality, see e.g. [4], with equality on both sides if and only if K is a circle with diameter $L(\partial K)/\pi$.

Remark 1 The upper bound in (3) is a celebrated result by T. Carleman published already in 1919, see Thm. 8.6.6 in [5] for generalizations to higher-order CPIs in any dimension. A hint to the lower bound is given in [1].

2 Second-Order CPIs for Some Convex Discs

For any circular disc $B_r = \{\, x \in \mathbb{R}^2 : \|x\| \le r \,\}$ with radius $r > 0$, it is a simple exercise to confirm that $I_2(B_r) = 16\,\pi\,r^3/3$ and together with $L(\partial B_r) = 2\,\pi\,r$, $A(B_r) = \pi\,r^2$ we see that lower and upper bound in (3) coincide.

For an ellipse $E_{ab} = \{\, (x_1, x_2) \in \mathbb{R}^2 : b^2\,x_1^2 + a^2\,x_2^2 \le a^2\,b^2 \,\}$ with semi-axis a, b satisfying $a \ge b > 0$ and numerical excentricity $\varepsilon = \sqrt{a^2 - b^2}/a$, we arrive after lengthy computations, see [3], at

$$I_2(E_{ab}) = \frac{32\,a\,b^2}{3} \int\limits_0^{\frac{\pi}{2}} \frac{\mathrm{d}\varphi}{\sqrt{1 - \varepsilon^2\,\sin^2\varphi}} = \frac{32\,a\,b^2}{3}\,\mathsf{F}(\frac{\pi}{2}, \varepsilon)\,,$$

where $\mathsf{F}(\frac{\pi}{2}, \varepsilon)$ is Legendre's notation for an elliptic integral of first kind. On the other hand, using the elliptic integral of second kind $\mathsf{E}(\frac{\pi}{2}, \varepsilon)$ we can

express the perimeter $L(\partial E_{ab})$ by

$$L(\partial E_{ab}) = 4\,a\,\mathsf{E}(\frac{\pi}{2},\varepsilon) = 4\,a\int\limits_0^{\frac{\pi}{2}} \sqrt{1-\varepsilon^2\,\sin^2\varphi}\,\mathrm{d}\varphi\,.$$

By applying the Cauchy-Schwarz inequality and the well-known area formula $A(E_{ab}) = \pi\,a\,b$ we obtain that

$$\begin{aligned}\frac{32}{3} &= \frac{32}{3}\left(\frac{2}{\pi}\int\limits_0^{\frac{\pi}{2}} \frac{(1-\varepsilon^2\,\sin^2\varphi)^{1/4}}{(1-\varepsilon^2\,\sin^2\varphi)^{1/4}}\,\mathrm{d}\varphi\right)^2 \;\le\; \frac{128}{3\,\pi^2}\,\mathsf{E}(\frac{\pi}{2},\varepsilon)\,\mathsf{F}(\frac{\pi}{2},\varepsilon)\\ &= \frac{128}{\pi^2}\,\frac{L(\partial E_{ab})}{4\,a}\,\frac{3\,I_2(E_{ab})}{32\,a\,b^2} = \frac{L(\partial E_{ab})\,I_2(E_{ab})}{A^2(E_{ab})}\,,\end{aligned}$$

where '=' holds iff $\varepsilon = 0$. Thus, we have proved

Theorem 1 *For any ellipse E_{ab} both inequalities in (3) hold and equality on each side is attained iff $a = b$.*

The computation of CPIs for a rectangle R_{ab} with sides a and b is an immediate consequence of a more general formula for convex $N-$gons P_N which will be derived in the next Sect. 3. We get the formula

$$I_2(R_{ab}) = \frac{2\,(\,a^3+b^3\,) - 8\,(\sqrt{a^2+b^2}\,)^3}{3} + 4\,a\,b^2\,I\Big(\frac{a}{b}\Big) + 4\,a^2\,b\,I\Big(\frac{b}{a}\Big)\,,$$

where

$$I(x) = \int\limits_0^x \sqrt{t^2+1}\,\mathrm{d}t = \frac{1}{2}\Big[\,x\,\sqrt{x^2+1} + \log\Big(\,x+\sqrt{x^2+1}\,\Big)\Big]\,. \qquad (4)$$

Note that $I(-x) = I(x)$, $I'(x) > 0$, $I''(x) > 0$ and $I'''(x) > 0$ for $x > 0$.

Theorem 2 *Given the semiperimeter $s = a + b$, the ratio $I_2(R_{ab})/a^2\,b^2$ takes its minimum for the square with side length $s/2$, i.e.*

$$\frac{I_2(R_{ab})}{A^2(R_{ab})} \ge \frac{8}{3\,s}\Big[\,3\,\log(\,1+\sqrt{2}\,) + 1 - \sqrt{2}\,\Big] \approx \frac{11.8928}{L(\partial R_{ab})}\,. \qquad (5)$$

Proof After tedious calculations we find that the relation (5) is equivalent to $3(a+b)\,I_2(R_{ab})/(2\,a^2\,b^2) = f(a/(a+b)) + f(b/(a+b)) \geq 2\,f(1/2)$, where

$$f(x) = \frac{3}{x}\,\log\frac{x+\sqrt{1-2\,x\,(1-x)}}{1-x} - \frac{1}{1-x+\sqrt{1-2\,x\,(1-x)}}$$

for $0 < x < 1$.
In fact, it can be shown that $f''(x) > 0$ for $0 < x < 1$, i.e., $f(\cdot)$ is strictly convex so that $(\,f(x)+f(1-x)\,)/2 \geq f(1/2) = 2\,(\,3\,\log(\,1+\sqrt{2}\,)+1-\sqrt{2}\,)$ exhibits a special case of Jensen's inequality. □

Finally, we consider an arbitrary triangle Δ_{abc} with side-lengths a, b and c with semiperimeter $s = (a+b+c)/2$ such that each side is shorter than the sum of the other two sides. We use the below formula (6) to rewrite $I_2(K_3)$ in terms of the function (4) and express the trigonometric functions of the angles by the sides a, b, c, and s. Summarizing all expession leads directly to the comparatively simple formula

$$\frac{I_2(\Delta_{abc})}{A^2(\Delta_{abc})} = \frac{4}{3}\,\left[\,\frac{1}{a}\,\log\Big(\,\frac{s}{s-a}\,\Big) + \frac{1}{b}\,\log\Big(\,\frac{s}{s-b}\,\Big) + \frac{1}{c}\,\log\Big(\,\frac{s}{s-c}\,\Big)\,\right]\,,$$

where Heron's formula gives $A(\Delta_{abc}) = \sqrt{s\,(s-a)\,(s-b)\,(s-c)}$.

Theorem 3 *Among all planar triangles with perimeter $2\,s = a+b+c$, the ratio $I_2(\Delta_{abc})/A^2(\Delta_{abc})$ attains its minimum for the equilateral triangle, i.e.* for $a = b = c = 2\,s/3$.

Proof Using the (strict) convexity of the function

$$g(x) = \frac{1}{x}\,\log\Big(\,\frac{s}{s-x}\,\Big) = \frac{1}{s}\,\sum_{k=1}^{\infty}\frac{1}{k}\,\Big(\frac{x}{s}\Big)^{k-1} \quad \text{for} \quad 0 < x < s\,,$$

we may apply Jensen's inequality yielding

$$\frac{I_2(\Delta_{abc})}{A^2(\Delta_{abc})} = \frac{4}{3}\,\Big(\,g(a)+g(b)+g(c)\,\Big) \geq 4\,g\Big(\,\frac{a+b+c}{3}\,\Big) = \frac{12\,\log 3}{L(\partial\Delta_{abc})}$$

with equality iff $a = b = c = 2s/3$. □

3 Higher-Order CPIs for Convex Polygons

Following the ideas of A. Pleijel (1956) and R.V. Ambartzumian (1970-74), see references in [4], we can express $I_n(K)$ as double integral over the boundary ∂K. Combining two formulas for $I_n(K)$ given in Chapt. I.3.5 [4], p. 43, we obtain

$$I_n(K) = -\frac{2\,(n-1)}{n} \int\limits_{\partial K} \int\limits_{\partial K} \|s_1 - s_2\|^{n-1} \cos(\theta_1 + \theta_2)\, \mathrm{d}s_1 \wedge \mathrm{d}s_2$$

for $n \geq 1$, where $\theta_1 = \theta_1(s_1)$ (resp. $\theta_2 = \theta_2(s_2)$) denotes the angle between the tangent at s_1 (resp. s_2) on ∂K and the chord joining s_1 and s_2.

Now, let $K = K_N$ be a convex polygon having N vertices $A_1, \ldots, A_N$ (anti-clockwise) with inner angle α_i at A_i and edges $L_i = \overline{A_i\, A_{i+1}}$, where $A_{N+i} = A_i$, $L_{N+i} = L_i$ and $\alpha_{N+i} = \alpha_i$ for $i = 1, \ldots, N$. Obviously, $\partial K_N = L_1 \cup \cdots \cup L_N$. If $s_1 \in L_i \setminus \{A_{i+1}\}$ and $s_2 \in L_{i+j} \setminus \{A_{i+j}\}$, then we get a $(j+2)-$gon with vertices $s_1, A_{i+1}, \ldots, A_{i+j}, s_2$ such that $\theta_1 + \theta_2 + \alpha_{i+1} + \cdots + \alpha_{i+j} = j\,\pi$ implying $\cos(\theta_1 + \theta_2) = (-1)^j \cos(\alpha_{i+1} + \cdots + \alpha_{i+j})$. After some simple rearrangement we find that nth-order CPI $I_n(K_N)$ equals

$$\sum_{i=1}^{N} \sum_{j=1}^{N-1} (-1)^{j+1} \cos\Big(\sum_{k=1}^{j} \alpha_{i+k}\Big)\, I_n(L_i, L_{i+j}) - \frac{4\,(n-1)}{n^2\,(n+1)} \sum_{i=1}^{N} |L_i|^{n+1}$$

$$= 2 \sum_{j=1}^{\lfloor \frac{N-1}{2} \rfloor} (-1)^{j+1} \sum_{i=1}^{N} \cos\Big(\sum_{k=1}^{j} \alpha_{i+k}\Big)\, I_n(L_i, L_{i+j}) - \frac{4\,(n-1)}{n^2\,(n+1)} \sum_{i=1}^{N} |L_i|^{n+1}$$

$$-\big(1 + (-1)^N\big)\,(-1)^{N/2} \sum_{i=1}^{N/2} \cos\Big(\sum_{k=1}^{N/2} \alpha_{i+k}\Big)\, I_n(L_i, L_{i+\frac{N}{2}})\,, \qquad (6)$$

where $|L_i| = \|A_i - A_{i+1}\|$ and

$$I_n(L_i, L_{i+j}) = \frac{2\,(n-1)}{n} \int\limits_{L_i} \int\limits_{L_{i+j}} \|s_1 - s_2\|^{n-1}\, \mathrm{d}s_1 \wedge \mathrm{d}s_2\,.$$

We will apply the previous formula only for $n = 2$ so that it remains to compute the integral $I_2(\overline{AB}, \overline{CD})$ for a convex quadrangle $\square ABCD$:

$$J_{\varepsilon_1,\varepsilon_2}(a,c,e) = \int_0^a \int_0^c \| A - C + \frac{s}{a}(B-A) - \frac{t}{c}(D-C) \| \, \mathrm{d}t \, \mathrm{d}s$$

$$= \int_0^a \int_0^c \sqrt{s^2 + t^2 + e^2 - 2\,s\,e\,\cos\varepsilon_1 - 2\,t\,e\,\cos\varepsilon_2 + 2\,s\,t\,\cos(\varepsilon_2 - \varepsilon_1)}\,\mathrm{d}t\,\mathrm{d}s\,,$$

where $a = \|A-B\|$, $c = \|C-D\|$, $e = \|A-C\|$, $\varepsilon_1 = \angle(CAB)$, and $\varepsilon_2 = \angle(ACD)$ determine $\square ABCD$. Remarkably, the double integral $J_{\varepsilon_1,\varepsilon_2}(a,c,e)$ can be expressed as closed formula in terms of the function (4). The details of the rather lengthy computation are omitted. We obtain that, for $\varepsilon_1 \neq \varepsilon_2$,

$J_{\varepsilon_1,\varepsilon_2}(a,c,e) =$

$$q(\varepsilon_1,0)\Big[I\Big(\frac{e\,\cos\varepsilon_1 - a}{e\,\sin\varepsilon_1}\Big) - I\big(\cot\varepsilon_1\big)\Big] - q(\varepsilon_2,0)\Big[I\Big(\frac{e\,\cos\varepsilon_2 - c}{e\,\sin\varepsilon_2}\Big) - I\big(\cot\varepsilon_2\big)\Big]$$

$$+ q(\varepsilon_1,c)\Big[I\Big(\frac{e\,\cos\varepsilon_1 - c\,\cos(\varepsilon_2-\varepsilon_1)}{e\,\sin\varepsilon_1 + c\,\sin(\varepsilon_2-\varepsilon_1)}\Big) - I\Big(\frac{e\,\cos\varepsilon_1 - c\,\cos(\varepsilon_2-\varepsilon_1) - a}{e\,\sin\varepsilon_1 + c\,\sin(\varepsilon_2-\varepsilon_1)}\Big)\Big]$$

$$- q(\varepsilon_2,-a)\Big[I\Big(\frac{e\,\cos\varepsilon_2 - a\,\cos(\varepsilon_2-\varepsilon_1)}{e\,\sin\varepsilon_2 - a\,\sin(\varepsilon_2-\varepsilon_1)}\Big) - I\Big(\frac{e\,\cos\varepsilon_2 - a\,\cos(\varepsilon_2-\varepsilon_1) - c}{e\,\sin\varepsilon_2 - a\,\sin(\varepsilon_2-\varepsilon_1)}\Big)\Big]$$

with $q(\varepsilon,x) = (\,e\,\sin\varepsilon + x\,\sin(\varepsilon_2 - e_1)\,)^3/3\,\sin(\varepsilon_2 - e_1)$ and, for $\varepsilon_1 = \varepsilon_2$, $J_{\varepsilon,\varepsilon}(a,c,e) =$

$$\frac{e^3\,\sin^3\varepsilon}{3}\Big[J\Big(\frac{a+c-e\,\cos\varepsilon}{e\,\sin\varepsilon}\Big) - J\Big(\frac{c-e\,\cos\varepsilon}{e\,\sin\varepsilon}\Big) - J\Big(\frac{a-e\,\cos\varepsilon}{e\,\sin\varepsilon}\Big) + J\big(\cot\varepsilon\big)\Big]$$

with $J(x) = 3\,x\,I(x) - (\sqrt{x^2+1})^3$. If $\varepsilon_1 = 0$, i.e. $e = a$ and $C \equiv B$, then $J_{0,\varepsilon}(a,c,a) =$

$$\frac{a^3\,\sin^2\varepsilon}{3}\Big[I\Big(\frac{c-a\,\cos\varepsilon}{a\,\sin\varepsilon}\Big) + I\big(\cot\varepsilon\big)\Big] + \frac{c^3\,\sin^2\varepsilon}{3}\Big[I\Big(\frac{a-c\,\cos\varepsilon}{c\,\sin\varepsilon}\Big) + I\big(\cot\varepsilon\big)\Big].$$

Inserting $J_{\varepsilon,\varepsilon}(a,a,e)$ resp. $J_{0,\varepsilon}(a,c,a)$ in (6) for $N = 4$ resp. $N = 3$ with adequately chosen angles expressed in terms of the sides leads to the formulas for $I_2(R_{ab})$ resp. $I_2(\Delta_{abc})$ given in Sect. 2.

4 Second-Order CPIs for Regular $N-$gons

We consider a regular $N-$gon P_N with vertices $A_1, ..., A_N$, edge length a giving the circumradius $r_N = a/2\,\sin\varphi_N$ with $\varphi_N = \pi/N$. The vertices $A_1, ..., A_N (= A_0)$ can be identified with multiples of the unit roots

$A_k = r_N\,(\cos(2k\varphi_N), \sin(2k\varphi_N))$. Hence, for $k = 0, 1, ..., N-1$, we have

$$\|\overline{A_0\,A_k}\| = 2\,r_N\,\sin(k\varphi_N) = a\,\frac{\sin(k\,\varphi_N)}{\sin(\varphi_N)}\,.$$

Applying formula (6) for $I_2(K_N)$ in case of a regular $N-$gon P_N combined with the integral expressions in Sect. 3 and $A(P_N) = N\,a^2/4\,\tan\varphi_N$ and $L(\partial P_N) = N\,a$ leads to the following closed-term expression of $I_2(P_N)$:

Theorem 4 *For any $N = 3, 4, 5, ...$ we have*

$$I_2(P_N) = \frac{A^2(P_N)}{L(\partial P_N)}\,c_N = \frac{a^3\,N\,c_N}{16\,\tan^2\varphi_N} \quad \textit{with} \quad c_N = b_N - a_N\,,$$

where

$$a_N = \frac{16}{3\,\cos\varphi_N}\sum_{k=1}^{\lfloor\frac{N-3}{2}\rfloor}\frac{\sin^2(k\,\varphi_N)\,\sin^2((k+1)\,\varphi_N)}{\cos(k\,\varphi_N)\,\cos((k+1)\,\varphi_N)}\,\log\Big(\frac{\tan\frac{(k+1)\,\varphi_N}{2}}{\tan\frac{k\,\varphi_N}{2}}\Big)$$

and

$$b_N = \frac{16\,\big(1+\cos\varphi_N\big)^3}{3\,\sin\varphi_N\,\sin(2\,\varphi_N)}\,\log\Big(\frac{1+\sin\frac{\varphi_N}{2}}{\cos\frac{\varphi_N}{2}}\Big) \qquad \textit{for odd } N \geq 3\,,$$

$$b_N = \frac{16}{3}\Big[\frac{1+\sin^2\varphi_N}{\sin^2\varphi_N}\,\log\Big(\frac{1+\sin\varphi_N}{\cos\varphi_N}\Big) - \tan\frac{\varphi_N}{2}\Big] \quad \textit{for even } N \geq 4\,.$$

For $N \in \{3, 4, 5, 6\}$ with $\cos\varphi_N$ expressible by square root terms we get :

$$c_3 = 12\,\log 3\;,\quad c_5 = \frac{10\,(2+\sqrt{5})}{3}\Big[2\,\log(2+\sqrt{5}) - (8-3\,\sqrt{5})\,\log 5\Big]$$

$$c_4 = \frac{16}{3}\Big[3\,\log(1+\sqrt{2}) + 1 - \sqrt{2}\Big]\;,\quad c_6 = c_3 + \frac{8}{3}\Big[\log(6-3\,\sqrt{3}) + 2\,\sqrt{3} - 4\Big]$$

Numerical values of the ratio $c_N = L(\partial P_N)\,I_2(P_N)/A^2(P_N)$

N	c_N	N	c_N	N	c_N	N	c_N
3	13.183347	11	10.812517	19	10.715294	40	10.677629
4	11.892838	12	10.789036	20	10.710545	50	10.673683
5	11.412043	13	10.770821	21	10.706460	60	10.671539
6	11.172030	14	10.756401	22	10.702921	70	10.670247
7	11.033211	15	10.744788	23	10.699834	80	10.669408
8	10.945188	16	10.735297	24	10.697126	90	10.668832
9	10.885692	17	10.727439	25	10.694736	100	10.668421
10	10.843523	18	10.720859	30	10.686156	1000	10.666684

We can prove that $c_N > 32/3$ for $N \geq 3$ and $C_N \downarrow 32/3$ as $N \to \infty$.

Taking into account the 'discrete isoperimetric inequality' for $N-$gons K_N, namely $4\,N\,\tan\varphi_N\,A(K_N) \leq L^2(\partial K_N)$, see [2] for a survey, and the above formulas for $I_2(R_{ab})$, $I_2(\Delta_{abc})$, $I_2(P_N)$ (and also as consequence of numerical experiments) we have enough reasons for

Conjecture II Among all convex N-gons K_N with fixed perimeter $L(\partial K_N)$ the ratio $I_2(K_N)/A^2(K_N)$ attains its minimum for the regular N-gon P_N with edge length $L(\partial K_N)/N$. More precisely, the 'discrete' variant of (3)

$$\frac{c_N}{L(\partial K_N)} \leq \frac{I_2(K_N)}{A^2(K_N)} \leq \frac{c_N}{\sqrt{4\,N\,\tan\varphi_N\,A(K_N)}} \tag{7}$$

should be possible to prove with the constants c_N defined in Theorem 4 . Equality on each side holds iff K_N is regular $N-$gons P_N .

Remark 2 The right-hand inequality is the 'discrete' counterpart of Carleman's inequality. To the best of the author's knowledge a rigorous proof of it seems to be unknown.

5 An Extension to Higher Dimensions

Let there be given a stationary and isotropic Poisson hyperplane tessellation $T_\lambda^{(d)} = \bigcup_{i\in\mathbb{Z}^1} H(P_i, V_i)$ in $\mathbb{R}^d$ driven by an independently marked stationary Poisson process $\Pi_\lambda = \{[P_i, V_i] : i \in \mathbb{Z}^1\}$ on the real line with intensity λ and typical mark V_0 uniformly distributed on the upper hemisphere $\mathbb{S}_+^{d-1}$ of the unit ball $B_1^{(d)}$, see [3] for details. An unoriented hyperplane in $\mathbb{R}^d$ is defined by $H(p,v) = \{x \in \mathbb{R}^d : \langle v, x\rangle = p\}$ for any $p \in \mathbb{R}^1$ and $v \in \mathbb{S}_+^{d-1}$. Further, by $\mathcal{H}_d$ (or $\mathcal{H}_{d-1}$) we denote the $d-$ resp. $(d-1)-$dimensional Hausdorff measure in $\mathbb{R}^d$ and put $\kappa_d = \mathcal{H}_d(B_1^{(d)})$.

The random number of vertices $\Psi_V(\varrho\,K)$ generated by $T_\lambda^{(d)}$ in $\varrho\,K$ is approximately normally distributed for large ϱ, see Thm. 3.1 in [3]:

$$\sqrt{\varrho}\,\Big(\frac{\Psi_V(\varrho\,K)}{\mathcal{H}_d(\varrho\,K)} - \kappa_d\,\Big(\lambda\,\frac{\kappa_{d-1}}{d\,\kappa_d}\Big)^d\Big) \underset{\varrho\to\infty}{\Longrightarrow} \mathcal{N}\Big(0\,,\,\frac{\kappa_{d-1}}{d-1}\,\Big(\lambda\,\frac{\kappa_{d-1}}{d\,\kappa_d}\Big)^{2d-1}\,\frac{J_2(K)}{\mathcal{H}_d^2(K)}\Big)$$

with

$$J_2(K) = \frac{2}{(d-1)\kappa_{d-1}} \int\limits_{\mathbb{R}^1} \int\limits_{\mathbb{S}_+^{d-1}} \mathcal{H}_{d-1}^2(K\cap H(p,v))\,\mathcal{H}_{d-1}(\mathrm{d}v)\mathrm{d}p = \int\limits_K \int\limits_K \frac{\mathrm{d}x\mathrm{d}y}{\|x-y\|}.$$

The right-hand equality is shown by combining the affine Blaschke-Petkantschin formula of Thm. 7.2.7 with Thm. 8.6.4 in [5]. As by-product it turns out that $J_2(K)$ coincides (up to a constant) with the dth-order CPI of the convex body $K \subset \mathbb{R}^d$. Hence, as a natural extension of (3) we formulate the following

Conjecture III For any convex body $K \subset \mathbb{R}^d$ with inner points, it holds

$$\frac{(2^d\, d!\,)^2\, \kappa_{d-1}}{(d-1)\,(2\,d)!\,\kappa_d} \left(\frac{d\,\kappa_d}{\mathcal{H}_{d-1}(\partial K)} \right)^{\frac{1}{d-1}} \leq \frac{J_2(K)}{\mathcal{H}_d^2(K)} \leq \frac{(2^d\, d!\,)^2\, \kappa_{d-1}}{(d-1)\,(2\,d)!\,\kappa_d} \left(\frac{\kappa_d}{\mathcal{H}_d(K)} \right)^{\frac{1}{d}}$$

with equality on each side iff K is a $d-$ball $B_r^{(d)}$ with some radius $r > 0$.

Due to the generalized Carleman inequality for CPIs, see Thm. 8.6.6 in [5], the upper bound is known for long time, whereas the lower bound seems to be still unproved. Using the relation $\mathcal{H}_{d-1}(\partial K)/d\,\kappa_d \leq \big(b(K)/2\big)^{d-1}$ between *mean breadth* $b(K)$ and the surface content $\mathcal{H}_{d-1}(\partial K)$ of K, we can replace the lower bound by a smaller one which is maybe easier to prove.

References

[1] Davy, P. J. (1984). Inequalities for moments of secant length. *Z. Wahrscheinlichkeitstheorie verw. Gebiete* **68**, 243–246.

[2] Florian, A. (1993). Extremum problems for convex discs and polyhedra, In: *Handbook of Convex Geometry*, P. M. Gruber and J. M. Wills (Eds.), Elsevier, North-Holland, 177–221.

[3] Heinrich, L. (2007). CLTs for motion-invariant Poisson hyperplanes in expanding convex bodies. Preprint 043/2007 (http://www.math.uni-augsburg.de/), submittd to *Rend. Circ. Mat. Palermo.*

[4] Santaló, L. A (1976). *Integral Geometry and Geometric Probability.* Addison-Wesley, Reading (Mass.).

[5] Schneider, R. and Weil, W. (2008). *Stochastic and Integral Geometry.* Springer, Berlin.

Postal address: Universität Augsburg, 86135 Augsburg, Germany
E-mail address: heinrich@math.uni-augsburg.de

RENDICONTI DEL CIRCOLO MATEMATICO DI PALERMO
Serie II, Suppl. 81 (2009), pp. 223-235

Graphs arising from ideals of mixed products

MAURIZIO IMBESI

Department of Mathematics, Faculty of Sciences, University of Messina
C.da Papardo, Sal. Sperone, 31 - I 98166 MESSINA
e-mail: imbesim@unime.it

Abstract

In this work we deal with term orders and in particular with the sorted and generalized bi-sorted orders on monomials in one and two sets of variables respectively.

We characterize the edge ideals of graphs that derive from the monomial algebra $K[F]$, where F is a minimal set of generators of an ideal of Veronese-type or an ideal of mixed products.

An application to security field is considered.

AMS 2000 Subject Classifications: Combinatorics, Graph Theory
AMS 2000 Classifications: 05C38, 05C50

The aim of this paper is to manage non usual term orders to obtain less known algebraic objects.

The most known term orders, commonly used in algebraic questions, are the lexicographic order, the degree lexicographic order and the reverse degree lexicographic order.

Different term orders were introduced in algebra, algebraic geometry and other fields.

One of these is the *diagonal term order* that was considered for studying algebraic varieties associated to subalgebras of polynomials generated by the minors of maximal order of a generic matrix.
Without establishing a term order in the corresponding polynomial ring, whose variables are the entries of the matrix, the initial monomial of a minor in this order is the product of the indeterminates in the main diagonal.

For example, if we consider the (2×3)-matrix $\begin{pmatrix} X_{11} & X_{12} & X_{13} \\ X_{21} & X_{22} & X_{23} \end{pmatrix}$ and its 2-minors

$$[1\,2]=X_{11}\,X_{22}-X_{12}\,X_{21}\,,\ [1\,3]=X_{11}\,X_{23}-X_{13}\,X_{21}\,,\ [2\,3]=X_{12}\,X_{23}-X_{13}\,X_{22}\,,$$

which belong to the ring $A=K[\,X_{11},X_{12},X_{13},X_{21},X_{22},X_{23}\,]$, K a field, the initial monomials of $[1\,2],[1\,3],[2\,3]$ are respectively $X_{11}\,X_{22}$, $X_{11}\,X_{23}$, $X_{12}\,X_{23}$, the products of the entries in the main diagonal of that minors.

The diagonal term order is very useful to determine the Sagbi basis of the ring $B=K[\,[1\,2],[1\,3],[2\,3]\,]$, a K-subalgebra of A, and to study several algebraic and geometric properties of B (see [2], [3], [6]).

Here we work with a term order which is more joined to combinatorial objects: the *sorted order* and its variations and generalizations.

In section 1 we recall the sorted order and the generalized bi-sorted order in a multivariate polynomial ring over a field K and some results about the toric ideal $\mathfrak{I}$ defined by the set $T_{(n,r),(m,s)}$, when r and s are respectively the lengths of the strings of a bi-string over the alphabets $A_1=\{1,2,\dots,n\}$ and $A_2=\{1,2,\dots,m\}$. The bi-strings can contain dots, so their lengths can be variable, respectively $\leqslant r$ and $\leqslant s$. The reduced Gröbner basis of $\mathfrak{I}$ is computed by utilizing the generalized bi-sorted order.

In section 2 we characterize the edge ideals of graphs that derive from the monomial algebra $K[F]$, where F is a minimal set of generators of an ideal of Veronese-type or an ideal of mixed products.

Finally, in section 3 we proceed, through an example, to find methods or algebraic objects for preserving secret data transmission.

1 Generalized bi-sorted orders

The sorted order was introduced and characterized in [7].
It is structured as follows.

For fixed r and $s_1,\dots,s_d$ positive integers, let's consider the set

$$T=\{(i_1,\dots,i_d)\in\mathbb{Z}^d \mid i_1+\dots+i_d=r\,,\ 0\leqslant i_1\leqslant s_1,\ \dots\,,\ 0\leqslant i_d\leqslant s_d\}\,.$$

There exists a natural bijection between the elements of T and weakly increasing strings of length r over the alphabet $\{1,2,\dots,d\}$ that have at most s_j occurrences of the letter j.
In this way $(i_1,\dots,i_d)$ is mapped to the increasing string

$$\underline{u}=u_1u_2\cdots u_r=\underbrace{11\cdots1}_{i_1\text{ times}}\ \underbrace{22\cdots2}_{i_2\text{ times}}\ \cdots\ \underbrace{dd\cdots d}_{i_d\text{ times}},$$

and $X_{\underline{u}} = X_{u_1 u_2 \cdots u_r}$ indicates the relating variable in $K[\underline{X}]$, K a field.

Definition 1 For a fixed integer $r > 0$, a monomial $X_{u_1 u_2 \cdots u_r} \cdots X_{z_1 z_2 \cdots z_r}$ of $K[\underline{X}]$ is said to be *sorted* if

$$u_1 \leqslant \ldots \leqslant z_1 \leqslant u_2 \leqslant \ldots \leqslant z_2 \leqslant u_3 \leqslant \ldots \leqslant u_r \leqslant \ldots \leqslant z_r \,.$$

Let $sort(\cdot)$ denote the operator which takes any string over the alphabet $\{1, 2, \ldots, d\}$ and sorts it into increasing order.

Let $\mathfrak{I}_T$ be the toric ideal defined by the set T,

$$\mathfrak{I}_T = \left(X_{\underline{u}} \cdots X_{\underline{w}} - X_{\underline{u'}} \cdots X_{\underline{w'}} \;\mid\; \text{sort}\,(\underline{u} \cdots \underline{w}) = \text{sort}\,(\underline{u'} \cdots \underline{w'}) \right),$$

where $\underline{w} = w_1 \cdots w_r$, $\underline{u'} = u'_1 \cdots u'_r$, $\underline{w'} = w'_1 \cdots w'_r$ ([7], Remark 14.1).

Theorem 1 There exists a term order $\prec$ on $K[\underline{X}]$ such that the sorted monomials are precisely the $\prec$ - standard monomials modulo $\mathfrak{I}_T$.
The initial ideal $\text{in}_{\prec}(\mathfrak{I}_T)$ is generated by square-free quadratic monomials. The corresponding reduced Gröbner basis of $\mathfrak{I}_T$ is

$$\{\underline{X_{u_1 u_2 \cdots u_r} X_{v_1 v_2 \cdots v_r}} - X_{z_1 z_3 \cdots z_{2r-1}} X_{z_2 z_4 \cdots z_{2r}} \quad \text{such that} \\ z_1\, z_2\, z_3 \cdots z_{2r} = \text{sort}\,(u_1 v_1 u_2 v_2 \cdots u_r v_r)\} \,.$$

Proof. See [7], Theorem 14.2 .

Recently, in [4] and in [1], the notion of sorted order was extended to strings of fixed length structured in double sets of integers, by defining the *generalized bi-sorted order*. It is characterized as specified below.

For fixed positive integers ℓ, r, s and $r_1, \ldots, r_n$, $s_1, \ldots, s_m$, let's consider the following set

$$\begin{aligned} T_{(n,r),\,(m,s)} = \{&(i_1, \ldots, i_n;\, j_1, \ldots, j_m) \in \mathbb{N}^n \oplus \mathbb{N}^m \;\text{ such that} \\ &i_1 + \ldots + i_n + j_1 + \ldots + j_m = \ell\,; \\ &0 \leqslant i_1 + \ldots + i_n = \rho \leqslant r, \quad 0 \leqslant i_1 \leqslant r_1,\; \ldots\,,\, 0 \leqslant i_n \leqslant r_n\,; \\ &0 \leqslant j_1 + \ldots + j_m = \sigma \leqslant s, \;\; 0 \leqslant j_1 \leqslant s_1,\; \ldots\,, 0 \leqslant j_m \leqslant s_m\} \,. \end{aligned}$$

There is a natural bijection between the elements of $T_{(n,r),\,(m,s)}$ and weakly increasing bi-strings of length $\ell \leqslant r + s$, the first string over the alphabet $A_1 = \{1, 2, \ldots, n\}$, the other one over $A_2 = \{1, 2, \ldots, m\}$, that have at most r_k and s_k occurrences of the letter k, respectively.

Under this bijection, $(i_1, \ldots, i_n;\, j_1, \ldots, j_m) \in T_{(n,r),\,(m,s)}$ is mapped to the increasing bi-string

$$u_1 u_2 \cdots u_\rho ; v_1 v_2 \cdots v_\sigma = \underbrace{11\cdots1}_{i_1 \text{ times}}\, \underbrace{22\cdots2}_{i_2 \text{ times}} \cdots \underbrace{nn\cdots n}_{i_n \text{ times}} ; \underbrace{11\cdots1}_{j_1 \text{ times}}\, \underbrace{22\cdots2}_{j_2 \text{ times}} \cdots \underbrace{mm\cdots m}_{j_m \text{ times}} .$$

Let's write $X_{\underline{u};\underline{v}} = X_{u_1 u_2 \cdots u_\rho;\, v_1 v_2 \cdots v_\sigma}$ for the relating variable in $K[\underline{X}]$.

Remark 1 For any $(i_1,\dots,i_n;\, j_1,\dots,j_m) \in T_{(n,r),\,(m,s)}$, since $i_1+\ldots+ +i_n=\rho$ is at most r, and $j_1+\ldots+j_m=\sigma$ is at most s, there could be variables $X_{u_1u_2\cdots u_\rho;\, v_1v_2\cdots v_\sigma} \in K[\underline{X}]$ such that $\rho \lneq r$ or $\sigma \lneq s$.
In such cases we'll add dots in the strings for reaching the fixed length.

Example 1 For fixed $\ell=3$, $r=3$, $s=3$, $r_1=r_2=r_3=s_1=s_2=s_3=1$, let $T_{(5,3),\,(4,3)}$ be the set of 9-tuples

$$\begin{aligned}\{&(1,1,1,0,0\,;0,0,0,0),(1,1,0,1,0\,;0,0,0,0),(1,1,0,0,1\,;0,0,0,0),\\ &(1,0,1,1,0\,;0,0,0,0),(1,0,1,0,1\,;0,0,0,0),(1,0,0,1,1\,;0,0,0,0),\\ &(0,1,1,1,0\,;0,0,0,0),(0,1,1,0,1\,;0,0,0,0),(0,1,0,1,1\,;0,0,0,0),\\ &(0,0,1,1,1\,;0,0,0,0),(0,0,0,0,0\,;1,1,1,0),(0,0,0,0,0\,;1,1,0,1),\\ &(0,0,0,0,0\,;1,0,1,1),(0,0,0,0,0\,;0,1,1,1)\}\,.\end{aligned}$$

The relating variables in $K[\underline{X}]$ are respectively

$$\begin{aligned}&X_{123;\bullet\bullet\bullet}\,,\ X_{124;\bullet\bullet\bullet}\,,\ X_{125;\bullet\bullet\bullet}\,,\ X_{134;\bullet\bullet\bullet}\,,\ X_{135;\bullet\bullet\bullet}\,,\ X_{145;\bullet\bullet\bullet}\,,\ X_{234;\bullet\bullet\bullet}\,,\\ &X_{235;\bullet\bullet\bullet}\,,\ X_{245;\bullet\bullet\bullet}\,,\ X_{345;\bullet\bullet\bullet}\,,\ X_{\bullet\bullet\bullet;123}\,,\ X_{\bullet\bullet\bullet;124}\,,\ X_{\bullet\bullet\bullet;134}\,,\ X_{\bullet\bullet\bullet;\,234}\,.\end{aligned}$$

Ten variables have bi-strings of length $3=\rho=r$, $0=\sigma<s$, so we add three dots in the second string of them. Similarly, for the remaining four variables, we add three dots in the first string of them.

Example 2 For fixed $\ell=5$, $r=3$, $s=3$, $r_1=r_2=r_3=s_1=s_2=s_3=1$, let $T_{(4,3),\,(3,3)}$ be the set of 7-tuples

$$\begin{aligned}\{&(1,1,0,0\,;1,1,1),(1,0,1,0\,;1,1,1),(1,0,0,1\,;1,1,1),\\ &(0,1,1,0\,;1,1,1),(0,1,0,1\,;1,1,1),(0,0,1,1\,;1,1,1),\\ &(1,1,1,0\,;1,1,0),(1,1,1,0\,;1,0,1),(1,1,1,0\,;0,1,1),\\ &(1,1,0,1\,;1,1,0),(1,1,0,1\,;1,0,1),(1,1,0,1\,;0,1,1),\\ &(1,0,1,1\,;1,1,0),(1,0,1,1\,;1,0,1),(1,0,1,1\,;0,1,1),\\ &(0,1,1,1\,;1,1,0),(0,1,1,1\,;1,0,1),(0,1,1,1\,;0,1,1)\}\,.\end{aligned}$$

The relating variables in $K[\underline{X}]$ are respectively

$$\begin{aligned}&X_{12_\bullet;123}\,,\ X_{13_\bullet;123}\,,\ X_{14_\bullet;123}\,,\ X_{23_\bullet;123}\,,\ X_{24_\bullet;123}\,,\ X_{34_\bullet;123}\,,\\ &X_{123;12_\bullet}\,,\ X_{124;12_\bullet}\,,\ X_{134;12_\bullet}\,,\ X_{234;12_\bullet}\,,\ X_{123;13_\bullet}\,,\ X_{124;13_\bullet}\,,\\ &X_{134;13_\bullet}\,,\ X_{234;13_\bullet}\,,\ X_{123;23_\bullet}\,,\ X_{124;23_\bullet}\,,\ X_{134;23_\bullet}\,,\ X_{234;23_\bullet}\,.\end{aligned}$$

Six variables have bi-strings of length $2=\rho<r$, $3=\sigma=s$, so we add one dot in the first string of them. Similarly, for the remaining twelve variables, we add one dot in the second string of them.

Let's now recall the definition of generalized bi-sorted monomial of degree two containing dots.

Definition 2 For fixed positive integers r and s, a monomial of degree two containing dots $X_{u_1u_2\cdots u_r;\, v_1v_2\cdots v_s}X_{z_1z_2\cdots z_r;\, w_1w_2\cdots w_s} \in K[\underline{X}]$ is said to be *generalized bi-sorted* if it holds both

$$u_1 \leqslant z_1 \leqslant u_2 \leqslant z_2 \leqslant \ldots \leqslant u_r \leqslant z_r \text{ and}$$
$$v_1 \leqslant w_1 \leqslant v_2 \leqslant w_2 \leqslant \ldots \leqslant v_s \leqslant w_s\,,$$

with the convention that

- dots are placed in the right side of its bi-strings,
- if some $u_i, z_i = \bullet$, or some $v_j, w_j = \bullet$, such elements must be skipped.

We need the following (see [1], Definition 1.4)

Definition 3 For fixed positive integers r and s, a monomial containing dots $X_{u_1u_2\cdots u_r;\, v_1v_2\cdots v_s}X_{u'_1u'_2\cdots u'_r;\, v'_1v'_2\cdots v'_s}\cdots X_{z_1z_2\cdots z_r;\, w_1w_2\cdots w_s} \in K[\underline{X}]$ is said to be *generalized bi-sorted* if it holds both

$$u_1 \leqslant u'_1 \leqslant \ldots \leqslant z_1 \leqslant u_2 \leqslant u'_2 \leqslant \ldots \leqslant z_2 \leqslant \ldots \leqslant u_r \leqslant u'_r \leqslant \ldots \leqslant z_r \text{ and}$$
$$v_1 \leqslant v'_1 \leqslant \ldots \leqslant w_1 \leqslant v_2 \leqslant v'_2 \leqslant \ldots \leqslant w_2 \leqslant \ldots \leqslant v_s \leqslant v'_s \leqslant \ldots \leqslant w_s\,,$$

with the same convention as in Definition 2.

Let *gen bi-sort*$(\cdot\,;\cdot)$ denote the operator which takes any bi-string over the alphabets $A_1 = \{1, 2, \ldots, n\}$ and $A_2 = \{1, 2, \ldots, m\}$ and sorts each string of it into increasing order.

Proposition 1 The toric ideal defined by the set $T_{(n,r),\,(m,s)}$ equals

$$\mathfrak{I}_{T_{(n,r),\,(m,s)}} = \Big(X_{\underline{u};\underline{v}}\cdots X_{\underline{z};\underline{w}} - X_{\underline{u'};\underline{v'}}\cdots X_{\underline{z'};\underline{w'}} \text{ such that}$$
$$\text{gen bi-sort}\,(\underline{u}\cdots\underline{z};\, \underline{v}\cdots\underline{w}) = \text{gen bi-sort}\,(\underline{u'}\cdots\underline{z'};\, \underline{v'}\cdots\underline{w'})\Big)\,,$$

where $\underline{u} = u_1u_2\cdots u_r$, $\underline{v} = v_1v_2\cdots v_s$, $\underline{z} = z_1z_2\cdots z_r$, $\underline{w} = w_1w_2\cdots w_s$, $\underline{u'} = u'_1u'_2\cdots u'_r$, $\underline{v'} = v'_1v'_2\cdots v'_s$, $\underline{z'} = z'_1z'_2\cdots z'_r$, $\underline{w'} = w'_1w'_2\cdots w'_s$.

Proof. See [1], Proposition 1.2.

Remark 2 The toric ideal $\mathfrak{I}_{T_{(n,r),\,(m,s)}}$ is generated by a Gröbner basis.

Theorem 2 There exists a term order $\prec$ on $K[\underline{X}]$ such that the generalized bi-sorted monomials are precisely the $\prec$-standard monomials modulo the ideal $\mathfrak{I}$ generated by the elements of a set $\mathcal{F}$ of marked binomials of $K[\underline{X}]$, where the variables are indexed by bi-strings of the same length, but containing dots

$$\{\underline{X_{u_1u_2\cdots u_r;\, v_1v_2\cdots v_s}\, X_{u'_1u'_2\cdots u'_r;\, v'_1v'_2\cdots v'_s}} -$$
$$X_{z_1z_3\cdots z_{2r-1};\, w_1w_3\cdots w_{2s-1}}X_{z_2z_4\cdots z_{2r};\, w_2w_4\cdots w_{2s}} \text{ such that}$$

$z_1 z_2 \cdots z_{2r};\ w_1 w_2 \cdots w_{2s} = \text{gen bi-sort}\,(u_1 u_1' u_2 u_2' \cdots u_r u_r';\ v_1 v_1' v_2 v_2' \cdots v_s v_s')\}$.

Because $\mathcal{F}$ is the reduced Gröbner basis of $\mathfrak{I}$, the initial ideal $\text{in}_\prec(\mathfrak{I})$ is generated by square-free quadratic monomials.

Proof. See [1], Theorem 1.3.

2 Edge ideals of graphs arising from ideals of mixed products

Let $K[F]$ be a monomial ring, $K[F] \subset K[\underline{X}]$, generated by a set F of monomials of the same degree.

Then $K[F] = K[\underline{X}]/\mathfrak{I}$, $\mathfrak{I}$ ideal generated by binomials.

If, for any monomial order $\prec$, the Gröbner basis of $\mathfrak{I}$ is square-free quadratic, the initial ideal $\text{in}_\prec(\mathfrak{I})$ is generated by the edges of a graph $\mathcal{G}$.

In general, $\text{in}_\prec(\mathfrak{I})$ is not a square-free quadratic ideal.

But, if $\prec$ is the sorted order or the generalized bi-sorted order, it can be shown that $\text{in}_\prec(\mathfrak{I})$ is square-free quadratic (see [7], [1]).

So, for such orders, it makes sense to study $\mathcal{G}(\text{in}_\prec(\mathfrak{I}))$.

$\mathcal{G}(\text{in}_\prec(\mathfrak{I}))$ is a graph having vertices all the variables that appear in $K[\underline{X}]$ and edges the generators of $\text{in}_\prec(\mathfrak{I})$.

Algebraically speaking, we characterize this problem by discussing Gröbner bases for families of toric ideals associated to ideals of Veronese-type and ideals of mixed products.

Let I be a monomial ideal of $K[X_1, \ldots, X_n]$, K a field.

Definition 4 Let $I \subset K[X_1, \ldots, X_n]$ generated in degree $q > 0$. We call I a *q-Veronese* ideal if I is generated by all monomials in $K[X_1, \ldots, X_n]$ of degree q.

Definition 5 Let $I \subset K[X_1, \ldots, X_n]$ generated in degree $q > 0$. We call I an ideal of *q-Veronese type* if I is generated by the set of monomials in $K[X_1, \ldots, X_n]$ of degree q such that

$$\left\{ X_1^{a_{i_1}} \cdots X_n^{a_{i_n}} \mid \sum_{j=1}^{n} a_{i_j} = q,\ \ 0 \leqslant a_{i_1} \leqslant s_1, \ldots,\ 0 \leqslant a_{i_n} \leqslant s_n \right\}.$$

Theorem 3 Let I be an ideal of Veronese type. Let $\prec$ denote the sorted order on $K[\underline{X}]$. Let $\mathfrak{I}$ be the toric ideal of the monomial subring $K[F]$ of $K[\underline{X}]$, where F is the minimal generating set of I that consists of square-free quadratic monomials.

If $\mathcal{G}$ is the graph whose edges are the generators of the ideal in$_\prec(\mathfrak{I})$, then

$$E(\mathcal{G}) = \{X_{u_1u_2\cdots u_r}X_{v_1v_2\cdots v_r} \mid \text{sort}\,(u_1v_1u_2v_2\cdots u_rv_r) = z_1\,z_2\,z_3\cdots z_{2r}\}\,,$$

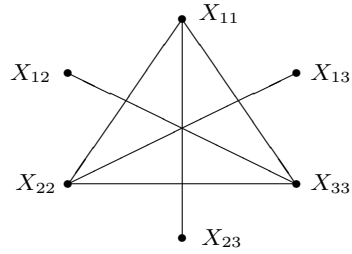
where $X_{z_1z_3\cdots z_{2r-1}}X_{z_2z_4\cdots z_{2r}}$ is the second term of the binomials constituting the reduced Gröbner basis of $\mathfrak{I}$.

Proof. The toric ideal $\mathfrak{I}$ coincides with the ideal $\mathfrak{I}_T$ defined by the set T introduced in section 1.
Its generators constitute the reduced Gröbner basis of $\mathfrak{I}$ with respect to the term order $\prec$ that selects as initial terms the not sorted monomials ([7]).
So in$_\prec(\mathfrak{I}) = (X_{u_1u_2\cdots u_r}X_{v_1v_2\cdots v_r} \mid \text{sort}\,(u_1v_1u_2v_2\cdots u_rv_r) = z_1\,z_2\,z_3\cdots z_{2r})$.

Example 3 Let $T = \{(2,0,0),(1,1,0),(1,0,1),(0,2,0),(0,1,1),(0,0,2)\}$.
Let $\mathcal{G}_T$ be the graph with vertices $X_{11}, X_{12}, X_{13}, X_{22}, X_{23}, X_{33}$ and whose edges are the initial terms of the reduced Gröbner basis of $\mathfrak{I}_T$. Then

$$E(\mathcal{G}_T) = \{X_{11}X_{33}, X_{11}X_{22}, X_{11}X_{23}, X_{12}X_{33}, X_{13}X_{22}, X_{33}X_{22}\}$$

$\mathcal{G}_T$



The graph $\mathcal{G}_T$ contains the complete subgraph with vertices X_{11}, X_{22}, X_{33}.
This is a general fact if the reduced Gröbner basis of $\mathfrak{I}_T$ contains binomials not square-free.

Remark 3 In Example 3, the reduced Gröbner basis of the toric ideal $\mathfrak{I}_T$ with respect to the sorted order is constituted by six binomials, which are the generators of the ideal of the Veronese surface in $\mathbb{P}^5$,

$$(\underline{X_{11}X_{33}} - X_{13}^2,\ \underline{X_{11}X_{22}} - X_{12}^2,\ \underline{X_{11}X_{23}} - X_{12}X_{13},$$
$$\underline{X_{12}X_{33}} - X_{13}x_{23},\ \underline{X_{13}X_{22}} - X_{12}X_{23},\ \underline{X_{33}X_{22}} - X_{23}^2)\,.$$

Let's now recall the notion of ideal of mixed products.

Definition 6 Let p, q, h, k be non-negative integers such that $p+q=h+k$.
We say *ideal of mixed products* to be the monomial ideal $L = I_p\,J_q + I_h\,J_k$ of the polynomial ring $R = K[X_1,\ldots,X_n;Y_1,\ldots,Y_m]$ such that I_p (resp. J_q) is the ideal generated by all the square-free monomials of degree p (resp. q) in the variables $X_1,\ldots,X_n$ (resp. $Y_1,\ldots,Y_m$).

The class of the ideals of mixed products L is the following:

- $I_p\, J_q$, when $p, q \geqslant 1$,
- $I_t + J_t$, when $t \leqslant \inf\{n, m\}$,
- $I_k J_{k+1} + I_{k+1} J_k$, when $k \geqslant 0$,
- $I_p\, J_h + I_q$, or $J_p + I_k\, J_q$, when $1 \leqslant h < q$, or $1 \leqslant k < p$,
- $I_p J_q + I_h J_k$, when $h \geqslant p+1$, or $k \leqslant q-1$.

The variables $X_{\underline{u};\,\underline{v}}$ arising from each of these ideals can contain dots in their bi-strings.

Let's characterize the edge ideals of graphs that derive from each class of ideals L of mixed products and give the list of graphs arising from each minimal generating set of L.

Theorem 4 Let $L = I_p\, J_q$, $p, q \geqslant 1$, be an ideal of mixed products. Let $\succ$ denote the generalized bi-sorted order on $K[\underline{X}]$. Let $\mathfrak{I}$ be the toric ideal of the monomial subring $K[F]$, where F is the minimal generating set of L consisting of square-free monomials. Let $\mathcal{G}$ be the graph whose edges are the generators of the ideal $\text{in}_{\prec}(\mathfrak{I})$. Then

$$E(\mathcal{G}) = \{X_{u_1u_2\cdots u_p;\, v_1v_2\cdots v_q} X_{u'_1u'_2\cdots u'_p;\, v'_1v'_2\cdots v'_q} \quad \text{such that}$$
$$\text{gen bi-sort}\,(u_1u'_1u_2u'_2\cdots u_pu'_p; v_1v'_1v_2v'_2\cdots v_qv'_q) = z_1z_2\cdots z_{2p}\,; w_1w_2\cdots w_{2q}\},$$

where $X_{z_1z_3\cdots z_{2p-1};w_1w_3\cdots w_{2q-1}} X_{z_2z_4\cdots z_{2p};w_2w_4\cdots w_{2q}}$ is the second term of the marked binomials in $K[\underline{X}]$.

Proof. By Proposition 1, the toric ideal $\mathfrak{I}$ has generators $X_{\underline{u};\underline{v}} X_{\underline{u}';\underline{v}'} - X_{\underline{u}'';\underline{v}''} X_{\underline{u}''';\underline{v}'''}$ such that $\text{gen bi-sort}\,(\underline{u}\,\underline{u}';\, \underline{v}\,\underline{v}') = \text{gen bi-sort}\,(\underline{u}''\,\underline{u}'''';\, \underline{v}''\,\underline{v}''')$, with $\underline{u}^{()} = u_1^{()}u_2^{()}\cdots u_p^{()}$, $\underline{v}^{()} = v_1^{()}v_2^{()}\cdots v_q^{()}$.
Such generators constitute the reduced Gröbner basis of $\mathfrak{I}$ with respect to the term order $\prec$ that selects as initial terms the not generalized bi-sorted monomials. So $\text{in}_{\prec}(\mathfrak{I}) = \Big(X_{\underline{u};\underline{v}} X_{\underline{u}';\underline{v}'}$ such that
$\text{gen bi-sort}\,(u_1u'_1u_2u'_2\cdots u_pu'_p; v_1v'_1v_2v'_2\cdots v_qv'_q) = z_1z_2\cdots z_{2p}\,; w_1w_2\cdots w_{2q}\Big)$.

Theorem 5 Let $L = I_t + J_t$, $t \leqslant \inf\{n, m\}$, be an ideal of mixed products. Let $\succ$ denote the generalized bi-sorted order on $K[\underline{X}]$. Let $\mathfrak{I}$ be the toric ideal of the monomial subring $K[F]$, where F is the minimal generating set of L consisting of square-free monomials. Let $\mathcal{G}$ be the graph whose edges are the generators of the ideal $\text{in}_{\prec}(\mathfrak{I})$. Then

$$E(\mathcal{G}) = \{X_{u_1u_2\cdots u_t;\bullet\bullet\cdots\bullet} X_{u'_1u'_2\cdots u'_t;\bullet\bullet\cdots\bullet}, X_{\bullet\bullet\cdots\bullet;\, v_1v_2\cdots v_t} X_{\bullet\bullet\cdots\bullet;\, v'_1v'_2\cdots v'_t}$$
$$\text{such that} \quad \text{gen bi-sort}\,(u_1u'_1\cdots u_tu'_t; v_1v'_1\cdots v_tv'_t) = z_1\cdots z_{2t}; w_1\cdots w_{2t}\},$$

where $X_{z_1 z_3 \cdots z_{2t-1}; \bullet\bullet\cdots\bullet} X_{z_2 z_4 \cdots z_{2t}; \bullet\bullet\cdots\bullet}$ and $X_{\bullet\bullet\cdots\bullet;\, w_1 w_2 \cdots w_{2t-1}} X_{\bullet\bullet\cdots\bullet;\, w_2 w_4 \cdots w_{2t}}$ represent the second terms of the marked binomials in $K[\underline{X}]$.

Proof. See [4], Theorem 3.2, for computation of the Gröbner basis of $\mathfrak{I}$.

Example 4 In $K[Y_1, \ldots, Y_5; Z_1, \ldots, Z_4]$, let $L = I_3 + J_3$, where
$I_3 = (Y_1 Y_2 Y_3,\ Y_1 Y_2 Y_4,\ Y_1 Y_2 Y_5,\ Y_1 Y_3 Y_4,\ Y_1 Y_3 Y_5,$
$\quad Y_1 Y_4 Y_5,\ Y_2 Y_3 Y_4,\ Y_2 Y_3 Y_5,\ Y_2 Y_4 Y_5,\ Y_3 Y_4 Y_5)$, and
$J_3 = (Z_1 Z_2 Z_3,\ Z_1 Z_2 Z_4,\ Z_1 Z_3 Z_4,\ Z_2 Z_3 Z_4)$.

Let $\mathcal{G}_{T_{(5,3),\,(4,3)}}$ be the graph having vertices the 14 variables (Example 1)

$$X_{123;\bullet\bullet\bullet},\ X_{124;\bullet\bullet\bullet},\ X_{125;\bullet\bullet\bullet},\ X_{134;\bullet\bullet\bullet},\ X_{135;\bullet\bullet\bullet},\ X_{145;\bullet\bullet\bullet},\ X_{234;\bullet\bullet\bullet},$$
$$X_{235;\bullet\bullet\bullet},\ X_{245;\bullet\bullet\bullet},\ X_{345;\bullet\bullet\bullet},\ X_{\bullet\bullet\bullet;123},\ X_{\bullet\bullet\bullet;124},\ X_{\bullet\bullet\bullet;134},\ X_{\bullet\bullet\bullet;\,234},$$

and edges the initial not generalized bi-sorted terms of the Gröbner basis of the toric ideal $\mathfrak{I}_{T_{(5,3),\,(4,3)}}$, as computed in [1], Example 2.1. Then

$$\begin{aligned} E(\mathcal{G}_{T_{(5,3),\,(4,3)}}) = \{ & X_{123;\bullet\bullet\bullet} X_{145;\bullet\bullet\bullet},\ X_{123;\bullet\bullet\bullet} X_{245;\bullet\bullet\bullet},\ X_{123;\bullet\bullet\bullet} X_{345;\bullet\bullet\bullet}, \\ & X_{124;\bullet\bullet\bullet} X_{345;\bullet\bullet\bullet},\ X_{125;\bullet\bullet\bullet} X_{134;\bullet\bullet\bullet},\ X_{125;\bullet\bullet\bullet} X_{234;\bullet\bullet\bullet}, \\ & X_{125;\bullet\bullet\bullet} X_{345;\bullet\bullet\bullet},\ X_{135;\bullet\bullet\bullet} X_{234;\bullet\bullet\bullet},\ X_{145;\bullet\bullet\bullet} X_{234;\bullet\bullet\bullet},\ X_{145;\bullet\bullet\bullet} X_{245;\bullet\bullet\bullet} \}. \end{aligned}$$

Theorem 6 Let $L = I_k J_{k+1} + I_{k+1} J_k$, $k \geqslant 0$, be an ideal of mixed products. Let $\succ$ denote the generalized bi-sorted order on $K[\underline{X}]$. Let $\mathfrak{I}$ be the toric ideal of the monomial subring $K[F]$, where F is the minimal generating set of L consisting of square-free monomials. Let $\mathcal{G}$ be the graph whose edges are the generators of the ideal $\text{in}_{\prec}(\mathfrak{I})$. Then

$$\begin{aligned} E(\mathcal{G}) = \{ & X_{u_1 u_2 \cdots u_k \bullet;\, v_1 v_2 \cdots v_{k+1}} X_{u'_1 u'_2 \cdots u'_k \bullet;\, v'_1 v'_2 \cdots v'_{k+1}}, \\ & X_{u_1 u_2 \cdots u_{k+1};\, v_1 v_2 \cdots v_k \bullet} X_{u'_1 u'_2 \cdots u'_{k+1};\, v'_1 v'_2 \cdots v'_k \bullet}, \\ & X_{u_1 u_2 \cdots u_k \bullet;\, v_1 v_2 \cdots v_{k+1}} X_{u'_1 u'_2 \cdots u'_{k+1};\, v'_1 v'_2 \cdots v'_k \bullet} \quad \text{such that} \end{aligned}$$

$$\text{gen bi-sort}(u_1 u'_1 \cdots u_{k+1} u'_{k+1};\, v_1 v'_1 \cdots v_{k+1} v'_{k+1}) = z_1 \cdots z_{2(k+1)};\, w_1 \cdots w_{2(k+1)}\},$$

where $X_{z_1 z_3 \cdots z_{2k-1} \bullet;\, w_1 w_3 \cdots w_{2k-1}\ w_{2k+1}} X_{z_2 z_4 \cdots z_{2k} \bullet;\, w_2 w_4 \cdots w_{2k}\ w_{2(k+1)}}$,
$X_{z_1 z_3 \cdots z_{2k-1}\ z_{2k+1};\, w_1 w_3 \cdots w_{2k-1} \bullet} X_{z_2 z_4 \cdots z_{2k}\ z_{2(k+1)};\, w_2 w_4 \cdots w_{2k} \bullet}$,
$X_{z_1 z_3 \cdots z_{2k-1} \bullet;\, w_1 w_3 \cdots w_{2k-1}\ w_{2k+1}} X_{z_2 z_4 \cdots z_{2k}\ z_{2k+1};\, w_2 w_4 \cdots w_{2k} \bullet}$
represent the second terms of the marked binomials in $K[\underline{X}]$.

Proof. See [4], Theorem 3.3, for computation of the Gröbner basis of $\mathfrak{I}$.

Example 5 In $K[Y_1, Y_2, Y_3, Y_4; Z_1, Z_2, Z_3]$, let $L = I_2 J_3 + I_3 J_2$, where
$I_2 = (Y_1 Y_2, Y_1 Y_3, Y_1 Y_4, Y_2 Y_3, Y_2 Y_4, Y_3 Y_4)$, $J_3 = (Z_1 Z_2 Z_3)$,
$I_3 = (Y_1 Y_2 Y_3, Y_1 Y_2 Y_4, Y_1 Y_3 Y_4, Y_2 Y_3 Y_4)$, $J_2 = (Z_1 Z_2, Z_1 Z_3, Z_2 Z_3)$.

Let $\mathcal{G}_{T_{(4,3),\,(3,3)}}$ be the graph having vertices the 18 variables (Example 2)

$$X_{12_\bullet;123}\,,\ X_{13_\bullet;123}\,,\ X_{14_\bullet;123}\,,\ X_{23_\bullet;123}\,,\ X_{24_\bullet;123}\,,\ X_{34_\bullet;123}\,,$$
$$X_{123;12_\bullet}\,,\ X_{124;12_\bullet}\,,\ X_{134;12_\bullet}\,,\ X_{234;12_\bullet}\,,\ X_{123;13_\bullet}\,,\ X_{124;13_\bullet}\,,$$
$$X_{134;13_\bullet}\,,\ X_{234;13_\bullet}\,,\ X_{123;23_\bullet}\,,\ X_{124;23_\bullet}\,,\ X_{134;23_\bullet}\,,\ X_{234;23_\bullet}\,,$$

and edges the initial not generalized bi-sorted terms of the Gröbner basis of the toric ideal $\mathfrak{I}_{T_{(4,3),\,(3,3)}}$, as computed in [1], Example 2.2. Then

$$\begin{aligned} E(\mathcal{G}_{T_{(4,3),\,(3,3)}}) \,=\, \{&X_{34_\bullet;123}\,X_{12_\bullet;123},\ X_{124;12_\bullet}\,X_{123;13_\bullet},\ X_{124;12_\bullet}\,X_{123;23_\bullet},\\ &X_{134;12_\bullet}\,X_{123;13_\bullet},\ X_{134;12_\bullet}\,X_{124;13_\bullet},\ X_{134;12_\bullet}\,X_{123;23_\bullet},\\ &X_{134;12_\bullet}\,X_{124;23_\bullet},\ X_{234;12_\bullet}\,X_{123;13_\bullet},\ X_{234;12_\bullet}\,X_{124;13_\bullet},\\ &X_{234;12_\bullet}\,X_{134;13_\bullet},\ X_{234;12_\bullet}\,X_{123;23_\bullet},\ X_{234;12_\bullet}\,X_{124;23_\bullet},\\ &X_{234;12_\bullet}\,X_{134;23_\bullet},\ X_{124;13_\bullet}\,X_{123;23_\bullet},\ X_{134;13_\bullet}\,X_{123;23_\bullet},\\ &X_{134;13_\bullet}\,X_{124;23_\bullet},\ X_{234;13_\bullet}\,X_{123;23_\bullet},\ X_{234;13_\bullet}\,X_{124;23_\bullet},\\ &X_{234;13_\bullet}\,X_{134;23_\bullet},\ X_{14_\bullet;123}\,X_{123;12_\bullet},\ X_{14_\bullet;123}\,X_{123;13_\bullet},\\ &X_{14_\bullet;123}\,X_{123;23_\bullet},\ X_{24_\bullet;123}\,X_{123;12_\bullet},\ X_{24_\bullet;123}\,X_{123;13_\bullet},\\ X_{24_\bullet;123}\,X_{123;23_\bullet},\ &X_{34_\bullet;123}\,X_{123;12_\bullet},\ X_{34_\bullet;123}\,X_{123;13_\bullet},\ X_{34_\bullet;123}\,X_{123;23_\bullet}\,\}\,. \end{aligned}$$

Theorem 7 Let $L = I_p\,J_h + I_q$, $p+h=q$, be an ideal of mixed products. Let $\succ$ denote the generalized bi-sorted order on $K[\underline{X}]$. Let $\mathfrak{I}$ the toric ideal of the monomial subring $K[F]$, where F is the minimal generating set of L consisting of square-free monomials. Let $\mathcal{G}$ be the graph whose edges are the generators of the ideal $\mathrm{in}_\prec(\mathfrak{I})$. Then

$$\begin{aligned} E(\mathcal{G}) = \{&X_{u_1\cdots u_p\,\bullet\cdots\bullet;\,v_1\cdots v_h}\,X_{u'_1\cdots u'_p\,\bullet\cdots\bullet;\,v'_1\cdots v'_h}\,,\\ &X_{u_1u_2\cdots u_q;\,\bullet\bullet\cdots\bullet}\,X_{u'_1u'_2\cdots u'_q;\,\bullet\bullet\cdots\bullet},\\ &X_{u_1\cdots u_p\,\bullet\cdots\bullet;\,v_1\cdots v_h}\,X_{u'_1u'_2\cdots u'_q;\,\bullet\bullet\cdots\bullet}\quad \text{such that}\\ \text{gen bi-sort}\,(u_1u'_1\cdots u_pu'_p\cdots u_qu'_q;\,v_1v'_1\cdots v_hv'_h) = z_1\cdots z_{2p}\cdots z_{2q};\,w_1\cdots w_{2h}\}\,, \end{aligned}$$

where $X_{z_1z_3\cdots z_{2p-1}\,\bullet\cdots\bullet;\,w_1w_3\cdots w_{2h-1}}X_{z_2z_4\cdots z_{2p}\,\bullet\cdots\bullet;\,w_2w_4\cdots w_{2h}}$,
$X_{z_1z_3\cdots z_{2q-1};\,\bullet\bullet\cdots\bullet}\,X_{z_2z_4\cdots z_{2q};\,\bullet\bullet\cdots\bullet}$,
$X_{z_1z_3\cdots z_{2p-1}\,\bullet\cdots\bullet;\,v_1v_2\cdots v_h}\,X_{z_2z_4\cdots z_{2p}\,z_{2p+1}\cdots z_q;\,\bullet\bullet\cdots\bullet}$
represent the second terms of the marked binomials in $K[\underline{X}]$.

Proof. See [1], Theorem 2.1, for computation of the Gröbner basis of $\mathfrak{I}$.

Example 6 In $K[\,Y_1,\ldots,Y_5;Z_1,Z_2\,]$, let $L = I_2\,J_2 + I_4$, where
$I_2 = (Y_1\,Y_2,\ldots,Y_1\,Y_5,\ Y_2\,Y_3,\ldots,Y_4\,Y_5)$, and $J_2 = (Z_1\,Z_2)$,
$I_4 = (Y_1\,Y_2\,Y_3\,Y_4,\ Y_1\,Y_2\,Y_3\,Y_5,\ Y_1\,Y_2\,Y_4\,Y_5,\ Y_1\,Y_3\,Y_4\,Y_5,\ Y_2\,Y_3\,Y_4\,Y_5)$.

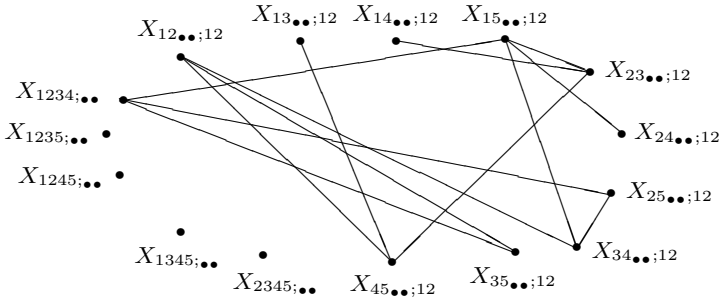
Let $\mathcal{G}_{T_{(5,4),\,(2,2)}}$ be the graph whose vertices are the 15 variables

$$X_{12_{\bullet\bullet};12},\ X_{13_{\bullet\bullet};12},\ X_{14_{\bullet\bullet};12},\ X_{15_{\bullet\bullet};12},\ X_{23_{\bullet\bullet};12},$$

$$X_{24_{\bullet\bullet};12},\ X_{25_{\bullet\bullet};12},\ X_{34_{\bullet\bullet};12},\ X_{35_{\bullet\bullet};12},\ X_{45_{\bullet\bullet};12},$$
$$X_{1234;_{\bullet\bullet}},\ X_{1235;_{\bullet\bullet}},\ X_{1245;_{\bullet\bullet}},\ X_{1345;_{\bullet\bullet}},\ X_{2345;_{\bullet\bullet}},$$

and whose edges are the initial not generalized bi-sorted terms of the Gröbner basis of $\mathfrak{I}_{T_{(5,4),\,(2,2)}}$, as computed in [1], Example 2.3. Then

$$\begin{aligned} E(\mathcal{G}_{T_{(5,4),\,(2,2)}}) = \{&X_{12_{\bullet\bullet};12}\,X_{34_{\bullet\bullet};12},\ X_{12_{\bullet\bullet};12}\,X_{35_{\bullet\bullet};12},\ X_{12_{\bullet\bullet};12}\,X_{45_{\bullet\bullet};12},\\ &X_{13_{\bullet\bullet};12}\,X_{45_{\bullet\bullet};12},\ X_{14_{\bullet\bullet};12}\,X_{23_{\bullet\bullet};12},\ X_{15_{\bullet\bullet};12}\,X_{23_{\bullet\bullet};12},\\ &X_{15_{\bullet\bullet};12}\,X_{24_{\bullet\bullet};12},\ X_{15_{\bullet\bullet};12}\,X_{34_{\bullet\bullet};12},\ X_{15_{\bullet\bullet};12}\,X_{1234;_{\bullet\bullet}},\\ &X_{23_{\bullet\bullet};12}\,X_{45_{\bullet\bullet};12},\ X_{25_{\bullet\bullet};12}\,X_{34_{\bullet\bullet};12},\ X_{25_{\bullet\bullet};12}\,X_{1234;_{\bullet\bullet}},\ X_{35_{\bullet\bullet};12}\,X_{1234;_{\bullet\bullet}}\} \end{aligned}$$



Note that the graph contains complete subgraphs.

Theorem 8 Let $L = I_p J_q + I_h J_k$, $p+q = h+k$, be an ideal of mixed products. Let $\succ$ denote the generalized bi-sorted order on $K[\underline{X}]$. Let $\mathfrak{I}$ the toric ideal of the monomial subring $K[F]$, where F is the minimal generating set of L consisting of square-free monomials. Let $\mathcal{G}$ be the graph whose edges are the generators of the ideal $\text{in}_{\prec}(\mathfrak{I})$.
Then elements in $E(\mathcal{G})$ are square-free quadratic monomials.

Proof. See [1], Theorem 2.1.

3 An approach to security field

In this section we would like to suggest some ideas to utilize the previous arguments for approaching to security problems.

The fact that the toric ideal $\mathfrak{I} \subset K[F]$ have a Gröbner basis of degree 2 helps us to construct simple combinatorial objects such as the graphs.

Classically, if $\mathfrak{I}$ is an ideal of a polynomial ring, we define *initial complex* $\text{in}_{\succ}(\mathfrak{I})$ to be the simplicial complex of the non-faces (see [7]).

But, in other way, we have utilized directly $\mathrm{in}_{\prec}(\mathfrak{I})$ to construct a graph. We will call *auxiliary graph* such a graph.

The difficulty to make out the auxiliary graph is the key for security.

Let's take in consideration Example 6 to explain our procedure in order to obtain a high level of security.

1st step

Determine a reduced Gröbner basis $\mathcal{H}$ for the toric ideal $\mathfrak{I}$ of $L = I_2\, J_2 + I_4$, marking the initial terms of the binomials in $\mathcal{H}$ for two different orders, the generalized bi-sorted order and the lexicographic order.

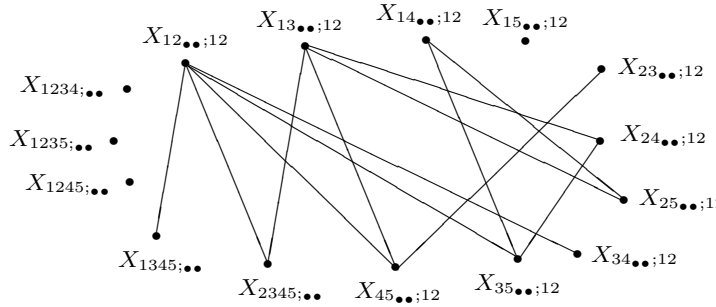
Here we write the reduced Gröbner basis $\mathcal{H}$ of $\mathfrak{I}$ where underline the initial terms in the lexicographic order.

$$\{\underline{X_{12_{\bullet\bullet};12}\, X_{34_{\bullet\bullet};12}} - X_{13_{\bullet\bullet};12}\, X_{24_{\bullet\bullet};12}\,,\ \underline{X_{12_{\bullet\bullet};12}\, X_{35_{\bullet\bullet};12}} - X_{13_{\bullet\bullet};12}\, X_{25_{\bullet\bullet};12}\,,$$
$$\underline{X_{12_{\bullet\bullet};12}\, X_{45_{\bullet\bullet};12}} - X_{14_{\bullet\bullet};12}\, X_{25_{\bullet\bullet};12}\,,\ \underline{X_{13_{\bullet\bullet};12}\, X_{45_{\bullet\bullet};12}} - X_{14_{\bullet\bullet};12}\, X_{35_{\bullet\bullet};12}\,,$$
$$X_{14_{\bullet\bullet};12}\, X_{23_{\bullet\bullet};12} - \underline{X_{13_{\bullet\bullet};12}\, X_{24_{\bullet\bullet};12}}\,,\ X_{15_{\bullet\bullet};12}\, X_{23_{\bullet\bullet};12} - \underline{X_{13_{\bullet\bullet};12}\, X_{25_{\bullet\bullet};12}}\,,$$
$$X_{15_{\bullet\bullet};12}\, X_{24_{\bullet\bullet};12} - \underline{X_{14_{\bullet\bullet};12}\, X_{25_{\bullet\bullet};12}}\,,\ X_{15_{\bullet\bullet};12}\, X_{34_{\bullet\bullet};12} - \underline{X_{14_{\bullet\bullet};12}\, X_{35_{\bullet\bullet};12}}\,,$$
$$\underline{X_{23_{\bullet\bullet};12}\, X_{45_{\bullet\bullet};12}} - X_{24_{\bullet\bullet};12}\, X_{35_{\bullet\bullet};12}\,,\ X_{25_{\bullet\bullet};12}\, X_{34_{\bullet\bullet};12} - \underline{X_{24_{\bullet\bullet};12}\, X_{35_{\bullet\bullet};12}}\,;$$
$$X_{15_{\bullet\bullet};12}\, X_{1234;_{\bullet\bullet}} - \underline{X_{12_{\bullet\bullet};12}\, X_{1345;_{\bullet\bullet}}}\,,\ X_{25_{\bullet\bullet};12}\, X_{1234;_{\bullet\bullet}} - \underline{X_{12_{\bullet\bullet};12}\, X_{2345;_{\bullet\bullet}}}\,,$$
$$X_{35_{\bullet\bullet};12}\, X_{1234;_{\bullet\bullet}} - \underline{X_{13_{\bullet\bullet};12}\, X_{2345;_{\bullet\bullet}}}\}\,.$$

2nd step

Let $\mathcal{G}_{\mathrm{lex}}$ be the graph having the same vertices of $\mathcal{G}_{T_{(5,4),\,(2,2)}}$ and edges the initial terms of $\mathcal{H}$ in the lexicographic order. Then

$$\begin{aligned} E(\mathcal{G}_{\mathrm{lex}}) = \{&X_{12_{\bullet\bullet};12}\, X_{34_{\bullet\bullet};12}\,,\ X_{12_{\bullet\bullet};12}\, X_{35_{\bullet\bullet};12}\,,\ X_{12_{\bullet\bullet};12}\, X_{45_{\bullet\bullet};12},\\ &X_{12_{\bullet\bullet};12}\, X_{1345;_{\bullet\bullet}}\,,\ X_{12_{\bullet\bullet};12}\, X_{2345;_{\bullet\bullet}}\,,\ X_{13_{\bullet\bullet};12}\, X_{24_{\bullet\bullet};12},\\ &X_{13_{\bullet\bullet};12}\, X_{25_{\bullet\bullet};12}\,,\ X_{13_{\bullet\bullet};12}\, X_{45_{\bullet\bullet};12}\,,\ X_{13_{\bullet\bullet};12}\, X_{2345;_{\bullet\bullet}},\\ X_{14_{\bullet\bullet};12}\, X_{25_{\bullet\bullet};12}\,,\ &X_{14_{\bullet\bullet};12}\, X_{35_{\bullet\bullet};12}\,,\ X_{23_{\bullet\bullet};12}\, X_{45_{\bullet\bullet};12}\,,\ X_{24_{\bullet\bullet};12}\, X_{35_{\bullet\bullet};12}\} \end{aligned}$$



Let's show how to have security.

3^{rd} step. The communicator transmits $\mathcal{G}_{\text{lex}}$.

4^{th} step. The receiver changes the message and draws $\mathcal{G}_{T_{(5,4),\,(2,2)}}$.

5^{th} step. The graph that must be utilized is $\mathcal{G}_{T_{(5,4),\,(2,2)}}$.

Since data must be condensed the more possible, we can follow a better way to transmit the previous information.

In particular, it is possible to give a sequence of integers that individualizes univocally the ideal of mixed products.

As regards our specific case, $L = I_pJ_q + I_hJ_k$ can be assigned through the sequence

$$n = 5, \quad m = 2, \quad p = 2, \quad q = 2, \quad h = 4, \quad k = 0\,.$$

Corollary 1 Let (n, m, p, q, h, k) be an ideal of mixed products. Suppose that the lexicographic Gröbner basis of the toric ideal of $K[F]$ is square-free quadratic. Then the generalized bi-sorted graph is an auxiliary graph.

References

[1] Imbesi M., Restuccia G. – *Bi-sorted orders and applications*, to appear in Afrika Matematika (2009).

[2] Kreuzer M., Robbiano L. – *Computational Commutative Algebra 2*, Springer-Verlag, Berlin (2005).

[3] Miller E., Sturmfels B. – *Combinatorial Commutative Algebra*, Springer GTM **227** (2004).

[4] Restuccia G. – *Monomial orders in the vast world of Mathematics*, Appl. Ind. Maths in Italy II, Ser. Adv. in Maths for Appl. Sc. **75** (2007), 525–536.

[5] Restuccia G., Villarreal R.H. – *On the normality of monomial ideals of mixed products*, Commun. Algebra, **29**, 8 (2001), 3571–3580.

[6] Robbiano L., Sweedler M. – *Subalgebra bases*, Proc. Comm. Alg. Salvador, Bruns and Simis eds., Springer LNM **1430** (1990), 61–87.

[7] Sturmfels B. – *Gröbner Bases and Convex Polytopes*, AMS Univ. Lect. Ser. **8** (1996).

RENDICONTI DEL CIRCOLO MATEMATICO DI PALERMO
Serie II, Suppl. 81 (2009), pp. 237-246

MINIMAL VERTEX COVERS AND MATCHING PROBLEMS ON PLANAR GRAPHS

MONICA LA BARBIERA

Abstract. We are interested to study the minimal vertex covers and the maximal matchings of a class of bipartite planar graphs useful to analyze connection problems.
Classification AMS: 05C99.

Introduction

A graph is a symbolic representation of a network and of its connectivity. More precisely a graph is a geometric model for several problems in which there are sets with relations between the elements. For this reason a graph can be used to analyze connection problems (for example street nets, railway nets, telephone nets, infrastructure nets, assignment problems). In particular urban and territorial analysis uses planar graphs. A graph is said planar if it is embedded in the plane that is each pair of edges is intersected only in common vertices and it is divided in some regions by its edges. A street net, the plant of a building can be represented by a planar graph.

In this paper we consider bipartite planar graphs. A graph is said bipartite if its vertex set can be partitioned into disjoint subsets V_1 and V_2, and every edge joins a vertex of V_1 with a vertex of V_2. More precisely we are interested in studying two sets associated to a bipartite planar graph G: the minimal vertex cover of G and the maximal matching of G. The problem of the vertex cover is a classic optimization problem. It consists in finding a vertex cover of minimum cardinality, that is a minimal subset $\mathcal{A}$ of the vertex set of G such that each edge of G is incident with one vertex in $\mathcal{A}$. The matching problems are particular optimization problems that require the subdivision in different pairs of elements linked by some relations. The matchings of a graph are studied for their applications as models of real problems, the so called assignment problems of maximum cardinality. For example they are useful to assignee employees to tasks or machines to production jobs or fleet of aircrafts to particular trips.
In particular, we consider the class of bipartite planar graphs B_{2t}, where $t \geq 1$ is an integer and $r = 2t$ is the number of its regions. These graphs have been introduced in [1] and they are known for their application in connection problems and in planimetry. In [4] some algebraic invariants of

their edge ideal are studied. In this paper we study the minimal vertex covers of the graphs B_{2t} using their geometry in the plane and its connection to the bipartite matching. As a consequence we extract specific informations about some algebraic aspects of the graphs B_{2t}. The paper is organized as follows. In the section 1 the minimal vertex covers of the bipartite planar graphs B_{2t} are described in order to apply this result to solve a security problem. Some algebraic aspects are connected to vertex covers. In fact there is a correspondence between the minimal vertex covers and the minimal primes of the edge ideal. If all minimal vertex covers have the same size, then the graph is unmixed. In [6] the unmixed bipartite graphs are characterized. Now we verify that the planar graphs B_{2t} are not unmixed. In section 2 the problem to find maximal matchings for the bipartite graphs B_{2t} is studied using their geometry in the plane and the connections to the minimal vertex covers. In [5] it is given the notion of matching of König type, that is a collection $e_1, \dots, e_g$ of pairwise disjoint edges of a graph such that the union of the vertices in which $e_1, \dots, e_g$ are incident is the vertex set and g is equal to the height of the edge ideal. We prove that the graphs B_{2t}, for t odd, have perfect matchings of König type and we give a complete description of these matchings.

The author is grateful to Professor Rosanna Utano for useful discussions about the results of this paper.

1. Planar graphs and Minimal vertex covers

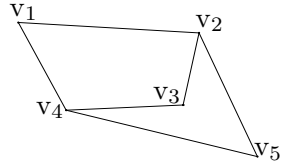
Let G be a graph with vertex set $V(G) = \{v_1, \dots, v_n\}$ and a collection $E(G)$ of subsets of V, that consists of pairs $\{v_i, v_j\}$, for some $v_i, v_j \in V$, called edges.

Definition 1.1. *A graph G is bipartite if its vertex set V can be partitioned into disjoint subsets V_1 and V_2, and every edge joins a vertex of V_1 with a vertex of V_2.*

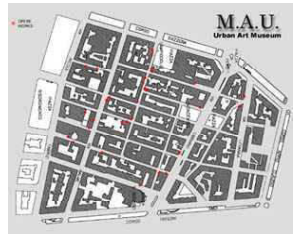
Definition 1.2. A bipartite graph G is said complete if all the vertices of V_1 are joined to all the vertices of V_2. If V_1 and V_2 have n and m vertices respectively, we denote such a complete bipartite graph by $K_{n,m}$.

Definition 1.3. A graph is said *planar* if it can be embedded in the plane and its edges are incident only in the common vertices ([3]).

Example 1.1. The following graph on the vertex set $V = \{v_1, v_2, v_3, v_4, v_5\}$ is planar.



Now we consider an application in the direction of the topic of security. More precisely we consider a security problem that can be solved via graph theory.
Problem: How is it possible to set the minimal number of guards in a museum such that they can control any points of the museum in the figure?

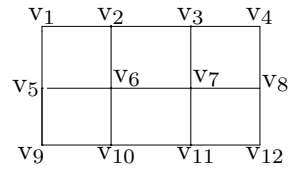


A suitable model to represent this situation is a planar graph and the problem can be solved studying its minimal vertex cover. The geometric model that we use is the class of bipartite planar graphs B_{2t} introduced in [1].

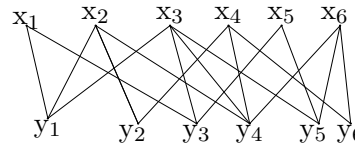
Let B_{2t} be the planar graph with $r = 2t$ regions, $t \geq 1$ an integer, with vertex set $V(B_{2t}) = \{v_1, \ldots, v_{3t+3}\}$ and edge set $E(B_{2t}) = \{\{v_i, v_{i+1}\} | 1 \leq i \leq 3t+2, \quad i \neq t+1, 2t+2, 3t+3\} \cup \{\{v_i, v_{i+t+1}\} | 1 \leq i \leq 2t+2\}$.
B_{2t} is a planar graph by Kuratowski's Theorem, for all $t \geq 1$.

Remark 1.1. B_{2t} is a bipartite planar graph ([4]). The vertex set of B_{2t} can be partitioned into disjoint subsets V_1 and V_2, with $|V_1| + |V_2| = 3t+3$. We distinguishing the two following cases:
• t even
$V_1 = \{v_i | i \quad odd, 1 \leq i \leq 3t+3\}$ with $|V_1| = \frac{3t+4}{2}$
$V_2 = \{v_i | i \quad even, 1 \leq i \leq 3t+3\}$ with $|V_2| = \frac{3t+2}{2}$
• t odd
$V_1 = \{v_1, v_3, \ldots, v_t\} \cup \{v_{2+(t+1)}, v_{4+(t+1)}, \ldots, v_{t+1+(t+1)}\} \cup \{v_{1+(2t+2)}, v_{3+(2t+2)}, \ldots, v_{t+(2t+2)}\}$,
$V_2 = \{v_2, v_4, \ldots, v_{t+1}\} \cup \{v_{1+(t+1)}, v_{3+(t+1)}, \ldots, v_{t+(t+1)}\} \cup \{v_{2+(2t+2)}, v_{4+(2t+2)}, \ldots, v_{t+1+(2t+2)}\}$,
Then $|V_1| = |V_2| = \frac{3t+3}{2}$.

Example 1.2. $G = B_6$, with $V(B_6) = \{v_1, \ldots, v_{12}\}$ and
$E(B_6) = \{\{v_1, v_2\}, \{v_2, v_3\}, \{v_3, v_4\}, \{v_5, v_6\}, \{v_6, v_7\}, \{v_7, v_8\}, \{v_9, v_{10}\}, \{v_{10}, v_{11}\}, \{v_{11}, v_{12}\}, \{v_1, v_5\}, \{v_2, v_6\}, \{v_3, v_7\}, \{v_4, v_8\}, \{v_5, v_9\}, \{v_6, v_{10}\}, \{v_7, v_{11}\}, \{v_8, v_{12}\}\}$



$V(B_6)$ can be partitioned into disjoint subsets:
$V(B_6) = \{v_1, v_3, v_6, v_8, v_9, v_{11}\} \cup \{v_2, v_4, v_5, v_7, v_{10}, v_{12}\} = V_1 \cup V_2$.
If we rename $\{x_1, \ldots, x_6\}$ the vertices of V_1 and $\{y_1, \ldots, y_6\}$ the vertices of V_2 , then the edge set can be written:
$E(B_6) = \{\{x_1, y_1\}, \{x_1, y_3\}, \{x_2, y_1\}, \{x_2, y_2\}, \{x_2, y_4\}, \{x_3, y_1\}, \{x_3, y_3\}, \{x_3, y_4\}, \{x_3, y_5\}, \{x_4, y_2\}, \{x_4, y_4\}, \{x_4, y_6\}, \{x_5, y_3\}, \{x_5, y_5\}, \{x_6, y_4\}, \{x_6, y_5\}, \{x_6, y_6\}\}$



The two pictures represent the same planar graph B_6.

Now we study the minimal vertex covers of B_{2t}.

Definition 1.4. Let G be a graph with vertex set $V(G)$. A subset $\mathcal{A} \subset V(G)$ is called a minimal vertex cover for G if:
(1) each edge of G is incident with one vertex in $\mathcal{A}$;
(2) there is no proper subset of $\mathcal{A}$ with this property.

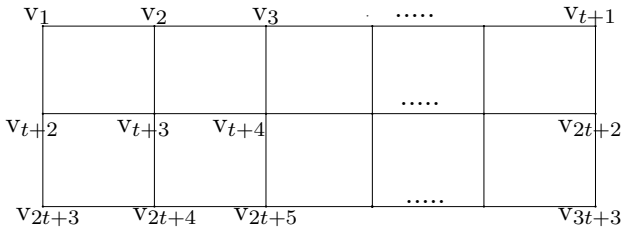
If $\mathcal{A}$ satisfies condition (1) only, then $\mathcal{A}$ is called a *vertex cover* of G and $\mathcal{A}$ is said to cover all the edges of G.
The smallest number of vertices in any minimal vertex cover of G is said *vertex covering number*. We denote it by $\alpha_0(G)$.

Proposition 1.1. *Let B_{2t} be the bipartite planar graph with $r = 2t$ regions and $t \geq 1$. Then:*

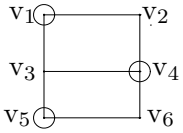
$$\alpha_0(B_{2t}) = \begin{cases} \frac{3}{4}r + \frac{3}{2} & \text{if } t \text{ odd} \\ \frac{3}{4}r + 1 & \text{if } t \text{ even} \end{cases}$$

Proof. Let $V(B_{2t}) = \{v_1, \ldots, v_{3t+3}\}$ and $E(B_{2t}) = \{\{v_i, v_{i+1}\} | 1 \leq i \leq 3t+2, \ \ i \neq t+1, 2t+2, 3t+3\} \cup \{\{v_i, v_{i+t+1}\} | 1 \leq i \leq 2t+2\}$. Hence the representation of B_{2t} in the plane is a sequence of squares without chords

disposed in 2 rows and t columns



For $t = 1$, $\alpha_0(B_2) = 3$



and $\mathcal{A}(B_2) = \{v_1, v_4, v_5\}$, $\mathcal{A}'(B_2) = \{v_2, v_3, v_6\}$ are minimal vertex covers of B_2.

For $t > 1$ a minimal vertex cover of $\alpha_0(B_{2t})$ is given by adjoining to the minimal vertex cover of B_2 one vertex for each even column and two vertices for each odd column. Hence

1) If t is odd

$$\alpha_0(B_{2t}) = \alpha_0(B_2) + 1(\frac{t-1}{2}) + 2(\frac{t-1}{2}) = \frac{3}{2}t + \frac{3}{2} = \frac{3}{4}r + \frac{3}{2},$$

where $\frac{t-1}{2}$ is the number of the even (odd) columns in the graph for $t > 1$.

2) If t is even

$$\alpha_0(B_{2t}) = \alpha_0(B_2) + 1(\frac{t}{2}) + 2(\frac{t}{2} - 1) = \frac{3}{2}t + 1 = \frac{3}{4}r + 1,$$

where $\frac{t}{2}$ is the number of the even columns and $\frac{t}{2} - 1$ is the number of the odd columns of the graph for $t > 1$. □

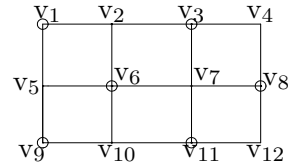
Proposition 1.2. *Let B_{2t} be the bipartite planar graph with $r = 2t$ regions and $t \geq 1$. Then the minimal vertex covers with cardinality $\alpha_0(B_{2t})$ are:*

$$\mathcal{A}(B_{2t}) = \begin{cases} V_1, V_2 & \text{if } t \text{ odd} \\ V_2 & \text{if } t \text{ even} \end{cases}$$

Proof. If t is odd $\alpha_0(B_{2t}) = \frac{3t+3}{2}$, that is the cardinality of the vertex sets V_1 and V_2, where $V_1 = \{v_1, v_3, \ldots, v_t\} \cup \{v_{2+(t+1)}, v_{4+(t+1)}, \ldots, v_{t+1+(t+1)}\} \cup \{v_{1+(2t+2)}, v_{3+(2t+2)}, \ldots, v_{t+(2t+2)}\}$ and $V_2 = \{v_2, v_4, \ldots, v_{t+1}\} \cup \{v_{1+(t+1)}, v_{3+(t+1)}, \ldots, v_{t+(t+1)}\} \cup \{v_{2+(2t+2)}, v_{4+(2t+2)}, \ldots, v_{t+1+(2t+2)}\}$ are two minimal sets of vertices that cover all edges of B_{2t}.

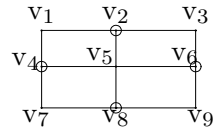
If t is even $\alpha_0(B_{2t}) = \frac{3t+2}{2}$, that is the cardinality of the vertex set $V_2 = \{v_i | i \text{ even}, 1 \leq i \leq 3t+3\}$. V_2 is the only subset of vertices with cardinality $\alpha_0(B_{2t})$ that covers all the edges of B_{2t}. □

Example 1.3. 1) $G = B_6$, $r = 6$, $t = 3$ odd



$\mathcal{A}_1(B_6) = V_1 = \{v_1, v_3, v_6, v_8, v_9, v_{11}\}$; $\mathcal{A}_2(B_6) = V_2 = \{v_2, v_4, v_5, v_7, v_{10}, v_{12}\}$
$\alpha_0(B_6) = |\mathcal{A}_1(B_6)| = |\mathcal{A}_2(B_6)| = 6$

2) $G = B_4$, $r = 4$, $t = 2$ even



$\mathcal{A}(B_4) = V_2 = \{v_2, v_4, v_6, v_8\}$
$\alpha_0(B_4) = |\mathcal{A}(B_4)| = 4$.

Now we consider some algebraic aspects linked to the minimal vertex covers of a graph G.
Let $R = K[X_1, \ldots, X_n]$ be the polynomial ring over a field K with one variable X_i for each vertex v_i. The edge ideal $I(G)$ associated to a graph G is the ideal of R generated by the square-free monomials of degree two X_iX_j such that $\{v_i, v_j\} \in E(G)$ for $1 \leq i \leq j \leq n$:

$$I(G) = (\{X_iX_j | \{v_i, v_j\} \in E(G)\}).$$

We recall the one to one correspondence between the minimal vertex covers of G and minimal primes of $I(G)$. In fact $\wp$ is a minimal prime ideal of $I(G)$ if and only if $\wp = (\mathcal{A})$ for some minimal vertex cover $\mathcal{A}$ of G ([7], 6.1.16). Thus the primary decomposition of the edge ideal of G is given by $I(G) = (\mathcal{A}_1) \cap \cdots \cap (\mathcal{A}_p)$, where $\mathcal{A}_1, \ldots, \mathcal{A}_p$ are the minimal vertex covers of G. Hence G is an *unmixed* graph if and only if all the minimal vertex covers of G have the same cardinality.
For the bipartite planar graphs B_{2t} we have the following results.

Corollario 1.1. *Let $\mathcal{I}$ be the edge ideal of B_{2t} with $r = 2t$ regions. Then:*

$$ht(\mathcal{I}) = \begin{cases} \frac{3}{4}r + \frac{3}{2} & \text{if } t \text{ odd} \\ \frac{3}{4}r + 1 & \text{if } t \text{ even} \end{cases}$$

Proof. It is known that the vertex covering number $\alpha_0(G)$ is equal to the height of the edge ideal $ht(I(G))$ ([7], 6.1.18). Hence the assertion follows by Proposition 1.1. □

Recall the following:

Theorem 1.1. *([6], Theorem 1.1)*
Let G be a bipartite graph without isolated vertices. Then G is unmixed if and only if there is a bipartition $V_1 = \{x_1, \ldots, x_m\}$, $V_2 = \{y_1, \ldots, y_m\}$ of G such that:
1) $\{x_i, y_i\} \in E(G)$ for all i;
2) if $\{x_i, y_j\}$ and $\{x_j, y_k\}$ are in $E(B_{2t})$ and i, j, k are distinct, then $\{x_i, y_k\} \in E(B_{2t})$.

Proposition 1.3. *B_{2t} is not unmixed for all $t > 0$.*

Proof. If t is odd, using the characterization of unmixed bipartite graphs (Theorem 1.1), it is enough to verify that: if $\{x_i, y_j\}, \{x_j, y_k\} \in E(B_{2t})$, then $\{x_i, y_k\} \notin E(B_{2t})$.
Let $V_1 = \{v_1, v_3, \ldots, v_t\} \cup \{v_{2+(t+1)}, v_{4+(t+1)}, \ldots, v_{t+1+(t+1)}\} \cup \{v_{1+(2t+2)}, v_{3+(2t+2)}, \ldots, v_{t+(2t+2)}\}$ and $V_2 = \{v_2, v_4, \ldots, v_{t+1}\} \cup \{v_{1+(t+1)}, v_{3+(t+1)}, \ldots, v_{t+(t+1)}\} \cup \{v_{2+(2t+2)}, v_{4+(2t+2)}, \ldots, v_{t+1+(2t+2)}\}$ the two disjoint vertex sets of B_{2t}. Replacing with $\{x_1, \ldots, x_{\frac{3t+3}{2}}\}$ the vertices of V_1 and with $\{y_1, \ldots, y_{\frac{3t+3}{2}}\}$ the vertices of V_2, then we have $v_1 = x_1$, $v_{1+(t+1)} = y_{\frac{t+1}{2}+1}$, $v_{2+(t+1)} = x_{\frac{t+1}{2}+1}$, $v_{3+(t+1)} = y_{\frac{t+1}{2}+2}$.
Then $\{x_1, y_{\frac{t+1}{2}+1}\}, \{x_{\frac{t+1}{2}+1}, y_{\frac{t+1}{2}+2}\} \in E(B_{2t})$, but $\{x_1, y_{\frac{t+1}{2}+2}\} \notin E(B_{2t})$.
2) If t is even, it is sufficient to observe that V_1 and V_2 are two minimal vertex covers with $|V_1| > |V_2|$.
Hence B_{2t} is not unmixed. □

2. Perfect matchings on planar graphs

Let G be a graph. A minimal vertex cover $\mathcal{A}$ of G is linked to the *set of the independent edges*. The edges of G that have no vertex in common are called *independent edges*. The *independence number* of a graph G, denoted by $\beta_1(G)$, is the maximum number of its independent edges.

Definition 2.1. A matching of G is a set $\mathcal{M}$ of independent edges.

G has a perfect matching if G has an even number of vertices and there is a set of independent edges "covering" all the vertices. This means that there is a pairing off of all the vertices of G.

Definition 2.2. A maximum matching is a matching $\mathcal{M}$ such that every other matching $\mathcal{M}'$ satisfies $|\mathcal{M}'| < |\mathcal{M}|$. In this case $|\mathcal{M}| = \beta_1(G)$.

Remark 2.1. Let $\mathcal{M}$ be a maximum matching and $\mathcal{A}$ a minimal cover of a graph G. Note that each edge of $\mathcal{M}$ must be covered by at least one vertex of $\mathcal{A}$ and each vertex of $\mathcal{A}$ can cover at most one edge of $\mathcal{M}$. It follows: $\beta_1(G) \leq \alpha_0(G)$.

Definition 2.3. A perfect matching of König type of a graph G is a collection $e_1, \ldots, e_g$ of pairwise disjoint edges such that the union of the vertices in which $e_1, \ldots, e_g$ are incident is the vertex set of B_{2t} and g is equal to the height of $I(G)$.

Remark 2.2. A graph G satisfies the König property if the maximum number of independent edges of G equals the height of $I(G)$. Hence a graph with a perfect matching of König type has the König property. In [2] it is proved that the converse is true for unmixed graphs.

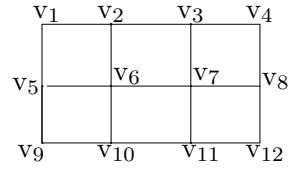
We are interested in the bipartite matching problem, that is to find a matching with the maximum number of edges. Clearly, the size of any matching is at most the size of any vertex cover. This follows from the fact that, given any matching $\mathcal{M}$, a vertex cover $\mathcal{A}$ must contain at least one of the vertices of each edge in $\mathcal{M}$. The maximum size of a matching is at most the minimum cardinality of a vertex cover. More precisely, it is known the following result.

Theorem 2.1. *(König,* [7]*, 6.1.7)*
For any bipartite graph G, the size of a maximum matching is equal to the size of a minimum vertex cover, that is $\beta_1(G) = \alpha_0(G)$.

Proposition 2.1. *Let B_{2t} be the bipartite planar graph with $r = 2t$ regions and t odd. Each maximal matching is a perfect matching of cardinality $\frac{3}{4}r + \frac{3}{2}$.*

Proof. B_{2t} is a bipartite graph, then by Theorem 2.1 $\beta_1(B_{2t}) = \alpha_0(B_{2t})$. Hence any vertex of the minimum vertex cover is incident upon independent edge. Then B_{2t} has maximal matching with cardinality $\beta_1(B_{2t}) = |\mathcal{M}(B_{2t})| = |V_1| = |V_2| = \frac{3}{4}r + \frac{3}{2}$, $r = 2t$. Moreover B_{2t} has an even number of vertices and $|V_1| = |V_2|$, this means that there is a pairing off of all the vertices of B_{2t}. It follows that each maximal matching is a perfect matching. □

Example 2.1. $G = B_6$, $r = 6$, $t = 3$ odd



A maximal perfect matching is

$$\mathcal{M} = \{\{v_1, v_2\}, \{v_3, v_4\}, \{v_5, v_6\}, \{v_7, v_8\}, \{v_9, v_{10}\}, \{v_{11}, v_{12}\}\}$$

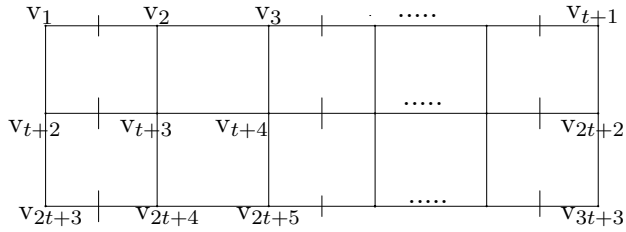
$\beta_1(B_6) = |\mathcal{M}| = 6 = \alpha_0(B_6)$

We give a description of the maximal perfect matchings of B_{2t}, t odd.

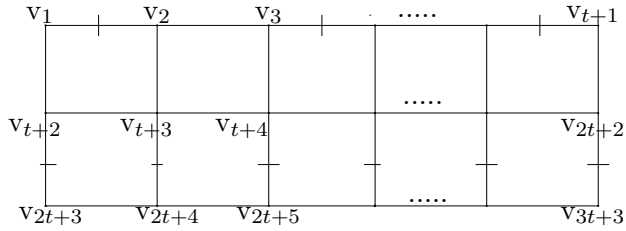
Proposition 2.2. *Let B_{2t} be the bipartite planar graph with $r = 2t$ regions and t odd. B_{2t} has perfect matching of König type.*

Proof. $V_1 = \{v_1, v_3, \ldots, v_t\} \cup \{v_{2+(t+1)}, v_{4+(t+1)}, \ldots, v_{t+1+(t+1)}\} \cup \{v_{1+(2t+2)}, v_{3+(2t+2)}, \ldots, v_{t+(2t+2)}\}$ and $V_2 = \{v_2, v_4, \ldots, v_{t+1}\} \cup \{v_{1+(t+1)}, v_{3+(t+1)}, \ldots, v_{t+(t+1)}\} \cup \{v_{2+(2t+2)}, v_{4+(2t+2)}, \ldots, v_{t+1+(2t+2)}\}$ are minimal vertex covers of B_{2t} with cardinality $\alpha_0(B_{2t}) = \frac{3}{4}r + \frac{3}{2}$. Notice that $\beta_1(B_{2t}) = \alpha_0(B_{2t}) = \frac{3}{4}r + \frac{3}{2}$ and any vertex of the minimum vertex cover is incident upon independent edge. Hence by the geometry of the planar graph B_{2t} we obtain the following maximal matchings:

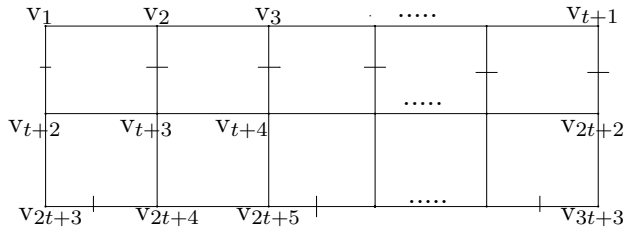
• $\mathcal{M} = \{\{v_{i-1}, v_i\} | i \text{ even}, 2 \leq i \leq 3t+3\}$



• $\mathcal{M} = \{\{v_{i-1}, v_i\} | i \text{ even}, 2 \leq i \leq t+1\} \cup \{\{v_{i+t}, v_{i+2t+1}\} | 2 \leq i \leq t+2\}$



• $\mathcal{M} = \{\{v_i, v_{i+t+1}\} | 1 \leq i \leq t+1\} \cup \{\{v_{i-1}, v_i\} | i \text{ even}, 2t+4 \leq i \leq 3t+3\}$

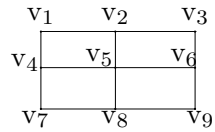


The other perfect matchings of König type are obtained by the previous schemes by different combinations of the columns in the representation of the graph. In all the cases $\mathcal{M}$ is a matching such that $|\mathcal{M}| = \alpha_0(B_{2t}) =$

$ht(I(B_{2t}))$ and the union of the vertices in which the edges of $\mathcal{M}$ are incident is the vertex set of B_{2t}. Hence B_{2t} has perfect matchings of König type. □

Remark 2.3. Let B_{2t} be the bipartite planar graph with $r = 2t$ regions and t even. Each maximal matching $\mathcal{M}(B_{2t})$ is a complete matching from V_2 to V_1 (being $|V_2| < |V_1|$), this means that $\mathcal{M}(B_{2t})$ covers each vertex of V_2, but not all the vertices of V_1. In fact: $|\mathcal{M}(B_{2t})| = \beta_1(B_{2t}) = |V_2| = \frac{3}{4}r + 1$.

Example 2.2. $G = B_4$, $r = 4$, $t = 2$ even.
$V_1 = \{v_1, v_3, v_5, v_7, v_9\}$, $V_2 = \{v_2, v_4, v_6, v_8\}$



A maximal matching is $\mathcal{M} = \{\{v_1, v_2\}, \{v_4, v_5\}, \{v_7, v_8\}\{v_3, v_6\}\}$
$\beta_1(B_4) = |\mathcal{M}(B_4)| = 4 = \alpha_0(B_4) = |V_2|$.
All the vertices of V_2 are incident upon the edges of the maximal matching $\mathcal{M}$, but $\mathcal{M}$ does not cover all the vertices of V_1.

References

[1] L. R.Doering and T. Gunston, Algebras arising from bipartite planar graphs, *Comm. Alg.* **24** (1996), pp. 3589-3598.
[2] I. Gitler, E. Reyes and R. H. Villarreal, Blowup algebras of ideals of vertex covers of bipartite graphs, *Contemp. Math.*, **376** (2000), pp. 273-279.
[3] F. Harary, *Graph Theory*, Addison-Wesley, Reading, MA, 1972.
[4] M. La Barbiera, On Betti numbers of a class of bipartite planar graphs, *Supplemento ai Rendiconti del Circolo Matematico di Palermo*, Serie II, **80** (2008), pp. 201-210.
[5] S. Morey, E. Reyes and R. Villarreal, Cohen-Macaulay, shellable and unmixed clutters with a perfect matching of König type, *J. Pure Appl. Algebra*, **212**(7) (2008), pp 1770-1786.
[6] R. H. Villarreal, Unmixed bipartite graphs, *Revista Colombiana de Matematicas*, **41** (2007), pp. 393-395.
[7] R. H. Villarreal, *Monomial Algebras*, Monographs and Textbooks in Pure and Applied Mathematics, 238, Marcel Dekker, Inc., New York, 2001.

University of Messina, Department of Mathematics,, C.da Papardo, salita Sperone, 31, 98166 Messina, Italy
E-mail address: monicalb@libero.it

RENDICONTI DEL CIRCOLO MATEMATICO DI PALERMO
Serie II, Suppl. 81 (2009), pp. 247-259

RISK IN AGRICULTURAL FIRM: A MATHEMATICAL APPROACH

M. Lanfranchi* C. Giannetto** A. Puglisi***

Abstract

In order to assess the positive and negative impacts associated with the agricultural products it is inevitably necessary to make use of a large number of variables which characterize completely the changes taken in the production process. So, it is necessary to use an appropriate mathematical instrument, which is able to synthesize, conveniently, the results obtained in a representational space with dimension more limited than those used initially; retaining, however, as far as possible the informations obtained by the data of leaving. In this paper we propose a methodological approach that is able to solve the problem for the risk analysis in agricultural firm .

Keywords: *correlation matrix, factorial axes, social utility, risk.*

1 Introduction

This paper has been articulated in two main parts. The first particularly dwelled upon the different typologies of the risk towards which the agricultural contractor goes during the course of the firm's activity and it dwelled upon the effects caused by the taking place of the risky event in the making process of the entrepreneurial decisions. In the second part have been underlined the limits of the traditional research methods and it has been guaranteed the hypothesis to search in the ambit of the *mathematical theory* a probable application to what concerns the management of the risk in the ambit of the agricultural firm.

---

* The work is the result of a complete cooperation and it is, therefore, of responsability of both the authors. The material drawing up of **Introduction** and paraghraph ***2,*** are attribuiting to Maurizio Lanfranchi, paragraph ***1.1*** to Carlo Giannetto, paragraph ***1.2*** to Maurizio Lanfranchi and Carlo Giannetto paragraphs ***3*** and ***4*** to Alessandro Puglisi.

* Professor of Agricultural Economy and Policy, University of Messina – Department of Economic, Financial, Social, Environmental Science – Faculty of Economy - Piazza Pugliatti 1 - 98124 Messina (Italy). mlanfranchi@unime.it.

** PhD student of Development of Substainable Tourism, , University of Messina – Department of Economic, Financial, Social, Environmental Science – Faculty of Economy - Piazza Pugliatti 1 - 98124 Messina (Italy).

*** PhD student of Economic, Business disciplines and Quantitative Methods, University of Messina – Department S.E.A. – Faculty of Economy - Piazza Pugliatti 1 - 98124 Messina (Italy). puglisia@unime.it

The agricultural activity is one of the most unforeseeable economic activities, it is in non-stop process, too. For this reason it is necessary a continuous adjustment of the traditional methods of the economic-business analysis.
One of the basilar concepts of the study that has been carried out is that about the risk, that is about the eventuality of an unfavourable proceeding in the taking place of perspective happenings, and that till the passing of time hasn't change the future in the present (Corbella).
On an economic point of view, the concept of "the risk" refers to the possibility to have a deficit and to the cognitive asymmetry about the taking place of this deficit. Taking care of the firms, the deficit that could derive from the risky, future and uncertain event, can be identified with the unsuccessful achievement of the aim for which the firms have been created, that is the profit maximization attainable by the maximization of the function of the production and the minimization of the function of the cost.
The existence of shiftier and shiftier risks to the possibility of a minimizing human control is implied in the nature of the activity carried out by the agricultural firm. Analyzing one by one the typical risks of an agricultural firm and supposing that the entrepreneurial choices (of short or long-term) are direct exclusively towards the maximization of the profit and that the condition, by which the aforesaid function target results optimized, is represented by the minimization of the general economic risk of the firm and by its single components, it has been planned a prospect of analysis in which the different categories of firm's risk are considered as variable-constraint in comparison with the need for the maximization of the function target. In few words, it deals with a problem of "bound maximization" about which it's preliminarily necessary understand in what manner and in what measure the principal decision-making processes tinged to the govern of the agricultural firm influence and are influenced by particular risks that hang over it, and at last, how the afore-said interactions have repercussions on the patrimonial, economic and financial balance of the firm.

1.1 The analysis of the risks in an agricultural firm

The typologies of the risk that has to face an agricultural contractor who works in any outlet or transformation market are surely different from those that agricultural contractors have to face in other productive sectors. These differences derive above all from the fact that an agricultural firm has to act taking into consideration some factors that condition the activity of the agricultural contractor, they refer to the inelasticity of the biological cycles, to the restricted bargaining power, to the perishability of the agricultural products, to the short attention to the requirements of the market. Generally the risks that an agricultural contractor has to take into consideration are different and greater than those that a business contractor has to face. The different sources of uncertainty, that have relevancy on the profit of the agricultural firm, can be schematized in:

- atmospheric and biological risk;

- risk of a right combination of productive factors;
- financial risk;
- market risk;
- infrastructural risk;
- social and personal risk;
- institutional risk;
- emerging risk.

Atmospheric and biological risk

It is typical of the agricultural firm, it refers to all those natural events as the hail[1], intense cold, drought, intense rainy rainfalls, extreme temperatures, squall, that represent concrete and strong threats for the agricultural productions, while they have no effect on the productive activities of the other economic sectors. These events can cause and compromise the technical result of the agricultural firm and, consequently, the economic, patrimonial and financial balance of the agricultural activity. Another "typical" risk of the agricultural firm is the biological one that is referable to the action of the insects, cattle's diseases and virus that damage the production (for example the virus of the swine plague, foot-and-mouth disease, spongiform encephalopathy, avian virus, etc..[2]). The atmospheric risk[3] can be defined as an abiotic risk referable to atmospheric and chemical agents; on the contrary, the biological risk is a biotic risk, and different from the former it's possible face it by inner variables (prevention, tools of control, agronomic actions) that have to place it at the agricultural contractor's disposal.

The risk of a correct combination of productive factors

It happens when the agricultural contractor makes wrong choices about the use or the choice of the combination of available productive factors. The combinatorial order of a productive process is fundamental and it depends on the conditions of decision to coordinate heterogeneous but complementary activities (such as for example the herbage and woody farming, or the agricultural farming and the zootechnic activity). The process of these economic activities suggests the existence of a particular state of order considered as systematic one being it characterized by a cyclical progress of combined operations. If these operations weren't respected some productive damages (caused by systematic risks) could arise. All these negative elements can significantly influence the levels of company profitability both during the managerial phase and during the organizing phase.

---

[1] In this case the damage can derive from the product depreciation or from a quantitative loss of the harvest.

[2] There are other diseases such as the corn diabrotica, peach sharka, ect…

[3] Generally, for every risk, the agricultural firms can make use of more or less suitable and adequate tools of defence, for example to face the atmospheric phenomena, the agricultural contractor can make use of tools of defence of active, passive or mixed nature. By the active defence can be adopted suitable techniques and instrumentations such as for example the anti-hail nets; the passive defence centres its action on the insurance contracts; at last the mixed defence characterizes the combined use of the anti-hail nets (or similar tools) and the insurance contract.

Financial risk

Agricultural firm frequently suffers risk concerning the productive activity's financing, this expression refers in particular to: the cost and the availability of borrowed capital; to the ability to face the current expenses without being late; to the power to keep and increase the stock of the starting capital (Harwood et all.,1999)[4]. For this reason it is possible that some financial imbalances are created during the productive process that is when there is a long period between the combination of the acquired productive factors and the achievement of the product that has to be placed in the market. The agricultural contractor often has to suffer the current expenses (input purchase) before achieving the proceeds (output sale), and for this reason he has to resort to his own financial reserves (self-financing) or to the credit. The meaning of this is that it is underlined the existence of a series of legislative interventions directed towards the support of the agricultural activity (for example the facilitate forms of financing precisely named "credit in farming" or "agricultural credit"). Certainly the greater the financial expenses the higher the risk will be (related to the lending rate). Generally the most negative variables that influence the financial risk are: the seasonal course state of productions, the rise in the market price of productive factors, the proceeding of financial markets, ect…

The market risk

The agricultural market, having often the form of an atomistic omeopoly (in some cases of oligopoly or monopolistic competition), is bending on the agricultural traders to influence the conditions of demand and offer, for this reason the agricultural contractor becomes "price-taker", that is he suffers the price that is fixed by the market or by the counterpart. For this reason, one of the most relevant components of the market risk is the price.[5] Often, in fact, the agricultural contractor can't fix and known the price of the products that he will sell or the price of the productive factors that he has to buy. The price risk isn't restricted only to the productive factors but to the cost of production, too. Another form of the market risk makes concrete in the low elasticity of the demand compared with the consumer's income or with the price of the products sold as the contractor doesn't succeed in having a considerable profit as a result of an increase in the consumer's income or of a reduction in the selling price of the products. Other market risks can be generated by the volatility of the quotation, the availability of the transport system, the breaches of contracts, the agreements related to the sell of the product, ect...

---

[4] To this category belong the financial risks due to the changes of the taxation or the changes on the firm's activity both on the labour's wages and the tax system in farming in general.

[5] With reference to the lower or higher price, we speak about uncertainty and not about risk when we know all the limits, but we disown the probabilities with which different possibilities could manifest themselves. In this case the producer behaves taking in consideration the lower price when he has to choose. According D.V. Lindley, in uncertain conditions, the choices of the traders depend on subjective, and not objective, probabilities linked to their personal trust to the future.

Institutional risk

These potential negative events can limit the production causing consequential economic deficit of the agricultural firm. An example of this are the decisions of a foreign Country to limit the importations; the amendments of the rules that regulate the use of pesticides, fertilizers, soils, or whatever else product used to the increase of the production; the politics that regulate the waste disposal of the animals; the changes of the tax and credit regulations. Finally, another example of the institutional risk is the risk of the "form" identifiable in the lack of flexibility that rises from the legal forms adopted in the institutional phase. This choice, in fact, could bind the whole business combination.

The social and personal risk

The farming is an economic sector characterized by a raised seasonal nature in the labour market, this implies several and substantial differences, one of these is the low culture managerial education of the contractors.[6] The risks concerning the "human factor" are also referable to the job of occasional and seasonal collaborators irregularly engaged (for this the black market extends), to the progressive ageing of the working population; to the delay of the technologies in relation to the innovations of the productive processes. The social or personal risks can rise from other events as the death, disability, disease, but also as the abandonment of the agricultural activity from a member of the family. All these events cause relevant effects on the business organization and on the incomes structure. In this context it doesn't matter the risk raising from the personal factors of the contractor, in fact, at the workplace he suffers his physical and psychological state, his action as exact as possible by operating logic is perpetually uncertain. (Bertini, 1999).

The infrastructural risk

This typology of risk refers to the assets of the agricultural firm, in particular to the productive plants that suffer a physical depreciation (senescence) or technological and economic depreciation (obsolescence). In this case the risk can rise from the calculation of the amortization allowance that can result by excess or by defect in negative cases. The agricultural contractor could adopt wrong or irrational managerial choices as for example the distribution of insufficient income or the realization of investment policy in the presence of an index of inadequate company profitability. Another infrastructural risk can rise from the non-replacement of the structures and this happens when during the managerial phase the contractor attains negative results, he squeezes the costs through a cut of the amortization allowances. The consequent inadequacy of the structures as regards to the remaining productive factors could imply the taking on of decisions that threaten the existence itself of the firm.

[6] The risk of a bad management can rise from the inadequate entrepreneurial abilities concerning both the different education degree and the informative want.

Emerging risks

This typology of risk comes from the change of the conditions and the aims of the production. Then, from the passage from one production that bases itself on the quantity to another that bases itself on the quality, or from a monoculture to a diversified agriculture. An example of this is the risk linked not to the products' correspondence but to the contract requirements for the typical productions, or for the biological productions. These are the less noticed and the measured hardly risks, but not for this they have to be undervalued.[7]

The total risk fro the agricultural firm doesn't correspond to the sum of every single category of risks because a space of interaction exists among each of them. In any case, with the direct damage referred to the capital good (for example the plantations' damaging), an indirect damage keeps company (Prestamburgo 1995), because of the product depreciations in the following years to those in which the event has taken place.

1.2 The management of the risk in an agricultural firm

The ability to manage, to minimize or to face the risks has been always the reason of the success of an economic activity or of a contractor. To face the risk is a problem that can be faced by whom conducts a business and succeeds in guessing at the right moment the adverse phenomena to the management cheapness, so that the firm can suffer as the least damage as possible. Actually, to reduce the risks in his own firm an agricultural contractor has to distinguish public instruments from private ones. The former essentially rise from agrarian policy interventions and among these the interventions for the market regulation, the assistance measures, the support of the active defence. With regard to this, in many Countries, the programs for the compensation for damages due to natural calamity also meet the damages to agricultural productions. The private instruments for the risk management in farming can be classified in:

- the planning of the management and of the business and familiar structure;
- the use of financial and commercial politics;
- the advance covering of the damage by special funds;
- the advance covering of the damage by policy.

By the shake-up of the business structure it is possible to diversify the productive activity or to realize a pluriactivity. In the first case, that is frequently realized, more farming are simultaneously adopted, it happens thanks to a technological evolution that allows an improvement in the combinations and in the use of the productive factors. On the contrary, by the pluriactivity there is a greater involvement of the family and of the agricultural contractor's collaborators who are interested in forming new activities compared with that which is traditionally carried out but that are always directly linked to it. An example of pluriactivity is the farm holiday centre or in general the rural tourism, it represents additional font of the agricultural contractor's profit. In fact, it allows to generate a new "portfolio" of activity which the agricultural risk is put on and it is easily amortized. Another example of shake-up is the adoption of "vertical integration" that consists of agreement among several contractors to gather in one firm to realize some common phases of their own productive process. The vertical integration can be a backward or a forward integration, and among the latter many examples are referable to horticultural and floricultural firms. By the vertical integrations the risks concerning the quantity and the quality of the offer of the productive factors and the transaction costs associated to the exchange of products along the process are reduced.

[7] The group of risks linked to the sanitary emergency is assuming a considerable weight.

Another instrument at contractor's disposal to face the risk in farming is to turn to financial practices. Till short time ago this instrument was unknown to European agricultural contractors and this can be justified by the fact that they could have operated in a firm price system for the products regulated by the Market Common Organizations. The lack of stability and the existence of guarantee of compensation from EU has leaded to the abandonment of the traditional methods of prevention in favour of specializations towards more guaranteed productions (Cafiero C.). But, nowadays, people think that the financial derivatives in farming can have a more and more important role also because the continuous technical progress increases the possibilities to use instruments supplying less expensive and more effective methods to make the firm's risk transferring to the whole economic system. In farming the most used financial derivatives to carry out the covering of the price risk are the forward contracts, the futures and the options on the futures. These instruments can be used in two different markets that is either in an organized market where the instruments are available to the small consumers, there are low transaction costs, they have a good liquidity and the price can be measured easily, or in a market over the counter (there is an exchange between brokers and customers without they are quoted on the public market) where the instruments are realized for specific user's exigencies.

When the risk is assumed, the firm has to know the entity of the greatest damage that can be produced and the chances that the damaging event has to manifest itself. With regard to this one of the most used forms of facing from agricultural firm is the settlement of special "internal funds". By these internal funds are funded annually some shares that are equal to the entity of the risk that probably can weight on the business concern. This typology of the risk management has an estimated vision of the firm life. For this reason the funds provision made ad hoc for these risks presents some difficulties because it bases itself on probabilistic and supposed data. Even so, one of the recent suggestions of the European Commission is that to form insurance funds by which, besides the traditional functions, it's possible to create a direct channel between the agricultural contractor and the financial market. Among the traditional insurance funds people remember the constitution of financial reserves created by the contribution of the business partners, that have to be used at the moment in which someone of them suffers heavy deficit during the business year.

The financial covering of the damage by policy is one of the most used instrument in farming. Generally three different typologies of insurances can be distinguished: *single risk policy* and *associate risk policy*, in this case the damages caused by a specific event (for example the hail) are covered; *profit policy* in which the profit, that is estimated through the relation between the output and the harvest price, is guaranteed. For this typology of policy it is offered a guarantee of the price variability and then of the relative fluctuation. Another typology of policy, that is present in farming, is the *income policy* that covers the total performance of the production that is realized taking into consideration the whole costs performance. This policy can consider either the income of the single production or the income of the whole business activity that can be gained in the space of a year. It's important to underline that to take out insurance policy in the ambit of the primary sector has never been easy and this depends on several reasons, first of all, because exists a real possibility of the risk realization that the insured suffers as the agro-ambient events are cyclic and they involve wide territorial areas. This situation causes damages to the agricultural contractors that, if all of them are assured, can generate serious financial consequences to the assurance companies at the same time. Another problem is that of the informative asymmetry because there is often a difference of information among the producers, who working in this sector and being more experienced, better know what could be the risks

that can take place during the agricultural year and the insurers who often aren't able to estimate the different typical risks of agricultural sector. Finally, another problem that could take place at the moment in which the insurance contract is stipulated is that of the *moral hazard,* the contractor, who knows that he can obtain a compensation in case of non-profit or inadequate production, has a lean incentive to fulfil all the dealings needed for the realization of the firm's managerial efficiency conscientiously.
After considering this, on an insurance company of view, it's possible to identify two typologies of risk that weights on the agricultural firm, the first is an independent category of risk, while, the second is a typology of risk that has a systematic nature, that is it is completely correlated. When the risk is independent, an insurance company covers the agricultural firm that has suffered the damage, in this case the event doesn't alter the probability that the same thing could happen to another agricultural firm; on the contrary, when the systematic risk takes place it happens that the negative event damages more firms located in an homogeneous area or belonging to the same market [8].

2. The asymmetry during the decisional phase and the model of decision under uncertainty

The reality of any for profit firm is deeply complex because of various factors that are part of it and for the different modalities of their combination. This complexity seems exaggerated if we take into consideration an agricultural firm and this is due to the distinctiveness of the principal activity that makes it a dynamic sector that requires a broad vocational training of the agricultural contractor so that he can be able to conduct in the best way possible the firm risk.
Before choosing, the contractor has to consider some important external factors (external to the firm) the taking place of which is independent from his will, and then he has to analyse the internal factors (internal to the firm). Among the external factors we have to consider the *territorial component*, that is considered as a landscape and environmental resource; the *anthropological component,* that involves the architectonic, cultural, gastronomic and craft made resources. Among the internal factors we analyze the agricultural, human and financial resources.
Every productive activity involves a risk because it is based on decisions taken in uncertain conditions and it is linked to the changes of economic situation. In fact, we generally speak about firm risk because it acquires a fundamental and basic importance in the theory of profit.
The contractor always tends to eliminate or, more or less, to minimize the risks either turning to the payment of the insurance premium, or forming proper risk funds by the business concern earmarking; and also either adding price revision clauses in the sale contract or at last resorting to suitable market surveys, to advertising campaigns in order to affect consumer's tastes.

Synoptic table of the risk system in an agricultural firm

RISK: PHENOMENA	SPECULATIVE RISKS	MERE RISKS
Natural	• The effects of the climate on the agricultural products' price • The effects of the climate on demand of the tourist services	• Floods • Earthquakes

[8] An example of systematic risk rises from the price volatility of the agricultural product, for a firm that deals on a competitive market.

	• The effects of the climate on demand of food goods	• Hurricanes, tempests
Socia*l*	• Fashion • Labour situation • Variation in the consumer models	• Common criminality • White collar crime • Hackering
Po*l* **itica***l*	• Nazionalizations/privatizations • Firm activities provisions	• Terrorist attacks • The arrest of managers or key men
ācr **o-economic**	• Variations in the consumer rates • Fluctuation of exchange • Fluctuation of the interest rates	• None
Tec*h***nica***l*	• Introduction of new product technologies • Introduction of new productive processes • The result of the firm projects of *R&S*	• Industrial injury • Malfunction of the products • Ecological disasters
inanci **a***l*	• Variations in the conditions practised by the credit institutions • The trend of the capital market • Variations in the conditions practised by the custormers and the suppliers	• None
Competiti*v* **e**	• The launching of substitutive products • The emerging of new distributive channels • The competitors price politics	• Industrial espionage • Counterfeit of the product • Sabotage

As it has been said, the agricultural contractor during his firm activity has to choose and to decide in condition of imperfect knowledge. This cognitive asymmetry, that characterizes the decisional phase, causes the taking place of the "risk" and it influences with its effects the total calculation of the agricultural firm's economic result. Therefore the decisional process of the agricultural contractor is conditioned by some factors among which we underline:

a) resources availability;
b) technological level and the consequent production's function that rises from the quality and the quantity of the available productive factors;
c) the market conditions and the price fluctuations related both to the productive factors and to final products;
d) social-institutional background where the firm acts;
e) targets settled by the contractor and his attitude towards the risk;
f) the uncertainty linked to the resources availability , the market conditions, the technological trend and the social-institutional background.

A simplified model of entrepreneurial decisions results structured to induce the contractor to the maximization of the profit that is correlated to an indifferent attitude towards the hypothesis of the risk (point e)

Simplified model of entrepreneurial decisions

Target	To Maximize the product	Point e)
Attitude towards the risk	Indifference	Point e)
Level of uncertainty	No use	Point f)

A Mathematical approach.

For the generic agricultural production we have:

$$P_{r_i} = \sum_{K=1}^{p} B_K - \sum_{K=1}^{q} C_h, \qquad i = 1,\ldots,n \tag{1}$$

All this, if we suppose to obtain all together p benefits and support q costs of different value with B_K and C_h.

This analysis need estimate of cost-benefits connected with the use of resources which aren't regulated by market's traditional mechanism. So all this means that the terms B_K and C_h can't always represent monetary terms. For the estimation of the alternatives, the variables will be expressed in unit of measurement not homogeneous, and sometimes they can be constituted by specific subjective risks. In order to analyze completely and correctly the system of variables is necessary before to transform all the risk indicators in a-dimensional variables, in order to compare each other. If we consider all the variables represented in (1), it is useful individualize an appropriate mathematic method which permits to choose, between $m=p+q$ risk indicators, $h<m$ most important for this problem without that we lose important information of analysis.

So, it is necessary to indicate appropriate mathematical methods which must give an appropriate representation of the reality and they must reduce the original dimensions of the examined variables with a selection of the most important informations. In this search a specific analytical criterion is proposed which is based on principles of factorial analysis. If we use appropriate linear functions not correlated, it is possible to express, with clear representation, the principal rule of each environmental indicator in the explanation of the investigation's table.

In order to find the most appropriate indicators for the estimation of the agricultural production P associated to n possible risks, we will use a matrix representation of the problem.

Let M be the matrix of the nxm variables of the (1), and we denote with x_i the costs C_h and B_k for the risk i

$$M=\| x_{ij} \|,\ i=1 \ldots.. n;\ j=1, \ldots., m.$$

In order to solve the problem of the homogeneous variables we estimate

arithmetic mean $\bar{x}_j$, and the root-mean-square deviation of the indicator j

$$\bar{x}_j = \frac{1}{n}\sum_{i=1}^{n} x_{ij} \qquad \sigma_j = \sqrt{\frac{1}{n}\sum_{i=1}^{n}\left(x_{ij} - \bar{x}_j\right)^2}, \quad (j = 1,\ldots,m)$$

we can find new variables that allow to make the variables homogeneous

$$X = \left\| x_{ij} \right\| = \frac{x_{ij} - \bar{x}_j}{\sigma_j \sqrt{n}}.$$

So we can compare the terms and standardize them.
In order to estimate the correlation degree between the synthetic risks, now we can compute the correlation matrix C:

(2) $$C = {}^{t}X \cdot X.$$

The (2) is a symmetric matrix of the correlation between the m considered variables, it is a square matrix of order m and it represents the matrix of deviations and co-deviations[9] in the statistical-mathematic view point.

Since, C is a symmetric matrix it has m positive real eingevalue $\lambda_1 > 0$, ..., these eingenvalues are the root of the characteristic equation

$$\det\left(C - \lambda I_m\right) = 0.$$

The corresponding eingenvalues λ_1, ..., λ_m are determinated by the equation

$$(C - \lambda_h I_m) \cdot V_h = O_{m,1}$$

where O_{m1} is the matrix which has all null elements, and V_h is the column matrix which the elements are the m components of eingenvector $\vec{v}_h$ corresponding to eingenvalue v_h.

In order to obtain the searched matrix

---

[9] The deviation is the sum of the difference's squares between the singular observations and the their mean; $devx_h \sum_{i=1}^{mn}\left(x_{ih} - \bar{x}_k\right)^2 = C_{hh}$. The Co-deviation is the sum of the difference's products of the consiterated variable values from respective mean; codev $(x_h, x_k) = \sum_{i=1}^{mn}\left(x_{ih} - \bar{x}_k\right)\left(x_{ik} - \bar{x}_k\right) = C_{hk} = C_{kh}$. The Value of the element C_{hk} denote the concordance and discordance between the variability of x_h and $x_k$is included between the limits + 1 and -1

$$R = \|r_{hk}\|$$

of components rhk in order to found the significance of any of the *m* considered variables for obtain the better management, we order the eingenvalue *h* in decreasing sens.

After, we can estimate the normalized eingenvalues with the expression:

$$\vec{e}_h = \frac{1}{\|\vec{v}_h\|} \cdot \vec{v}_h$$

where $\|\vec{v}_h\|$ is the norm of the eingenvector $\vec{v}_h$.

We can obtain the matrix *R* by computing the elements r_{hk}. In fact we have that:

$$R = \|r_{hk}\| = \|\lambda_k \; e_{hk}^2\|$$

where λ_k is the eingenvalue *k-th* and b_{hk}^2, is the square of element b_{hk} of matrix $E = \|\vec{e}_{hk}\|$ of the normalized eingenvalue. So we have a good solution to our problem.

. n Eampe

We can find these examples of the complex agricultural reality in economic-agrarian literature. Clearly the decisions that the contractor has to take are conditioned by several factors and by the probability that the risks take place (De Benedictis-Cosentino, 1979). As a consequence of this, if we take into consideration many aleatory variables the system of decisions becomes complex, so it's necessary to resort to the processing of the *decisional mathematical models under uncertainty condition.*

E PCTO			
System of Risks of Atmospheric Precipitations In Agriculture			
TECHC ECOOC PRETER S		EVROE T PRETRES	
r1	Introduction new technologies of products	r h-1	Effect climate on the prices of the agricultural products
r2	Variation consumption rates	r h-1	Effect climate on the offer of the agricultural products
r3	Oscillation change and rates of interest	r h-1	Effect climate on agricultural products demand
…		r h-1	Smottamenti e dissesti idrogeologici
…		…	
rh	Variation models of consumption	rh	Ecological disasters

EET RE CTO			
TECHC ECOOC PRETER S		EVROE T PRETRES	
r1	Variation course of capital market them	r h-1	Effect climate on the capital market
r2	Variation interests of the credit institutions	r h-1	Effect climate on the interests practiced from the credit institutions
…		…	
…		…	
rh	Variation quotes financial markets	r h-1	Effect climate on the value of the share quotas the companies

References

[1] - Caristi G. – La scelta di investimenti pubblici alternativi: Un Modello di ottimizzazione, tesi di dottorato, Università di Messina, Novembre 2000.

[2] - Caristi G., Ferrara M., A model for the screening of alternative public investments, *Seminarberichte aus der FACULTÄT für Mathematik und Informatik der FernUniversität in Hagen, Band 71-2001.*

[3] - De Benedictis M. Cosentino V., Economia dell'azienda agraria, Bologna, 1979.

[4] - Lanfranchi M., Sulla multifunzionalità dell'agricoltura aspetti e problemi, Edas, Messina, 2002.

[5] - Lanfranchi M., Il ruolo della tassazione ambientale nello sviluppo dell'agricoltura sostenibile, Edas, Messina, 2004.

[6] - Lanfranchi M., Corso di economia dell'azienda agraria, Edas, Messina, 2008.

[7] - Lo Bosco D. – un criterio matematico per l'analisi sistemica degli indicatori sintetici adoperati nello studio del binomio strada-ambiente, Autostrade, n.1, gennaio-marzo 1995.

[8] - Prestamburgp M., Saccomandi V., Economia agraria, Serie di scienze per l'economia, Etas libri, 1995.

[9] - Stoka M. – Corso di Geometria, ed. CEDAM, Padova, 1995.

[10] - Stoka M. – Calcolo delle probabilità e statistica matematica, Ed. Leprotto&Bella, Torino, 1991.

RENDICONTI DEL CIRCOLO MATEMATICO DI PALERMO
Serie II, Suppl. 81 (2009), pp. 261-272

On Some Explicit Semi-stable Degenerations of Toric Varieties

Marina Marchisio, Vittorio Perduca

Abstract

We study semi-stable degenerations of toric varieties determined by certain partitions of their moment polytopes. Analyzing their defining equations we prove a property of uniqueness [1].

1 Background

1.1 Polytopes and semi-stable partitions

In his paper [5], Hu provides a toric construction for semi-stable degenerations of toric varieties. We study the uniqueness of this construction for a toric variety X in the particular case of a semi-stable partition of its moment polytope in two subpolytopes. Adapting a theorem by Sturmfels on toric ideals (Lemma 4.1 in [9] and Section 2 in [8]) to particular open polytopes, we investigate the equations of the degeneration of X as embedded variety.

Let $M \simeq \mathbb{Z}^n$ be a lattice and N its dual. We consider polytopes $\Delta \subset M$ which describe smooth algebraic varieties X_Δ; Δ determines the normal fan $\Sigma_{X_\Delta} \subset N$. Recall that convex polytopes Δ determine a toric manifold X_Δ together with an ample line bundle $\mathcal{L}_\Delta$: $(X_\Delta, \mathcal{L}_\Delta)$. If the polytope is non singular of dimension n, then $\mathcal{L}_\Delta$ is very ample, we then have an embedding $X_\Delta \hookrightarrow \mathbb{P}^\ell$, for some ℓ [7].

Now fix a (compact) polytope Δ and suppose $\Delta \cap M = \{\mathbf{m}_0, \dots, \mathbf{m}_\ell\}$. Take $x_0, \dots, x_l$ as homogeneous coordinates in $\mathbb{P}^\ell$. We can define $X = X_\Delta$ as the closure in $\mathbb{P}^\ell$ of the image of the map

$$\begin{aligned} \varphi : (\mathbb{C}^*)^n &\to \mathbb{P}^\ell \\ \mathbf{t} &\mapsto [\mathbf{t}^{\mathbf{m}_0}, \dots, \mathbf{t}^{\mathbf{m}_\ell}], \end{aligned} \tag{1}$$

[1] The authors would like to thank Antonella Grassi for stimulating their interest in this project and for many useful conversations.

where $\mathbf{t} = (t_1, \ldots, t_n) \in (\mathbb{C}^*)^n$ and given $\mathbf{u} = (u_1, \ldots, u_n) \in \mathbb{Z}^n$ we use the notation $\mathbf{t}^{\mathbf{u}} = t_1^{u_1} \cdot \ldots \cdot t_n^{u_n}$. Taking homogeneous coordinates in X_Δ, this map extends to a map $X_\Delta \to \mathbb{P}^\ell$, which is an embedding under the assumption X_Δ smooth (see [2]).

We assume that there exists a suitable finite partition Γ of Δ in subpolytopes $\{\Delta_j\}_{j=1}^k$. We will assume that the toric varieties X_{Δ_j} corresponding to each Δ_j are also smooth. We call an open l-face σ of Δ_j an l-face of Γ and we declare that the 0-faces of Δ are *not* 0-faces of Γ. Following [1, 5] we ask Γ to be *semi-stable*:

Definition 1.1 *Γ is semi-stable if for any l-face σ of Γ, if θ is a k-face of Δ such that $\sigma \subset \theta$, then there are exactly $k - l + 1$ Δ_j's such that θ is a face of each of them.*

In fact:

Theorem 1.2 [1, 5] *If $\{\Delta_j\}_{j=1}^k$ is a semi-stable partition of Δ, then there exists a semi-stable degeneration of X, $f : \tilde{X} \to \mathbb{C}$ with central fiber $f^{-1}(0) = \cup_{j=1}^k X_{\Delta_j}$; the central fiber is completely described by the polytope partition $\{\Delta_j\}_{j=1}^k$.*

$\tilde{X}$ is constructed by a *lift* of Δ (see Definition (1.3)). From Theorem 2.8 in [5], $\tilde{X}$ is unique: we study the uniqueness of $\tilde{X}$ for semi-stable partitions of Δ in two subpolytopes Δ_1, Δ_2, and we describe its defining equations. In particular, in Section 2 of [5], Hu shows that the ordering (arbitrarily fixed) $\{\Delta_1, \ldots, \Delta_k\}$ of the polytopes in Γ determines a piecewise affine function on the partition $F : \Delta \to \mathbb{R}$, which takes rational values on the points in the lattice M. F can be chosen to be concave and it is called *lifting function*.

Definition 1.3

$$\tilde{\Delta}_F = \{(m, \tilde{m}) \in M \times \mathbb{Z} \text{ such that } m \in \Delta \text{ and } \tilde{m} \geq F(m)\}$$

is an open lifting (here simply lift) of Δ with respect to Γ.

There are many possible lifts of Δ with respect to Γ; if Γ consists of two subpolytopes, then two lifts exist. By construction there exists a morphism $f : \tilde{X}_F := X_{\tilde{\Delta}_F} \to \mathbb{C}$ which realizes a semi-stable degeneration of X. As

before we have embeddings $X \hookrightarrow \mathbb{P}^\ell$ and $\tilde{X}_F \hookrightarrow \mathbb{P}^\ell \times \mathbb{C}$. In particular we can define $\tilde{X}_F$ as the closure in $\mathbb{P}^\ell \times \mathbb{C}$ of the image of the map:

$$\begin{array}{rcl} \psi_F : (\mathbb{C}^*)^n \times \mathbb{C} & \to & \mathbb{P}^\ell \times \mathbb{C} \\ (\mathbf{t}, \lambda) & \mapsto & ([\lambda^{F(\mathbf{m}_0)}\mathbf{t}^{\mathbf{m}_0}, \lambda^{F(\mathbf{m}_1)}\mathbf{t}^{\mathbf{m}_1}, \ldots, \lambda^{F(\mathbf{m}_\ell)}\mathbf{t}^{\mathbf{m}_\ell}], \lambda). \end{array} \tag{2}$$

Theorem 2.8 in [5] claims that the image of $\psi := \psi_F$, and hence $\tilde{X}_F$, is independent of the lifting function F.

We explicitly study this statement for semi-stable partitions of Δ in two subpolytopes. If Γ consists of two subpolytopes Δ_1, Δ_2, then we can construct two possible lifting functions F, G and then Δ has two lifts, say $\tilde{\Delta}_F$ and $\tilde{\Delta}_G$. In particular let $y_1, \ldots, y_n$ be coordinates in $\mathbb{R}^n \supset \Delta$ and let

$$a_1 y_1 + \ldots + a_n y_n + a_{n+1} = 0$$

be an equation of the *cut* $\Delta_1 \cap \Delta_2$ *in the lattice*, where we take $a_1, \ldots, a_{n+1} \in \mathbb{Z}$ such that for all $\mathbf{m}_j = (m_{1j}, \ldots, m_{nj}) \in \Delta_2 \cap M$ we have

$$a_1 m_{1j} + \ldots + a_n m_{nj} + a_{n+1} \geq 0.$$

Following the construction in [5], the functions F, G we obtain look like:

$$F(\mathbf{m}_j) = \begin{cases} 0 & \text{if } \mathbf{m}_j \in \Delta_1 \\ L_F(\mathbf{m}_j) := a_1 m_{1j} + \ldots + a_n m_{nj} + a_{n+1} & \text{if } \mathbf{m}_j \in \Delta_2, \end{cases}$$

$$G(\mathbf{m}_j) = \begin{cases} L_G(\mathbf{m}_j) := -a_1 m_{1j} - \ldots - a_n m_{nj} - a_{n+1} & \text{if } \mathbf{m}_j \in \Delta_1 \\ 0 & \text{if } \mathbf{m}_j \in \Delta_2. \end{cases}$$

We prove that the two non-compact toric varieties defined by the open polytopes $\tilde{\Delta}_F$ and $\tilde{\Delta}_G$ have the same toric ideals. To do this we adapt a Sturmfels's theorem on toric ideals (Lemma 4.1 in [9] and Section 2 in [8]) to this non-compact context.

1.2 Toric ideals

In [8] Sottile describes the ideal I of the compact toric variety X (*toric ideal*) defined as the closure of the image of a map (1), following Sturmfels's book [9].

Take $x_0, \dots, x_l$ as homogeneous coordinates in $\mathbb{P}^\ell$. With the notation of the previous section, suppose $\mathbf{m}_j = (m_{1j}, \dots, m_{nj})$, $j = 0, \dots, \ell$ and consider the $(n+1) \times (\ell+1)$ matrix

$$\mathcal{A}^+ = \begin{pmatrix} 1 & 1 & \dots & 1 \\ m_{10} & m_{11} & \dots & m_{1\ell} \\ \vdots & \vdots & & \vdots \\ m_{n0} & m_{n1} & \dots & m_{n\ell} \end{pmatrix}.$$

Observe that if $\mathbf{u} \in \mathbb{Z}^{\ell+1}$, then we may write $\mathbf{u}$ uniquely as $\mathbf{u} = \mathbf{u}^+ - \mathbf{u}^-$, where $\mathbf{u}^+, \mathbf{u}^- \in \mathbb{N}^{\ell+1}$, but $\mathbf{u}^+$ and $\mathbf{u}^-$ have no non-zero components in common. For instance, if $\mathbf{u} = (1, -2, 1, 0)$, then $\mathbf{u}^+ = (1, 0, 1, 0)$ and $\mathbf{u}^- = (0, 2, 0, 0)$ (Sottile's notation).

We therefore have:

Theorem 1.4 ([8], Corollary 2.3)

$$I = \langle \mathbf{x}^{\mathbf{u}^+} - \mathbf{x}^{\mathbf{u}^-} | \mathbf{u} \in \ker(\mathcal{A}^+) \text{ and } \mathbf{u} \in \mathbb{Z}^{\ell+1} \rangle.$$

There are no simple formulas for a finite set of generators of a general toric ideal. An effective method for computing a finite set of equations defining X_Δ in $\mathbb{P}^\ell$ is applying elimination theory algorithms to its parametrization in homogeneous coordinates. These algorithms are implemented in the well known computer algebra system Maplesoft [4].

2 First examples

To illustrate the previous section, we describe the semi-stable degenerations of a curve and a surface determined by a subdivision of their moment polytopes in two subpolytopes.

2.1 The twisted cubic

The twisted cubic $X \subset \mathbb{P}^3$ can be defined as $\mathbb{P}^1$ embedded in $\mathbb{P}^3$ by cubics, that is, as the toric curve $(X_\Delta, \mathcal{L}_\Delta) = (\mathbb{P}^1, \mathcal{O}(3))$, where Δ is the polytope below.

Here $M = \mathbb{Z}$, $\Delta \cap M = \{\mathbf{m}_j = j,\, j = 0, \dots, 3\}$, X is the closure of the image of

$$\begin{array}{rccl} \varphi : \mathbb{C}^* & \to & \mathbb{P}^3 \\ t & \mapsto & [1, t, t^2, t^3], \end{array}$$

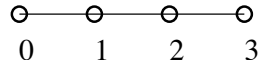


Figure 1: The moment polytope Δ of the twisted cubic $X \subset \mathbb{P}^3$.

which extends to the embedding

$$\begin{array}{ccc} X_\Delta & \hookrightarrow & \mathbb{P}^3 \\ (v_0, v_1) & \mapsto & [v_1^3, v_0 v_1^2, v_0^2 v_1, v_0^3], \end{array}$$

where v_0, v_1 are homogeneous coordinates in X_Δ.

The toric ideal of X is of course computed to be

$$I = \langle x_0 x_2 - x_1^2, x_1 x_3 - x_2^2, x_0 x_3 - x_1 x_2 \rangle.$$

Now consider the semi-stable partition $\{\Delta_1, \Delta_2\}$ of Δ, where $\Delta_1 = [0,1] \subset \mathbb{R}$ and $\Delta_2 = [1,3] \subset \mathbb{R}$. This partition gives the semi-stable degeneration of X to the union of two curves $X_1 \cup X_2$, where $X_1 = (\mathbb{P}^1, \mathcal{O}(1))$ and $X_2 = (\mathbb{P}^1, \mathcal{O}(2))$.

The two possible lifting functions are

$$F(j) = \begin{cases} 0 & j = 0,1 \\ j-1 & j = 2,3 \end{cases}, \; G(j) = \begin{cases} 1 & j = 0 \\ 0 & j \neq 0 \end{cases}.$$

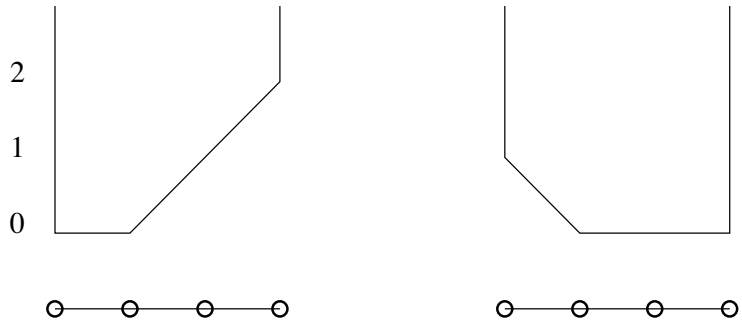


Figure 2: Δ_F and Δ_G.

Using the notation of (2), in local coordinates the embeddings of $\tilde{X}_F$ and $\tilde{X}_G$ in $\mathbb{P}^3 \times \mathbb{C}$ are $([1, t, \lambda t^2, \lambda^2 t^3], \lambda)$ and $([\lambda, t, t^2, t^3], \lambda)$, while in homogeneous coordinates these are

$$([v_1^3, v_0 v_1^2, \lambda v_0^2 v_1, \lambda^2 v_0^3], \lambda)$$

and

$$([\lambda v_1^3, v_0 v_1^2, v_0^2 v_1, v_0^3], \lambda).$$

We therefore observe that $\tilde{X}_F$ and $\tilde{X}_G$ have different parametric equations, nevertheless it is easy to see that both of them are defined in $\mathbb{P}^3 \times \mathbb{C}$ by the equations

$$x_0 x_2 - \eta x_1^2 = 0, x_1 x_3 - x_2^2 = 0, x_0 x_3 - \eta x_1 x_2 = 0,$$

where η is the non-homogeneous coordinate in $\mathbb{C}$. These equations can also be found applying elimination theory algorithms to the two parametrizations in homogeneous coordinates, computations can be performed by hand or using computer algebra systems.

2.2 $\mathbb{P}^1 \times \mathbb{P}^1$ blown up in a point

Consider the polytope Δ in figure 3 with its associated normal fan. The toric

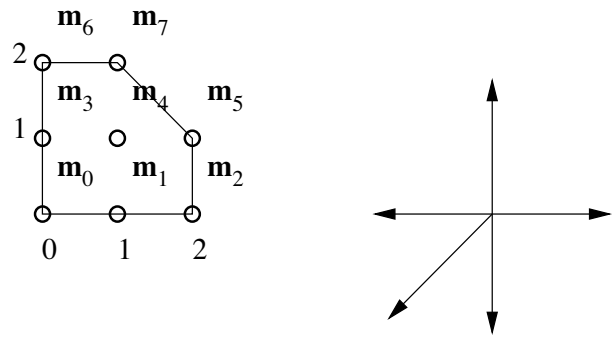


Figure 3: $\mathbb{P}^1 \times \mathbb{P}^1$ blown up in a point and its normal fan.

surface X determined by Δ is $\mathbb{P}^1 \times \mathbb{P}^1$ blown up in a point and embedded in $\mathbb{P}^7$. In local coordinates it is the closure of the image of

$$\begin{aligned} \varphi : (\mathbb{C}^*)^2 &\to \mathbb{P}^7 \\ (t_1, t_2) &\mapsto [1, t_1, t_1^2, t_2, t_1 t_2, t_1^2 t_2, t_2^2, t_1 t_2^2], \end{aligned}$$

while taking homogeneous coordinates $v_0, \ldots, v_4$ for X_Δ (one for each facet of Δ), the embedding is

$$\begin{aligned} X_\Delta &\hookrightarrow \mathbb{P}^7 \\ (v_0, \ldots, v_4) &\mapsto [v_2^2 v_3^3 v_4^2, v_0 v_2 v_3^2 v_4^2, v_0^2 v_3 v_4^2, v_1 v_2^2 v_3^2 v_4, v_0 v_1 v_2 v_3 v_4, \\ &\quad v_0^2 v_1 v_4, v_1^2 v_2^2 v_3, v_0 v_1^2 v_2 v_4]). \end{aligned} \tag{3}$$

Consider the semi-stable partition $\{\Delta_1, \Delta_2\}$ of Δ:

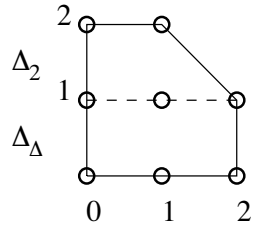


Figure 4: A semistable partition of X.

This partition gives the semi-stable degeneration of X to the union of two surfaces $X_1 \cup X_2$, where $X_1 = \mathbb{P}^1 \times \mathbb{P}^1$ and $X_2 = \mathbb{F}^1$.

The two possible lifting functions are

$$F(\mathbf{m}_j) = \begin{cases} 0 & j = 0, \ldots, 5 \\ 1 & j = 6, 7 \end{cases}, \; G(\mathbf{m}_j) = \begin{cases} 1 & j = 0, 1, 2 \\ 0 & j = 3, \ldots, 7 \end{cases}.$$

In local coordinates the embdeddings of $\tilde{X}_F$ and $\tilde{X}_G$ in $\mathbb{P}^7 \times \mathbb{C}$ are

$$([1, t_1, t_1^2, t_2, t_1t_2, t_1^2t_2, \lambda t_2^2, \lambda t_1 t_2^2], \lambda)$$

and

$$([\lambda, \lambda t_1, \lambda t_1^2, t_2, t_1t_2, t_1^2t_2, t_2^2, t_1t_2^2], \lambda).$$

We have embeddings

$$\begin{array}{rcl} \iota_F : \tilde{X}_F & \hookrightarrow & \mathbb{P}^7 \times \mathbb{C} \\ (v_0, \ldots, v_4, \lambda) & \mapsto & ([v_2^2v_3^3v_4^2, v_0v_2v_3^2v_4^2, v_0^2v_3v_4^2, v_1v_2^2v_3^2v_4, v_0v_1v_2v_3v_4, \\ & & v_0^2v_1v_4, \lambda v_1^2v_2^2v_3, \lambda v_0v_1^2v_2v_4], \lambda), \end{array}$$

and

$$\begin{array}{rcl} \iota_G : \tilde{X}_G & \hookrightarrow & \mathbb{P}^7 \times \mathbb{C} \\ (v_0, \ldots, v_4, \lambda) & \mapsto & ([\lambda v_2^2v_3^3v_4^2, \lambda v_0v_2v_3^2v_4^2, \lambda v_0^2v_3v_4^2, v_1v_2^2v_3^2v_4, v_0v_1v_2v_3v_4, \\ & & v_0^2v_1v_4, v_1^2v_2^2v_3, v_0v_1^2v_2v_4], \lambda). \end{array}$$

$\tilde{X}_F$ and $\tilde{X}_G$ have different parametric equations. We find that $\tilde{X}_F, \tilde{X}_G$ are both defined in $\mathbb{P}^7 \times \mathbb{C}$ by the following nine quadratic equations:

$$\begin{array}{c} x_3x_5 - x_4^2 = 0, x_2x_6 - \lambda x_4^2 = 0, x_1x_6 - \lambda x_3x_4 = 0 \\ x_1x_5 - x_2x_4 = 0, x_1x_4 - x_2x_3 = 0, x_0x_6 - \lambda x_3^2 = 0 \\ x_0x_5 - x_2x_3 = 0, x_0x_4 - x_1x_3 = 0, x_0x_2 - x_1^2 = 0. \end{array}$$

Omitting λ in these equations we obtain a set of equation for X_Δ embedded in $\mathbb{P}^7$: these are the same equations one can compute from (3) trough elimination.

3 Main results

We use the notation of the previous sections.

Let I_F be the ideal of all polynomials in the coordinates $x_0, \dots, x_\ell, \eta$ homogeneous in $x_0, \dots, x_\ell$ and vanishing on $\tilde{X}_F$, where η is the non-homogeneous coordinate in $\mathbb{C}$. In analogy with the compact case we use the notation

$$\mathbf{z}^{\mathbf{u}} = x_0^{u_0} \dots x_\ell^{u_\ell} \eta^{u_{\ell+1}},$$

with $\mathbf{u} = (u_0, \dots, u_\ell, u_{\ell+1}) \in \mathbb{Z}^{\ell+2}$.

Consider the $(n+2) \times (\ell+2)$ matrix

$$\mathcal{B}^+ = \mathcal{B}_F^+ = \begin{pmatrix} 1 & 1 & \dots & 1 & 0 \\ m_{10} & m_{11} & \dots & m_{1\ell} & 0 \\ \vdots & \vdots & & \vdots & \vdots \\ m_{n0} & m_{n1} & \dots & m_{n\ell} & 0 \\ F(\mathbf{m}_0) & F(\mathbf{m}_1) & \dots & F(\mathbf{m}_\ell) & 1 \end{pmatrix}.$$

Lemma 3.1 *I_F is the linear span of all binomials $\mathbf{z}^{\mathbf{u}} - \mathbf{z}^{\mathbf{v}}$ with vectors $\mathbf{u}, \mathbf{v} \in \mathbb{N}^{\ell+2}$ such that $\mathcal{B}^+ \mathbf{u} = \mathcal{B}^+ \mathbf{v}$.*

Proof. We follow Theorems 2.1 and 2.2 [8].

A binomial $\mathbf{z}^{\mathbf{u}} - \mathbf{z}^{\mathbf{v}}$, with $\mathbf{u}, \mathbf{v} \in \mathbb{N}^{\ell+2}$, vanishing on $\psi((\mathbb{C}^*)^n \times \mathbb{C})$ needs to be homogeneous in the coordinates $x_0, \dots, x_\ell$, i.e.

$$\sum_{i=0}^{\ell} u_i = \sum_{i=0}^{\ell} v_i. \tag{4}$$

Therefore we prove that I_F is the linear span of all binomials $\mathbf{z}^{\mathbf{u}} - \mathbf{z}^{\mathbf{v}}$ with vectors $\mathbf{u}, \mathbf{v}$ such that (4) holds and $\mathcal{B}\mathbf{u} = \mathcal{B}\mathbf{v}$, where

$$\mathcal{B} = \mathcal{B}_F = \begin{pmatrix} m_{10} & m_{11} & \dots & m_{1\ell} & 0 \\ \vdots & \vdots & & \vdots & \vdots \\ m_{n0} & m_{n1} & \dots & m_{n\ell} & 0 \\ F(\mathbf{m}_0) & F(\mathbf{m}_1) & \dots & F(\mathbf{m}_\ell) & 1 \end{pmatrix}.$$

Consider a monomial $\mathbf{z}^{\mathbf{u}}$ and restrict it to $\psi((\mathbb{C}^*)^n \times \mathbb{C})$:

$$\begin{aligned}
\mathbf{z}^{\mathbf{u}}_{|\psi((\mathbb{C}^*)^n\times\mathbb{C})} &= (x_0^{u_0}\dots x_\ell^{u_\ell}\eta^{u_{\ell+1}})_{|\psi((\mathbb{C}^*)^n\times\mathbb{C})} = \\
&= (t_1^{m_{10}}\dots t_n^{m_{n0}}\lambda^{F(\mathbf{m}_0)})^{u_0}\dots(t_1^{m_{1\ell}}\dots t_n^{m_{n\ell}}\lambda^{F(\mathbf{m}_\ell)})^{u_\ell}\cdot \\
&\cdot\ \lambda^{u_{\ell+1}} = \\
&= t_1^{m_{10}u_0+\dots+m_{1\ell}u_\ell}\dots t_n^{m_{n0}u_0+\dots+m_{n\ell}u_\ell}\cdot \\
&\cdot\ \lambda^{F(\mathbf{m}_0)u_0+\dots+F(\mathbf{m}_\ell)u_\ell+u_{\ell+1}} = \\
&= T^{\mathcal{B}\mathbf{u}},
\end{aligned}$$

with $T = (t_1, \dots, t_n, \lambda)$.

This shows that in the hypothesis (4), $\mathbf{z}^{\mathbf{u}} - \mathbf{z}^{\mathbf{v}}$ vanishes on $\psi((\mathbb{C}^*)^n \times \mathbb{C})$ (and hence belongs to I_F) if and only if $\mathcal{B}\mathbf{u} = \mathcal{B}\mathbf{v}$.

Now we show that these binomials generate I_F as a $\mathbb{C}$-vector space: we follow Sturmfels's book [9]. Sturmfels considers the (compact) toric variety defined as in (1) and doesn't deal with the homogeneous vs. non-homogeneous question.

Fix a monomial ordering $>$ on $\mathbb{C}[x_0, \dots, x_\ell, \eta]$, and remember that this is a well-ordering on the set of monomials $\mathbf{z}^{\mathbf{u}}$. Suppose the set R of polynomials $f \in I_F$ which cannot be written as a $\mathbb{C}$-linear combination of binomials as above is non-empty and take $f \in R$ such that

$$LM_>(f) = \min_{g\in R} LM_>(g),$$

where $LM_>(f)$ is the leading monomial of f with respect to $>$. We can suppose f to be monic, so that its leading term $LT_>(f)$ is its leading monomial, let this be the monomial $\mathbf{z}^{\mathbf{u}}$.

When we restrict f to $\psi((\mathbb{C}^*)^n \times \mathbb{C})$ we get an expression containing $T^{\mathcal{B}\mathbf{u}}$ as a term and which is equal to zero. Hence the term $T^{\mathcal{B}\mathbf{u}}$ must cancel in this expression. This means that there is some other monomial $\mathbf{z}^{\mathbf{v}}$ appearing in f such that $\mathcal{B}\mathbf{u} = \mathcal{B}\mathbf{v}$ and (4) holds.

Moreover $\mathbf{z}^{\mathbf{u}} > \mathbf{z}^{\mathbf{v}}$. The polynomial

$$f' := f - \mathbf{z}^{\mathbf{u}} + \mathbf{z}^{\mathbf{v}}$$

belongs to I_F and to R but since $LM_>(f) > LM_>(f')$, we get a contradiction. □

Theorem 3.2 $I_F = \langle \mathbf{z}^{\mathbf{u}^+} - \mathbf{z}^{\mathbf{u}^-} | \mathbf{u} \in \ker(\mathcal{B}^+) \text{ and } \mathbf{u} \in \mathbb{Z}^{\ell+2}\rangle$.

Proof. On one hand, $\mathbf{u} \in \ker(\mathcal{B}^+)$ if and only if $\mathcal{B}^+\mathbf{u}^+ = \mathcal{B}^+\mathbf{u}^-$. On the other hand we show that if $\mathcal{B}^+\mathbf{v} = \mathcal{B}^+\mathbf{w}$ (and (4) holds), then $\mathbf{z}^{\mathbf{v}} - \mathbf{z}^{\mathbf{w}} = h(\mathbf{z}^{\mathbf{u}^+} - \mathbf{z}^{\mathbf{u}^-})$, for some polynomial h and vector $\mathbf{u} \in \ker(\mathcal{B}^+) \cap \mathbb{Z}^{\ell+2}$; the statement will then follow from the theorem.

If $\mathcal{B}^+\mathbf{v} = \mathcal{B}^+\mathbf{w}$, then $\mathbf{v} - \mathbf{w} \in \ker(\mathcal{B}^+)$.

$$\begin{aligned} \mathbf{z}^{\mathbf{v}} - \mathbf{z}^{\mathbf{w}} = \mathbf{z}^{\mathbf{w}}(\mathbf{z}^{\mathbf{v}-\mathbf{w}} - 1) &= \mathbf{z}^{\mathbf{w}}\mathbf{z}^{-(\mathbf{v}-\mathbf{w})^-}(\mathbf{z}^{(\mathbf{v}-\mathbf{w})^+} - \mathbf{z}^{(\mathbf{v}-\mathbf{w})^-}) \\ &= \mathbf{z}^{\mathbf{w}-(\mathbf{v}-\mathbf{w})^-}(\mathbf{z}^{(\mathbf{v}-\mathbf{w})^+} - \mathbf{z}^{(\mathbf{v}-\mathbf{w})^-}) \end{aligned}$$

It is easy to show that $\mathbf{w} - (\mathbf{v} - \mathbf{w})^- \in \mathbb{N}^{\ell+2}$. □

Now let G be the second lift, then we can consider the matrix $\mathcal{B}_G^+$ and characterize the toric ideal I_G of $\tilde{X}_G$ as above. In general $\tilde{X}_G$ will have a different parametrization from the one of $\tilde{X}_F$, moreover the normal fans are different.

Our main result is

Theorem 3.3 *$\tilde{X}_F$ and $\tilde{X}_G$ have the same equations in $\mathbb{P}^\ell \times \mathbb{C}$, i.e. $I_F = I_G$.*

Proof. Reorder the $\mathbf{m}_j$'s such that $\mathbf{m}_0, \ldots, \mathbf{m}_r \in \Delta_1 - \Delta_2$, $\mathbf{m}_{r+1}, \ldots, \mathbf{m}_s \in \Delta_1 \cap \Delta_2$ and $\mathbf{m}_{s+1}, \ldots, \mathbf{m}_\ell \in \Delta_2 - \Delta_1$, then we have

$$\mathcal{B}_F^+ = \begin{pmatrix} 1 & .. & 1 & 1 & .. & 1 & 1 & .. & 1 & 0 \\ m_{10} & .. & m_{1r} & m_{1,r+1} & .. & m_{1s} & m_{1,s+1} & .. & m_{1\ell} & 0 \\ \vdots & & \vdots & \vdots & & \vdots & \vdots & & \vdots & \vdots \\ m_{n0} & .. & m_{nr} & m_{n,r+1} & .. & m_{ns} & m_{n,s+1} & .. & m_{n\ell} & 0 \\ 0 & .. & 0 & 0 & .. & 0 & L_F(\mathbf{m}_{s+1}) & .. & L_F(\mathbf{m}\ell) & 1 \end{pmatrix},$$

and

$$\mathcal{B}_G^+ = \begin{pmatrix} 1 & .. & 1 & 1 & .. & 1 & 1 & .. & 1 & 0 \\ m_{10} & .. & m_{1r} & m_{1,r+1} & .. & m_{1s} & m_{1,s+1} & .. & m_{1\ell} & 0 \\ \vdots & & \vdots & \vdots & & \vdots & \vdots & & \vdots & \vdots \\ m_{n0} & .. & m_{nr} & m_{n,r+1} & .. & m_{ns} & m_{n,s+1} & .. & m_{n\ell} & 0 \\ L_G(\mathbf{m}_0) & .. & L_G(\mathbf{m}_r) & 0 & .. & 0 & 0 & .. & 0 & 1 \end{pmatrix}.$$

Let E be the $(n+2) \times (n+2)$ elementary matrix

$$\begin{pmatrix} 1 & 0 & \ldots & 0 & 0 \\ 0 & 1 & \ldots & 0 & 0 \\ \vdots & \vdots & & \vdots & \vdots \\ 0 & 0 & \ldots & 1 & 0 \\ a_{n+1} & a_1 & \ldots & a_n & 1 \end{pmatrix} \in SL_{n+2}(\mathbb{Z})$$

we have

$$E \cdot \mathcal{B}_G^+ = \mathcal{B}_F^+,$$

and hence

$$\ker \mathcal{B}_F^+ = \ker \mathcal{B}_G^+.$$

The theorem follows from Theorem (3.2). □

Going back to the examples above, if X is the twisted cubic, we have

$$\mathcal{B}_F^+ = \begin{pmatrix} 1 & 1 & 1 & 1 & 0 \\ 0 & 1 & 2 & 3 & 0 \\ 1 & 0 & 0 & 0 & 1 \end{pmatrix}, \mathcal{B}_G^+ = \begin{pmatrix} 1 & 1 & 1 & 1 & 0 \\ 0 & 1 & 2 & 3 & 0 \\ 0 & 0 & 1 & 2 & 1 \end{pmatrix},$$

and E is the 3×3 elementary matrix

$$\begin{pmatrix} 1 & 0 & 0 \\ 0 & 1 & 0 \\ 1 & -1 & 1 \end{pmatrix} \in SL_3(\mathbb{Z}).$$

In the case of $\mathbb{P}^1 \times \mathbb{P}^1$ blown up in a point, we have

$$\mathcal{B}_F^+ = \begin{pmatrix} 1 & 1 & 1 & 1 & 1 & 1 & 1 & 1 & 0 \\ 0 & 1 & 2 & 0 & 1 & 2 & 0 & 1 & 0 \\ 0 & 0 & 0 & 1 & 1 & 1 & 2 & 2 & 0 \\ 1 & 1 & 1 & 0 & 0 & 0 & 0 & 0 & 1 \end{pmatrix},$$

$$\mathcal{B}_G^+ = \begin{pmatrix} 1 & 1 & 1 & 1 & 1 & 1 & 1 & 1 & 0 \\ 0 & 1 & 2 & 0 & 1 & 2 & 0 & 1 & 0 \\ 0 & 0 & 0 & 1 & 1 & 1 & 2 & 2 & 0 \\ 0 & 0 & 0 & 0 & 0 & 0 & 1 & 1 & 1 \end{pmatrix},$$

and

$$E = \begin{pmatrix} 1 & 0 & 0 & 0 \\ 0 & 1 & 0 & 0 \\ 0 & 0 & 1 & 0 \\ 1 & 0 & -1 & 1 \end{pmatrix} \in SL_4(\mathbb{Z}).$$

It would be interesting to extend such results to semi-stable partitions of a polytope Δ in an arbitrary number of subpolytopes.

References

[1] V. Alexeev, *Complete moduli in the presence of semiabelian group action*, Ann. Math., **155** (2002) 611–708.

[2] D. Cox, *What is a toric variety?*, Topics in algebraic geometry and geometric modeling, 203–223, Contemp. Math., **334**, Amer. Math. Soc., Providence, RI, (2003); also avalaible at http://www.amherst.edu/ dacox/

[3] W. Fulton, *Introduction to Toric Varieties*, Ann. of Math. Studies, **13**, Princeton University Press, (1993).

[4] Maplesoft. Maple10. [http://maplesoft.com].

[5] S. Hu, *Semistable Degeneration of Toric Varieties and Their Hypersurfaces*, Communications in Analysis and Geometry, Volume 14, Number 1 (2006), 59–89; arXiv:math.AG/0110091, (2001) 1-26.

[6] M. Marchisio - V. Perduca, *On Some Properties of Explicit Toric Degenerations*, Bollettino U.M.I. (8) **9**-B (2006), 779-784.

[7] T. Oda, *Convex Bodies and Algebraic Geometry*, **15**, Springer-Verlag, Berlin Heidelberg (1988).

[8] F. Sottile, *Toric ideals, real toric varieties, and the moment map*, Topics in algebraic geometry and geometric modeling, 225–240, Contemp. Math., **334**, Amer. Math. Soc., Providence, RI, (2003); arXiv:math.AG/0212044.

[9] B. Sturmfels, *Gröbner Bases and Convex Polytopes*, American Mathematical Society, University Lecture Series, Volume 8, Providence, RI (1996). MR **97b:**13034.

Marina Marchisio
Università di Torino
Dipartimento di Matematica
Via Carlo Alberto, 10
10123 Torino (Italy)
marina.marchisio@unito.it

Vittorio Perduca
Università di Torino
Dipartimento di Matematica
Via Carlo Alberto, 10
10123 Torino (Italy)
vittorio.perduca@unito.it

RENDICONTI DEL CIRCOLO MATEMATICO DI PALERMO
Serie II, Suppl. 81 (2009), pp. 273-287

Assessing the quality of local development through an input-output model

Domenico Marino[1] *and Raffaele Trapasso*[2]

Introduction

This paper discusses the qualitative patterns of regional development using the input-matrix as an instrument to understand what happens when a regional economy changes its productivity function or when, on the contrary, it retains the same productivity function. As in the case of national economies (Arrow and Hahn 1972), each individual region can be modelled as a linear input-output system to assess whether the local community has transformed its factors of production or not; i.e. whether a new production function has been implemented or not. If the region has adopted a new production function, local growth can be intended as a collective development of skills, human capital and investment capacity, which influence the sustainability of growth. Otherwise, the region is just exploiting in an extensive way its resources and factors of production. Such condition may affect the sustainability of growth, since the community is not investing its energies in developing new skills or human capital: the local community has not created *a new competitive advantage*.

Because of globalisation many regions have achieved a remarkable growth thanks to local specialisation in a given sector or activity. This is due to international division of labour and increased factor mobility. On the one hand, in a number of regions this phenomenon has brought about the possibility of concentrating capital and labour in new sectors characterised by an high level of productivity and, thus, by an higher potential of development. In this case, the economy has gone through a process of technological transformation that impacts on (*i*) factor productivity, and (*ii*) knowledge, skills, and occupational structure of employment. This is the most desiderable pattern of development, even though in some cases the impact on the employment (creation of jobs) may be neutral.[3] On the other hand, in some regions growth depends on an extensive use of resources and factors of productions. This means that the region has not changed its productivity function or the sectoral composition of the economy. Such a pattern of growth is based on the *multiplication* of factor of production. Far to be the exception, regional development due to factor multiplication is very common also in industrialised countries that can use the large influx of low-skilled workers (e.g.

[1] Mediterranea University of Reggio Calabria.

Adress: Domenico Marino via Lia, 35 - 89100 Reggio Cal.

Tel.: +393389092929 Fax: +390965651042

e-mail:dmarino@unirc.it

[2] OECD

3 . This phenomenon is often labelled as “job-less growth” or employment neutral growth (Gordon, 1993).

immigrants coming from less developed countries), an outcome of globalisation, to improve sectors characterised by low per capita productivity such as construction, traditional manufacturing, or proximity and personal services.[4] This pattern of growth may lead to a paradox: that economic growth does not depend on movement from less efficient to more efficient technology, yet the higher (regional) income is associated with higher employment rate but lower productivity per capita.[5]

To evaluate the *quality* of regional development, this essay uses the input/output analysis. The input/output analysis is a method used to characterise economic activity in a given time period, and to predict the reaction of a regional economy to stimulation, for example, from increased consumption or changes in government policy. For instance, the input/output analysis can be used to describe the way in which the productive system satisfies final demand (consisting of consumption, investments and exports). An input-output matrix represents the links between an economy's resources and its consumption. The matrix may vary from the simple (three sectors: industry, services and agriculture) to the complex (over 500 branches). It is one of the only techniques applicable to the evaluation of the sectoral impacts of structural interventions, because it allows for the detailed division of an economy's productive structure. An input-output matrix can be compared to a macro-economic model that is highly simplified regarding the economic mechanisms represented, but which is extremely detailed from the sectoral point of view.

Input-output analysis is used primarily in scenario analysis and simulation, where it serves to verify policy scenarios, based on the technological structure of the economy of a given country (or region, as in this case) and on the state of final demand. Also, it can be used in predicting dynamics. For instance, there are numerous applications of input-output matrices to the evaluation of development programmes, including estimating impacts differentiated according to the different branches of an economy. Following the aim of this essay, the input-output analysis will be used to assess the typology (or, as stated above, the *quality*) of regional development.

---

4 . Growth can occur through factor multiplication process or factor transformation process (Barewald, 1970). Factor multiplication involves increase in the quantity of the same factor inputs of the given quality to be transformed into highest output of the same type and quality through the use of the same production function. But the factor transformation process involves a different production function resulting in more and different quality output per unit of factor inputs. New production function generally embodies different technology. Technology affects the nature, direction and magnitude of relationship between employment and income. Development of technology has generally been capital intensive and labour displacing, and hence, labour augmenting. Besides, new technology is often more knowledge and skill intensive. Knowledge and skill requirements are not only greater in magnitude and superior in quality but these are also very different from earlier ones. This makes some occupations and types of knowledge/skills redundant and obsolete, while some new occupations and types of education emerge

5 . Classical economics states that economic growth is generally characterized with a movement from less efficient to more efficient technology (Mathur, 1962). The technological change leads to growth of income, through improvements in employment and productivity. However, technological development has generally been capital intensive and labour displacing. This may lead to a paradox: on the one hand, economic growth can be associated with higher productivity and income but lower employment; on the other hand, a higher income can be associated with higher employment rate but lower productivity per capita.

Input-output matrices are based on the notion that the production of outputs requires inputs. These inputs may take the form of raw materials or semi-manufactured goods, or inputs of services supplied by households or the government. Households, provide labour inputs, while the government supplies a wide range of services such as national security, social services and the road system. Having purchased inputs from other producing sectors, or primary inputs from households, an industry then produces output and sells this output either to other industries or to final demanders, such as households or residents of other regions. Thus, a wide range of inputs is used to produce an equally wide range of outputs.

Assessing inputs and outputs through an input-output model it is possible to detect the (regional) productive specialization. For instance, the industrial mix of the region is clearly depicted by the transaction matrix and key sectors are easily detectable. Thus, if the previous part of this essay studied the agglomeration forces that concentrate factors in a given territory, this part aims at understanding whether the achieved agglomeration (i.e. the local specialization) is characterized by (*i*) a specialisation in high-tech sectors, or mature sectors enjoying a large and stable international demand, and (*ii*) a higher level of productivity.[6]

Detecting backward and forward linkages through an input-output analysis

In a regional assessment is obviously important to know how closely "linked" sectors are with each other, and which sectors may considered as the *drivers* of the economy. Of course, the direct linkages are shown in the matrix of technological coefficients (the so-called *A* matrix), and the direct plus the indirect linkages are revealed by the Leontief inverse (Mathallah, 1996). However, we need to distinguish between *backward* linkages and *forward* linkages. Backward linkages are the relationship between the activity in a sector and its purchases. Forward linkages are the relationship between the activity in a sector and its sales. These linkages may give rise to the agglomeration of activity in a given region.[7] Input-output models are based on the assumption that export demand (or the ability of industries to sell to the external economy) is the engine that generates activity in the regional economy. Changes in final demand (direct effects) infuse local industries with new funds, which increase output and employment.[8] The present essay assumes that a region with stronger backward and

6 . It is important to bear in mind that it is very difficult to evaluate the quantity of technology that a sector embodies. To have a clear assessment of the level of technology used by a given industry one should look at the supply-chain rather than at the sectors. Empirical evidence demonstrates that often in some mature production such as textile there are specific activities that can be considered as high tech ones. On the contrary in other sectors commonly defined like "high tech sectors" or capital intensive sectors, there are some activities that are rather labour intensive.

7 . New economic geography theory argues that although flexibility in location decisions exists a priori, once the agglomeration process has begun, spatial differences become quite rigid. Krugman and Venables (1995) and Venables (1996) have shown how this feature can be explained by backward and forward linkages. The same result of lock-in dynamics is achieved with different hipotesis as the possibility that location decisions are influenced by previous equilibria of the system, as it was stated in the first part of this essay.

forward linkages in sectors with high rate of export is in a more favourable condition than a region with weak linkages in export oriented sectors (Cfr. Aoki 2002).

The analysis of linkages, used to examine the interdependency in production structures, has a long history within the field of input-output analysis. Since the pioneering work of Chenery & Watanabe (1958), Rasmussen (1956) and Hirschman (1958) on the use of linkages to compare international productive structures, this analytical tool has been improved and expanded in several ways, and many different methods have been proposed for the measurement of linkage coefficients. The measures, including backward and forward linkages, have extensively been used for the analysis of both interdependent relationships between economic sectors, and for the formation of development strategies (Hirschman, 1958). In the 1970s, these traditional measures were widely discussed and several adapted forms were put forward (Yotopoulos & Nugent, 1973; Laumas, 1976; Riedel, 1976, Jones, 1976; Schultz, 1977). Moreover, linkage analysis methods have attracted increasing attention from the part of input-output analysts (Cella, 1984; Clements, 1990; Heimler, 1991; Sonis et al, 1995; Dietzenbacher, 1997).

In this essay both backward linkages and forward linkages are taken into account. Such choice can expose the analysis to a possible criticism. There is some literature against the reliability of this methodology (Cardenete and Sancho, 2006). In fact, while backward linkages are constructed from the Leontief inverse matrix, forward linkages use the inverse matrix from the Ghosh model.[9] While the Leontief model has a clear technological interpretation well rooted in production theory, the Ghosh model lacked a corresponding embedding in standard micro theory until Dietzenbacher (1997) suggested to interpret the model as a price model. For a long time therefore, more conceptual credit has been given to backward linkages than to forward linkages since only the former were believed to trace the ripple effects implicit in the underlying technology.

The output multipliers, defined as the column sum of the Leontief inverse matrix, obviously indicate backward linkages. Using the row sums of the Leontief inverse, the output multipliers are given by $(I-A)^{-1}\, i$. This shows the effect on the total activity in each sector if every sector increases its final demand by unity. This is sometimes referred to as "sensitivity" of the sector. This is true if we assume that intermediate inputs are proportional to total output. Otherwise we would assume that intermediate flows are supply led rather than demand led. For most economies this is a less acceptable assumption (Matallah and Proof, 1994).

---

8 . A sector's outputs are demanded both inside and outside the regional economy. Final demand in an input-output framework is that portion of demand that is not used in the production of other outputs inside the regional economy (intermediate demand). Final demand includes consumption, investment, government and exports.

9 . Ghosh's "supply-driven" input-output model is a well-known alternative for Leontief's traditional "demand-driven" input-output model. The Ghosh model calculates changes in gross sectoral outputs for exogenously specified changes in the sectoral inputs of primary factors. Typically, the model is interpreted so as to describe physical output changes as caused by changes in the physical inputs of primary factors (Dietzenbacher, 1997).

The backward linkages of each given sector represented in the matrix can be represented as an index derived by the *i*th(s) sectoral multipliers. In this case, the result is an index in which z_{ij} is an element of $(I\text{-}A)^{-1}$(*). The index is constructed to measure the relative strength of the backward linkages by dividing each of the sectors' backward linkages by their respective averages for the whole economy.

$$n\sum_i z_{ij} / \sum_j \sum_i z_{ij} \qquad (*)$$

Concerning forward linkages, rather than using the inverse matrix from the Ghosh model (see above) and assuming that intermediate inputs are proportional to total output, one might assume that they are proportional to total inputs (Jones, 1976); i.e. rather than using

$$x_{ij} = a_{ij} X_j$$

we might use

$$x_{ij} = b_{ij} X_j.$$

This means that the intermediate flows are supply led rather than demand led. Therefore, if the matrix (*B*) is defined as above, then the row sums of $(I\text{-}B)^{-1}$ are measures of forward linkages. In other words, thanks to this method it is possible to define forward linkages by using the Leontief inverse matrix. Accordingly, the "input multiplier" (that is the result of our assumption) will generate the index (**) measuring the intensity of forward linkages per each sector:

$$n\sum_i q_{ij} / \sum_j \sum_i q_{ij} \qquad (**)$$

where q_{ij} is an element of $(I\text{-}B)^{-1}$.

Finally, these indexes can be used to measure the relative strength of the forward and backward linkages within the regional economy. Sectors possessing weak forward linkage indices meant that these industries sell their output mostly to final demand and hence do not figure significantly in the measures as they depend on intermediate flows. Sectors possessing weak backward linkage indices meant that their dependence on other sectors for their inputs is relatively low, i.e., their principal inputs are provided mainly by imports. Key sectors, according to Hirschman (1958), are those sectors with both backward and forward indices greater than unity. However, it is possible to consider some nuances rather than a dicotomic approach (Matallah, Proops, 1996).

A numerical application of these indexes and a calculation of the strengths of linkages within the regional economy is presented in the last part of the essay, where the case of the Madrid metropolitan region will be analysed through this *lens*.

Backward and forward linkages in the Madrid productive framework

The paragraph above has showed that there is not any clear specialisation within the Madrid-based productive framework, thus it is possible to state that many different sectors act as drivers for of the regional economy. However, the analysis has been conducted without taking into account the functional linkages among sectors, yet their position and distance on the LIM. A more robust way to understand which sectors

represent the pillars of the local economy is to detect and evaluate the intensity of backward and forward linkages among the 61 branches of the I-O tables. Recalling what we stated in the first chapter of this essay, we detect both backward linkages and forward linkages within the Madrid productive framework.[10]

The output multipliers, defined as the column sum of the Leontief inverse indicate backward linkages. Using the row sums of the Leontief inverse, the output multipliers are given by $(I\text{-}A)^{-1}\, i$. Table 1, below, shows the *i*th(s) sectoral multipliers and report the backward linkages of each given sector as in index in which z_{ij} is an element of $(I\text{-}A)^{-1}$.

Table 1 – Sectoral output multipliers in the Madrid metro-region (2002)

Sector	output multiplier	index $n\sum_i z_{ij} / \sum_j \sum_i z_{ij}$ (BW linkages)
Servicio doméstico	1,0000	0,393589724
Educación de no mercado	1,3090	0,515228072
Administraciones públicas	1,5792	0,621570029
Intermediación finanziera	1,5817	0,622552568
Otro comercio menor y reparación	1,6401	0,645536018
Energía y minería	1,6419	0,646229961
Servicios anexos al transporte	1,6706	0,657544692
Seguros y planes de pensiones	1,7925	0,705494021
Sanidad de no mercado	1,9489	0,767062403
Actividades asociativas	1,9796	0,779135537
Servicios recreativos de no mercado	1,9822	0,780153911
Inmobiliarias y alquileres	1,9962	0,785681129
Servicios de saneamiento	2,1250	0,836367296
Otros servicios profesionales	2,1374	0,841260785
Educación de mercado	2,1791	0,857675023
Comercio mayorista	2,1806	0,858257168
Asesoramiento	2,2408	0,881949956
Servicios personales	2,2723	0,894343866
Comunicaciones	2,3073	0,908145636
Agricultura y ganadería	2,3317	0,917730445
Sanidad de mercado	2,3820	0,937549932
Bebidas y tabaco	2,4729	0,973322004
Hostelería	2,4735	0,973562204
Servicios recreativos de mercado	2,4982	0,983271898

10 See pag. 26.

Vidrio	2,5033	0,985261172
Actividades informáticas	2,5281	0,995048717
Comercio vehículos y combustibles	2,5283	0,995124964
Cemento y derivados	2,5374	0,998698916
Construcción	2,5517	1,004337101
Otras industrias no metálicas	2,6716	1,051508962
Transporte no terrestre	2,6911	1,059198688
Caucho y plástico	2,7080	1,065848445
Transporte terrestre	2,7237	1,072031256
Otro material de transporte	2,7299	1,074479011
Edición	2,7411	1,078850376
Publicidad	2,7646	1,088135968
Imprentas	2,7793	1,093889925
Servicios tecnico	2,7962	1,100567751
Industrias lácteas	2,8152	1,108028498
Maquinaria industrial	2,8263	1,112409731
Industria textil	2,8332	1,115115596
Máquinas oficina y precisión	2,8497	1,121620548
Forja y talleres	2,8541	1,123327932
Estructuras metálicas	2,8642	1,127319803
Industria del papel	2,8767	1,132227608
Industrias cárnicas	2,9200	1,14929122
Industria del mueble	2,9462	1,159601117
Otras alimenticias	2,9673	1,167897434
Metálicas básicas	2,9714	1,169494306
Artículos metálicos	3,0005	1,180974132
Confección	3,0059	1,183095952
Material eléctrico	3,0072	1,18359186
Material electrónico	3,0180	1,187862445
Productos farmacéuticos	3,0578	1,203530056
Otras manufacturas	3,1444	1,237586273
Cuero y calzado	3,1892	1,255234406
Madera	3,2261	1,269745252
Otra química final	3,2551	1,281180642
Química industrial	3,3204	1,306886568
Química de base	3,3671	1,325244527
Vehículos y sus piezas	3,6905	1,452538566

Similarly, according to the model presented above in the essay to determine forward linkages we will assume that intermediate inputs are proportional to total inputs (Jones, 1976)

$$x_{ij} = b_{ij} X_j.$$

This means that the intermediate flows are supply led rather than demand led. Such hypothesis can be considered as true over the short run, even in a regional economy, such as of Madrid, that has shown a remarkable capacity to expand its output. Then the row sums of $(I\text{-}B)^{-1}$ are measures of forward linkages. The table below (Table 2) shows the "input multiplier" and an index measuring the intensity of forward linkages per each sector where q_{ij} is an element of $(I\text{-}B)^{-1}$.

Table 2 – Sectoral input multipliers in the Madrid metro-region (2002)

Sector	Input multiplier	Index $n\sum_i q_{ij} / \sum_j \sum_i q_{ij}$ (FW linkages)
Servicio doméstico	1,0000	0,39359
Servicios de administración pública	1,0000	0,39359
Servicios recreativos de no mercado	1,0067	0,396237
Servicios sanitarios de no mercado	1,0310	0,40578
Servicios de educación de no mercado	1,0439	0,410859
Servicios personales	1,0627	0,418266
Servicios de asociaciones	1,0994	0,432713
Servicios sanitarios de mercado	1,1664	0,459083
Servicios de comercio al por menor y reparación	1,2020	0,473095
Productos lácteos	1,2358	0,486398
Servicios de saneamiento público	1,2458	0,49034
Productos de la edición	1,2576	0,494991
Otros productos químicos	1,2716	0,500473
Servicios de educación de mercado	1,2989	0,511237
Servicios recreativos de mercado	1,3809	0,543499
Productos de la confección	1,3921	0,547924
Productos cárnicos	1,3961	0,549475
Muebles	1,4082	0,554248
Servicios anexos al transporte	1,4873	0,585379
Servicios de transporte no terrestre	1,5177	0,597358
Productos de cuero y calzado	1,6534	0,650768
Bebidas y tabaco	1,7109	0,673409
Productos del vidrio	1,7531	0,69001
Cemento y derivados	1,8457	0,726457
Servicios de informática	1,9050	0,749808
Productos de la metalurgia básica y fundición	1,9115	0,752354
Servicios de seguros y planes de pensiones	1,9629	0,772596
Otros productos alimenticios	1,9896	0,783106
Servicios de hostelería	1,9945	0,785014
Servicios de comercio de vehículos y combustibles	2,0032	0,78843
Productos farmacéuticos	2,1770	0,856862
Otro material de transporte	2,1886	0,861424
Otras manufacturas	2,2938	0,902811
Maquinaria industrial	2,3381	0,920263
Servicios tecnico	2,4315	0,957003
Productos impresos	2,6257	1,033446
Productos textiles	2,7913	1,098645
Productos de la agricultura y ganadería	2,9272	1,1521
Servicios de asesoramiento	3,0147	1,186545
Servicios de intermediación finanziera	3,0938	1,217671
Servicios de comercio al por mayor e intermediarios	3,1150	1,226046
Productos de forja y talleres	3,1411	1,236305
Trabajos de construcción	3,2093	1,263153

Productos de otras industrias no metálicas	3,3005	1,299031
Estructuras metálicas	3,4059	1,340521
Material eléctrico	3,4514	1,358422
Madera, corcho y sus produco	3,4518	1,35861
Máquinas oficina y precisión	3,5152	1,383537
Productos de caucho y materias plásticas	3,5870	1,411824
Minerales no energéticos	3,6257	1,427019
Otros servicios profesionales	3,6571	1,439409
Comunicaciones	3,7144	1,461947
Servicios de publicidad	3,8233	1,504823
Productos de la química básica	4,0709	1,602252
20. Papel y productos de papel	4,2021	1,653887
Material electrónico	4,3167	1,699006
Vehículos y sus piezas	4,5266	1,781607
Servicios inmobiliarios y de aquile	5,0641	1,99317
Electricidad, gas, agua y combustibles	5,3715	2,114181
Servicios de transporte terrestre	5,7599	2,267043
Productos de la química industrial	7,5585	2,974949

According to Hirschman (1958) key sectors of the local economy are those sectors with both backward and forward indices greater than unity. However, the most interesting aspect which might emerge, for developing economies, is the appearance of sectors that "nearly" qualify as key sectors. This conclusion was first introduced by Matallah and Proops (1994), and further developed by the same authors (Matallah, Proops, 1996), and can be summarized by defining "strong", "intermediate", and "weak" as in table 3 below (Matallah, Proops, 1996).

Table 3 – Three different intensities of backward (forward) linkages

Strong linkage index	*index* > 1
Intermediate linkage index	0.9 > *index* = 1
Weak linkage index	*index* < 0.9

Source: Matallah, Proops, 1996

Following the methodology showed in the table above it is possible to understand what the key sectors in the Madrid economy are: i.e. those sectors acting as pillars of the local economy by generating a large number of bw and fw linkages. The table 49, below, is the rank of the indexes used as a measure of bw and fw linkages. It is very interesting to note that the traditional manufacturing (and particularly the automotive industry) plays an important role in the regional economy, that, as was assessed in chapter two, it is mainly a post-industrial economy in which the service sector generates the larger part of the regional GDP.

Through this new piece of analysis it possible to assess that the service sector is not autonomous in the region and depends on manufacturing activities. What it is important to note is that these manufacturing activities are probably changing following the evolution of the local technology and the local capacity to innovate. However, to verify this hypothesis it would be necessary to have a long time series and to apply the same methodology at each period to assess how the ranking evolves.

Table 4 – Rank of Backward and Forward linkages in the Madrid metro-region

Sector	BW	FW
Servicio doméstico	0,39359	0,39359
Educación de no mercado	0,51523	0,410859
Administraciones públicas	0,62157	0,39359
Intermediación finanziera	0,62255	1,217671
Otro comercio menor y reparación	0,64554	0,473095
Energía y minería	0,64623	2,114181
Servicios anexos al transporte	0,65754	0,585379
Seguros y planes de pensiones	0,70549	0,772596
Sanidad de no mercado	0,76706	0,40578
Actividades asociativas	0,77914	0,432713
Servicios recreativos de no mercado	0,78015	0,396237
Inmobiliarias y alquileres	0,78568	1,99317
Servicios de saneamiento	0,83637	0,49034
Otros servicios profesionales	0,84126	1,439409
Educación de mercado	0,85768	0,511237
Comercio mayorista	0,85826	1,226046
Asesoramiento	0,88195	1,186545
Servicios personales	0,89434	0,418266
Comunicaciones	0,90815	1,461947
Agricultura y ganadería	0,91773	1,1521
Sanidad de mercado	0,93755	0,459083
Bebidas y tabaco	0,97332	0,673409
Hostelería	0,97356	0,785014
Servicios recreativos de mercado	0,98327	0,543499
Vidrio	0,98526	0,69001
Actividades informáticas	0,99505	0,749808

Comercio vehículos y combustibles	0,99512	0,78843
Cemento y derivados	0,99870	0,726457
Construcción	1,00434	1,263153
Otras industrias no metálicas	1,05151	1,299031
Transporte no terrestre	1,05920	0,597358
Caucho y plástico	1,06585	1,411824
Transporte terrestre	1,07203	2,267043
Otro material de transporte	1,07448	0,861424
Edición	1,07885	0,494991
Publicidad	1,08814	1,504823
Imprentas	1,09389	1,033446
Servicios tecnico	1,10057	0,957003
Industrias lácteas	1,10803	0,486398
Maquinaria industrial	1,11241	0,920263
Industria textil	1,11512	1,098645
Máquinas oficina y precisión	1,12162	1,383537
Forja y talleres	1,12333	1,236305
Estructuras metálicas	1,12732	1,340521
Industria del papel	1,13223	1,653887
Industrias cárnicas	1,14929	0,549475
Industria del mueble	1,15960	0,554248
Otras alimenticias	1,16790	0,783106
Metálicas básicas	1,16949	0,752354
Artículos metálicos	1,18097	1,427019
Confección	1,18310	0,547924
Material eléctrico	1,18359	1,358422
Material electrónico	1,18786	1,699006

Productos farmacéuticos	1,20353	0,856862
Otras manufacturas	1,23759	0,902811
Cuero y calzado	1,25523	0,650768
Madera	1,26975	1,35861
Otra química final	1,28118	0,500473
Química industrial	1,30689	2,974949
Química de base	1,32524	1,602252
Vehículos y sus piezas	1,45254	1,781607

Limits of – and objections to – this methodology

The results obtained are not neutral to the level of aggregation. In fact, a high level of aggregation may have the following results. First, aggregation reduces the technological factor of the intersectoral relationship described by the input-output table, i.e. reducing the impact of a sector on the economy. Second, it reduces the homogeneity of sectors. In an input-output table, classification and division of the economic sectors might affect the sectoral hierarchy. Another limitation of this approach is that the inter-sectoral relationship derived from an input-output table should reflect the technological structure of the regional economy. However, the elements of an input-output table are the result of a complex interaction of several factors, i.e. economic, technical, institutional, etc. Thus it is challenging for a model to consider all this variables and to take them into account while assessing the regional productive framework.

There are also external limits. The methods used and the results obtained are based mainly on the current interindustry flow matrices. They do not take into account the transaction of fixed capital within the economy. The integration of fixed capital would modify the results already obtained. Their integration would necessitate the construction of the capital matrices and the utilisation of a dynamic Leontief model (Miernyk, 1977). Moreover, the effects induced by the spending of revenues paid to households are not included. Their integration once more would modify the classification of the economic sectors. Theoretically speaking, their integration is seen as possible by making them endogenous within the economic system (Morrisson and Smith, 1979).

Finally, some objections could be raised against this approach. The first objection concerns the hypothesis of stable technical coefficients, which is based on the assumptions of the static Leontief model. The economy is mainly in a continuous dynamic state, which means that the sectoral hierarchy might not be stable. Given that this essay takes into account very close periods, this objection may not be valid in this context. The second objection is advanced from the relation between linkages and the efficiency of the economy. The indices calculated do not take into account the differential efficiency of the several branches of the national economy. For instance,

backward linkages might favour those sectors with limited efficiency with regard to intermediate consumption. The third and last objection concerns the problem of employment. The methods used do not take the variable of employment into account, bearing in mind that economic sectors have different potential with regard to this aspect. In a region like Madrid the labour market is buoyant, it would have been extremely difficult to take into account the dynamics of local employment.

Bibliography

Aoki, M. (1999), *Analysis of an open model of share markets with several types of participats*, UCLA, working paper.

Aoki, M. (2003), *A new model of labour dynamics: Ultrametrics, Okun's law, and transient dynamics,* UCLA, working paper.

Aoki, M (2004), *New frameworks for macroeconomic modelling: some illustrative examples*, UCLA, working paper 2004.

Arrow, K. J. and F. Hahn (1971). *General Competitive Analysis*. Holden-Day, San Francisco

Arthur, W. B. (1988), *Self-Reinforcing Mechanisms in Economics*, in Anderson, P. W., Arrow, K. J. and Pines, D.,(eds.), *The Economy as an Evolving Complex System, Reading*, MA: Addison-Wesley.

Arthur, W. B. (1989), "Competing technologies, increasing returns and lock in by historical events". *The economic journal* vol. 99.

Arthur, W. B. (1989), "Complexity and the Economy", *Science*, vol. 284, pp.107-109

Arthur, W. B. (2005), "Out-of-equilibrium and Agent-based Modelling", *Hand-book for computational economics*, Vol. 2.

Barro, R. J. and X. Sala-i-Martin (1995), *Economic Growth*, McGraw-Hill.

Baumol, W.J and Oates, (1988) W.E. The Theory of Environmental Policy. Cambridge: Cambridge University Press.

Becattini G. (1979), "Dal "settore" al "distretto" industriale. Alcune considerazioni sull'unità di indagine nell'economia industriale", *Rivista di Economia e Politica Industriale*, n.1.

Becattini G., and E. Rullani (1993), "Sistema locale e mercato globale", in *Economia e Politica industriale*, n. 80.

Bianchi, P. (1995), *Le politiche industriali dell'Unione Europea,* Bologna, Il Mulino.

Dosi, G. (1984), *Technical change and industrial transformation*, St. Martin Press, New York.

Florida, R. (2002), *The Rise of the Creative Class and How It's Transforming Work, Leisure and Everyday Life*, Basic Books, New York.

Foster, G. (1973), *Traditional Societies and Technological Change*, Harper & Row, New York, NY.

Frenken, K. (2005), *Technological innovation and complexity,* Urban and Regional research centre Utrecht (URU), working paper.

Freeman, A. (2004), "Measuring and Comparing World Cities", GLA-Economics, working paper n. 9.
Friedmann, J. (1986), "The World Cities Hypothesis", *Development and Change*, Vol. 17, No. 1, pp. 69-84.
Hall, P. (2000), "Creative Industries and Economic Development", *Urban Studies*, Vol. 37, No. 4, pp. 639-649.
Hirschman, A. O. (1959), *The Strategy of Economic Development*, Yale University Press, New Haven, CT.
Jacobs, J (1984). *Cities and the wealth of nations*. Vintage Books, New York.
Krugman, P. (1991), "History Versus Expectations"*, Quarterly Journal of Economics*, vol. 106.
Krugman, P. (1991), *Geography and Trade*, MIT Press.
Krugman, P and A. J. Venables, (1995) *The Seamless World: A Spatial Model of International Specialization*, 1230, C.E.P.R. Discussion Papers.
Krugman, P. R., A. J. Venables and M. Fujita (1999), *The Spatial Economy*, The MIT Press, Cambridge, MA.
Latella, F. and D. Marino (1996), "Diffusione della conoscenza ed innovazione territoriale: verso la costruzione di un modello*", Quaderni di Ricerca di Base dell' Università Bocconi,* n. 2, 1996.
Marino, D. (1998), "Territorial Economic Systems and Artificial Interacting Agents: Models Based on Neural Networks", *International Journal of Chaos Theory and Applications*", vol.3, 1/2.
Moreno L. (2001), *The Federalization of Spain*, Frank Cass, London.
Matallah, K. and J. L. R. Proops, (1992), *Algerian Economic Development; 1968-1979: A Multiplier and Linkage Analysis*, Economic Systems Research, vol. 4, pp. 257-267.
Matallah, K. and J. L. R. Proops, (1994), *An Input-Output Assessment of Algerian development*, Working Paper Series, Department of Economics, University of Keele, U.K.
Miernyk, W. H. (1977). *The Projection of Technical Coefficients for Medium-Term Forecasting,* in William F. Gossling (ed.), *Medium-Term Dynamic Forecasting*. London: Input-Output Publishing Company, pp. 29–41.
Morrisson, W. I. And P. Smith (1979), *Input-Output Methods in Urban and Regional Planning: a Practical Guide*, Pergamon Press, Oxford.
Myrdal, G. (1957), *Economic Theory and Underdeveloped Regions*, London Duckworth.
Nelson, R.R. and S.G. Winter (1977). "In Search a Useful Theory of Innovation", *Research Policy*, vol. 6, pp. 36-76.
Nelson, R. R. and S. G. Winter (1982), *An Evolutionary Theory of Economic Change*, The Belknap Press of Harvard University Press, Cambridge, MA.
Porter, M. (1990). *The Competitive advantage of nations*. The Free Press, New York.

Ringrose, D. R. (1984), "Madrid and the Spanish Economy, 1560-1850", *The Hispanic American Historical Review*, Vol. 64, No. 4, pp. 785-786.

Venables, A. J. (1996), "Equilibrium locations of vertically linked industries" *International*

Williamson, O. E. (1981). *The economics of organization: The transaction cost approach*. The American journal of sociology, vol. 87, n. 2, p. 233.

RENDICONTI DEL CIRCOLO MATEMATICO DI PALERMO
Serie II, Suppl. 81 (2009), pp. 289-298

A distance decay model for local spatial statistics

Massimo Mucciardi

Department of Economics, Statistics, Mathematics and Sociology "V. Pareto"
University of Messina massimo.mucciardi@unime.it

Summary

The main objective of this work is to develop an alternative version of the DSMA procedure to improve the local measures of spatial autocorrelation. According to a distance decay model, we introduced a transform in the DSMA so that the spatial weights generated are sensitive to the effective distance of each territorial unit. Finally, an application related to the railway density of 107 Italian provinces is discussed.

1. Introduction

A rising interest in clustering spatial data is emerging in numerous areas, such as economic development, epidemiology, demography etc.. In this context, local measures of spatial autocorrelation aim at identifying patterns of spatial dependence within the study region. Mapping these measures provides the basic building block for identifying spatial clusters of units. Recently, interest has shifted to the identification of local patterns of spatial association. In fact, while global measures can be used to summarize the typical features of spatial autocorrelation for the entire region, local measures of spatial autocorrelation have been proposed for identifying the presence of deviations from global patterns of spatial association, and "hot spots", such as local clusters or local outliers (Boots, 2002). Whatever local statistic is used, there is a need to define a "local neighbourhood" (Mucciardi, 2008a). Generally, most local spatial indices utilize a classical (0-1) matrix of weight as the interconnection system. We should remember that the main problem of classical (0-1) matrixes (queen and rook case) is that they are invariant with regard to topological transformations of the territory (Mucciardi, 2008b). In fact, if we consider a number of zones of equal numerousness, each characterised by the same group of observations and by the same weight matrix, the spatial indices always assume the same value independently of the topographical configuration of each spatial system considered. Recently, the criterion of a "flexible weight matrix" (Mucciardi, 2008a) has been proposed in relation to the phenomenon under investigation, which takes into consideration the effective distance between spatial units represented as points (or centroid for spatial areal data) and returns final weights proportional to the intensity of the links between adjacent units.

With this aim, in this paper we present a modified version of the DSMA (Double State Maximin Algorithm - Mucciardi, 1998) procedure using a distance decay model to determine a new system interconnection for point and areal spatial data. The outline of the paper is as follows. In section 2, we briefly examine one of the most utilized spatial local index; section 3 we discuss the proposed change to the DSMA method. Finally, section 4 looks at an application related to the railway density of 107 Italian provinces.

2. A brief description of the Local Moran statistic

There are different proposals for local measures, but in this paper we focus on a local Moran statistic. The local Moran I_i (Anselin, 1995) detects local spatial autocorrelation and can be used to identify local clusters (regions where adjacent areas have similar values) or spatial outliers (areas distinct from their neighbours). The Local Moran statistic decomposes Moran's I (Moran, 1950), the equivalent of the global measure, into contributions for each location I_i. The sum of I_i for all observations is proportional to Moran's I.

In formula, Local Moran's I_i statistic for each observation i may be defined as follows:

$$I_i = z_i \sum_{j, j \neq i}^{n} w_{ij} z_j \qquad (1)$$

where the observation z_i and z_j are in standardized form and the weight w_{ij} are generic elements of the interconnection matrix $\mathbf{W}$ (generally in row-standardized form). As we can observe, the local index is the product of the standardized local value and the mean of the standardized neighbouring value. Thus, similarly to the global index, it can be positive, negative or equal to zero. It is negative when there is an association of opposite values at neighbouring locations, and positive in the case of spatial association of similar values. From the statistical inference point of view, the distribution of I_i can be approximated by a normal distribution, with a mean just below zero, but it is preferable to use a permutation (Monte Carlo) approach to simulate a significance level (Anselin, 1995). Ord and Getis (1995) recommend a Bonferroni adjustment as a conservative correction, but also suggest that since the focus is on spatial pattern rather than the underlying values themselves the use of z scores in the calculations for I_i may be sufficient.

3. Use of the "distance decay model" in DSMA procedure

If we consider n territorial units (point or areal data), the $n \times n$ spatial weight matrix $\mathbf{W}$ (also called spatial connectivity matrix) defines the interconnection system for each location or zone with non-zero elements for neighbours, zero for others and has zero on the diagonal by convention (by convention, w_{ii} is also defined as zero). It is commonly assumed that closer zones will exert more influence than those farther away. Furthermore, many studies have shown that the decline in spatial relationship between two locations is not simply proportional to distance (Fotheringham and O'Kelly, 1989). As a result, a power or exponential function modifying the distance weight is often used to model spatial interaction between places. In order to solve this problem, we specify a spatial weight (π_{ij}^{k}) as a continuous and monotone decreasing function of distance:

$$\pi_{ij}^{k} = f(d_{ij}) = e^{-\varphi\left(\frac{d_{ij}}{h^k}\right)^{\alpha}} \quad \text{if} \quad 0 < d_{ij} \le h^k \quad \forall\, i \neq j \quad \text{with} \quad k = 1,..,t \qquad (2)$$

$$\pi_{ij}^{k} = f(d_{ij}) = 0 \quad \text{if} \quad d_{ij} > h^k \quad \forall\, i \neq j \quad \text{with} \quad k = 1,..,t$$

where φ is the decay parameter, α is a smoothing parameter, d_{ij} is the distance between the "n" units in the study area and h^k is a threshold distance (or interconnection ray) which is generated by the DSMA procedure in the k-th spatial order (Mucciardi, 1998). Distance has been assumed to be the simple Euclidean distance between points (or centroids for areal data) ignoring barriers and other factors. Other features of the function are the following:

$$\lim_{dij \to 0} = 1 \text{ and } \lim_{dij \to \infty} = 0$$

Moreover in formula (2) with φ=0.5 and α=2 we obtain a Gaussian distance decay function (the weighting diminishes at a rate determined by a normal curve). In the first stage of the DSMA procedure, the threshold distance h^k (also called MaxMin distance), is chosen in such way to satisfy the relation:

$$h^k = \max\left(\mathbf{e}^k{}_1, \mathbf{e}^k{}_2, \ldots \mathbf{e}^k{}_j \ldots \mathbf{e}^k{}_n\right), \qquad j = 1,..,n \qquad (3)$$

where the $\mathbf{e}^{k}{}_{j}$ represents minimum distance between the unit j (with $i \neq j$) and each of the other units[1]. According to procedure, the function (3) excludes zones that are further from "i" than a specified (radius) distance h^{k}, which is equivalent to setting a zero weight on zones "j" whose distance from i are greater than h. For the zones included, in other words those within the radius h^{k}, the function assigns weights according to function (2). Finally, to ensure the compatibility of the elements $\pi_{ij} \in \mathbf{\Pi}$ with a local measure of spatial autocorrelation we introduce a specific reweighing (Mucciardi et al, 2006), so that the weights are in row-standardized form and that for each unit the sum of the weights equals 1

4. Spatial analysis of railway density of Italian provinces

To show the properties of the new connectivity matrix, we considered an application regarding the railway density (DR) of 107 Italian provinces expressed in km per 100 km^2 of municipal territory (Istat, 2009). In this analysis the results obtained using the new spatial weights (Distance Decay method) will be compared with reference to the classic binary weights (Classic Binary method with rook case[2]), to the binary weights originating from the threshold distance (MaxMin method) and to the weights produced using the DSMA procedure (DSMA method). As far as regards geographical information for the territory, the calculation is made by considering a matrix of distance between the Italian provinces' territorial centroids (km). Applying (3) to the 107 Italian provinces we obtain for the first spatial lag[3] $h^{1} = 80.1$ km. At this point we may consider various specifications of function (2) appropriately varying the parameters φ and α (see figure 1). As we can observe, by increasing the parameter φ we emphasise the weight of the nearer units compared to the more distant ones within the interconnection radius h^{1} (threshold distance), while parameter α acts above all on the "cut-off" distance we established. Beyond this distance, the function in fact begins to decrease rapidly, tending from "1" to "0". From the various simulations performed on the territorial partition analysed, we decided to use a function with φ=5 and α=2 since this better differentiates the geographically closer territorial units. The Gaussian model (φ=0.5 and α=2) in practice does not differ significantly from the classic contiguity (Classic Binary method), similarly to the model with φ=1 and α=1

[1] We should remember that this distance ensures that no zone remains isolated.
[2] In Rook case, "wij" is set to 1 if the pair shares a common edge and 0 otherwise.
[3] In this study only the first spatial lag was taken into consideration.

(results not showed). Having established the parameters for the distance decay model, we can now concentrate on analysing the results obtained for local spatial index considering the various neighbourhood models. It should be highlighted that in formula (1), the quantity $\sum_{j,j\neq i}^{n} w_{ij} z_j$ for the "Classic Binary" and "MaxMin" methods becomes a simple mean, while for the "DSMA" and "Distance Decay" methods it becomes a weighted mean with weightings sensitive to the effective distance between the interconnected units. The main results are shown in tables 1,2 and 3.

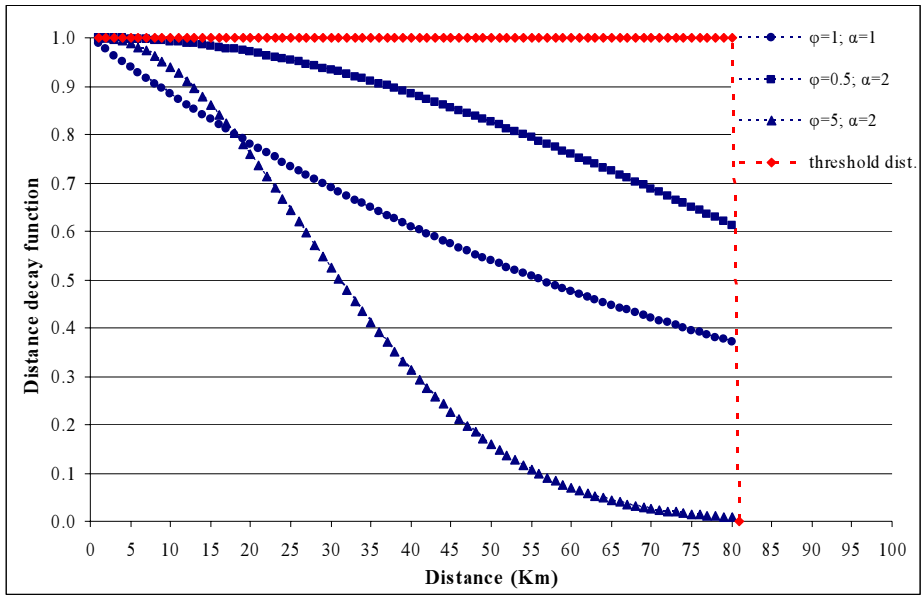


Fig. 1 – Distance decay function for various values assumed by the parameters

At the level of overall spatial autocorrelation, we note that the four methods do not show statistically significant autocorrelation of the data (tab. 1). In practice, the variable railway density does not show at an overall level to be statistically correlated with the territory. The situation is differentiated, however, by analysing the results at a local level. As said before, the spatial data may often fail to show territorial dependence at a global level but show it at a local level. In the case in point, tables 2 and 3 show the Local Moran values only in the provinces in which the data was found to be statistically significant. For the various methods compared, the analysis identifies situations of marked local autocorrelation. Specifically, the spatial outliers detected were found to be the same for the "MaxMin" and "DSMA" methods, while they differed for the "Classic Binary" and "Distance Decay" methods. In particular, this latter

method proposed seems to make the Local Moran values more extreme than with all the other methods assuming always either highest or lowest value in the province of reference. This characteristic is also confirmed by the Moran scatter plots for all the provinces (see figure 2, 3, 4 and 5 in appendix). It is evident that in the "Distance Decay" method, the cluster of points appears less concentrated than with other methods.

Method	Global Moran	Z-value
Bin	0.120	1.4786
MM	0.086	1.4220
DSMA	0.090	1.4680
DD	0.112	1.3986

Tab. 1 – Global Moran indexes

Provinces	zi	LM (Bin)	*Z-value (Bin)*	LM (MM)	*Z-value (MM)*
Novara	1.16	0.3263	*0.7807*	0.7214	*2.1816*
Como	2.77	2.0405	*4.2423*	1.4866	*4.1559*
Milano	1.27	0.8251	*3.1073*	0.7246	*2.4747*
Lecco	1.11	1.2737	*2.6560*	0.7678	*2.3201*
Savona	2.92	0.9977	*2.3408*	0.9977	*2.3408*
Genova	1.66	1.1594	*2.7189*	1.0120	*2.8390*
Firenze	2.68	0.0263	*0.1138*	-0.3604	*-1.0476*
Napoli	2.59	1.5735	*2.8245*	0.1046	*0.2035*
Bari	2.17	-0.8589	*-3.1750*	-1.3320	*-2.3606*
Catania	2.11	-1.3334	*-3.0800*	-1.3334	*-3.0800*
Nuoro	-1.16	0.9880	*2.3195*	1.0268	*2.1451*

zi= DR standardized; LM= Local Moran index; Bin = classical Classic Binary weights (rook case); MM = MaxMin method; shadow area = significant at p< 0.05

Tab. 2 – Local Moran indexes for "Classic Binary" and "MaxMin" methods

Provinces	zi	LM (DSMA)	*Z-value (DSMA)*	LM (DD)	*Z-value (DD)*
Novara	1.16	0.6646	*2.0030*	0.1233	*0.2860*
Como	2.77	1.5522	*4.3148*	2.1322	*3.9181*
Milano	1.27	0.7703	*2.6199*	1.0554	*2.9263*
Lecco	1.11	0.8472	*2.5385*	1.7126	*3.1630*
Savona	2.92	0.9595	*2.2503*	0.4715	*0.9446*
Genova	1.66	0.9750	*2.7316*	0.4056	*0.8995*
Firenze	2.68	-0.4311	*-1.2522*	-1.2531	*-2.0970*
Napoli	2.59	0.3334	*0.6097*	2.9356	*4.0827*
Bari	2.17	-1.3638	*-2.4155*	-1.8945	*-2.8216*
Catania	2.11	-1.3506	*-3.1120*	-1.6140	*-2.5896*
Nuoro	-1.16	1.0266	*2.1429*	1.0337	*1.8095*

zi= DR standardized; LM= Local Moran index; DSMA = DSMA method; DD = "distance decay" method; shadow area = significant at p< 0.05

Tab. 3 – Local Moran indexes for "DSMA" and "Distance Decay" methods

4. Conclusion

The main objective of this paper is to develop an alternative version of the DSMA procedure to improve the local measures of spatial autocorrelation. According to a distance decay function, we introduced a transform in the DSMA so that the spatial weights generated are sensitive to the effective distance of each territorial unit. The performance of the new weights was assessed considering the Local Moran, the most widely used index for local spatial analysis, and comparing the results obtained for the same index with various neighbourhood models (Classic Binary, MaxMin, and DSMA). The results confirm that the "Distance Decay" method tends to produce a more extreme neighbourhood situation in the interconnection radius "h", giving greater weight than even the DSMA procedure to the zones nearest to the centre of the circumference of radius "h", and less to the territorial units furthest from the centre of the circumference. Clearly, this property may be an advantage when, on the basis of the type of research and nature of the variable examined, it is necessary to attribute greater weight to the territorially closest zones. An aspect which should however be studied in more detail is the set-up of the parameters, which must be performed on the basis of the territory and in particular of the type of territorial unit analysed (municipalities, provinces, regions etc.).

Appendix: Moran scatter plots for railway density of Italian provinces

Legend: *Upper right quadrant* (called High–High) indicates high railway density point with high railway density neighbours; *Lower left quadrant* (called Low–Low) indicates low railway density point with low railway density neighbours; *Lower right quadrant* (called High–Low) indicates high railway density point with low railway density neighbours; *Upper left quadrant* (called Low–High) indicates low railway density point with high railway density neighbours.
Point= province

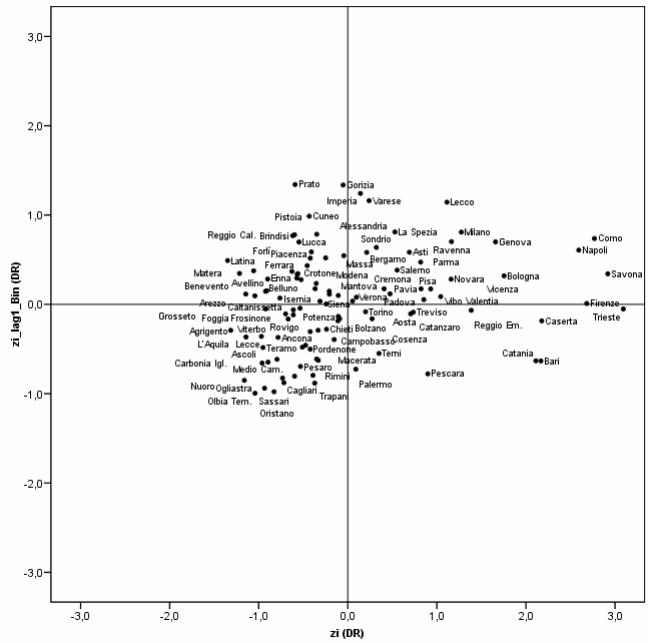


Fig. 2 – Moran scatter plot for "Classic Binary" method
x-axis = zi (DR) y-axis = spatial lag of zi

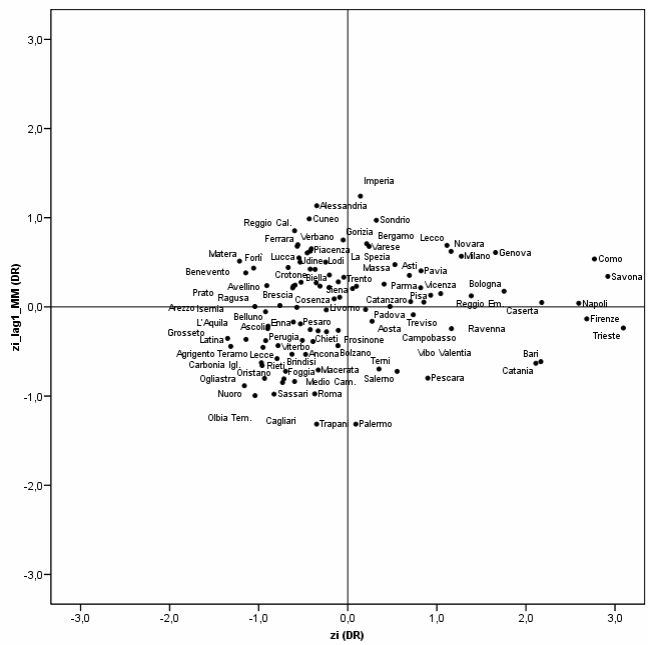


Fig. 3 – Moran scatter plot for "MaxMin" method
x-axis = zi (DR) y-axis = spatial lag of zi

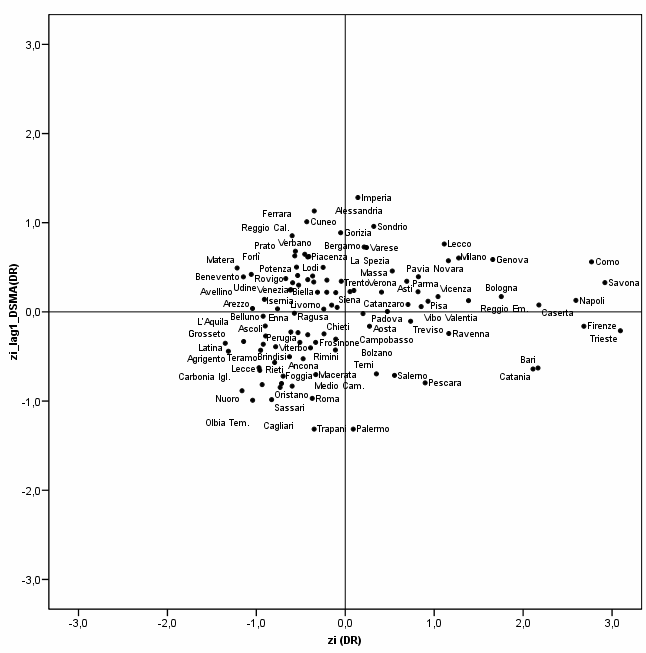
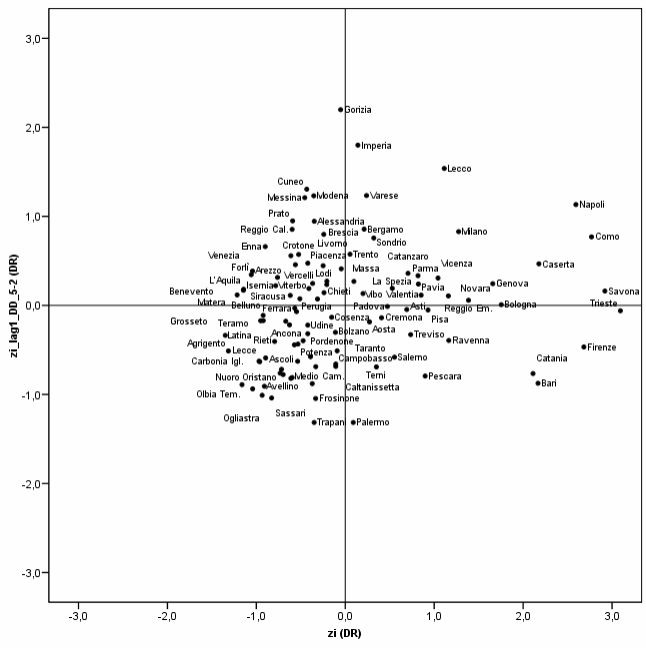


Fig. 4 – Moran scatter plot for “DSMA” method
x-axis = zi (DR) y-axis = spatial lag of zi



. Fig. 5 – Moran scatter plot for “Distance Decay” method
x-axis = zi (DR) y-axis = spatial lag of zi

Principal references

Anselin L. (1995), Local Indicator of Spatial Association. Geographical Analysis, n°27.

Boots B. (2002), Local Measures of Spatial Association. Ecoscience, 9, pp. 168-176.

Fotheringham, A.S., O'Kelly M.E., (1989), Spatial Interaction Models: Formulations and Applications. Kluwer, Boston, pp. 224.

ISTAT (2009), Indicatori sui Trasporti Urbani - Anno 2007, on-line document.

La Tona L., Mazza A., Mucciardi M. (2006), A Generalized Weight Matrix for Autocorrelated Superficial Data. Proceeding of Spatial Data Methods for Environmental and Ecological Processes, Cafarelli B, Lasinio G.J. and Pollice A. (Eds), Wip edition.

Mucciardi M. (2008a), Use of a Flexible Weight Matrix in a Local Spatial Statistic. Proceeding of first joint meeting of the Société Francophone de Classification and the Classification and Data AnalysisGroup of the Italian Society of Statistics, Caserta 11-13 giugno 2008, pp. 385-388.

Mucciardi M. (2008b), Geographic Information and Global Index of Spatial Autocorrelation. Proceeding of VI International Conference in Stochastics Geometry, Convex Bodies, Empirical Measures, in Rendiconti del Circolo dei Matematici di Palermo, Vol. n° 80.

Mucciardi M. (1998), La Procedura D.S.M.A. per la Misura dell'Intensità dei Legami tra Unità Spaziali di Tipo Puntuale. Proceeding of Italian Statistical Society, Sorrento, pp. 773-779.

Ord J.K., Getis A. (1995), Local Spatial Autocorrelation Statistics: Distributional Issues and an Application. Geographical Analysis 27, pp. 286–305.

RENDICONTI DEL CIRCOLO MATEMATICO DI PALERMO
Serie II, Suppl. 81 (2009), pp. 299-310

Railtracksubstructure resistan ce to Hazmat spil ɬage:an experim entalstudy

Praticò Filippo Giammaria, Moro Antonino, Ammendola Rachele

ABSTR ACT

Nowadays industries and economies of nations depend, in part, on the large numbers of hazardous materials (Hazmat) transported from the supplier to the user and, ultimately, to the waste disposer. Hazardous materials are transported by road, rail, water, air and pipeline. The vast majority reach their destination safely and without accidents.
When fuel or lubricant, for example, accidentally comes into contact with ground this can constitute a big issue for the environment around the rail track. On the other hand, many studies demonstrated that the use of HMA (Hot Mix Asphalt) sub-ballast or HMA support tracks can constitute a reliable technical option and many rail track substructures include such systems. In the light of above facts chemical resistance of HMA layers in rail substructures is becoming a new scientific and technical problem.
Spillages can require the replacement of the asphalt course, and many parameters are involved: mix effective porosity, diameter of the pores, quantity and type of fuel, course thickness, immersion time, asphalt binder characteristics, size and shape of the flow paths, Reclaimed Asphalt Pavement Content, etc.
Though important studies on this topic have been proposed, some new and old issues on management and interpretation still need answers.
In particular, it is not clear how asphalt binder properties can affect these phenomena.
Given this, in this paper a model has been formalized and experimentally validated.
Results demonstrate that, especially for some classes of hazmats, HMA properties are the basis for the interpretation of the involved phenomena and this can be useful in deciding the suitable typology of Hot Mix Asphalt to use in rail track substructures, especially in rail tracks where conditions of high vulnerability or/and high probability of fuel release do occur.

1. BAC K R U

As is well-known the design of rail track sub-structure largely depends on bearing strength. The resistance to Hazmat spillage is therefore a supplementary requirement that interacts with this important property. Therefore, this section deals with bearing strength as first factor required in rail track substructure design.
Figures 1 to 3 refer to typical cross section: slab (figure 2) and ballasted (figure 3) tracks are shown. Figure 3, in particular, shows possible paths of Hazmat materials.

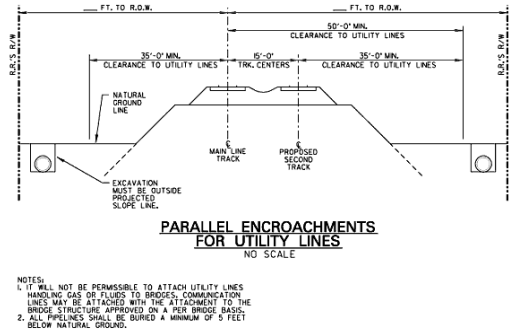


Figure 1: Typical cross sections (two tracks)

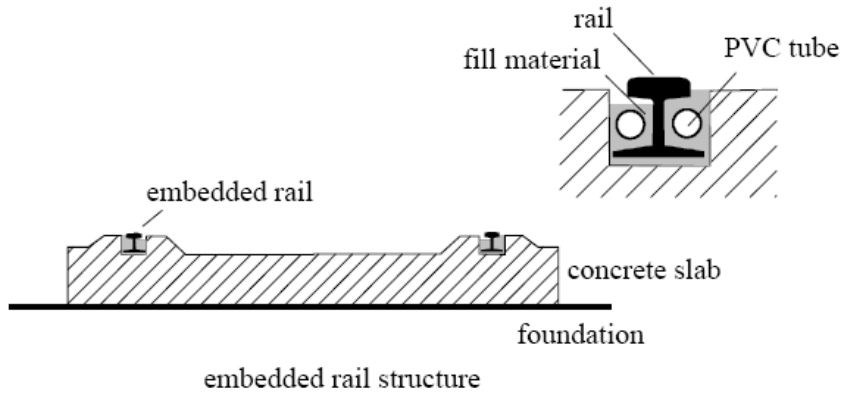


Figure 2: slab tracks: embedded rail structure
[http://www.rail.tudelft.nl/Publications/portugal.PDF]

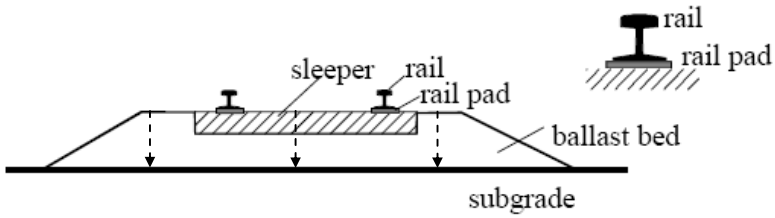


Figure 3: Ballasted tracks (arrows refer to possible paths of Hazmat materials)

The requirements for the bearing strength and quality of the track depend to a large extend on the following parameters:
- Axle load: static vertical load per axle;
- Tonnage borne: sum of the axle loads;
- Running speed.

In principle, the static axle load level, to which the dynamic increment is added, determines the required strength of all the layers of the track. The accumulated tonnage is a measure well correlated to the deterioration of the track quality and it provides an indication of when maintenance and renewal will be necessary [Mittal et al., 2006]. The dynamic load component, which depends on speed and horizontal and vertical track geometry, can also play an essential role.
The nominal axle loads applied to the track are shown in table 1.

	Number of axles	Empty	Loaded
Trams	4	50 kN	70 kN
Light – rail	4	80 kN	100 kN
Passenger coach	4	100 kN	120 kN
Passenger motor coach	4	150 kN	1700 kN
Locomotive	4 or 6	215 kN	--
Freight wagon	2	120 kN	225 kN
Heavy haul (USA, Australia)	2	120 kN	250 – 350 kN

Table 1: Number of axles and axle weight of several rolling stock

With very high axle load the number of rail defects increases considerably and the track requires more maintenance.
When line classification is concerned, it's important to observe that the UIC (International Union of Railways), which is the organisation for railway cooperation and which counts standardization among its tasks, makes a distinction between load categories [Esveld, 2001].
An example of such categories is shown in table 2.

Category	Axle load [kN]	Weight/m [kN/m]
A	160	48
B_1	180	50
B_2	180	64
C_2	200	64
C_3	200	72
C_4	200	80
D_4	225	80

Table 2: UIC load classification

Daily tonnage is used to express the intensity or capacity of rail traffic on a specific line. The average daily tonnage is about 20,000 t. The most heavily loaded sections have a daily load of 60,000 t. Abroad, on what are known as heavy haul lines, daily tonnage of 300,000 t can occur (see figure 4).

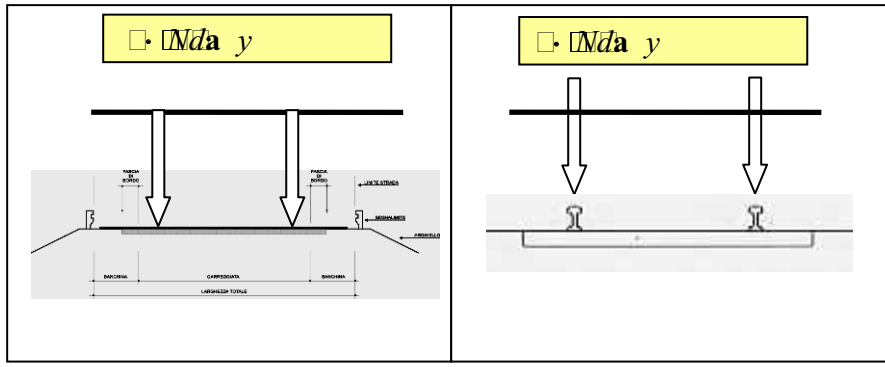


Figure 4: Rough estimation of daily traffic load on roads and tracks

Furthermore, all types of track deterioration features, such as increase in geometrical deviations, increase in rail fractures, and rail wear, can be expressed as a function of tonnage. This is often expressed as MGT = million gross tonnes (note: 1 MGT (US) = 8896 MN).
For the sake of dimensioning and maintenance of the permanent way, the track network is divided into classes determined by the equivalent tonnage (T_f) defined in UIC leaflet 714 according to:

$$\mathbf{T_f} = \mathbf{T}_p \frac{V}{100} + \mathbf{T_g} \frac{P_c}{18 \cdot D}$$

In which:

T_p : Real load for daily passenger traffic (t);
T_g : Real load for daily freight traffic (t);
V : Maximum permissible speed [km/h];
D : Minimum wheel diameter [m];
P_c : Maximum axle load with wheels of diameter D [tonnes].

For example, if T_p = 10,000 t, v = 100km/h, T_g = 10,000 t, P_c = 20 t, D = 0.6 m, it is $T_f \cong$ 12,000t.
The groups used by the NS are globally speaking as follows:

Class I	40.000 <	T_f	
Class II	20.000 <	T_f	< 40.000
Class III	10.000 <	T_f	< 20.000
Class IV		T_f	< 10.000

The maximum speed on a specific section is expressed in km/h. An example of line section speeds is given in table 3 [Esveld, 2001].

	Passenger trains	Freight trains
Branch lines	--	30 – 40 km/h
Secondary lines	80 – 120 km/h	60 – 80 km/h
Main lines	160 – 200 km/h	100 – 120 km/h
High speed lines*	250 – 300 km/h	
world record 515,3 km/h (TGV SNCF, May 1990		

Table 3: Maximum speeds: example

The forces acting on the track as a result of train load are considerable and are quite impulsive. The loads can be considered from three main angles:
- Vertical;
- Horizontal, transverse to the track;
- Horizontal, parallel to the tracks.

Generally, the loads are unevenly distributed over the two rails and are often difficult to quantify. Depending on the nature of the loads they can be divided as follows:
- Quasi-static loads as a result of the gross tare, the centrifugal force and the centering force in curves and switches, and cross winds;
- Dynamic loads caused by (see figure 5):
  - Track irregularities (horizontal and vertical) and irregular track stiffness due to variable characteristics and settlement of ballast bed ad formation;
  - Discontinuities at welds, joints, switches, etc.;
  - Irregular rail running surface (corrugations);

- Vehicle defect such as wheels flats, natural vibrations.

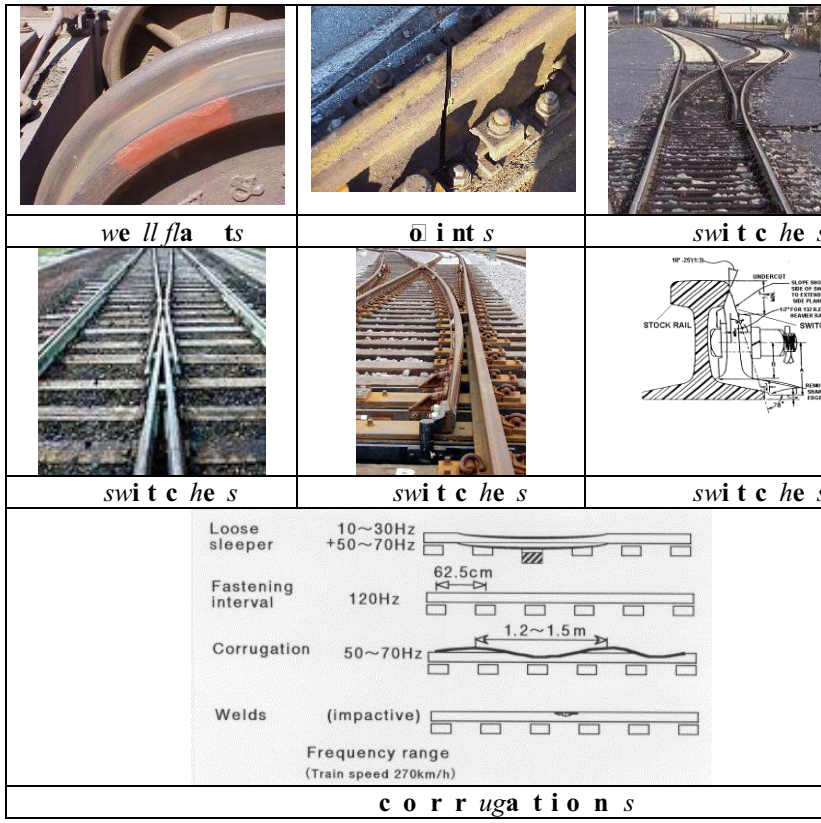


Figure 5 Joints, switches, corrugation, well flats [www.tsb.gc.ca]

In addition, the effect of temperature on CWR (Continuous Welded Rail) track can cause considerable longitudinal tensile an compressive forces, which in the latter case can result in instability (risk of buckling-curling) of the track.
By referring to the total vertical wheel load on the rail, it's made up of the following components [Esveld, 2001]:

$$Q_{tot} = Q_{stat} + Q_{centr} + Q_{wind} + Q_{dyn}$$
$$quasi - static\ forces$$

where:
Q_{stat} : static wheel load = half the static axle load, measured on straight horizontal track;
Q_{centr} : increase in wheel load on the outer rail in curves in connection with non – compensated centrifugal forces;
Q_{wind} : idem for cross winds;

Q_{dyn} : dynamic wheel load components resulting from:

- Sprung mass 0 – 20 Hz;
- Unsprung mass 20 – 125 Hz;
- Corrugation, welds, wheel flats 0 - 2000 Hz.

The proportion of Q_{centr} is usually 10 to 25% of the static wheel load.
In the light of above – mentioned facts, it results that in order to better distribute the vertical loads, an HMA (Hot Mix Asphalt) is often placed between the sleepers-ballast and the subgrade.
This accomplishes for a better quality of rail track substructure but it can constitute a problem in the case of Hazmat spillage.
Therefore experiments have been planned and carried out to analyse how HMA properties can affect the resistance to Hazmat spillage.

2. E□PERME N TS

Experiments have been planned according to the following procedures and standards:

1) Volumetric tests:
   1a) %b = asphalt binder content as a percentage of aggregates (B.U. CNR n.38/73; ASTM 6307); carbon tetrachloride has been used as solvent;
   1b) G = aggregate gradation (B.U. CNR n. 4/53);
   1c) NMAS = Nominal Maximum Aggregate Size;
   1d) f (%) = filler content ($d \leq 0.075$ mm);
   1e) s(%) = sand content (0.075 mm$\leq d \leq 2$ mm);
   1f) γ_g = aggregate apparent specific gravity (B.U. CNR n. 63/78);
   1g) G_{mb} = mix bulk specific gravity (ASTM D6752; ASTM D6857);
   1h) G_{mbAO} = mix bulk specific gravity after opening (ASTM D6752; ASTM D6857); 1i) $n_{eff.}$ = mix effective porosity (ASTM D6752; ASTM D6857);
2) Permeability tests (K_{cv}), using a Flexible Wall Permeameter – FWP (ASTM PS 129-01);
3) Brush tests in order to estimate A, B and C (EN 12697-43:2005), where:
   3a) A, mean value of the loss of mass after soaking in fuel, has been defined (together with $m_{1,i}$ and $m_{2,i}$) in section 1 (see equations (9) and (10));
   3b) B(%) = mean value of the loss of mass after the brush test, where $B=\Sigma_i B_i/3$, with i□*2, 3* (specimens), $B_i=((m_{2,i} - m_{5,i})/ m_{2,i})\cdot 100$, $m_{5,i}$= mass of the test specimen i after soaking and 120 s in the brush test, in grams (g);
   3c) C(%) =mean value of the loss of mass of the specimens, where $C=\Sigma_i C_i/3$, with i□□*2, 3* (n° specimen), $C_i=((m_{1,i} - m_{5,i})/ m_{1,i})\cdot 100$. Note that the parameter C is not defined in the EN standard; it has been introduced

in order to have a descriptor able to combine the two different actions (soaking + brushing).

Figures 6 and 7 illustrate the main phases of the brushing test: i) soaking in fuel and removing the fuel; ii) brushing. Note that if A results greater than 5%, then only the first phase is usually performed (poor resistance). When A≤5%, if B<1% there is good resistance, if 1≤B%≤5% there is moderate resistance, while if B>5% there is still poor resistance to that fuel.



Figure 6 Brush test - I PHASE: Soaking in fuel; removing the fuel



Figure 7 Brush test - II PHASE: A≤5% - Brushing

During the 1st phase all the examined HMAs had the same asphalt binder grade. Owing to the necessity to test the influence of mix parameters over a consistent range of variation, four different bituminous mixes have been tested. Average Air voids in DGFCs, BICs and BACs resulted 9%, while, for PEMs, a mean value of 22% has been detected. Note that PEMs have been considered only as a limit case. Each mix type has been subdivided into sets: 7 sets of DGFC (for a total amount of 7×4 = 28 specimens), 2 sets of BIC, 2 sets of BAC and 23 sets of PEM. For each set of 4 specimens one of them has been used to control composition parameters and the other three for the Brush test (see Figure 8).

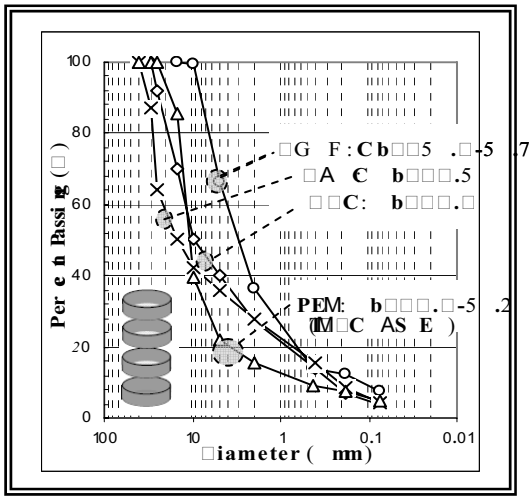


Figure 8 Summary of the design of experiments (BAC = BAse Course; BIC= BInder Course; DGFC= Dense Graded Friction Course; PEM = Porous European Mixes).

Figure 9 deals with the dependence of the effects (selected indicators A, B, C) on composition parameters (n_{eff}).

Though the statistic characteristics of the investigation need to be optimized, some observations can be here remarked.

As far as the susceptibility to the effective porosity is concerned, the obtained results show a strong dependence on n_{eff} of the mass loss after soaking (A), of the mass loss after brush test (B) and of the mass loss for combined action (soaking + brushing, C). R-square values (logarithmic curves) range from 0.55 (vs A) up to 0.89 (vs B). Linear trendlines give slightly lower R-square values (from 0.37 up to 0.78).

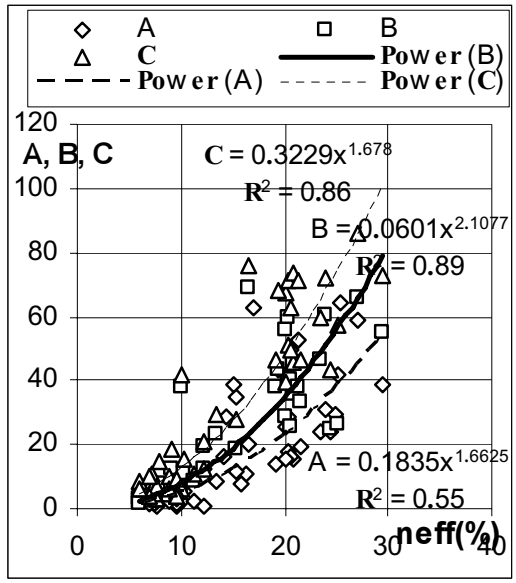


Figure 9 Sensitivity of the parameters A, B, C to the effective porosity n_{eff}.

In the second phase, the main aim of the experiments was to assess the influence of the asphalt binder characteristics (viscosity in particular) on chemical resistance.

In order to pursue the above-mentioned objectives and scope, asphalt binder properties have been previously analyzed.

The following tests have been performed:

a) Penetration test according to CNR BU N.24 -1971 (Norme per l'accettazione dei bitumi per usi Stradali; EN 1426:2007: Bitumen and bituminous binders - Determination of needle penetration);
b) Softening point (Ball and ring) according to CNR BU N.35-1973; EN 1427: 2007: Bitumen and bituminous binders - Determination of the softening point - Ring and Ball method);
c) Viscosity at 135, 160, 170°C according to ASTM D4402-02 (Standard test method for viscosity determinations of unfilled asphalts using the Brookfield thermosel apparatus; EN 14896:2006: Bitumen and bituminous binders - Dynamic viscosity of bituminous emulsions, cut-back and fluxed bituminous binders -Rotating spindle viscometer method).

On the basis of the obtained results, two main sets of asphalt binder typologies have been detected (see figures 10 and 11): 1) the first group includes asphalt binders with low penetration (pen, 35 dmm c.a), high softening point (PA, 70°C circa), high viscosity (η, ≅0.3Pas at 170°C, ≅0.4Pas at 160°C, ≅0.8Pas at

135°C); 2) the second group includes asphalt binders with high penetration grade (≅65 dmm), quite low softening point (45~50°C), quite low viscosity (≅0.1Pas at 170°C, ≅0.15Pas at 160°C, ≅0.4Pas at 135°C).
Figure 10 shows the relationships between pen (25°C, dmm) and η (Pa ·s), for three different asphalt binders, the three curves represent the three different temperature chosen to determine η. Similarly, figure 11 describes how softening point (PA, °C) and viscosity (η, Pa ·s) relate each other, for the three selected asphalt binder, for three different temperatures (135, 160, 170).
It's possible to observe that:

- The higher the softening point of the given asphalt binder, the higher the viscosity it possesses;
- For a given asphalt binder, the higher the test temperature the lower the viscosity.

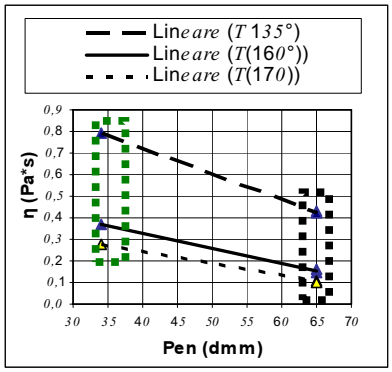


Figure 10 Pen vs η

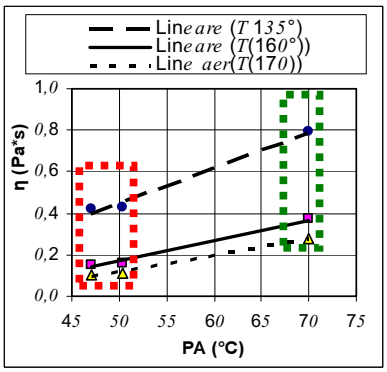


Figure 11 PA vs η

Following the model above discussed, in the design of experiments attention has been paid to the control of the other main factors affecting chemical resistance (n_{eff}, etc.)
After asphalt binder characterization, the selected specimens have been subjected to the Brush test and experiments are still in progress.
First experiments didn't give reliable results on asphalt binder influence and more research is still needed.
Similar researches carried out on road HMAs [Praticò et al., 2007] are still in progress.

□ □ □ S

The following conclusions may be drawn:

i) Rail tack substructure, when HMA layers are placed, must be checked for bearing properties and also for chemical resistance;
ii) the composition parameters of Hot Mix Asphalts (air voids content, etc…) can affect chemical resistance; anyhow, correlations with asphalt binder quality (viscosity) resulted unsatisfactory;
iii) first experiments seem to suggest a possible influence of viscosity on chemical resistance; more research is needed.

References

[Mittal et al., 2006] Mittal A.V., Maurya S.K., Bansal SHRI. G., "Ballast specification for high axle load (32.5 tonnes) and high speed (250 kmph)", iricen_gov, India Ministry of Railways, 2006.
[Praticò et al., 2007] Praticò F. G., Ammendola R., Moro A., "Asphalt binder influence on chemical resistance of HMAs: a theorical and experimental study", submitted at the 4th International SIIV Congress, "Advances in transport infrastructures and stakeholders expectations", Palermo 2007
[www.tsb.gc.ca] www.tsb.gc.ca/.../1998/r98t0042/r98t0042.asp, Transportation Safety Board of Canada, 1988
[Esveld, 2001] Esveld Coenraad, Modern Railway Track. TuDelft, 2001

RENDICONTI DEL CIRCOLO MATEMATICO DI PALERMO
Serie II, Suppl. 81 (2009), pp. 311-322

Assessing rail track sub-ballast resistance through density testing: experiments

Praticò Filippo Giammaria, Moro Antonino, Ammendola Rachele,
Dattola Vincenzo

Abstract: As is well known, much of the performance, reliability and deterioration of track components can be attributed to the railway track substructure.
The track substructure, consisting of the ballast, sub-ballast, and subgrade layers, has an outstanding influence on track performance. Sub-ballast are often HMAs (Hot Mix Asphalts).
The primary benefits of the HMA layer are to optimize load distribution to the subgrade, to protect from water and to confine the subgrade. The waterproofing effects are particularly relevant since the impermeable HMA mat essentially eliminates sub-grade moisture fluctuations; this effectively improves and maintains the load carrying capability. Additionally, HMAs can provide a positive separation of ballast from subgrade and thereby can eliminate subgrade pumping without substantially increasing the stiffness of the track-bed. The resultant trackbed has the potential to be more stable, to provide increased operating efficiency and to decrease maintenance costs; this could result in long-term economic benefits for the railroad and rail transit industries.
On the other side many research demonstrate that performance (permeability, moduli, etc.) are strictly related to air voids content. As is well-known, the main input parameter in the determination of air voids content is bulk specific parameter but many question on this topic still need answers.
In the light of above, the objective of this paper is to analyse the problem of bulk specific gravity estimation for compacted HMA samples, as key-factor for checking HMA permeability and mechanical properties.
As is well known, the Bulk Specific Gravity of the Compacted Asphalt Mixture is the ratio of the mass in air of a unit volume of a permeable material (including both permeable and impermeable voids normal to the material) at a stated temperature to the mass in air (of equal density) of an equal volume of gas-free distilled water at a stated temperature.
There are several different ways to measure bulk specific gravity; all of these use slightly different ways to determine specimen volume: a) Water displacement methods (Saturated Surface Dry (SSD); Paraffin; Parafilm; vacuum sealing device); b) Dimensional; c) others (Gamma ray, etc.).
Given that, in this paper, a model has been formalized and experiments have been designed and performed. Results demonstrate the prevailing influence of several factors in selecting the method and in estimating the void content and

so, in providing better track substructure performance. Critical issues are provided.

1. Background

As is well-known, ballasted tracks as very common (figures 1 to 3). Figure 1 refers to typical cross sections (lengths are in feet), while in figures 2 and 3 typical ballast tracks are shown.

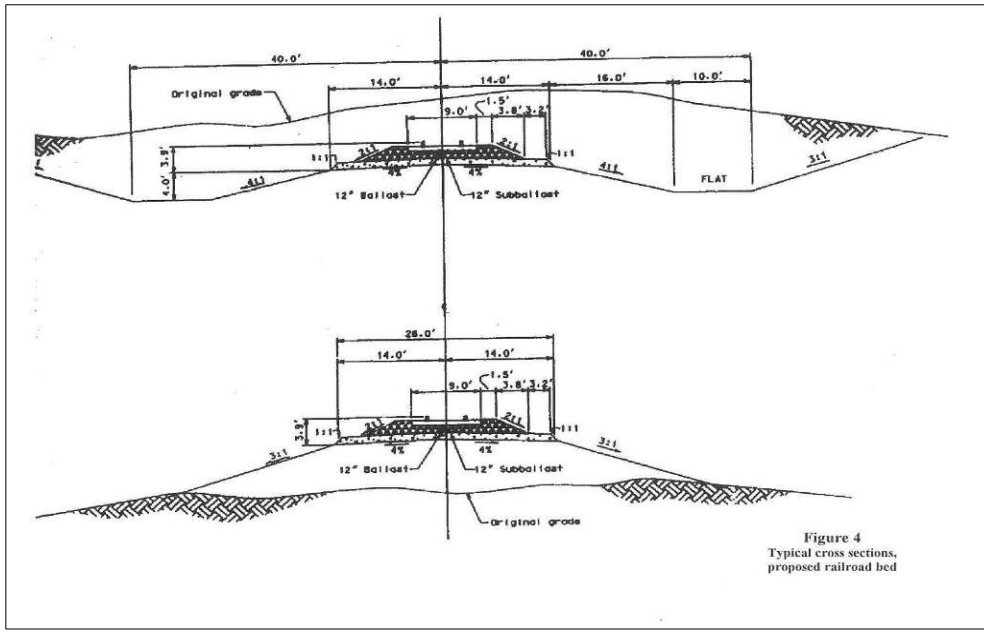


Figure 1: Typical cross sections

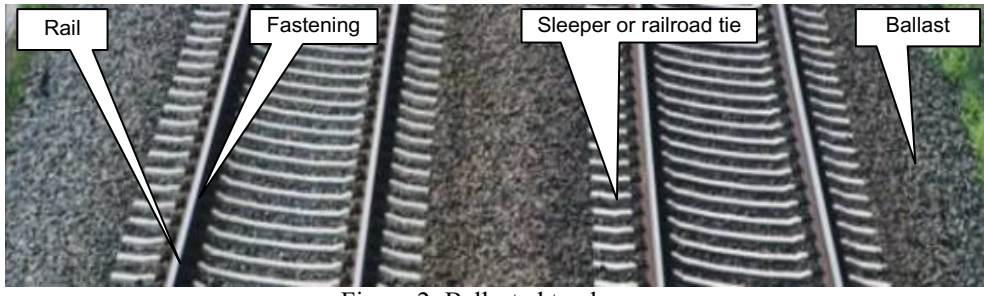


Figure 2: Ballasted tracks

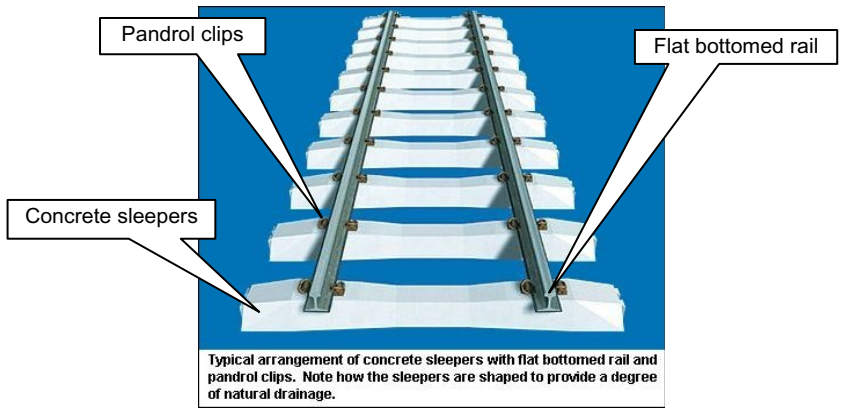


Figure 3: Ballasted tracks: Concrete sleepers
[http://www.railway-technical.com/Sleepers-Concrete.jpg]

Apart from ballasted tracks, another solution is becoming more and more important: slab tracks (see figures 4 and 5). Figure 4 deals with main construction phases, while in figure 5 the bearings between slab and sub-structure are shown.

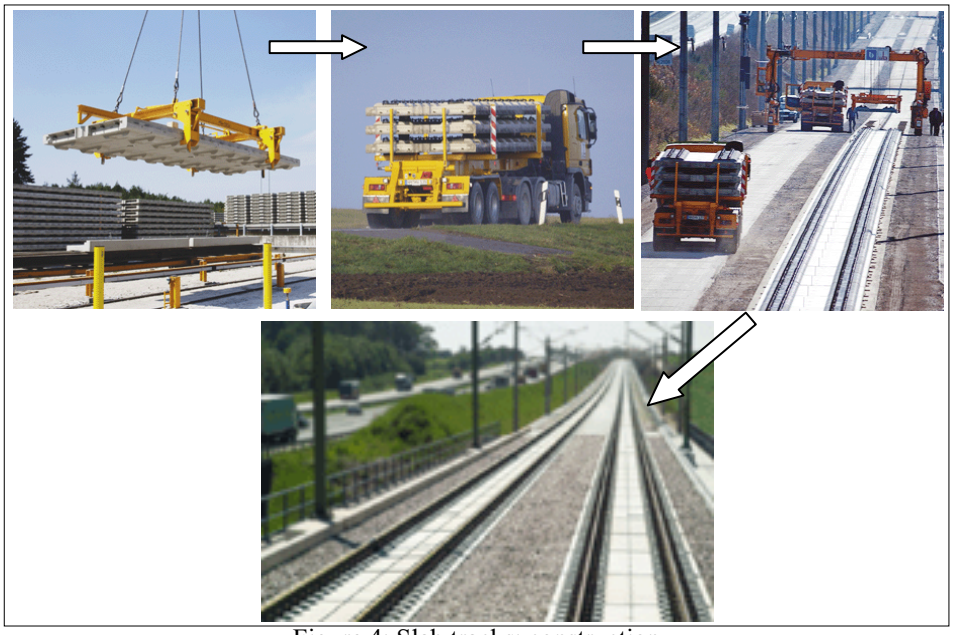


Figure 4: Slab tracks: construction
[http://www.max-boegl.de/boegldip/web/content.jsp?nodeId=1109]



Figure 5: Bearings

It's important to observe that natural rubber is the most widely used material for bearings, mainly because of its appreciable dynamic characteristics and a proven service record in bridges (sometimes for over 100 years).
As is well-known, there are two principal designs for floating slab track bearings: 1) Discrete bearings can be installed under pre-cast concrete slabs in the traditional manner; 2) Alternatively, a soft continuous layer of resilient material, similar to a ballast material, can be installed. Concrete can then be cast on top of this layer to create the slab [ESVELD, 2001].
In order to improve load-bearing function a layer of HMA (Hot Mix Asphalt) is often placed under the ballast.
On the other hand many studies demonstrate a strong correlation between HMA mechanical properties and density, and density it self can be determinated according to many methods.
So the main objective of this paper is confined to the theoretical and experimental analysis of relationships among different density measurements.

2. Load-bearing function of the track

It is well known that the purpose of track is to transfer train loads to the formation (subgrade included). Conventional track still in use consist of a discrete system made up of rails, sleepers and ballastbed. Figure 6 shows a principal sketch with the main elements, while in figure 7 normal stresses are estimated for a conventional track structure.

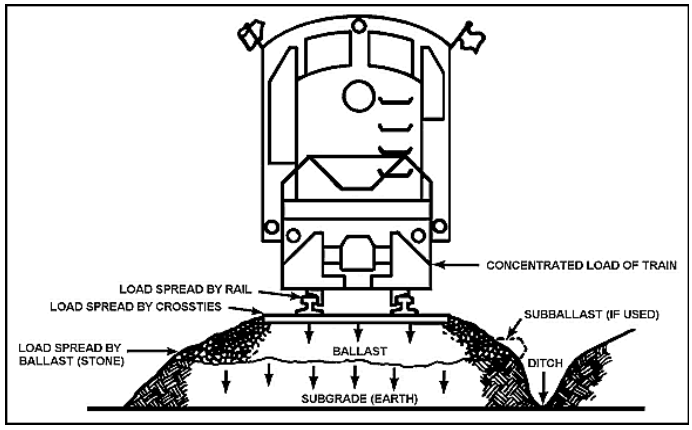


Figure 6 Load distribution in Ballasted tracks [http://www.globalsecurity.org/military/library/policy/army/fm/5520/fig7-1.gif]

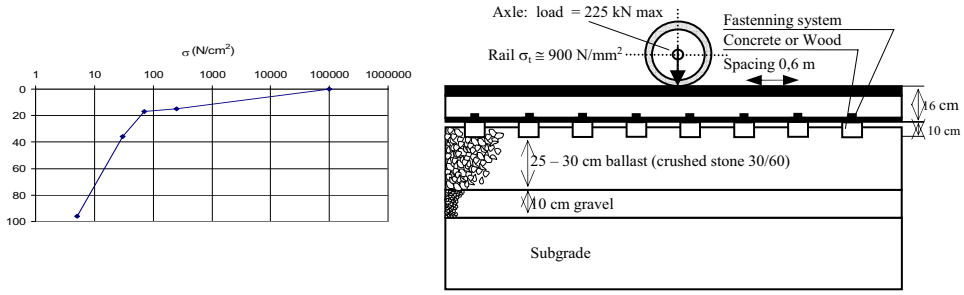


Figure 7: Conventional track structure – estimate of stresses

$$(1\,N/cm^2 = 10^{-2}\,MPa = 10^{-2}\,N/mm^2)$$

Load transfer works on the principal stress reduction, by operating layer by layer, as depicted schematically in figure 8. The greatest stress occurs between wheel and rail and it is in the order of 30 ~ 100 kN/cm^2 (=300 ~ 1000 MPa). Note that even higher values may occur in particular conditions. Between rail and sleeper the stress is two orders smaller (e.g. 2,5 MPa) and diminishes between sleeper and ballast - bed down to about 30 N/cm^2 (0,3 MPa). Finally the stress on the formation (subgrade) is only about, for example, 5 N/cm^2.

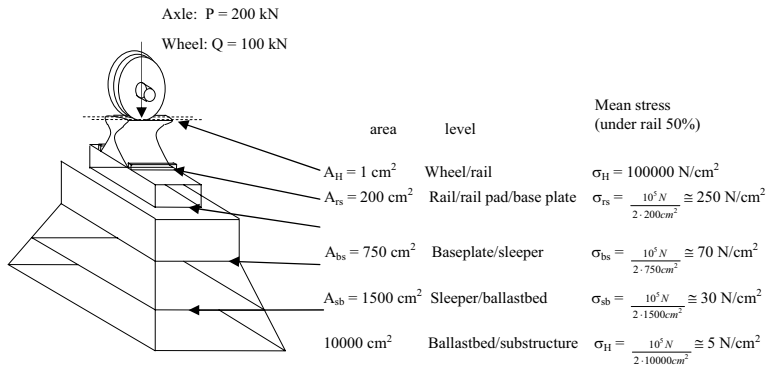


Figure 8: Principle of load transfer

3. Stresses on ballast bed and formation

Conventional ballast bed and formation are conceived as a two-layer system [MITTAL et al., 2006]. The vertical stresses on the ballast bed and on the formation which are due to wheel loads are often considered as the determining stresses for the load – bearing capacity of the layer system. Overloading of the ballast bed causes rapid deterioration of the quality of the track geometry. Overloading of the formation raise the material in the ballast bed, especially in the case of materials susceptible to moisture. This phenomenon is known as pumping. Membranes can be used to mitigate such phenomena.

The compressive stresses which the sleepers exert on the ballast bed, are considered evenly distributed. The material from which the sleeper is made thus doesn't play any important role here. To determine the mean values of the stress the calculation is often based on Zimmermann's theory, whereas the dynamic amplitude is taken into account by means of Eisenmann's increment factor. The maximum stress σ_{sbmax} between sleeper and ballast bed under a wheel load Q is expressed as [ESVELD, 2001; IRIGEN, 2006]:

$$\sigma_{sb\,max} = DAF\ \sigma_{sb\,mean} \tag{1}$$

where:

$$\sigma_{sb\,mean} = \frac{F_{mean}}{A_{sb}} = \frac{Q \cdot a}{2A_{sb}} \sqrt[4]{\frac{k_d a^3}{4EI}}$$

DAF = dynamic amplification factor (for ballast: t = 2);(?)
Q = effective wheel load [t];
a = sleepers spacing [cm];
A_{sb} = contact area between sleeper and ballast bed for half sleeper [mm^2];
U = modulus of elasticity of rail support [kg/cm^2];
E = modulus of elasticity of rail steel [kg/cm^2];
I = moment of inertia of rail section [cm^4].

Permissible contact pressure on the ballast bed is usually: $\sigma_{sb} \leq 0{,}50$ N/mm^2, while sleeper rotation can give rise to high local edge pressure, and sometimes this is taken into account by introducing an increment factor.
It can be seen from the above equation that sleeper spacing (a) and the extend of the support area (A_{sb}) have a relatively important influence on the mean stress ($\sigma_{sb\ mean}$). A high value for the foundation coefficient can give high values for the stresses on the ballast bed. In the case of a ballast bed on a structure, the foundation modulus should be lowered. A heavier rail profile has a positive effect in this respect. Some authors [ESVELD, 2001] report that use of UIC 54 instead of NP 46, can lead to a stress reduction in the ballast bed of about 10% (see table 1).

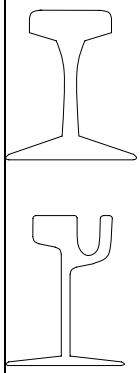
Rail profile	Rail section	S41	S49	NP46	UIC54	UIC60	Ri60
	Height h_r [mm]	138	149	142	159	172	180
	Head width b_h [mm]	67	67	72	70	72	113
	Foot width b_f [mm]	125	125	120	140	150	180
	Area A [cm^2]	52,7	63,0	59,3	69,3	76,9	77,1
	Mass/meter m [kg/m]	41,3	49,4	46,6	54,4	60,3	60,5
	Moment of inertia $I=I_y$ [cm^4]	1368	1819	1605	2346	3055	3334
	Moment of inertia I_z [cm^4]	276	320	310	418	513	884
	Section modulus W_{yh} [cm^3]	196	240	224	279	336	387
	Section modulus W_{yf} [cm^3]	200,5	248	228	313	377	355
	Section modulus W_z [cm^3]	44,2	51,2	52	60	68	135

Table 1: Rail dimensions and strength data [ESVELD, 2001]

The rail foot stress and the stress between sleeper and ballast bed can be calculated by means of particular equations [ESVELD, 2001]. For Q = 170 kN, $C_{sb} = 100$ N/cm^3, $a = 60$ cm, $A_{sb} = 2850$ cm^2, the data in table 2 are obtained:

	Rail		Ballast	
	σ_r [N/mm^2]	Ratio	σ_r [N/mm^2]	Ratio
UIC 60	97	–	0,21	–
UIC 54	110	13 %	0,22	7 %
NP 46	137	41 %	0,25	18 %

Table 2: Stresses resulting from Q = 170 kN [ESVELD, 2001]

A heavier rail profile has a great influence on rail stress reduction. The effect on ballast stress is approximately half of the effect on rail stress.
The relation between vertical stress and deterioration in the quality of track geometry is still ambiguous. On the basis of the AASHO Road Test for road structure, it is nevertheless assumed that:

$$\textit{Decrease in track geometry quality} = (\textit{increase in stress on ballast bed})^m$$

In which m = 3 to 4.
In order to calculate the maximum vertical stress on the formation the contributions of the various sleepers have to be superimposed. Figure 9 shows the stress pattern on the ballast bed along the length of the track.

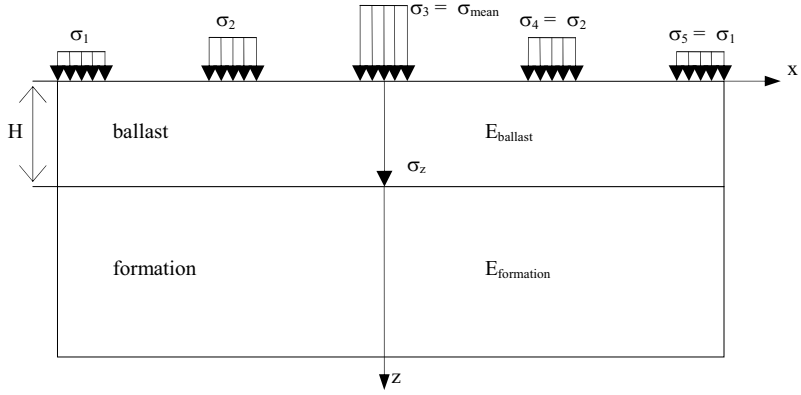


Figure 9: Ballast bed and formation represented as two-layer system

For each sleeper the stress is assumed to be evenly distributed over the sleeper surface. The magnitude of this stress beneath the various sleepers caused by wheel load Q is:

$$\sigma_{max} = DAF\ \frac{Qa}{2LA_{sb}}$$

$$\sigma_i = \sigma_{max}\ \eta(x_i) \qquad \text{in which:}$$

$$\eta(x_i) = e^{-x_i/L}\left[\cos\frac{x_i}{L} + \operatorname{sen}\frac{x_i}{L}\right] \qquad x_i \geq 0$$

To determine the vertical stress on the formation the value of factor t = 1 can be taken, as adjacent sleepers cannot all be subjected to an unfavourable load at the same time.
The evenly distributed stresses per sleeper are then replaced by equivalent strip load covering the sleeper width. Assuming this, the problem can be described

by the well-known two – dimensional stress distribution for a plane strain situation.
Softening of the subgrade can cause major problems, especially in combination with vibration. High-speed lines in Japan and Italy are therefore laid on a waterproof asphalt concrete layer between 5 cm and 8 cm thick. In order to distribute – and hence reduce – subgrade stresses, this bituminous concrete layer can be increased to 15 cm or 20 cm (see figure 10). Easy maintenance of the track geometry which is inherent in classic ballasted track is thus retained.
Asphalt layers may offer major advantages when constructing new track designed for relatively high axle load and high gross annual tonnage. In addition, the use of reinforcing layers on conventional track designed for passenger services could lead to a significant reduction in the frequency with which the track geometry has to be maintained (see figure 10).

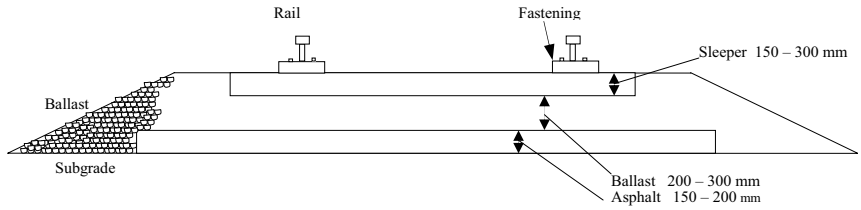


Figure 10: Hot Mix Asphalt in Railway Trackbeds

In such cases, HMA density measurement becomes a QC/QA (Quality Control / Quality Assurance) problem.

4. Design of experiments

This section deals with the design of experiments, carried out in order to pursue the above- mentioned objective. Mixes are described in § 4.1, while procedures are summarized in § 4.2.

4.1. Mixes

Five sets of DGFCs (Dense-Graded Friction Courses), have been tested (see table 3). For each set a sub set of specimens has been used for composition analyses (asphalt binder content b – CNR n.38/73, aggregate grading – CNR n.4/53, aggregate apparent specific gravity γ_g– CNR n. 63/78. The Nominal Maximum Aggregate (NMAS) was 10 mm circa.

b	%	4,78÷5,35
γ_g	g/cm^3	2,749÷2,783
NMAS	mm	10
Compaction		Marshall

Table 3: HMA Composition/compaction

4.2. Procedures

Four different methods have been considered (see Table 4 and figure 11).

(**)	Indicator	Algorithm	Standard
1.	G_{mb} *(geom)(dimensional)*	$\frac{A}{V_{Geom} \cdot \gamma_w}$	AASHTO T 269
2.	G_{mb} *(parafilm)*	$\frac{A}{D'-E'-\frac{D'-A}{F} \cdot \gamma_w^{(*)}}$	ASTM D 1188 (abs>2%)
3.	G_{mb} *(VSD)*	$\frac{A}{B'-E'-\frac{B'-A}{F_t}}$	ASTM D 6752
4.	G_{mb} *(paraffin)*	$\frac{A}{D'-E'-\frac{D'-A}{F_p} \cdot \gamma_w^{(*)}}$	BU N40-1973 / AASHTO T 275-A (abs>2%)

Legend: A = mass of the dry specimen in air; abs>2%: absorption more than 2%; B' = mass of dry and sealed specimen; D'=mass of the dry, coated specimen; E' = mass of sealed/coated specimen under water; F =specific gravity of the coating determined at 25°C; F_p = specific gravity of the paraffin at 25°C; F_t = apparent specific gravity of plastic bag; G_{mb} = Bulk Specific Gravity; V_{Geom} = geometric volume of HMA sample; *VSD* = Vacuum Sealing Device. (*) the γ_w is not included in the standard. (**) test order; note that experiments are in progress and the data here reported are only a part of the entire research plan.

Table 4: Main procedures for G_{mb}

Figure 11 deals with the main phases of each of the four methods.

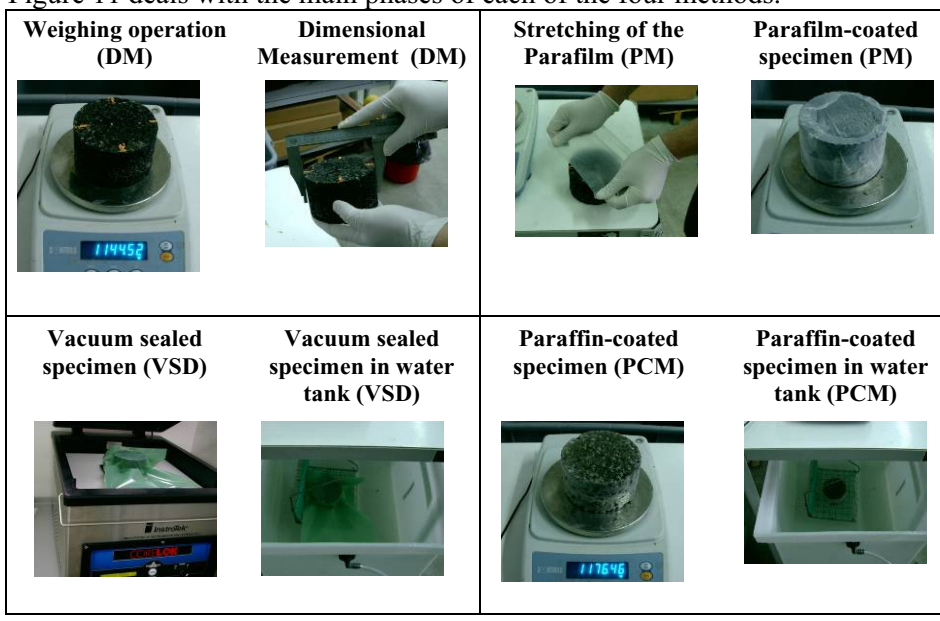


Figure 11 Main Phases for the four procedures

5. Experiments and results

Figures 12 shows the obtained results (the line of equality is dotted).
Note that it results:

$$G_{mbparaffin} > G_{mbVSD} > G_{mbparafilm} > G_{mbgeom}$$

And, then:

$$V_{mbparaffin} < V_{mbVSD} < V_{mbparafilm} < V_{mbgeom}$$

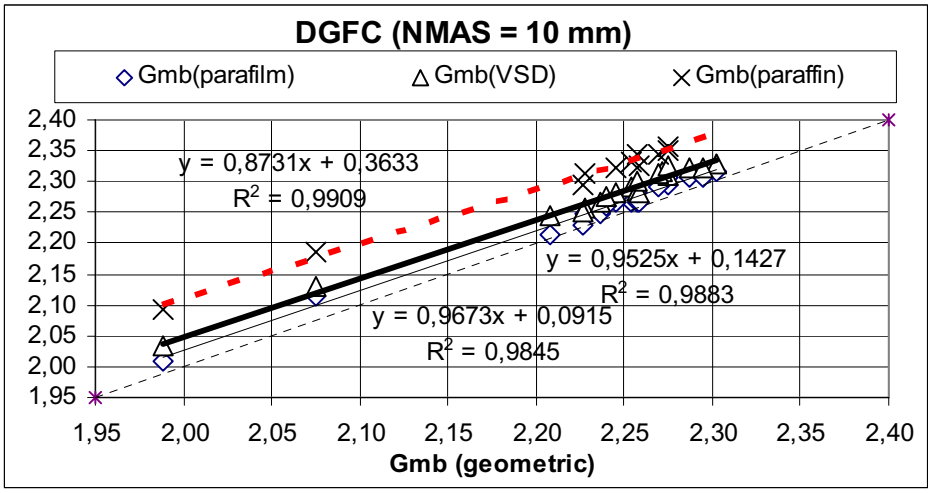


Figure 12

The following observations can be drawn (see figure 12): 1) the simplest method (dimensional) and the Italian most used method (paraffin coated) have the greatest distance (2% ~ 5%); 2) the other methods have a lower gap; 3) many hypotheses should be proposed in the field of the "best descriptor"; it remains quite unclear the assessment of the best G_{mb} indicator; research is still needed on this topic.

Main findings

In the light of the above, the following conclusions may be drawn:
1) research prove that HMA layers in rail track sub-ballast can have an outstanding importance.
2) bulk volumes estimated by the dimensional method are greater than that estimated by the parafilm, VSD (Vacuum Sealing Device) and paraffin method;

3) Physical explanations may be related to the texture considered as a part of the bulk volume: maximum values for the dimensional method, minimum values for the paraffin coated specimens;
4) fitting curves have been obtained; this could constitute a former support, well-grounded in experiments, for QC/QA (Quality Controls/Quality Assurance) procedures.

References

[BROWN et al., 2004] BROWN E. R., HAININ M. R., COOLEY A., HURLEY G. (2004) - Relationship of Air Voids, Lift Thickness, and Permeability in Hot Mix Asphalt Pavements - NCHRP Report 531, National Center for Asphalt Technology—Auburn University, Auburn, AL, TRANSPORTATION RESEARCH BOARD, WASHINGTON, D.C.
[CROUCH et al., 2003] CROUCH L.K., BADOE D.A., CATES M., BORDEN T.A., COPELAND A.R., WALKER C.T., DUNN T., MAXWELL R.A., GOODWIN W.A. (2003) - Bulk specific gravity of compacted Bituminous mixtures: finding a more widely applicable method - Final Report, State of Tennessee, Department of Transportation, July.
[ESVELD, 2001] ESVELD COENRAAD, "Modern Railway Track, TuDelft, 2001.
[IRIGEN, 2006]
[KVASNAK et al., 2006] KVASNAK A., WILLIAMS C.R., WILLIAMS B., STANTON B. (2006) - Evaluation of methods used to determine bulk specific gravity of Hot Mix Asphalt - ICAP.
[MITTAL et al., 2006] MITTAL A.V., MAURYA S.K., BANSAL SHRI. G., "BALLAST SPECIFICATION FOR HIGH AXLE LOAD (32.5 TONNES) AND HIGH SPEED (250 KMPH)", iricen_gov, India Ministry of Railways, 2006.
[MOHAMMAD et al., 2005] MOHAMMAD L.N., HERATH A., WU ZHONG, COOPER S., A (2005) - Comparative study of factors influencing the permeability of hot-mix asphalt mixtures, Volume 74E Electronic Journal 2005, AAPT Publications, 2005.
[SPELLERBERG et al., 2004] SPELLERBERG P., SAVAGE D. (2004) - An investigation of the cause of variation in HMA Bulk Specific Gravity test results using non-absorptive aggregates - National Cooperative Highway Research Program Web Document 66 (Project 9-26 (Phase 2)), July.
[WILLIAMS et al., 2005] WILLIAMS R.C., WILLIAMS B., STANTON B., KVASNAK A., VAN DAM T. (2005) - Development of acceptance criteria of compacted hot mixture asphalt bulk specific gravity based on vacuum sealed specimens - Final report, Michigan Department of Transportation - Construction and Technology division, Lansing, Mi, US, October.
[http://www.railway-technical.com/Sleepers-Concrete.jpg]
[http://www.max-boegl.de/boegldip/web/content.jsp?nodeId=1109]
[http://www.globalsecurity.org/military/library/policy/army/fm/5520/fig7-1.gif]

RENDICONTI DEL CIRCOLO MATEMATICO DI PALERMO
Serie II, Suppl. 81 (2009), pp. 323-331

Joint density and related performance in HMA subballast

Praticò Filippo Giammaria, Ammendola Rachele, Moro Antonino, Dattola Vincenzo

Abstract: Nowadays we are demanding more performance from our railtrack substructures than ever before.
Therefore the behaviour of the overall structure is often improved by interposing a bituminous sub-ballast layer.
On the other hand, because of the difficulty in compacting the unconfined edges of such bituminous layers, lower density zones can occur at the longitudinal joints in HMAs (Hot Mix Asphalts); these joints can deteriorate faster than other areas and this contributes to the ultimate performance, then to HMA life and life cycle cost. The main goal of this paper is to investigate on longitudinal joint density in HMA sub-ballast.
In order to pursue this objective, in-lab and on-site experiments were designed and performed. On the basis of the obtained results, specific findings have been drawn.

1. Background

As is well known, two main designs of HMA subballast are very common: HMA underlayment and HMA overlayment (see figures 1 and 2).
For the solution of HMA underlayment, the HMA layer is usually placed and compacted (figure 2) directly on the subgrade. Then a layer of ballast is placed between the HMA layer and the railroad ties. This design changes little from normal trackbed design, since the HMA layer merely replaces the granular subballast layer.
In the case of HMA overlayment, the design involves placing the HMA layers in a similar manner, except that no ballast is used between the HMA layer and the railroad ties. Therefore, the ties are placed directly on the HMA surface. Cribbing aggregate is then placed between the ties and at the end of the ties to restrain track movement.

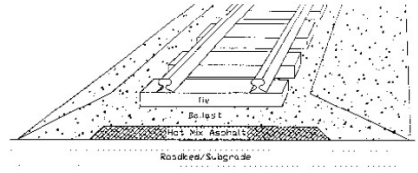


Figure I.—Underlayment

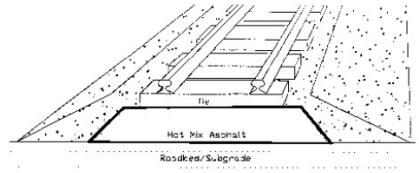


Figure II. —Overlayment

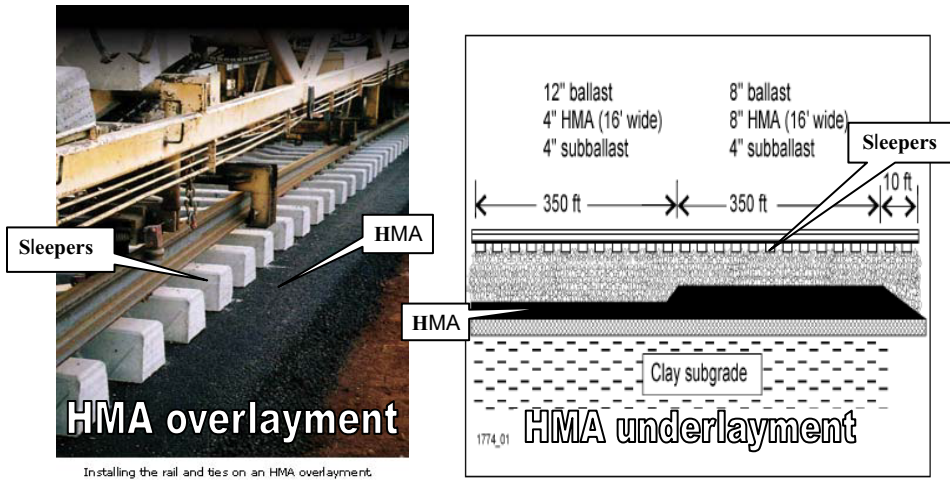


Figure 1: Hot Mix Asphalt in Railway Tracks: two solutions [Hensley, 2000]

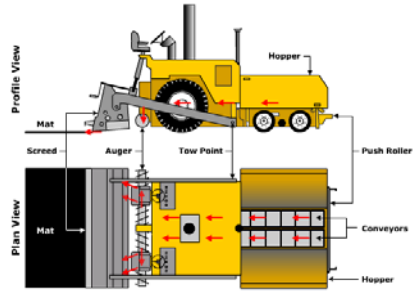


Figure 2: HMA placement – Pavers

On the other hand, both for Quality Controls and Quality Assurance procedures, testing and acceptance are necessary and this fact can positively affect HMA layers.

Testing and acceptance can address component or structural issues.

Component testing and acceptance (rail profile, fastening system, sleepers, ballast, track support system, etc.) deal with:

- Mechanical properties;
- Elasticity properties;
- Stability properties;
- Durability and fatigue properties;
- Specific component properties;
- …

On the contrary structural testing and acceptance refer to:

- Noise and vibration testing of track structures;
- Passenger comfort and ride quality
- Dynamic properties of track structures;
- …

By referring to component testing and acceptance, and, in particular, to mechanical properties, it is well-known that track components are supposed to have specific mechanical properties that enable the track to support and guide railway vehicles [Esveld, 2001]. In table 1 a number of track components and properties are listed (see also figure 3). Mechanical properties are not necessarily the most important ones, but they reflect the principle of considering the track as a mechanical system subjected to vehicle loading.

	PROPERTY			
COMPONENT	Elasticity	Strength	Stability	Durability
Rail profile		x		x
Fastening system	x		x	x
Sleepers		x	x	x
Ballast	x		x	x
Slabs		x		x
Track support system	x		x	x
HMA layer		x	x	x

Table 1: Overview of the most important track properties of each component

It is important to remark that [Esveld, 2001]

- Track elasticity is dominated by the stiffness properties of the track components such as rail pad and ballast (see figure 3). Damping, also known as energy loss or imaginary stiffness, is also very relevant regarding low, medium or high frequency loading;

- *Track stiffness* depends on the ballast, the subgrade and the quality of the used materials. It is specified by the elastic settlement (and wear) of rails, concrete sleepers, or HDM slabs;
- *Track stability* by the weight of sleepers also by the good resistance of sleepers in ballast;
- *Fixing* for long term performance and for rapid maintenance and replacement. The fixing and loading conditions, however, influence the rail.



Fastening system



Slabs



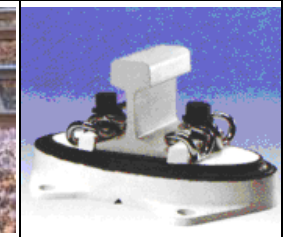
Cologne Egg



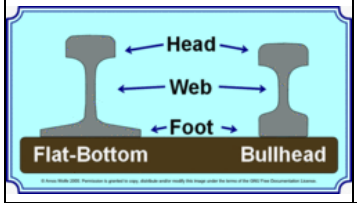
Sleepers



Ballast



Cologne Egg



Railroprofile



Welsd



Railpad

Figure 3 - Components of a railway track

[http://www.railtech.com/Slabtrack/Slabtrack_files/image001.gif]

[http://www.gjtse.com/pix/spar1.gif]

[http://www.vip-pompeiana.com/images/railpad_m1.jpg]

Given that, one must remark that the importance of HMA subballast is relative not only to bearing properties but also to ride comfort.
In fact, as is well-known, in the case of ballasted tracks, vibrations may be reduced by [Esveld, 2001] :

- Increasing the ballast depth. Tests have shown a reduction of 6 dB at frequencies below 10 Hz by increasing the ballast depth from 30 to 75 cm. This is not a very important solution because of the costs, the weight and the extra height;
- Installing resilient mats between the bottom of the ballast and the tunnel invert;
- Installing pads between sleeper and ballast;
- Installing super-elastic fastenings system, for instance the "Cologne Egg" (see figure 3).

On the basis of above-mentioned facts, HMA subballast can have an outstanding role. In this case, however, critical points such as joints can cause damages and can affect both quality assurance and performance.
Therefore, controls on affective density of HMA subballast can be a key -factor.

TEST PLAN

In order to investigate on the effective density of HMA subballasts, in-lab and on-site experiments were designed and performed. The Factorial plan of the experiments is summarised in table 2.

	wedge			
C	any			
RT	Rolling from the hot side 150 mm circa away from the joint			
PT	Proper mat overlap			
roller	Steel roller, 80KN			
	Hot lane	Joint	Cold lane	Tests
cores	17	4	8	G_{mbgeom} G_{mb}, G_{mbAO}, n_{eff}, %b, G
MPD	4	4	4	SH

Sum bo MP: Measurement Points; J=Joint; SH= Sand Height; G_{mbgeom}: mix bulk specific gravity (dimensional method, AASHTO T 269); G_{mb}=mix bulk specific gravity (vacuum seal method, ASTM D6752; ASTMD6857); G_{mbAO}=mix bulk specific gravity after opening (vacuum seal method, ASTMD6752; ASTMD6857); n_{ff}=mix effective porosity (ASTM D6752; ASTMD6857). Note: The MPD (Mean Profile Depth) has been derived from SH according to PIARC experiment [AA.VV., 1995].

Table 2: A summary of the experiments performed

Note that the experimental plan followed the scheme adapted in [Praticò et alia, 2007] for PEMs, except that in this case dense–grade mixes have been addressed.

During the experiments, after the construction of the so-called Cold Lane (CL, the 1st one) and Hot Lane (HL-the 2nd one), in-site (SH, etc.) and in-lab (on the extracted cores) measurements have been performed.
Locations have been divided into three main classes (HL, J, CL, see table 2).
The following parameters have been determined on the extracted cores (see figure 4): b (%) = asphalt binder content as a percentage of aggregate weight (B.U. CNR n.38/73; ASTM 6307); G = aggregate gradation (B.U. CNR n. 4/53); γ_g = aggregate apparent specific gravity (B.U. CNR n. 63/78); G_{mb} = mix bulk specific gravity (ASTM D6752; ASTM D6857); G_{mbAO} = mix bulk specific gravity after opening (ASTM D6752; ASTM D6857); n_{eff} = mix effective porosity (ASTM D6752; ASTM D6857). The effective porosity (n_{eff}) has been calculated from G_{mb} and G_{mbAO}: $n_{eff} = (G_{mbAO} \cdot \gamma_w - G_{mb} \cdot \gamma_w) \cdot (G_{mbAO} \cdot \gamma_w)^{-1}$, γ_W = water density.



Extraction: b (%) (CNR n. 38/73; ASTM 6307)



Sieves, screens, sieve shaker: G (CNR n. 4/53)



Vacuum Sealing: G_{mb}, G_{mbAO}, n_{eff} (ASTM D6752; D6857)

Figure 4 Main devices used

RESULTS

Figures 5 and 6 show the obtained results.
Note that a vertical line (bolded) is reported at the abscissa (360.0 cm from the left shoulder): it represents the joint position and divides the hot lane (HL, the left) from the cold lane (CL, on the right).

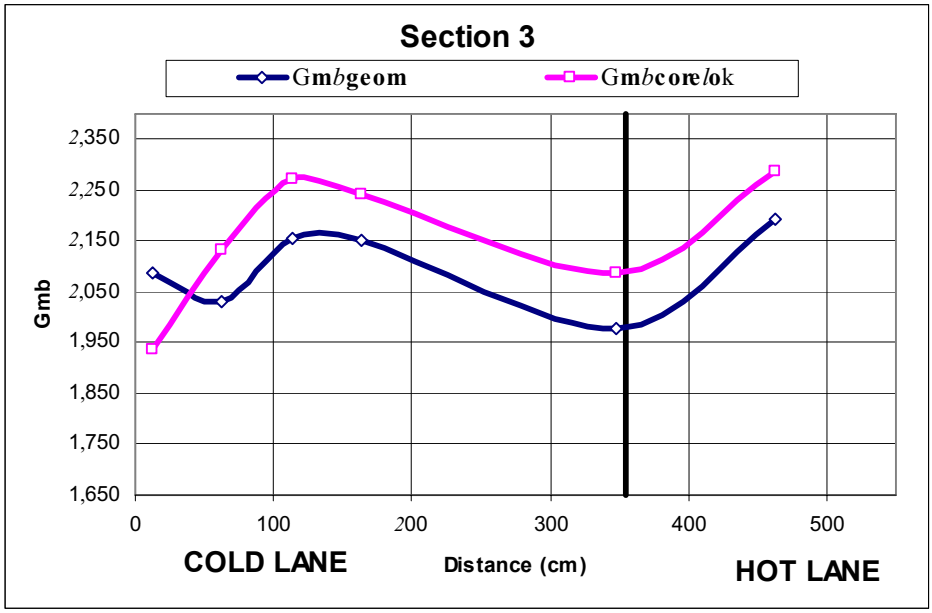


Figure 5

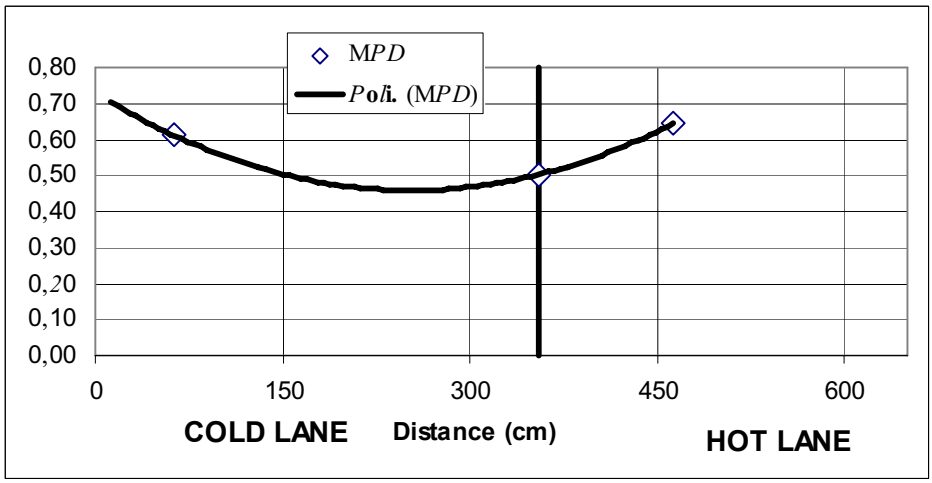


Figure 6

The following observations are worked:

1. it is recurrent practice to allow, in some European countries, the presence in surface layers of a certain amount of air voids (typically 10%) for the sole reason that the layer is left open to traffic for a short period of time. No attempt has been made in this case to study dense-graded mixes;
2. specific gravities determined by means of dimensional (G_{mbgeom}) and volumetric principles ($G_{mbcorelok}$) are compared; the latter is

a well-known problem of intrinsic correlation between G_{mbgeom} and G_{mb} (Vacuum sealing device); it must be remarked that G_{mbgeom} is greatly affected by core integrity

3. the hypothesis of homogeneity of material and of construction procedures, which supports a common G_{mb} of reference could be too strong; this fact may be the reason of some of the detected variations in G_{mb} behaviour; more research is needed on this topic.

Finally, figure 6 shows texture variations for the selected points; just a few measurements have been performed; however, it is possible to observe that the negative correlation between G_{mb} and SH seems to be confirmed at the Joint location. More research is needed into this issue.

CONCLUSIONS

On the basis of the studies on HMA subballast, the primary benefits of HMA layers seem to be to improve load distribution, to waterproof and to confine the subgrade.
On the other hand, the factors affecting density and texture for longitudinal joints of HMAs appear to be numerous and a large number of experiments is needed in order to mitigate "noise" in data analysis.
When SH variability is concerned, other research is needed on this topic and the use of more precise and accurate devices could make the difference.
Future research will aim to mitigate the influence of the involved boundary conditions in order to make it possible to pursue more reliable inferences.

Acknowledgment
Authors are grateful to Domenico Papalia (*Mediterranea* University, IT), Sylvia Neufeld (Houston, USA), Maria Rodà (*Mediterranea* University, IT) for suggestions and help.

References

[AA.VV., 1995] International PIRC experiment to compare and harmonise texture and skid resistance measurements, PIARC, France, 1995.
[AA.VV., 2003] Longitudinal Joint Construction techniques, Tech Notes, Washington State Department of Transportation, February 2003.
[AA.VV., 2004] TRB of the National Academies, National Cooperative Highway Research Program, Quality characteristics for use with performance-related specifications for hot mix asphalt, Research Result Digest 291, August 2004.
[AA.VV., 2006] TRB Circular Number E-C105, Transportation Research Board, General Issues in Asphalt Technology Committee, Factors Affecting Compaction of Asphalt Pavements, September 2006.

[Esveld , 2001] Esveld Coenraad, "Modern Railway Track, TuDelft, 2001.
[Kandhall et al., 1996] Kandhall P.S., Mallik R.B., A study of longitudinal Joint Construction techniques in HMA pavements (interim report – Colorado project), National Center for Asphalt Technology Report No 96-03, August 1996.
[Kandhall et al., 1997] Kandhall P.S., Mallik R.B., Longitudinal Joint Construction techniques for asphalt pavements, National Center for Asphalt Technology Report No 97-04, August 1997.
[Kandhall et al., 2002] Kandhal P.S., Ramirez T.L., Ingram P.M., Evaluation of eight longitudinal techniques for asphalt pavements in Pennsylvania, National Center for Asphalt Technology Report No 02-03, February 2002.
[Mittal et al., 2006] Mittal A.V., Maurya S.K., Bansal SHRI. G., "BALLAST SPECIFICATION FORHIGH AXLE LOAD (32.5 TONNES) AND HIGH SPEED (250KMPH)", iricen_gov, IndiaMinistry of Railways, 2006.
[Praticò et alia, 2007] Praticò F. G., Moro A., Ammendola R., Joints in porous asphalt concretes: density and texture singularities, submitted at the 4th International SIIV Congress Palermo (Italy) 12-14 September 2007.
[Sebaaly et al., 2004] Sebaaly P.E. and Barrantes J.C., Development of a joint density specification: phase I: literature review and test plan, Western Regional superpave center, Nevada Department of Transportation, Carson City, NV, USA, 2004.
[Sebaaly et al., 2005a] Sebaaly P.E. and Barrantes J.C., Fernandez G., Development of a joint density specification: phase II: evaluation of test sections, Nevada Department of Transportation, Carson City, NV, USA, 2005.
[Sebaaly et al., 2005b] Sebaaly P.E., Barrantes J.C., Fernandez G., Loria L., Development of a joint density specification: phase II: evaluation of 2004 and 2005 test sections, Nevada Department of Transportation, Carson City, NV, USA, December 2005.
[Yoichi Sunaga Isao Sano et al.] Yoichi Sunaga Isao Sano, "A practical use of axlebox acceleration to control the short wave track irregularities"
[Hensley, M.J. and J.G. Rose] Hensley, M.J., "Design, Construction, and Performance of Hot Mix Asphalt for Railway Trackbeds", " Proceedings, 1st World Conference on Asphalt Pavements, Sydney, Australia, 2000
[http://www.asphaltinstitute.org/upload/Design_Construction_Performance_HMA_RR_Trackbeds.pdf]
[http://www.rail.tudelft.nl/Slabtrack_files/image.gif]

RENDICONTI DEL CIRCOLO MATEMATICO DI PALERMO
Serie II, Suppl. 81 (2009), pp. 333-336

On Pareto minimum solutions

Alfio Puglisi
University of Messina
Faculty of Economy department SEA
e-mail: puglisia@unime.it

Abstract

In 1973 ([2]), I. A. Marusciac defined a class of extremal approximate solution of a linear inconsistent system that contains as particular cases the least square solution and the Tschebychev's best approximation solution of the system, the two main methods used to obtain an approximate solution of an inconsistent system. The least squares method was applied by M. Fekete and J.M Walsh in 1951 ([1]) in order to obtain an approximate solution of an inconsistent system, whereas the Tschebychev's best approximation method was used for the same reason by R.L. Remez in 1969 ([3]). In this paper we obtain a first approach in order to show a connection between the "Pareto minimum solutions" of an inconsistent system and the "infrasolutions" of this system. First of all we will start with some definitions and known results.
AMS-2000 Mathematics Subject Classification: **49K10**.

1 Preliminaries

Let consider the following system of m equations and n unknowns:

$$f_k(z) = \sum_{j=1}^{n} a_{kj} z - b_j = 0, \quad k \in M = \{1, 2, \ldots, m\} \tag{1}$$

or, equivalently,

$$Az - b = 0$$

where the notations are obvious:

$$A = (a^k)_{k=1,2,\ldots,m} := (a_{k1}, a_{k2} \ldots, a_{kn})_{k=1,2,\ldots,m} \in \mathcal{M}_{m,n}(\mathbb{C}), b =$$

$$(b_1, b_2, \ldots b_m) \in \mathcal{M}_{m,1}(\mathbb{C})$$

and

$$z = (z_1, z_2, \ldots, z_n) \in \mathcal{M}_{n,1}(\mathbb{C})$$

here

$$a^k := (a_{k1}, a_{k2}, \ldots, a_{kn})$$

Definition 1.1 *$z \in \mathbb{C}^n$ is an infrasolution of the system (1) if there is no $u \in \mathbb{C}^n$ so that:*

- *$Au \neq Az$*
- *If, for $k \in M$, $f_k(z) = 0$, then $f_k(u) = 0$*
- *If, for $k \in M$, $f_k(z) \neq 0$, then $|f_k(u)| < |f_k(z)|$*

Let denote the set of all infrasolutions of (1) by $\mathrm{I}S(A, b)$

Directly from the Definition 2.1 we have:

Lemma 1.1 *The system (1) is consistent if and only if every solution z of the system is also an infrasolution,* **i.e.** $\mathrm{I}S(A, b)$ *coincides with the set of <u>all</u> solutions of (1).*

Definition 1.2 *([2]) $z \in \mathbb{C}^n$ is a Pareto minimum solution or Pareto minimum point of the system (1) if there is no $u \in \mathbb{C}^n$ such that:*

- *$|f_k(u)| \leq |f_k(z)|$ for all $k \in M$.*
- *There is a $k_0 \in M$ so that $|f_{k_0}(u)| < |f_{k_0}(z)|$*

We denote by $\mathrm{P}A(A, b)$, and, respectively by $\mathrm{P}A^*(A, b)$ the sets of all Pareto minimum solutions, respectively of all weak Pareto minimum solutions of the system (1).

Definition 1.3 *An approximate solution $z_0 \in \mathbb{C}^n$ of the system (1) is called Tschebychev uniform best approximation solution of (1), or a Tschebychev's point for the system (1) if*

$$\max_{k\in M}\{|f_k(z_0)|\} = \inf_{z\in\mathbb{C}^n} \max_{k\in M}\{|f_k(z)|\} \tag{2}$$

Definition 1.4 *Let now $(\lambda_k)^n$ be a system of weights, so that $\lambda_k > 0$, $\sum_{k=1}^n \lambda_k = 1$ and let also $p > 0$. An approximate solution $z^* \in \mathbb{C}^n$ of the system (1) is called solution of the least deviaton from 0 in weighted mean of order p of (1), if*

$$\left(\sum_{k=1}^n \lambda_k |f_k(z^*)|^p\right)^{1/p} = \inf_{z\in\mathbb{C}^n} \left(\sum_{k=1}^n \lambda_k |f_k(z)|^p\right)^{1/p} \tag{3}$$

In the particular case $p = 2$ and $\lambda_k = 1/n$ for all $k \in M$, the solution of the least deviation from 0 of the system (1) is called the least squares solution of the system (1).

2 Main Results

Definition 2.1 *A matrix $A \in \mathcal{M}_{m,n}(\mathbb{C})$, $m \geq n$ is said to have the "H-property" (Haar property) if all quadratic submatrices of A of order n have the rank exactly n.*

Theorem 2.1 *If $z_0 \in \mathbb{C}^n$ and $A \in \mathcal{M}_{m,n}$, $m \geq n$ and A has the H-property and if there exist $l \geq n$ and $k_1, k_2, \ldots, k_l \in M$ so that*

$$f_{k_j}(z_0) = 0 \quad for \quad j = 1, 2, \ldots, l$$

then

$$z_0 \in \mathrm{P}A(A, b)$$

Proof. If z_0 satisfies the assertion we can suppose first that $z_0 \notin \mathrm{P}A(A, b)$. In this case we can find $v \in \mathbb{C}^n$ so that: $|f_k(v)| \leq |f_k(z_0)|$ for all $k \in M$ and there is a $k_0 \in M$ so that $|f_{k_0}(v)| < |f_{k_0}(z_0)|$. Because $f_{k_j} = 0$ for $j = 1, 2, \ldots, l$, it follows that: $a^{k_j}v - b_{k_j} = 0$ for $j = 1, 2, \ldots, l$ and v is considered as a column vector. Thus, if we put $u = z_0 - v \in \mathbb{C}^n$, we deduce that $a_{k_j}(u) = 0$ for $j = 1, 2, \ldots, l$. Because A has the H-property, it follows

that the rank of the matrix ${}^t(a_{k_1}, a_{k_2}, \dots a_{k_l})$ is exactly n and hence the last system has only the trivial solution $u = 0$. It follows that $v = z_0$, which contradicts the hypotesis. ■

Example 1 *Let consider the system:*

$$\begin{cases} y - 1 = 0 \\ y + 1 = 0 \\ x = 0 \end{cases}$$

Obviously, here

$$A = \begin{bmatrix} 0 & 1 \\ 0 & 1 \\ 1 & 0 \end{bmatrix}$$

and

$$b = \begin{bmatrix} 1 \\ -1 \\ 0 \end{bmatrix}$$

A simple calculation shows that:

- $\mathrm{I}S(A,b) = \{z \in \mathbb{R}^2 : x \in \mathbb{R}, y \in [-1,1]\}$
- $\mathrm{P}A(A,b) = \{z \in \mathbb{R}^2 : x = 0, y \in [-1,1]\}$
- $\mathrm{P}A^*(A,b) = \{z \in \mathbb{R}^2 : x \in \mathbb{R}, y \in [-1,1]\} \bigcup \{z \in \mathbb{R}^2 : x = 0, y \in \mathbb{R}\}$

From the example it follows that

$$\mathrm{I}S(A,b) \neq \mathrm{P}A(A,b) \neq \mathrm{P}A^*(A,b)$$

Also, for example, $z_0 = (1,0)$ is a Tschebychev point of the system, whereas it is not a Pareto minimum point (because $u = (0,0)$ is a point that satisfies the two conditions in the Definition 2.2, that should be **not** satisfied by any point in $\mathbb{C}^n$)

References

[1] M. Fekete, J.L. Walsh, *On restricted infrapolynomials*, Proceedings of the National Academy of Sciences, U.S.A., 37(1951), 95-103.

[2] I. Marusciac, *Infrapolynomials and Pareto optimization*, Mathematica (Cluj), 22(45), (1980), no. 2, 297-307.

[3] E.I. Remez, *Basis of the Numerical Methods in Tchebycheff's Approximation*, Izd. Kiev, 1969.

RENDICONTI DEL CIRCOLO MATEMATICO DI PALERMO
Serie II, Suppl. 81 (2009), pp. 337-344

On a simple class of staircase polytopes

Gaetana Restuccia
University of Messina, Department of Mathematics,
C.da Papardo, salita Sperone, 31, 98166 Messina, Italy.
E-mail: restucciag@tiscali.it

Dedicato al Chiarissimo Prof. Marius Stoka, per il Suo compleanno.

Abstract: The monomial Borel ideals are very important for algebraic, geometric and combinatoric reasons. We employ the principal Borel ideals to building geometric objects, useful in many fields.
Keywords: Monomial Ideals, Poytopes
Classification AMS: 13F20, 52BXX

Introduction

In a recent paper ([1]) we were interested to staircase diagrams in bi-dimensional and three-dimensional cases, introduced by E. Miller and B. Sturmfels ([2]). The reason was that these geometric objects arise from monomial ideals that, for a combinatorial point of view, are more easy to manage than in general case (ideals generated by polynomials). We utilize them in order to solve security problems, as reserved paths, reserved building and places of targets. To achieve one's aim rapidly, the set of dates we would to transmit has to be the smallest possible, then we have to individualize classes of monomial ideals for which the objective is reached. In this paper we consider the class of principal Borel ideals generated only by a monomial (the Borel generator), and the class of principal Borel polytopes. In this way, we have only to transmit a pair or a tern of numbers. In this case the selection procedure, described in ([1]), didn't have much sense, nevertheless we try to select points, for example, bounding the degree of a variable, and so the corresponding ideal has a smaller number of generators than in usual case, when the degree of Borel generators is big. In section N.1 we recall some definitions useful for the following. In section N.2 we give, with comments, the list of principal Borel ideals and staircase diagrams in two variables. In section N.3 we give the list of principal Borel ideals and corresponding polytopes in three variables with comments and pictures. At the end, we suggest some selection procedures.

1

Let $S = K[x_1, \ldots, x_n]$ be a polynomial ring over a field K, supposed of characteristic zero. Let $x^j = x_1^{j_1} x_2^{j_2} \cdots x_n^{j_n}$ be a monomial of S.

Definition 1.1 ([3], pag. 128, Def. 1.24) *An elementary move e_k, $1 \leq k \leq n-1$ is defined by $e_k\left(x^j\right) = x^{\hat{j}}$, where $\hat{j} = (j_1, \ldots, j_{k-1}, j_{k+1-1}, j_{k+2}, \ldots, j_n)$ and with the convention $x^{\hat{j}} = 0$, if some $j_m < 0$*

Definition 1.2 ([3], pag. 128, Def. 1.25) *A monomial ideal $I \subset S$ is said to be Borel-fixed if it satisfies the following condition: if $x^j \in I$, then for every elementary move $e_k\left(x^j\right) \in I$, $1 \leq k \leq n-1$.*

Example 1.1 *$I = \left(x_1^2, x_2^2\right) \subset K[x_1, x_2]$ is not Borel-fixed. In fact:*

$$e_1(x_1^2) = 0, \text{ but}$$
$$e_1(x_2^2) = x_1 x_2 \notin I$$

Example 1.2 *The following ideals are Borel-fixed*

$$I = \left(x_1^2, x_1 x_2, x_2^2\right) \subset K[x_1, x_2],$$
$$I = \left(x_1^3, x_1^2 x_2 x, x_1 x_2^2, x_2^3, x_1^2 x_3^2\right) \subset K[x_1, x_2, x_3],$$
$$I = \left(x_1^2, x_1 x_2, x_1 x_3, x_2^3\right) \subset K[x_1, x_2, x_3],$$

Definition 1.3 *Let I be a monomial ideal of $K[x_1, \ldots, x_n]$ generated by monomials of the same degree. The ideal I is said a principal Borel ideal with generator the monomial x^j, called the Borel generator, if I is the smallest Borel-fixed ideal containing x^j.*

A Borel-fixed ideal I will be indicated by $\left[x^j\right]$, if x^j is the Borel generator of I.

Example 1.3 *$I = \left(x_1^2, x_1 x_2, x_2^2\right) \subset K[x_1, x_2]$ is a principal Borel ideal and $I = \left[x_1^2\right]$.*

Definition 1.4 ([1], pag. 4, Def. 1.8)*A monomial ideal I in three variables is said strongly generic, if for every pair of generator $x_1^i x_2^j x_3^k$ and $x_1^{i'} x_2^{j'} x_3^{k'}$ we have:*

$$i \neq i' \text{ or } i = i' = 0,\ j \neq j' \text{ or } j = j' = 0,\ k \neq k' \text{ or } k = k' = 0.$$

We are interested to principal Borel ideals in bi or three-dimensional case. For these classes, the lattice points of the Borel generator will be indicated by $[i_1, i_2]$ or $[i_1, i_2, i_3]$. In this way the date associated to the ideals and, as a consequence, to the polytopes they represent, are very small.

2 Bi-dimensional principal Borel polytopes

Our project is to give the list of principal Borel ideals by lattice points corresponding to the Borel generator.

Example 2.1 (in degree 1,2,3)

$$\begin{array}{lcl}
[1,0] & \mapsto & [x_1] = (x_1, x_2) \\
[0,1] & \mapsto & [x_2] = (x_2) \\
[2,0] & \mapsto & \left[x_1^2\right] = \left(x_1^2, x_1x_2, x_2^2\right) \\
[1,1] & \mapsto & [x_1, x_2] = \left(x_1x_2, x_2^2\right) \\
[0,2] & \mapsto & \left[x_2^2\right] = \left(x_2^2\right) \\
[3,0] & \mapsto & \left[x_1^3\right] = \left(x_1^3, x_1^2x_2, x_1x_2^2, x_2^3\right) \\
[2,1] & \mapsto & \left[x_1^2x_2\right] = \left(x_1^2x_2, x_1x_2^2, x_2^3\right) \\
[1,2] & \mapsto & \left[x_1x_2^2\right] = \left(x_1x_2^2, x_2^3\right) \\
[0,3] & \mapsto & \left[x_2^3\right] = \left(x_2^3\right)
\end{array}$$

Proposition 2.1 *Let I be a principal Borel ideal of $K[x_1, x_2]$, generated in the same degree $m \geq 1$. Then I is one of the following types:*

1. $I = [x_1^m]$,
2. $I = \left[x_1^i x_2^j\right]$, $1 \leq i, j \leq m-1$, $i + j = m$,
3. $I = [x_2^m]$, *with* 1. *and* 2. *strongly generic ideals and* 3. *a principal ideal of* $K[x_1, x_2]$.

Proof: For the case 1., by applying the moves e_1 and e_2, we have:

$$I = [x_1^m] = \left(x_1^m, x_1^{m-1}x_2, \ldots, x_2^m\right)$$

For the case 2., by applying the moves e_1 and e_2, we have:

$$I = \left[x_1^i x_2^j\right] = \left(x_1^i x_2^j, x_1^{i-1}x_2^{j+1}, \ldots, x_2^m\right)$$

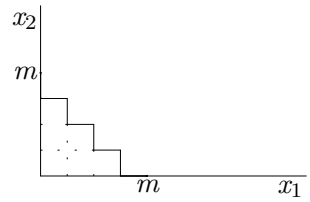
For the case 3., we obtain the simple form:

$$I = [x_2^m] = \left(x_2^m\right),$$

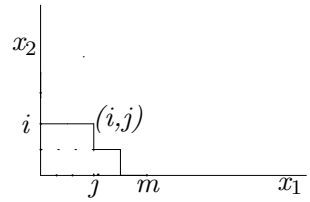
since no move can be applied.
We call the staircase diagrams, corresponding to the ideals of the Proposition 2.1, $P^{[m,0]}$, $P^{[i,j]}$, $P^{[0,m]}$. We have the following characterization:

Proposition 2.2 *Let $N^2_{\geq 0}$ the orthant consisting in all the positive lattice points (x_1, x_2). Then*

1. *The staircase diagram $P^{[m,0]}$ is a complete stair in $N^2_{\geq 0}$, between the points $(m, 0)$ and $(0, m)$ and no step is skipped.*

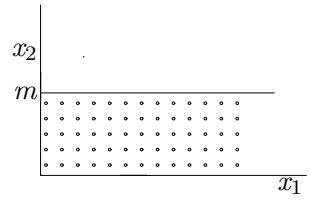


2. *The staircase diagram $P^{[i,j]}$, with $i + j = m$, $1 \leq i, j \leq m - 1$, has the following picture*



The surface of $P^{[i,j]}$ is a segment of the line $x_2 = i$, starting from the point $(0, i)$ until the lattice point (i, j). The stair is complete until the point $(0, m)$ and it has a jump in the lattice point (i, j).

3. *The staircase diagram $P^{[0,m]}$ has the line $x_2 = m$ as a surface and it is not finite.*



Proof: By easy considerations.

We propose a selection procedure only for the staircase diagram $P^{[0,m]}$. More precisely, we give:

Definition 2.1 *Let $P^{[m,0]}$ be the staircase polytope in the orthant $N^2_{\geq 0}$. Then a selection procedure consists in skipping one or more lattice points of the complete diagram.*

Example 2.2 *In* $P^{[4,0]}$ *we can delete the point* $(3,1)$ *or* $(2,2)$ *and so on.*

3 Three-dimensional principal Borel polytopes

Let $S = K[x_1, x_2, x_3]$ be the polynomial ring in three variables. In three-dimensional case, after the study of the principal Borel ideals by the Borel monomial generator, it will possible to give the picture of the corresponding staircase polytopes by the lattice points corresponding to the Borel generator and to introduce some selection procedures for security problems.

Proposition 3.1 *Let* $I \subset S = K[x_1, x_2, x_3]$ *be a principal Borel ideal, generated in the same degree* m*. Then* I *is one of the following types:*

1. $I = [x_1^m]$,
2. $I = \left[x_1^i x_2^j\right]$, $1 \leq i, j \leq m-1$, $i + j = m$,
3. $I = \left[x_1^i x_2^j x_3^k\right]$, $1 \leq i, j, k \leq m-2$, $i + j + k = m$,
4. $I = \left[x_1^i x_3^k\right]$, $1 \leq i, k \leq m-1$, $i + k = m$,
5. $I = [x_2^m]$,
6. $I = \left[x_2^j x_3^k\right]$, $1 \leq j, k \leq m-1$, $j + k = m$,
7. $I = [x_3^m]$,

Proof: The ideals 1., 2., 3., 4., are monomial ideals in three variables and we have:

1′. $[x_1^m] = \left(x_1^m, x_1^{m-1}x_2, \ldots, x_1x_2^{m-1}, x_2^m, x_1^{m-1}x_3, \ldots, x_3^m\right)$, the Veronese ideal of S in degree m.

2′. $\left[x_1^i x_2^j\right] = \left(x_1^i x_2^j, x_1^{i-1}x_2^{j+1}, \ldots, x_1x_2^{i+j-1}, x_2^m, x_1^{i-1}x_2^j x_3, \ldots, x_3^m\right)$

3′. $\left[x_1^i x_2^j x_3^k\right] = \left(x_1^i x_2^j x_3^k, x_1^{i-1}x_2^{j+1}x_3^k, \ldots, x_2^{i+j}x_3^k, x_1^i x_2^{j-1}x_3^{k+1}, \ldots, x_1^i x_3^{j+k}, \ldots\right.$

4′. $[x_1^i x_3^k] = \left(x_1^i x_3^k, x_1^{i-1}x_2x_3^k, \ldots, x_2^i x_3^k, x_2^{i-1}x_3^{k+1}, \ldots, x_3^m\right)$

The ideals 5., 6. are:

5′. $[x_2^m] = \left(x_2^m, x_2^{m-1}x_3, \ldots, x_3^m,\right)$

6′. $\left[x_2^j x_3^k\right] = \left(x_2^j x_3^k, x_2^{j-1} x_3^{k+1}, \ldots, x_3^{j+k}\right)$

that are strongly generic ideals. Finally the ideal 7. is

7′. $[x_3^m] = (x_3^m)$, a principal ideal.

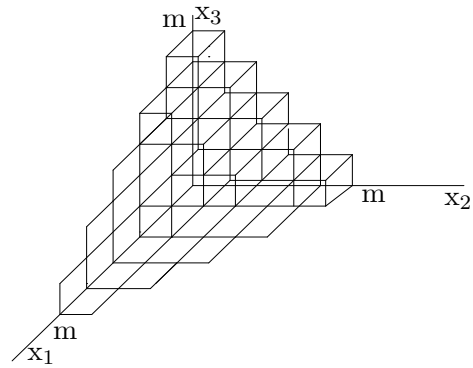
Theorem 3.1 *Let $N^3_{\geq 0}$ the orthant consisting in all the positive lattice points (x_1, x_2, x_3). Then we have:*

a. The staircase polytopes $P^{[m,0,0]}$, $P^{[i,j,0]}$, $P^{[i,j,k]}$, $P^{[i,0,k]}$, corresponding to the ideals 1., 2., 3., 4. of Proposition 3.1, have a three dimensional finite representation given by a′

b. The staircase polytopes $P^{[0,m,0]}$, $P^{[0,j,k]}$, $P^{[0,0,m]}$, corresponding to the ideals 5., 6., 7. of Proposition 3.1, are infinite staircase polytopes and their description is given by b′.

Proof:

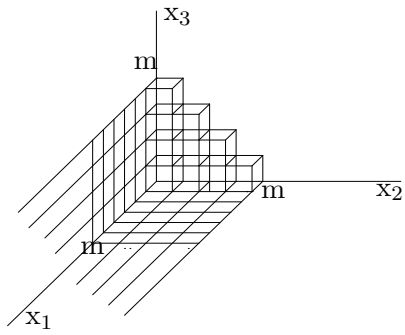
a'. The polytope $P^{[m,0,0]}$ has the following picture:



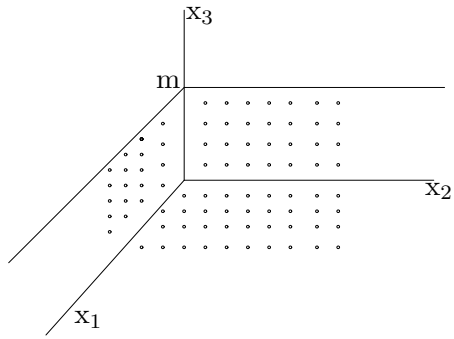
The polytope has the same staircase diagram as projections in the three orthants x_1x_2, x_1x_3, x_2x_3. It is full, in the sense that no step is skipped. Every point (i, j, k), $0 \leq i, j, k \leq m$, is inside the polytope. The polytopes $P^{[i,j,0]}$, $P^{[i,j,k]}$, $P^{[i,0,k]}$ are sub-polytopes of $P^{[m,0,0]}$ and their differ only by bounds on the three eights.

b'. The polytope $P^{[0,m,0]}$ has a staircase diagram as projection on the plane x_1x_3 and it extends along the x_1-axis. Every point (i, j, k), for

$j < m$, $i, k > m$, is inside the polytope, that is infinite:



In the same way for $P^{[0,j,k]}$, with bounds for the final corners of the projection staircase diagram on the plane x_1x_3. Finally, for $P^{[0,0,m]}$, we have the picture



The polytope is infinite along the two directions of the x_1-axis and x_2-axis. We have an infinite plane of height m, starting from the orthants x_1x_2 and x_2x_3.

Concerning selection procedures, they can consist in the deletion of lattice points on the polytope surface, as explained in [1]. But, since the notion of Borel generator is a mathematical notion which needs a background of different notions, then we can use the principal Borel polytopes in the finite three-dimensional case, as the objects that we have to transmit, without other operations or changes. Then we transmit only two or three natural numbers, that are the coordinates of the lattice point (Borel generator of the polytope) and the receiver can utilize directly the polytope that a software graphic program will build.

References

[1] A.Fabiano, G.Restuccia *Staircase polytopes and visualization of targets*, Communications to SIMAI Congress,ISSS 1827-9015.Vol.3 (2008), 317 (pp11).

[2] E.Miller, B.Sturmfels *Combinatorial Commutative Algebra*, Springer GTM 227 (2004).

[3] J.Elias, J.M.Giral, R.M.Mir *Roig, S.Zarzuela Editors.Six Lectures on Commutative Algebra*, Progress in Mathematics 166, Birkhaeuser.

RENDICONTI DEL CIRCOLO MATEMATICO DI PALERMO
Serie II, Suppl. 81 (2009), pp. 345-351

COMPUTING THE INTEGRAL CLOSURE OF POWERS OF MIXED PRODUCTS IDEALS

Paola L. Staglianò
University of Messina, Department of Mathematics,
C.da Papardo, salita Sperone, 31, 98166 Messina, Italy.
E-mail: paolasta@dipmat.unime.it

Abstract: The combinatorics of the integral closure of monomial ideals in two sets of variables is studied. We consider not normal ideals of mixed products and we obtain an expression for the not integrally closed powers of a particular class of mixed products ideals.
Keywords: Monomial Ideal, Integral Closure.
Classification AMS: 13B22, 13F20.

Introduction

Let $\mathbf{R} = K[x_1, x_2, \ldots, x_m]$ be a polynomial ring over K.The class of monomial of $\mathbf{R}$ has been intensively studied and many problems arise when we would like to study good properties of monomial ideals, such that integral closure, normality. Let $R = K[x_1, x_2, \ldots, x_m; y_1, y_2, \ldots, y_n]$ be a polynomial ring in two disjoint sets of variables, K a field of characteristic 0 and let $L = I_k J_r + I_s J_t$ be a mixed products ideals, with $k + r = s + t$ and where I_k (resp. J_r) is the ideal generated by all the square-free monomials of degree k (resp. r) in the variables x_i (resp. y_j). This class of ideals has been introduced in [4] and a complete classification of the normal ideals is given. An interesting problem is to give a description for the integral closure of the powers not integrally closed of mixed products ideals. In this direction the program `Normaliz` [1] can help us to find information when we work with low values of n and m and to formulate some conjectures. In this paper we are interested to study the integral closure for the powers not integrally closed of the ideals of the type $L = I_1 J_n + I_m J_1 \subset R = K[x_1, x_2, \ldots, x_n; y_1, y_2, \ldots, y_n]$. In 1 we recall some results about the integral closure of monomial ideals. In 2 we compute the integral closure for powers of ideals of mixed products not integrally closed of the type $L = I_1 J_n + I_n J_1 \subset R$.

The author is grateful to Professor Gaetana Restuccia for useful discussions about the results of this paper.

1

Let A be a commutative noetherian ring with unit, we recall some definitions and results that will use in this paper.

Definition 1.1 *Let A be a ring, and $I \subset A$ an ideal of A. The integral closure of I is the set of all elements of A which are integral over I.*

Remark 1.1 *For a monomial ideal $I \subset \mathbf{R} = K[x_1, x_2, \ldots, x_m]$ the definition is more clear because the integral closure of a monomial ideal I is again a monomial ideal and in* [6] *we have the following description for the integral closure of I:*

$$\overline{I} = \{f | f \text{ is a monomial in } R \text{ and } f^i \in I^i, \text{ for some } i \geqslant 1 \}$$

Definition 1.2 *If $I = \overline{I}$, I is said to be integrally closed. If $I^k = \overline{I^k}$ for all k then I is said to be normal.*

Now we study the integral closure of a particular class of monomial ideal, called mixed products ideal. This class of monomial ideals has been introduced by Restuccia and Villarreal in [4]. They are square-free monomial ideals generated in the same degree.

Definition 1.3 *Let $R = K[x_1, x_2, \ldots, x_m; y_1, \ldots, y_n]$ be a polynomial ring in two disjoint sets of variables over a field K. Given non negative integers k, r, s, t such that $k + r = s + t$, the ideals of mixed products L are:*

$$L = I_k J_r + I_s J_t$$

where I_k is the ideal of R generated by the square-free monomials of degree k in the variables x_i and J_r is the ideal of R generated by the square-free monomials of degree r in the variables y_j.

Theorem 1.1 *Let $R = K[x_1, x_2, \ldots, x_m; y_1, \ldots, y_n]$ be a polynomial ring over a field K. If*

$$L = I_k J_r + I_s J_t \neq R$$

is an ideal of mixed products with $k + r = s + t$, then L is normal if and only if L can be written (up to a permutation of k,s and r, t) in one of the following forms:

(a) $L = I_k J_r + I_{k+1} J_{r-1}$, $k \geq 0$ *and* $r \geq 1$.

(b) $L = I_k J_r$, $k \geq 1$ *or* $r \geq 1$.

(c) $L = I_k J_r + I_s J_t$, $0 = k < s = m$, *or* $0 = t < r = n$, *or* $k = t = 0$, $s = 1$

Proof: [6], Theorem 7.5.8

We are interested to study the mixed products ideals of the ring $R = K[x_1, x_2, \ldots, x_m; y_1, \ldots, y_n]$ which are not normal and, up to a permutation of k,s and r, t, they can be written in one of the following forms:

(a) $k = t = 0$, $L = I_s + J_s$, $2 \leq s < inf\,\{m, n\}$

(b) $k = 0$, $t \geq 1$, $L = J_r + I_s J_t$, $2 \leq s < m$

(c) $k \geq 1$, $t = 0$,$L = I_k J_r + I_s$, $2 \leq r < n$

(d) $k \geq 1$, $t \geq 1$, $L = I_k J_r + I_s J_t$, $s \geq k + 2$

A particular class of the ideals of type (a) has been studied in [2]. The integral closure of monomial ideals generated by monomials of degree two and not necessary square-free has been studied in [5].

2

In this section we would like to give a description for the integral closure of powers not integrally closed for ideals of type (d). For these ideals L^i is integrally closed for $i = 1, 2$ ([3]).

Theorem 2.1 *Let* $R = K[x_1, x_2, \ldots, x_m; y_1, y_2, \ldots, y_n]$ *be the polynomial ring in two disjoint sets of variables. Let*

$$L = I_k J_r + I_s J_t \subset R.$$

If $s > k + 1 \geq 2$, $t \geq 1$ *and* $k + r = s + t$, *then* L *is not normal.*

Proof: ([6], Proposition 7.5.6)

In particular we will examine the case $L = I_1 J_n + I_n J_1 \subset R = K[x_1, x_2, \cdots, x_n; y_1, y_2, \cdots, y_n]$.

Example 2.1 *Let* $L = I_1 J_3 + I_3 J_1 \subset K[x_1, x_2, x_3; y_1, y_2, y_3]$ *be a mixed products ideal.*

$$L = (x_1y_1y_2y_3, x_2y_1y_2y_3, x_3y_1y_2y_3, x_1x_2x_3y_1, x_1x_2x_3y_2, x_1x_2x_3y_3)$$

A computation of L^3, L^4 *using the software* `Normaliz` ([1]) *gives the following results:*

- $\overline{L^3} = \left(L^3, f\right)$ *with* $f = x_1^2x_2^2x_3^2y_1^2y_2^2y_3^2$
- $\overline{L^4} = \left(L^4, fL\right)$

Theorem 2.2 *Let* $K\left[x_1, x_2, x_3; y_1, y_2, y_3\right]$ *be the polynomial ring in two disjoint set of variables,* $L = I_1J_3 + I_3J_1$ *and* $f = x_1^2x_2^2x_3^2y_1^2y_2^2y_3^2$.
Then we have:

i. $\overline{L^3} = \left(L^3, f\right)$

ii. $\overline{L^{2+i}} = \left(L^{2+i}, fL^{i-1}\right)$, $i \geq 1$ *and the generators of* $\overline{L^{2+i}}$ *are of the same degree.*

Proof:

i. Using the program `Normaliz`, (Cf. example 2.1).

ii. By induction. For $i = 1$

$$\overline{L^3} = \left(L^3, f\right)$$

For $i > 1$. Let M be the following quotient $M = \overline{L^{2+i}}/\left(L^{2+i}, fL^{i-1}\right)$ and let I be the following ideal $I = \left(L^{1+i}, fL^{i-2}\right)$, by induction hypothesis $\overline{L^{1+i}} = \left(L^{1+i}, fL^{i-2}\right)$ and then $\overline{L^{1+i}}/I = 0$. As $\overline{L^{2+i}} \subset L^{1+i}$, we have

$$\overline{L^{2+i}}/I \cap L^{2+i} \subset \overline{L^{1+i}}/I \qquad (2.1)$$

Now we prove that

$$\left(L^{2+i}, fL^{i-1}\right) \subset I \cap \overline{L^{2+i}} \qquad (2.2)$$

In fact $\left(L^{2+i}, fL^{i-1}\right) \subset I$ and $\left(L^{2+i}, fL^{i-1}\right) \subset \overline{L^{2+i}}$, because $L^{2+i} \subset \overline{L^{2+i}}$ and $fL^{i-1} \subset \overline{L^{2+i}}$ ($h \in fL^{i-1} \Rightarrow h \in fL^{i-2}$, but by induction hypothesis $\left(L^{1+i}, fL^{i-2}\right) = \overline{L^{1+i}} \supset \overline{L^{2+i}} \Rightarrow h \in \overline{L^{1+i}}$). Using (2.2) the inclusion (2.1) becomes

$$\overline{L^{2+i}}/\left(L^{2+i}, fL^{i-1}\right) \subset \overline{L^{1+i}}/\left(L^{1+i}, fL^{i-2}\right) = 0$$

It follows that $\overline{L^{2+i}}/\left(L^{2+i}, fL^{i-1}\right) = 0$, and then $\overline{L^{2+i}} = \left(L^{2+i}, fL^{i-1}\right)$.

Example 2.2 *Let* $L = I_1J_4 + I_4J_1 \subset K\left[x_1, x_2, x_3, x_4; y_1, y_2, y_3, y_4\right]$ *be a mixed products ideal.*

$$L = (x_1y_1y_2y_3y_4, x_2y_1y_2y_3y_4, x_3y_1y_2y_3y_4, x_4y_1y_2y_3y_4, x_1x_2x_3x_4y_1, x_1x_2x_3x_4y_2, x_1x_2x_3x_4y_3, x_1x_2x_3x_4y_4)$$

Then we have

- $\overline{L^3} = \left(L^3, f\right)$ *with* $f = x_1^2x_2^2x_3^2x_4^2y_1^2y_2^2y_3^2y_4^2$
- $\overline{L^4} = \left(L^4, x_1^2x_2^2x_3^2x_4^2y_1^3y_2^3y_3^3y_4^3, x_1^3x_2^3x_3^3x_4^3y_1^2y_2^2y_3^2y_4^2\right)$

Remark 2.1 *$\overline{L^3}$ is not generated by monomials of the same degree.*

Theorem 2.3 *Let $K\left[x_1, x_2, x_3, x_4; y_1, y_2, y_3, y_4\right]$ be the polynomial ring in two disjoint set of variables, $L = I_1J_4 + I_4J_1$, $f = x_1^2x_2^2x_3^2x_4^2y_1^3y_2^3y_3^3y_4^3$, $g = x_1^3x_2^3x_3^3x_4^3y_1^2y_2^2y_3^2y_4^2$.*
Then we have:

i. $\overline{L^4} = \left(L^4, f, g\right)$

ii. $\overline{L^{3+i}} = \left(L^{3+i}, (f,g)L^{i-1}\right)$ *and* $i \geq 1$

Proof:

i. Cf. example 2.2.

ii. By induction. For $i = 1$

$$\overline{L^4} = \left(L^4, f, g\right)$$

For $i > 1$. Let M be the following quotient $M = \overline{L^{3+i}}/\left(L^{3+i}, fL^{i-1}, gL^{i-1}\right)$ and let I be the following ideal $I = \left(L^{2+i}, fL^{i-2}, gL^{i-2}\right)$, by induction hypothesis $\overline{L^{2+i}} = \left(L^{2+i}, fL^{i-2}, gL^{i-2}\right)$ and then $\overline{L^{2+i}}/I = 0$. As $\overline{L^{3+i}} \subset L^{1+i}$, we have

$$\overline{L^{3+i}}/I \cap L^{3+i} \subset \overline{L^{2+i}}/I \qquad (3.1)$$

Now we prove that

$$\left(L^{3+i}, fL^{i-1}, gL^{i-1}\right) \subset I \cap \overline{L^{3+i}} \qquad (3.2)$$

In fact $\left(L^{3+i}, fL^{i-1}, gL^{i-1}\right) \subset I$ and $\left(L^{3+i}, fL^{i-1}, gL^{i-1}\right) \subset \overline{L^{3+i}}$, because $L^{3+i} \subset \overline{L^{3+i}}$ and $\left(fL^{i-1}, gL^{i-1}\right) \subset \overline{L^{3+i}}$. Using (3.2) the inclusion (3.1) becomes

$$\overline{L^{3+i}}/\left(L^{3+i}, fL^{i-1}, gL^{i-1}\right) \subset \overline{L^{2+i}}/\left(L^{2+i}, fL^{i-2}, gL^{i-1}\right) = 0$$

It follows that $\overline{L^{3+i}}/\left(L^{3+i}, fL^{i-1}, gL^{i-1}\right) = 0$, and then $\overline{L^{3+i}} = \left(L^{3+i}, fL^{i-1}, gL^{i-1}\right)$.

Example 2.3 *Let $L = I_1J_n + I_nJ_1 \subset K[x_1, x_2, \ldots, x_n; y_1, y_2, \ldots, y_n]$ be a mixed products ideal with $n = 3, 4, 5, 6, 7$. Using the software* `Normaliz`*, we obtain:*

i. $\overline{L^n} = (L^n, f_1, f_2, \ldots, f_{n-2})$

ii. $\overline{L^{n-1+i}} = \left(L^{n-1+i}, (f_1, f_2, \ldots, f_{n-2})\, L^{i-1}\right)$ *and* $i \geq 1$

with:

$$f_1 = x_1^{2+\alpha}x_2^{2+\alpha}\cdots x_n^{2+\alpha}y_1^2y_2^2\cdots y_n^2 \quad \alpha = n-3$$
$$f_2 = x_1^2x_2^2\cdots x_n^2y_1^{2+\alpha}y_2^{2+\alpha}\cdots y_n^{2+\alpha} \quad \alpha = n-3$$
$$f_3 = x_1^{3+\beta}x_2^{3+\beta}\cdots x_n^{3+\beta}y_1^3y_2^3\cdots y_n^3 \quad \beta = n-5$$
$$f_4 = x_1^3x_2^3\cdots x_n^3y_1^{3+\beta}y_2^{3+\beta}\cdots y_n^{3+\beta} \quad \beta = n-5$$
$$f_5 = x_1^{4+\gamma}x_2^{4+\gamma}\cdots x_n^{3+\gamma}y_1^4y_2^4\cdots y_n^4 \quad \gamma = n-7$$

Thanks to the example 2.3, we can suppose the following conjecture:

Conjecture 2.1 *Let $K[x_1, x_2, \ldots, x_n; y_1, y_2, \ldots, y_n]$ be the polynomial ring in two disjoint sets of variables, $L = I_1J_n + I_nJ_1$.*
Then we have:

i. $\overline{L^n} = (L^n, f_1, f_2, \ldots, f_{n-2})$

ii. $\overline{L^{n-1+i}} = \left(L^{n-1+i}, (f_1, f_2, \ldots, f_{n-2})\, L^{i-1}\right)$ *and* $i \geq 1$

with:

$$f_1 = x_1^{2+\alpha}x_2^{2+\alpha}\cdots x_n^{2+\alpha}y_1^2y_2^2\cdots y_n^2 \quad \alpha = n-3$$
$$f_2 = x_1^2x_2^2\cdots x_n^2y_1^{2+\alpha}y_2^{2+\alpha}\cdots y_n^{2+\alpha} \quad \alpha = n-3$$
$$f_3 = x_1^{3+\beta}x_2^{2+\beta}\cdots x_n^{2+\beta}y_1^3y_2^3\cdots y_n^3 \quad \beta = n-5$$
$$f_4 = x_1^3x_2^3\cdots x_n^3y_1^{2+\beta}y_2^{2+\beta}\cdots y_n^{2+\beta} \quad \beta = n-5$$
$$\cdots$$
$$f_{2n-3} = x_1^{2n-5}x_2^{n-5}\cdots x_n^{2n-5}y_1^{2n-5}y_2^{2n-5}\cdots y_n^{2n-5} \quad \text{if } n = 2n-1$$
$$f_{2n-2} = x_1^nx_2^n\cdots x_n^ny_1^{n+1}y_2^{n+1}\cdots y_n^{n+1} \quad \text{if } n = 2n$$

We will conclude this research enouncing an almost evident conjecture suggested by the examples 2.1, 2.2 and by the following:

Example 2.4 *Let* $K[x_1, x_2, x_3, x_4, x_5; y_1, y_2, y_3, y_4, y_5]$ *be the polynomial ring in two disjoint set of variables and* $L = I_1J_5 + I_5J_1$*, then*

$$\overline{L^3} = \left(L^3, x_1^2x_2^2x_3^2x_4^2x_5^2y_1^2y_2^2y_3^2y_4^2y_5^2\right)$$

Conjecture 2.2 *Let* $K[x_1, x_2, \ldots, x_n; y_1, y_2, \ldots, y_n]$ *be the polynomial ring in two disjoint set of variables,* $L = I_1J_n + I_nJ_1$ *the class of ideals of mixed products not normal*
Then the first power not integrally closed L^3 *is given by:*

$$\overline{L^3} = \left(L^3, f\right) \text{ with } f = x_1^2x_2^2\cdots x_n^2y_1^2y_2^2\cdots y_n^2$$

References

[1] W. Brums, R. Koch, *Normalize*-a program for computing normalizations of affine semigroups, 1998. Available via anonymous ftp from `ftp.mathematik.Uni-Osnabrueck.DE/pub/osm/kommalg/software`

[2] M. La Barbiera, M. Paratore, *Convex sets associated to monomial ideals in two sets of variables*, Rendiconti del circolo matematico di Palermo, Serie II, 77, pp. 355-362, 2006.

[3] M. La Barbiera, M. Paratore, *Complete Powers of Mixed Products Ideals* , Atti dell'Accademia Peloritana dei Pericolanti, vol LXXX, pp. 35-42, 2002.

[4] G. Restuccia, R. H. Villarreal, *On the Normality of Monomial Ideals of Mixed Products*, Communication in Algebra, **29(8)**, pp. 3571, 2001.

[5] P.L. Staglianò, *Integral Closure of Monomial Ideals*, Communications to SIMAI Congress, Vol 3, 2009.

[6] R. H. Villarreal, *Monomial Algebras*, Marcel Dekker Inc., 2001.

RENDICONTI DEL CIRCOLO MATEMATICO DI PALERMO
Serie II, Suppl. 81 (2009), pp. 353-361

Statistical tests for point processes obtained from martingale central limit theorems

Franz Streit

ABSTRACT

Martingale central limit theorems are reviewed and applied to derive new tests of hypotheses concerning point processes.

Key Words: Point processes, martingale central limit theorems, statistical tests.
AMS Classification 2000: 60G55,62F03,62F05.

1.) ON THE USEFULNESS OF LARGE SAMPLE THEORY IN STATISTICAL INFERENCE FOR POINT PROCESSES

When developing methods of statistical inference for point processes it is only in exceptional and very simple cases feasible to determine the exact sampling distribution of the relevant statistics. This explains why results of the large sample theory are so important in this field. As main tools, which have been found to be very convenient in this situation, the standard central limit theorem for independent and identically distributed random variables and central limit theorems of the Ljapunov type for independent random variables with different probability laws have to be mentioned.
If however the future evolution of the point process is influenced by its past central limit theorems for dependent random variables are often needed. In the following martingale central limit theorems, which find applications in the described context, are reviewed and their utility demonstrated by discussing three problems of inference for point processes.

2.) ON MARTINGALE CENTRAL LIMIT THEOREMS

In the literature one finds a great variety of martingale central limit theorems, but the following result is particularly appropriate for our purpose:

Theorem (Billingsley,P.) [5, pp.52 ff.]:
Let the sequence of random variables $\{S(n) = \sum_{k=1}^{n} V(k); n = 1, 2, 3, \ldots\}$ be a zero-mean martingale with respect to the σ-fields $\mathcal{F}_n$ generated by our knowledge of the process up to and including the instant $t = n$ and put $S(0) = 0$ with probability 1. Then $E[S(n)|\mathcal{F}_{n-1}] = S(n-1)$ with probability 1 and $E[S(1)] = 0$. Suppose that the $V(k)$'s possess a moment of order 3 and that
(1) $\lim_{n\to\infty} n^{-1} \sum_{k=1}^{n} E[V^2(k)|\mathcal{F}_{k-1}] = \beta^2$ and
(2) $\lim_{n\to\infty} n^{-3/2} \sum_{k=1}^{n} E[|V(k)|^3|\mathcal{F}_{k-1}] = 0$
with probability 1, where β^2 is a non-negative constant.
Then
$n^{-1/2} S(n) \to_L N^*(0, \beta^2)$,
where $\to_L$ denotes convergence in distribution and $N^*(a, g)$ the normal distribution with expectation a and variance g.

Remark:
Condition (1) may be written equivalently as
$\lim_{n\to\infty} [Var[S(n)]]^{-1} \sum_{k=1}^{n} E[V^2(k)|\mathcal{F}_{k-1}] = 1$
with probability 1.

As shown in [8] the conclusion of the above theorem may also be demonstrated under certain sets of conditions other than {(1) and (2) }. Furthermore the fact that (2) implies the conditional Lindeberg condition admits the following generalization due to [6] and [4] (see also [3, Appendix 1]):

Extension of the theorem:
If the condition (1) in the preceding theorem is replaced by
(1*) $Var[S(n)]^{-1} \sum_{k=1}^{n} E[V^2(k)|\mathcal{F}_{k-1}] \to_p \Psi$
where Ψ is a random variable which is almost surely positive and $\to_p$ denotes convergence in probability then
$[Var[S(n)]]^{-1/2} S(n) \to_L N^*(0, \sigma^2) \wedge_{\sigma^2} F_\Psi$,
where F_Ψ is the distribution function of Ψ and $\wedge_{\sigma^2}$ indicates the mixture of the variance σ^2 with the distribution of Ψ.

3.) SOME APPLICATIONS OF MARTINGALE CENTRAL LIMIT THEOREMS TO INFERENCE PROBLEMS FOR POINT PROCESSES

To exhibit the usefulness of the theorems of section 2, we show their application to the construction of tests for point processes related to three

problems of statistical inference.
In all three cases we deal with orderly point processes with state space $\mathcal{R}^+ = \{t > 0\}$ or a subset of it. $T(i)$ $[i \in \mathcal{N} = \{1, 2, 3, \ldots\}]$ designates the occurrence time of the ith point event after $t = 0$ and t_i the realized value of this random variable (with an analogous notation for other random variables). We denote by $\{U(i); i \in \mathcal{N}\}$ the sequence of gap lengths $U(i) = T(i) - T(i-1)$ between consecutive point events. Of course $(T(1), \ldots, T(i))$ and $(U(1), \ldots, U(i))$ are equivalent indications. $N(t, t+\delta)$ stands for the random number of point events in $(t, t+\delta]$ and $N(t)$ for the random number of point events in $(0, t]$. $\sim$ means 'distributed as' and $Poi(\lambda)$ designates the Poisson distribution with parameter λ.

Problem A
Testing independence versus a particular dependence relation among Poisson distributed count data.
It is supposed that a point process of the Poisson type is analyzed over the fixed period from $t = 0$ to $t = n_0$ with (n_0 an integer number greater than 1), but that we are only informed of the numbers $K_i = N(i-1, i)$ $[i = 1, \ldots, n_0]$ of the point events realized in the subintervals $(i-1, i]$. In the stochastic model considered, which is motivated by work of [9, p.227, formula (16)] on the specification of bivariate Poisson distributions, the K_i's may be independent or exhibit a dependence relation in the sense that K_i is influenced by K_{i-1} as specified by the relations

$$\begin{aligned} K_1 = N(0,1) &\sim Poi(\lambda) \\ K_2 = N(1,2) | K_1 = k_1 &\sim Poi(\lambda \rho^{\lambda - k_1}) \\ K_3 = N(2,3) | K_1 = k_1, K_2 = k_2 &\sim Poi(\lambda \rho^{\lambda - k_2}) \\ &\vdots \\ K_{n_0} = N(n_0 - 1, n_0) | K_1 = k_1, K_2 = k_2, & \\ \ldots, K_{n_0 - 1} = k_{n_0 - 1} &\sim Poi(\lambda \rho^{\lambda - k_{n_0 - 1}}). \end{aligned}$$

It is of interest to distinguish the case of independence, where all counts are independently Poisson distributed with parameter λ and the case of dependence, where K_i depends on K_{i-1} $[i = 2, 3, \ldots]$ in such a way that small (large) counts have the tendency to be followed by large (small) counts, by selecting the hypotheses $H_0 : \rho = 1$ and $H_1 : \rho > 1$.
A locally most powerful test is looked for, which should recognize whether the process disposes of a self-regulation property leading to counts clustered nearer to the mean value λ than under the independence assumption. In fact, values of ρ greater than 1 but near 1 imply that the point process

reacts against rather low (high) counts by an increase (decrease) of the intensity rate.
In order to find such a test we analyse the likelihood function L of ρ for the observed count data and for fixed λ, which is given by
$L(\rho : K_1 = k_1, \ldots, K_{n_0} = k_{n_0}; \lambda) =$
$((\lambda)^{k_1}/(k_1!)) \exp[-\lambda] \prod_{i=2}^{n_0} [(\lambda\rho^{\lambda - k_{i-1}})^{k_i} \exp[-\lambda\rho^{\lambda-k_{i-1}}]/(k_i!)]$
The efficient score test statistic is determined based on the statements
$\log(L(\rho : K_1 = k_1, \ldots K_{n_0} = k_{n_0}; \lambda)) =$
$k_1 \log(\lambda) - \lambda - \log(k_1!) + \sum_{i=2}^{n_0} [k_i(\log(\lambda) + (\lambda - k_{i-1}) \log(\rho)) - \lambda\rho^{\lambda-k_{i-1}} - \log(k_i!)]$
and
$(\partial \log(L(\rho : K_1 = k_1, \ldots, K_{n_0} = k_{n_0}; \lambda)/\partial\rho)|_{\rho=1} = \sum_{i=2}^{n_0} [(\lambda - k_{i-1})(k_i - \lambda)]$.
Thus the test statistic to be used is
${}_K T_{n_0,\lambda}(1) = \sum_{l=2}^{n_0} [(\lambda - K_{l-1})(K_l - \lambda)] = \sum_{l=2}^{n_0} {}_K T_\lambda^{(l)}(1)$
and is obtained by summation of the $n_0 - 1$ contributions
${}_K T_\lambda^{(l)}(1) = (\lambda - K_{l-1})(K_l - \lambda)\, [l = 2, \ldots, n_0]$.
Since $E[{}_K T_\lambda^{(l)}(1) | K_1, \ldots, K_{l-1} : \rho = 1] = (\lambda - K_{l-1})(\lambda - \lambda) = 0$ and therefore also $E[{}_K T_{n_0,\lambda}(1) : \rho = 1] = 0$,
$\{{}_K T_{2,\lambda}(1),\ {}_K T_{3,\lambda}(1), \ldots\}$ is a zero-mean martingale and
$\{{}_K T_\lambda^{(2)}(1),\ {}_K T_\lambda^{(3)}(1), \ldots\}$ is a sequence of martingale differences under H_0.
It turns out that the suppositions of the theorem of section 2 are fulfilled.
In fact, we find
$(n_0 - 1)^{-1} \sum_{l=2}^{n_0} E[{}_K T_\lambda^{(l)2}(1) | K_1, \ldots, K_{l-1} : \rho = 1] =$
$(n_0 - 1)^{-1} \sum_{l=2}^{n_0} [(\lambda - K_{l-1})^2 E[(K_l - \lambda)^2 : \rho = 1] = (\lambda/(n_0 - 1)) \sum_{l=2}^{n_0} (\lambda - K_{l-1})^2$
$\to \lambda E[(\lambda - K_{l-1})^2 : \rho = 1] = \lambda^2$
with probability 1, taking into account the strong law of large numbers and the fact, that for $\rho = 1$ the K_l's are independent identically distributed. Condition(1) is thus satisfied with $\beta^2 = \lambda^2$.
On the other hand
$(n_0 - 1)^{-3/2} E[|{}_K T_\lambda^{(l)3}(1)| | K_1, \ldots, K_{l-1} : \rho = 1] =$
$(n_0 - 1)^{-3/2} \sum_{l=2}^{n_0} E[(|\lambda - K_{l-1}|^3 |K_l - \lambda|^3 | K_1, \ldots, K_{l-1} : \rho = 1] =$
$(n_0 - 1)^{-3/2} \sum_{l=2}^{n_0} |\lambda - K_{l-1}|^3 E[|X - \lambda|^3 : \rho = 1] \to$
$(n_0 - 1)^{-1/2} E[|X - \lambda|^3 : \rho = 1]^2 \to 0$
with probability 1, where X denotes a random variable with a Poisson distribution with parameter λ. The strong law of large number has again been used together with the finiteness of $E[|X - \lambda|^3 : \rho = 1] \le \max\{\lambda^3, E[X^3 : \rho = 1]\} = \lambda^3 + 3\lambda^2 + \lambda$. Condition (2) holds thus also.
According to the theorem of section 2 we find for $n_0 \to \infty$ and under H_0 that

$[\sqrt{n_0-1}\lambda]^{-1}\,{}_K T_{n_0,\lambda}(1) \sim N^*(0,1)$.
The critical region of the locally most powerful test of H_0 versus H_1 of level of significance α for large n_0 is thus given by
$[\sqrt{n_0-1}\lambda]^{-1}\,{}_K t_{n_0,\lambda}(1) > z(1-\alpha)$
with $\Phi(z(1-\alpha)) = 1-\alpha$ and Φ designating the distribution function of the standard normal distribution. The test rejects H_0 if and only if the realization ${}_K t_{n_0,\lambda}(1)$ of our test statistic satisfies the above inequality.
So far we have considered the parameter λ as known. There may however be some doubt about the effective value of the parameter λ. Suppose λ_0 is the most likely value of λ, assumed to be taken with large probability $1-p$, but that there exists an alternative value λ_1 which may be correct with a small probability p. In such a set-up, we consider the parameter as a random variable Λ with its distribution function F_Λ specified by
$P(\Lambda = \lambda_0) = 1-p$ and $P(\Lambda = \lambda_1) = p$.
Our previous considerations lead to
${}_K T_{n_0,\Lambda}(1) \sim \sqrt{n_0-1}\lambda_0 Z$ with probability $1-p$ and
${}_K T_{n_0,\Lambda}(1) \sim \sqrt{n_0-1}\lambda_1 Z$ with probability p
and therefore the test statistic follows the variance-mixed normal distribution
${}_K T_{n_0,\Lambda}(1) \sim N^*(0,(n_0-1)\lambda^2) \wedge_{(n_0-1)\lambda^2} F_{(n_0-1)\Lambda^2}$
where $F_{(n_0-1)\Lambda^2}$ stands for the mixing distribution specified by
$P((n_0-1)\Lambda^2 = (n_0-1)\lambda_0^2) = 1-p$ and $P((n_0-1)\Lambda^2 = (n_0-1)\lambda_1^2) = p$.
The critical region of the test is now
$[n_0-1]^{-1/2}\,{}_K t_{n_0,\Lambda}(1) > [(1-p)\lambda_0 + p\lambda_1]z(1-\alpha)$.
Our result is in good agreement with the statement of the extension of the theorem, since condition (1^*) is satisfied with
$(Var[{}_K T_{n_0,\Lambda}(1)])^{-1} \sum_{l=2}^{n_0} E[{}_K T_\Lambda^{(l)2}(1)|\mathcal{F}_{l-1}] \to_p \Psi$
with
$P(\Psi = \lambda_0^2/[(1-p)\lambda_0^2 + p\lambda_1^2]) = 1-p$ and $P(\Psi = \lambda_1^2/[(1-p)\lambda_0^2 + p\lambda_1^2]) = p$.
What has been explained in the simple special case of a two-point distribution for Λ, holds by analogy for an arbitrary F_Λ- distribution provided that $F_\Lambda(0) = 0$. The technique amounts to replace classical statistical analysis by a Bayesian statistical analysis in case of uncertainty about the effective value of a nuisance parameter. By this procedure we may extend the statistical analysis to point processes involving an external randomization as for instance when Cox processes are chosen instead of Poisson point processes.

Problem B
Testing whether the gap lengths between successive point events of a point process with state space $\mathcal{N}$, which are supposed to follow (displaced) Pois-

son distributions, are independent or not.

The gap lengths of the considered point process may only take positive integer values and have a discrete enumerative distribution according to the stochastic model specified by the relations

$$\begin{aligned} U(1)-1 &\sim Poi(\lambda) \\ U(2)-1|U(1)=u_1 &\sim Poi(\lambda\rho^{\lambda-u_1+1}) \\ U(3)-1|U(1)=u_1, U(2)=u_2 &\sim Poi(\lambda\rho^{\lambda-u_2+1}) \\ &\cdot \\ &\cdot \\ &\cdot \\ U(n_0)-1|U(1)=u_1, U(2)=u_2, \dots, & \\ U(n_0-1)=u_{n_0-1} &\sim Poi(\lambda\rho^{\lambda-u_{n_0-1}+1}). \end{aligned}$$

We want to test the hypotheses

$H_0 : \rho = 1$, implying that all gap lengths follow a displaced Poisson distribution with the same parameter λ and that the point process is a renewal point process, which places single point events at some of the points $t = i\,[i \in \mathcal{N}]$

versus

$H_1 : \rho > 1$, which leads to a point process which places point events at some of the time points $t = i\,[i \in \mathcal{N}]$ with gap lengths following different displaced Poisson distributions. Under this hypothesis long (short) gap lengths have the tendency to be followed by short (long) gap lengths.

Note that in this stochastic model the distribution is used to choose the distance between consecutive point events and not to select the number of point events appearing in a given time interval as in problem A.

We assume that the point process is observed in the time period $(0, T(n_0)]$ and use the abbreviation $\pi(\nu, d) := d^\nu \exp[-d]/(\nu!)\,[\nu = 0, 1, \dots; d > 0]$ for the probabilities generated by a Poisson distribution with parameter d.

The intensity function under the general hypothesis takes the form

$\lambda^*(t_{i-1} + s_i) = [\sum_{\nu=s_i-1}^{\infty} \pi(\nu, \lambda\rho^{\lambda-u_{i-1}+1})]^{-1} \pi(s_i - 1, \lambda\rho^{\lambda-u_{i-1}+1})$
$[i = 1, \dots, n_0 - 1; s_i = 1, \dots, u_i; t_0 = 0; u_0 := \lambda + 1]$ and
$\lambda^*(t_{i-1} + s_i) = 0$ [otherwise].

The likelihood function may be written as integral-product [2, Chapter 2]

$L(\rho : u_1, \dots, u_{n_0}; \lambda) = \prod_{t\in(0,t_{n_0}]} \{(\lambda^*(t))^{\Delta N(t)} (1 - \lambda^*(t))^{1-\Delta N(t)}\} =$
$\prod_{i=1}^{n_0} \{(\sum_{\nu=1}^{\infty} \pi(\nu, \lambda\rho^{\lambda-u_{i-1}+1})/1) \cdot$
$(\sum_{\nu=2}^{\infty} \pi(\nu, \lambda\rho^{\lambda-u_{i-1}+1}) / \sum_{\nu=1}^{\infty} \pi(\nu, \lambda\rho^{\lambda-u_{i-1}+1})) \cdot$
$\dots (\sum_{\nu=u_i-1}^{\infty} \pi(\nu, \lambda\rho^{\lambda-u_{i-1}+1}) / \sum_{\nu=u_i-2}^{\infty} \pi(\nu, \lambda\rho^{\lambda-u_{i-1}+1})) \cdot$
$(\pi(u_i - 1, \lambda\rho^{\lambda-u_{i-1}+1}) / \sum_{\nu=u_i-1}^{\infty} \pi(\nu, \lambda\rho^{\lambda-u_{i-1}+1}))\} =$
$\prod_{i=1}^{n_0} \pi(u_i - 1 : \lambda\rho^{\lambda-u_{i-1}+1})$.

Since $K_i \sim U_i - 1\,[i \in \mathcal{N}]$, all the calculations concerning the likelihood

function and the test statistic lead to the same result as in problem A, when K_i is replaced by $U(i) - 1$. In particular the statistic to be used for the test is now
$T_{n_0,\lambda}(1) = \sum_{i=2}^{n_0}\{(\lambda - U(i-1) + 1)(U(i) - 1 - \lambda)\}$ and all the comments on the testing procedure made in the previous section remain valid.

Problem C
Testing a homogeneous Poisson point process versus a particular Poisson type process.
The problem consists to devise a locally most powerful test based on the observation period $(0, T(n_0)]$ with $n_0 \in \mathcal{N}$ and $n_0 > 1$ for the hypotheses
H_0 : The point process is a Poisson point process with global rate λ and
H_1 : The point process is a Poisson type process. The value of its complete intensity function depends on the position of the last realized point event and increases if this point event presents itself late.
The complete intensity function of the stochastic model is chosen as
$\lambda^*(t : \lambda, \delta) = \lambda$ for $0 < t \leq t_1$ and
$\lambda^*(t : \lambda, \delta) = \lambda + \delta 1_{\{t_{n-1} > 2(n-1)/\lambda\}}(t_{n-1})$ for $t_{n-1} < t \leq t_n\, [n = 2, 3, \ldots]$.
Here $1_A(x) = 1$ for $x \in A$ and $1_A = 0$ for $x \notin A$. Note that we have $H_0 : \delta = 0$ and $H_1 : \delta > 0$.
λ^* attains a value above λ if the last realized point event appears at a time point later than the double of its mean value under H_0. The likelihood function is given by
$L(\delta : t_1, \ldots, t_{n_0}; \lambda) =$
$\lambda e^{-\lambda u_1} \prod_{i=2}^{n_0}\{(\lambda + \delta 1_{\{t_{i-1} > 2(i-1)/\lambda\}}(t_{i-1})) \exp[-(\lambda + \delta 1_{\{t_{i-1} > 2(i-1)/\lambda\}}(t_{i-1}))u_i]\}$.
For the determination of the efficient score test statistic we remark that
$\log(L(\delta : t_1, \ldots, t_{n_0}; \lambda) = \log(\lambda) - \lambda u_1 +$
$\sum_{i=2}^{n_0} \log(\lambda + \delta 1_{\{t_{i-1} > 2(i-1)/\lambda\}}(t_{i-1})) - \sum_{i=2}^{n_0}\{(\lambda + \delta 1_{\{t_{i-1} > 2(i-1)/\lambda\}}(t_{i-1}))u_i\}$
and thus
$T_{n_0,\lambda}(0) = \partial \log(L(\delta : T(1), \ldots, T(n_0); \lambda)/\partial\delta|_{\delta=0} =$
$\sum_{i=2}^{n_0}\{1_{\{T(i-1) > 2(i-1)/\lambda\}}(T(i-1))[(1/\lambda) - U(i)]\}$.
It turns out that we can apply the theorem of section 2. In fact we find
$E[1_{\{T(i-1) > 2(i-1)/\lambda\}}(T(i-1)((1/\lambda) - U(i))|T(1), \ldots, T(i-1) : \delta = 0] =$
$1_{\{T(i-1) > 2(i-1)/\lambda\}}(T(i-1)[1/\lambda - 1/\lambda] = 0$ and thus also
$E[1_{\{T(i-1) > 2(i-1)/\lambda\}}(T(i-1)((1/\lambda) - U(i)) : \delta = 0] = 0$.
Condition (1) is satisfied, although only in the for our purpose sufficient mode of convergence in probability, since
$E[\sum_{i=2}^{n_0} 1_{\{T(i-1) > 2(i-1)/\lambda\}}(T(i-1))[(1/\lambda) - U(i)]^2|T(1), \ldots, T(i-1) : \delta =$
$0][n_0 - 1]^{-1} =$

$[(n_0-1)\lambda^2]^{-1}\sum_{i=2}^{n_0} 1_{\{T(i-1)>2(i-1)/\lambda\}}(T(i-1)) \to_p$
$((n_0-1)\lambda^2)^{-1}\sum_{i=2}^{n_0} P(T(i-1)>2(i-1)/\lambda : \delta=0) =$
$((n_0-1)\lambda^2)^{-1}\sum_{i=2}^{n_0}(1-P(i-1,2(i-1))),$
where
$P(i-1,2(i-1)) :=$
$\int_0^{2(i-1)/\lambda} \lambda^{i-1}t_{i-1}^{i-2}\exp[-\lambda t_{i-1}]dt_{i-1}/\Gamma(i-1)$
stands for a value of the normed incomplete Γ-function as defined in [1, p.260] and we have applied a general ergodic theorem [7, pp.73–75] which states the sample mean of a stochastic process is ergodic, if and only if as the sample size n_0 is increased there is less and less correlation between the sample mean and the last observation. It is enough to observe that for $n_0 \to \infty$
$P(1_{\{T(n_0-1)>2(i-1)/\lambda\}}(T(n_0-1)) = 1 : \delta = 0) \to_L$
$1-\Phi((\sqrt{(n_0-1}/\lambda)^{-1}((n_0-1)/\lambda)) = 1-\Phi(\sqrt{n_0-1}) \to 0$
since $T(n_0-1) \sim N^*((n_0-1)/\lambda,(n_0-1)/\lambda^2)$ for $n_0 \to \infty$. Thus
$1_{\{T(n_0-1)>2(n_0-1)/\lambda\}}(T(n_0-1) \to_p 0.$
Condition(2) is also fulfilled due to
$\sum_{i=2}^{n_0} E[1_{\{T(i-1)>2(i-1)/\lambda\}}(T(i-1))|(1/\lambda)-U(i)|^3|T(1),\ldots,T(i-1) :$
$\delta=0]/(n_0-1)^{3/2} \leq$
$\sum_{i=2}^{n_0} 1_{\{T(i-1)>2(i-1)/\lambda\}}(T(i-1)\max\{1/\lambda)^3, 6/\lambda^3\}(n_0-1)^{-3/2} \leq$
$6[(n_0-1)\lambda^6]^{-1/2} \to 0$ for $n_0 \to \infty$.
Therefore
$T_{n_0,\lambda}(0) \sim N^*(0,[(n_0-1)\lambda^2]^{-1}\sum_{i=2}^{n_0}(1-P(i-1,2(i-1))))$
for $n_0 \to \infty$ under H_0.
Again the locally most powerful test is based on a critical value of the standard normal distribution and any doubt about the true value of the nuisance parameter λ may be expressed by a prior distribution and leads to tests involving critical values of variance-mixed normal distributions.

REFERENCES

[1] Abramowitz,M. & Stegun,I.A.
Handbook of mathematical functions.
National Bureau of Standards, Washington, 1964.

[2] Andersen,P.K., Borgan,Ø., Gill,R.D. & Keiding,N.
Statistical models based on counting processes.
Springer, New York, 1993.

[3] Basawa,I.V. & Prakasa Rao,D.L.S.
Statistical inference for stochastic processes.
Academic Press, London, 1980.

[4] Basawa,I.V. & Scott,D.J.
Efficient tests for stochastic processes.
Sankhyā 39, Series A, 21–31, 1977.

[5] Billingsley,P.
Statistical inferences for Markov processes.
The University of Chicago Press (Midway), Chicago, 1974.

[6] Hall,P.
Martingale invariance principles.
Annals of Probability 5, 875–887, 1977.

[7] Parzen,E.
Stochastic processes.
Holden–Day, San Francisco, 1965.

[8] Scott,D.J.
Central limit theorems for martingales and for processes with stationary increments using a Skorokhod representation approach.
Adv. Appl. Prob. 5, 119-137, 1973.

[9] Wesolowski,J.
Bivariate discrete measures via a power series conditional distribution and a regression function.
Journal of Multivariate Analysis, 55, 2, 219–229, 1995.

Section de Mathématiques de l'Université de Genève
Case Postale 64, CH-1211 Genève 4, Suisse.
e-mail: streit@unige.ch

RENDICONTI DEL CIRCOLO MATEMATICO DI PALERMO
Serie II, Suppl. 81 (2009), pp. 363-367

ISOPERIMETRIC DEFICIT UPPER LIMIT OF A PLANAR CONVEX SET

JIAZU ZHOU*, CHUANTING ZHOU AND FANG MA

Abstract. We investigate the convex set K of area A and length L with the continuous radius of curvature ρ of ∂K. Then we obtain some upper limits of the isoperimetric deficit of K. The upper bounds obtained are invariants involving area A, length L, the maximum and minimum of curvature ρ. As we expected, those upper limits are attained for circles.

1. Introductions and Prelimilaries

Perhaps the well-known geometric inequality is the isoperimetric inequality. And its analytic proofs root back to centuries ago. One can find some simplified and beautiful proofs that lead to generalizations of higher dimensions and applications to other branches of mathematics ([1], [3], [5], [9], [10], [11], [12], [14], [15]).

The classical isoperimetric inequality says that: for a simple closed curve Γ of length L in the Euclidean plane R^2, the area A enclosed by Γ satisfies

$$L^2 - 4\pi A \geq 0. \tag{1}$$

The equality sign holds if and only if Γ is a circle. It follows that the circle is the only curve of constant length L enclosing maximum area.

Let K be a domain with the boundary composing of the simple curve of length L and area A. Then the isoperimetric deficit of K is defined as

$$\Delta(K) = L^2 - 4\pi A. \tag{2}$$

The isoperimetric deficit measures the deficit between a domain and a disc. During the 1920's, Bonnesen proved a series of inequalities of the form

$$\Delta(K) \geq B, \tag{3}$$

where the equality B is an invariant of geometric significance having the following basic properties:

1. B is non-negative;
2. B is vanish only when K is a disc.

Many Bs are found in the last century and mathematicians are still working on those unknown invariants of geometric significance. See reference [1], [3], [5], [9], [10], [11], [12], [14], [15] for more details.

Date: May, 2009.
2000 Mathematics Subject Classification. Primary 52A10, 52A27; Secondary 52A22.
Keywords: Convex set, isoperimetric deficit, inscribed radius, circumscribed radius.
*Supported in part by CNSF (grant number: 10671159).

A set of points K in R^n is called *convex* if for each pair of points $x \in K$, $y \in K$ it is true that the line segment $\overline{xy}$ joining x and y is contained in K. Let $D \neq \emptyset$ be a set, $D^* = \bigcup_{x,y \in D} \overline{xy}$ is called the *convex hull* of D. Since for any domain D in R^2, its convex hull D^* increases the area A^* and decreases the length L^*. Then we have $L^2 - 4\pi A \geq L^{*2} - 4\pi A^*$, that is $\Delta(D) \geq \Delta(D^*)$. Therefore the isoperimetric inequality and the Bonnesen-type inequality are valid for all domains in R^2 if they are valid for convex domains.

When mathematicians are mainly interested in and focus on the lower bound of the isoperimetric deficit, there is another question: is there invariant C of geometric significance such that

$$\Delta(K) \leq C? \tag{4}$$

Of course we expect that the upper bound be attained when K is a disc. This is a long standing unsolved problem in geometry. Unfortunately we are not aware of any upper bound up today except for few special convex domains ([2], [8], [12]).

Assume that the boundary ∂K of the convex set K has a continues radius of curvature ρ. Let ρ_m and ρ_M be the smallest and the greatest values, respectively, of ρ. Bottema (see [2], [12]) finds an upper isoperimetric deficit limit of K, that is:

Proposition 1. Let K be a convex set of area A and length L with the continuous radius of curvature ρ of ∂K. Let ρ_m and ρ_M be the smallest and the greatest values, respectively, of ρ. Then

$$\Delta(K) \leq \pi^2(\rho_M - \rho_m)^2. \tag{5}$$

The equality sign holds if and only if $\rho_M = \rho_m$, that is, if K is a circle.

Pleijel (see [8], [12]) has an improvement of Bottema's result as follows:

Proposition 2. Let K be a convex set of area A and length L with the continuous radius of curvature ρ of ∂K. Let ρ_m and ρ_M be the smallest and the greatest values, respectively, of ρ. Then

$$\Delta(K) \leq \pi(4 - \pi)(\rho_M - \rho_m)^2. \tag{6}$$

The equality sign holds if and only if K is a circle.

Recently Li and Zhou generalize Bottema's result to surface of constant curvature (see [6]). Mathematicians have been working very hard on those yet known isoperimetric deficit upper limits. We are not aware of any progress until recent works of Zhou, Li and Ma (see [16], [17], [18]).

In this paper, we first investigate the convex polygon Γ and we find some inequalities among the invariants of Γ (Lemma 1). Since any convex curve can be approximated by convex polygons. Then we obtain some upper bounds of isoperimetric deficit $\Delta(K)$ of a convex set K with the continuous radius of curvature ρ of ∂K. As we expect, these upper bounds (Theorem 1 and Theorem 2) are the geometric significance, and are attained when K is a disc.

2. The isoperimetric deficit upper limit of a convex set

Let Γ be a convex polygon of length L in R^2 and be composed of finite sides Γ_k of length L_k, that is, $\Gamma = \bigcup_{k=1}^{n} \Gamma_k$, $L = \sum_{k=1}^{n} L_k$. Assume that Γ encloses area A and an inscribed circle of radius r_I and is circumscribed in a circle of radius r_E. Denote by d the diameter of Γ. Zhou and Ma (see [18]) prove the following

Proposition 3. Let Γ be a convex polygon of length L in the plane, and A the area enclosed by Γ. Then the diameter d, the in-radius r_I and the circum-radius r_E of Γ satisfy the following inequalities

$$r_I \leq \frac{2A}{L} \leq \sqrt{\frac{A}{\pi}} \leq \frac{L}{2\pi} \leq \frac{d}{2} \leq r_E. \tag{7}$$

Let K be a convex set of area A and length L with the continuous radius of curvature ρ of ∂K. Let ρ_m and ρ_M be the smallest and the greatest values, respectively, of ρ. Since any convex set can be approximated by polygons, therefore inequalities (7) valid for all convex sets. We have the following

Lemma 1. Let K be a convex set of area A and length L with the continuous radius of curvature ρ of ∂K. Let ρ_m and ρ_M be the smallest and the greatest values, respectively, of ρ. Denote by d the diameter, r_I the in-radius, r_E the circum-radius r_E of ∂K, respectively. Then we have

$$\rho_m \leq r_I \leq \frac{2A}{L} \leq \sqrt{\frac{A}{\pi}} \leq \frac{L}{2\pi} \leq \frac{d}{2} \leq r_E \leq \rho_M. \tag{8}$$

Each equality holds if and only if K is a disc.

Theorem 1. Let K be a convex set of area A and length L with the continuous radius of curvature ρ of ∂K. Let ρ_m and ρ_M be the smallest and the greatest values, respectively, of ρ. Then we have

$$\begin{array}{rcl} \Delta(K) & \leq & 2\pi L(\rho_M - \rho_m); \\ \Delta(K) & \leq & \frac{\pi L^2}{A}(\rho_M^2 - \rho_m^2); \\ \Delta(K) & \leq & 4\pi^2(\rho_M^2 - \rho_m^2). \end{array} \tag{9}$$

Each equality sign holds if and only if $\rho_M = \rho_m$, that is, if K is a circle.

Proof: Via inequalities

$$\rho_m \leq \frac{2A}{L} \leq \frac{L}{2\pi} \leq \rho_M,$$

we have

$$\frac{L}{2\pi} - \frac{2A}{L} \leq \rho_M - \rho_M,$$

that is,

$$L^2 - 4\pi A \leq 2\pi L(\rho_M - \rho_m). \tag{10}$$

From

$$\rho_m \leq \frac{2A}{L} \leq \sqrt{\frac{A}{\pi}} \leq \rho_M,$$

we have

$$\rho_m^2 \leq \frac{4A^2}{L^2} \leq \frac{A}{\pi} \leq \rho_M^2,$$

and then

$$\frac{A}{\pi} - \frac{4A^2}{L^2} \leq \rho_M^2 - \rho_m^2.$$

Therefore we have

$$L^2 - 4\pi A \leq \frac{\pi L^2}{A}(\rho_M^2 - \rho_m^2). \tag{11}$$

By inequalities

$$\rho_m \leq \sqrt{\frac{A}{\pi}} \leq \frac{L}{2\pi} \leq \rho_M,$$

we have

$$\rho_m^2 \leq \frac{A}{\pi} \leq \frac{L^2}{4\pi^2} \leq \rho_M^2,$$

and then

$$\frac{L^2}{4\pi^2} - \frac{A}{\pi} \leq \rho_M^2 - \rho_m^2,$$

that is,

$$L^2 - 4\pi A \leq 4\pi^2(\rho_M^2 - \rho_m^2). \tag{12}$$

We have completed the proof of Theorem 1.

Since $L \leq 2\pi\rho_M$, then we have

Theorem 2. Let K be a convex set of area A and length L with the continuous radius of curvature ρ of ∂K. Let ρ_m and ρ_M be the smallest and the greatest values, respectively, of ρ. Then we have

$$\Delta(K) \leq 4\pi^2\rho_M(\rho_M - \rho_m). \tag{13}$$

The equality sign holds if and only if $\rho_M = \rho_m$, that is, if K is a circle.

As we expect that the invariant C in (4) can be expressed as the form of

$$\Delta(K) \leq C(\rho_M, \rho_m), \tag{14}$$

and is of geometric significance. All isoperimetric deficit upper limits obtained are attained when and only when K is a circle.

References

[1] Yu. D. Burago & V. A. Zalgaller, Geometric Inequalities, Springer-Verlag Berlin Heidelberg (1988).

[2] O. Bottema, Eine obere Grenze für das isoperimetrische Defizit ebener Kurven, Nederl. Akad. Wetensch. Proc., A66 (1933), 442-446.

[3] E. Grinberg, D. Ren & J.Zhou, The symetric isoperimetric deficit and the containment problem in a plan of constant curvature, preprint.

[4] R. Howard, The sharp Sobolev inequality and the Banchoff-Pohl inequality on surfaces, Proc. Amer. Math. Soc., 126(1998), 2779 - 2787.

[5] W. Y. Hsiung, An elementary proof of the isoperimetric problem, Chin. Ann. Math., 23A: 1(2002), 7-12.

[6] M. Li & J. Zhou, An upper limit for the isoperimetric deficit of convex set in a plane of constant curvature, preprint submitted.
[7] E. Lutwak, D. Yang & G. Zhang, Sharp affine L_p Sobolev inequality, J. Diff. Geom., 62(2002), 17 - 38.
[8] A. Pleijel, On konvexa kurvor, Nordisk Math. Tidskr. 3(1955), 57-64.
[9] R. Osserman, The isoperimetric inequality, Bull. Amer. Math. Soc., 84(1978), 1182-1238.
[10] R. Osserman, Bonnesen-style isoperimetric inequality, Amer. Math. Monthly, 86(1979),1-29.
[11] Delin Ren , Topics in Integral Geometry, World Scientific, Sigapore (1994).
[12] L. A. Santaló, Integral Geometry and Geometric Probability, Reading, MA: Addison-Wesley, 1976.
[13] G. Zhang, The affine Sobolev inequality, J. Diff. Geom., 53 (1999), 183 - 202.
[14] J. Zhou, On Bonnesen-type inequalitiesActa Math. Sinica no.6. 50(2007), 1397 - 1402.
[15] J. Zhou & F. Chen, The Bonnesen-type inequalities in a plane of constant curvature, Journal of Korean Math. Sco. no.6. 44(2007), 1363 - 1372.
[16] J. Zhou & L. Ma, The isoperimetric deficit upper bounds for polygons, preprint submitted.
[17] J. Zhou, & M. Li, The Isoperimetric Deficit Upper Bounds for convex sets in space, preprint submitted.
[18] J. Zhou & L. Ma, Upper Bound of the Isoperimetric Deficit, preprint preprint.

School of Mathematics and Statistics, Southwest University, Chongqing, 400715, People's Republic of China
E-mail address: zhoujz@swu.edu.cn

RENDICONTI DEL CIRCOLO MATEMATICO DI PALERMO
Serie II, Suppl. 81 (2009), pp. 369-378

A PERMUTATION APPROACH TO EVALUATE HYPERHOMOCYSTEINEMIA IN EPILEPTIC PATIENTS

AGATA ZIRILLI, ANGELA ALIBRANDI

Abstract. In this paper we want to evaluate if the variations of homocysteine and folates levels in epileptic patients are in relation to the genetic mutations of the MTHFR enzyme. We have studied a group of 178 epileptic patients followed in the Neurological Clinic of Messina University. All the subjects have been classified in relationship to their different genotype: 677TT (homozygote); 677CT (heterozygote); C677T/1298AC (diplotipo or composed heterozygote). The statistical analysis has been performed by a non parametric approach, using permutation tests; we applied the NPC test in order to compare the three genotype in relationship to homocysteine and folates and the Stochastic Ordering procedure in order to assess the existence of a monotonous trend for homocysteine and folates levels in time.

1. Introduction

The epilepsy is a pathological syndrome that interests about 1% of the Italian population. It can arise in every age, even if the periods of greater incidence are the infancy (<10 years) and, above all, the seniority (>60 years) when the pathology is also increased by circulatory troubles, by tumours and by cerebral atrophic trials. The epilepsy is characterized by the repetition of crises or by a variety of neurological symptoms.

In the 60-70% of the cases the epilepsy can be treated through medicines that stabilize the electric properties of the membrane of the nervous cells. The required time for the antiepileptic therapy depends on the type, on the cause and on the spontaneous evolution of the illness. Because the medicines effects finish few times after the care is interrupted, the therapy has to continue in precise way and for a long period of time and, not rarely, for the whole life. It is, therefore, a symptomatic therapy that doesn't eliminate the cause of the epilepsy; nevertheless it guarantees a normal life to many patients.

The patients submitted to antiepileptic therapy are often interested by hyperhomocysteinemia. The homocysteine is a sulphurated amino-acid that is formed as intermediate product of the metionine; it is introduced by the feeding. Three enzymes have involved in the transformation of the homocysteine: ligase metionine; methylene tetrahydrofolate reductase (MTHFR); betaligase cystathionine. A genetic defect frequently found in the population is a mutation of MTHFR

This note, though it is the result of a close collaboration, was specifically elaborated as follows: paragraphs 1, 2, 3, 3.1, 3.2 by A. Zirilli and paragraphs 3.3, 3.4, 4 by A. Alibrandi.

gene. Rare mutations can cause the serious deficiency of MTHFR, with appearance of homocystinuria (more serious form of the hyperhomocysteinemia) and low plasmatic levels of folic acid. Some variants are been identified with serious deficiency of MTHFR: 677TT (homozygote); 677CT (heterozygote); C677T/1298AC (diplotipo or composed heterozygote).

Various studies have been performed on the polymorphisms of patients submitted to antiepileptic therapy; in Caccamo et al. (2004) the prevalence of the MTHFR C677T and A1298C polymorphisms and their impact on the hyperhomocysteinemia is investigated. This paper suggests that both the MTHFR polymorphisms must be examined for verifying risk factors for hyperhomocysteinemia in epilepsy. In Ono et al.(2002) the C677T mutation is studied in patients that assume one or more anticonvulsivantes; the authors affirm that the mutation C677T is tightly connected to the hyperhomocysteinemia and to the lack of folates in epileptic patients that assume multiple anticonvulsivantes.

2. The Data

The purpose of the present paper is to examine the homocysteine and folates levels in epileptic patients; in particular, we want to verify if the variations that occur are associated to genetic mutations of the MTHFR enzyme. The study has been lead on a sample of 178 subjects with epilepsy diagnosis (98 males and 80 females); they have ambulatorily been followed in the Neurological Clinic of Messina University. They has furnished their consent to the their data treatment for scientific finalities. In our analysis, all the subjects have been gathered in three categories, in relationship to their different genotype:

- the first one includes the belonging subjects to the 677TT genotype (homozygote);
- the second includes the belonging subjects to the 677CT genotype (heterozygote);
- the third includes the belonging subjects to the C677T/1298AC genotype (diplotype or composed heterozygote).

Initially, homocysteine and folate levels have been measured (Pre-treatment = $P.T.$). Folic acid (5mg/die) has been administered to them for a month. After the suspension of folic acid, the haematic levels of homocysteine and folates have been measured after one month (T_1), two months (T_2), four months (T_3), six months (T_4). The patients, in chronic therapy with anticonvulsive medicines, showed high-levels of homocysteine and low levels of folic acid.

Table 1 shows the descriptive statistics (mean $\pm$ standard deviation, minimum, maximum and confidence interval C.I. at α level $= 0.05$) for the numerical variables for every genotype. The percentage composition for sex in the three genotypes is the following: 58% males and 42% females for 1 and 3 genotypes; 53% males and 47% females for 2 genotype.

TABLE 1. Descriptive statistics for genotype

Genotype 1					
Variables	Times	Mean ± S.D.	Min	Max	C.I.
Age		32,90 ±13,33	16	56	27,06-38,74
Weight		65,75 ± 8,33	53	77	62,10-69,40
	P.T.	27,23 ± 3,35	21,90	32,00	25,76-28,69
	T_1	13,36 ± 3,68	7,60	19,00	11,74-14,97
Homocysteine	T_2	20,58 ± 3,13	12,80	25,46	19,21-21,95
	T_3	22,58 ± 2,89	16,90	28,00	21,31-23,84
	T_4	30,63 ± 3,44	25,00	35,00	29,12-32,14
	P.T.	3,89 ± 2,07	2,13	9,23	2,98-4,80
	T_1	22,91 ± 1,96	20,12	25,83	22,05-23,77
Folates	T_2	5,54 ± 2,19	3,20	8,96	4,57-6,50
	T_3	10,76 ± 7,93	3,10	24,14	7,28-14,23
	T_4	4,20 ± 2,08	2,13	8,17	3,29-5,11
Genotype 2					
Age		38,30 ±14,68	16	61	31,52-45,08
Weight		68,72 ± 8,39	58	82	64,85-72,59
	P.T.	23,40 ± 3,15	18,62	28,45	21,94-24,86
	T_1	1,60 ± 3,39	6,36	18,83	9,04-12,17
Homocysteine	T_2	13,36 ± 3,03	8,22	16,36	11,96-14,76
	T_3	13,71 ± 3,47	8,830	19,45	12,10-15,31
	T_4	22,42 ± 2,21	18,23	25,28	21,40-23,44
	P.T.	4,23 ± 2,13	2,07	8,44	3,24-5,21
	T_1	28,98 ± 2,11	26,20	32,53	28,00-29,96
Folates	T_2	6,70 ± 2,17	3,39	10,06	5,70-7,70
	T_3	6,05 ± 2,21	3,22	10,33	5,03-7,07
	T_4	3,97 ± 2,11	2,11	9,24	3,00-4,95
Genotype 3					
Age		41,88 ± 11,90	21	56	36,66-47,09
Weight		70,57 ± 5,09	60	80	68,34-72,80
	P.T.	28,39 ± 4,30	23,51	35,34	26,50-30,27
	T_1	9,18 ± 4,12	3,35	17,28	7,38-10,99
Homocysteine	T_2	12,83 ± 3,02	8,40	20,22	11,50-14,15
	T_3	16,34 ± 2,49	12,50	20,41	15,25-17,43
	T_4	21,59 ± 1,53	19,33	23,52	20,92-22,27
	P.T.	4,62 ± 2,19	2,30	9,11	3,66-5,58
	T_1	25,95 ± 2,98	20,50	29,90	24,64-27,25
Folates	T_2	7,02 ± 2,25	3,20	9,70	6,04-8,01
	T_3	4,94 ± 1,66	3,21	8,74	4,21-5,67
	T_4	3,98 ± 2,06	2,04	7,84	3,08-4,88

All patients have also been submitted to anticonvulsive therapy, with different medicines according to their different type of epilepsy.

3. Statistical analysis by means of Multivariate Permutation Test

The low sampling dimension and the non-normality of the distribution don't guarantee valid asymptotic results. For this reason, the statistical analysis has been performed through a non parametric approach, using the permutation tests (Pesarin, 2001). We have chosen such technique because we needed to use a non parametric methodology to test multidimensional hypotheses, without implying the knowledge of the statistical distributions for the studied variables, neither their structure of dependence. Moreover, the inferences associated to permutation tests are extendible to the whole population, being guaranteed the properties of non-distortion and consistence. By means of permutation tests, we performed:

- the Non Parametric Combination test or NPC Test (Pesarin, 2001) in order to evaluate the existence of possible statistically significant differences among the three groups of subjects, (according to the genotype) in relationship to homocysteine and folates levels;
- the Stochastic Ordering procedure (Terpstra and Magel, 2003) in order to verify the existence of a monotonous increasing or decreasing for homocysteine and folates levels in time.

3.1. **NPC test.** This multivariate and multistrata procedure allows to reach effective solutions concerning problems of multidimensional hypothesis verifying within the non parametric permutation inference (Pesarin, 1997); it is used in different application fields that concern verifying of multidimensional hypotheses with a complexity that can't be managed in parametric context. NPC test is released to distributional assumptions because doesn't assume normality and homoscedasticity; it draws any type of variable; it also assumes a good behavior in presence of missing data; it is also powerful in low sampling dimension; it resolves multidimensional problems, without the necessity to specify the structure of dependence among variables; it allows to test multivariate restricted alternative hypothesis (allowing the verifying of the directionality for a specific alternative hypothesis); it allows stratified analysis; it can be applied also when the sampling number is smaller than the number of variables. All these properties make NPC test very flexible and widely applicable in several fields; in particular we cite recent applications in medical context (Bonnini et al., 2003; Bonnini et al., 2006; Zirilli et al., 2005; Callegaro et al., 2003; Arboretti et al., 2005; Salmaso, 2005; Alibrandi and Zirilli, 2007) and in genetics (Di Castelnuovo et al., 2000; Finos et al., 2004).

The null hypothesis, that postulates the indifference among the distributions, and the alternative one are expressed as follows:

$$H_0 : \left\{ X_{11} \stackrel{d}{=} X_{12} \right\} \cap \cdots \cap \left\{ X_{n1} \stackrel{d}{=} X_{n2} \right\} \tag{3.1}$$

$$H_1 : \left\{ X_{11} \stackrel{d}{\neq} X_{12} \right\} \cup \cdots \cup \left\{ X_{n1} \stackrel{d}{\neq} X_{n2} \right\} \tag{3.2}$$

In presence of a stratification variable, the hypotheses system is:

$$H_{0i} : \left\{ X_{11i} \stackrel{d}{=} X_{12i} \right\} \cap \cdots \cap \left\{ X_{n1i} \stackrel{d}{=} X_{n2i} \right\} \tag{3.3}$$

$$H_{1i} : \left\{ X_{11i} \overset{d}{\neq} X_{12i} \right\} \cup \cdots \cup \left\{ X_{n1i} \overset{d}{\neq} X_{n2i} \right\} \tag{3.4}$$

The hypotheses systems are verified by the determination of partial tests (first order) that allow to evaluate the existence of statistically significant differences. By means of this methodology we can preliminarily define a set of k (k>1) unidimensional permutation tests (partial tests); they allow to examine every marginal contribution of answer variable, in the comparison among the examined groups. The partial tests are combined, in a non parametric way, in a second order test that globally verifies the existence of differences among the multivariate distributions. A procedure of conditioned resampling CMC (Conditional Monte Carlo, Pesarin, 2001) allows to estimate the p-values, associated both to partial tests and to second order tests.

3.2. **Application of NPC test for the evaluation of differences among genotypes.** Through the aforesaid methodology, we have realized the comparisons among the three examined groups of subjects, stratifying for each of five times (before the treatment = T_0, after a month = T_1, after two months = T_2, after four months = T_3 and after six months =T_4). The hypothesis system can be defined through the following relationships:

$$H_{0i} : \left\{ homoc._{1i} \overset{d}{=} ... \overset{d}{=} homoc._{3i} \right\} \cap \left\{ fol._{1i} \overset{d}{=} ... \overset{d}{=} fol._{3i} \right\} \tag{3.5}$$

$$H_{1i} : \left\{ homoc._{1i} \overset{d}{\neq} ... \overset{d}{\neq} homoc._{3i} \right\} \cup \left\{ fol._{1i} \overset{d}{\neq} ... \overset{d}{\neq} fol._{3i} \right\} \tag{3.6}$$

where $1, \ldots, 3$ are referred to the three typologies of genotype and the stratification i index ($i = 0, \ldots, 4$) is referred to times. The table 2 shows the results of the test.

TABLE 2. Comparison among genotypes

Times	*Homocysteine*	*Folates*		*Comb.*
P.T.	**0,001**	0,557	→	**0,003**
T_1	**0,003**	**0,000**	→	**0,000**
T_2	**0,000**	0,093	→	**0,000**
T_3	**0,000**	**0,001**	→	**0,000**
T_4	**0,000**	0,930	→	**0,001**
				↓
				0,000

The results show that, in reference to homocysteine and in every considered time, all the comparisons are statistically significant except those concerning the folates at T_0, T_2 and T_4 times. So, we have performed all the "two by two" comparisons with the purpose to individualize the most significant group (table 3), stratifying for times of observation. For only significant results the directionality (direct.) is shown.

TABLE 3. Two by two comparison between genotypes

Times	Homocystene		Folates			
	Genotype 1 vs Genotype 2					
	p-value	direct.	p-value	direct.		Comb.
$P.T.$	**0,001**	$>$	0,618	-	$\rightarrow$	0,106
T_1	**0,024**	$>$	**0,000**	$<$	$\rightarrow$	**0,000**
T_2	**0,000**	$>$	0,107	-	$\rightarrow$	**0,000**
T_3	**0,000**	$>$	**0,022**	$>$	$\rightarrow$	**0,000**
T_4	**0,000**	$>$	0,738	-	$\rightarrow$	**0,000**
	Genotype 1 vs Genotype 3					
$P.T$	0,345	-	0,283	-	$\rightarrow$	0,327
T_1	**0,003**	$>$	**0,000**	$<$	$\rightarrow$	**0,000**
T_2	**0,000**	$>$	**0,039**	$<$	$\rightarrow$	**0,000**
T_3	**0,000**	$>$	**0,002**	$>$	$\rightarrow$	**0,000**
T_4	**0,000**	$>$	0,739	-	$\rightarrow$	0,327
	Genotype 2 vs Genotype 3					
$P.T$	**0,000**	$<$	0,580	-	$\rightarrow$	**0,001**
T_1	0,252	-	**0,001**	$>$	$\rightarrow$	**0,002**
T_2	0,594	-	0,654	-	$\rightarrow$	0,752
T_3	**0,013**	$<$	0,088	-	$\rightarrow$	**0,009**
T_4	0,185	-	0,988	-	$\rightarrow$	0,496

The results show that 1 and 2 genotypes are significantly different for the homocysteine levels; for the folates the two groups are different only at T_1 and T_3 times. The comparison between 1 and 3 genotypes results significant for both the variables and at every time, except the one referred to $P.T.$; we can find another non significant p-value at time T_4 for the folates (p =0,739). A smaller number of statistically significant differences can be noticed for the comparison between 2 and 3 genotypes.

3.3. **The Stochastic Ordering procedure.** With reference to C independent samples, the researchers sometimes had to verify if the answer to a treatment is independent from the order with which the means of treatments are disposed, performing test with unilateral alternative hypotheses also when there are more groups. Such problematic can be faced through a permutation solution, applying the so-called "Stochastic Ordering" (Pesarin, 2001), in which an increasing (or decreasing) effect is hypothesized to the growth (or to decrease) of the examined variable values. We consider a C-sample univariate problem concerning an experiment where units are randomly assigned to C groups which are defined according to increasing levels of a treatment. Let's assume that responses are quantitative or ordered categorical and the related model is:

$$X_{ji} = \mu + \Delta_{ji} + Z_{ji}, \qquad \text{with} \quad i = 1, \ldots, n \quad \text{and} \quad j = 1, \ldots, C \tag{3.7}$$

where μ is a population constant, Z are exchangeable random errors, and Δ_j are the stochastic effects on the jth group. Moreover, let's assume that effects satisfy

the monotonic stochastic ordering condition $\Delta_1 \overset{d}{\leq} ... \overset{d}{\leq} \Delta_C$, so that the condition $F_1(t) \overset{d}{\geq} ... \overset{d}{\geq} F_C(t), \forall t \in R^1$ is satisfied. The following hypoteses system has to be verified:

$$H_0 : \{X_1 \overset{d}{=} ... \overset{d}{=} X_C\} = \{\Delta_1 \overset{d}{=} ... \overset{d}{=} \Delta_C\} \tag{3.8}$$

$$H_1 : \{X_1 \overset{d}{\leq} ... \overset{d}{\leq} X_C\} = \{\Delta_1 \overset{d}{\leq} \ldots \overset{d}{\leq} \Delta_C\}. \tag{3.9}$$

where $X_j (j = 1, ..., C)$ is the dataset in the jth group and Δ_j the stochastic effects.

In a permutation context, in order to tackle this problem of isotonic inference, let's imagine that for any j ∈ {1,...,C-1}, the whole data set is split into two pooled pseudo-groups, where the first is obtained by pooling together data of the first j (ordered) groups and the second by pooling the rest. In particular, the first pooled pseudo-group is $Y_{1(j)} = X_1 \uplus ... \uplus X_j$ and the second is $Y_{2(j)} = X_{j+1} \uplus ... \uplus X_C$, with $j = 1, \ldots, C-1$; $\uplus$ is the symbol for pooling data into one pseudo-group and $X_j = \{X_{ji}, i = 1, ..., n_j\}$ is the data set in the jth group. In the null hypothesis, data of every pair of pseudo-groups are exchangeable because related pooled variables satisfy the relationship $Y_{1(j)} \overset{d}{=} Y_{2(j)}$, with $j = 1, ..., C-1$. The alternative hypothesis $Y_{1(j)} \overset{d}{\leq} Y_{2(j)}$ corresponds to the monotonic stochastic ordering (dominance) between any pair of pseudo-groups. For this, the equivalent form of hypotheses system is:

$$H_0 : \{\cap_j (Y_{1(j)} \overset{d}{=} Y_{2(j)})\} \tag{3.10}$$

$$H_1 : \{\cup_j (Y_{1(j)} \overset{d}{\leq} Y_{2(j)})\}. \tag{3.11}$$

Focusing our attention on the jth sub-hypothesis $H_{oj} : \{Y_{1(j)} \overset{d}{=} Y_{2(j)}\}$ against $H_{1j} : \{Y_{1(j)} \overset{d}{\leq} Y_{2(j)}\}$, the permutation solution is based on test statistics

$$T_j^* = \sum_{1 \leq i \leq N_{2(j)}} Y_{2(j)i}^* \tag{3.12}$$

where $N_{2(j)} = \sum_{r>j} n_r$ is sample size of $Y_{2(j)}$. Then, all the T_j^* $(j = 1, \ldots, C-1)$ represent a set of appropriate partial solutions for the problem; since these partial tests are all exact and marginally unbiased, their non-parametric combination represents an exact overall solution. This monotonic inference problem can be also faced in multivariate context. Recent application of Stochastic Ordering can be found in Zirilli et al., 2008; Alibrandi and Finos, 2005.

3.4. **Application of Stochastic Ordering procedure.** For every genotype, the attention has been focused on the observation times (T_1, T_2, T_3, T_4), assessing the possible increasing tendency for homocysteine and decreasing tendency for folates. So, we had to verify the hypothesis of existence of an increasing monotonous stochastic ordering in the different times for homocysteine and decreasing for folates. The multivariate and multistrata Stochastic Ordering procedure has been applied

with the purpose to verify the existence of such monotonicity in the trend, testing directional ordinate alternative hypotheses.

$$H_{0j} : \{homoc._{T1j} \overset{d}{=} ... \overset{d}{=} homoc._{T4j}\} \cap \{fol._{T1j} \overset{d}{=} ... \overset{d}{=} fol._{T4j}\} \tag{3.13}$$

$$H_{1j} : \{homoc._{T1j} \overset{d}{\neq} ... \overset{d}{\neq} homoc._{T4j}\} \cup \{fol._{T1j} \overset{d}{\neq} ... \overset{d}{\neq} fol._{T4j}\} \tag{3.14}$$

The stratification j index refers to the three genotypes. The results of Stochastic Ordering procedure are shown in table 4.

TABLE 4. Stochastic Ordering results for different times

HOMOCYSTEINE			
Comparisons	Genotype 1	Genotype 2	Genotype 3
$T_1 < T_2$	**0.000**	**0.008**	**0.001**
$T_2 < T_3$	**0.024**	0,376	**0.000**
$T_3 < T_4$	**0.000**	**0.000**	**0.000**
	↓	↓	↓
Stoch. Ord.	**0.000**	**0.000**	**0.000**
FOLATES			
$T_1 > T_2$	**0.000**	**0.000**	**0.000**
$T_2 > T_3$	0.696	0.185	**0.002**
$T_3 > T_4$	**0.000**	**0.000**	**0.039**
	↓	↓	↓
Stoch. Ord.	**0.004**	**0.000**	**0.000**

Examining the highly significant values of the combined tests, we assess the existence of an increasing monotone Stochastic Ordering for homocysteine and decreasing for folates. Particularly, for homocysteine and with reference to 1 and 3 genotypes, a meaningful increasing trend is verified for each time, while for 2 genotype the increasing tendency isn't statistically significant in the comparison between T_2 and T_3 times. For folates the decreasing tendency is always statistically significant, except in the comparison between T_2 and T_3 times for 1 and 2 genotypes. In figure 1 we report the means of homocysteine and folates to illustrate such order in the different times and for each genotype.

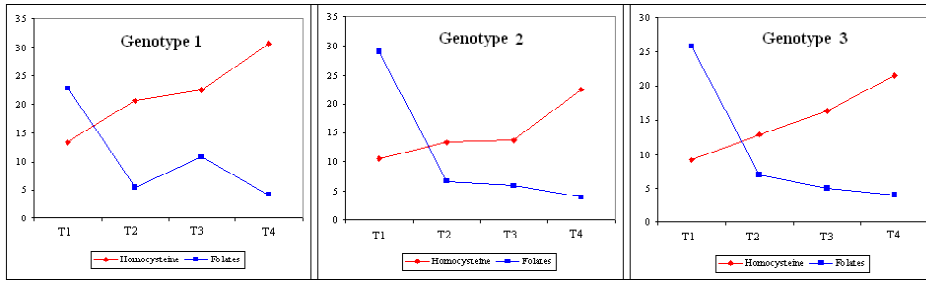


FIGURE 1. Stochastic Ordering for genotype

4. Final remarks

The low sample size and the non-normal distribution of the considered phenomenon led us to use a non parametric approach; in particular we have chosen a based permutation tests approach, for its several properties of goodness. By means of this metodology, we have performed two analysis: the Non Parametric Combination test or NPC Test for the evaluation the existence of possible statistically significant differences among the three groups of subjects in relationship to homocysteine and folates levels and the Stochastic Ordering procedure to verify the existence of a monotonous increasing or decreasing for homocysteine and folates levels in time. Analyzing the obtained results we can notice that all the examined patients show more elevated homocysteine levels than the physiological ones. The comparison among the three genotypes showed that the most remarkable significant differences in homocysteine levels are been found among the first group belonging subjects, i.e. the 677TT genotype (homozygote). The comparison performed within every group, for the different periods of observation, showed that the times to get levels of surplus homocysteine than the physiological ones vary in considerable way among the patients. Particularly, the patients with 1 genotype (homozygous mutation 677TT) already develop hyperhomocysteinemia conditions after two months from the folates suspension. Contrarily, in the holder patients of 2 genotype (heterozygous mutation 677CT) the homocysteine levels maintain below the physiological levels up to four months from the suspension of the folates, therefore the conditions of hyperhomocysteinemia occur only after six months. In the patients with 3 genotype (diplotype C677T/1298AC) it is observed that, after four months from the suspension of the treatment, the levels of homocysteine exceed, although of few, the physiological values and come back in the conditions of hyperhomocysteinemia after six months. Therefore the results show that the levels of homocysteine vary in a significant way both on the base of patients genetic mutation and in relationship to the periods in which the levels of homocysteine have been noticed. Moreover, we have verified, by the Stochastic Ordering inferential procedure, the existence of a significant increasing tendency for homocysteine and a decreasing tendency for folates. In conclusion, in order to maintain normal the levels of homocysteine in the blood, the carriers of the 677TT MTHFR mutation need more elevated doses of folates, for a more prolonged time, in comparison to the other analyzed genotypes carriers.

References

Alibrandi A., Finos L. (2005), Building abusiveness in the City of Messina: analysis of the trend in the year 1990-2003. *Atti XLI Riunione Scientifica SIS: Statistics and Environment*, CLEUP, Padova, 29–33.

Alibrandi A., Zirilli A. (2007), A statistical evaluation on high seric levels of D-Dimer: a case control study to test the influence of ascites, *Atti S.Co.2007 Conference*, CLEUP, Padova, 9–14.

Arboretti Giancristofaro R., Marozzi M., Salmaso L. (2005), Repeated measures designs: a permutation approach for testing for active effects, *Far East Journal of Theoretical Statistics, Special Volume on Biostatistics*, vol. 16, 2, 303–325.

Bonnini S., Corain L., Muna F., Salmaso L. (2006), Neurocognitive Effects in Welders Exposed to Aluminium: An Application of the NPC Test and NPC Ranking Methods, *Statistical Methods and Applications, Journal of the Statistical Society*, 15, 2, 191–208.

Bonnini S., Pesarin F., Salmaso L. (2003), Statistical Analysis in biomedical studies: an application of NPC Test to a clinical trial on a respiratory drug. *Atti 5º Congresso Nazionale della Societ Italiana di Biometria*, 107–110.

Caccamo D., Condello S., Gorgone G., Crisafulli G., Belcastro V., Gennaro S., Striano P., Pisani F., Ientile R. (2004), Screening for C677T and A1298C MTHFR polymorphisms in patients with epilepsy and risk of hyperhomocysteinemia, *Neuromolecular Med.*, 6(2-3), 117–26.

Callegaro A., Pesarin F., Salmaso L. (2003), Test di permutazione per il confronto di curve di sopravvivenza, *Statistica Applicata*, vol. 15, 2, 241–261.

Di Castelnuovo A., Mazzaro D., Pesarin F., Salmaso L. (2000), Test di permutazione multidimensionali in problemi d'inferenza isotonica: un'applicazione alla genetica, *Statistica*,60,4, 691–700.

Finos L., Pesarin F., Salmaso L., Solari A.(2004), Nonparametric iterated procedure for testing genetic differentiation, *Atti XLIII Riunione Scientifica SIS*, CLEUP, Padova.

Ono H., Sakamoto A., Mizoguchi N., Sakura N. (2002), The C677T mutation in the methylenetetrahydrofolate reductase gene contributes to hyperhomocysteinemia in patients taking anticonvulsants, *Brain Dev.*, 24,4, 223–226.

Pesarin F. (1997), *Permutation testing of multidimensional Hypotheses*, CLEUP, Padova.

Pesarin F. (2001), *Multivariate Permutation Test*, John Wiley & Sons, Chichester, England.

Salmaso L. (2005), Permutation tests in screening two-level factorial experiments, *Advances and Applications in Statistics*, vol. 5, 1, 91–110.

Terpstra J. T., Magel R. (2003), A new non parametric test for the ordered alternative problem, *Nonparametric statistic*, 15, 3, 289–301.

Zirilli A. , Alibrandi A., D'Amico S.M.I., D'Amico S.(2008) Statistical analysis on volcanic sismicity: applications and comparisons, Atti della XLIV Riunione Scentifica SIS, CLEUP, Padova, 87–88.

Zirilli A., Alibrandi A., Spadaro A., Freni M.A. (2005), Prognostic factors of survival in the cirrhosis of the liver: A statistical evaluation in a multivariate approach, *Atti S.Co.2005 Conference*, CLEUP, Padova, 173–178.

Agata Zirilli, Angela Alibrandi – Department of Economical, Financial, Social, Environmental, Statistical and Territorial Sciences (SEFISAST) - University of Messina

Tipografia A.C.
Finito di stampare dalla
Tipografia A. C.
Via Filippo Marini, 15 - Palermo
Novembre 2009
E-mail: tipografiaac@alice.it